ISSN 0181-0642

BULLETIN du MUSÉUM NATIONAL d'HISTOIRE NATURELLE

PUBLICATION TRIMESTRIELLE

SECTION C

Sciences de la Terre

paléontologie
géologie
minéralogie

4e SÉRIE, T. 18, 1996 (2-3)

ÉDITIONS SCIENTIFIQUES DU MUSÉUM, PARIS

ÉDITIONS SCIENTIFIQUES DU MUSÉUM, PARIS

BULLETIN DU MUSÉUM NATIONAL D'HISTOIRE NATURELLE

57, rue Cuvier, 75005 Paris

—

Section C : SCIENCES DE LA TERRE

Rédacteur en chef : Hervé LELIÈVRE

Secrétariat de rédaction : Florence KERDONCUFF

S'adresser

pour les échanges :

au Service des périodiques et des échanges de la Bibliothèque Centrale
du Muséum national d'Histoire naturelle
38, rue Geoffroy Saint-Hilaire, 75005 Paris
Tél. : [33] (1) 40 79 36 41

pour les abonnements et achats au numéro :

aux Éditions Scientifiques du Muséum, Paris - Diffusion
57, rue Cuvier, 75005 Paris
Tél.: [33] (1) 40 79 37 00
Fax : [33] (1) 40 79 38 40
e-mail : dhenay@mnhn.fr

pour l'envoi de manuscrits :

aux Éditions Scientifiques du Muséum, Paris - Rédaction du Bulletin
57, rue Cuvier, 75005 Paris
Tél.: [33] (1) 40 79 34 38
Fax : [33] (1) 40 79 38 58
e-mail: bulletin@mnhn.fr

Abonnements pour l'année 1996 (prix HT) :

Abonnement général : 1800 FF
Section A : zoologie, biologie et écologie animales : 800 FF
Section B : botanique *Adansonia* : 500 FF
Section C : sciences de la Terre, paléontologie, géologie et minéralogie : 600 FF.

Numéro d'inscription à la Commission paritaire des publications et agences de presses : 1405 AD

BULLETIN DU MUSÉUM NATIONAL D'HISTOIRE NATURELLE, Paris
4[e] sér., **18**, 1996, n[os] 2-3, Section C, (Sciences de la Terre : Paléontologie, Minéralogie, Géologie)

SOMMAIRE

Bulletin du Muséum national d'Histoire naturelle, Paris, 4e sér., **18**, 1996
Section C, nos 2-3 : 179-232

Révision des ammonites du Cénomanien supérieur et du Turonien inférieur du Tinrhert (Sahara algérien) : implications biostratigraphiques

par Francis AMÉDRO, Georges BUSSON et Annie CORNÉE

Résumé. — Le Tinrhert central et oriental, région du Sahara algérien située entre le Grand Erg oriental au nord et le bassin d'Illizi au sud, fournit une succession du Cénomanien supérieur-Turonien inférieur particulièrement précieuse étant donné son isolement : les affleurements des régions plissées du Maghreb sont situées près de 1 000 km plus au nord et les premiers affleurements au sud du Massif central saharien (Niger, Nigeria) à une distance du même ordre. En outre, la série comparée à celle des plateaux qui prolongent vers l'ouest le Tinrhert (Tademaït en particulier) est remarquablement riche et se prête donc à une zonation excellente. Enfin, cette série qui a échappé à la dolomitisation fournit des données pour dater les calcaires massifs du Cénomano-Turonien connus tant au Sahara algérien (à l'extrême est du Tinrhert, sur le Haut d'El Biod, sur le Mzab), en Libye (Nord-Tripolitaine, hamada El Homra) et sur une grande partie du Maghreb, de l'extrême sud tunisien (Dahar) jusqu'au littoral atlantique. La récolte de plus de 200 ammonites déterminables spécifiquement dans ces formations cénomano-turoniennes du Tinrhert (Sahara algérien) sert de base à une étude systématique et à la révision des travaux de COLLIGNON (1957, 1965). La mise en synonymie d'un certain nombre de taxons décrits par COLLIGNON conduit à une réduction sensible du nombre des espèces qui passe de 34 à 15. La localisation d'une grande partie du matériel sur des coupes métrées permet de distinguer six intervalles biostratigraphiques successifs, soit du bas vers le haut : 1) *Neolobites vibrayeanus* (d'Orbigny, 1841) et *Cunningtoniceras tinrhertense* (Collignon, 1965) ; 2) *N. vibrayeanus, Forbesiceras* sp., *Calycoceras (Calycoceras) naviculare* (Mantell, 1822) et *Eucalycoceras pentagonum* (Jukes-Browne, 1896) ; 3) *Nigericeras gadeni* (Chudeau, 1909) ; 4) *Vascoceras gamai* (Choffat, 1898) et *V. cauvini* (Chudeau, 1909) associés vers le bas à *N. gadeni* et au sommet à *Pseudaspidoceras grecoi* (Collignon, 1965), *Fikaites subtuberculatus* (Collignon, 1965) et *F. laffitei* (Collignon, 1965) ; 5) *Pseudotissotia nigeriensis* (Woods, 1911) ; 6) *P. nigeriensis, Choffaticeras* gr. *quaasi* (Peron, 1904) –*pavillieri* (Pervinquière, 1907) et *Choffaticeras* sp. En tenant compte de la disparition de *V. cauvini* au sommet du 4e intervalle et de l'apparition de *P. nigeriensis* à la base du 5e, la limite Cénomanien-Turonien est placée entre les intervalles 4 et 5. Ceci revient à remonter sensiblement la position de la limite Cénomanien-Turonien au Tinrhert par rapport aux interprétations antérieures de COLLIGNON (1957, 1965) et BUSSON (1965, 1972) où toutes les faunes à *Nigericeras* et les faunes plus récentes étaient attribuées au Turonien. Ces divisions nouvelles sont particulièrement précieuses pour assurer des corrélations tant avec les séries du Maghreb qu'avec les séries du Niger et du Nigeria.

Mots-clés. — Tinrhert, Sahara algérien, Cénomanien supérieur, Turonien inférieur, Ammonites, nouveaux taxons, biostratigraphie.

Revision of the upper Cenomanian-Lower Turonian ammonites of Tinrhert (Algerian Sahara): biostratigraphic implications

Abstract. — In central and eastern Tinrhert of the Algerian Sahara, located between the "Grand Erg Oriental" in the north and the Illizi basin in the south, an Upper Cenomanian-Lower Turonian succession is exposed. This occurrence is of particular interest because of its remoteness to other outcrops of the same age: the outcrops from the Maugrabin folded areas in the north are about 1000 km away; the distance from the nearest outcrops of the Saharan Central Massif (Niger, Nigeria) in the south is the same magnitude. In comparison with the plateaus which extend from the Tinrhert westwards (particularly the Tademait), the sequence is rich in ammonites and suitable for detailed zonation. Furthermore, the rocks are not dolomitized and thus provide means of dating the extensive Cenomanian-Turonian limestones from the Algerian Sahara (in the easternmost Tinrhert, High of

El Biod, Mzab), Libya (northern Tripolitania, Hamada El Homra), and a large part of the Magrab, the extreme south of Tunisia (Dahar) to the Atlantic coast. From this Cenomanian-Turonian sequence in Tinrhert more than 200 ammonites have been collected, which are determinable to species. The material has permitted a systematic study and revision of the work of COLLIGNON (1957, 1965). A number of taxa described by COLLIGNON have been placed in synonymy and the number of species has been reduced from 36 to 15. The positioning of a large part of the material within measured sections allows the recognition of six successive biostratigraphic intervals: interval 1 containing *Neolobites vibrayeanus* (d'Orbigny, 1841) and *Cunningtoniceras tinrhertense* (Collignon, 1969); interval 2 containing *N. vibrayeanus*, *Forbesiceras* sp., *Calycoceras (Calycoceras) naviculare* (Mantell, 1822) and *Eucalycoceras pentagonum* (Jukes-Browne, 1896); interval 3 containing *Nigericeras gadeni* (Chudeau, 1909); interval 4 containing *Vascoceras gamai* (Choffat, 1898) and *V. cauvini* (Chudeau, 1909) associated to *N. gadeni* at the bottom and to *Pseudaspidoceras grecoi* (Collignon, 1965), *Fikaites subtuberculatus* (Collignon, 1965) and *F. laffitei* (Collignon, 1965) at the top; interval 5 containing *Pseudotissotia nigeriensis* (Woods, 1911); interval 6 containing *P. nigeriensis*, *Choffaticeras* gr. *quaasi* (Peron, 1904) – *pavillieri* (Pervinquière, 1907) and *Choffaticeras sp.* On account of the disappearance of *V. cauvini* at the top of interval 4 and the appearance of *P. nigeriensis* at the base of interval 5, the Cenomanian-Turonian boundary is placed between intervals 4 and 5. This means that the Cenomanian-Turonian boundary in the Tinrhert is now placed considerably higher than in previous studies (Collignon, 1957, 1964; Busson, 1965, 1972), where the beds with *Nigericeras* and above were ascribed to the Turonian. These new subdivisions allow correlations with both the Maugrabin and the Niger-Nigeria successions.

Key-words. — Tinrhert, Algerian Sahara, Upper Cenomanian, Lower Turonian, ammonites, new taxon, biostratigraphy.

F. AMÉDRO, *26, rue de Nottingham, 62100 Calais.*
G. BUSSON & A. CORNÉE, *Muséum national d'Histoire naturelle, Laboratoire de Géologie, 43, rue de Buffon, F-75231 Paris cedex 05.*

INTRODUCTION (G. B. & A. C.)

L'intérêt de la série du Tinrhert oriental

Dans le Nord-Ouest africain, les dépôts marins du Cénomanien-Turonien correspondent à la plus vaste transgression de l'histoire post-carbonifère. Ces dépôts marins, particulièrement étendus à partir du Cénomanien supérieur, se présentent souvent sous la forme de carbonates massifs, d'une épaisseur de l'ordre d'une centaine de mètres, fréquemment dolomitisés et, de ce fait, peu ou pas fossilifères. À peu près isopiques et isopaques, ils prennent en écharpe le domaine nord-saharien et le domaine atlasique, de la hamada el Homra (Libye) jusqu'à l'Atlantique (BUSSON 1972, Fig. XIII.2). Ces carbonates massifs, attribués globalement au Cénomanien-Turonien, occupent ainsi – pour s'en tenir au domaine nord-saharien – le Dahar tunisien, le Tinrhert extrême-oriental, le Mzab (Fig. 1).

Au sud de 31°N, une intercalation marneuse se développe, pouvant atteindre une épaisseur de 65 m, aux dépens de la partie moyenne de cette barre carbonatée, le total représentant toujours une centaine de mètres d'épaisseur.

Dans cette « province argileuse méridionale » (BUSSON 1972), la série cénomano-turonienne est alors occupée par une triade comprenant :

1) les calcaires inférieurs {c2-t1 de la carte Fort-Flatters (BUSSON 1964)};
2) des marnes médianes (t2);
3) des calcaires supérieurs (t3) (Fig. 2).

Or les « calcaires inférieurs », de même que les quelques bancs calcaires intercalés dans les « marnes médianes » ont été remarquablement préservés de la dolomitisation et sont souvent ri-

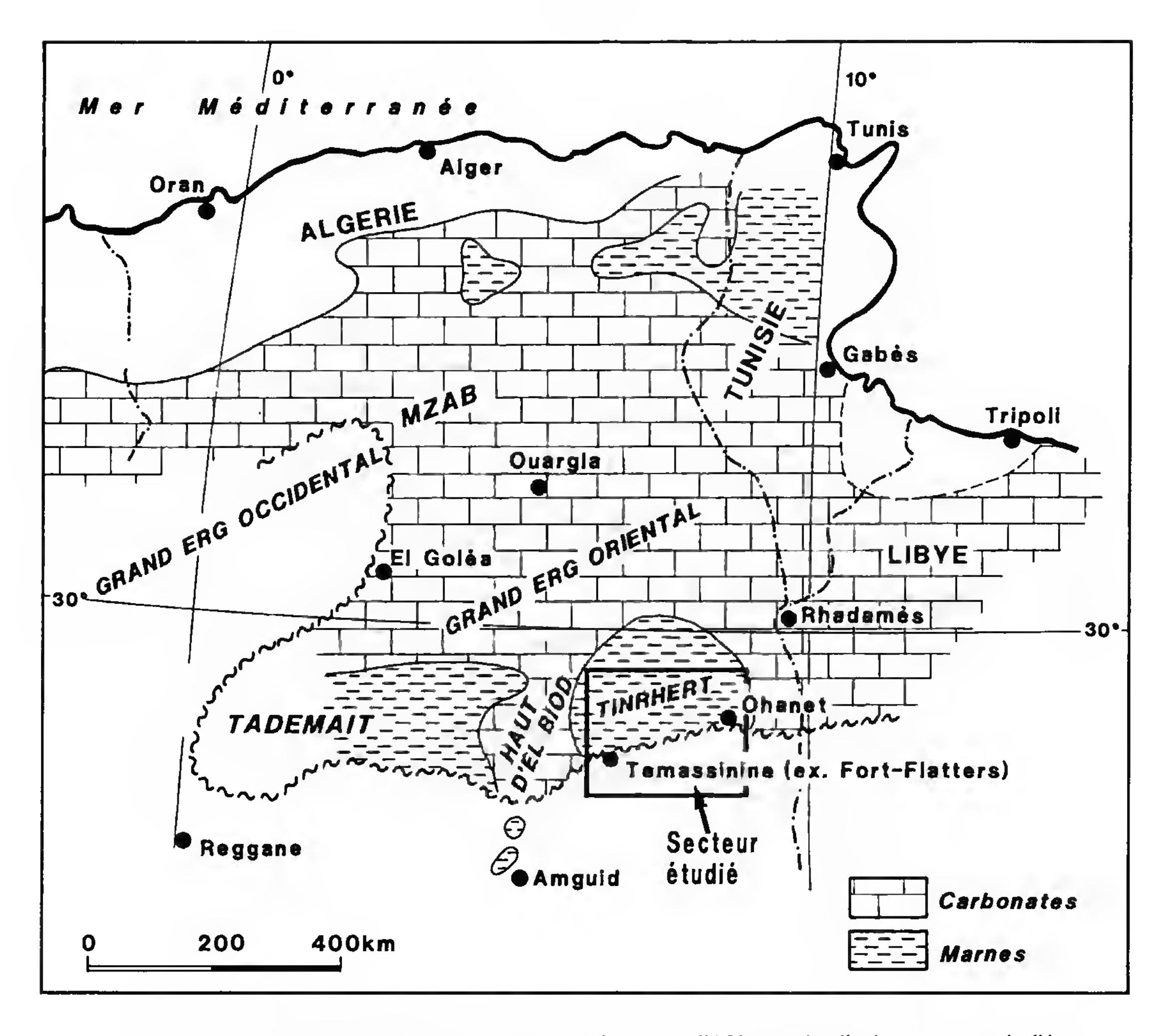


FIG. 1. — Situation géographique du Tinrhert dans le nord de l'Afrique et localisation du secteur étudié.

chement fossilifères. De telles séries offrent donc une opportunité sérieuse et rare dans tout le Nord-Ouest africain de dater plus précisément cet ensemble cénomano-turonien. Une telle datation est d'autant plus précieuse que l'unité sous-jacente aux «calcaires inférieurs» consiste, dans la plus grande partie du domaine considéré, en argiles à gypse pratiquement azoïques (BUSSON 1970) et que l'unité sus-jacente – souvent attribuée dubitativement au Sénonien – revêt le même faciès et n'a jamais pu être datée.

Si l'on ajoute à ces faits que le Nord-Est du Sahara algérien étant occupé par les atterrissements du Bas-Sahara et du Grand Erg oriental est dépourvu d'affleurements crétacés, la série de la province argileuse mériodionale (Tademaït et Tinrhert) est particulièrement importante. Ces

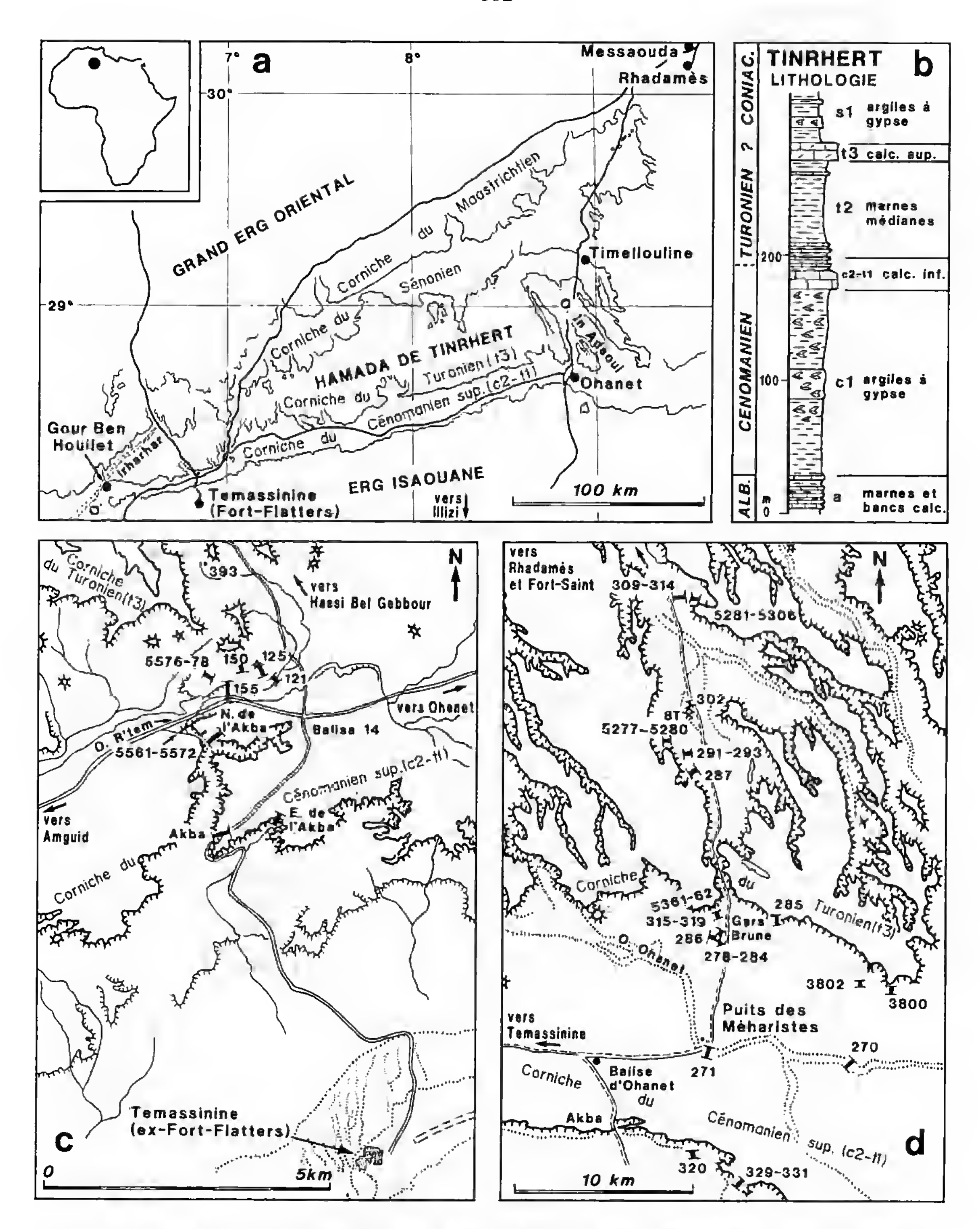


FIG. 2. — a, cadre géographique. b, coupe géologique du secteur étudié dans la hamada de Tinrhert et localisation des gisements d'ammonites dans les régions de Témassinine. c, Fort-Flatters et d, d'Ohanet.

affleurements en effet sont isolés, distants de près de mille kilomètres au sud des affleurements plissés et fossilifères des régions atlasiques et à une distance du même ordre de grandeur des affleurements du sud des massifs centraux sahariens (Niger et Nigeria). Cet isolement même en fait des jalons particulièrement précieux.

Or, dans cette province, les affleurements du Tinrhert oriental offrent des séries relativement épaisses comparées à celles du Tademaït et particulièrement fossilifères.

Les ammonites

La faune ici révisée a été récoltée par l'un de nous (G. B.) entre 1957 et 1965. Ces ammonites ont déjà été décrites en détail sur le plan systématique par COLLIGNON en 1957, puis en 1965. Trente-quatre espèces, réparties en dix-neuf genres, ont été citées ou figurées par cet auteur, dont dix étaient nouvelles. Ces ammonites récoltées sur des coupes métrées (voir annexe 1) nous ont paru mériter une révision systématique et biostratigraphique détaillée.

En effet, il y a une vingtaine d'années, l'ensemble des faunes à *Nigericeras* et à *Vascoceras* était attribué au Turonien. Aujourd'hui, une part substantielle des Vascoceratidae est datée du Cénomanien supérieur (BERTHOU *et al.* 1985; KENNEDY & COBBAN 1991). D'autre part, le concept de l'espèce en paléontologie a considérablement évolué, passant d'une vision typologique, avec comme résultat un fractionnement des espèces, à une interprétation plus biologique, acceptant un large spectre de variations morphologiques.

Les objectifs de ce travail sont d'abord d'ordre systématique. Ils incluent, outre de préciser la répartition de ces faunes d'ammonites au sein des formations cénomano-turoniennes du Tinrhert central et oriental, d'y établir des divisions biostratigraphiques fines. Grâce à elles, la limite Cénomanien-Turonien se trouve placée avec une certaine précision.

HISTORIQUE DE TRAVAUX ANTÉRIEURS (G. B. & A. C.)

Nous ne ferons que citer quelques noms parmi les premiers explorateurs (CORTIER, LAVAUDAN, ROCHE, ROLLAND, BASSE & LAPPARENT) dont la mémoire, les travaux et les résultats – très méritoires même quand ils n'étaient que ponctuels – ont récemment été fort bien évoqués par LEFRANC (1976). Le premier travail systématique a été celui de la mission BRP-Tinrhert 1955-1956 (RUMEAU *et al.* 1957). Ces auteurs donnaient, pour la première fois, une carte géologique au 1/200000 d'une bonne partie de la hamada de Tinrhert. Pour ce qui est du Cénomano-Turonien, ils reconnaissaient la triade lithologique caractéristique (calcaires inférieurs, marnes médianes et calcaires supérieurs) dont ils attribuaient les termes respectivement au Turonien inférieur, au Turonien moyen et au Turonien supérieur. Ils recueillaient des fossiles en particulier dans le Cénomano-Turonien (*cf.* ci-dessous, COLLIGNON 1957) et distinguaient cartographiquement le Cénomanien supérieur (calcaires bruns dolomitiques, massifs) du bord du plateau, du Turonien (calcaires blancs, crayeux, tendres, fossilifères) du bas de la cuesta turonienne. Il s'est avéré que cette distinction ne pouvait être retenue car il ne s'agit là que de deux modes d'altération dépendant des conditions d'affleurement. Les calcaires du bord du plateau affleurant depuis longtemps ont été soumis à de fortes actions tardi-diagénétiques ; les affleurements apparaissant dans

les ravinements du plateau ou au pied de la falaise argileuse sont beaucoup plus frais et offrent le faciès crayeux. Mais des couches représentées à la partie supérieure du bord du plateau se retrouvent à la base des calcaires crayeux. Cette confusion a amené ces auteurs à exagérer l'épaisseur de ce qu'ils imputaient au Cénomanien supérieur et au Turonien.

COLLIGNON* (1957) déterminait les fossiles ramassés au cours de cette mission. Selon les conceptions alors en usage, au moins dans le domaine africain, il attribuait au Turonien inférieur les faunes à *Nigericeras* et toutes les faunes sus-jacentes. Traduisant la grande variabilité morphologique des céphalopodes en termes spécifiques, il déterminait sur une cinquantaine d'exemplaires dix-huit espèces ou variétés dont six nouvelles.

Cénomanien : *Angulithes fleuriausi, Neolobites vibrayei, N. peroni, N. fourteaui.*

Turonien inférieur : cf. *Nigericeras jacqueti, Mammites subconciliatus* Choffat var., *flattersi* nov. var., *Mammites* cf. *pseudonodosoides, Vascoceras gamai, Paravascoceras rumeaui* nov. sp., *Discovascoceras* cf. *amieirense, D. tesselitense* nov. sp., *D. defrennei* nov. sp., *Hoplitoides* aff. *ingens, Pseudotissotia gallienei* var. *inflata* nov. var., *Bauchioceras nigeriense, Furoniceras trumpyi* nov. gen., nov. sp., *Leoniceras pavillieri.*

BUSSON (1960) précisait la lithologie de la triade de la partie centrale du Tinrhert oriental. Il interprétait les mécanismes du passage de ces trois termes à la série carbonatée massive vers l'est et vers l'ouest. Il mettait l'accent sur la zone intermédiaire – entre le domaine des marnes médianes et le domaine d'une série carbonatée massive unique – en particulier dans la région de Gour ben Houilet où la partie supérieure des marnes médianes s'enrichit considérablement en fossiles (*Hemiaster semicavatus, Bauchioceras*) permettant dès lors de confirmer l'âge turonien de ces marnes, affirmé depuis ROCHE (1880) sans arguments paléontologiques. Il justifiait d'attribuer au Cénomanien inférieur et moyen (?) les argiles à gypse sous-jacentes aux calcaires inférieurs, argiles à gypse qui auraient été trop souvent placées dans le Continental intercalaire.

Peu après, BUSSON publiait la carte géologique régulière au 1/500000 Fort-Flatters (1964) puis une note (1965) introduisant l'étude paléontologique des premières faunes récoltées (*cf.* COLLIGNON 1965, ci-dessous). Par une étude de très nombreuses coupes et une cartographie complète sur le terrain et avec l'aide des photos aériennes, il avait mis en évidence l'erreur cartographique ci-dessus imputée à RUMEAU *et al.* La limite Cénomanien-Turonien, coïncidant à cette époque encore avec la base des couches à *Nigericeras*, se situait dans un ensemble de calcaires crayeux parfaitement monotones ou dissimulés sous les hamadas et regs séparant la falaise cénomanienne au sud de la falaise turonienne au nord. Cartographiquement, il était possible seulement de définir une unité Cénomanien supérieur-Turonien inférieur (c2-t1 de la carte) correspondant aux «calcaires inférieurs» ci-dessus évoqués et parfaitement individualisée par les diagraphies dans les sondages. Les cartes et coupes fournies dès cette époque (BUSSON 1965, fig. 2 A, B ; fig. 3 A, B) correspondent aux documents de base des figures ci-jointes (Figs 2-4).

Les affleurements de Cénomanien supérieur et de Turonien inférieur des régions d'Ohanet-In Adaoui, de Fort-Flatters devenue Témassinine et de Gour ben Houilet principalement avaient fourni des centaines de fossiles, en particulier de céphalopodes. Il apparaissait manifeste que loin de s'agir de deux faunes globales (l'une cénomanienne, l'autre turonienne), une évolution verticale et une zonation s'imposaient nettement. COLLIGNON (1965) étudiant les ammonites de

* Cette étude de fossiles de la hamada de Tinrhert était située par son auteur au Fezzan. Cela s'écartait d'un usage qui limite cette province au territoire de la Libye.

ces récoltes créait encore neuf formes nouvelles dans ces faunes où la diversité morphologique n'est pas moins remarquable que l'extrême abondance des individus. L'inventaire des formes déterminées consistait en :

– ammonites cénomaniennes : *Neolobites vibrayei, N. fourtaui, N. peroni, N. bussoni* nov. sp., *Calycoceras grossouvrei, C. boulei, Calycoceras* sp., *Euralycoceras pentagonum, Protacanthoceras* sp. ;

– ammonites turoniennes : *Kamerunoceras tinrhertense* nov. sp., *Pseudaspidoceras footei* Stol. var. *grecoi* nov. var., *Nigericeras gignouxi, N. lamberti, N. jacqueti, N. jacqueti* Schneegans var. *crassecostata, N.* (?) vel. *Furoniceras* (?), *Discovascoceras tesselitense, D. defrennei, Paravascoceras* aff. *cauvini, Vascoceras gamai, Paramammites laffittei* nov. sp., *P. subtuberculatus* nov. sp., *Neoptychites* sp. aff. *taelingaeformis* Solger var. *discrepans, Pseudotissotia (Bauchioceras) nigeriensis* Woods var. *egrediens* nov. var., *Pseudotissolia bussoni* nov. sp., *Leoniceras pavillieri, Leoniceras luciae, L. segne, Hoplitoides* aff. *ingens, H. hourcqui* nov. sp.

Les données géologiques et paléontologiques lui permettaient de proposer la zonation suivante, de bas en haut :

1) *Neolobites* seul ;
2) *Neolobites* plus *Calycoceras, Eucalycoceras*, etc. ;
3) les mêmes plus *Nigericeras* ;
4) *Nigericeras* plus divers Vascoceratidae ;
5) divers Vascoceratidae plus *Bauchioceras* ;
6) *Bauchioceras* plus divers *Choffaticeras, Leoniceras, Hoplitoides.*

Dans BUSSON (1965), une note ajoutée en cours d'impression faisait savoir qu'à la lumière de nouvelles études de terrain, la zone 3 devait être amendée : une récolte plus fine montrait qu'à quelques centimètres près les *Nigericeras* étaient toujours superposés aux *Neolobites* et *Calycoceras*. Les trois premières zones étaient attribuées au Cénomanien supérieur et terminal ; les suivantes au Turonien inférieur. BUSSON (1965) notait en outre quelques traits différenciant la région d'Ohanet-In Adaoui de la région de Témassinine (*ex* Fort-Flatters) : manque possible des *Calycoceras* à Ohanet ; extrême amincissement de la série sus-jacente au niveau à *Nigericeras* et tout spécialement de la série à *Bauchioceras* des coupes d'Ohanet à celles de Témassinine (*ex* Fort-Flatters).

À la suite de nouvelles récoltes (dont les déterminations par COLLIGNON sont restées inédites) et d'une synthèse générale sur le Mésozoïque saharien, BUSSON (1969, 1972) amendait légèrement la succession proposée. On peut la schématiser avec un Cénomanien supérieur et terminal comprenant :

1) une zone à *Neolobites* divers ;
2) une zone à *Neolobites* et *Calycoceras boulei, Eucalycoceras pentagonum* ;

puis un Turonien inférieur avec :

1) un niveau à *Nigericeras* ;
2) un niveau à *Vascoceras gamai, Paravascoceras* aff. *cauvini, Paramammites laffittei, P. subtuberculatus, Pseudouspidoceras footei* var. *grecoi.* ;
3) un niveau à *Pseudotissotia* (*Bauchioceras*) *nigeriensis*,
4) un niveau à *Leoniceras luciae, L. segne, L. pavillieri, Discovascoceras defrennei, Hoplitoides ingens* et *H. hourcqui*.

Notons que le même travail imputait pour la première fois le banc calcaire de la partie supérieure des marnes médianes de Fort-Flatters au Turonien inférieur.

Depuis 1972 aucune étude importante n'a été publiée sur le Cénomanien-Turonien de la Hamada du Tinrhert oriental ou central. Toutefois, sur un plan général, on sait qu'à la suite des études de LAUVERJAT & BERTHOU (1974) menées au Portugal, confirmées par tous les travaux postérieurs, les faunes à *Vascoceras gamai* et *V. cauvini* – et *a fortiori* les couches sous-jacentes – ne doivent plus être datées du Turonien inférieur comme cela a été le cas dans tant de travaux africains, mais du Cénomanien supérieur.

Une étude sur les échinides de ces niveaux et de cette région vient d'être publiée (NÉRAUDEAU *et al.* 1993).

LE CADRE GÉOLOGIQUE (G. B., A. C. & F. A.)

LA COUPE DU CRÉTACÉ MOYEN

Sur le glacis méridional du bassin nord-saharien, la hamada de Tinrhert est comprise entre le Grand Erg oriental au nord et l'erg Isaouane et le bassin d'Illizi au sud, et s'allonge sur une distance d'environ 300 km suivant une direction est-ouest (Fig. 2a).

Plus précisément, la région d'où proviennent les fossiles ici étudiés correspond à la partie sud de la hamada de Tinrhert (ou Tinrhert oriental) couvert par la feuille au 1/500000 Fort-Flatters et limitée par les parallèles 28 et 29° N et les méridiens 6 et 10° E.

Le modelé du paysage est marqué par la présence de corniches parallèles, couronnées par les principales « barres » carbonatées ou gréso-carbonatées, soit du sud vers le nord (ou du bas vers le haut dans l'ordre stratigraphique) : corniche du Cénomanien supérieur (partie inférieure de l'ensemble c2-t1 du log lithologique et de la carte géologique au 1/500 000 de Fort-Flatters); corniche du Turonien (t3); corniche du « Santonien-Campanien indifférencié » ; corniche du Maastrichtien. Ces corniches fournissent d'excellents repères visuels, à la fois sur le terrain et lors de l'examen des photographies aériennes. La continuité des deux premières est à peu près générale. La troisième est souvent beaucoup plus indécise. Les deux dernières, de toute façon, ne sont nettement définissables qu'à l'est de l'oued Irharhar. Du bas vers le haut, la succession des ensembles lithologiques attribués au Cénomanien et au Turonien dans la hamada de Tinrhert est la suivante (les index reprennent la classification des formations utilisées sur la carte géologique au 1/500000 de Fort-Flatters et reportées sur la figure 2b :

Albien, partie supérieure :

a : alternance de marnes sableuses et de bancs carbonatés.

Cénomano-Turonien :

c1 : sur 130 à 140 m : argiles à bancs de gypse massif avec trois unités :

– les 30 à 50 m de base sont constitués de couches argileuses homogènes, en général rouges ou brun rouge, à peu près dépourvues de gypse ;

– les 25 à 35 m en position médiane sont particulièrement riches en gypse massif;

– les 60 à 70 m derniers mètres sont constitués d'une alternance d'argiles vertes ou rouges, parcourues de filons de gypse, de bancs de gypse massif stratifié et, dans les 40 m sommitaux,

de bancs de dolomie blanchâtre, parfois pétrie de débris y compris, dans la région d'Alrar, un oursin nain (BUSSON 1960);

c2-t1 : 25 m à 35 m : «calcaires inférieurs», avec deux unités :

– à la base, sur 10 à 15 m : calcaires massifs, peu ou pas stratifiés, de teinte claire, riches en ammonites (*Neolobites* et, au sommet, *Calycoceras*). Cette unité forme en général la plus grande partie de la première corniche du Tinrhert qui s'étend depuis Ohanet jusqu'au-delà de Témassinine (Fort-Flatters) et que l'on retrouve à l'ouest au Tinrhert central, occidental, puis sur le pourtour du Tadémaït;

– au-dessus, sur 15 à 20 m : bancs de calcaires crayeux, parfois intercalés de marnes. Les ammonites y abondent encore (*Nigericeras*, *Vascoceras*, *Pseudotissotia*, *Choffaticeras*) réparties en plusieurs faunes successives.

t2 : 40 à 60 m : «marnes médianes» constituées de marnes et d'argiles vertes, intercalées de quelques bancs calcaires à l'ouest de Takouazet et surtout à proximité du mole de la dorsale d'El Biod, soit à l'est (Gour Ben Houilet), soit à l'ouest (Chebka Tinrhert). Du gypse peut être discrètement présent. Cet ensemble marneux forme la partie principale du front de la cuesta turonienne. À Gour Ben Houilet, des *Choffaticeras* et *Pseudotissotia* du Turonien inférieur sont encore présents à 3 m du sommet.

t3 : 10 à 15 m : «calcaires supérieurs»; calcaires du Turonien massifs, parfois dolomitiques, et souvent abondamment silicifiés en bancs durs, argileux, bien réglés. Malgré leur faible épaisseur et grâce au fait qu'ils sont intercalés entre deux masses argileuses également importantes, ils constituent non seulement le couronnement de la cuesta turonienne, mais aussi la surface d'un immense plateau rocheux qui peut-être considéré, à proprement parler comme étant véritablement la hamada de Tinrhert.

«*Coniacien*»-«*Santonien*» :

S1 : 50 m : argiles rouges et vertes incluant du gypse et, plus rarement, des bancs dolimitiques. À noter l'identité de faciès de ces argiles attribuées au Coniacien-Santonien sans aucun argument paléontologique avec les argiles à gypse (c1) du Cénomanien.

Les calcaires inférieurs (c2-t1) et les marnes médianes (t 2) ont été datés grâce aux faunes d'ammonites (*cf.* ci-dessous). Les argiles à gypse sous-jacentes n'ont pas livré d'ammonites : leur attribution au Cénomanien paraît néanmoins extrêmement probable, ainsi que cela a été admis de la Tripolitaine au Maroc (*cf.* BUSSON 1960, 1972). Par contre, la datation des calcaires supérieurs (t3) et des argiles à gypse sus-jacentes («Coniacien-Santonien ?») est très incertaine. Des éléments de discussion se trouvent dans BUSSON (1960, 1972). La confirmation présente de l'attribution au Turonien inférieur de la partie supérieure des marnes médianes pose plus que jamais la question de l'âge des deux unités sus-jacentes (t_3 et S_1).

Les ammonites considérées ici (225 spécimens déterminés au total, *cf.* annexe 2) proviennent principalement de trois séries de gisements répartis dans la région d'Ohanet, dans la région de Témassinine (Fort-Flatters), et au lieu-dit Gour Ben Houilet, localisé à une quarantaine de kilomètres à l'ouest de Témassinine (Fig. 2). La quasi-totalité du matériel a été récoltée dans les «calcaires inférieurs» (ensemble c2-t1), les quelques spécimens restants provenant des calcaires crayeux équivalents de la partie supérieure des «marnes médianes» (ensemble t2).

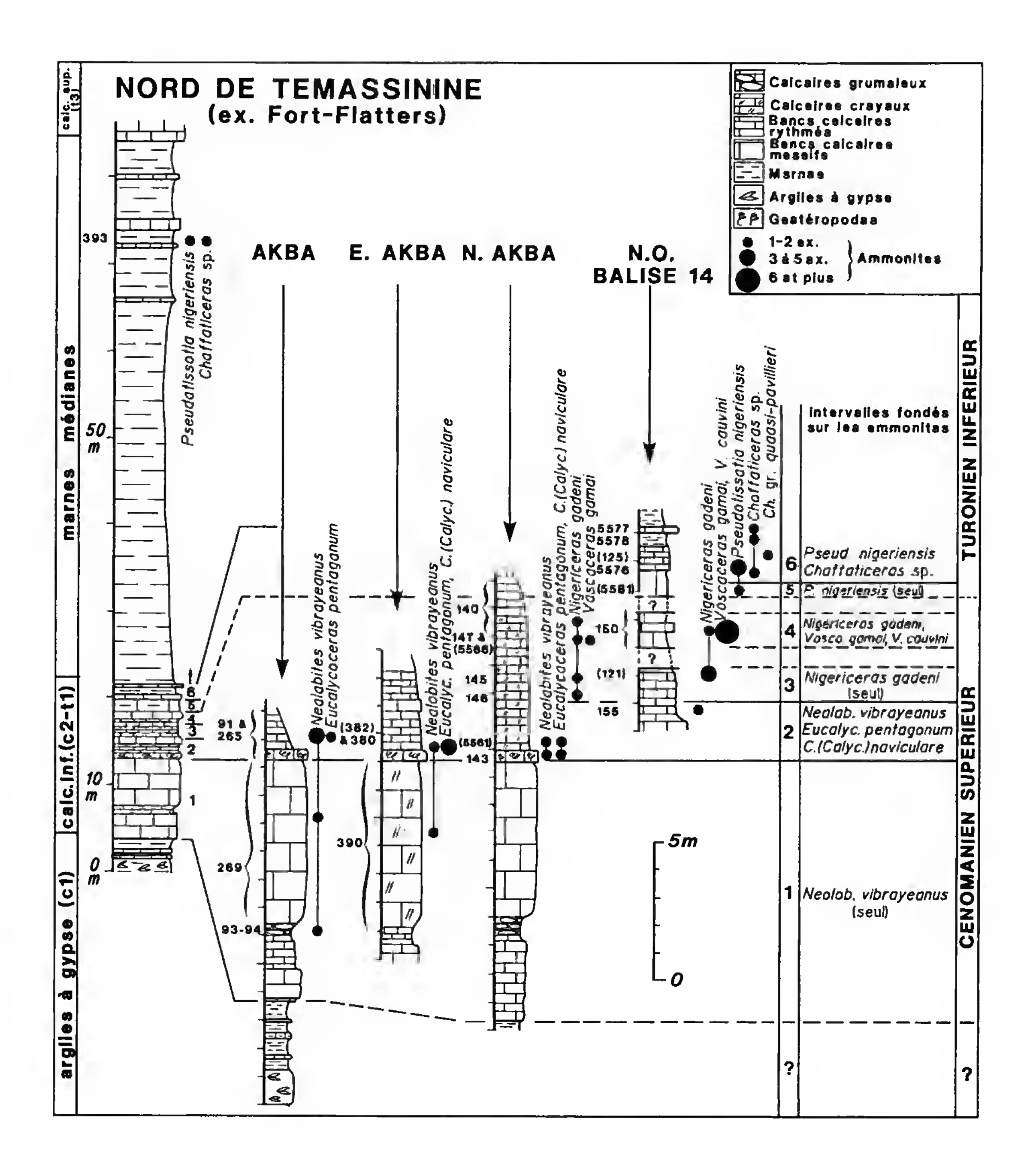


FIG. 3. — Distribution verticale des ammonites de la série calcaire du Cénomanien supérieur-Turonien inférieur dans la région de Témassinine, *ex.* Fort-Flatters, Sud algérien.

LES GISEMENTS DES ENVIRONS DE TÉMASSININE

La figure 2c présente le cadre géographique du secteur étudié. Tout un ensemble de gisements se localise à une dizaine de kilomètres au nord de Témassinine. Au total, quatre coupes sont considérées. Les trois premières (Akba de Témassinine, est de l'Akba, et au nord de l'Akba) exposent la base des «calcaires inférieurs», depuis le contact avec les «argiles à gypse» sous-jacentes. Le calage vertical entre ces trois coupes est fondé sur des corrélations lithologiques. Celles-ci sont facilitées par la quasi-horizontalité de ces terrains, mais en revanche compliquées par l'extrême monotonie des faciès et par la discontinuité due aux regs et aux surfaces altérées. Un banc à trous situé immédiatement au-dessus du gisement 143 fournit un niveau-repère local (Fig. 3). La quatrième coupe, composite, est établie à partir de trois coupes partielles sises près de la balise 14. Cette section est placée plus haut au sein des marnes et bancs calcaires formant la seconde unité de l'ensemble c2-t1, mais en l'absence de repère lithologique commun, sa position exacte par rapport aux trois coupes précédentes reste incertaine.

Au sein de ces quatre coupes, comme dans celles des secteurs d'Ohanet et de Gour Ben Houilet, les récoltes d'ammonites sont localisées par leurs numéros de gisements. Les gisements situés le long de la coupe ou à proximité immédiate sont indiqués sur la gauche des logs lithologiques par des numéros écrits en chiffres arabes. Les gisements un peu plus lointains, mais corrélés avec l'une de ces coupes sont figurés par des numéros entre parenthèses.

Une remarque doit être formulée sur :

«*la présence de nombreux gisements compréhensifs, c'est-à-dire insuffisamment localisés dans le sens vertical et s'étalant de ce fait sur plus d'une zone stratigraphique. Deux raisons en rendent compte. D'une part, dans une série de calcaires crayeux très monotone, il est parfois impossible de repérer à quelques décimètres près le niveau précis d'un affleurement fossilifère isolé. D'autre part, les récoltes ont été effectuées il y a longtemps (de 1957 à 1964), à un stade de l'exploration où l'on visait à reconnaître le Cénomanien et le Turonien et où l'on ne pressentait pas que les zones d'ammonites qui pourraient être définies un jour seraient très minces – parfois de l'ordre de quelques décimètres, exigeant un ramassage très finement différencié dans le sens vertical*» (NÉRAUDEAU *et al.* 1993).

Malgré ces limites, la distribution verticale des ammonites recueillies dans la région de Témassinine (Fort-Flatters) permet de définir six intervalles valables pour tout le Tinhert, soit du bas vers le haut :

– 1 : intervalle à *Neolobites vibrayeanus* seul (sur 7 à 9 m d'épaisseur);

– 2 : intervalle à *N. vibrayeanus* associé à *Forbesiceras* sp., *Calycoceras (Calycoceras) naviculare* et *Eucalycoceras pentagonum* (1 à 2 m);

– 3 : intervalle à *Nigericeras gadeni* seul (2 m);

– 4 : intervalle à *Vascoceras gamai* et *V. cauvini* associés à *N. gadeni* (1 m);

– 5 : intervalle à *Pseudotissotia nigeriensis* seul (1 à 2 m);

– 6 : intervalle à *P. nigeriensis* associé à *Choffaticeras* gr. *quaasi – pavillieri* et *Choffaticeras* sp. (2 m sommitaux des «calcaires inférieurs» et «marnes médianes», soit environ 50 m).

Au total, six intervalles peuvent être différenciés dans les «calcaires inférieurs» et les «marnes médianes» de la région de Témassinine, sur 65 m d'épaisseur.

Rappelons la correspondance entre les intervalles ici définis pour la description de l'ammonitofaune et les unités utilisées, pour les mêmes coupes et les mêmes gisements, lors de la

description de l'échinofaune (NÉRAUDEAU *et al.* 1993) : intervalle 1 = Cs1 ; 2 = Cs2 ; 3 = Cs3 ; 4 = Cs4 ; 5 = Ti1 ; 6 = Ti2.

LES GISEMENTS DES ENVIRONS D'OHANET IN ADAOUI

Les coupes, indiquées sur la figure 2d, s'échelonnent du sud vers le nord sur une vingtaine de kilomètres dans la dépression d'Ohanet-In Adaoui. L'échantillonnage le plus bas stratigraphiquement se localise à 2 km et 8 km à l'est de l'Akba d'Ohanet sur le rebord de la corniche du Cénomanien supérieur. Là affleurent sur une dizaine de mètres d'épaisseur les calcaires massifs, blancs, à *Neolobites vibrayeanus* qui constituent l'unité inférieure de l'ensemble c2-t1 de la carte géologique à 1/500 000 de Fort-Flatters. En terme d'ammonites, il s'agit du premier intervalle à *N. vibrayeanus* précédemment reconnu à Témassinine.

Nous n'avons pas relevé de coupes assurant une continuité stratigraphique entre cette première coupe et les suivantes, prises une dizaine de kilomètres plus au nord au pied de la corniche du Turonien. La lacune d'observation liée à cette discontinuité des affleurements peut être de plusieurs mètres. La deuxième série de coupes (trois au total) porte sur les marnes et bancs calcaires de la partie supérieure de l'ensemble Cénomanien-Turonien. La distribution des ammonites conduit à distinguer ici quatre intervalles, soit du bas vers le haut et en reprenant la numérotation définie dans le secteur de Témassinine (Fig. 4) :

– 1 : intervalle à *Neolobites vibrayeanus*, associé à *Cunningtoniceras tinrhertense* ;

– 2 et 3 : non individualisés, certainement par la lacune d'observation ;

– 4 : intervalle à *Vascoceras gamai*, *V. cauvini*, *Pseudaspidoceras grecoi*, *Fikaites laffitei* et *F. subtuberculatus* (vu sur 3 m) ;

– 5 : intervalle à *Pseudotissotia nigeriensis* seul (8 à 9 m) ;

– 6 : intervalle à *P. nigeriensis* associé à *Choffaticeras* sp. (identifié sur 2 m).

Malgré la discontinuité des affleurements échantillonnés, on retrouve dans la région d'Ohanet, au sein des « calcaires inférieurs » (ensemble c2-t1), les mêmes divisions fondées sur la distribution verticale des ammonites que dans le secteur de Témassinine. À noter toutefois, l'augmentation d'épaisseur dans la région d'Ohanet de l'intervalle 5 à *Pseudotissotia nigeriensis* qui passe de 1 à 2 m dans les environs de Témassinine à 8 à 9 m près d'Ohanet. D'un autre côté, l'intervalle 4, dont seule la partie supérieure a fait l'objet de recherches dans le secteur d'Ohanet, ne contient pas de *Nigericeras gadeni* associé aux *Vascoceras gamai* et *V. cauvini*, mais des *Fikaites* et *Pseudaspidoceras grecoi*. Cette différence suggère qu'il existe peut-être deux faunes successives dans ce que nous appelons aujourd'hui l'intervalle 4 ; l'association recueillie dans les environs d'Ohanet pouvant être légèrement plus récente que celle de Témassinine. La mise en évidence au Nigeria où les successions sont comparables à celle du Tinhrert d'un horizon à *Fikaites* aux confins de la limite Cénomanien-Turonien, au-dessus du niveau de disparition des *Nigericeras* rend cette hypothèse très probable (MEISTER 1989 ; ZABORSKI 1993, 1995).

GOUR BEN HOUILET

La région des Gour Ben Houilet située à une quarantaine de kilomètres à l'ouest de Témassinine (Fig. 2a) présente un double intérêt. D'une part, géographiquement, il s'agit d'une zone de transition dans laquelle les « marnes médianes » tendent à passer latéralement dans leur

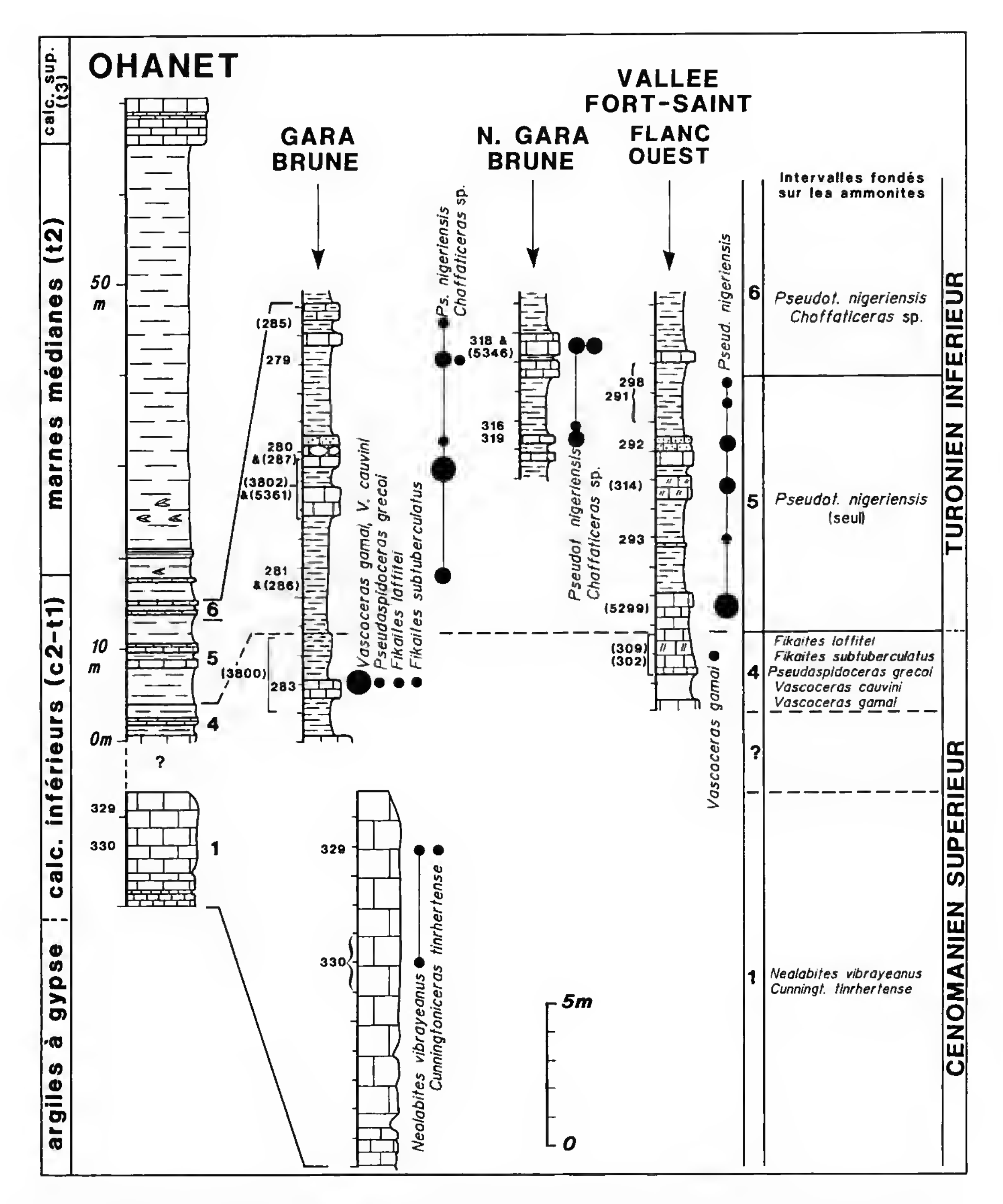


FIG. 4. — Distribution verticale des ammonites de la série calcaire Cénomanien supérieur-Turonien inférieur dans la région d'Ohanet, Sud algérien.

partie supérieure au faciès carbonaté massif que l'on retrouve sur les hauts-fonds de la dorsale d'El Biod. Cette transition se fait par l'intermédaire d'un enrichissement généralisé en bancs calcaires riches en échinides (NÉRAUDEAU *et al.* 1993). D'autre part, la région des Gour Ben Houilet est une des seules localités où la partie supérieure des «marnes médianes» passe à un faciès ayant livré des ammonites déterminables spécifiquement, en nombre significatif. C'est, avec le gisement 393 situé à la partie supérieure des «marnes médianes» dans les environs de Témassinine (Fort-Flatters), le deuxième point où une attribution stratigraphique peut être apportée pour une partie élevée de la formation dans le Tinrhert.

La figure 5 présente la distribution verticale des ammonites recueillies. L'inventaire de l'ammonito-faune qui inclut *Pseudotissotia nigeriensis* et *Choffaticeras* sp., est très comparable à celui de l'intervalle 6 de Témassinine (Fort-Flatters) et d'Ohanet.

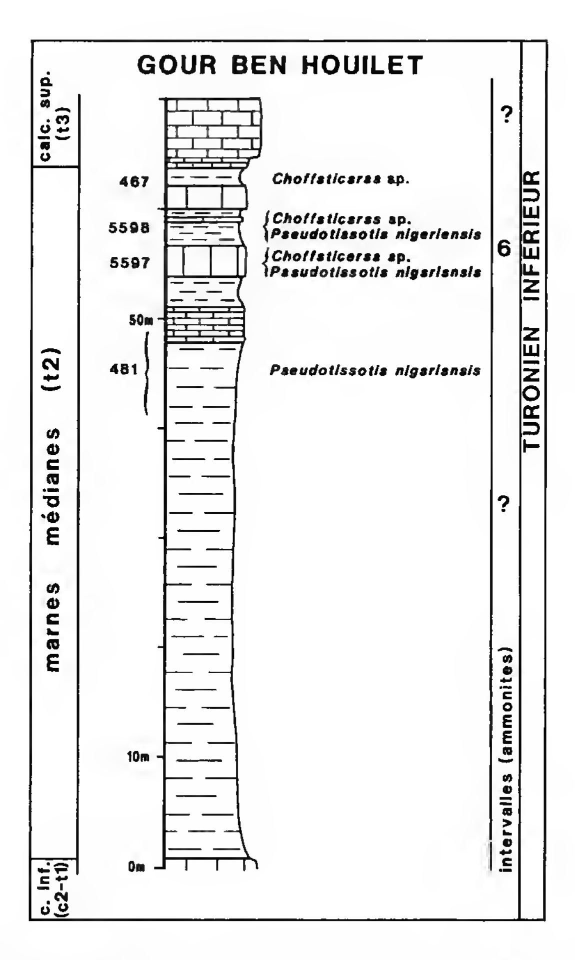


FIG. 5. — Localisation des récoltes d'ammonites dans le Turonien inférieur de la coupe des Gour Ben Houilet, Sud algérien.

Synthèse biostratigraphique

La détermination de deux cent ving cinq spécimens d'ammonites récoltés sur près de 300 km dans le Tinrhert conduit à individualiser six intervalles biostratigraphiques successifs résumés dans la figure 6, soit du bas vers le haut à :

– 1 : *Neolobites vibrayeanus* et *Cunningtoniceras tinrhertense*;

– 2 : *N. vibrayeanus*, *Forbesiceras* sp., *Calycoceras (Calycoceras) naviculare* et *Eucalycoceras pentagonum*;

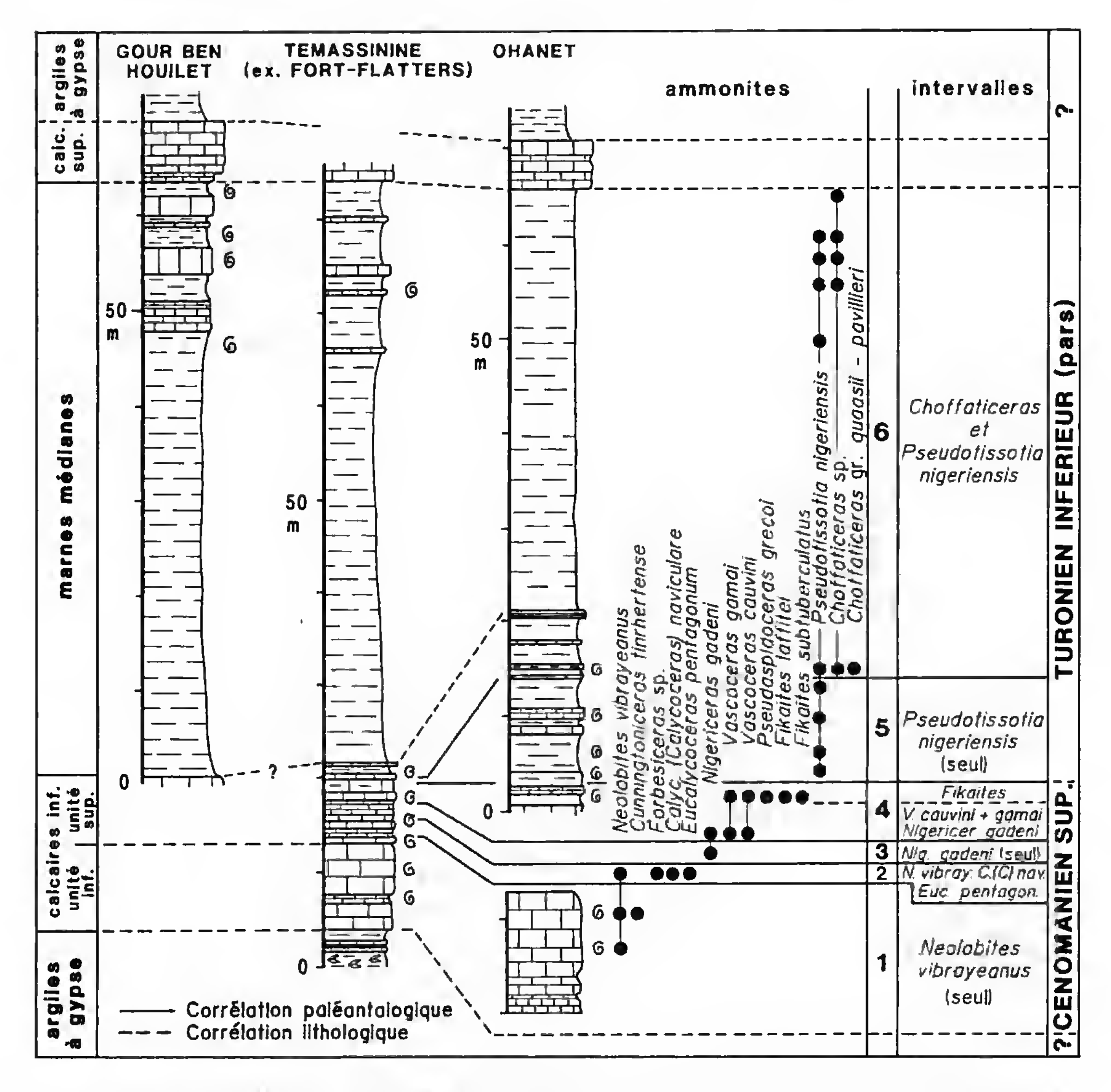


Fig. 6. — Synthèse biostratigraphique dans les formations du Cénomanien supérieur-Turonien inférieur des régions de Gour Ben Houilet, Témassinine et Ohanet au Tinrhert, Sahara algérien.

– 3 : *Nigericeras gadeni* ;

– 4 : *Vascoceras gamai* et *V. cauvini* associés vers le bas à *N. gadeni* et au sommet à *Pseudaspidoceras grecoi*, *Fikaites subtuberculatus* et *F. laffitei* ;

– 5 : *Pseudotissotia nigeriensis* ;

– 6 : *P. nigeriensis*, *Choffaticeras gr. quaasi-pavillieri* et *Choffaticeras* sp.

Il apparaît qu'une succession identique existe à l'ouest de la dorsale d'El Biod, en particulier dans le Tinrhert central (feuille Tilmas El Mra, à l'angle N.-E. de la feuille au 1 500 000 Amguid, *cf.* annexe 1).

LA LIMITE CÉNOMANIEN-TURONIEN AU TINRHERT

Tracer la limite Cénomanien-Turonien dans la hamada de Tinrhert n'est pas commode en raison du provincialisme marqué de ses faunes d'ammonites. La plate-forme saharienne dont fait partie le Tinrhert appartient au domaine téthysien alors dominé par le développement des Vascoceratidae. Comme les stratotypes des étages Cénomanien et Turonien se trouvent en domaine boréal où les faunes d'Acanthoceratidae sont très différentes, aucune corrélation directe n'est possible dans l'état actuel des connaissances.

Suivant les recommandations émises par la Sous-commission internationale de stratigraphie du Crétacé (BIRKELUND *et al.* 1984), le Turonien pourrait débuter avec la zone d'ammonite à *Pseudaspidoceras flexuosum*. Dans des travaux plus récents, KENNEDY & COBBAN (1991) ont proposé de décaler légèrement cette limite vers le bas en la faisant coïncider avec la base de la zone à *Watinoceras devonense* qui précède la zone à *P. flexuosum*. Quelle que soit l'opinion retenue, ni *W. devonense* ni *P. flexuosum* ne sont connus sur la plate-forme saharienne et la position de la limite Cénomanien-Turonien au Tinrhert ne peut être appréciée que de manière indirecte en tenant compte des éléments suivants.

– *Neolobites vibrayeanus*, *Calycoceras (C.) naviculare* et *Eucalycoceras pentagonum* (intervalles 1 et 2 du Tinrhert) sont connus à la base du Cénomanien supérieur dans la zone à *C. (C.) naviculare* du domaine boréal.

– *Nigericeras gadeni* est, dans la partie inférieure de son extension (intervalle 3 du Tinrhert), associé à *Metoicoceras geslinianum* dans les niveaux équivalents du Niger (MEISTER *et al.* 1992) et du Nigeria (ZABORSKI 1990). *M. geslinianum* est également un index de zone du Cénomanien supérieur du domaine boréal.

– *Vascoceras* cf. *gamai* et *V. cauvini* (intervalle 4) sont connus aux États-Unis et en Israël dans la zone à *Neocardioceras juddii* ou ses équivalents et dans des niveaux immédiatement inférieurs (LEWY *et al.* 1984 ; COBBAN *et al.* 1989). *N. gadeni* est également présent aux États-Unis dans la Zone à *N. juddii* toujours attribuée au Cénomanien supérieur (KENNEDY *et al.* 1989).

– L'apparition de *Pseudotissotia nigeriensis* (base de l'intervalle 5) coïncide au Nigeria avec celle de *Pseudaspidoceras flexuosum* (MEISTER 1989) à la base du Turonien ou se produit légèrement avant (ZABORSKI 1993, 1995).

– Enfin, *Choffaticeras* gr. *quaasi-pavillieri* (intervalle 6) apparaît en Israël immédiatement avant *Mammites nodosoides* dans le Turonien inférieur (FREUND & RAAB 1969).

En tenant compte de ces informations, même si la corrélation est entachée d'une légère imprécision, la limite Cénomanien-Turonien peut être raisonnablement placée au Tinrhert entre les intervalles 4 et 5.

À noter que l'interprétation proposée a pour résultat de remonter sensiblement la position de la limite Cénomanien-Turonien par rapport aux travaux antérieurs de COLLIGNON (1957, 1965) et BUSSON (1965, 1972) où toutes les faunes à *Nigericeras* et à *Vascoceras* et les faunes plus récentes étaient considérées comme turoniennes.

PALÉONTOLOGIE SYSTÉMATIQUE (F. A.)

Ordre AMMONOIDEA Zittel, 1884
Sous-ordre AMMONITINA Hyatt, 1889
Superfamille HOPLITACEAE Douvillé, 1890
Famille ENGONOCERATIDAE Hyatt, 1900

Genre **NEOLOBITES** Fischer, 1882

ESPÈCE-TYPE. — *Ammonites vibrayeanus*, d'Orbigny, 1841, par désignation originale.

Neolobites vibrayeanus (d'Orbigny, 1841)
(Fig. 7)

Ammonites vibrayeanus d'Orbigny, 1841 : 322, pl. 96, fig. 1-3.

Synonymes :
Neolobites choffati Hyatt, 1903 : 178, pl. 30, figs 1-4.
Neolobites peroni Hyatt, 1903 : 179.
Neolobites bussoni Collignon, 1965 : 171, pl. C, figs 1a-c

Autres références :
Neolobites vibrayei — COLLIGNON 1965 : 170, text.-fig. 1
Neolobites fourtaui Pervinquière — COLLIGNON 1965 : 170, text.-fig. 2
Neolobites peroni Hyatt — COLLIGNON 1965 : 179, text.-fig. 3
Neolobites vibrayeanus — KENNEDY & JUIGNET 1981 : 23, figs 3 a-c, 4 a-c, 5, 6 a (avec synonymie). — LEFRANC 1981 : 158, figs 1-3. — MOREAU, FRANCIS & KENNEDY 1983 : 319, figs 10 a-b. — LUGER & GRÖSCHKE 1989 : 366, pl. 39, fig. 3, text.-fig. 5. — MEISTER, ALZOUMA, LANG & MATHEY 1992 : 60, pl. 1, figs 1-4, 6, text.-fig. 8. — THOMEL 1992 : 184, pl. 80, fig. 4.

HOLOTYPE. — Muséum national d'Histoire naturelle Paris, n° 1896 –27. Suivant KENNEDY & JUIGNET (1981), le spécimen proviendrait d'une couche d'argile du Cénomanien supérieur passant latéralement aux sables à *Catopygus obtusus*.

MATÉRIEL. — Trente-cinq spécimens dont une vingtaine sont repérés stratigraphiquement par rapport aux coupes décrites; à Témassinine, gisements 91, 93, 94, 143, 155, 269, 382, 390 et 5561 et, à Ohanet, gisements 329 et 330.

DISTRIBUTION VERTICALE. — En Europe, Israël et au Niger où les séries sont bien datées, *N. vibrayeanus* est connu à la base du Cénomanien supérieur, juste sous le niveau d'apparition de *Metoicoceras geslinianum* (KENNEDY & JUIGNET 1981 ; MEISTER *et al.* 1992). Au Tinrhert, *N. vibrayeanus* est présent dans les intervalles 1 et 2, associé dans l'intervalle 2 à *Eucalycoceras pentagonum* et *Calycoceras (Calycoceras) naviculare*, c'est-à-dire dans une position équivalente.

DISTRIBUTION GÉOGRAPHIQUE. — France, Espagne, Portugal, Maroc, Algérie, Tunisie, Égypte, Niger, Israël, Liban, Arabie, Pérou, Bolivie.

DESCRIPTION

Coquille très involute et comprimée avec des flancs légèrement convexes et une région ventrale étroite et plane. L'épaisseur maximale de la section du tour est obtenue au tiers interne du flanc. L'ornementation, peu accentuée, est constituée de côtes plutôt fines, qui naissent sur la bordure ombilicale ou sont intercalaires. D'abord étroites et rectilignes, les côtes se renforcent

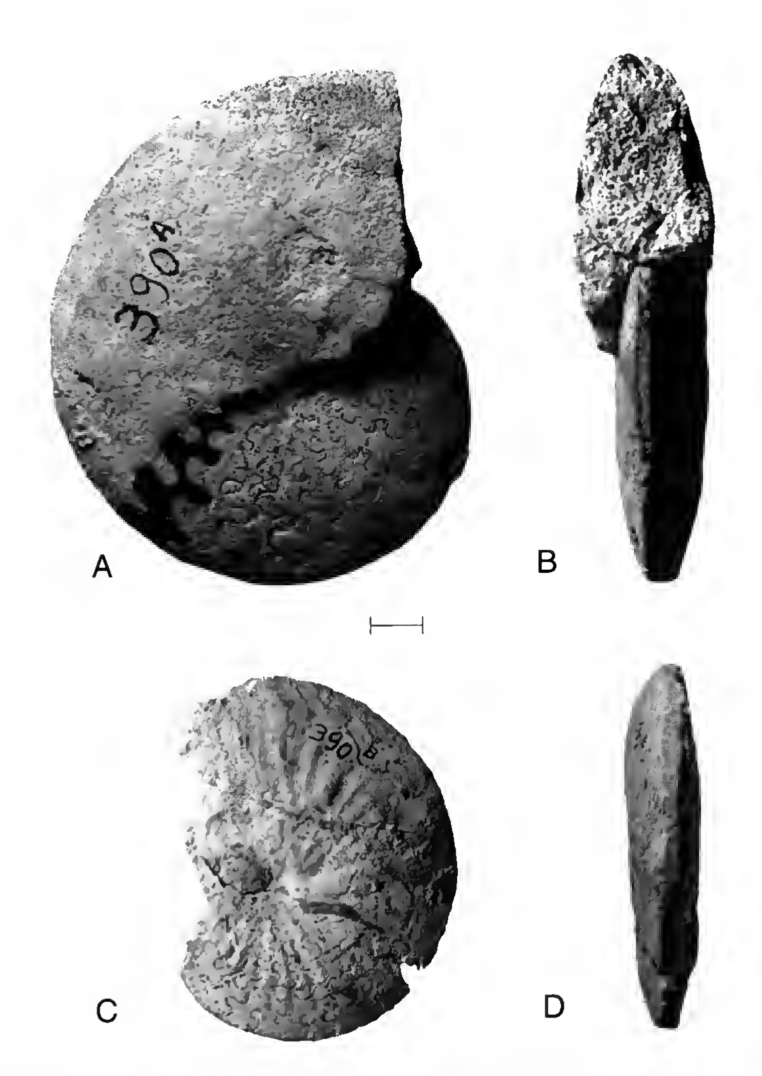


FIG. 7. — A-D, *Neolobites vibrayeanus* (d'Orbigny, 1841). Les deux spécimens proviennent du gisement 390 au nord de Témassinine. A-B, n° 390A ; C-D, n° 390B. Cénomanien supérieur, intervalle 1 du Tinrhert, (échelle : 1 cm).

au tiers interne du flanc, prennent un aspect sigmoïde, et enfin s'élargissent et s'atténuent sur la partie la plus externe de la coquille. Les épaules ventro-latérales portent chacune une ligne de petits tubercules allongés et serrés qui sont parfois indistincts. Enfin, la cloison est typiquement pseudocératiforme avec des selles larges et des lobes plus étroits.

DISCUSSION

Les études de COLLIGNON (1965), KENNEDY & JUIGNET (1981) et plus récemment MEISTER *et al.* (1992) ont révélé une grande variabilité au sein des populations contemporaines de *Neolobites* avec une série continue de transitions reliant *N. vibrayeanus* (d'Orbigny, 1841) (comprimé), *N. choffati* (Hyatt, 1903) (forme moyenne) et *N. peroni* (Hyatt, 1903) (épais). Suivant la proposition formulée par KENNEDY & JUIGNET (1981), les trois espèces sont maintenant mises en synonymie, *N. vibrayeanus* restant la seule espèce valide par application de la règle d'antériorité.

Neolobites bussoni, Collignon, 1965 a été créé à partir d'un spécimen unique provenant du gisement 91 de la coupe de l'Akba de Témassinine. L'holotype, illustré par COLLIGNON (1965, pl. C, Fig. 1 a-c) et réexaminé ici est un exemplaire de grande taille (17 cm de diamètre) dont seule la moitié du dernier tour de spire est préservée. Selon COLLIGNON, les caractères spécifiques de *N. bussoni* sont l'épaisseur de la coquille (36% du diamètre) et la largeur de la région ventrale bordée de tubercules fins et serrés. La population de *Neolobites vibrayeanus* du Niger figurée par MEISTER *et al.* (1992) illustre bien la variabilité de l'épaisseur du tour, de l'ornementation et de l'ouverture de l'ombilic de l'espèce. Dans la mesure où les variants les plus ornés ont une épaisseur du tour pouvant atteindre 35 à 38% du diamètre avec une région ventrale corrélativement très large, *N. bussoni* est considéré ici comme un simple variant de *N. vibrayeanus*.

Neolobites fourtaui Pervinquière, 1907, possède des tubercules ombilicaux proéminents, de fortes côtes concaves sur la partie externe du flanc et un ombilic plus ouvert, et constitue en revanche une espèce séparée.

À noter enfin que la majorité des *Neolobites* du Tinrhert sont des formes assez comprimées, involutes et relativement peu ornées.

Superfamille ACANTHOCERATACEAE de Grossouvre, 1894
Famille FORBESICERATIDAE Wright, 1952

Genre **FORBESICERAS** Kossmat, 1897

ESPÈCE-TYPE. — *Ammonites largilliertianus* d'Orbigny, 1841 ; par désignation subséquente de Diener, 1925.

Forbesiceras sp.
(Fig. 8)

Neoptychites sp. aff. *taelingaeformis* Solger var. *discrepans* Solger. — COLLIGNON 1965 : 188.

MATÉRIEL. — Deux fragments de moules internes provenant du gisement 380 situé dans le secteur de Témassinine.

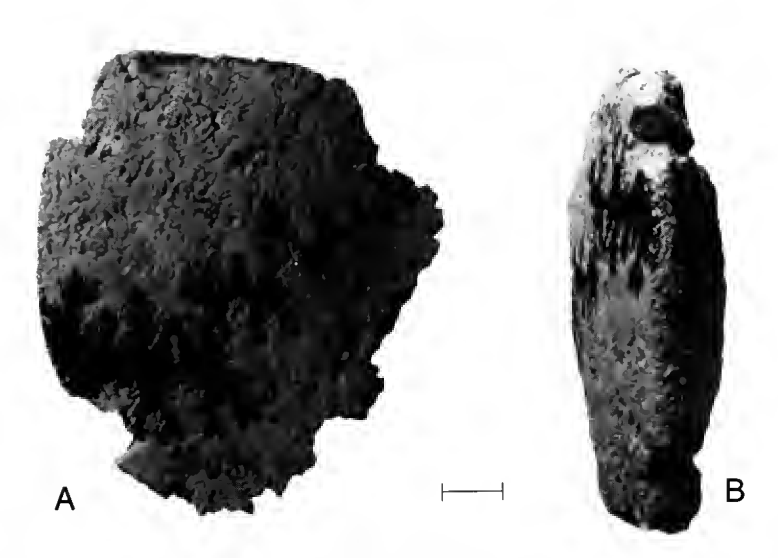


FIG. 8. — A-B, *Forbesiceras* sp. Gisement 380D Témassinine. Cénomanien supérieur, intervalle 2 du Tinrhert (échelle : 1 cm).

DISTRIBUTION VERTICALE. — Intervalle 2 du Tinrhert. Dans le gisement 380, les deux *Forbesiceras* décrits ici sont associés à *Calycoceras (Calycoceras) naviculare* et *Eucalycoceras pentagonum*. Cénomanien supérieur.

DISCUSSION

Les deux échantillons sont des portions de phragmocônes correspondant à des coquilles discoïdales, lisses et très comprimées, d'assez grande taille (10 à 15 cm de diamètre). L'enroulement est involute. La section du tour, beaucoup plus haute que large, est subtriangulaire avec des flancs légèrement convexes, convergents, et une région ventrale étroite et arrondie. La cloison est très divisée.

Par leur section du tour, ces deux spécimens rappellent le genre *Metengonoceras* Hyatt, 1903 ; cependant, la comparaison des cloisons les en sépare nettement, les *Metengonoceras* ayant une ligne de suture pseudocératiforme très simple et non très découpée comme ici. Ce même critère de la cloison les rapproche beaucoup plus des *Forbesiceras* Kossmat, 1897, qui ont une suture avec des lobes incisés et des selles phyllocératiformes (KENNEDY *et al.* 1981 ; WRIGHT & KENNEDY 1984). La morphologie générale de la coquille est aussi très comparable avec la perte, à de grands diamètres, du méplat ventral et l'acquisition d'une région ventrale étroite et arrondie. Le fragment de grande taille du Nouveau-Mexique (États-Unis) illustré par COBBAN *et al.* (1989, 77, fig. 66 a-b) comme *Forbesiceras* sp. ressemble beaucoup aux spécimens du Tinrhert (voir également la cloison dessinée par COBBAN *et al.*, 21, fig. 2). Sans l'observation des tours internes, une détermination spécifique est toutefois impossible. À noter que COLLIGNON (1965) avait déterminé ces spécimens comme *Neoptychites* sp. aff. *taelingaeformis* var. *discrepans* Solger (espèce turonienne), malgré leur association à des ammonites typiques du Cénomanien supérieur dans le gisement 380 : *Calycoceras (C.) naviculare* et *Eucalycoceras pentagonum.*

Famille ACANTHOCERATIDAE de Grossouvre, 1894
Sous-famille ACANTHOCERATINAE de Grossouvre, 1894

Genre **CUNNINGTONICERAS** Collignon, 1937

ESPÈCE-TYPE. — *Ammonites cunningtoni* Sharpe, 1855, par désignation originale.

Cunningtoniceras tinrhertense (Collignon, 1965)
(Fig. 9)

Kamerunoceras tinrhertense Collignon, 1965 : 175, pl. D
non *Kamerunoceras tinrhertense* — ZABORSKI 1985 : 51, fig. 57-59 (= *Romaniceras* sp.)

HOLOTYPE. — Muséum national d'Histoire naturelle Paris, n° R53926, d'Ohanet, Algérie.

MATÉRIEL. — L'holotype provenant du gisement 329 dans le secteur d'Ohanet.

DISTRIBUTION VERTICALE. — Intervalle 1 du Tinrhert à *Neolobites vibrayeanus*. Cénomanien supérieur.

DISTRIBUTION GÉOGRAPHIQUE. — Algérie.

DESCRIPTION

L'holotype (Fig. 9A) est un moule interne de 19 cm de diamètre. Seuls le flanc droit et une partie de la région ventrale sont préservés. L'enroulement est très évolute, l'ombilic représentant 43 % du diamètre. La section du tour est sensiblement carrée avec un mur ombilical arrondi, des flancs plats, parallèles jusqu'à l'épaule ventro-latérale, puis convergents entre les tubercules ventro-latéraux internes et externes. La région ventrale est plane.

Sur les tours internes, les côtes longues naissent seules ou occasionnellement par paires au niveau de tubercules ombilicaux saillants et sont effacées à mi-flanc. Elles sont fréquemment séparées par une courte intercalaire qui apparaît au tiers externe du flanc. La région ventrale porte cinq rangées de tubercules : ventro-latéraux internes qui tendent à devenir épineux, ventro-latéraux externes et siphonal. Au diamètre de 127 mm, on compte 22 tubercules ombilicaux par tour contre 34 tubercules ventro-latéraux et siphonaux.

Sur le dernier tour de spire, la densité costale diminue sensiblement tandis que toutes les côtes longues deviennent simples et portent seules des tubercules ventro-latéraux internes saillants, les côtes intercalaires étant très effacées.

DISCUSSION

COLLIGNON (1965) en créant l'espèce *Kamerunoceras tinrhertense* était hésitant sur son attribution générique. Les récoltes récentes effectuées aux États-Unis par KENNEDY *et al.* (1987) et KENNEDY & COBBAN (1991) ont clairement démontré que le genre *Kamerunoceras* (Reyment, 1954) dérive du genre *Euomphaloceras* (Spath, 1923), aux confins de la limite Cénomanien-Turonien. Or le gisement 329 d'où provient le type de *K. tinrhertense* a également fourni plusieurs exemplaires de *Neolobites vibrayeanus* (d'Orbigny, 1841), ce qui indique un niveau bas dans le



FIG. 9A. — *Cunningtoniceras tinrhertense* (Collignon, 1965). Holotype, du gisement 329A (échelle : 1 cm).

Cénomanien supérieur (sensiblement équivalent à la partie inférieure de la Zone à *Calycoceras naviculare* du domaine boréal).

En fait, les *Kamerunoceras* ont le plus souvent des côtes légèrement concaves vers l'arrière, des tubercules ombilicaux situés assez haut sur la bordure ombilicale et pincés radialement, et des tubercules ventro-latéraux internes peu saillants à l'inverse de ce que l'on observe chez *K. tinrhertense*. La morphologie de la coquille, la section du tour quadrangulaire et les tubercules ventro-latéraux internes épineux rappellent beaucoup plus le genre *Cunningtoniceras* (Collignon, 1937). L'espèce la plus proche semble être *Cunningtoniceras arizonense* (Kirkland & Cobban, 1986) du Western Interior aux États-Unis qui a également une densité costale élevée et paraît contemporaine. L'absence de côtes intercalaires et le développement de véritables cornes sur la chambre d'habitation de *C. arizonense* permettent cependant aisément de distinguer les deux espèces.

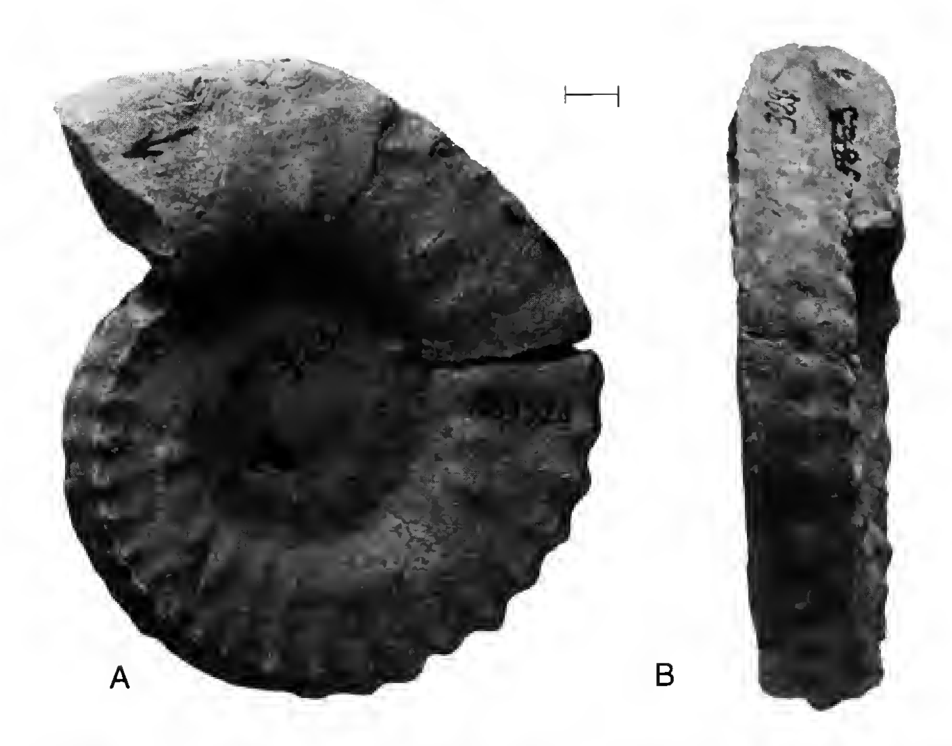


FIG. 9B-C. — *Cunningtoniceras tinrhertense* (Collignon, 1965). Phragmocône de l'holotype, gisement 329A, Ohanet. Cénomanien supérieur, intervalle 1 du Tinrhert, (échelle : 1 cm).

Genre et sous-genre **CALYCOCERAS** Hyatt, 1900

ESPÈCE-TYPE. — *Ammonites navicularis* Mantell, 1822, par désignation de la Commission internationale de nomenclature zoologique (Opinion 557).

Calycoceras (Calycoceras) naviculare (Mantell, 1822)
(Fig. 10)

Ammonites navicularis Mantell, 1822 : 198, pl. 22, fig. 5.

Autres références :

Calycoceras grossouvrei (Spath) — COLLIGNON 1965 : 172, pl. B, fig. 2 a, b.

Calycoceras boulei — COLLIGNON 1965 : 173, pl. B, figs 3, 4. (non *Calycoceras (Metacalycoceras) boulei* Collignon, 1937 : 43 (pars), pl. 5, fig. 2 seulement; pl. 8, figs 9-11 seulement (= *Calycoceras (Calycoceras) bathyomphalum* (Kossmat, 1895)).

Calycoceras naviculare — COBBAN 1971 : 13, pl. 1, figs 1-3; pl. 10, figs 1-8; pl. 11, figs 1-5; pl. 12, figs 1, 2; pl. 13, figs 1-5; pl. 14, figs 1-3; pl. 15, figs 1, 2; pl. 16, figs 1, 2; pl. 17; text.-figs 12-14.

Calycoceras (Calycoceras) naviculare — Wright & Kennedy 1981 : 34, pl. 4 ; pl. 5, figs 1-3, text. figs 13, 14 c-e (avec synonymie). — Wright & Kennedy 1990 : 236, pl. 61, fig. 1 ; pl. 62, figs 1-6 ; pl. 63, figs 1-3 ; text figs 88E, 1 ; 89 D ; 110 C (avec synonymie additionnelle).

Holotype. — Natural History Museum London, n° 5681, des Marnes à *Actinocamax plenus* à Offham, Sussex (R.-U.).

Matériel. — Neuf exemplaires provenant des environs de Témassinine, dans les gisements 143, 380, 382 et 5561.

Distribution verticale. — Intervalle 2 du Tinrhert, associé à *Eucalycoceras pentagonum*. Cénomanien supérieur.

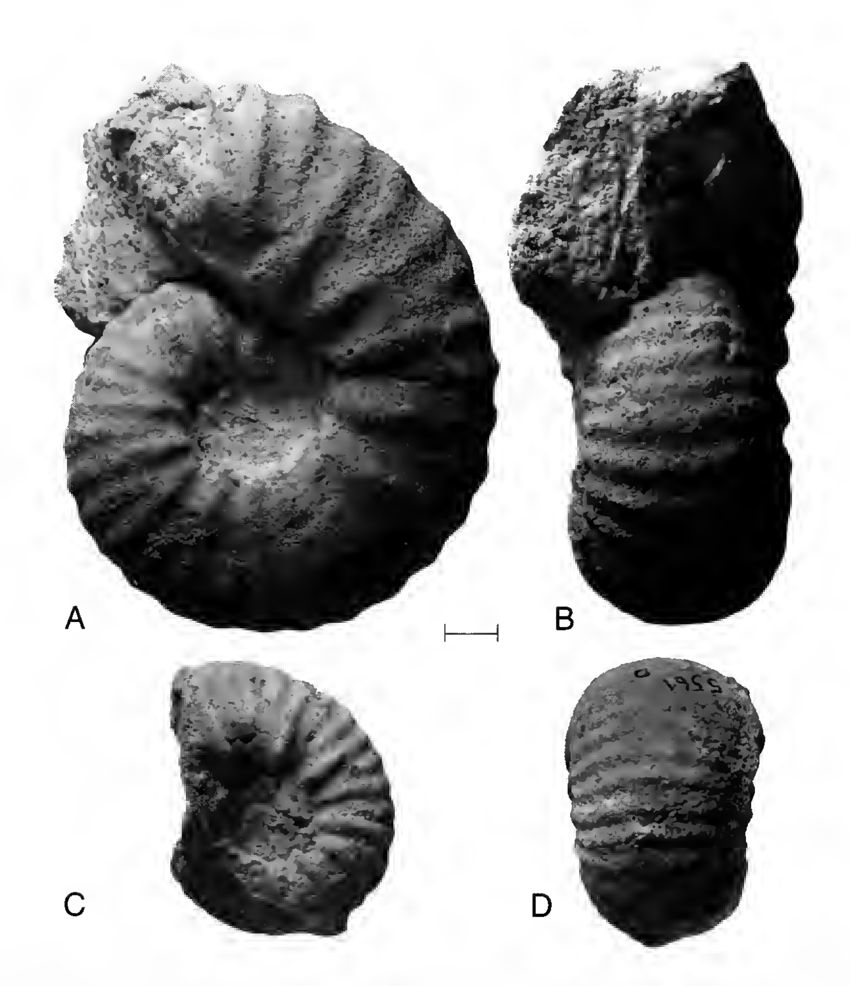


Fig. 10. — A-C, *Calycoceras (Calycoceras) naviculare* (Mantell, 1822). A-B, gisement 382A, Témassinine. C, gisement 5561.B, Témassinine. Cénomanien supérieur, intervalle 2 du Tinrhert, × 1. D, *Calycoceras (Calycoceras) naviculare* (Mantell, 1822). Gisement 5561B, Témassinine. Cénomanien supérieur, intervalle 2 du Tinrhert (échelle : 1 cm).

Distribution géographique. — Angleterre, France, Allemagne, Espagne, Portugal, États-Unis (Western Interior), Californie, Afrique du Nord, Angola, Madagascar, Proche-Orient, Inde, Japon.

Discussion

L'espèce *Calycoceras (Calycoceras) naviculare* (Mantell, 1822) vient d'être révisée à plusieurs reprises par Cobban (1971), Kennedy (1971) et Wright & Kennedy (1981, 1990). L'espèce est un *Calycoceras* à section du tour déprimée, à flancs arrondis sur les tours internes, où l'épaisseur maximale de la coquille est observée au niveau des tubercules ombilicaux. Suivant Cobban (1971), on compte 12 à 25 côtes par demi-tour sur les tours internes, mais la densité costale diminue quand la coquille s'agrandit. Les spécimens du Tinrhert s'intègrent bien dans cette variation morphologique et deux exemplaires pris à des diamètres de 5 et 10 cm sont illustrés (Fig. 10A-B, C-D). Collignon (1965) a figuré plusieurs *Calycoceras* provenant des coupes de la région de Témassinine sous les noms de *Calycoceras grossouvrei* (Spath, 1926) (Collignon 1965 ; pl. B, Fig. 2 a-b) et *Calycoceras boulei* (Collignon 1937, pl. B, figs 3, 4). Suivant Wright & Kennedy (1990), les deux espèces sont respectivement des synonymes juniors de *C. (C.) naviculare* et de *C. (C.) bathyomphalum* (Kossmat, 1895). Si la première espèce n'appelle pas de remarque particulière, les spécimens déterminés par Collignon (1965), comme *C. boulei*, ne montrent pas la section plus comprimée, ni les flancs plats et la rétention jusqu'au diamètre de 4 cm des tubercules ventro-latéraux internes épineux caractéristiques de *C. (C.) bathyomphalum*. À notre avis, il s'agit également de *C. (C.) naviculare*.

Genre **EUCALYCOCERAS** Spath, 1923

Espèce-type. — *Ammonites pentagonus* Jukes-Browne, 1896, par désignation originale.

Eucalycoceras pentagonum (Jukes-Browne, 1896)
(Fig. 11)

Ammonites pentagonus Jukes-Browne, 1896 : 156, pl. 5, fig. 1

Synonyme :

Eucalycoceras pentagonum saharense Collignon, *in* Amard *et al.*, 1983 : 101, pl. 14 ; fig. 1.

Autres références :

Eucalycoceras aff. *pentagonum* — Collignon 1965 : 174.

Protacanthoceras sp. — Collignon 1965 : 174.

Eucalycoceras pentagonum — Cobban 1988 : 9, pl. 3 ; text.-figs 6, 7 (avec synonymie). – Wright & Kennedy 1990 : 282, pl. 78, figs 1, 3 ; pl. 79, figs 1-5 ; text.-figs 89 E, 123 A, B. – Thomel 1992 : 180, pl. 78, figs 1, 5 ; pl. 79, figs 1-5.

Holotype. — Geological Survey Museum London, n° 53481, du Bed C du Cenomanian Limestone à Humble Point, Devon (R.-U.)

Matériel. — Cinq exemplaires de la région de Témassinine, dont quatre dans les gisements 91, 265, 380 et 5561.

Distribution verticale. — Intervalle 2 du Tinrhert, associé à *C. (C.) naviculare* et *N. vibrayeanus*. Cénomanien supérieur

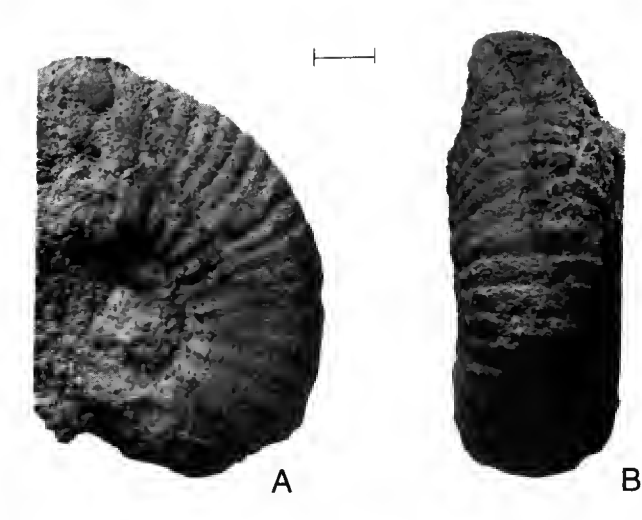


FIG. 11. — *Eucalycoceras pentagonum* (Jukes-Browne, 1896). Gisement 5561A, Témassinine. Cénomanien supérieur, intervalle 2 du Tinrhert (échelle : 1 cm).

DISTRIBUTION GÉOGRAPHIQUE. — Angleterre, France, Espagne, Portugal, Roumanie, Tunisie, Algérie, Égypte, Madagascar, Inde, Russie, Japon, États-Unis (Western Interior).

DISCUSSION

Eucalycoceras pentagonum (Jukes-Browne, 1896) est une espèce d'*Eucalycoceras* aisément identifiable par la présence de cinq rangées de tubercules ventraux plus ou moins équidistants, par ses flancs plats, parallèles et par la disparition fréquente des côtes à mi-flanc à la fin du phragmocône. Un autre élément également caractéristique est la modification de l'ornementation sur la deuxième moitié de la chambre d'habitation avec disparition des tubercules ventraux, arrondissement de la région ventrale et augmentation de la densité costale, les espaces intercostaux devenant alors très étroits.

Le matériel du Tinrhert est identique aux spécimens recueillis dans les craies du bassin anglo-parisien ou des formations du Cénomanien supérieur du Western Interior aux États-Unis (COBBAN 1988; WRIGHT & KENNEDY 1990).

***Eucalycoceras* sp.**
(Fig. 12)

MATÉRIEL. — Deux exemplaires de la région de Témassinine dans le gisement 380.

DISTRIBUTION VERTICALE. — Intervalle 2 du Tinrhert, associés dans le gisement 380 à *C. (C) naviculare, E. pentagonum* et *Forbesiceras* sp.

DISCUSSION

À côté des spécimens typiques d'*Eucalycoceras pentagonum* existent, dans le gisement 380 des environs de Témassinine, des Acanthoceratinae très voisins, mais à ornementation des tours

internes plus robuste. Ces exemplaires, déterminés comme *Eucalycoceras* sp., sont illustrés (Fig. 12). La morphologie du phragmocône rappelle celle des *Pseudocalycoceras* et, en particulier, *P. angolaense* (Spath, 1931), espèce révisée par COOPER (1978) et COBBAN (1988). Mais, alors que les côtes restent fortes et largement espacées jusqu'au péristome chez *P. angolaense*, les exemplaires du Tinrhert montrent le même changement d'ornementation qu' *Eucalycoceras pentagonum* sur la deuxième moitié de la chambre d'habitation. Il s'agit d'un exemple de protérogenèse et ces spécimens sont des intermédiaires entre *E. pentagonum* (espèce ancestrale connue dans la zone à *Calycoceras naviculare* et la moitié inférieure de la Zone à *Metoicoceras geslinianum* du domaine boréal) et *P. angolaense* (qui apparaît dans la Zone à *M. geslinianum*), confirmant la filiation proposée par COBBAN (1988).

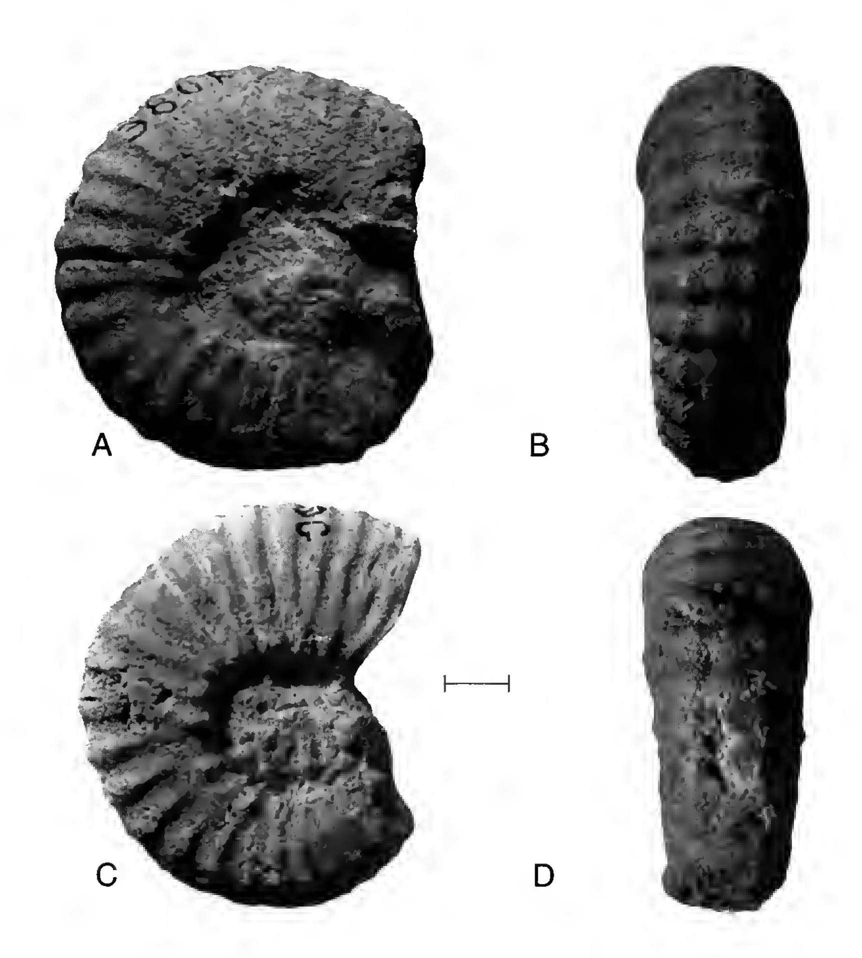


FIG. 12. — A-B, *Eucalycoceras* sp. Gisement 380F, Témassinine. Cénomanien supérieur du Tinrhert, intervalle 2 du Tinrhert, × 1. C-D, *Eucalycoceras* sp. Gisement 380G, Témassinine. Cénomanien supérieur, intervalle 2 du Tinrhert (échelle : 1 cm).

Genre **NIGERICERAS** Reyment, 1955

ESPÈCE-TYPE. — *Nigericeras gignouxi* Schneegans, 1943, par désignation subséquente de Reyment, 1955.

Le nom de genre *Nigericeras* ne satisfait pas aux dispositions de l'article 13b du code de nomenclature, nonobstant la désignation subséquente d'une espèce-type.

Nigericeras gadeni (Chudeau, 1909)
(Fig. 13)

Acanthoceras? gadeni Chudeau, 1909 : 71, pl. 3, fig. 6.

Synonymes :

Nigericeras gignouxi Schneegans, 1943 : 119, pl. 5, figs 10-15, text.-figs 1,2.
Nigericeras lamberti Schneegans, 1943 : 121, pl. 6, figs 1-5, 7, text.-figs 3-4.
Nigericeras jacqueti Schneegans, 1943 : 125, pl. 6, fig. 8, text.-fig. 7.
Nigericeras jacqueti var. *crassecostata* Collignon, 1965 : 178, pl. E, fig. 4 a-b.

Autres références :

Nigericeras gadeni — SCHNEEGANS 1943 : 123, pl. 7, figs 3-4; text.-Fig. 5. – SCHÖBEL 1975 : 117, pl. 6. figs 1-3 (avec synonymie additionnelle). – KENNEDY, COBBAN, HANCOCK & HOOK 1989 : 62, figs 9L, 11, O, P. – ZABORSKI 1990 : 4, figs 4-7. – MEISTER, ALZOUMA, LANG & MATHEY 1992 : 67, pl. 3, figs 1-3, 5, 7; pl. 4, fig. 1, text. fig. 13.

Nigericeras gignouxi — COLLIGNON 1965 : 177, pl. E, fig. 2 a, b; pl. F, fig. 1.

Nigericeras lamberti — COLLIGNON 1965 : 178. — COLLIGNON *in* AMARD *et al.* 1983 : 56, pl. 8, fig. 1 a-b.

Nigericeras jacqueti — COLLIGNON 1965 : 178, pl. E, fig. 3 a-c. – AMARD, COLLIGNON & LEFAVRAIS-HENRY, 1978 : pl. 1, fig. 2 a-b, – MEISTER 1989 : 11, pl. 2, figs 3-4; pl. 4, fig. 1. – MEISTER, ALZOUMA, LANG & MATHEY 1992 : 68, pl. 3, figs 4, 6; pl. 4, fig. 2.

Nigericeras cf. gignouxi — WRIGHT & KENNEDY 1981 : 85, pl. 15, fig. 6.

non Nigericeras gadeni, N. lamberti — MEISTER 1989 : 10, pl. 3, figs 1-3 (= *Vascoceras cauvini* Chudeau, 1909).

HOLOTYPE. — Muséum national d'Histoire naturelle Paris n° R 52466, coll. CHUDEAU, de Béréré, Damergou, Niger.

MATÉRIEL. — Vingt exemplaires dont huit sont situés sur les coupes retenues dans le secteur de Témassinine; gisements 121, 140, 145, 146 et 150.

DISTRIBUTION VERTICALE. — *N. gadeni* est connu au Niger et Nigeria en association avec *Metoicoceras geslinianum*, index de zone du Cénomanien supérieur (MEISTER *et al.* 1992; ZABORSKI 1990). Aux États-Unis, l'espèce est également présente dans la zone suivante à *Neocardioceras juddii*, toujours du Cénomanien supérieur (KENNEDY *et al.* 1989). Au Tinrhert, *Nigericeras gadeni* est recueilli dans l'intervalle 3 à *N. gadeni* seul, et dans l'intervalle 4 à *N. gadeni*, *Vascoceras gamai* et *V. cauvini*. Cénomanien supérieur.

DISTRIBUTION GÉOGRAPHIQUE. — Angleterre, France, Algérie, Niger, Nigeria, Égypte, Angola, Israël, Inde, Japon, États-Unis (Western Interior).

DESCRIPTION

Coquille modérément évolute, dont l'épaisseur varie depuis des formes relativement comprimées (rapport H/E de la hauteur du tour sur l'épaisseur = 1,6) jusqu'à des formes déprimées

(H/E = 0,75). La section du tour, subovale à subtrapézoïdale, montre une région ventrale arrondie et des flancs convergents, plats ou légèrement convexes. L'épaisseur maximale de la coquille est observée près du bord ombilical. L'ornementation des tours internes est typiquement « acanthocératiforme », en particulier chez les variants épais, avec des côtes droites, simples ou naissant

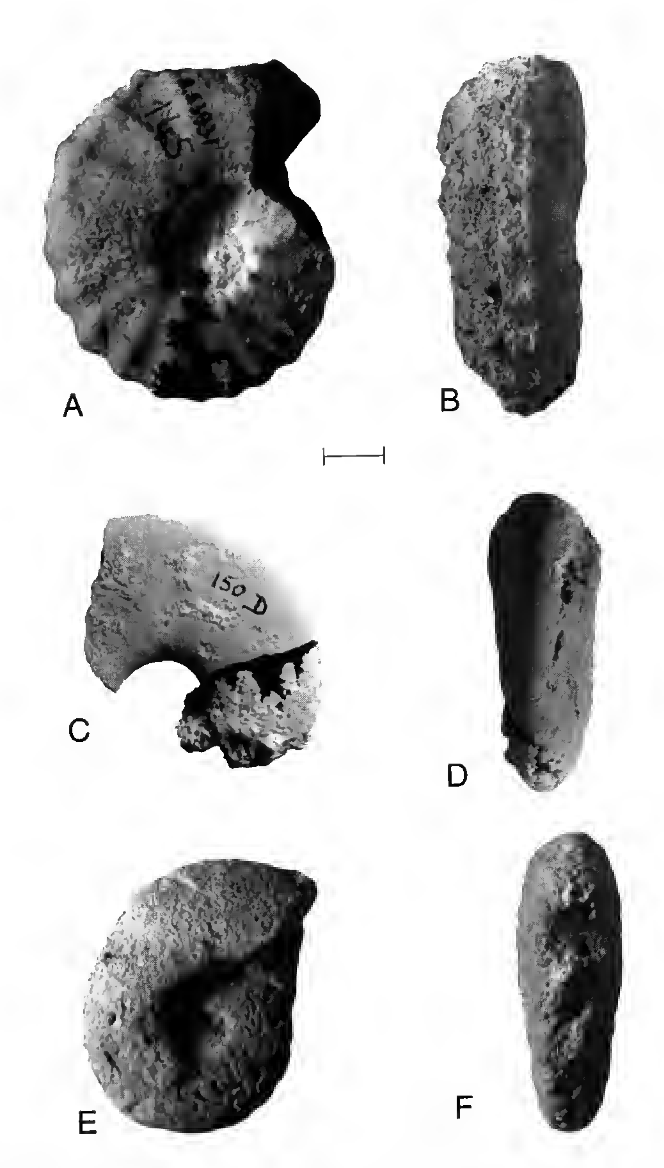


FIG. 13. — A-B, *Nigericeras gadeni* (Chudeau, 1909). Variant épais du gisement 145, Témassinine. Cénomanien supérieur, intervalle 3 du Tinrhert, × 1. *Nigericeras gadeni* (Chudeau, 1909), C-D gisement 150D et E-F, gisement 121A ; tous deux dans le secteur de Témassinine. Cénomanien supérieur, intervalles 3 et 4 du Tinrhert (échelle : 1 cm).

par paires et qui portent des tubercules ombilicaux, ventro-latéraux internes et externes, et siphonaux. Entre les côtes primaires s'intercalent fréquemment une ou deux côtes secondaires qui naissent au tiers interne ou à mi-flanc. Sur les tours externes, l'ornementation disparaît très rapidement et la morphologie de la coquille devient alors homéomorphe de celle de certains *Vascoceras*. À noter que chez les variants comprimés, la perte de l'ornementation s'effectue très tôt et la coquille est alors rapidement lisse, des nodosités péri-ombilicales persistant seulement chez certains individus.

DISCUSSION

SCHÖBEL (1975) a clairement démontré à l'aide d'une étude statistique des *Nigericeras* du Niger que *N. gignouxi* Schneegans, 1943, *N. lamberti* Schneegans, 1943 et *N. jacqueti* Schneegans, 1943, sont des synonymes juniors de *N. gadeni* (CHUDEAU 1909), et sont de simples morphotypes illustrant un large spectre de variation d'une seule espèce biologique. Les *Nigericeras gadeni* du Tinrhert sont totalement identiques à ceux du Niger et montrent la même variabilité morphologique avec des formes comprimées et d'autres plus épaisses, et une perte rapide de l'ornementation. Ce dernier caractère permet d'ailleurs de différencier facilement *N. gadeni* de *Nigericeras scotti* (COBBAN 1971) du Western Interior aux États-Unis, qui garde son ornementation «acanthocératiforme» à un diamètre beaucoup plus grand que *N. gadeni*.

À noter que les *Nigericeras* ont été longtemps considérés comme le lien phylétique unissant les *Acanthoceras* (ou les *Protacanthoceras*) du Cénomanien supérieur aux *Vascoceras* cénomano-turoniens. Ils étaient de plus inclus comme premiers représentants de la famille des Vascoceratidae. En fait, il est maintenant clair que les *Vascoceras* dérivent directement des *Protacanthoceras* à un niveau bas du Cénomanien supérieur (WRIGHT & KENNEDY 1980; KENNEDY & WRIGHT 1994) et que leur apparition est antérieure à celle des *Nigericeras*. C'est la raison pour laquelle les *Nigericeras* sont traités aujourd'hui comme des Acanthoceratidae chez lesquels la perte de l'ornementation au stade adulte conduit simplement à une morphologie homéomorphe de celle des Vascoceratidae.

Genre **FIKAITES** Zaborski, 1993

ESPÈCE-TYPE. — *Fikaites varicostatus* Zaborski, 1993.

Fikaites laffitei (Collignon, 1965)
(Fig. 14)

Paramammites laffitei Collignon, 1965 : 186, pl. A, fig. 2.

HOLOTYPE. — Muséum national d'Histoire naturelle Paris, n° R53920, d'Ohanet, Algérie.

MATÉRIEL. — L'holotype du gisement 283; secteur d'Ohanet.

DISTRIBUTION VERTICALE. — Intervalle 4 du Tinrhert, associé à *Vascoceras gamai* et *V. cauvini*. Cénomanien supérieur. Au Nigeria, les *Fikaites* coexistent avec les derniers *Pseudaspidoceras pseudonodosoides*, *Vascoceras* aff. *gamai*, *V. nigeriense* et les premiers *Thomasites gongilensis* aux confins de la limite Cénomanien-Turonien.

DISTRIBUTION GÉOGRAPHIQUE. — Algérie.

DESCRIPTION DE L'HOLOTYPE.

Il s'agit d'un spécimen de 82 mm de diamètre montrant le dernier tour de spire du phragmocône et une portion de la chambre d'habitation. La coquille est modérément évolute et globuleuse. La section du tour, légèrement déprimée (rapport H/E = 0,80), est d'abord subtrapézoïdale sur la première partie du phragmocône, avec des flancs convergents, légèrement convexes, et un ventre faiblement arqué, puis devient plus ou moins arrondie vers la fin du phragmocône et sur la chambre d'habitation. L'épaisseur maximale de la section est observée près du bord ombilical. L'ornementation, atténuée, est constituée de fines côtes longues ou courtes qui traversent sans interruption la région ventrale. Les côtes primaires naissent sur la bordure ombilicale au niveau d'un petit tubercule allongé radialement, puis s'infléchissent progressivement vers l'avant. Entre les côtes primaires s'intercalent fréquemment une, parfois deux côtes secondaires. Toutes les côtes longues et la plupart des courtes portent sur l'épaule ventro-latérale de faibles tubercules qui sont plutôt des renflements des côtes. Sur le dernier demi-tour de phragmocône visible, on compte dix-huit tubercules ventro-latéraux contre huit tubercules ombilicaux.

DISCUSSION

Fikaites laffitei a été considéré lors de sa création par COLLIGNON (1965) comme un *Paramammites*. Le genre *Paramammites* Furon, 1935, avec comme espèce-type *P. polymorphus* (Pervinquière, 1907) est caractérisé par des côtes saillantes, alternativement longues et courtes, pourvues sur les tours internes de tubercules épineux. Les côtes primaires portent des tubercules ombilicaux, latéraux, ventro-latéraux internes et externes, tandis que les côtes secondaires possèdent seulement les tubercules latéraux. Les spécimens-types de *Paramammites polymorphus*

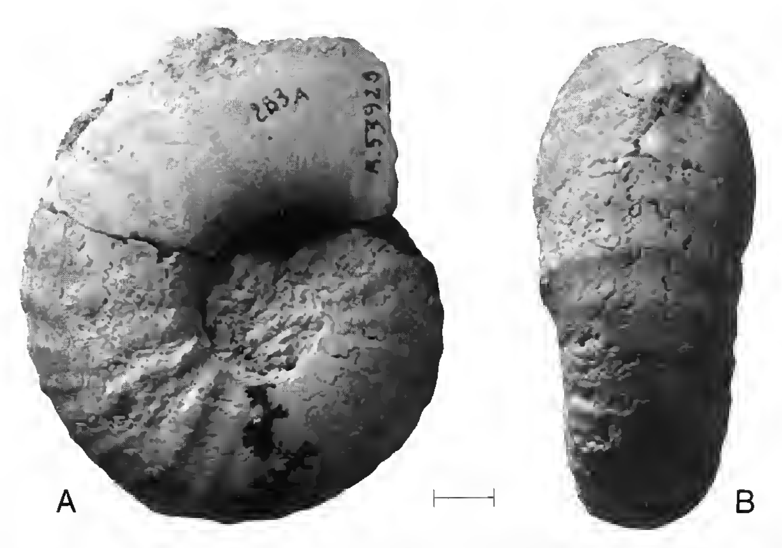


FIG. 14. — *Fikaites laffitei* (Collignon, 1965). Holotype du gisement 283A, Ohanet. Cénomanien supérieur, intervalle 4 du Tinrhert (échelle : 1 cm).

viennent d'être refigurés et discutés par CHANCELLOR *et al.* (1994). La comparaison du matériel montre que l'on ne retrouve pas l'ornementation très vigoureuse de *P. polymorphus* chez les «*Paramammites*» décrits au Nigeria par BARBER (1957) puis MEISTER (1989), et au Tinrhert par COLLIGNON (1965). En revanche, la costulation relativement dense et parfois irrégulière avec des côtes longues séparées par une à trois côtes intercalaires est beaucoup plus caractéristique du genre *Fikaites* récemment créé par ZABORSKI (1993).

Comme COLLIGNON (1965) le note, *Fikaites laffitei* se rapproche des «*Paramammites*» à ornementation réduite décrits par BARBER (1957) au Nigeria. L'espèce la plus proche paraît être «*P.*» *inflatus* (Barber, 1957) qui est cependant beaucoup plus épaisse, avec un ombilic plus profond et une ornementation plus atténuée. *Fikaites varicostatus* (Zaborski, 1993) est également très voisin, mais avec des flancs plus plats et des côtes légèrement flexueuses et non concaves vers l'avant.

Fikaites subtuberculatus (Collignon, 1965)
(Fig. 15)

Paramammites subtuberculatus Collignon, 1965 : 187, pl. A, fig. 3.

HOLOTYPE. — Muséum national d'Histoire naturelle Paris, n° R53921, d'Ohanet, Algérie.

MATÉRIEL. — L'holotype du gisement 3800 dans les environs d'Ohanet.

DISTRIBUTION VERTICALE. — La position du gisement 3800 est incertaine mais correspond vraisemblablement à l'intervalle 4 du Tinrhert (voir la discussion dans le paragraphe consacré à *Pseudaspidoceras grecoi*). Cénomanien supérieur élevé. Au Nigeria, *Fikaites varicostatus* (très voisin, sinon identique à *F. subtuberculatus*) est connu aux confins de la limite Cénomanien-Turonien (ZABORSKI 1993, 1995).

DISTRIBUTION GÉOGRAPHIQUE. — Algérie et, peut-être, Nigeria.

DESCRIPTION DE L'HOLOTYPE.

Coquille modérément évolute. Section du tour subrectangulaire avec des flancs plats, parallèles jusqu'à l'épaule ventro-latérale, puis convergents entre les tubercules ventro-latéraux internes et externes jusqu'à la région ventrale légèrement convexe. Bien que le flanc gauche soit seul préservé, la hauteur et l'épaisseur de la section du tour semblent très comparables. Sur le phragmocône, les côtes atténuées naissent par paires au niveau d'un tubercule ombilical rond et mousse. D'abord radiales ou légèrement convexes vers l'avant, elles deviennent franchement obliques vers l'avant entre les tubercules ventro-latéraux internes et externes, puis traversent la région ventrale en étant presque droites. Quelques intercalaires apparaissent très haut sur les flancs, au niveau de l'épaule ventro-latérale. Sur la chambre d'habitation, malgré la conservation partielle du spécimen, les côtes semblent ne plus naître par faisceaux de deux, mais deviennent alternativement longues et courtes. Les côtes primaires portent au total six rangées de tubercules bien visibles : ombilicaux, ventro-latéraux internes et externes. Un léger renflement des côtes, décelable sur la ligne siphonale, suggère cependant l'existence possible d'une septième rangée de tubercules siphonaux sur les tours internes. La ligne du suture, bien visible, présente une première selle latérale large et un premier lobe latéral large avec de nombreuses denticulations.

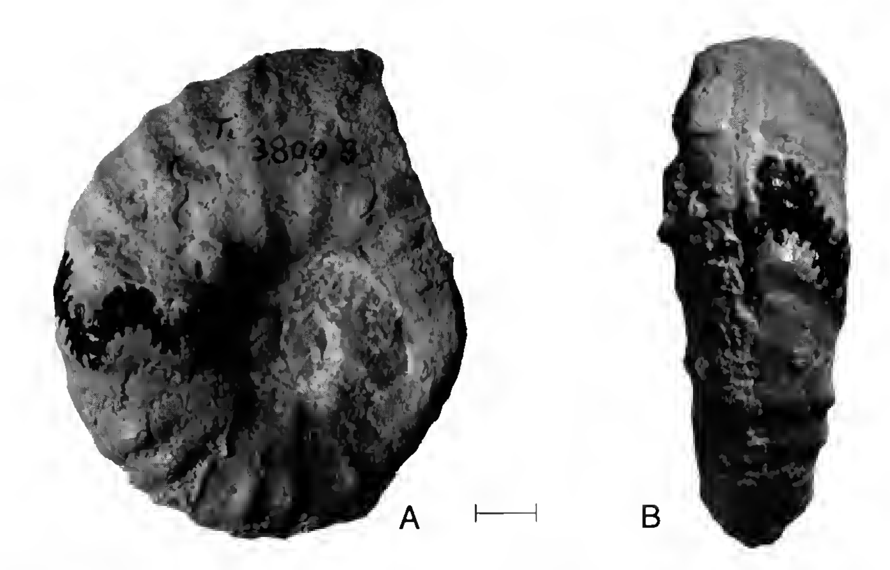


FIG. 15. — *Fikaites subtuberculatus* (Collignon, 1965). Holotype du gisement 3800B, Ohanet. Cénomanien supérieur, vraisemblablement de l'intervalle 4 du Tinrhert (échelle : 1 cm).

DISCUSSION

Morphologiquement, *Fikaites subtuberculatus* Collignon, 1965 est très voisin de *Fikaites varicostatus* Zaborski, 1993. Le paratype illustré par ZABORSKI (1993 : 363, fig. 2-P-Q) comme variant épais de l'espèce est en particulier quasiment identique à *F. subtuberculatus*. Il n'est pas impossible qu'une comparaison ultérieure du matériel conduise à la mise en synonymie des espèces, mais pour l'instant une position conservatrice est adoptée.

Sous-famille EUOMPHALOCERATINAE Cooper, 1978

Genre **PSEUDASPIDOCERAS** Hyatt, 1903

ESPÈCE-TYPE. — *Ammonites footeanus* Stoliczka, 1864, par désignation originale.

Pseudaspidoceras footei "var." ***grecoi*** Collignon, 1965[1]
(Fig. 16)

Mammites (*Pseudaspidoceras*) *footeanus* (?) Stol. — GRECO 1915 : 208, pl. 17, fig. 5.
Pseudaspidoceras footei var. *grecoi* Collignon, 1965 : 176, pl. E, fig. 1a, b.

---

1. COLLIGNON (1965) a décrit sous le nom *Pseudaspidoceras footei* var. *grecoi* une ammonite que nous considérons spécifiquement distincte de *P. footeanus*. En application de l'art. 16 du Code de Nomenclature, le nom *grecoi* n'est pas disponible. Cependant, compte tenu de la similitude de cette variété *grecoi* avec *P. pseudonodosoides* Choffat, 1898 nous nous abstenons de valider formellement le nom *grecoi* et remettons à une publication ultérieure l'évaluation de ces différents noms.

?*Pseudaspidoceras footei* var. *grecoi* — COLLIGNON *in* AMARD *et al.* 1983 : 50, pl. 5, fig. 1a-b.

HOLOTYPE. — Museum national d'Histoire naturelle Paris, n° R53927, d'Ohanet, Algérie.

MATÉRIEL. — L'holotype et unique exemplaire provenant du gisement 3800 dans le secteur d'Ohanet.

DISTRIBUTION VERTICALE. — Le gisement 3800 est un affleurement isolé situé à 16,5 km au N.E. de la balise d'Ohanet. Toute corrélation lithologique avec les coupes décrites est impossible. La récolte dans le même gisement de *Vascoceras* aff. *cauvini* Chudeau, 1909 et *Fikaites subtuberculatus* Collignon, 1965 suggère cependant que l'on se trouve dans un équivalent de l'intervalle 4 à *Vascoceras gamai*, *V. cauvini* et *Nigericeras gadeni*. Au Nigeria, *Pseudaspidoceras pseudonodosoides* (très voisin, sinon identique à *P. grecoi*) est également associé à *Vascoceras cauvini*, dans des niveaux attribués au Cénomanien supérieur élevé (POPOFF *et al.* 1986; MEISTER 1989; ZABORSKI 1990). Aux États-Unis, *P. pseudonodosoides* et *V. cauvini* sont présents dans la Zone à *Neocardioceras juddii* (KENNEDY *et al.* 1989).

DISTRIBUTION GÉOGRAPHIQUE. — Algérie, Égypte.

DESCRIPTION DE L'HOLOTYPE

Il s'agit d'une chambre d'habitation montrant un demi-tour de spire. La coquille est évolute. La section du tour, presque carrée, est légèrement déprimée (rapport H/E = 0,90) avec des flancs

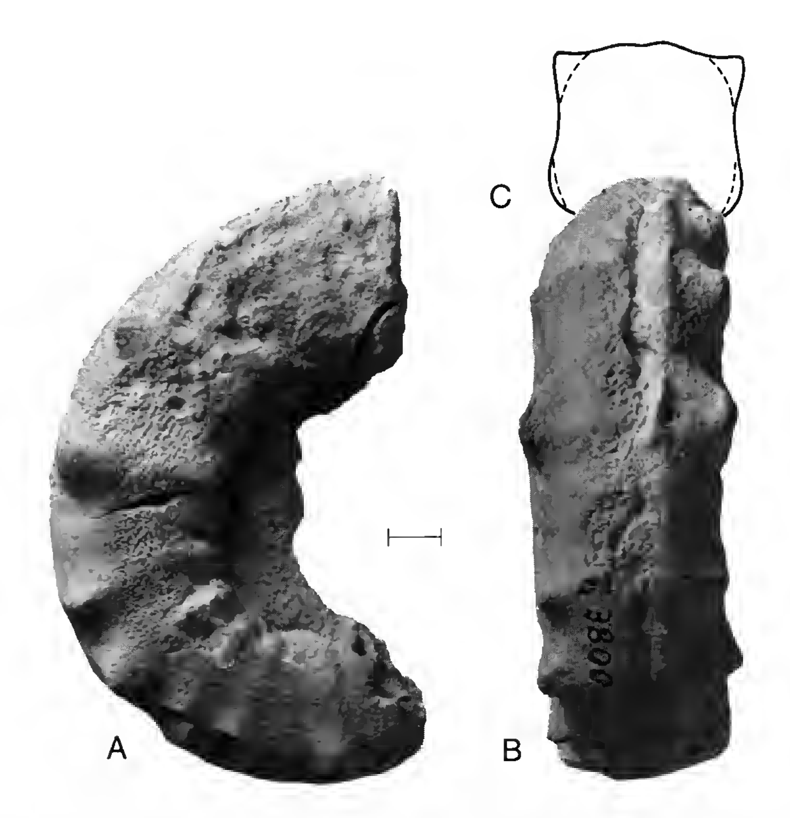


FIG. 16. — A-B, *Pseudaspidoceras grecoi* Collignon, 1965. Holotype du gisement 3800, Ohanet. Cénomanien supérieur, équivalent probable de l'intervalle 4 du Tinrhert. C, *Pseudaspidoceras grecoi* Collignon, 1965 (holotype prise au niveau de la chambre d'habitation, au diamètre approximatif de 90 mm) (échelle : 1 cm).

faiblement convexes et une région ventrale arrondie. L'épaisseur maximale de la section est observée au niveau des tubercules ventro-latéraux internes (Fig. 16C). L'ornementation est constituée de côtes simples, droites, assez serrées, qui naissent au niveau d'un tubercule ombilical allongé radialement, s'effacent à mi-flanc, et redeviennent saillantes sur l'épaule ventro-latérale où elles portent un tubercule ventro-latéral interne qui tend à se développer en corne. Entre les côtes longues s'intercale parfois une côte courte non tuberculée. La région ventrale, large et légèrement arrondie, est en relief par rapport aux tubercules ventro-latéraux externes en nombre identique aux précédents. On compte douze côtes longues et courtes sur le demi-tour de chambre d'habitation préservé.

DISCUSSION

Pseudaspidoceras grecoi Collignon, 1965 diffère des espèces ultérieures comme *P. flexuosum* Powell, 1963 par l'absence de côtes flexueuses, bouclées, et comme du génotype : *P. footeanum* Stoliczka, 1864 par ses côtes droites et non convexes vers l'avant, et par le développement des tubercules ventro-latéraux internes saillants. *P. paganum* Reyment, 1954, récemment révisé par ZABORSKI (1995) a des côtes moins saillantes, souvent plus denses et des flancs plus convergents. La morphologie de *P. grecoi* le rapproche en revanche beaucoup de *Pseudaspidoceras pseudonodosoides* (CHOFFAT 1898) qui semble contemporain et ce n'est pas sans hésitation qu'une séparation spécifique est maintenue pour l'instant. Les larges collections de *P. pseudonodosoides* illustrées par COBBAN *et al.* (1989) du Nouveau-Mexique montrent en effet des spécimens très comparables – *cf.* fig. 83 1-J. L'holotype de *P. grecoi* s'en sépare cependant par la rétention des tubercules ventro-latéraux internes et externes qui restent séparés et bien marqués jusque sur la chambre d'habitation. De plus, la région ventrale du type de *P. grecoi* est large et convexe tandis que chez les spécimens figurés de *P. pseudonodosoides*, celle-ci forme plutôt une dépression étroite au niveau de la chambre, séparant les terminaisons ventro-latérales des côtes. Il n'est pas impossible que des récoltes futures permettent d'inclure *P. grecoi* dans le spectre de variation de *P. pseudonodosoides* mais une position d'attente est adoptée pour le moment.

Famille VASCOCERATIDAE Douvillé, 1912
Sous-famille VASCOCERATINAE Douvillé, 1912

Genre **VASCOCERAS** Choffat, 1898

(= *Paravascoceras* Furon, 1935; *Pachyvascoceras* Furon, 1935; *Paracanthoceras* Furon, 1935; *Broggiiceras* Benavides-Caceres, 1956; *Discovascoceras* Collignon, 1957; *Greenhornoceras* Cobban & Scott, 1972 et *Provascoceras* Cooper, 1979). Voir pour la discussion de la synonymie BERTHOU *et al.* (1985)).

ESPÈCE-TYPE — *Vascoceras gamai* Choffat, 1898 par désignation subséquente de Roman, 1938.

Vascoceras gamai Choffat, 1898
(Fig. 17)

Vascoceras gamai Choffat, 1898 : 54, pl. 7, figs 1-4; pl. 8, fig. 1; pl. 10, fig. 2; pl. 21, figs 1-4.

Autres références :

Vascoceras gamai — COLLIGNON 1965 : 183, figs 5-7. – BERTHOU, CHANCELLOR & LAUVERJAT 1985 : 66, pl. 2, figs 1-12; pl. 3, figs 1-3, 5-7, 10, 13, 14 (avec synonymie). – LUGER & GROSCHKE 1989 : 378, pl. 40, figs 5-7; text-fig. 6c. – THOMEL 1992 : 320, pl. 121, figs 1, 2.

LECTOTYPE. — Service géologique du Portugal, coll. CHOFFAT, n° 808-2, de Meirinhas Baixo, Portugal.

MATÉRIEL. — Dix exemplaires dont sept sont repérés par rapport aux coupes décrites, soit dans la région de Témassinine les gisements 150, et 5566 et, dans le secteur d'Ohanet, les gisements 283, 302 et 309.

DISTRIBUTION. — Intervalle 4 du Tinrhert, associé à *V. cauvini* et *Nigericeras gadeni*. Cénomanien supérieur. Au Portugal et au Nouveau Mexique aux États-Unis, *V. gamai* occupe une position similaire dans la zone à *Neocardioceras juddii* et dans la zone précédente à *Burroceras clydense* (COBBAN *et al.* 1989).

DISTRIBUTION GÉOGRAPHIQUE. — France, Portugal, Espagne, Nigeria, Maroc, Algérie, Tunisie, Égypte, Brésil, Nouveau-Mexique.

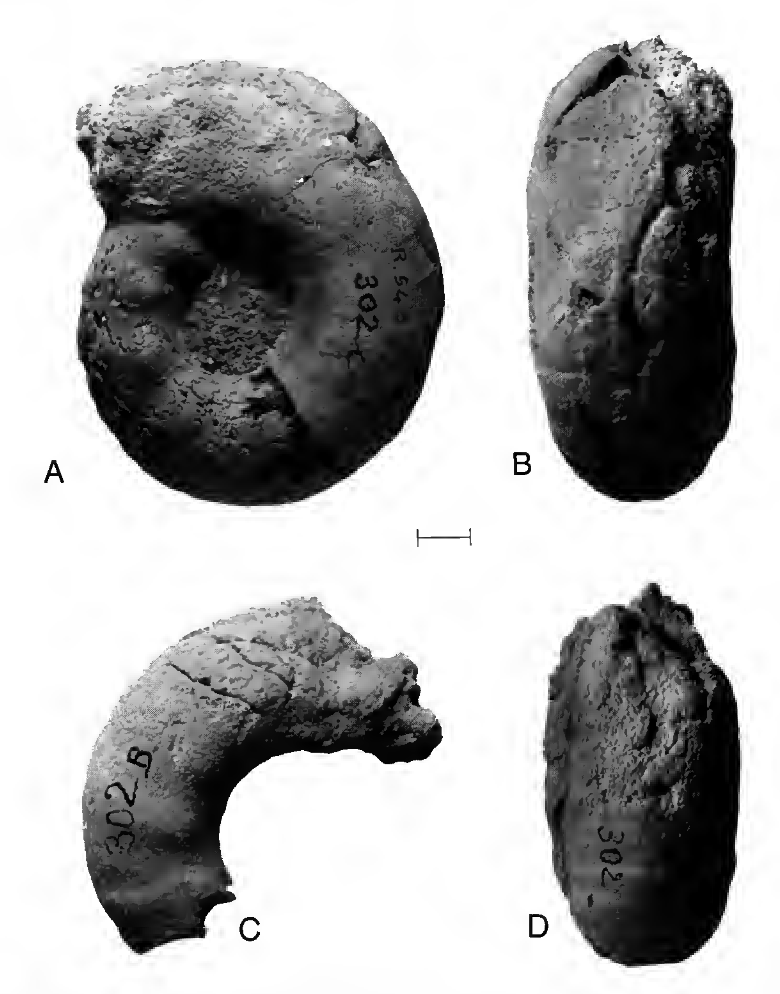


FIG. 17. — *Vascoceras gamai* Choffat, 1898. Tous deux du gisement 302 dans la région d'Ohanet. A-B, n° 302C. C-D, n° 302B. Cénomanien supérieur, intervalle 4 du Tinrhert (échelle : 1 cm).

DISCUSSION

Vascoceras gamai Choffat, 1898, récemment révisé au Portugal par BERTHOU *et al.* (1985), est un *Vascoceras* typiquement évolute, modérément comprimé, qui possède une chambre d'habitation arrondie, lisse ou très faiblement costulée, et des tours internes pourvus de forts tubercules ombilicaux au nombre de huit à dix par tour. Les spécimens du Tinrhert, dont certains ont déjà été illustrés par COLLIGNON (1965 : 183, figs 5-7) sont comparables aux exemplaires de la série type.

Vascoceras cauvini Chudeau, 1909
(Fig. 18)

Vascoceras cauvini Chudeau, 1909 : 68, pl. 1, figs 1,2; pl. 2, figs 1-3; pl. 3, figs 1, 2, 4.

Synonyme :
Paravascoceras rumeaui Collignon, 1957 : 122, pl. 1, fig. 2.

Autres références :
Paravascoceras aff. cauvini — COLLIGNON 1965 : 183.
Paravascoceras cauvini — SCHÖBEL 1975 : 119, pl. 4, figs 1-3; pl. 5, figs 1-4 (avec synonymie).
Vascoceras cauvini — KENNEDY *et al.* 1989 : 82, figs 96, 20 c-g. – ZABORSKI 1990 : figs 8a-b, 12-15.
Vascoceras (Paravascoceras) cauvini — MEISTER *et al.* 1992 : 71; pl. 4, fig. 6; pl. 5, fig. 1-3; pl. 6, figs 1-4; pl. 7, fig. 1 (avec synonymie additionnelle).
Nigericeras gadeni, N. lamberti — MEISTER 1989 : 10, pl. 3, figs 1-3.

LECTOTYPE. — Muséum national d'Histoire naturelle Paris, coll. CHUDEAU, n° R52488 de Gjadjidouna, Damergou, Niger.

MATÉRIEL. — Sept exemplaires dont cinq des gisements 150 (secteur de Témassinine) et 283 (environs d'Ohanet).

DISTRIBUTION VERTICALE. — *Vascoceras cauvini* est présent au Tinrhert dans l'intervalle 4 avec *V. gamai* et *Nigericeras gadeni.* L'espèce est également connue en Israël, associée à *Metoicoceras geslinianum* (LEWY *et al.* 1984) et son extension monte jusque dans la zone à *Neocardioceras juddii* et ses équivalents, en particulier en Israël et aux États-Unis (KENNEDY *et al.* 1989). Cénomanien supérieur.

DISTRIBUTION GÉOGRAPHIQUE. — Israël, Égypte, Algérie, Niger, Nigeria, Soudan, Pérou, Texas, Nouveau-Mexique.

DISCUSSION

Vascoceras cauvini Chudeau est aujourd'hui bien connu grâce à l'excellent travail de SCHÖBEL (1975), réalisé sur les populations du Niger d'où provient le type. Les tours internes sont presque lisses avec des flancs aplatis et convergents, mais l'espèce est surtout aisément reconnaissable si la chambre d'habitation est préservée, avec sa section du tour qui tend à devenir triangulaire et sa costulation caractéristique constituée de côtes arrondies et larges. La comparaison du matériel du Tinrhert avec les spécimens du Niger figurés par SCHNEEGANS (1943) et SCHÖBEL (1975) montre que les deux populations sont identiques.

À noter que tous les « *Vascoceras* », « *Paravascoceras* » et « *Pachyvascoceras* » décrits dans l'ouest du Tinrhert et au Tademaït par COLLIGNON & ROMAN *in* AMARD *et al.* (1983) sont, selon BERTHOU *et al.* (1985), dont l'opinion est acceptée ici, spécifiquement indéterminables. Tous les spécimens concernés sont en effet de grande taille et très usés.

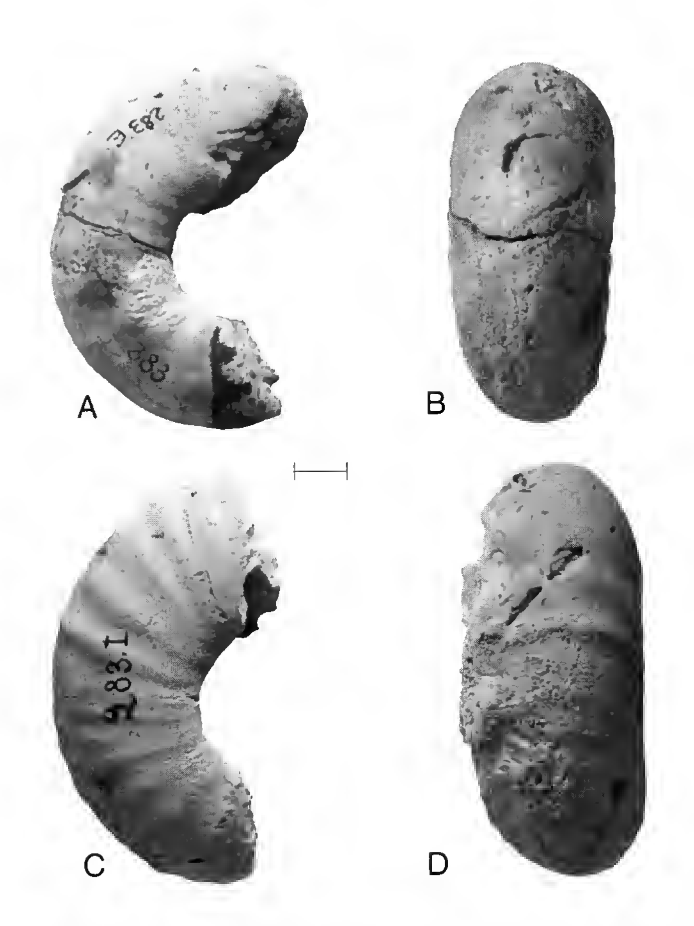


FIG. 18. — A-B, *Vascoceras cauvini* Chudeau, 1909. Gisement 283, Ohanet. Cénomanien supérieur, intervalle 4 du Tinrhert, × 1. C-D, *Vascoceras cauvini* Chudeau, 1909. Gisement 283I, Ohanet. Cénomanien supérieur, intervalle 4 (échelle : 1 cm).

Sous-famille PSEUDOTISSOTIINAE Hyatt, 1903

Genre **PSEUDOTISSOTIA** Peron, 1897
(= *Bauchioceras* Reyment, 1954; *Furoniceras* Collignon, 1957)

ESPÈCE-TYPE. — *Ammonites galliennei* d'Orbigny, 1850, par désignation originale.

Pseudotissotia nigeriensis (Woods, 1911)
(Figs 19-22)

Hoplitoides nigeriensis Woods, 1911 : pl. 23, fig. 3; pl. 24, figs 1-5.

Synonymes :

Pseudotissotia (*Bauchioceras*) *nigeriensis macrocarinata* Barber, 1957 : 49, pl. 21, fig. 5ab; pl. 34, fig. 7, 15;

Pseudotissotia (*Bauchioceras*) *nigeriensis plana* Barber, 1957 : 49, pl. 20, fig. 2a-b; pl. 21, fig. 2a-b; pl. 22, figs 5, 6a-b; pl. 23, fig. 1a-b; pl. 34, figs 2, 8-10.

Pseudotissotia (*Bauchioceras*) *nigeriensis bicarinata* Barber, 1957 : 49, pl. 22, figs 1a-b, 2a-b, 3a-b. 4a-b; pl. 34, figs 4, 12.

Furoniceras trumpyi Collignon, 1957 : 17, pl. 3, fig. 1-1a.

Pseudotissotia (*Bauchioceras*) *nigeriensis* var. *egrediens* Collignon, 1965 : 188, pl. H, fig. 1a-c.

Pseudotissotia (*Bauchioceras*) *bussoni* Collignon, 1965 : 190, pl. H, fig. 2a-b.

Autres références :

Pseudotissotia (*Bauchioceras*) *nigeriensis nigeriensis* — BARBER 1957 : 47, pl. 21, fig. 3a-b; pl. 22, fig. 6a-b; pl. 34, figs 3, 16.

Pseudotissotia (*Bauchioceras*) *nigeriensis tricarinata* (Reyment) — BARBER 1957 : 47, pl. 20, fig. 1a-b; pl. 21, fig. 4a-b; pl. 34, figs 6, 14.

Discovascoceras tesselitense — COLLIGNON 1965 : 181, pl. G, fig. 1a-b. (non *Discovascoceras tesselitense* Collignon, 1957 : 125, pl. 1, fig. 1-1a (= *Vascoceras* indéterminé).)

Discovascoceras defrennei — COLLIGNON 1965 : 182, fig. 4a-b. (*non Discovascoceras defrennei* Collignon, 1957 : 125, pl. 2, fig. 3-3a (= *Vascoceras* indéterminé).)

Pseudotissotia nigeriensis — HIRANO 1983 : 46, pl. 1, figs 1-10; pl. 2, fig. 110; pl. 3, figs 1-18; pl. 4, figs 1-6 (avec synonymie additionnelle). — COURVILLE 1992 : pl. 12, fig. 4; pl. 13, figs 1-3. — ZABORSKI 1993 : 369, fig. 6 J.L.

« *Pseudotissotia* » *nigeriensis* — MEISTER 1989 : 44, pl. 21, figs 4-6; pl. 22, figs 1-4; pl. 23, figs 1-5; pl. 24, fig. 1; pl. 25, figs 1-7; pl. 26, figs 1-3; pl. 27, figs 1-3.

Thomasites nigeriensis — MEISTER *et al.* 1992 : 78, pl. 10, figs 4-6; pl. 11, figs 3, 4; text.-fig. 19.

HOLOTYPE. — Sedgwick Museum Cambridge, coll. WOODS, du N.-E. du Nigeria.

MATÉRIEL. — Une centaine de spécimens dont près de la moitié sont situés sur les coupes décrites ici, soit dans la région de Témassinine des gisements 125, 393 et 5581, et dans le secteur d'Ohanet des gisements 279, 280, 281, 286, 287, 292, 293, 298, 314, 316, 319, 3802, 5299 et 5361.

DISTRIBUTION VERTICALE. — Intervalle 5 à *Pseudotissotia nigeriensis* (seul) et intervalle 6 à *P. nigeriensis* et *Choffaiceras* sp. du Tinrhert. Turonien inférieur. En Israël, *P. nigeriensis* est connu dans la zone à *Choffaticeras securiforme* à la base du Turonien inférieur (FREUND & RAAB 1969). Au Nigeria, l'espèce occupe une position équivalente dans les niveaux les plus bas du Turonien (POPOFF *et al.* 1986; MEISTER 1989; ZABORSKI 1990, 1993, 1995).

DISTRIBUTION GÉOGRAPHIQUE. — Niger, Nigeria, Algérie, Israël, Mexique, Brésil.

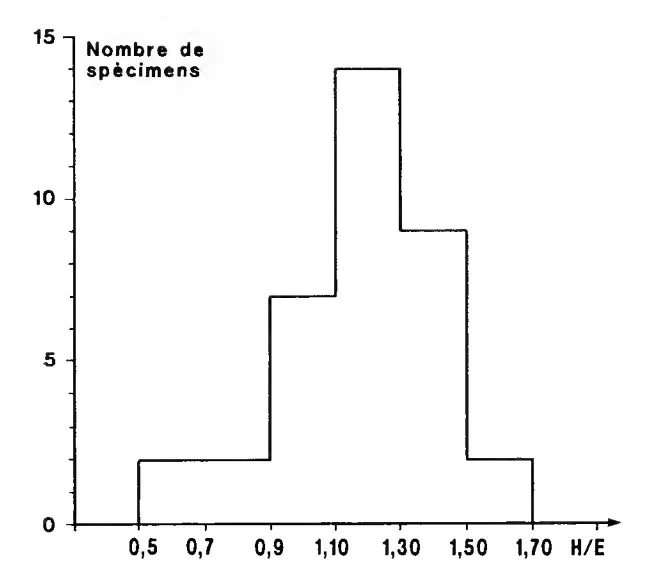


FIG. 19. — Variation du rapport H/E (hauteur du tour sur l'épaisseur mesuré sur 42 exemplaires de *Pseudotissotia nigeriensis* (Woods, 1911) du Tinrhert. La majorité des spécimens sont modérément comprimés (H/E compris entre 1,10 et 1,30, mais le spectre de variation s'étend de spécimens épais (H/E = 0,59 à des formes très comprimées (H/E = 1,68).

DESCRIPTION

Coquille discoïdale, involute à très involute, avec un ombilic étroit et profond. La section du tour, subtrapézoïdale, présente le maximum d'épaisseur au tiers interne du flanc, parfois même plus bas, avec des flancs légèrement arrondis qui convergent vers la région ventrale plane ou légèrement tectiforme, modérément large et ornée de trois carènes. La population du Tinrhert montre une variation considérable dans l'épaisseur du tour, allant de formes involutes et comprimées à des formes évolutes et très renflées. Le spectre de variation apparaît bien dans l'histogramme de la figure 19 qui classe les spécimens en fonction du rapport de la hauteur sur l'épaisseur du tour (H/E). Si la majorité des exemplaires ont un rapport H/E compris entre 1,10 et 1,30 et correspondent à des coquilles modérément comprimées, les deux extrémités du spectre vont de 1,68 (variants les plus comprimés) à 0,59 (variants déprimés). À noter que chez les variants comprimés, la région ventrale tend parfois à devenir plane ou même plus rarement légèrement concave, et la carène siphonale peut disparaître plus ou moins.

Au diamètre de préservation du matériel qui est généralement supérieur à 8 cm l'ornementation est inexistante ou très atténuée. Sur les tours internes des variants les plus épais, on distingue cependant des côtes primaires larges et mousses qui naissent sur un renflement ombilical, traversent le flanc en étant radiales ou légèrement concaves vers l'avant, et se terminent sur l'épaule ventro-latérale. Entre les côtes longues s'intercalent fréquemment deux ou trois côtes courtes. Cette ornementation disparaît cependant très vite, en particulier chez les variants comprimés et le stade adulte est entièrement lisse. Les carènes ventrales sont le plus souvent entières et saillantes, mais dans quelques spécimens les carènes ventro-latérales et, plus rarement, la carène siphonale apparaissent onduleuses, formées de *clavi* pincés dans le sens de l'enroulement, en correspondance avec les terminaisons ventrales des côtes et en nombre identique sur les différentes carènes (Fig. 22C).



FIG. 20. — *Pseudotissotia nigeriensis* (Woods, 1911). Variant épais du gisement 5361F. Ohanet. Turonien inférieur, intervalle 5 du Tinrhert (échelle : 1 cm).

La ligne de suture possède un lobe externe étroit et profond, une première selle latérale haute et large denticulée et un premier lobe latéral souvent bifide.

DISCUSSION

BARBER (1957) et HIRANO (1983), ont décrit en détail la grande variabilité morphologique de *Pseudotissotia nigeriensis* (Woods, 1911). Les formes comprimées, faiblement ornementées, portent trois carènes bien individualisées; tandis qu'à l'autre extrémité du spectre de variation, les variants épais sont costulés et les carènes développent des *clavi* qui correspondent à la terminaison ventrale des côtes, ce fait étant particulièrement net sur les tours internes du phragmocône. Le matériel du Tinrhert illustre bien cette large diversité morphologique et tous les représentants du spectre de variation sont récoltés à travers l'ensemble des gisements, les formes modérément comprimées étant néanmoins les plus communes.

Pseudotissotia nigeriensis var. *egrediens* Collignon, 1965 est un variant comprimé à flancs plats pour lequel une séparation sous-spécifique est superflue (HIRANO 1983). De la même façon, *Pseudotissotia bussoni* Collignon, 1965 à coquille comprimée, ombilic étroit, carène siphonale saillante et flancs modérément convexes, entre dans le spectre de variation de *P. nigeriensis* dont il constitue un synonyme junior. Quant aux spécimens épais figurés par COLLIGNON (1965) sous les noms de *Discovascoceras tesselitense* Collignon, 1957 (COLLIGNON, 1965 : 181, pl. 6, fig. 1a-b) et *Discovascoceras defrennei* Collignon, 1957 (COLLIGNON 1965 : 182, fig. 4a-b), ce sont des variants déprimés et évolutes proches de *Pseudotissotia nigeriensis tricarinata* Reyment, 1954 (*cf.* l'exemplaire du Nigeria illustré par BARBER 1957, pl. 20, fig. 1a-b). À noter en revanche que les types de *D. tesselitense* et *D. defrennei* de Collignon (1957) sont vraisemblable-

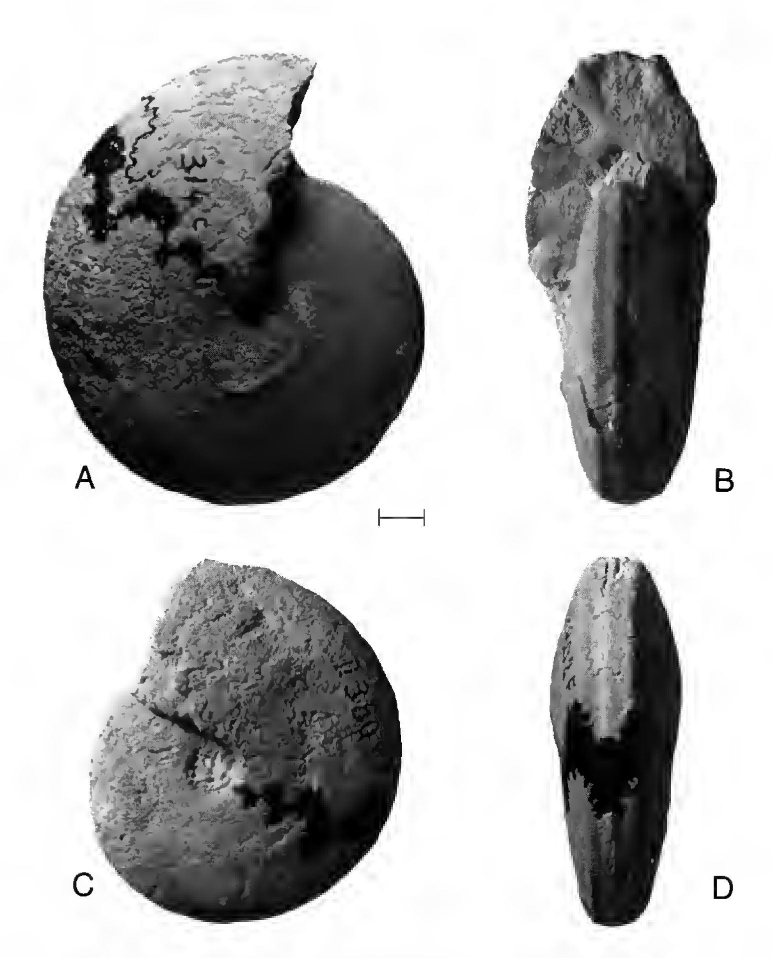


FIG. 21. — *Pseudotissotia nigeriensis* (Woods, 1911). A-B, variant moyennement épais du gisement 314C, Ohanet. C-D, variant comprimé du gisement 3802F, Ohanet. Turonien inférieur, intervalles 5 et 6 du Tinrhert (échelle : 1 cm).

ment, selon l'avis de BERTHOU *et al.* (1985) des *Vascoceras* usés indéterminables spécifiquement. Enfin, *Furoniceras trumpyi* Collignon, 1957 est également un synonyme junior de *P. nigeriensis* dont la cloison aberrante «semble liée à l'usure éolienne du fossile» (REYMENT 1978).

P. nigeriensis diffère du génotype *Pseudotissotia gallienei* (d'Orbigny, 1850) par son enroulement plus involute, la perte rapide de toute ornementation et son stade adulte entièrement lisse (KENNEDY *et al.* 1979). La tuberculation des carènes ventrales sur les tours internes des formes épaisses rappelle dans une moindre mesure ce que l'on observe chez les *Thomasites* Pervinquière, 1907, et en particulier *Thomasites gongilensis* (Woods 1911). Ceci a conduit MEISTER *et al.* (1992) à proposer un changement d'attribution générique de *P. nigeriensis* sous le nom de *Thomasites nigeriensis*. Dans la mesure où l'espèce-type du genre *Pseudotissotia*, *P. gallienei*, possède également des *clavi* et des carènes onduleuses sur les tours internes et puisque, dans tous les variants de *P. nigeriensis*, le dernier tour de spire est entièrement lisse

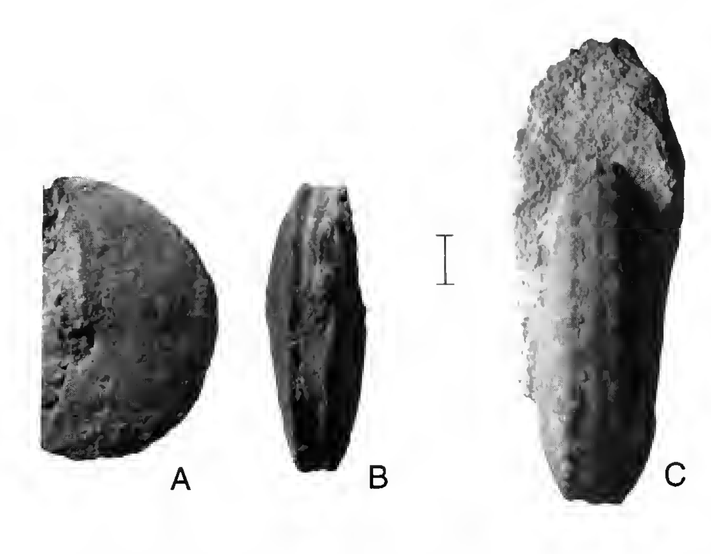


FIG. 22. — *Pseudotissotia nigeriensis* (Woods, 1911). A-B, variant comprimé à région ventrale légèrement concave, du gisement 461, Gour Ben Houilet. Turonien inférieur, intervalles 5 et 6 du Tinrhert, × 1. C, *Pseudotissotia nigeriensis* (Woods, 1911). Vue ventrale d'un variant dont les carènes portent des *clavi*; gisement 5299, Ohanet. Turonien inférieur, intervalle 5 du Tinrhert (échelle : 1 cm).

et les trois carènes ne sont pas tuberculées, cette proposition n'est pas suivie, ce qui est également l'avis de ZABORSKI (1990, 1993) et de CHANCELLOR *et al.* (1994).

Genre **CHOFFATICERAS** Hyatt, 1903
(= *Leoniceras* Douvillé, 1912)

Choffaticeras gr. *quaasi* (Peron, 1904) – *pavillieri* Pervinquière, 1907 pl. 10, fig. 1.

ESPÈCE-TYPE — *Pseudotissotia meslei* Peron, 1897, par désignation originale.

MATÉRIEL. — Un spécimen du gisement 125 situé à l'ouest de la balise 14 dans les environs de Témassinine.

DISTRIBUTION VERTICALE. — Intervalle 6 à *Pseudotissotia nigeriensis* et *Choffaticeras* sp. du Tinrhert. Turonien inférieur. En Israël, *Ch. quaasi* et *Ch. pavillieri* sont connus au sommet du Turonien inférieur dans la zone à *Choffaticeras quaasi* et, pour la première d'entre elles, dans la zone suivante à *Choffaticeras luciae trisellatum* qui est équivalente à la zone à *Mammites nodosoides* du domaine boréal (FREUND & RAAB 1969). En France, *Ch. pavillieri* est présent dans la zone à *Kamerunoceras turoniense* à la base du Turonien moyen (AMÉDRO & HANCOCK 1985).

DISTRIBUTION GÉOGRAPHIQUE. — *Ch. quaasi* est connu actuellement en Égypte, Israël et Tunisie. La dispersion de *Ch. pavillieri* est plus vaste et comprend Israël, l'Égypte, la Tunisie, la Roumanie, la France, le Zaïre, Madagascar et les États-Unis (Western Interior).

DISCUSSION

Choffaticeras quaasi (Péron, 1904) et *Choffaticeras pavillieri* (Pervinquière, 1907) font partie selon FREUND & RAAB (1969) du groupe des *Choffaticeras* comprimés à ombilic étroit. Contrairement à *Choffaticeras sinaiticum* (Douvillé, 1928) où la section devient rapidement tranchante, *Ch. quaasi* garde une section du tour ogivale et un ventre arrondi ; tandis que *Ch. pavillieri*

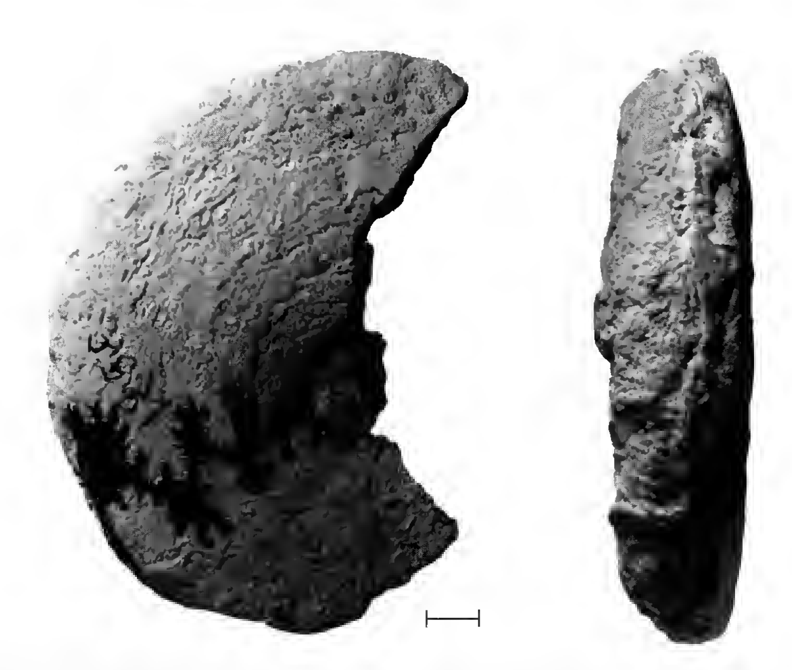


FIG. 23. — *Choffaticeras* gr. *quaasi* (Peron, 1904) – *pavillieri* Pervinquière, 1907. Gisement 125C, Témassinine. Turonien inférieur, intervalle 6 du Tinrhert (échelle : 1 cm).

possède une région ventrale tectiforme avec une carène siphonale qui persiste même sur la chambre. Un exemplaire du gisement 125, malheureusement assez mal conservé, rassemble plusieurs caractères communs à *Ch. quaasi* et *Ch. pavillieri* : coquille comprimée, ombilic étroit et région ventrale non tranchante. L'altération de la région ventrale ne permet pas de choisir entre les deux espèces même si l'aspect général de la section du tour avec des flancs sub-parallèles, peu convergents, rappelle plus *Ch. pavillieri* (*cf.* les spécimens illustrés par PERVINQUIÈRE (1907), pl. 23, fig. 6a-b, et par AMÉDRO & HANCOCK 1985 : 30, fig. 10a-b).

Choffaticeras sp.
(Fig. 24)

MATÉRIEL. — Une quinzaine de spécimens dont la plupart proviennent de gisements intégrés dans les coupes décrites, soit les gisements 279, 318 (six exemplaires) et 5346 (région d'Ohanet); 393, 5576, 5577 et 5578 (secteur de Témassinine) et, 461, 467, 5597 et 5598 (Gour Ben Houilet).

DISTRIBUTION VERTICALE. — Intervalle 6 à *Pseudotissotia nigeriensis* et *Choffaticeras* sp. du Tinrhert. Turonien inférieur.

DISCUSSION

Un certain nombre d'ammonites de 15 à 20 cm de diamètre, à coquille discoïdale, modérément comprimée à comprimée, ombilic étroit et profond avec un mur anguleux, et section

tranchante, sont considérés comme *Choffaticeras* indéterminés. La plupart sont des phragmocônes légèrement écrasés, ce qui renforce le caractère comprimé de la section du tour. Certains ont des flancs légèrement convexes jusqu'au niveau de la carène siphonale tandis que chez d'autres, les flancs deviennent concaves sur la partie la plus externe.

Le caractère comprimé de la coquille, l'ombilic étroit et la section lancéolée rappellent les formes d'Égypte et du Sinaï décrites par DOUVILLÉ (1928) et, en particulier, *Choffaticeras sinaiticum* (Douvillé, 1928) (dont *Ch. luciae* var. *stricta* Pervinquière, 1907 pourrait être un synonyme antérieur selon FREUND & RAAB 1969). La différence de diamètre (7 cm pour le type contre 15 à 20 cm pour les spécimens du Tinrhert) et l'écrasement du matériel algérien rendent cependant la comparaison difficile. Certains *Choffaticeras pavillieri* Pervinquière, 1907 acquièrent par exemple également une section lancéolée à des diamètres supérieurs à 10 cm (FREUND & RAAB 1969, fig. 11b).

COLLIGNON (1965 : 29, text-fig. 8a-b) a figuré sous le nom de *Leoniceras luciae* Perv. un spécimen plus épais provenant du gisement 3827. Cette détermination, actualisée sous le nom de *Choffaticeras luciae* semble exacte, malheureusement la position du gisement qui est isolé ne peut être précisée par rapport aux coupes décrites.

Hoplitoides hourcqui Collignon, 1965 (193, pl. F, fig. 3a-b), dont le type provient du gisement 318 dans le secteur d'Ohanet, possède enfin une morphologie comparable à certains spécimens considérés ici comme *Choffaticeras* sp. Selon COLLIGNON (1965), *H. hourcqui* est distingué par sa cloison, caractérisée par un très fin découpage des selles et des lobes. Si certains



FIG. 24. — *Choffaticeras* sp. Gisement 318C, Ohanet. Turonien inférieur, intervalle 6 du Tinrhert (échelle : 1 cm).

TABLEAU 1. — Comparaison des déterminations anciennes (COLLIGNON 1957, 1965) et actualisées des ammonites cénomano-turoniennes du Tinrhert (Sahara algérien).

COLLIGNON, 1957, 1965	Ce travail
Neolobites vibrayei d'ORBIGNY *Neolobites fourtaui* PERVINQUIÈRE *Neolobites peroni* HYATT *Neolobites bussoni* COLLIGNON	*Neolobites vibrayeanus* (d'ORBIGNY)
Kamerunoceras tinrhertense COLLIGNON	*Cunningtoniceras tinrhertense* (COLLIGNON)
Calycoceras grossouvrei (SPATH) *Calycoceras boulei* COLLIGNON	*Calycoceras (C.) naviculare* (MANTELL)
Eucalycoceras pentagonum JUKES-BROWNE & HILL *Protacanthoceras* sp.	*Eucalycoceras pentagonum* (JUKES-BROWNE)
Nigericeras gignouxi SCHNEEGANS *Nigericeras lamberti* SCHNEEGANS *Nigericeras jacqueti* SCHNEEGANS *Nigericeras jacqueti* var. *crassecostata* COLLIGNON	*Nigericeras gadeni* (CHUDEAU)
Pseudaspidoceras footei var. *grecoi* COLLIGNON	*Pseudaspidoceras grecoi* COLLIGNON
Paramammites laffitei COLLIGNON	*Fikaites laffitei* (COLLIGNON)
Paramammites subtuberculatus COLLIGNON	*Fikaites subtuberculatus* (COLLIGNON)
Mammites cf. *pseudonodosoides* CHOFFAT	? «*Paramammites*» sp.
Vascoceras gamai CHOFFAT	*Vascoceras gamai* CHOFFAT
Paravascoceras aff. *cauvini* CHUDEAU *Paravascoceras rumeaui* COLLIGNON	*Vascoceras cauvini* CHUDEAU
Neoptychites sp. aff. *taelingaeformis* var. *discrepans* SOLGER	*Forbesiceras* sp.
Discovascoceras tesselitense COLLIGNON, 1957 *Discovascoceras defrennei* COLLIGNON, 1957	*Vascoceras* sp. ind.
Discovascoceras tesselitense COLLIGNON, *sensu* 1965 *Discovascoceras defrennei* COLLIGNON, *sensu* 1965 *Furoniceras trumpyi* COLLIGNON *Pseudotissotia nigeriensis* var. *egrediens* COLLIGNON *Pseudotissotia bussoni* COLLIGNON	*Pseudotissotia nigeriensis* (WOODS)
Leoniceras luciae PERVINQUIÈRE	*Choffaticeras luciae* PERVINQUIÈRE
Leoniceras pavillieri PERVINQUIÈRE	*Choffaticeras* gr. *quaasi* (PERON)-*pavillieri* PERVINQUIÈRE
Leoniceras segne SOLGER	*Choffaticeras* sp.
Hoplitoides hourcqui COLLIGNON	? *Choffaticeras* sp. ou ? *Hoplitoides* sp.

Hoplitoides montrent également une cloison très découpée (*cf.* la ligne de suture d'*H.* cf. *wohltmanni* (von Koenen) illustrée par COBBAN & HOOK 1980), la plupart, tel *Hoplitoides ingens* (von Koenen, 1897), ont une cloison beaucoup plus pseudocératiforme (REYMENT 1955). Selon COBBAN & HOOK (1980), la suture des *Choffaticeras* rappelle celle des *Hoplitoides*. D'un autre côté, les *Hoplitoides* ont un ombilic très fermé et un ventre plat sur les tours internes, deux caractères qui n'apparaissent pas sur les deux spécimens de la série type d'*H. hourcqui* conservés dans les collections du Muséum national d'Histoire naturelle à Paris. Aussi n'est-il pas impossible qu'*Hoplitoides hourcqui* puisse être interprété dans le futur comme étant un *Choffaticeras*, mais des récoltes complémentaires dans la localité-type seraient nécessaires pour soutenir l'option.

CONCLUSION

La révision d'une collection de plusieurs centaines d'ammonites recueillies entre 1957 et 1965 dans les formations du Cénomanien supérieur et du Turonien inférieur du Tinrhert (Sahara algérien) conduit à inventorier quinze espèces, ce qui constitue une réduction sensible par rapport aux études antérieures de COLLIGNON (1957, 1965) qui admettait la présence de trente-quatre taxons. La différence tient à la mise en synonymie d'un certain nombre d'espèces définies dans un concept typologique où la moindre variation d'un caractère morphologique externe était le prétexte pour la création d'une « espèce » n'ayant probablement pas une valeur, ni un sens biologiques. La comparaison des déterminations anciennes et actualisées est résumée dans le tableau 1.

D'un autre côté, malgré la relative monotonie des faciès, la localisation des spécimens sur des coupes permet de distinguer six intervalles biostratigraphiques fondés sur la répartition des espèces. La limite Cénomanien-Turonien, interprétée jusqu'alors à l'apparition du genre *Nigericeras* est placée maintenant au niveau de disparition de *Vascoceras cauvini*, ce qui s'accorde mieux avec l'usage actuel dans le domaine boréal. Cet ajustement revient à remonter sur le terrain de 2 à 5 m la limite au sein de la première masse calcaire, c'est-à-dire des « calcaires inférieurs » (c2-t1). Enfin, la position stratigraphique de plusieurs espèces significatives est précisée. Tel est le cas par exemple de « *Kamerunoceras* » *tinrhertense* (COLLIGNON 1965) interprété à l'origine comme un taxon turonien et associé en réalité à *Neolobites vibrayeanus* à la base du Cénomanien supérieur.

Manuscrit soumis pour publication le 7 février 1995 ; accepté le 20 octobre 1995.

RÉFÉRENCES

AMARD B., COLLIGNON M. & LEFAVRAIS-HENRY M. 1978. — Le Cénomanien d'El Goléa (Tademaït N., Sahara algérien) : coexistence de *Calycoceras* avec *Nigericeras* et implications stratigraphiques. *Cahiers de Micropaléontologie* **4** : 29-39, pls 1-5.

AMARD B., COLLIGNON M. & ROMAN J. 1983. — Étude stratigraphique et paléontologique du Crétacé supérieur et Paléocène du Tinrhert-W et Tademaït-E (Sahara algérien). *Documents du Laboratoire de Géologie de Lyon*, H. S. **6** : 15-173.

AMÉDRO F. & HANCOCK J. M. 1985. — Les ammonites de l'autoroute « L'Aquitaine », France (Turonien et Santonien). *Cretaceous Research* **6** : 15-32.

BARBER W. 1957. — Lower Turonian ammonites from north-eastern Nigeria. *Bulletin of the Geological Survey of Nigeria* **26**, 86 p., 34 pls.

BENAVIDES-CACERES V. E. 1956. — Cretaceous system in northern Peru. *Bulletin of the American Museum of natural History* **108** : 353-494, pls 31-66.

BERTHOU P. Y., CHANCELLOR G. R. & LAUVERJAT J. 1985. — Revision of the Cenomanian-Turonian Ammonite *Vascoceras* Choffat, 1898, from Portugal. *Comunicaçoes dos Servicos Geologicos de Portugal* **71** (1) : 55-79, 6 pls.

BIRKELUND T., HANCOCK J. M., HART M. B., RAWSON P. F., REMANE J., ROBASZYNSKI F., SCHMID F. & SURLYK F. 1984. — Cretaceous stage boundaries - Proposals. *Bulletin of the Geological Society of Denmark* **33** : 3-20.

BUROLLET P.F. 1956. — Contribution à l'étude stratigraphique de la Tunisie centrale. *Annales des Mines et de la Géologie*, Tunis **18**, 345 p.

BUSSON G. 1960. — Sur la coupe du Crétacé supérieur et de l'Éocène inférieur du Tinrhert central (Sahara algérien). *Travaux de l'Institut de Recherches sahariennes* **19** : 141-149, 4 pls.

— 1964. — Carte géologique de l'Algérie au 1/500000. Feuille Fort-Flatters. *Publication du Centre de Recherches sur les Zones Arides*, Paris (CNRS).

— 1965. — Sur les gisements de céphalopodes crétacés sahariens. *Annales de Paléontologie (Invertébrés)* **51** (2) : 153-161.

— 1969. — Sédimentation, transgression et paléogéographie sur les grandes plates-formes du Mésozoïque : l'exemple du Cénomanien-Turonien du nord-est de la plate-forme saharienne et de Berbérie. *Bulletin de la Société géologique de France* **7** (11) : 687-703.

— 1970. — Le Mésozoïque saharien : 2e partie. Essai de synthèse des données des sondages algéro-tunisiens. *Publication du Centre de Recherches sur les Zones Arides*, Paris (CNRS). 811 p., 5 pls.

— 1972. — Principes, méthodes et résultats d'une étude stratigraphique du Mésozoïque saharien. *Mémoire du Muséum national d'Histoire naturelle, Paris (Sciences de la Terre)* N.S. C **26** . 1-442.

CHANCELLOR G. R., KENNEDY W. J. & HANCOCK J. M. 1994. — Turonian ammonite faunas from Central Tunisia. *Special Papers in Palaeontology* **50**, 118 p., 37 pls.

CHOFFAT P. 1898. — Recueil d'études paléontologiques sur la faune crétacique du Portugal. 1. Espèces nouvelles ou peu connues. Deuxième série, Les ammonées du Bellasien, des couches à *Neolobites vibrayeanus*, du Turonien et du Sénonien. *Travaux de géologie du Portugal* : 41-86, pl. 3-22.

CHUDEAU R. 1909. — Ammonites du Damergou (Sahara méridional). *Bulletin de la Société géologique de France* **4** (9) : 67-71, pl. 1-3.

COBBAN W. A. 1971. — New and little-known ammonites from the Upper Cretaceous (Cenomanian and Turonian) of the Western Interior of the United States. *Professional Paper U.S. Geological Survey* **699**: 1-24, 18 pls.

— 1988. — *Tarrantoceras* Stephenson and related Ammonoid genera from Cenomanian (Upper Cretaceous) rocks in Texas and the Western Interior of the United States. *Professional Paper U.S. Geological Survey* **1473**, 30 p., 10 pls.

COBBAN W. A. & HOOK S. C. 1980. — The Upper Cretaceous (Turonian) ammonite family Coilopoceratidae Hyatt in the Western Interior of the United States. *Professional Paper U.S. Geological Survey* **1192**, 28 p., 21 pls.

COBBAN W. A., HOOK S. C. & KENNEDY W. J. 1989. — Upper Cretaceous rocks and ammonites faunas of southwestern New Mexico. *New Mexico Bureau of Mines & Mineral Resources* **45**, 137 p.

COBBAN W. A. & SCOTT G. R. 1972. — Stratigraphy and ammonite faunas of the Graneros Shale and Greenhorn Limestone near Pueblo, Colorado. *Professional Paper U.S. Geological Survey* **645**, 108 p., 41 pls.

COLLIGNON M. 1937. — Ammonites cénomaniennes du Sud-Ouest de Madagascar. *Annales géologiques du Service des Mines de Madagascar* **8** : 29-72, pl. 1-11.

— 1957. — Céphalopodes néocrétacés du Tinrhert (Fezzan). *Annales de Paléontologie (Invertébrés)* **43** : 113-136, pl. 16-18.

— 1965. — Nouvelles ammonites néocrétacées sahariennes. *Annales de Paléontologie (Invertébrés)* **5** : 165-202, pl. A-H.

COOPER M. R. 1978. — Uppermost Cenomanian-basal Turonian ammonites from Salinas, Angola. *Annals of the South African Museum* **75** : 51-152.

— 1979. — Ammonite evolution and its bearing on the Cenomanian-Turonian boundary problem. *Paläontologie Zeitschrift* **53** : 120-128.

COURVILLE Ph. 1992. — Les Vascoceratinae et les Pseudotissotiinae (Ammonitina) d'Ashaka (N.-E. Nigeria) : relations avec leur environnement biosédimentaire. *Bulletin du Centre de Recherches Exploration Production Elf Aquitaine* **16** : 407-457. 14 pls.

DIENER C. 1925. — *Ammonoidea neocretacea.* Fossilium Cat., 244 p.

DOUVILLÉ H. 1890. — Sur la classification des cératites de la Craie. *Bulletin de la Société géologique de France* **3** (18) : 275-292.

— 1912. — Évolution et classification des Pulchelliidés. *Bulletin de la Société géologique de France* **4** (11) : 285-320.

— 1928. — Les ammonites de la Craie supérieure en Égypte et au Sinaï. *Mémoire de l'Académie des Sciences, Institut de France* **60**, 44 p., 7 pl.

FISCHER P. 1882. — *Manuel de Conchyliologie et de Paléontologie conchyliologique.* Masson (ed.). Paris, 1369 p., 23 pls.

FREUND R. & RAAB M. 1969. — Lower Turonian ammonites from Israel. *Special Papers in Palaeontology* **4**, 83 pp., 10 pl.

FURON R. 1935. — Le Crétacé et le Tertiaire du Sahara soudanais (Soudan, Niger, Tchad). *Archives du Muséum national d'Histoire naturelle de Paris* **6** (13). 96 p., 7 pl.

GRECO B. 1915. — Fauna cretacea dell' Egitto raccolta dal Figari Bey. *Palaeontographica Italica* **21**: 189-231, pls 17-22.

GROSSOUVRE A. DE 1894. — Recherches sur la Craie supérieure, 2 : Paléontologie. Les Ammonites de la Craie supérieure. *Mémoire du Service de la Carte géologique détaillée de France*, 264 p., 39 pls.

HIRANO H. 1983. — Revision of two Vascoceratid Ammonites from the Upper Cretaceous of Nigeria. *Bulletin of Science and Engineering Research Laboratory, Waseda University* **105**: 44-79, 5 pls.

HYATT A. 1889. — Genesis of the Arietidae. *Smithsonian Contribution to Knowledge*, 238 p., 14 pls.

— 1900. — Cephalopoda. *In* K. A. VON ZITTEL (ed.). *Textbook of Palaeontology.* Eastman, London : 502-604.

— 1903. — Pseudoceratites of the Cretaceous. *Monography U.S. Geological Survey* **44**, 351 p., 47 pls.

JUKES-BROWNE A. J. 1896. — Critical remarks on some of the fossils. *In* A. J. JUKES-BROWNE & HILL (eds). A delimitation of the Cenomanian : being a comparison of the corresponding beds in South-Western England and Western France. *Quaterly Journal of the Geological Society of London* **52** : 99-178, pl. 5.

KENNEDY W. J. 1971. — Cenomanian ammonites from southern England. *Special Papers in Palaeontology* **8**, 133 p., 64 pls.

KENNEDY W. J. & COBBAN W. A. 1991. — Stratigraphy and interregional correlation of the Cenomanian-Turonian transition in the Western Interior of the United States near Pueblo, Colorado, a potential boundary stratotype for the base of the Turonian stage. *Newsletters in Stratigraphy* **24**: 1-33.

KENNEDY W. J, COBBAN W. A., HANCOCK J. M. & HOOK S. C. 1989. — Biostratigraphy of the Chispa Summit Formation at its type locality : a Cenomanian through Turonian reference section for Trans-Pecos Texas. *Bulletin of the Geological Institutions of the University of Uppsala* **15**: 39-119.

KENNEDY W. J., COOPER M. R. & WRIGHT C. W. 1979. — On *Ammonites gallienei* d'Orbigny, 1850. *Bulletin of the Geological Institutions of the University of Uppsala* **8**: 5-15.

KENNEDY W. J. & JUIGNET P. 1981. — Upper Cenomanian Ammonites from the Environs of Saumur, and the provenance of the types of *Ammonites vibrayeanus* and *Ammonites geslinianus. Cretaceous Research* **2**: 19-49.

KENNEDY W. J., JUIGNET P. & HANCOCK J. M. 1981. — Upper Cenomanian Ammonites from Anjou and the Vendée, Western France. *Palaeontology* **24** (1): 25-84. pls 3-17.

KENNEDY W. J. & WRIGHT C. W. 1994. — The affinities of *Nigericeras* Schneegans, 1943 Cretaceous Ammonoidea. *Geobios* **27** (5): 583-589, 2 pl.

KENNEDY W. J., WRIGHT C. W. & HANCOCK J. M. 1987. — Basal Turonian ammonites from West Texas. *Palaeontology* **30**: 27-74, pls 1-10.

KIRKLAND J. I. & COBBAN W. A. 1986. — *Cunningtoniceras arizonense* n. sp., a large acanthoceratid ammonite from the upper Cenomanian (Cretaceous of eastern central Arizona). *Hunteria* **1**: 1-14.

KOENEN A. VON 1897-1898. — Ueber Fossilien der unteren Kreide am Ufer des Mungo in Kamerun. *Abhandlungen der Königlische Gesellschaft der Wissenschaften zu Göttingen.* 65 p., 7 pls.

KOSSMAT F. 1895-1898. — Untersuchungen über die südindische Kreideformation. *Beiträge zur Paläontologie und Geologie Österreich-Ungarns und des Orients.* 217 p., 19 pls.

LAUVERJAT J. & BERTHOU P. Y. 1974. — Le Cénomanien-Turonien de l'embouchure du Rio Mondego, Beira littoral, Portugal. *Communicaçoes dos Servicos geologicos de Portugal* **57** : 263-301.

LEFRANC J.-Ph. 1976. — État des connaissances actuelles sur les zonations biostratigraphiques du milieu du Crétacé (Albien à Turonien au Sahara. *Annales du Muséum d'Histoire naturelle de Nice* 4, **19** : 1-19.

— 1981. — Étude de *Neolobites vibrayeanus*, ammonite cénomanienne du Sahara algérien. *106ᵉ Congrès national des Sociétés savantes.* Perpignan : 155-166, 2 pls.

LEWY Z., KENNEDY W. J. & CHANCELLOR G. 1984. — Co-occurence of *Metoicoceras geslinianum* d'Orbigny, and *Vascoceras cauvini* Chudeau (Cretaceous Ammonoidea in the Southern Negev Israel and its stratigraphic implications. *Newsletters in Stratigraphy* **13** (2): 67-76, 4 figs, 1 pl.

LUGER P. & GRÖSCHKE M. 1989. — Late Cretaceous ammonites from the Wadi Qena area in the Egyptian eastern desert. *Palaeontology* **32**: 355-407, pls 38-49.

MANTELL G. A. 1822. — *The fossils of the South Downs; or illustrations of the geology of Sussex*, London, 327 p., 42 pl.

MEISTER C. 1989. — Les ammonites du Crétacé superieur d'Ashaka, Nigeria. *Bulletin Centres de Recherches Exploration Production Elf Aquitaine* **13**, 84 p., 28 pl.

MEISTER C., ALZOUMA K., LANG J. & MATHEY B. 1992. — Les ammonites du Niger (Afrique occidentale) et la transgression Transsaharienne au cours du Cénomanien-Turonien. *Geobios* **25** : 55-100, 11 pls.

MOREAU P., FRANCIS I. H. & KENNEDY W. J. 1983. — Cenomanian ammonites from Northern Aquitaine. *Cretaceous Research* **4**: 317-339.

NÉRAUDEAU D., BUSSON G. & CORNÉE A. 1993. — Les échinides du Cénomanien supérieur et du Turonien inférieur du Tinrhert oriental et central (Sahara algérien). *Annales de Paléontologie (Invertébrés)* **4** : 273-313.

ORBIGNY A. D' 1840-1842. — *Paléontologie française. Description des Mollusques rayonnés fossiles. Terrains Crétacés, 1 – Céphalopodes*, Masson, Paris, 662 p., 151 pls.

— 1850. — *Prodrome de Paléontologie stratigraphique universelle des animaux mollusques et rayonnés.* (2), Masson, Paris, 428 p.

PÉRON A. 1896-1897. — Les ammonites du Crétacé supérieur de l'Algérie. *Mémoire de la Société géologique de France, Paléontologie* **17**, 88 p., 18 pl.

— 1904. — *In* FOURTAU. Contribution à l'étude de la faune crétacique d'Égypte. *Bulletin de l'Institut égyptien* **4**, 255 p., pl. 1.

PERVINQUIÈRE L. 1907. — Études de paléontologie tunisienne. 1. Céphalopodes des terrains secondaires. *Carte géologique de la Tunisie*, 438 p., 27 pls.

POPOFF M., WIEDMANN J. & DE KLASZ I. 1986. — The Upper Cretaceous Gongila and Pindiga formations, Northern Nigeria : subdivisions, age, stratigraphic correlations and paleogeographic implications. *Eclogae geologica Helvetiae* **79** (2): 343-363.

POWELL J. D. 1963. — Cenomanian-Turonian (Cretaceous ammonites from Trans-Pecos Texas and North-Eastern Chihuahua, Mexico. *Journal of Paleontology* **37**: 309-322, pl. 31-34.

REYMENT R. A. 1954. — Some new Upper Cretaceous Ammonites from Nigeria. *Colonial Geological Mineral Resources* **4**: 149-164.

— 1955. — The Cretaceous Ammonoidea of Southern Nigeria and the Southern Cameroons. *Bulletin of Geological Survey of Nigeria* **25**, 112 p., 25 pls.

— 1978. — Analyse quantitative des Vascoceratidés à carènes. *Cahiers de Micropaléontologie* **4** : 57-64.

ROBASZYNSKI F., CARON M., DUPUIS C., AMÉDRO F., GONZALEZ DONOSO J. M., LINARES D. HARDENBOL J., GARTNER S., CALANDRA F. & DELOFFRE R. 1990. — A tentative integrated stratigraphy in the Turonian of Central Tunisia : formations, zones and sequential stratigraphy in the Kalaat Senan area. *Bulletin des Centres de Recherche Exploration, Production Elf-Aquitaine* **14** (1) : 213-384, 44 pls.

ROCHE J. 1880. — Sur la géologie du Sahara septentrional. *Comptes Rendus de l'Académie des Sciences, Paris* **91** : 890-893

ROMAN F. 1938. — *Les ammonites jurassiques et crétacées. Essai de genera.* Masson, Paris, 554 p., 53 pls.

RUMEAU J. L., DEBRENNE P. & DECREMPS P. 1957. — Mission BRP Tinrhert. Rapport de fin de campagne 1955-1956. *Publication Institut française du Pétrole*, réf. 1241, 33 p.

SCHNEEGANS D. 1943. — Invertébrés du Crétacé supérieur du Damergou (Territoire du Niger). *Bulletin de la Division des Mines d'Afrique occidentale française* 7 : 87-150, 8 pl.

SCHÖBEL J. 1975. — Ammoniten der Familie Vascoceratidae aus dem Unterturon des Damergou-Gebietes, République du Niger. *Publications from the Palaeontological Institution of the University of Uppsala* Special Volume 3, 136 p., 6 pls.

SHARPE D. 1853-1857. — Description of the fossil remains of Mollusca found in the Chalk of England. I., Cephalopoda. *Monograph of the Palaeontographical Society*, 68 p., 27 pls.

SPATH L. F. 1923. — On the ammonite horizons of the Gault and contiguous deposits. *Summary of Progress geological Survey of Great Britain*, London: 139-149.

— 1926. — On new ammonites from the English Chalk. *Geological Magazine* **63**: 77-83.

— 1931. — A monograph of the Ammonoidea of the Gault, Part 8. *Monograph of the Palaeontographical Society* **83**: 313-378, pl. 31-36.

STOLICZKA F. 1863-1866. — The fossil cephalopoda of the Cretaceous rocks of Southern India : Ammonitidae, with revision of the Nautilidae. *Memoir of the Geological Survey of India, Palaeontologica Indica*, 216 p., 94 pls.

THOMEL G. 1992. — *Ammonites du Cénomanien et du Turonien du Sud-Est de la France.* Serre. Nice, **2**, 381 p., 130 pls.

WOODS H. 1911. — The palaeontology of the Upper Cretaceous deposits of Northern Nigeria. *In* J. D. FALCONER (ed.). *The Geology and Geography of Northern Nigeria.* London: 273-286, pl. 19-24.

WRIGHT C. W. 1952. — A classification of the Cretaceous ammonites. *Journal of Paleontology* **26**: 213-222.

WRIGHT C. W. & KENNEDY W. J. 1980. — Origin, evolution and systematics of the dwarf acanthoceratid *Protacanthoceras* Spath. 1923 (Cretaceous Ammonoidea. *Bulletin of the British Museum (Natural History) Geology series* **34**: 65-107.

— 1981. — The Ammonoidea of the *Plenus* Marls and the Middle Chalk. *Monograph of the Palaeontographical Society*. 148 p., 32 pls.

— 1984-1990. — The Ammonoidea of the Lower Chalk (part. 1-3). *Monograph of the Palaeontographical Society*, 294 p., 86 pls.

ZABORSKI P. M. P. 1985. — Upper Cretaceous ammonites from the Calabar region, South-East Nigeria. *Bulletin of the British Museum (Natural History) Geology series* **39**, 72 p.

— 1990. — The Cenomanian and Turonian (mid-Cretaceous ammonite biostratigraphy of North-Eastern Nigeria. *Bulletin of the British Museum (Natural History) Geology series* **46**: 1-18.

— 1993. — Some new and rare Upper Cretaceous ammonites from North-Eastern Nigeria. *Journal of African Earth Sciences* **17** (3): 359-371.

— 1995. — The Upper Cretaceous ammonite *Pseudaspidoceras* Hyatt, 1903, in North-Eastern Nigeria. *Bulletin of the Natural History Museum London (Geology)* **51** (1): 53-72.

ZITTEL K. A. 1884. — *Handbuch der Palaeontologie, Cephalopoda.* Munich & Leipzig: 329-522.

ANNEXE 1. — Situation stratigraphique des principaux gisements fossilifères de la hamada de Tinrhert. Un certain nombre de gisements n'ont pas fourni d'ammonites décrites dans ce texte, mais leur examen a permis leur localisation stratigraphique. Il a paru important de les localiser dans cette annnexe car la plupart fournira la matière à l'étude d'autres taxons.

INTERVALLES (ammonites)						NOM	Localisation
1	2	3	4	5	6	DES	sur cartes
CENOMANIEN SUPÉRIEUR				TURON. INF.		GISEMENTS	et coupes
AC						Akba de Témassinine (ex. Fort-Flatters)	fig. 1c
			8T			Vallée de la route de Fort Saint	fig. 1d
	91					Akba de Témassinine	figs 1c et 2
93						Akba de Témassinine	figs 1c et 2
94						Akba de Témassinine	figs 1c et 2
		121				W. Balise 14	figs 1c et 2
					125	W. Balise 14	figs 1c et 2
		133				14 km N.N.W. Témassinine	figs 1c et 2
	137					14 km N.N.W. Témassinine	figs 1c et 2
			140			N. Akba de Témassinine	figs 1c et 2
143						N. Akba de Témassinine	figs 1c et 2
		145				N. Akba de Témassinine	figs 1c et 2
		146				N. Akba de Témassinine	figs 1c et 2
			147			N. Akba de Témassinine	figs 1c et 2
			150			W. Balise 14	figs 1c et 2
	155					W. Balise 14	figs 1c et 2
	265					Akba de Témassinine	figs 1c et 2
269						Akba de Témassinine	figs 1c et 2
270						15 km W. Balise d'Ohanet	fig. 1d
271						Berge de l'oued au puits d'Ohanet	fig. 1d
					279	Gara brune (flanc nord)	figs 1d et 3
				280		Gara brune (flanc nord)	figs 1d et 3
				281		Gara brune (flanc nord)	figs 1d et 3
			283			Gara brune (flanc nord)	figs 1d et 3
					285	Environs de Gara brune	figs 1d et 3
				286		Flanc W. Gara brune	figs 1d et 3
				287		N. de gara brune	figs 1d et 3
				291		Vallée route de Fort Saint. Flanc W.	fig. 1d
				298		Vallée route de Fort Saint. Flanc W.	fig. 3
			302			Vallée route de Fort Saint. Flanc W.	figs 1d et 3
				306		15 km N.W. de la Balise d'Ohanet	-
			309			Vallée route de Fort Saint. Rive nord	figs 1d et 3
			312			Vallée route de Fort Saint. Rive sud	fig. 1d
				314		Vallée route de Fort Saint. Rive sud	figs 1d et 3
				315		Nord de Gara brune	fig. 1d
				316		Nord de Gara brune	figs 1d et 3
					318	Nord de Gara brune	figs 1d et 3
				319		Nord de Gara brune	figs 1d et 3
320						4 km E.S.E. Akba d'Ohanet	fig. 1d
329						8 km S.E. Akba d'Ohanet	figs 1d et 3
330						8 km S.E. Akba d'Ohanet	figs 1d et 3
331						8 km S.E. Akba d'Ohanet	fig. 1d
	380					Est Akba Témassinine	figs 1c et 2
	382					Est Akba Témassinine	fig. 1c
	387					Est Akba Témassinine	fig. 1c
		388				Est Akba Témassinine	fig. 1c
		389				Est Akba Témassinine	fig. 1c
390						Est Akba Témassinine	figs 1c et 2
					393	Nord de Témassinine	figs 1c et 2
		455				Akba d'Amguid	-

INTERVALLES (ammonites)						NOM DES GISEMENTS	Localisation sur cartes et coupes
1	2	3	4	5	6		
CENOMANIEN SUPÉRIEUR				TURON. INF.			
					461	Gour Ben Houilet	figs 1a et 4
					467	Gour Ben Houilet	figs 1a et 4
					3015	Gour Ben Houilet	figs 1a et 4
			3800			Est de Gara brune	figs 1d et 3
				3802		Est de Gara brune	figs 1d et 3
				5277		Flanc W. de la vallée de Fort Saint	fig. 1d
				5278		Flanc W. de la vallée de Fort Saint	fig. 1d
				5279		Flanc W. de la vallée de Fort Saint	fig. 1d
				5280		Flanc W. de la vallée de Fort Saint	fig. 1d
				5281		Gara blanche d'In Adaoui	fig. 1d
				5282		Gara blanche d'In Adaoui	fig. 1d
				5283		Gara blanche d'In Adaoui	fig. 1d
				5285		Gara blanche d'In Adaoui	fig. 1d
				5286		Gara blanche d'In Adaoui	fig. 1d
				5299		Gara blanche d'In Adaoui	figs 1d et 3
				5300		Gara blanche d'In Adaoui	fig. 1d
				5301		Gara blanche d'In Adaoui	fig. 1d
				5303		Gara blanche d'In Adaoui	fig. 1d
				5304		Gara blanche d'In Adaoui	fig. 1d
				5305		Gara blanche d'In Adaoui	fig. 1d
				5306		Gara blanche d'In Adaoui	fig. 1d
					5312	Gara d'In Adaoui	fig. 1d
				5345		Gara brune	fig. 1d
					5346	Gara brune	figs 1d et 3
				5380		Est de Gara brune	fig. 1d
				5381		Route de Fort Saint	fig. 1d
				5382		Route de Fort Saint	fig. 1d
	5561					Coupe de l'Oued R'tem 8 km N.NW de Témassinine	figs 1c et 2
			5566			Coupe de l'Oued R'tem 8 km N.NW de Témassinine	figs 1c et 2
			5569			Coupe de l'Oued R'tem 8 km N.NW de Témassinine	fig. 1c
			5571			Coupe de l'Oued R'tem 8 km N.NW de Témassinine	fig. 1c
			5572			Coupe de l'Oued R'tem 8 km N.NW de Témassinine	fig. 1c
					5576	W. Balise 14	figs 1c et 2
					5577	W. Balise 14	figs 1c et 2
					5578	W. Balise 14	figs 1c et 2
			5580			14 km W.N.W. de Témassinine	-
				5581		14 km W.N.W. de Témassinine	fig. 2
					5597	Gour Ben Houilet	figs 1a et 4
					5598	Gour Ben Houilet	figs 1a et 4
5751						Chebkha Tinrhert (200 000ème Tilmas El Mra)	-
	5755					Chebkha Tinrhert (200 000ème Tilmas El Mra)	-
		5759				Chebkha Tinrhert (200 000ème Tilmas El Mra)	-
		5769				Chebkha Tinrhert (200 000ème Tilmas El Mra)	-
		5799				25 km W. Chebkha Tinrhert	-
			5800			25 km W. Chebkha Tinrhert	-
				5850		Sud Tin Bidder	-
			5851			Sud Tin Bidder	-

ANNEXE 2. — Liste des gisements d'ammonites cités dans le texte.

TÉMASSININE (FORT-FLATTERS)
Akba : 91, 93-94, 265, 269
Est Akba : 380, 382, 390
Nord Akba : 140, 143, 145, 146, 147, 5561, 5566
W. Balise 14 : 121, 125, 150, 155, 5576, 5577, 5578, 5581
sommet des Marnes médianes sur le log. synthétique : 393

OHANET
Gara brune : 279, 280, 281, 283, 286, 287, 3800, 3802, 5361
N. Gara brune : 316, 318, 319, 5346
Vallée Fort-Saint-Flanc W : 292, 293, 298, 302, 309, 314, 5299
Bord de la corniche cénomanienne : 329, 330

GOUR BEN HOUILET
461, 467, 5597, 5598.

Bulletin du Muséum national d'Histoire naturelle, Paris, 4[e] sér., **18**, 1996
Section C, n[os] 2-3 : 233-347

The phylogeny of the Antiarcha (Placodermi, Pisces), with the description of Early Devonian antiarchs from Qujing, Yunnan, China

by Min ZHU

Abstract. — Five new antiarchs (*Yunnanolepis porifera* n. sp., *Mizia longhuaensis* n. gen., n. sp., *Phymolepis guoruii* n. sp., *Chuchinolepis robusta* n. sp. and *C. sulcata* n. sp.) are described on the basis of the new material from the Early Devonian of Qujing, Yunnan Province, south-western China. *Y. chii* is reexamined to show the CHANG's apparatus and lateroventral fossa of the trunk-shield. New material of Qujing comprises also *Heteroyunnanolepis qujingensis*, *Y.* sp. from the Xitun Formation, *P. cuifengshanensis* and *Zhanjilepis aspratilis* from the Xishancun Formation, *C. gracilis* and *C. qujingensis* from the Xishancun and Xitun Formations, and an unnamed antiarch from the Xitun Formation. It is proposed that *Procondylolepis*, as well as *Qujinolepis*, is the junior synonym of *Chuchinolepis*. The pectoral fin articulation of the Chuchinolepididae is argued to have only one dermal joint. It is suggested that the pectoral fin of the Chuchinolepididae is laterally compressed and that the fossa on the parabrachial process is the attachment area for the abductor muscle of the fin. A cladistic analysis of antiarchs is presented. Thirty two equally parsimonious trees are found, and a strict consensus tree is constructed. The monophyly of the Yunnanolepidoidei is corroborated in the cladogram, with an emended definition of the group. The Chuchinolepididae, *Vanchienolepis*, and an unnamed antiarch are included in the Yunnanolepidoidei. *Minicrania* (ZHU & JANVIER 1996) is the sister-group of the antiarchs possessing the brachial process and funnel pit. The Bothriolepidoidei, as previously defined, turn out to be a paraphyletic group. The Microbrachiidae are at the base of the Euantiarcha. *Nawagiaspis* is assumed to be the nearest sister-group of the Asterolepidoidei, and *Hunanolepis* is placed at the base of the Asterolepidoidei.

Key-words. — Antiarcha, Early Devonian, morphology, phylogeny, China.

Phylogénie des Antiarches (Placodermi, Pisces) et description d'antiarches du Dévonien inférieur de Qujing, Yunnan, Chine

Résumé. — Cinq nouveaux antiarches (*Yunnanolepis porifera* n. sp., *Mizia longhuaensis* n. gen., n. sp., *Phymolepis guoruii* n.sp., *Chuchinolepis robusta* n. sp. et *C. sulcata* n. sp.) sont décrits sur la base de nouveau matériel du Dévonien inférieur de Qujing (province de Yunnan), dans le sud-ouest de la Chine. *Y. chii* est réétudié, afin de montrer l'appareil de CHANG et la fosse ventrolatérale de la cuirasse thoracique. Le nouveau matériel comprend aussi *Heteroyunnanolepis qujingensis* et *Y.* sp. de la Formation de Xitun, *P. cuifengshanensis* et *Zhanjilepis aspratilis* de la Formation de Xishancun, *C. gracilis* et *C. qujingensis* des Formations de Xishancun et Xitun, et un antiarche non nommé de la Formation de Xitun. Il est proposé que *Procondylolepis*, ainsi que *Qujinolepis*, est le synonyme plus récent de *Chuchinolepis*. L'articulation de la nageoire pectorale des Chuchinolepididae est considérée comme n'ayant qu'une seule articulation dermique. Il est suggéré que la nageoire pectorale des Chuchinolepididae est comprimée latéralement et que la fosse sur le processus parabrachial sert à l'insertion du muscle abducteur de nageoire. Une analyse cladistique des antiarches est proposée. Trente-deux arbres également parsimonieux sont obtenus, et un arbre de strict consensus est construit. La monophylie des Yunnanolepidoidei est confirmée dans le cladogramme, avec une définition émendée. Les Chuchinolepididae, *Vanchienolepis* et un antiarche non nommé sont inclus dans les Yunnanolepidoidei. *Minicrania* (ZHU & JANVIER 1996) est le groupe-frère des antiarches possédant un processus brachial pourvu d'un canal en entonnoir. Les Bothriolepidoidei définis auparavant se trouvent être un groupe paraphylétique. Les Microbrachiidae sont à la racine des Euantiarcha. *Nawagiaspis* est supposé être le groupe-frère le plus proche des Asterolepidoidei, et *Hunanolepis* est placé à la racine des Asterolepidoidei.

Mots-clés. — Antiarcha, Dévonien inférieur, morphologie, phylogénie, Chine.

M. ZHU, *Institute of Vertebrate Paleontology and Paleoanthropology, Chinese Academy of Sciences, P.O. Box 643, Beijing 100044, China.*

ABBREVIATIONS

a anterior angle of AMD plate
aa anterior angle of PMD plate
adg anterodorsal sensory-line groove of trunk-shield
ADL anterior dorsolateral plate
AL anterior lateral plate
alr postlevator thickening of AMD plate
AMD anterior median dorsal plate
ar3v external articular area of Cv1 plate
art.v ventral articular depression for dermal process of pectoral fin
AVL anterior ventrolateral plate
c1 corner between anterior and middle divisions of mesial margin of ventral lamina of AVL plate.
C.Chang cavity of CHANG's apparatus
c.al anterolateral corner of subcephalic division of ventral lamina of AVL plate
Ca.o opening of CHANG's apparatus
Cd1-4 dorsal central plate 1-4
cf.ADL area overlapping ADL plate
cf.AMD area overlapping AMD plate
cf.AVL area overlapping AVL plate
cf.MV area overlapping MV plate
cf.PDL area overlapping PDL plate
cf.PVL area overlapping PVL plate
cf.PL area overlapping PL plate
cit *crista transversalis interna anterior*
cr.tp *crista transversalis interna posterior*
Cv1-4 ventral central plate 1-4
d dorsal corner of PDL plate
dlg posterior oblique dorsal sensory-line groove
dlm dorsal lamina of ADL and PDL plates
dlr dorsolateral ridge of trunk-shield
dma tergal angle of trunk-shield
dm,ppbr dorsal margin of parabrachial process
dmr median dorsal ridge of trunk-shield
f.ab fossa of AVL plate for abductor muscle of fin
f,ad fossa of AVL plate for adductor muscle of fin
f.art articular fossa of ADL plate
fe.orb orbital fenestra
f.lv lateroventral fossa of trunk-shield
f.pec pectoral fenestra
f.retr levator fossa of AMD plate
g.Chang groove of trunk-shield caused by CHANG's apparatus
gpbr parabrachial groove
grm median ventral groove of dorsal wall of trunk-shield
L lateral plate
l.Chang inner lamina of CHANG's apparatus
lc lateral corner of AMD plate
lcg main lateral-line groove
llm lateral lamina of ADL, AVL, PDL and PVL plates
l.pbr postbranchial lamina or ridge
Ml2-4 lateral marginal late 2-4
Mm1-4 mesial marginal plate 1-4
MV median ventral plate
mvr median ventral ridge of dorsal wall of trunk-shield
m.SL margin of AVL plate in contact with SL plate
mx sedimentary matrix of fossil
MxL mixilateral plate
Nu nuchal plate
n node formed by tubercles
oa.ADL area overlapped by ADL plate
oa,AMD area overlapped by AMD plate
oa.PDL area overlapped by PDL plate
oa.PL area overlapped by PL plate
oa,PMD area overlapped by PMD plate
oa,PVL area overlapped by PVL plate
pa posterior angle of PMD plate
p.AL process of AL plate
pda posterior dorsal angle of trunk-shield
pdg posterodorsal sensory-line groove of trunk-shield
PDL posterior dorsolateral plate
PL posterior lateral plate
plc posterolateral corner of PMD plate
plg posterolateral groove of trunk-shield
plr posterolateral ridge of trunk-shield
PM postmarginal plate
pma posterior marginal area of PMD plate
PMD posterior median dorsal plate
PNu paranuchal plate
Pp postpineal plate
p.PMD pit on external surface of PMD plate
ppbr parabrachial process
prc prepectoral corner
pr.p posterior process of PMD plate
prv1 anterior ventral process of dorsal wall of trunk-shield
prv2 posterior ventral process of dorsal wall of trunk-shield
pt1 anterior ventral pit of dorsal wall of trunk-shield
pt2 posterior ventral pit of dorsal wall of trunk-shield
PVL posterior ventrolateral plate
r.Chang ridge caused by CHANG's apparatus
r.ibr infrabrachial ridge
r.obl oblique ridge on dorsal wall of trunk-shield
r.semi semicircular ridge of skull-roof
scap scapulocoracoid
SL semilunar plate
Sp spinal plate
vlm ventral lamina of AVL and PVL plates
vlr ventrolateral ridge of trunk-shield
vm.ppbr ventral margin of parabrachial process

INTRODUCTION

The Paleozoic early vertebrates of China were first reported from Panxi (Po-Si), Huaning County, Yunnan by MANSUY (1907). However, the remains (an "ichthyodorulite") were impossible to be identified by MANSUY and no further description or photo was given. From the same locality, three brachythoracid arthrodires and some acanthodian spines were collected later from the Middle Devonian deposits (J.-Q. WANG 1979, 1982, 1991c). The first figured early vertebrate from China (MANSUY 1912) was an antiarch from near Xundian, north-east of Kunming (Yun-Nan-Fou), the capital of Yunnan Province. MANSUY assigned this fossil (part of a trunk-shield) to a placoderm similar to *Bothriolepis*, but he referred it to the "Silurian" (in the sense of this time, that is, including most of the Lower Devonian). According to the photograph, the only information we have about this specimen, MANSUY 's fossil is possibly to be referred to as *Dianolepis*, which has later been found in the same region. If it is true, the age of this antiarch should be Middle Devonian. This began the discoveries of antiarchs in China.

The forerunner of antiarch research in China is Y.-S. CHI (1940), who described a species of *Bothriolepis* (*B. sinensis*), from the Middle Devonian of Chansha, Hunan. Later, CHI (1942) and H.-C. WANG (1942) reported the occurrence of *Bothriolepis* from the Devonian of Yunnan, and PIEN (1948) noted the finding of *Bothriolepis* in Guangdong. By this time, all antiarchs found in China were euantiarchs, no older than Middle Devonian in age ; that, is consistent with the age of antiarchs in Europe, North America and Australia.

The subsequent studies of Chinese antiarchs are related to the discoveries of new antiarch groups, which have a major significance in the understanding of antiarch evolution and biogeography. Moreover, the antiarchs found in China have extended the history of the group back to Early Silurian (J.-Q. WANG 1991b), since before 1963, when *Yunnanolepis* was formally described by Y.-H. LIU, antiarchs were restricted to Middle and Late Devonian. The exception is the remains described by MANSUY (1915) in North Vietnam, near the frontier between China and Vietnam. These fossils, originally referred to as an ostracoderm, ?*Homostius* and *Asterolepis*, turned out to be yunnanolepidoids or galeaspids (TONG-DZUY & JANVIER 1987), which are the major components of the highly endemic Early Devonian fish fauna in South China and North Vietnam.

The first new antiarch group found in China is the Sinolepididae (LIU & P'AN 1958). *Sinolepis*, the type genus of the family, was discovered in the Upper Devonian Wutung Series near Nanjing, in association with a bothriolepidoid *Jiangxilepis sinensis* (LIU & P'AN 1958; P'AN 1964; ZHANG & LIU 1991) which was originally referred to as *Asterolepis*. *Sinolepis* is the first indication of the highly endemic feature of the early vertebrate fauna in the Silurian and Devonian of China (including South China, Tarim and Ningxia) and Vietnam. The further research on the Sinolepididae (RITCHIE *et al.* 1992), which are now known to be unique to China and Australia, indicates a close paleogeographic affinity between these two regions, and shows that the Sinolepididae are the closest relatives of the Euantiarcha.

The second new group is the Yunnanolepidoidei (Y.-H. LIU 1963; GROSS 1965; MILES 1968; G.-R. ZHANG 1978; M.-M. ZHANG 1980), exemplified by the Yunnanolepididae. The Yunnanolepididae is a distinctive element of the Early Devonian endemic vertebrate fauna of South China and North Vietnam, and was assumed to be the most primitive antiarch group because of its plesiomorphies shared with other placoderms, and thus having bearings on the problems

of antiarch relationships and interrelationships. The yunnanolepidoid *Shimenaspis* (J.-Q. WANG 1991b) found in the Early Silurian (Llandovery) of Lixian, Hunan (Fig. 2) is the earliest placoderm record. However, since the Yunnanolepidoidei, as previously defined, was mainly based on symplesiomorphies, its monophyly had been doubted (JANVIER & P'AN 1982), and the suborder was generally referred to as the stemgroup of antiarchs. The relationships among the various genera of the Yunnanolepidoidei are still vague. Therefore, a further study and strict definition of the Yunnanolepidoidei is essential to research on antiarch evolution.

The third new group is the Chuchinolepididae (G.-R. ZHANG 1984; YOUNG & ZHANG 1992), which is characterized by its peculiar pectoral fin articulation. This group was found in the Early Devonian of Yunnan and Guangxi, China, and was discovered later in the Early Devonian of North Vietnam (TONG-DZUY & JANVIER 1990). G.-R. ZHANG (1984) and YOUNG & ZHANG (1992) proposed a hypothesis where the Chuchinolepididae are intermediate between the Yunnanolepidoidei and the other advanced antiarchs (the Sinolepididae and Euantiarcha), as to the pectoral fin articulation. In contrast, ZHU & JANVIER (1996) suggest that the Chuchinolepididae and the Sinolepididae + Euantiarcha represent two distinct evolutionary paths towards the formation of the pectoral fin articulation.

These discoveries have established the Chinese antiarchs, especially those from the Early Devonian, as being of crucial importance in the understanding of antiarch evolution. The first aim of this work is to describe new antiarch material from the Early Devonian of Qujing (Yunnan, China), and clarify certain aspects of yunnanolepidoid comparative morphology. The second aim is to discuss the structure of the pectoral fin articulation of the Chuchinolepididae, which has been an interesting subject as to its origin and fate. A new hypothesis about the placement of the pectoral fin in this bizarre fish is proposed, and contrasts with those of G.-R. ZHANG (1984) and YOUNG & ZHANG (1992). The third aim of this work is to explore the phylogeny of antiarchs in the light of character analysis. Since the Chinese antiarchs were taken into consideration, the phylogeny of antiarchs has been discussed in depth, in the framework of either Cladistics or Evolutionary Systematics (JANVIER & PAN 1982; G.-R. ZHANG 1984; YOUNG 1984c, 1988; PAN *et al.* 1987; YOUNG & ZHANG 1992; RITCHIE *et al.* 1992; ZHU & JANVIER 1996). With the aid of the information provided by the Yunnanolepidoidei, the phylogeny of the Sinolepididae and Euantiarcha is now better corroborated (RITCHIE *et al.* 1992), even though *Yunnanolepis* as the root of the antiarch cladogram sometimes biases the determination of character polarity. In fact, *Yunnanolepis* is a relatively derived antiarch (ZHU & JANVIER 1996). However, turning to the early evolution of antiarchs, the scheme becomes more or less obscure, and this ambiguity affects the understanding of the phylogeny of the advanced antiarchs. The obstacle is the deficiency of the character analysis on the Yunnanolepidoidei, including the Chuchinolepididae, and the fact that the relationships among the various primitive genera are unavailable by now. Moreover, the previous cladograms of antiarchs, except that of bothriolepidoids (ZHANG & YOUNG 1992), were somewhat empirical, and were not strictly based on the principle of parsimony. In addition, the cladogram of bothriolepidoids included the assumption of their monophyly, which will be refuted below. The phylogenetic analysis in this work includes all well-understood antiarch taxa, and is achieved using Hennig 86 (FARRIS 1988).

REVIEW OF THE EARLY DEVONIAN ANTIARCHS FROM CHINA

Eleven localities yielding Early Devonian antiarchs in China are reviewed below (Fig. 1).

1) The first Early Devonian antiarch described in China is *Yunnanolepis chii* (Y.-H. LIU 1963), which was represented by a skull-roof in visceral view, and was found in the Xishancun Formation (Y.-H. LIU pers. comm.) of the Cuifengshan Group of Qujing, Yunnan. This antiarch was originally regarded as belonging to the Pterichthyodidae (=the Asterolepidoidei), and was later placed in the Bothriolepididae by GROSS (1965). At the Paris meeting on vertebrate paleontology (1966), M.-M. CHANG reported on the research advances on the Early Devonian antiarchs of Qujing, and indicated that the Yunnanolepididae are very primitive in some features of the trunk-shield. Since a close relationship to the Bothriolepidoidei was unlikely, MILES (1968) erected a new suborder Yunnanolepidoidei, of equal rank to the Bothriolepidoidei.

Detailed descriptions of the Early Devonian antiarchs from Qujing, Yunnan (mainly from the Xitun Formation of the Cuifengshan Group) have not been published until 1978. The works of K.-J. CHANG (1978), P'AN & WANG (1978), G.-R. ZHANG (1978, 1979) and M.-M. ZHANG (1980) showed that the pectoral fin and fin articulation of the Yunnanolepididae fill the mor-

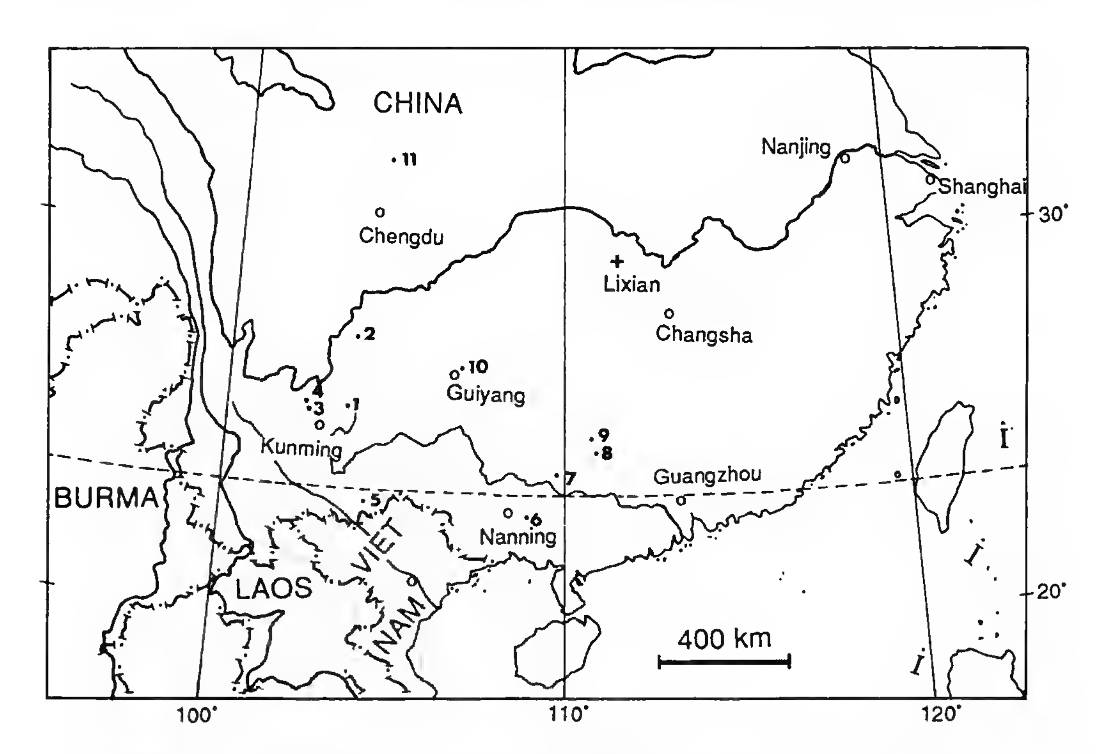


FIG. 1. — Sketch map showing the localities of Early Devonian antiarchs in China. 1. Qujing, Yunnan; 2. Zhaotong, Yunnan; 3. Wuding, Yunnan; 4. Luquan, Yunnan; 5. Wenshan, Yunnan; 6. Liujing, Hengxian, Guangxi; 7. Dale, Xiangzhou, Guangxi; 8. Pingle, Guangxi; 9. Xindu, Hexian, Guangxi; 10. Wudang, Guiyang, Guizhou; 11. Longmenshan, Sichuan.

phological gap between euantiarchs and other placoderms. YOUNG (1984c) stated that the Early Devonian antiarchs of South China play a very important role in the discussion of the antiarch phylogeny and paleobiogeography. G.-R. ZHANG (1984) described an antiarch, *Procondylolepis*, from the Xitun Formation of Qujing, which bears a more derived pectoral fin articulation than the Yunnanolepididae. The taxon Procondylolepiformes was erected to distinguish it from the Yunnanolepiformes. It is shown below that, *Procondylolepis*, as well as *Qujinolepis*, is the junior synonym of *Chuchinolepis*.

JANVIER (1995) described two antiarchs, referred to as sinolepids, from the Xitun Formation of Qujing which were collected during the field trip of the Early Vertebrate Symposium held in Beijing (1987). These two antiarchs bear the large rectangular fenestra in the ventral wall of the trunk-shield, like the Sinolepididae, however, their pectoral fin articulations are most suggestive of that of the Yunnanolepididae.

The Early Devonian antiarchs of Qujing are best preserved in the Xitun Formation of the Cuifengshan Group, but ZHU *et al.* (1994) pointed out that the antiarchs were also abundant in the other three formations of the group (Xishancun, Guijiatun and Xujiachong Formations), and recorded *Y. chii* and *Chuchinolepis (Procondylolepis) qujingensis* from the Guijiatun Formation. Z.-S. WANG (1994) described *Heteroyunnanolepis qujingensis* from the Xishancun Formation. *Minicrania lirouyii* (ZHU & JANVIER 1996), a very tiny yunnanolepidoid-like antiarch, is also found in this formation.

It is suggested by ZHU & WANG (in press) that the Chuandong Formation of Qujing is mainly of Emsian in age, and *Wudinolepis* has never been reported in this horizon.

2) From the Pusongchong Formation of Zhaotong, Yunnan, were described galeaspids (Y.-H. LIU 1973; PAN & WANG 1981; WANG & ZHU 1994) and an onychodontiform (ZHU & JANVIER 1994). A yunnanolepidoid-like trunk-shield with pectoral fins attached, as well as a porolepiform and a possible petalichthyid, was discovered in 1991 and is under study (WANG *et al.* in prep.).

3) It is argued that the Jiucheng Formation of Wuding, Yunnan, is of Emsian age (WANG & ZHU 1995). *Wudinolepis* (K.-J. CHANG 1965), in addition to abundant arthrodires (LIU & WANG 1981; WANG & WANG 1983, 1984), has been described from this formation. More antiarchs, including two new forms, have been collected during the past years (S.-F. LIU in prep.).

4) An Early Devonian euantiarch *Luquanolepis* was described from Luquan, Yunnan (ZHANG & YOUNG 1992). In 1991, *Wudinolepis* was also found in the same locality, and it is not yet clear whether it is from the same horizon as *Luquanolepis*.

5) Many Early Devonian antiarchs have been collected from the Pusongchong Formation of Wenshan, Yunnan (J.-Q. WANG pers. comm.). These specimens have not been described.

6) P'AN (1973) described an Early Devonian antiarch, *Kwangsilepis kwangsiensis*, from the Lianhuashan Formation of Liujing, Hengxian, Guangxi. This was the first report of Early Devonian antiarchs from the Guangxi Province. The referred material included an internal mould and several detached plates of the trunk-shield, which probably belong to *Yunnanolepis chii* (S.-F. LIU 1992). S.-F. LIU (1974) reported *Yunnanolepis* sp. from the Lianhuashan Formation of Liujing, and compared the Lianhuashan Formation to the Xitun Formation of Qujing, Yunnan. In 1978, P'AN & WANG described two new antiarchs (*Orientolepis neokwangsiensis* and *Lianhuashanolepis liukiangensis*) from the same horizon and locality. G.-R. ZHANG (1979) and

S.-F. LIU (1992) later pointed out that *Lianhuashanolepis* was a junior synonym of *Yunnanolepis*, whereas *Orientolepis* was the junior synonym of *Chuchinolepis*. S.-F. LIU (1992) described and reviewed the antiarchs from the Lianhuashan Formation of Liujing, *i.e. Y. chii*, *C. gracilis* and *Zhanjilepis* sp., as in the Xitun Formation of Qujing, Yunnan.

7) S.-T. WANG (1987) described an antiarch, *Liujiangolepis suni*, from Dale, Xiangzhou, Guangxi. The fish-bearing horizon is referred to as the "Nagaoling Formation" (also the Xiaoshan Sandstone) of Late Gedinnian or Early Siegenian age by S.-T. WANG (1987), and is about 100 meters below the Tonggeng Formation, which roughly corresponds to the Pojiao Formation with its typical "*Euryspirifer tonkinensis-Dicoelostrophia punctata*" fauna. This fish-bearing bed is also incorporated into the Dayaoshan Group (HOU *et al.* 1988b). *Liujiangolepis* turns out to be a sinolepid (RITCHIE *et al.* 1992 : 362), although it shows many similarities with the Yunnanolepidoidei (S.-T. WANG 1987).

8) S.-T. WANG *in* RITCHIE *et al.* (1992) described another sinolepid, *Dayaoshania youngi*, from Pingle, Guangxi. The horizon is the upper part of the Dayaoshan Group, for which RITCHIE *et al.* (1992) provisionally proposed an Emsian-Eifelian age. However, by comparison to the horizon of *Liujiangolepis* from the neighbouring region, which is also at the top of the Dayaoshan Group, it is reasonable to assume the age of *Dayaoshania* is no younger than the Emsian.

9) P'AN *in* P'AN & WANG (1978) described *Hohsienolepis hsintuensis* from Xindu, Hexian, Guangxi. The horizon was referred to as the Xindu Formation, of Middle Devonian age (P'AN & WANG 1978, 331; also see P'AN 1981; PAN & DINELEY 1988). In the same volume, P'AN *et al.* (1978, 250) assigned the fish-bearing horizon to the "Yujiang Formation", of Early Devonian age. Even though their "Yujiang Formation" is not the exactly like the type Yujiang Formation and may include part of Middle Devonian sediments, the age of *Hohsienolepis* is definitely no younger than the Emsian, since it occurs at the bottom of the "Yujiang Formation" which overlies directly the Nagaoling Formation.

10) P'AN *et al.* (1978) reported Early Devonian antiarchs from the Wudang Formation of Guiyang, Guizhou Province, which are very suggestive of *Yunnanolepis*. Associated are the galeaspid *Neoduyunaspis minuta*, the arthrodire *Kueichowlepis sinensis* and the petalichthyid *Sinopetalichthys kueiyangensis* (P'AN *et al.* 1975; P'AN & WANG 1978).

11) The Early Devonian vertebrates from the Pingyipu Formation of Longmenshan, Sichuan, were first reported by Y.-H. LIU (1973), including the galeaspid *Sanqiaspis rostrata* and the petalichthyid *Neopetalichthys yenmenpaensis*. P'AN *et al.* (1975) and P'AN & WANG (1978) described two other galeaspids (*Lungmenshanaspis kiangyouensis* and *Sinoszechuanaspis yanmenpaensis*) and a petalichthyid *Xinanpetalichthys shendaowanensis*. P'AN *et al.* (1978 : 246) reported on the detached plates of antiarchs found in the same horizon. The formal description of the antiarchs from the Early Devonian of Longmenshan has been made by S.-T. WANG *in* HOU *et al.* (1988a), who described two antiarch genera (*Chuanbeiolepis* and *Yunlongolepis*). Comments on these two genera will be made below.

MATERIAL AND METHODS

As generally acknowledged, the Early Devonian deposits of Qujing (Yunnan, China, Fig. 2) are referred to as the Cuifengshan Group and can be subdivided into the Xishancun, Xitun, Guijiatun and Xujiachong Formations, in ascending order (ZHU *et al.* 1994; Fig. 2C). ZHU (in prep.) argued that the overlying Chuandong Formation is mainly Emsian (Fig. 2C), instead of Middle Devonian. All the material used in the preparation of this work comes from the Cuifengshan Group of Qujing, mainly the Xishancun and Xitun Formations, and is housed in the Institute of Vertebrate Paleontology and Paleoanthropology, Chinese Academy of Sciences, Beijing. Some specimens of the Xitun Formation were collected by Prof. M.-M. CHANG, whose contributions to this work are acknowledged.

The specimens have been prepared by the standard mechanical methods. In some cases, the acetic acid technique has been used on specimens from the Xitun Formation. The material from the Xishancun Formation was preserved as internal and/or external moulds, and elastomer casts were made after the mechanical preparation.

The line drawings in the text were made by means of the camera-lucida. The abbreviations used in the figures and text are mainly after the works of MILES (1968) and YOUNG (1988).

TERMINOLOGY

The placoderm classification of DENISON (1978) is used here, *i.e.* the Antiarcha is ranked as one of the orders of the class Placodermi.

As to the classification of the Antiarcha, the works of MILES (1968), YOUNG (1984c, 1988) and RITCHIE *et al* (1992) have been used as a reference, and the major subgroups are ranked as suborders. The monophyly of the suborder Bothriolepidoidei *sensu* ZHANG & YOUNG (1992) was provisionally acknowledged before the phylogenetic analysis of antiarchs in this paper. The Microbrachiidae and Bothriolepididae are two widely recognized families of the Bothriolepidoidei. The family Asterolepididae is a representative of the suborder Asterolepidoidei. The Sinolepididae (MILES 1968) is a justified emendation of the Sinolepidae (LIU & P'AN 1958; RITCHIE *et al.* 1992) which is an incorrect original spelling in accordance with the International Code of Zoological nomenclature (RIDE *et al.* 1985, Art. 29A, Art. 32c-d, Art. 33b). However, according to the Code (Art. 11f, Art. 33b), the name thus corrected retains the author and date of the original spelling (Sinolepididae LIU et P'AN 1958).

Since the Antiarcha is ranked as an order, the order Yunnanolepiformes (a subgroup of the Antiarcha), commonly used in the recent literature, is replaced here by the suborder Yunnanolepidoidei Miles, 1968. In this work, the Yunnanolepidoidei comprise the Yunnanolepididae, Chuchinolepididae, and related forms. The Yunnanolepididae takes the authorship and date of GROSS 1965. According to the Code (RIDE *et al.* 1985, Art. 50c), the change in the rank of a taxon within the family group (subfamily and family) does not affect the authorship of the name of the taxon. In the same way, the Chuchinolepididae is attributed to K.-J. CHANG 1978.

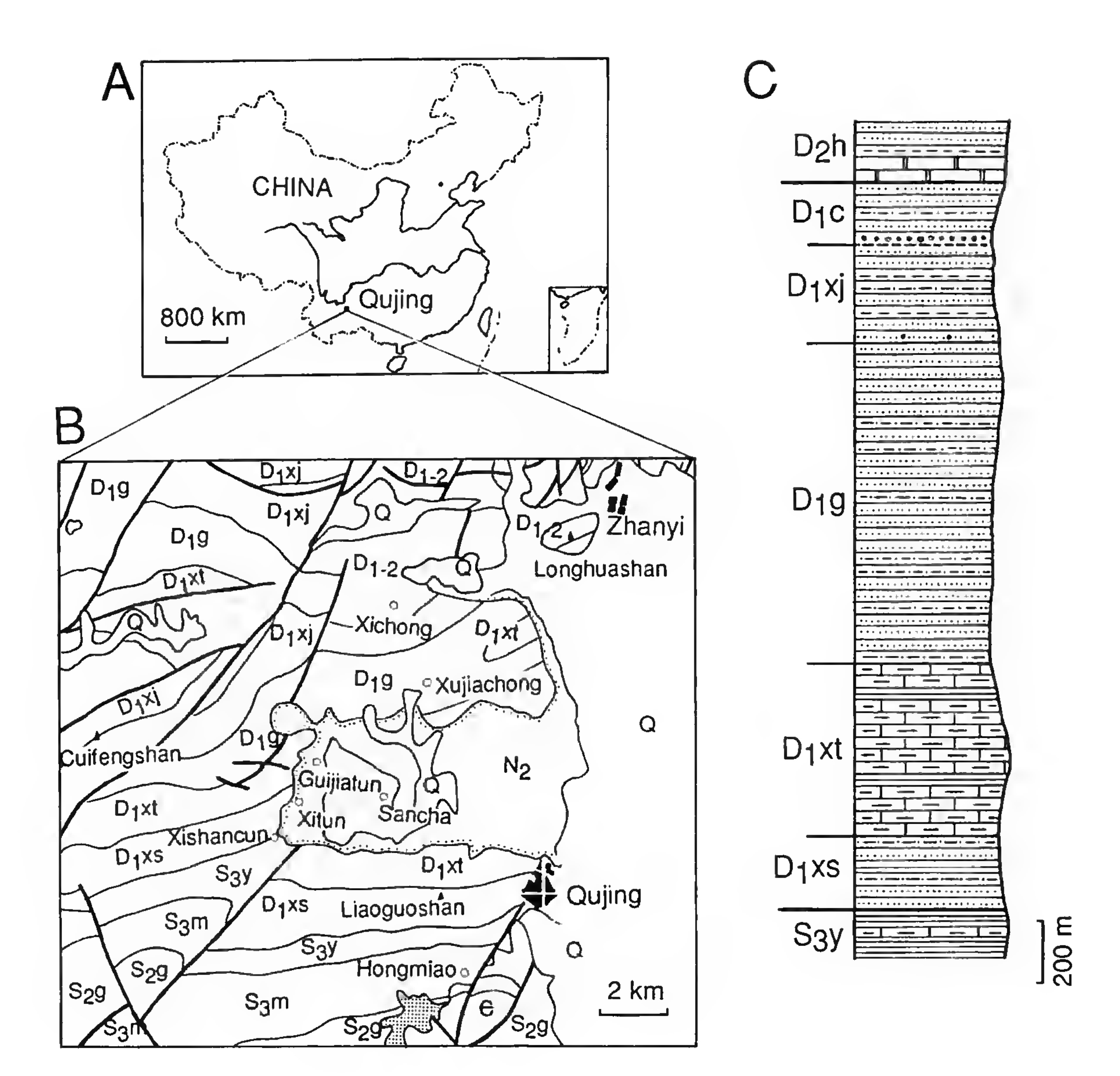


FIG. 2. — A, sketch map of China, showing the position of Qujing, where the material under study was collected; B, geological sketch map of the Qujing area in south-eastern Yunnan (modified from FANG *et al.* 1985, fig. 1); C, synthetic log of the Early Devonian in Qujing, Yunnan, China. S_2g – Guandi Formation, S_3m – Miaogao Formation, S_3y – Yulongsi Formation, D_1xs – Xishancun Formation, D_1xt – Xitun Formation, D_1g – Guijiatun Formation, D_1xj – Xujiachong Formation, D_1c – Chuandong Formation, D_2h – Haikou Formation, D_{1-2} – Chuandong and Haikou Formations.

As to the terminology for morphological characters, STENSIÖ's (1948) nomenclature, as modified by MILES (1968) and YOUNG (1988), is adopted here with minor changes. The terminology of the dermal plates of the pectoral fin in the Chuchinolepididae is discussed below.

SYSTEMATIC DESCRIPTIONS

Class PLACODERMI M'Coy, 1848
Order ANTIARCHA Cope, 1885
Suborder YUNNANOLEPIDOIDEI Miles, 1968

EMENDED DEFINITION. — Antiarcha in which the skull-roof is broad and short, with a broad lateral plate; anterior margin of the AMD plate pointed.

REMARKS. — Since the characters such as the absence of the brachial process, the large preorbital depression, are plesiomorphic for antiarchs, they are not included in the diagnosis of the suborder. These symplesiomorphies are also present in *Minicrania* (ZHU & JANVIER 1996). None of the characters in this definition are unique to this taxon. All appear at various levels of the Euantiarcha, as homoplasies.

Family YUNNANOLEPIDIDAE Gross, 1965

EMENDED DIAGNOSIS. — Yunnanolepidoidei in which the *crista transversalis interna posterior* turns forward on the visceral surface of the PMD plate, and lies in front of the posterior ventral process and pit.

TYPE GENUS *Yunnanolepis* Y.-H. Liu, 1963

REFERRED GENERA. — *Phymolepis* G.-R. Zhang, 1978; *Mizia* n. gen.

REMARKS. — Many diagnostic characters of the Yunnanolepididae (K.-J. CHANG 1978; G.-R. ZHANG 1978) turn out to be the symplesiomorphies, such as the preorbital depression, and the large postpineal plate which excludes the nuchal plate from the orbital fenestra. Therefore, a more restricted diagnosis based on unique characters is given here.

The *crista transversalis interna posterior* of antiarchs would be homologous to the transverse ventral crest of the median dorsal plate of other placoderms, if we accept Y.-H LIU's suggestion (1991) that the PMD plate of antiarchs is homologous to the median dorsal plate of other placoderms. In outgroups of antiarchs, *e.g.*, arthrodires and petalichthyids, the transverse ventral crest generally lies lateral to the median ventral process, which could be assigned to the plesiomorphic state for antiarchs. Among antiarchs, this ancestral state is seen in *Zhanjilepis* (G.-R. ZHANG 1978), *Minicrania* (ZHU & JANVIER 1996), and *Chuchinolepis*. In the Sinolepididae, exemplified by *Grenfellaspis* and *Xichonolepis* (G.-R. ZHANG 1980; RITCHIE *et al.* 1992), the *crista transversalis interna posterior* lies slightly in front of the posterior ventral process. However, the condition in the Sinolepididae is different from that in the Yunnanolepididae. The *crista transversalis interna posterior* in the Sinolepididae runs dorsally without a twist and has the same path as that in *Zhanjilepis*, *Minicrania* and *Chuchinolepis*, whereas that in the Yunnanolepididae turns forward on the visceral surface of the PMD plate.

In the Yunnanolepidoïdei, the lateroventral fossa on the visceral surface of the trunk-shield is found to lie at the junction of three plates (the AVL, PL and PVL plates). The portions of the trunk-shield which encircle the fossa are thickened, implying the attachment of some muscles in the fossa. This depression was mentioned by G.-R. ZHANG (1978) in the AVL plate of *Y. chii*. Since then, it had been overlooked until TONG-DZUY & JANVIER (1990) described the so-called "lateral thoracic recess" in the internal trunk-shield mould of *Yunnanolepis* cf. *Y. parvus*. However, this fossa is also found in *Zhanjilepis*. The Yunnanolepidoidei *Heteroyunnanolepis* lacks this unique structure.

Genus **YUNNANOLEPIS** Y.-H. Liu, 1963

Yunnanolepis Y.-H. Liu, 1963: 39, fig. 1, pl. I.

Synonyms:
Eoantiarchilepis P'an & Wang. 1978: 319, fig. 10, pl. 31.1-2.
Tsuifengshanolepis P'an & Wang, 1978: 320, pl. 30.2.
Lianhuashanolepis P'an & Wang, 1978: 323, pl. 32.1-5.

Others references:
Yunnanolepis K.-J. CHANG 1978: 293, pl. 25.1-4. — G.-R. ZHANG 1978: 148, figs 1-7, pls I-IV, V.3-6. — TONG-DZUY & JANVIER 1990: 159, pls II-IV. – S.F. LIU 1992: 212, pl. I. — ZHU, WANG & FAN 1994: 3, pl. I.1-3.

EMENDED DIAGNOSIS. — Yunnanolepididae in which the opening of the CHANG's apparatus is visible in lateral aspect.

TYPE SPECIES. — *Yunnanolepis chii* Y.-H. Liu, 1963.

REMARKS. — The opening of the CHANG's apparatus (a name erected here after Prof. M.-M. CHANG) was first figured by M.-M. ZHANG (1980, Fig. 3), and neither the description nor the explanation of this strange opening was given. As described below, the CHANG's apparatus consists of an internal cavity and an external opening which straddles the suture between the ADL and AVL plates. Since the CHANG's apparatus is completely separated from the interior of the trunk-shield, it cannot function as a mechanoreceptor system, like the sensory-line system which penetrates the dermal plates. However, this structure may function as an expanded ampullary electoreceptor and its opening is covered by the epidermis. Another explanation is that the CHANG's apparatus was glandular and had a role in mucus secretion. The goblet cells and compound mucus glands would have been integrated in the cavity of the CHANG's apparatus. Among the Yunnanolepididae, only *Yunnanolepis* and *Phymolepis* share the CHANG's apparatus. The differences between them are following:

1) *Phymolepis* retains the AL plate which hides the opening of the CHANG's apparatus from the outside;
2) In *Yunnanolepis* the posterolateral margin of the AMD plate is as long as the anterolateral margin, whereas in *Phymolepis* the posterolateral margin is obviously longer the anterolateral margin;
3) the PMD plate of *Phymolepis* bears a strong posterior process.

Yunnanolepis chii Liu, 1963
(Fig. 3)

Yunnanolepis chii Y.-H. Liu, 1963: 39, fig. 1, pl. 1.

Synonyms:
Eoantiarchilepis xitunensis P'an & Wang, 1978: 319, fig. 10, pl. 31.1-2.
Tsuifengshanolepis diantungensis P'an & Wang, 1978: 320, pl. 30.2.
Lianhuashanolepis liukiangensis P'an & Wang, 1978: 323, pl. 32.1-5.

Others references:
Yunnanolepis chii K.-J. CHANG, 1978: 293, pl. 25.1-4. — G.-R. ZHANG 1978: 148, figs × 1-7, pls I-IV, V.3-6. — S. F. LIU 1992: 212, pl. I. — ZHU, WANG & FAN 1994: 3, pl. 1.1-3.

EMENDED DIAGNOSIS. — A *Yunnanolepis* with a head-shield length of at least 3 cm; AMD plate with a central elevation; semilunar plate rectangular and broad.

HOLOTYPE. — A complete head-shield preserved ventrally and its mould, V2960.1 and V2960.2 (Y.-H. LIU 1963, Fig. 1, pl. I).

LOCALITY AND HORIZON. — Qujing (Chutsing), Yunnan, Cuifengshan Group, Early Devonian.

OTHER CONCERNED MATERIAL. — ADL plate, V4423.16 (G.-R. ZHANG 1978, pl. III, 1-2); AVL plate, V4423.18 (*ibid.*, pl. IV, 3-6); PL plate, V4423.23 (*ibid.*, pl. III, 3-4); PVL, V4463.30 (*ibid.*, pl. III, 6).

REMARKS. — Many diagnostic characters of *Yunnanolepis chii* (Y.-H. LIU 1963; K.-J. CHANG 1978; G.-R. ZHANG 1978) turn out to be plesiomorphic. Some of them, such as the position of the *crista transversalis interna posterior* and the hexagonal head-shield are synapomorphies of the higher taxonomic units, whereas those like the preorbital depression and the simple pectoral joint are symplesiomorphies even for antiarchs. This species has been described in detail by Y.-H. LIU (1963) and G.-R. ZHANG (1978). However, since *Y. chii* is the type species of *Yunnanolepis*, a supplementary description is noteworthy, even if mainly made on the basis of new observations on the specimens figured by G.-R. ZHANG (1978). *Y. chii* differs from the other *Yunnanolepis* species by its size, the large MV plate and an elevation at the centre of the AMD plate.

DESCRIPTION

CHANG's apparatus (Fig. 3A-D)

The CHANG's apparatus is poorly preserved in V4423.8, a fairly complete trunk-shield (G.-R. ZHANG 1978, pl. I, 6-7). However, the detached ADL and AVL plates described by G.-R. ZHANG (1978) clearly exhibit the CHANG's apparatus.

The upper margin of the opening of the CHANG's apparatus (Ca.o, Fig. 3C, D) is seen on the ventral margin of the ADL plate (V4423.16), slightly behind the anterior extremity of the plate. The ridge caused by the CHANG's apparatus (r.Chang, Fig. 3C, D) lies above the opening in external view. Internally, an additional lamina (l.Chang, Fig. 3D) lies just behind the *crista transversalis interna anterior* (cit, Fig. 3D). This lamina extends ventrally and forms a relatively large fossa (C.Chang, Fig. 3D), together with the lateral lamina of the plate.

The dorsal margin of the AVL plate (V4423.18, Fig. 3A, B) shows an conspicuous notch which represents the lower margin of the opening of the CHANG's apparatus (Ca.o, Fig. 3B). G.-R. ZHANG (1978) described prominent dorsal and anterodorsal processes on the dorsal margin of the AVL plate, and compared them to those of *Remigolepis*. In fact, these two corners are due to the opening of the CHANG's apparatus, and are different from those processes in *Remigolepis*. A ridge (r.Chang, Fig. 3B) is situated below the notch in external view. As for the ADL plate, an extra lamina (l.Chang, Fig. 3A) is seen behind the *crista transversalis interna anterior* (cit) and bounds off a fossa internally (C.Chang, Fig. 3A). This fossa, together with the corresponding fossa of the ADL plate (C.Chang, Fig. 3D), constitutes a large, enclosed cavity which communicates only with the outside by the opening of the CHANG's apparatus and is completely isolated from the interior of the trunk-shield.

Lateroventral fossa of the trunk-shield (f.lv, Fig. 3A, E)

The lateroventral fossa is an internal structure of the trunk-shield, and lies at the junction of three plates (the AVL, PL and PVL plates). Part of this fossa has been mentioned by G. R. ZHANG (1978, 163, Fig. 6B) on the AVL plate, and has also been figured on the PVL plate. The lateroventral fossa consist of three depressions on the AVL, PL and PVL plates, and that of the AVL plate is the largest (f.lv, Fig. 3A, E). The plate portions encircling the fossa are thickened, presumably for the attachment of some muscles. The same fossa is found in *Yunnanolepis* cf. *Y. chii* (TONG-DZUY & JANVIER 1990, Fig. 15).

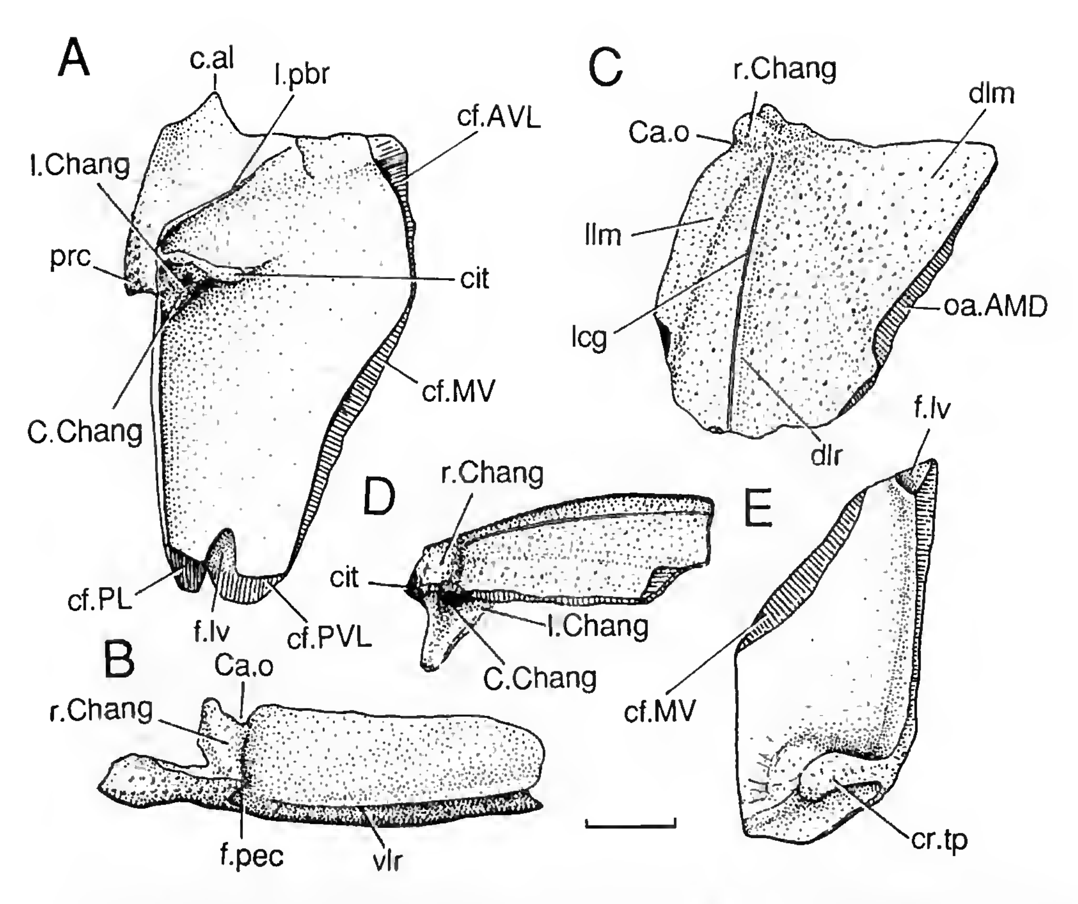


FIG. 3. — *Yunnanolepis chii* Liu, Xitun Formation, Qujing. A-B, left AVL plate (V4423.27) in visceral (A) and lateral (B) views; C-D, left ADL plate (V4423.23) in dorsal (C) and lateral (D) views; E, right PVL plate (V4423.30) in visceral view. (Scale bar 10 mm.)

Yunnanolepis porifera n. sp.
(Figs 4-7; pls I, 1-7; II, 1-7; III, 1-8)

Yunnanolepis parvus pars G.-R. Zhang, 1978: 164, pl. V, 3-6
"form probably akin to *Y. chii*" (pars) V4424.5, V4424.20, M.-M. Zhang, 1980: 179, 185, fig. 3, pls III, 2-4, IV, 2-4, V2-3.

DIAGNOSIS. — *Yunnanolepis* in which the PMD plate has a cone-shaped posterior dorsal angle.

ETYMOLOGY. — From *porus* (Lat.), "pore", by reference to the opening of the CHANG's apparatus.

HOLOTYPE. — V4424.20 (see M.-M. ZHANG 1980, pl. III, 2-4, fig. 3).

LOCALITY AND HORIZON. — Qujing, Yunnan, Xishancun Formation and Xitun Formation, Early Devonian.

New material. — V10499.1-3, trunk-shields; V10499.4-20, AMD plates; V10499.21-23, PMD plates; V10499.24-28, ADL plates; V10499.29-34, AVL plates; V10499.35-37, PDL plates; V10499.38-42, PL plates; V10499.43-44, PVL plates; V10499.45, MV plate. The specimens whose number begins with V10499 are from the Xishancun Formation, and V10507 (V10507.1-7) from the Xitun Formation.

Remarks. — By now, four species have been referred to *Yunnanolepis* (*Y. chii*, *Y. bachoensis*, *Y. deprati* and *Y. porifera*). The Chang's apparatus has not been described in the two Vietnam species *Y. bachoensis* and *Y. deprati* (Tong-Dzuy & Janvier 1990), however, it can be inferred from the notch and the anterior vertical ridge of the ADL plate. *Y. porifera* resembles both *Y. deprati* and *Y. bacboensis* by its small MV plate. As to the plate proportion, *Y. porifera* is more suggestive of *Y. deprati*. However, the trunk-shield of *Y. deprati* is quite different from that of *Y. porifera* in lacking ridges.

Y. porifera from the Xitun Formation has been described under the name of *Y. parvus* (G.-R. Zhang 1978; M.-M. Zhang 1980). It is found that the holotype of *Y parvus* (V4424.3) definitely differs from the other specimens which were referred to as *Y. parvus* by G.-R. Zhang (1978). V4424.3 has a different skull-roof from that of *Y. chii*, and its trunk-shield is most suggestive of that of *Mizia pani* n. g., n. sp., therefore this holotype should be more reasonably referred to as *Mizia parvus* rather than *Y. parvus*. Subsequently, those specimens removed from *Mizia parvus* should be referred to a new species of *Yunnanolepis*. Until now, the head-shield of *Y. porifera*, as well as that of *Y. deprati* or *Y. bacboensis*, is still unknown to us. The specimens of *Y. porifera* are first described here from the Xishancun Formation, providing us with more information about the shape of its semilunar plate.

Description

Material from the Xitun Formation (Figs 4, 5A, 6; pls I, 1-7; II, 5-7)

The material of *Y. porifera* n. sp. from the Xitun Formation has been described by G.-R. Zhang (1978) and M.-M. Zhang (1980). Complementary notes are given here in order to clarify several features.

Y. porifera is a small-sized yunnanolepid (Fig. 4), which is characterized by its sharp posterior dorsal angle of the PMD plate (pda, Fig. 4B). The skull-roof of *Y. porifera* cannot be identified from the material of the Xitun Formation. The trunk-shield of *Y. porifera* is somewhat higher than that of *Y. chii*. However, its relative height is variable. V10507.1 and V10507.2 (pl. I, 3-5) have a relatively low trunk-shield in comparison to the holotype. The AMD plate is generally ornamented with eight faint ridges radiating from the tergal angle. The tubercles on ridges are slightly larger than the others. V10507.1 (pl. I, 3) has its dorsal wall partly eroded to expose the internal mould. It is observed that the anterior ventral process and pit are situated just beneath the tergal angle, and the *crista transversalis interna posterior* lies in front of the posterior ventral process and pit. V10507.3 (pl. I, 1-2) is more or less distinctive from other specimens. It is similar to the other specimens of *Y. porifera* in size, high trunk-shield and structure of the Chang's apparatus. However, this trunk-shield is devoid of radiating ridges on the AMD plate and probably lacks the sharp posterior dorsal angle of the PMD plate, as inferred from the visible portion. Since only this specimen is available, V10507.3 is provisionally thought to represent an individual variation of *Y. porifera*. V10507.7 is a fragment of the AMD and PDL plates (Fig. 5A). Its AMD plate is gently arched and lacks ridges in external view, as in V10507.3. In visceral view (pl. II, 5), the median ventral ridge (mvr, Fig. 5A) extends from the anterior median process forwards and backwards.

The opening of the Chang's apparatus (Ca.o, Figs 4A-C, 6A1, 3C), which lies close to the anterior extremity of the trunk-shield and at the suture between the ADL and AVL plates, has been sketched by M.-M. Zhang (1980). Several specimens of *Y. porifera* have been prepared and examined in order to explain the function of the Chang's apparatus. It has been shown that

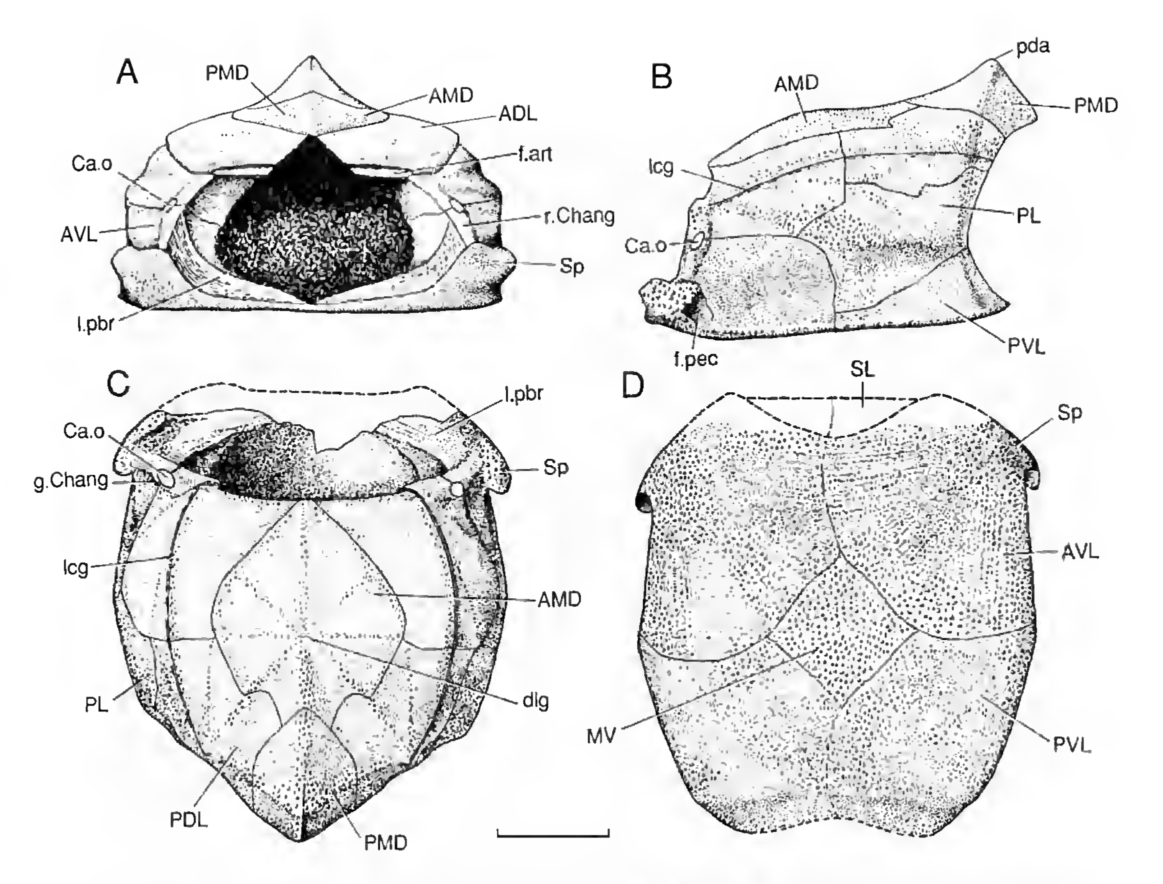


FIG. 4. — *Yunnanolepis porifera* n. sp., Xitun Formation, Qujing. Restoration of the trunk-shield in anterior (A), lateral (B), dorsal (C) and ventral (D) views (modified from M.-M. ZHANG 1980, fig. 3) (Scale bar 5 mm.)

the cavity of the CHANG's apparatus (C. Chang, Fig. 6A3) is a blind tube which extends downwards and slightly upwards. In external view, this tube produced a vertical ridge (r.Chang, Fig. 6A1, B) along the anterior margin of the trunk-shield. Behind this ridge is a vertical groove. In comparison to that of *Y. chii*, the cavity of the CHANG's apparatus of *Y. porifera* is smaller and narrower, somewhat like that of *Phymolepis*. In contrast to *Phymolepis*, the opening of the CHANG's apparatus of *Y. porifera* is directly exposed to the outside and there is no anterior lateral plate.

The lateroventral fossa of the trunk-shield, at the junction of the AVL, PL, PVL plates, is as in *Y. chii*. In V10507.5, a portion of the lateroventral fossa is clearly seen at the posterior end of the AVL plate in visceral view (f.lv, Fig. 6A2).

As to the pectoral fenestra, *Y. porifera* has a similar structure to other yunnanolepids and *Minicrania* (ZHU & JANVIER 1996). Noteworthy is an AVL plate, probably belonging to *Y. porifera*, which has its pectoral fenestra filled by the perichondrally ossified scapulocoracoid

(scap, Fig. 6B-D, pl. I, 6-7). This scapulocoracoid, extending from the bottom of the pectoral fenestra, is conical in shape and has its outmost end oval in section. In contrast to the dermal skeleton, its outer surface is smooth and devoid of ornamentation. Its mesial surface is closely in contact with the lateral wall of the plate.

Material from the Xishancun Formation (Figs 5B-G, 7, pls II, 1-4; III, 1-8)

Numerous specimens of *Y. porifera*, including three articulated trunk-shields, have been collected from the Xishancun Formation. Forty five of them are numbered for the study, and the isolated plates are identified by comparison with the articulated trunk-shields, in addition to their size and ornamentation. The material from the Xishancun Formation is very similar to that from the Xitun Formation, either in shape or in size. It bears the ventrolateral fossa and CHANG's apparatus as that from the Xitun Formation. The ornament is composed of small, closely set tubercles. Its dorsal wall is slightly narrower than the ventral wall, and the lateral wall is relatively high. The dorsal wall bears a sharp posterior dorsal angle on the PMD plate, and the median ventral plate is fairly small.

The AMD plate (Fig. 5B-G) is roughly rhombic in shape, with a pointed anterior margin (a, Fig. 5C-D). Its posterior margin (oa.PMD, Fig. 5C-D), which is by the PMD plate, is fairly narrow. The plate shows apparent lateral corners (lc, Fig. 5C-D), and its anterolateral margin is slightly longer than the posterolateral one. In external view, the plate is gently arched at the tergal angle (dma, Fig. 5C), which is almost halfway along the mid-line. Eight faint ridges radiate from the tergal angle to the margins, and the small tubercles are getting a little larger on the ridges. The short posterior oblique abdominal pit-line grooves (dlg, Fig. 5C) are sometimes visible behind the tergal angle. The overlap relationships with the adjoining plates are normal, as in other yunnanolepids. In visceral view, there exist many individual variations as to the development of the anterior ventral process (prv1, Fig. 5B, E, G), median ventral groove (grm, Fig. 5B, F) and ridge (mvr, Fig. 5G). In general, the AMD plate of *Y. porifera* bears the anterior ventral process and pit (prv1, pt1, Fig. 5B) as in *Y. chii*, just beneath the tergal angle. However, in some specimens, *e.g.* V10499.6 (Fig. 5F), the plate is devoid of the anterior ventral process and pit. Behind the anterior ventral process, or in the corresponding position relative to the tergal angle, the plate generally displays a median ventral groove (grm, Fig. 5F), contrary to the AMD plate of *Y. chii* (G.-R. ZHANG 1978). The exception is seen in V10499.12, which lacks the median ventral groove and has the median ventral ridge extending to the posterior end of the plate (mvr, Fig. 5G), like that of *Y. chii*. In front of the anterior ventral process, or in the corresponding position relative to the tergal angle, the plate is generally devoid of any ridge or groove. However, a short median ventral ridge is found in some specimens, such as V10499.11 (pl. III, 8).

The PMD plate is characterized by its dorsally projecting posterior dorsal angle (pda, Fig. 7B). In visceral view, the *crista transversalis interna posterior* (cr.tp) is developed in front of the posterior ventral process and pit (prv2, Fig. 7E).

The ADL plate (pl. III, 4) is subdivided into the dorsal and lateral laminae by the dorsolateral ridge of the trunk-shield. On the dorsal lamina, the articular fossa lies beneath its broad anterior margin. On the lateral lamina, the ridge and groove caused by the CHANG's apparatus are seen next to its anterior margin. Along the ventral margin there is the notch of the opening of the CHANG's apparatus, as in *Y. chii*. The main lateral-line groove runs through the plate below the dorsolateral ridge.

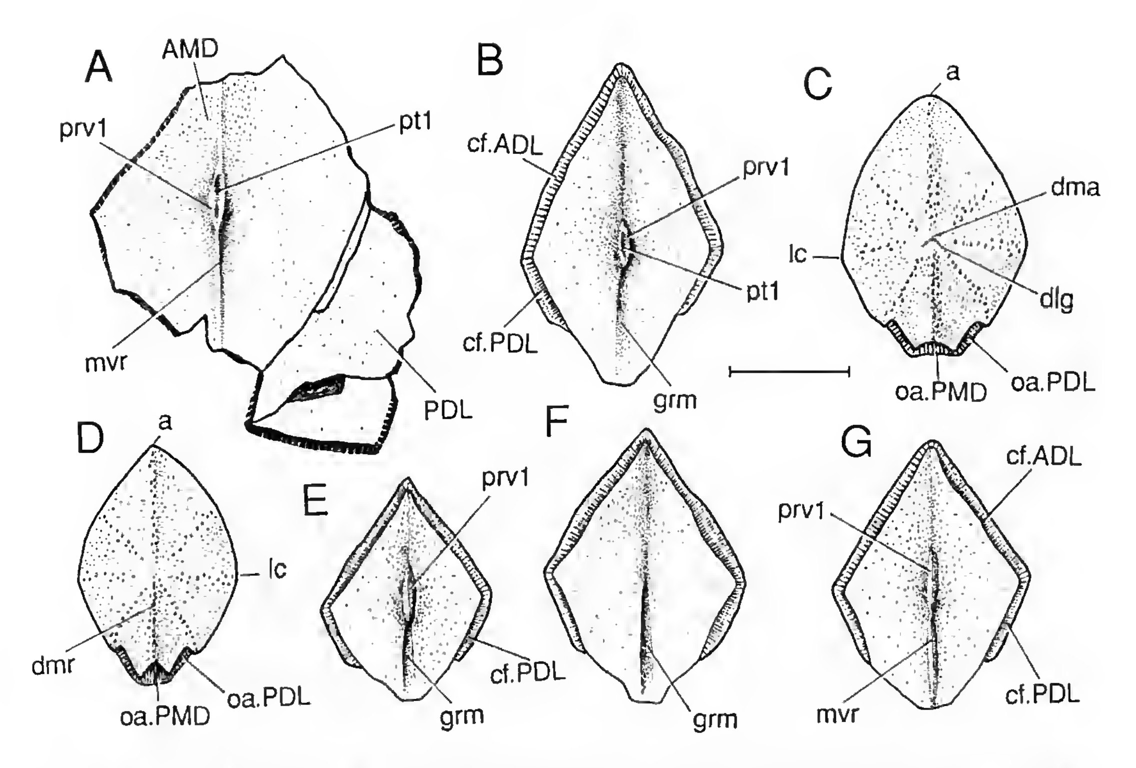


FIG. 5. — *Yunnanolepis porifera* n. sp., Xitun Formation (A) and Xishancun Formation (B-G), Qujing. A, incomplete AMD and PDL plates in visceral view, V10507.7; B-G, AMD plates (elastomer casts). B, V10499.18 in visceral view; C, V10499.16 in dorsal view; D, V10499.4 in dorsal view; E, 10499.7 in visceral view; F, V10499.6 in visceral view; G, V10499.12 in visceral view. (Scale bar 5 mm.)

The PDL plate (Fig. 7D, pl. III, 5) also comprises dorsal and lateral laminae. The dorsal lamina has a conspicuous dorsal corner. The lateral lamina is fairly low and, along its ventral margin, it overlaps the PL plate anteriorly and is overlapped by the PL plate posteriorly. The area which is overlapped by the PL plate (oa.PL, Fig. 7D) extends ventrally to form a process near its posterior end.

The PL plate (Fig. 7F) is elongated, low, and posteriorly descending. The *crista transversalis interna posterior* (cr.tp, Fig. 7F) is situated next to the posterior end of the plate. In visceral view, at the anteroventral corner of the plate, there is a shallow depression which is part of the lateroventral fossa of the trunk-shield (f.lv, Fig. 7F).

The AVL plate consists of the lateral and ventral laminae. Since there is no detached semilunar plate which could be definitely assigned to *Y. porifera*, the shape of the SL plate is inferred from the corresponding notch in the anteromesial margin of the AVL plate. As the AVL plates of *Y. porifera* from the Xitun Formation are generally broken at their anterior end, those from the Xishancun Formation are worthwhile in their completeness. The lateral lamina is relatively low. Anteriorly, the cavity of the CHANG's apparatus can be inferred from the internal mould of the plate. The plate has a conspicuous prepectoral corner, which is continuous with the

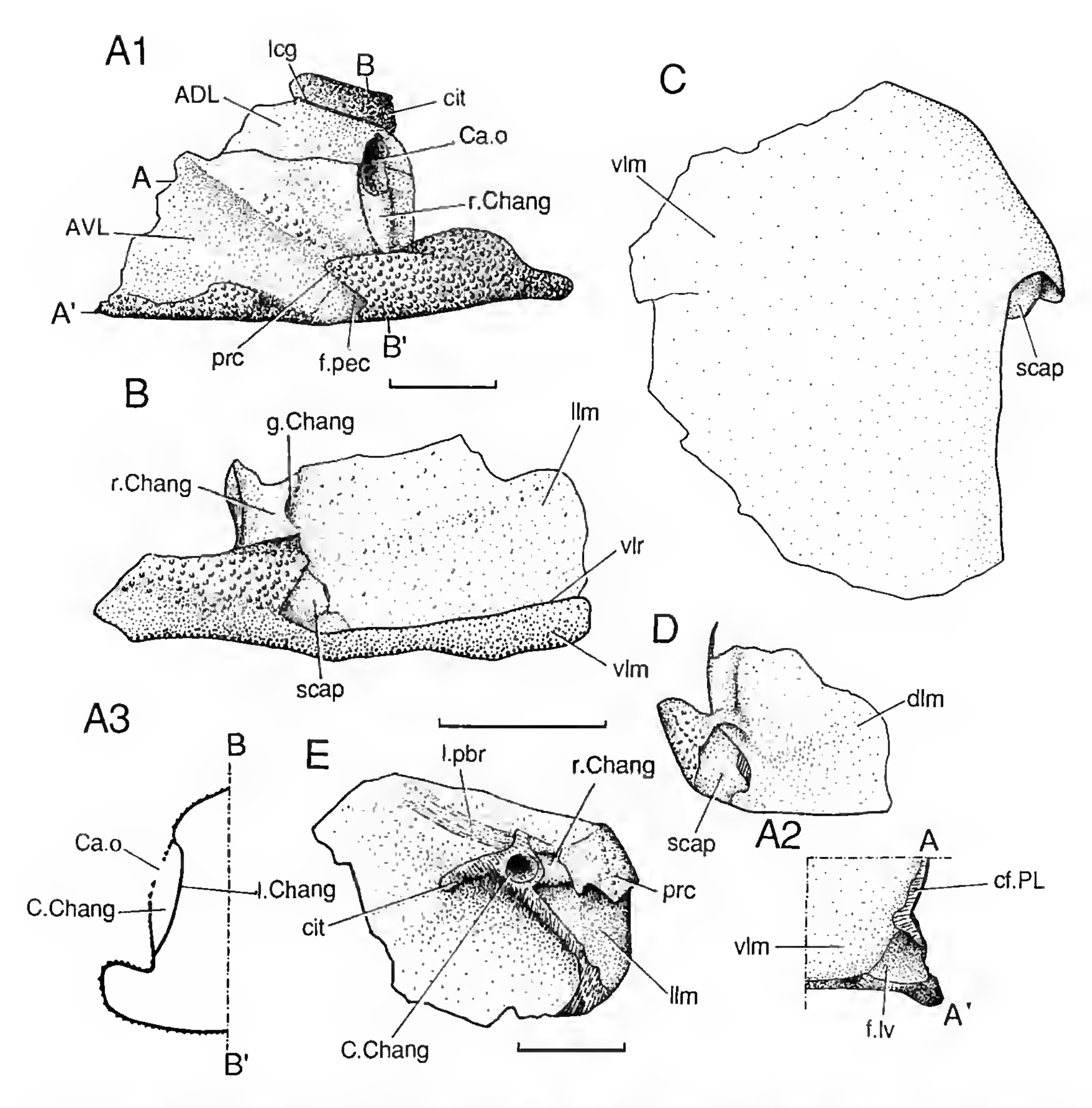


FIG. 6. — *Yunnanolepis porifera* n. sp., Xitun Formation, Qujing. A, right ADL and AVL plates in lateral (A1) and posterior (A2) views, A3 represents the section through the Chang's apparatus, V10507.5; B-D, left AVL plate in lateral (B), ventral (C) and posterolateral (D) views, V10507.4; E, incomplete right AVL plate in dorsal view, V10507.6. (Scale bar 5 mm.)

independent spinal plate. The anterior extremity of the plate is the anterolateral corner (c.al, Fig. 7A), from which the anterior division of the mesial margin extends posteromesially and straight. According to this portion of margin, it is reasonable to assume that the semilunar plate of *Y. porifera* is more or less triangular in shape, unlike that of *Y. chii*. The posterior division of the mesial margin, along which the plate overlaps the MV plate (cf. MV, Fig. 7G), is com-

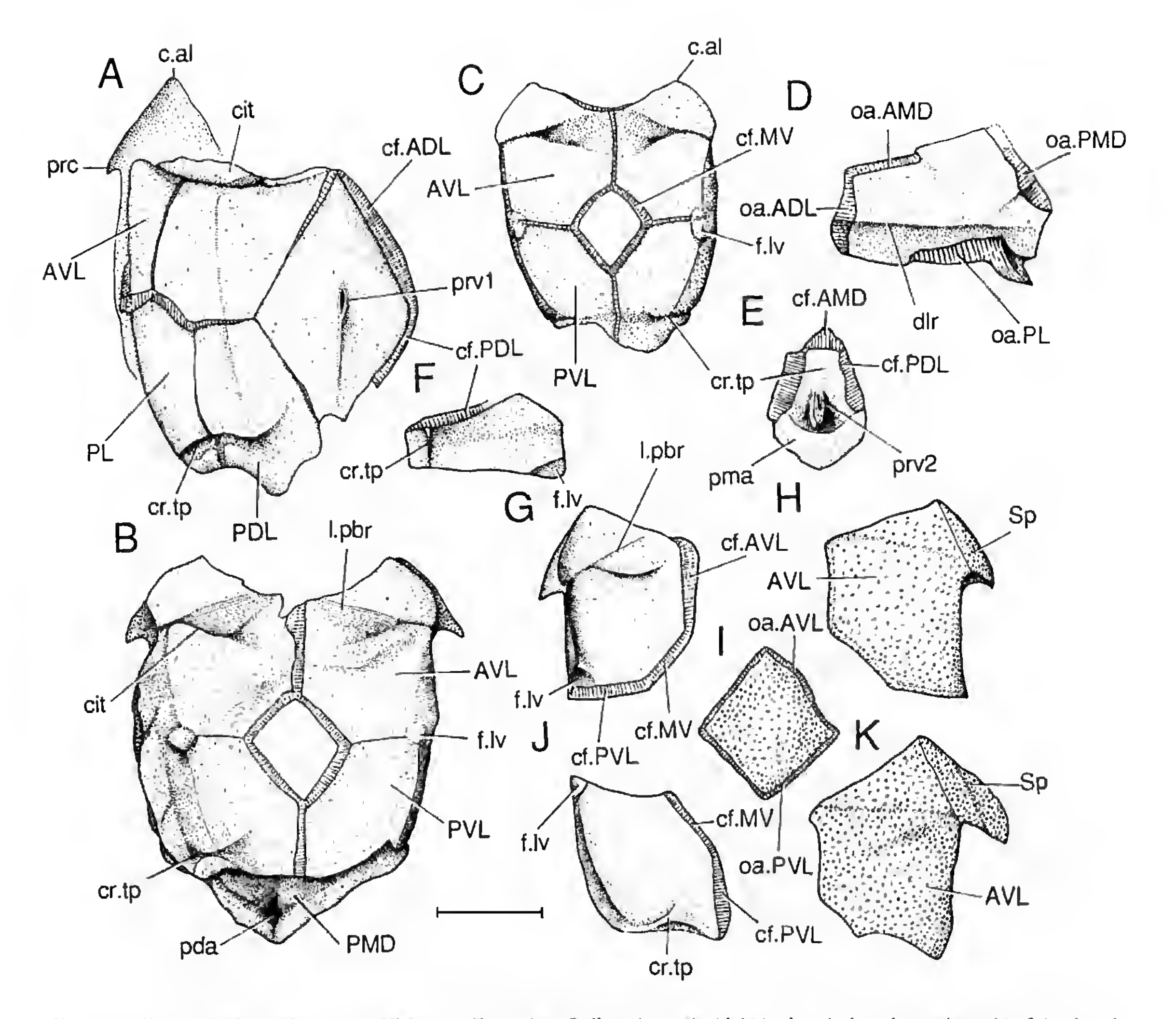


FIG. 7. — *Yunnanolepis porifera* n. sp., Xishancun Formation, Qujing. A, trunk-shield in dorsal view (internal mould of the dorsal and lateral walls, and external mould of the ventral wall), V10499.3; B, trunk-shield in ventral view (internal mould of the ventral wall and external mould in dorsal wall), V10499.1; C, trunk-shield in ventral view (internal mould of ventral and lateral walls), V10499.2; D, PDL plate in external view (elastomer cast), V10499.35; E, PMD plate in visceral view (elastomer cast), V10499.23; F, PL plate in visceral view (elastomer cast), V10499.38; G-H, left AVL and Sp plates in visceral (G) and external (H) views, V10499.37; I, MV plate in external view (elastomer cast), V10499.45; J, left PVL plate in visceral view (elastomer cast), V10499.43; K, left AVL and Sp plates in external view (elastomer cast), V10499.36 (Scale bar 5 mm.)

paratively short. In visceral view, there is a posterior depression which is part of the lateroventral fossa (f.lv, Fig. 7C, G). The postbranchial lamina (l.pbr, Fig. 7B-C, G) extends slightly anteromesially from near the small pectoral fenestra, and behind it is the transversely directed *crista transversalis interna anterior* (cit, Fig. 7B).

An independent Sp plate is present in *Y. porifera*. In general, this plate is fairly small but bears a conspicuous suture with the AVL plate as in V10499.37 (Fig. 7H). In V10499.36, this plate is somewhat enlarged, more or less similar to the small spinal plate of some arthrodires (Fig. 7K, pl. II, 4).

The PVL plate (Fig. 7B-C) has a low lateral lamina and relatively narrow ventral lamina, whose contact margin with the median ventral plate is fairly short. In visceral view, the component of the lateroventral fossa (f.lv, Fig. 7J) is seen at its anterolateral corner. The *crista transversalis interna posterior* (cr.tp, Fig. 7J) is situated next to the posterior end of the plate.

The MV plate (Fig. 7I) is fairly small and rhombic in shape. It is overlapped by the AVL and PVL plates.

Yunnanolepis sp.
(Figs 8-9, pl. II, 11)

Vanchienolepis sp. Janvier, 1995: 153, MNHN-CHD01, Fig. 6.

New material. — A trunk-shield associated with part of skull-roof, V10514.

Locality and horizon. — Qujing, Yunnan, Xitun Formation, Early Devonian.

Remarks. — Janvier (1995) described an antiarch (MNHN-CHD01) referred to as *Vanchienolepis* sp. or "*Vanchienolepis*-like specimen from Qujing" (p. 157). MNHN-CHD01 came from the Xitun Formation of Qujing, and is excellent in the preservation of the pectoral fin which had the natural position to the trunk-shield. However, its assignment as *Vanchienolepis* is doubtful, since its brachial articulation is poorly preserved, and is more suggestive of the simple one of the Yunnanolepididae rather than that of *Vanchienolepis*. Moreover, MNHN-CHD01 has a head-shield which is just same as that of Yunnanolepis, which is confirmed by my new specimen and was implied by Janvier (1995). The new material described here came from the same bed as MNHN-CHD01, and was prepared to show the visceral surface of the shield.

This antiarch is quite different from *Vanchienolepis* (Tong-Dzuy & Janvier 1990) except for the large rectangular fenestra on the ventral wall of the trunk-shield. They have different pectoral fin structures, AMD and ADL plates. As far as we know, the head-shield, the dorsal trunk-shield wall and the pectoral fin structure of MNHN-CHD01 and V10514 are just same as those of *Yunnanolepis*. It is referred to *Yunnanolepis* by its typical Chang's apparatus, whose opening, unlike that of *Phymolepis*, is visible in lateral aspect.

Description

V10514 is a small individual, whose trunk-shield length is shorter than 15 mm (Fig. 8). The preserved skull-roof plates include the nuchal, paranuchal and lateral plates (Nu, PNu, L, Fig. 8), which are just same as those of other *Yunnanolepis* species. The semicircular ridges (r.semi, Fig. 8A) are seen on the external surface of the nuchal plate.

The trunk-shield has lost its posterior margin, and part of the ventral wall was damaged during the preparation of the visceral surface of the shield (Fig. 8A, B). However, it is quite certain that its ventral wall is similar to that described by Janvier (1995), *i.e.* possessing a large opening instead of the MV plate.

Externally, the Chang's apparatus is well-preserved. The opening of the Chang's apparatus (Ca.o, Figs 8A, 9) is fairly elongated in shape and lies on a vertical ridge (r.Chang) next to the anterior extremity of the trunk-shield. The suture between the ADL and AVL plates delineates its upper margin. The cavity of the Chang's apparatus is narrowed, as in *Y. porifera*. The *crista*

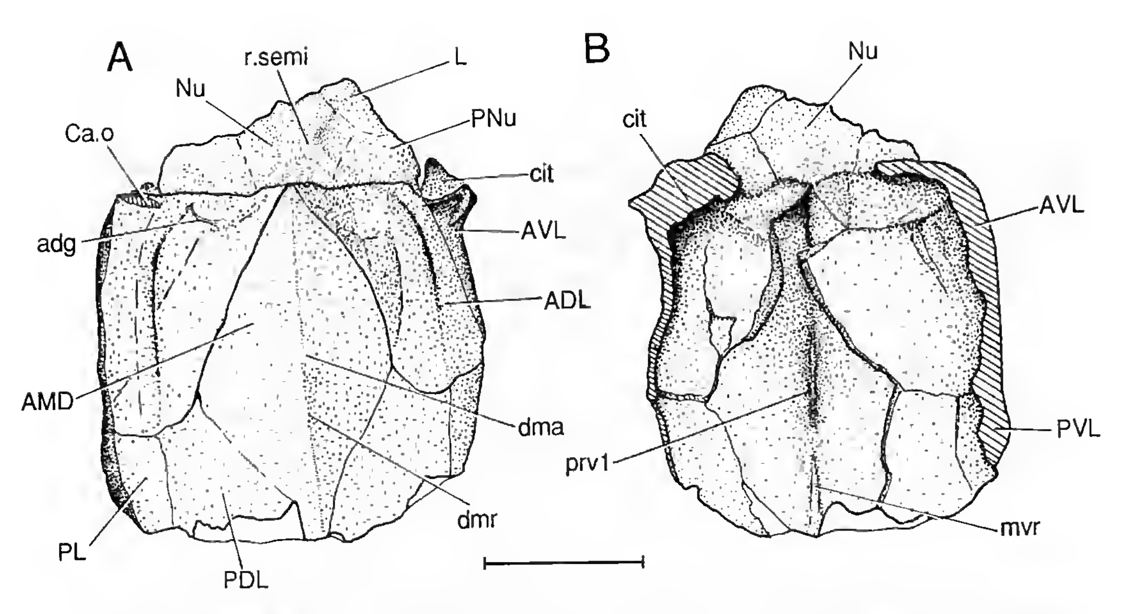


FIG. 8. — *Yunnanolepis* sp., Xitun Formation, Qujing. Incomplete trunk-shield and skull-roof in dorsal (A) and ventral (B) views, V10514. (Scale bar 5 mm.)

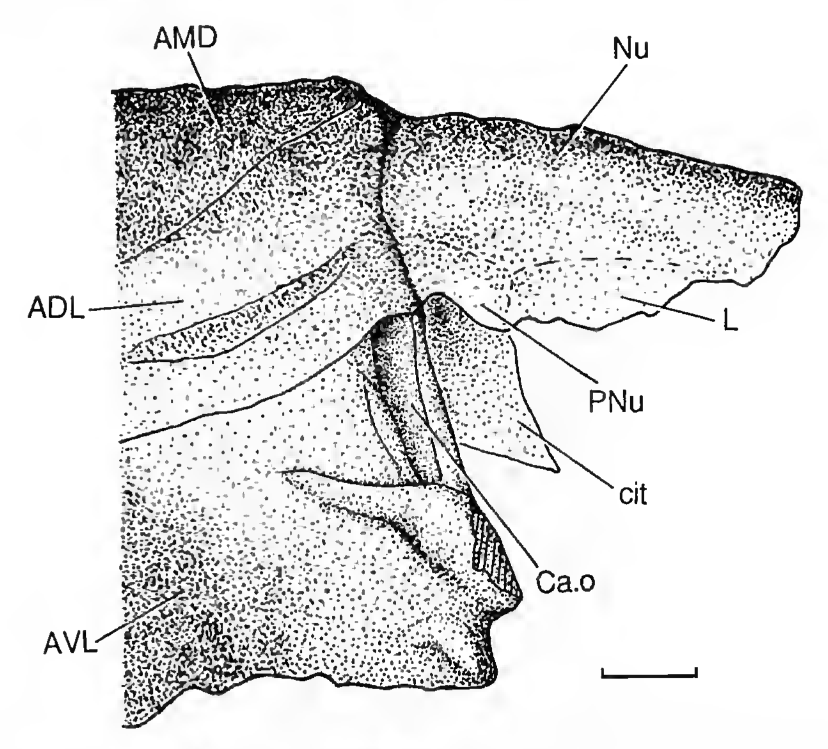


FIG. 9. — *Yunnanolepis* sp., Xitun Formation, Qujing. Incomplete trunk-shield and skull-roof in lateral view (anterior portion, showing the details of the CHANG's apparatus), V10514. (Scale bar 1 mm.)

transversalis interna anterior (cit, Figs 8A, 9) is in front of the CHANG's apparatus and beneath the skull-roof.

Internally, there is no anterior ventral process and pit on the AMD plate. Instead, there is a short median ventral ridge (mvr, Fig. 8B) which corresponds in position to the tergal angle (dma, Fig. 8A). The ridge reappears next to the posterior end of the AMD plate, yet it is relatively faint.

Genus **MIZIA** n. g.

DIAGNOSIS. — Yunnanolepididae in which small tubercles on the dorsal and lateral walls of the trunk-shield are arranged into regular ridges, with tiny tubercles between ridges.

ETYMOLOGY. — After the Chinese character 米 (Mi, in the Chinese phonetic alphabet), Zi = word, character; indicating the ridges on the dorsal wall of the trunk-shield looks like the Chinese character (Mi).

TYPE SPECIES. — *Mizia longhuaensis* n. sp. (Fig. 10; pl. II, 8-10).

REFERRED SPECIES. — *Mizia parvus* (G.-R. ZHANG 1978).

REMARKS. — *Mizia* is referred to the Yunnanolepididae because of its *crista transversalis interna posterior* in front of the posterior ventral process. *M. longhuaensis* bears an independent AL plate in front of the suture between the ADL and AVL plates and is devoid of CHANG's apparatus. As stated above, the specimen previously described as the holotype of *Yunnanolepis parvus* (V4424.3, G.-R. ZHANG 1978; also see M.-M ZHANG 1980), which has lost the anterior extremity of the dorsal wall of its trunk-shield, differs from the other material assigned to this species by G.-R. ZHANG (1978), and its skull-roof clearly differs from that of *Y. chii* in the pattern of sensory-line grooves. Since its ornamentation is quite suggestive of that of *M. longhuaensis*, *Y. parvus* is referred here to *Mizia*. The anterior region of the lateral wall of the trunk-shield is poorly preserved in V4424.3, and the available evidence suggests it may be similar to that in *M. longhuaensis*.

Mizia longhuaensis n. sp.
(Fig. 10; pl. II, 8-10)

DIAGNOSIS. — *Mizia* in which the median dorsal ridge branches into two parallel ridges behind the tergal angle.

ETYMOLOGY. — After the fossil locality of Longhua hill, Qujing, Yunnan.

HOLOTYPE. — A complete trunk-shield, V10515.

LOCALITY AND HORIZON. — Longhua hill, Qujing, Yunnan, Xujiachong Formation, Early Devonian.

REMARKS. — The new species differs from *M. (Yunnanolepis) parvus* mainly by its median dorsal ridge, which branches into two parallel ridges behind the tergal angle.

DESCRIPTION

The holotype is a small-sized trunk-shield, characterized by its regular ridges on the slightly arched dorsal and lateral walls. In general, the ridges converge toward the growth centre of the plate, and transect the sutures. For example, the ridges radiate from the tergal angle (dma, Fig. 10A, C) on the AMD plate. The tubercles on the ridges are small, however, they are apparently larger than those between ridges. The lateral wall is relatively low. Most of the bone on the ventral wall was eroded to leave the internal mould. The ventral wall is flat and has the

same breadth as the dorsal wall. It is a little longer than the dorsal wall, since its subcephalic portion is fairly short and its posterior end is situated slightly in front of the level of the posterior extremity of the dorsal wall.

The AMD plate (AMD, Fig. 10A) has a length/breadth index of about 125, and is pentagonal in shape. The lateral corner is distinct. The anterolateral margin is slightly longer than the posterolateral margin. The posterior margin is relatively broad and about two fifth of the plate breadth. The plate is somewhat arched with the tergal angle at the level of the lateral corners. In external view, the plate is adorned with radiating ridges, which are fairly high and delimit grooves. The development of the median dorsal ridge (dmr, Fig. 10A) in *M. longhuaensis* is not typical as in other yunnanolepids. In front of the tergal angle, the ridge becomes broader toward the anterior edge of the trunk-shield. Behind the tergal angle, the median dorsal ridge diverges into two

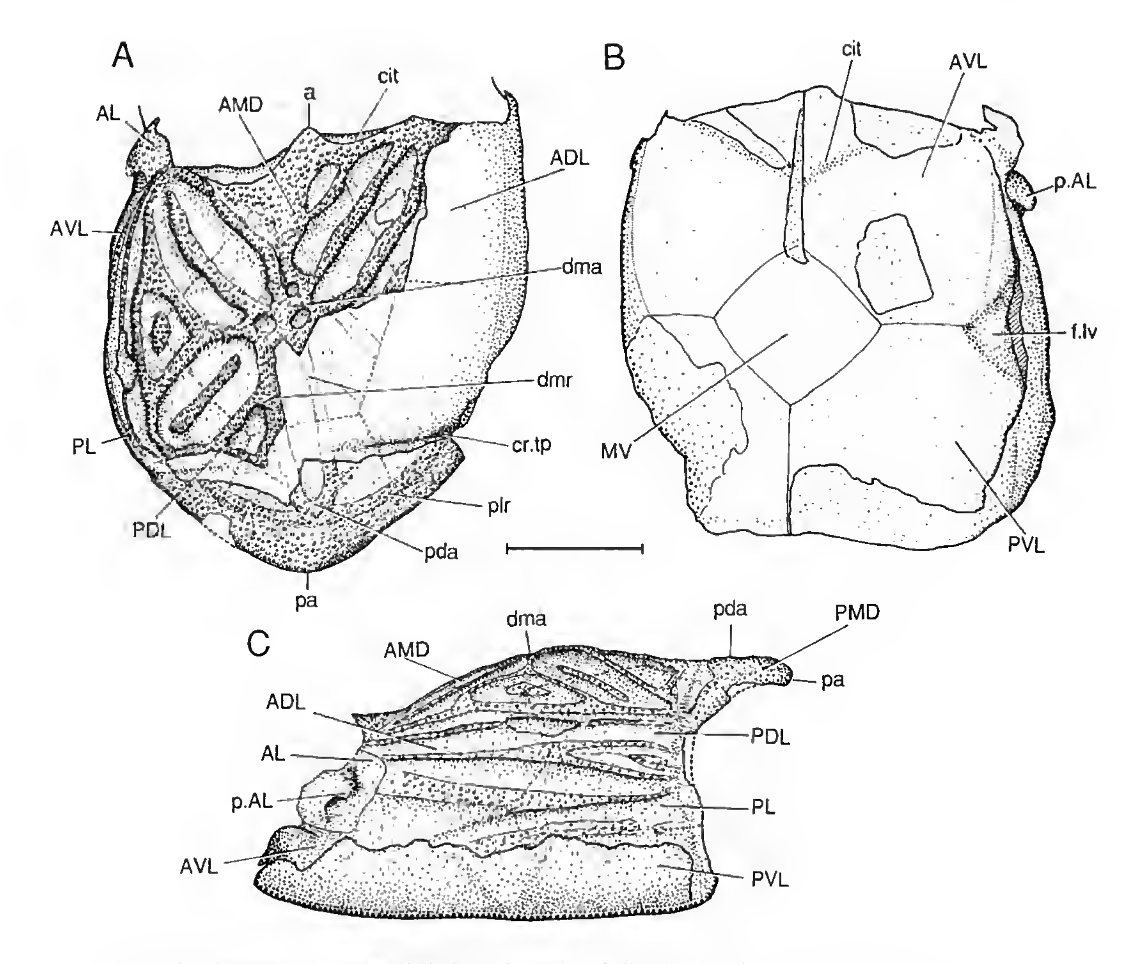


FIG. 10. — *Mizia longhuaensis* n. g., n. sp., Xujiachong Formation, Qujing. Trunk-shield (holotype, V10515) in dorsal (A), ventral (B) and lateral (C) views. (Scale bar 5 mm.)

parallel ridges extending to the PMD plate (part of the ridges were damaged during the preparation, however they still left the impressions). Between the parallel ridges is a conspicuous groove. At the tergal angle, the ridge bounds off three small, rounded depressions. The ridges of *M. longhuaensis* are different from those of *Yunnanolepis*, which has only eight ridges radiating from the tergal angle towards the margins and not forming grooves in between. In *M. longhuaensis*, there are at least ten ridges radiating from the tergal angle, and some of them branch outwards. The ridges form almost right angles with plate margins. Either the anterolateral margin or posterolateral margin is transected by three ridges. Four ridges, among which two ridges are derived from the median dorsal ridge, traverse the posterior margin. The visceral surface cannot be observed in the specimen.

The PMD plate (PMD, Fig. 10A, C) is relatively broad, with a length/breadth index of about 78, and its posterior margin is slightly protruding. On the external surface, there is no angle or hump as generally seen in *Yunnanolepis*. There are four ridges extending from the AMD plate. A ridge proceeds to the PDL plate in front of the faint posterolateral ridge (plr. Fig. 10A). Since part of the bone was crushed, the internal mould of the plate is exposed, showing that the *crista transversalis interna posterior* (cr.tp, Fig. 10A) arises from the PDL plates towards anterior portion of the plate, close to its anterior edge, as in other yunnanolepids. The posterior ventral process is not exposed in the specimen, and must have been situated far behind the *crista transversalis interna posterior*.

The ADL plate (ADL, Fig. 10A, C) is composed of dorsal and lateral laminae. The dorsal lamina has a very broad anterior margin, below which the articular fossa and *crista transversalis interna anterior* (cit, Fig. 10A) are visible in anterior view. Except for those four ridges coming from the AMD plate, there is a ridge above the dorsolateral ridge extending towards the PDL plate. The lateral lamina contacts the AVL plate ventrally, PDL and PL plates posteriorly and AL plate anteriorly. There are two, somewhat parallel ridges extending posteriorly. The main lateral-line groove is not observed in the specimen.

The PDL plate (PDL, Fig. 10A, C) is similar to that of other yunnanolepids in having a very low lateral lamina and a distinct dorsal corner. On the dorsal lamina, three ridges extend from the AMD plate, one in addition to the faint posterolateral ridge from the PMD plate and one from the ADL plate. Internally, the *crista transversalis interna posterior* (cr.tp, Fig. 10A) is situated near the posterior margin of the plate.

The AL plate of *M. longhuaensis* (AL, Fig. 10A, C) is most interesting. It is a small plate on the anterior extremity of the lateral wall. It shows distinct sutures with the ADL and AVL plates, and is remarkable by its posteriorly extending process (p.AL, Fig. 10A, C) which is easily confused with the prepectoral corner, a structure of the AVL plate. This AL process has a relatively dorsal position and is situated just below the dorsolateral ridge. With the rest of the plate, it delimits a blind fossa.

The PL plate (PL, Fig. 10A, C) is a long and low plate ornamented with ridges. Internally, the *crista transversalis interna posterior* lies next to its posterior end.

The AVL plate (AVL, Fig. 10B, C) has lateral and ventral laminae. The lateral lamina is very low and extends behind the AL plate. The pectoral region is poorly preserved. Part of the prepectoral corner is preserved, and it seems that *M. longhuaensis* has a simple pectoral joint like other yunnanolepids. The ventral lamina is somewhat similar to that of *Y. porifera*, since

it has narrow contact margin with the MV plate. However, as to the notch for the semilunar plate, *M. longhuaensis*, as well as *M. parvus* (M.-M. ZHANG 1980, pl. I, 2), is more suggestive of *Y. chii* (G.-R. ZHANG 1978, Fig. 6). The *crista transversalis interna anterior* (cit, Fig. 10B) extends from the level of the prepectoral corner to the mesial margin, and, halfway bends somewhat backwards. The ventrolateral fossa (f.lv, Fig. 10B, C) is clearly visible in the specimen, as in *Yunnanolepis*.

The PVL plate (PVL, Fig. 10B, C) is very similar to that of *Y. porifera*. It shows part of the ventrolateral fossa (f.lv) at its anterior end and the *crista transversalis interna posterior* lying close to its posterior margin.

The MV plate (MV, Fig. 10B) is a very small rhombic plate. Its breadth is less than two fifth of the trunk-shield breadth, as in *Y. porifera*.

Genus **PHYMOLEPIS** K.J. Chang, 1978

Phymolepis K.-J. Chang, 1978: 295, pl. 25, 5-7.

Other reference:
Phymolepis G.-R. ZHANG 1978: 168, figs 10-12, pl. VI.

EMENDED DIAGNOSIS. — Yunnanolepididae in which there is a strong posterior process of the PMD plate; AMD plate with anterior division longer than posterior division; anterior ventral process and pit situated slightly behind the level of the lateral corners of the AMD plate; conspicuous median dorsal ridge between the tergal and posterior dorsal angles.

TYPE SPECIES. — *Phymolepis cuifengshanensis* K.-J. Chang, 1978.

REMARKS. — *Phymolepis* is more suggestive of *Yunnanolepis* by its CHANG's apparatus. The other similarities are due to characters of the Yunnanolepididae or the Yunnanolepidoidei. They differ by the fact that the former retains the AL plate which hides the opening of the CHANG's apparatus from the outside.

Phymolepis cuifengshanensis K.-J. Chang, 1978
(Figs 11-12; pl. I, 8-10, IV, 1-9)

Phymolepis cuifengshanensis K.-J. Chang, 1978: 295, pl. 25, 5-7.

Other reference:
Phymolepis cuifengshanensis G.-R. ZHANG 1978: 168, figs 10-12, pl. VI.

EMENDED DIAGNOSIS. — *Phymolepis* species in which the strong posterior process of the PMD plate is rounded in shape, reaching one third of the plate length.

HOLOTYPE. — A trunk-shield, V4425.3 (K.-J. CHANG 1978, pl. 25, 5)

NEW MATERIAL. — Several detached trunk-shield plates from the Xishancun Formation, V10500; several PMD plates from the Xitun Formation, V10508.

LOCALITY AND HORIZON. — Qujing, Yunnan, Xitun Formation, Early Devonian.

REMARKS. — *P. cuifengshanensis*, characterized by its ball-shaped posterior process of the PMD plate, was erected by K.-J. CHANG (1978) on the basis of the material from the Xitun Formation, Qujing, Yunnan. This species is also found in the underlying Xishancun Formation (see below). The material of *P. cuifengshanensis*

from the Xitun Formation has already been studied in detail by G.-R. ZHANG (1978). However, since the posterior process of the PMD plate is the defining character for the species, its variations should be described.

Since the posterior process of *Phymolepis* is a fairly variable structure as seen in *P. cuifengshanensis*, the length/breadth index of the PMD plate is easily biased and this index is hard to be used for comparisons. The length/breadth index of the PMD plate proper is proposed here as a substitute. The portion of the PMD plate proper is the extent in front of the level of the posterolateral corners. This region corresponds to the plate portion which is in contact with the adjoining plates.

DESCRIPTION

Material from the Xishancun Formation (Fig. 11, pl. IV, 1-9)

The new material includes detached PMD, ADL, AVL, PDL, PL and PVL plates. The assignment of the PMD plate is unequivocal since it bears the typical posterior process and distinct median dorsal ridge. The other plates are more or less similar to those of *Y. porifera* from the same horizon, however, the plates referred to *P. cuifengshanensis* are evidently larger than those of *Y. porifera* which is a small-sized antiarch as seen above. At least AVL and PVL plates could not belong to *Y. chii* which has a large MV plate. They are distinguished from the plates of *Liaoguolepis* by the presence of the CHANG's apparatus and ventrolateral fossa.

The PMD plate (Fig. 11B, C, pl. IV, 2-4) bears a distinct median dorsal ridge (dmr, Fig. 11C) and posterolateral ridges (plr, Fig. 11C), like that of *P. cuifengshanensis* from the Xitun Formation. The median dorsal ridge ends at the posterior dorsal angle (pda, Fig. 11C), which forms a conspicuous dome. The posterolateral ridges and grooves (plr, plg, Fig. 11C) extend laterally from the posterior dorsal angle to the lateral margins. Behind the posterior dorsal angle and posterolateral grooves, there is a well-developed posterior process (pr.p, Fig. 11C), which is more or less rounded, about one third the length of the plate, and apparently larger than that of *Yunnanolepis* and *Chuchinolepis*. The lateral corners are poorly preserved. However, the posterolateral corners (plc, Fig. 11B, C) are conspicuous. The length/breadth index of the proper portion is about 100, a little larger than that of *P. cuifengshanensis* in the Xitun Formation, however smaller than that of *P. guoruii*.

In visceral view, the posterior ventral process and pit (prv2, pt2, Fig. 11B) are well-developed in the centre. The area in front of the process is thickened, as it represents the position of the *crista transversalis interna posterior* (cr.tp, Fig. 11B). Along the anterior and lateral margins are the overlap areas for the AMD and PDL plates (cf.AMD, cf.PDL, Fig. 11B).

The ADL plate (Fig. 11A, pl. IV, 1) consists of dorsal and lateral laminae (dlm, llm, Fig. 11A), forming an angle of about 160° at the dorsolateral ridge (dlr, Fig. 11A). The dorsal lamina has a broad anterior margin, which is about three quarters of the plate length and three times the posterior margin breadth. In anterior view, the transverse articular fossa (f.art, Fig. 11A) is situated beneath the anterior margin of the dorsal lamina. The plate is overlapped by the AMD plate along its mesial margin (oa.AMD, Fig. 11A). The main lateral-line groove (lcg, Fig. 11A) extends just below the dorsolateral ridge. The lateral lamina becomes deeper towards the posterior end. The ridge caused by the CHANG's apparatus (r.Chang, Fig. 11A) is seen on the surface, near the anterior extremity. The notch for the opening of the CHANG's apparatus (Ca.o, Fig. 11A) is situated at the ventral margin of the lateral lamina.

The PDL plate (Fig. 11D, pl. IV, 5) is represented by an internal mould, which has the dorsal and lateral laminae with a fairly blunt angle (dlm, llm, Fig. 11D). The plate has a

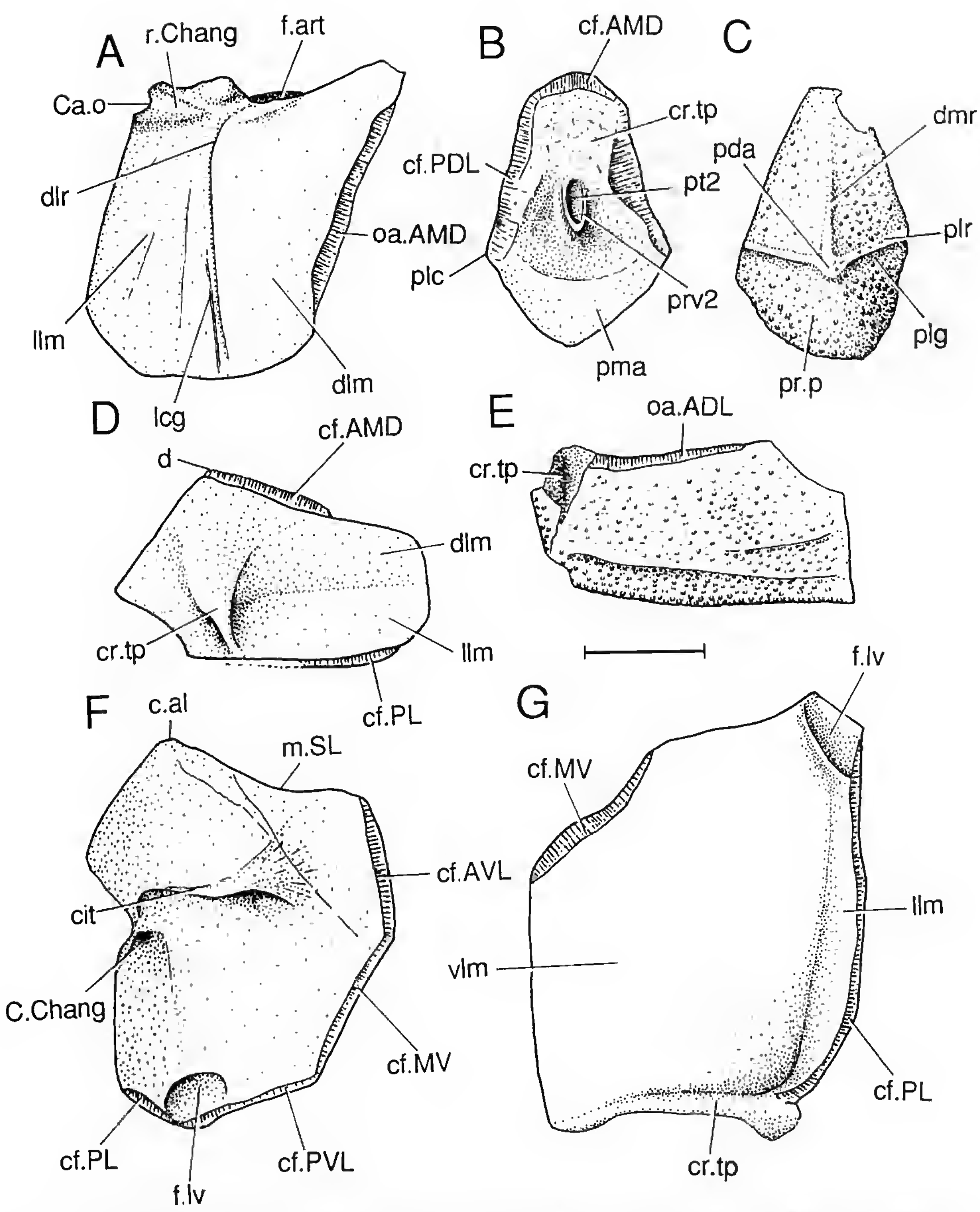


FIG. 11. — *Phymolepis cuifengshanensis* K.-J. Chang, Xishancun Formation, Qujing. All specimens are elastomer casts. A, left ADL plate in dorsolateral view, V10500.2; B-C, PMD plate in visceral (B) and dorsal (C) views, V10500.1; D, left PDL plate in visceral view, V10500.3; E, right PL plate in external view, V10500.4; F, left AVL plate in visceral view, V10500.5; G, right PVL plate in visceral view, V.10500.6. (Scale bar 5 mm.)

conspicuous dorsal corner (d, Fig. 11D), in front of which is the overlap area for the AMD plate (oa.AMD, Fig. 11D). It overlaps the PL plate along its ventral margin. The *crista transversalis interna posterior* (cr.tp, Fig. 11D) is seen to extend from the lateral lamina, where it is sharp, to the area near the dorsal corner where it becomes less distinct.

The PL plate (Fig. 11E, pl. IV, 6) is the same as that of *P. cuifengshanensis* from the Xitun Formation (G.-R. ZHANG 1978). It is relatively high in comparison with that of *Remigolepis* and *Stegolepis*, and the anterior portion is higher than the posterior portion. It is overlapped by the PDL plate along its dorsal margin (oa.PDL, Fig. 11E). The *crista transversalis interna posterior* (cr.tp, Fig. 11E) is developed close to the posterior end of the plate.

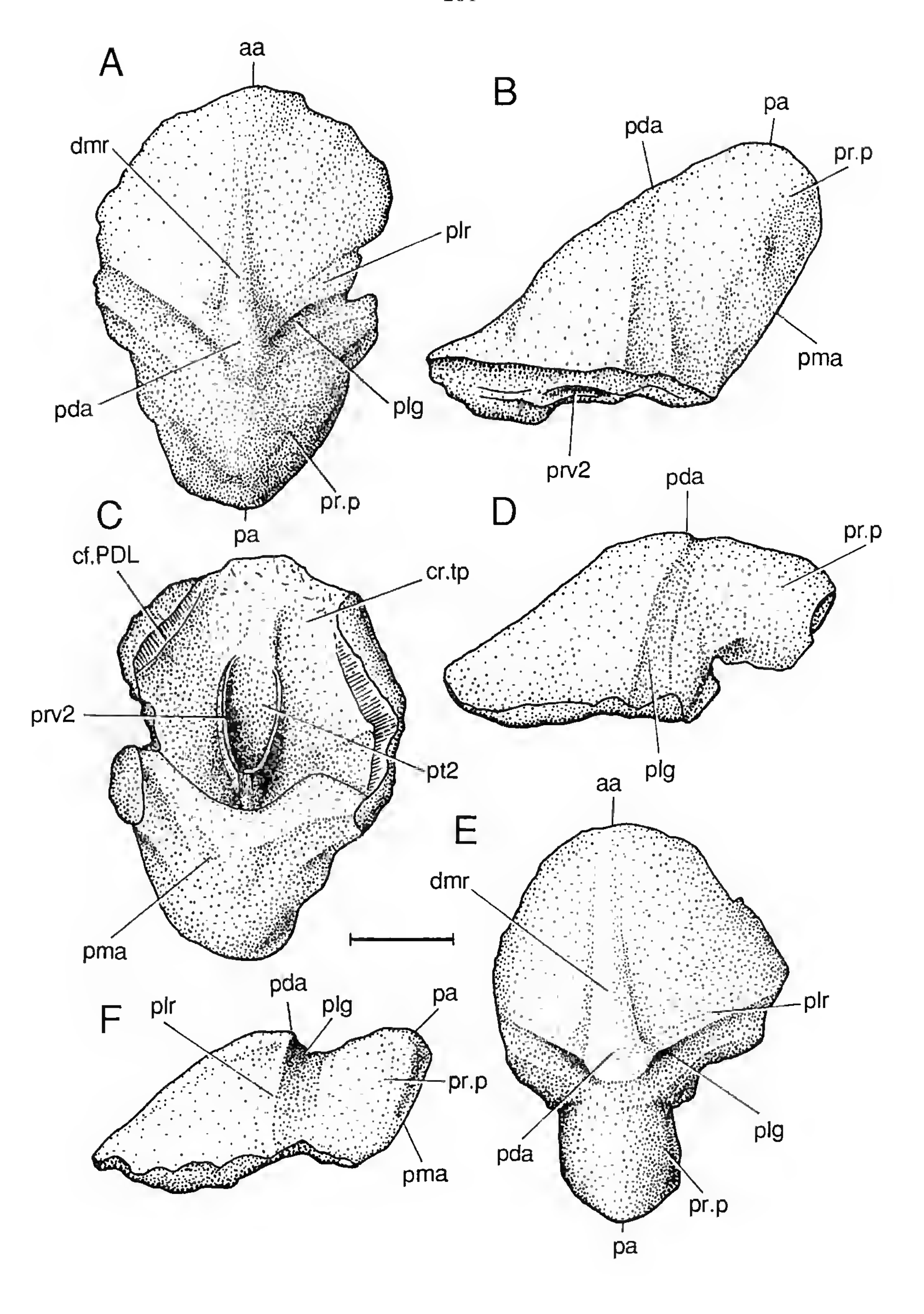
The AVL plate (Fig. 11F, pl. IV, 7-8) is exemplified by an internal mould. The plate is composed of ventral and lateral laminae, forming an almost right angle in visceral view. Posteriorly, the plate thickens to form a depression which is part of the ventrolateral fossa (f.lv, Fig. 11F). The *crista transversalis interna anterior* (cit, Fig. 11F) extends mesially on the relatively broad ventral lamina. The oblique mesial margin behind the anterolateral corner (c.al, Fig. 11F) is relatively long and straight. The overlap area for the MV plate (cf.MV, Fig. 11F) is comparably short. Since the plate under description is a left AVL plate, it bears the overlap area along its mesial margin for the right AVL plate (cf.AVL, Fig. 11F). The anterior part of the lateral lamina displays the wall of the CHANG's apparatus (C. Chang, Fig. 11F). The overlap areas for the PL and PVL plate are seen along its posterior margin (cf.PL, cf. PVL, Fig. 11F).

The PVL plate (Fig. 11G, pl. IV, 9) is also an internal mould, showing its visceral surface. Its anterior extremity bears a depression which forms part of the ventrolateral fossa (f.lv, Fig. 11G). The lateral lamina (llm, Fig. 11G) is fairly low at its anterior end, and gets slightly higher posteriorly. Along its dorsal margin is the overlap area for the PL plate (cf.PL, Fig. 11G). The ventral lamina is relatively broad, as that of the AVL plate, and the overlap area for the MV plate (cf.MV, Fig. 11G) is short. The *crista transversalis interna posterior* (cr.tp, Fig. 11G) lies very close to the posterior extremity of the plate.

Material from the Xitun Formation (Fig. 12, pl. I, 8-10)

Some detached PMD plates from the Xitun Formation are described to show variation in the posterior process. In external view, the PMD plate bears a distinctive median dorsal ridge and posterolateral ridges (dmr, plr. Fig. 12). The median dorsal ridge forms a relatively large angle with the contact margin plane of the plate. In V10508.2, this angle reaches about 45° (Fig. 12B). From the anterior margin of the plate, the median dorsal ridge stretches posteriorly to the posterior dorsal angle (pda, Fig. 12), which in general forms a conspicuous dome. The posterolateral ridges, as well as the posterolateral groove (plg, Fig. 12) behind them, extend laterally from the posterior dorsal angle to the lateral margins, slightly in front of the posterolateral corners. The length/breadth index of the proper portion of the plate is less than 100.

FIG. 12. — *Phymolepis cuifengshanensis* K.-J. Chang, Xitun Formation, Qujing. A-C, PMD plate in dorsal (A), lateral (B) and visceral (C) views, V10508.2; D-E, PMD plate in lateral (D) and dorsal (E) views, V10508.3; F, PMD plate in lateral view, V10508.1. (Scale bar 5 mm.)


A
aa
dmr
plr
pda
plg
pr.p
pa
B
pa
pda
pr.p
pma
prv2
C
cf.PDL
cr.tp
prv2
pt2
pma
D
pda
pr.p
plg
E
aa
dmr
plr
pda
plg
pr.p
pa
F
plr
pda
plg
pa
pr.p
pma

Behind the posterior dorsal angle is the well-developed posterior process (pr.p, Fig. 12), which is quite variable in shape as described below.

In visceral view, the overlap areas for PDL plates (cf.PDL, Fig. 12C) extend along the lateral margins, which form a contact margin plane together with the anterior margin. The posterior ventral process and pit (prv2, pt2, Fig. 12C) are strongly developed in the centre, and elongated in shape. The *crista transversalis interna posterior* (cr.tp. Fig. 12C) lies in front of the posterior ventral process.

The posterior process is quite variable, in both size and shape. Its length is about one third to two fifths of the plate length. In general, it has a rounded arched dorsal face and a flat ventral face (G.-R. ZHANG 1978, Fig. 10). The tubercles on the ventral face, *i.e.* of the posterior marginal area (pma, Fig. 12B, C, F), are much smaller than those on the dorsal face. In V10508.4, the dorsal lamina with larger tubercles bends toward the ventral face to form three small triangular lobes at the posterior end of the process. V10508.1 has the posterior end of the process raised (Fig. 12F). V10508.2 is remarkable by its swollen posterior process (pr.p, Fig. 12A, B), which extends posteriorly along the direction of the median dorsal ridge, and the lack of distinct limit between its dorsal and ventral faces. In contrast, V10508.3 has a cylindrical, and more or less slender posterior process (pr.p, Fig. 12D), which forms a conspicuous bend with the median dorsal ridge.

Phymolepis guoruii n. sp.
(Figs 13-14; pl. V)

DIAGNOSIS. — *Phymolepis* in which the tergal angle of the AMD plate forms a low cockscomb-shaped ridge; proper portion of the PMD plate with L/W index between 130 and 150; median dorsal ridge behind the tergal angle sharp.

ETYMOLOGY. — After Dr G.-R. ZHANG, Beijing.

HOLOTYPE. — A trunk-shield, V10509.1 (Fig. 13, pl. V, 1-3).

OTHER MATERIAL. — A trunk-shield (V10509.2) and several AMD or PMD plates, V10509.3-9.

LOCALITY AND HORIZON. — Qujing, Yunnan, Xitun Formation, Early Devonian.

REMARKS. — This new species resembles very much *P. cuifengshanensis* by its strong posterior process of the PMD plate and the conspicuous median dorsal ridge between the tergal and posterior dorsal angles. It is distinguished from *P. cuifengshanensis* mainly by the following three characters :

1) the AMD plate of *P. guoruii* forms a low cockscomb-shaped crest at its tergal angle, whereas the tergal angle of *P. cuifengshanensis* is just a simple rise;

2) the median dorsal ridge of this new species is fairly sharp;

3) the proper portion of the PMD plate in *P. guoruii* is relatively long and narrow, with the L/W index between 130 and 150, whereas it is less than 100 in *P. cuifengshanensis*.

DESCRIPTION

The available specimens of *P. guoruii* include two trunk-shields and several detached AMD or PMD plates. No skull-roof plate is referred to this new species. The holotype is a relatively complete trunk-shield, although its left half is distorted and the PMD plate is missing. V10509.2 (pl. V, 4) is an almost undistorted trunk-shield, but unfortunately, its bones in the ventral and lateral walls have been partly eroded in the internal mould. In overall aspect, the trunk-shield

of *P. guoruii* resembles very much that of *P. cuifengshanensis*. Its dorsal wall is slightly narrower than its ventral wall, and the lateral wall is comparatively high. The dorsolateral and ventrolateral ridges are fairly conspicuous. Moreover, it retains the separate AL plate which shelters the opening of the CHANG's apparatus. However, it differs from *P. cuifengshanensis* in possessing a low cockscomb-shaped crest at its tergal angle. Between the tergal and posterior dorsal angles, its median dorsal ridge is sharper than that of *P. cuifengshanensis*. Although the PMD plate is absent in these two articulated trunk-shields, several detached PMD plates are assigned to this new species by the sharp median dorsal ridge and the long contact margin for the PMD plate on the PDL plate. *P. guoruii* bears the same developed posterior process of the PMD plate as *P. cuifengshanensis*, however, its proper portion of the PMD plate is relatively long and narrow in contrast with that of the latter.

The AMD plate is well preserved in V10509.2 (pl. V, 4), whereas in the holotype (Fig. 13A, pl. V, 1) its posterior portion is partly damaged. The AMD plate has the similar shape as that of *P. cuifengshanensis*. Its anterior margin is pointed and the posterior margin is fairly narrow. The lateral corners are conspicuous and slightly posteriorly located, the anterior portion of the plate being longer than the posterior portion, as in *P. cuifengshanensis*. In dorsal view, the plate is arched by its elevated tergal angle which is situated slightly behind the level of the lateral corners. The very peculiar tergal angle (dma, Figs 13A, 14D-F), is a low cockscomb-shaped crest which is bordered by an elongated U-shaped ridge. This ridge is ornamented by slightly larger tubercles and encircles a central space of the tergal angle which is almost devoid of tubercles. This central space is flat in its anterior part, which is continuous with the area anterior to it, and is slightly expanded laterally in the posterior direction. This space is a little arched in its posterior part to form a summit. The U-shaped ridge of the tergal angle prolongs posteriorly to form the sharp median dorsal ridge (dmr, Fig. 14F, pl. V, 4) on the AMD plate. Two AMD fragments of *P. guoruii* have been found in the collection, characterized by their specialized tergal angles (dma, Fig. 14D, F). They correspond to the posterior half of the cockscomb-shaped crest seen in the holotype and V10509.2. In visceral view, the elongated anterior median process and pit (prv1, pt1, Fig. 14E, G), and part of the median ventral ridge (mvr, Fig. 14G) in front of them are visible.

The PMD plate is represented by several detached specimens. As in *P. cuifengshanensis*, it has the conspicuous posterior dorsal angle (pda, Fig. 14A-B), and the developed posterior process (pr.p, Fig. 14A-B) behind the angle. From the posterior dorsal angle radiate three ridges, one is the median dorsal ridge (dmr, Fig. 14A-B) prolonged from the AMD plate, while the others are the posterolateral ridges (plr, Fig. 14A-B) extending to the lateral margins near the posterolateral corners. The posterior process is arched on the dorsal surface and somewhat flattened ventrally (pma, Fig. 14C), and occupies about one third of the plate length. The proper portion of the plate is different from that in *P. cuifengshanensis*. Firstly, it is somewhat narrow and elongated in shape. The L/W index is between 130 and 150, whereas that in *P. cuifengshanensis* is less than 100. Secondly, the median dorsal ridge in the new species is sharper than that in the latter. In visceral view, the overlap areas for PDL plates are observed along the lateral margins. The anterior margin is fractured off. In the middle, the elongated posterior ventral process and pit (prv2, pt2, Fig. 14C) are developed as in *P. cuifengshanensis*. In front of them, the plate is thickened to form the *crista transversalis interna posterior* (cr.tp, Fig. 14C).

The ADL plate has a distinct dorsolateral ridge (dlr, Fig. 13A). As in other yunnanolepids, its dorsal lamina has a broad anterior margin. In anterior view, the articular fossa and *crista transversalis interna anterior* are situated beneath the anterior margin. The lateral lamina is fairly high, and the posterior portion is higher than the anterior one. The main lateral-line groove (lcg,

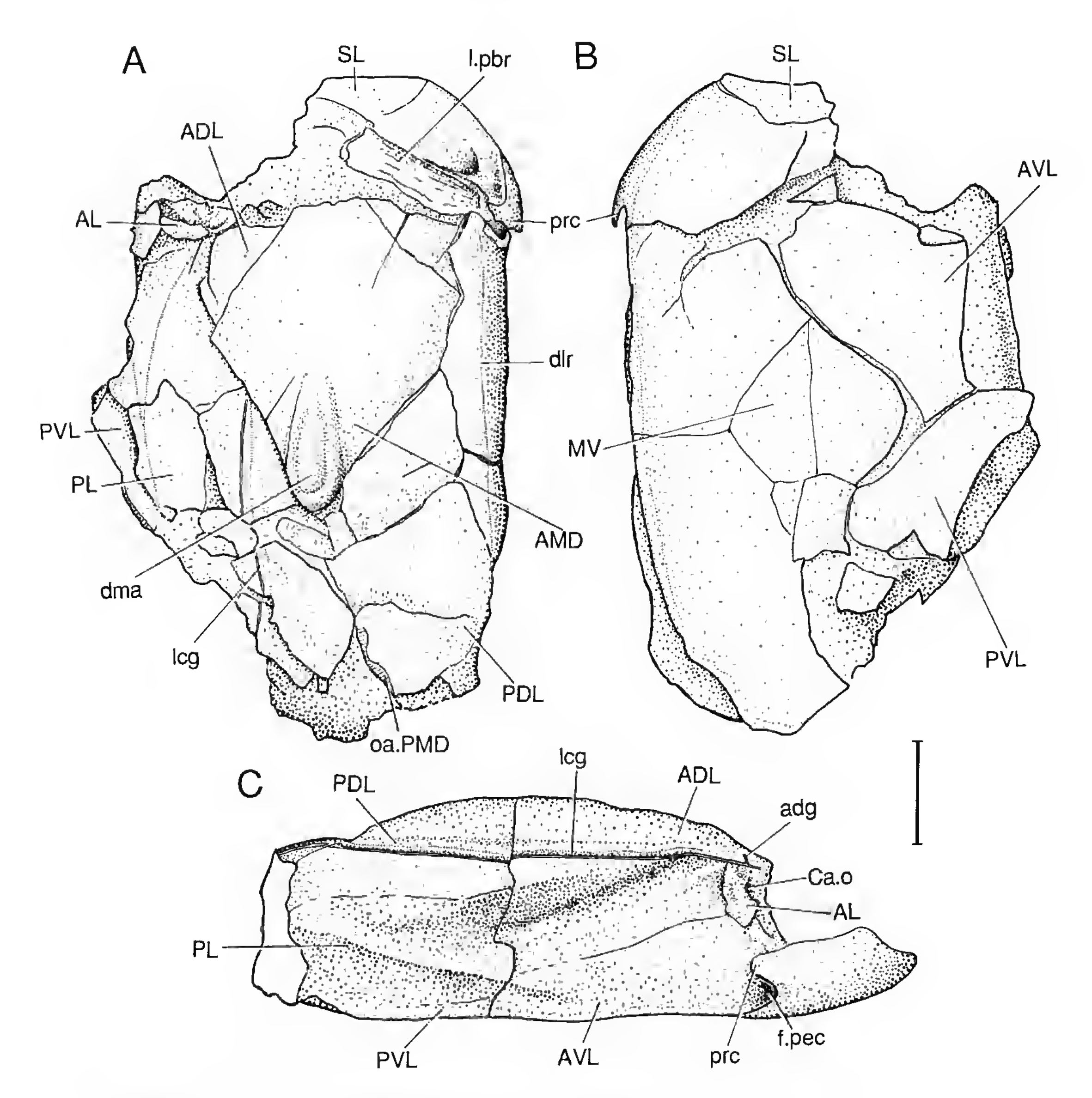


FIG. 13. — *Phymolepis guoruii* n. sp., Xitun Formation, Qujing. Trunk-shield (holotype, V10509.1) in dorsal (A), ventral (B) and lateral (C) views. (Scale bar 10 mm.)

Fig. 13A, C) runs just below the dorsolateral ridge. A short pit line (adg. Fig. 13C) branches off dorsally from the main lateral-line groove near its anterior end, as in *Y. porifera* (M.-M. ZHANG 1980, Fig. 3). The region of the lateral lamina near its anterior extremity is complicated by the overlapping AL plate. The ADL portion dorsal or posterodorsal to the AL plate seems to be thickened. An oblique ridge lies between the dorsolateral ridge and the AL plate, and diminishes posteriorly. The opening of the CHANG's apparatus (Ca.o. Fig. 13C) is hidden by the overlying AL plate and cannot be directly seen from the outside.

The AL plate (Fig. 13A, C) is a small plate, adjacent to the anterior extremity of the lateral wall of the trunk-shield. However, it does not form the anterior margin of the trunk-shield, as in *Mizia*. It looks like a large node on the lateral wall, across the suture between the ADL and AVL plates, but it is indeed an independent element of the trunk-shield and belongs neither to the ADL plate, nor to the AVL plate. A large part of the AL plate is situated above the ADL plate, and posteriorly forms a fossa between the AL and ADL plates. In anterior view, an even larger fossa is visible between the AL and ADL plates. The opening of the CHANG's apparatus (Ca.o, Fig. 13C) is located in this fossa and is invisible in lateral view.

The AVL plate forms an almost right angle at the ventrolateral ridge. The dorsal margin of the lateral lamina descends posteriorly and the ridge caused by the CHANG's apparatus is faintly seen near its anterior margin (Fig. 13C, pl. V, 3). It bears the typical yunnanolepid pre-pectoral corner (prc, Fig. 13A) and pectoral fenestra. The ventral lamina has a relatively short contact margin for the MV plate, as in *P. cuifengshanensis*. The postbranchial lamina (l.pbr, Fig. 13A) bears many parallel striations, and is a rod-shaped structure which extends anteromesially from near the pectoral fenestra. Immediately behind the postbranchial lamina is the mesially directed *crista transversalis interna anterior*.

The SL plate (Fig. 13A-B) is partly preserved in the holotype. It is broad and trapezoid in shape, intermediate in shape between the SL plates of *Y. chii* and *Y. porifera*.

The PDL plate (Fig. 13A) is well preserved in the right half of the holotype. The dorsal lamina has a distinct dorsal corner, behind which is the relatively long area overlapped by the PMD plate (oa.PMD, Fig. 13A). On the lateral lamina, the main lateral-line groove runs below the well-defined dorsolateral ridge. V10509.2 has preserved the internal mould of the plate, from which the *crista transversalis interna posterior* is inferred to be situated near the posterior end of the plate and extends dorsally close to the suture between the AMD and PMD plate.

The PL plate (Fig. 13C) is relatively high. Along its ventral margin, it is overlapped by the PVL plate. In visceral view, the *crista transversalis interna posterior* lies almost at its posterior end.

The PVL plate (Fig. 13B-C) has a fairly low lateral lamina. Its ventral lamina is similar to that of *P. cuifengshanensis* in having a short contact margin for the MV plate.

The MV plate (Fig. 13B) is a relatively small, rhombic plate. As in *Y. porifera* and *P. cuifengshanensis*, its breadth is smaller than two fifth of the ventral wall breadth of the trunk-shield.

The ornamentation of the trunk-shield consists of fine-grained and closely set tubercles. Along the ridges, and on the region anterior to the pectoral fenestra, the tubercles are slightly larger.

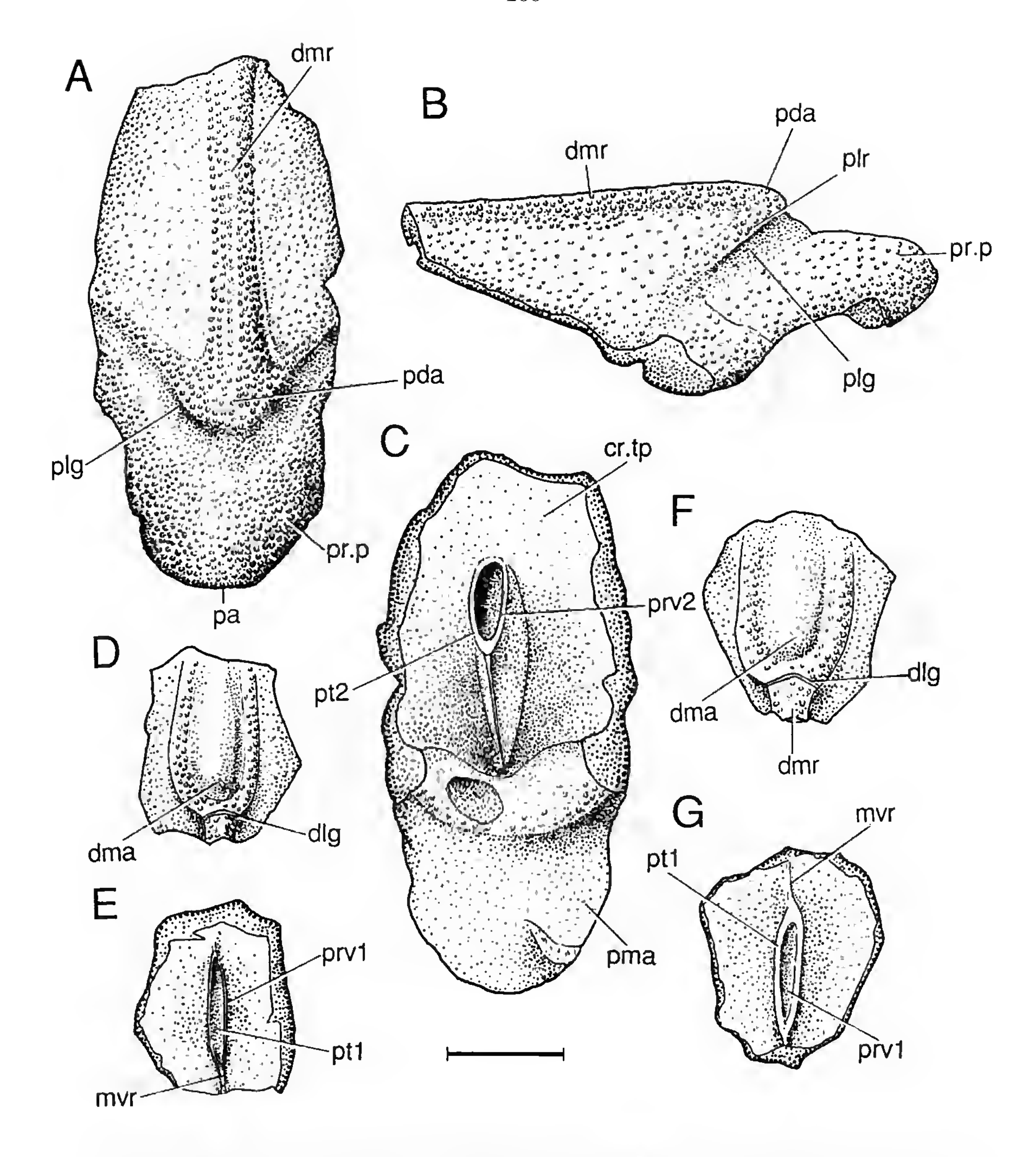


FIG. 14. — *Phymolepis guoruii* n. sp., Xitun Formation, Qujing. A-C, PMD plate in dorsal (A), lateral (B) and visceral views (C), V10509.5; D-E, incomplete AMD plate in dorsal (D) and visceral (E) views, V10509.4; F-G, incomplete AMD plate in dorsal (F) and visceral (G) views, V10509.3. (Scale bar 5 mm.)

Family indet.
Genus **ZHANJILEPIS** G.-R. Zhang, 1978

Zhanjilepis G.-R. Zhang, 1978: 178: figs 18-21, pl. VIII.

Other reference:
Zhanjilepis S.-F. LIU 1992: 216, pl. II, 8-9.

EMENDED DIAGNOSIS. — Same as for the type species (monotype).

TYPE SPECIES. — *Zhanjilepis aspratilis* G.-R. Zhang, 1978.

REMARKS. The genus was erected on the basis of several detached trunk-shield plates (G.-R. ZHANG 1978). The best diagnostic character is its ornamentation. *Zhanjilepis* resembles the Yunnanolepididae in the shape of its AMD plate, the position of the anterior ventral process and pit, and the presence of the ventrolateral fossa. But *Zhanjilepis* differs in the position of the *crista transversalis interna posterior*, which is suggestive of *Chuchinolepis* and *Minicrania* (ZHU & JANVIER 1996). However, as discussed below, the lateral position of the *crista transversalis interna posterior*, relatively to the posterior ventral process, as in *Chuchinolepis*, is a plesiomorphic feature.

Zhanjilepis aspratilis G.-R. Zhang, 1978
(Fig. 15, pl. III, 9-11, IV, 10)

Zhanjilepis aspratilis G.-R. Zhang, 1978: 178, figs 18-21, pl. VIII.

EMENDED DIAGNOSIS. — Yunnanolepidoidei in which the ornamentation is composed of coarse, scattered tubercles.

HOLOTYPE. — An AMD plate (V4427.1) from the Xitun Formation.

NEW MATERIAL. — Detached trunk-shield plates from the Xishancun Formation, including four AMD, an ADL, three PDL and a PVL plates, V10501.1-10.

LOCALITY AND HORIZON. — Qujing, Yunnan, Xishancun Formation and Xitun Formation, Early Devonian.

REMARKS. — Since *Z. aspratilis* was described from the Xitun Formation, Qujing, Yunnan (G.-R. ZHANG 1978), the distribution of *Zhanjilepis*, either stratigraphic or paleogeographic, has not been expanded until S.-F. LIU (1992) reported *Z.* sp. from the Lianhuashan Formation (Early Devonian) of Liujing, Guangxi. Here, *Z. aspratilis* is described from the Xishancun Formation (Lochkovian), the stratigraphic unit underlying the Xitun Formation.

DESCRIPTION

All the specimens referred to as *Z. aspratilis* in the Xishancun Formation are characterized by their coarse tubercle ornamentation, like those in the type horizon, *i.e.*, the Xitun Formation. However, the individual size of the specimens in the Xishancun Formation is definitely smaller than in those from the Xitun Formation.

The AMD plate is similar to that of the Yunnanolepididae and Chuchinolepididae with the pointed anterior end (a, Fig. 15A). Its posterior margin is relatively narrow, and about one fifth of the plate breadth. Its lateral corners (lc, Fig. 15A-B) are noticeable, and the anterior portion of the plate is slightly longer than its posterior portion. When compared with the holotype of *Z. aspratilis*, which is an AMD plate from the Xitun Formation, the AMD plates referred to here are slightly narrower, as in *Y. porifera*. V10501.1 (Fig. 15A-B) has a length/breadth index of about 145, and the index between the anterior and posterior portions is about 128. In external

view, the plate is gently arched with the tergal angle at the level of the lateral corners. The median dorsal ridge is faintly developed behind the tergal angle. In visceral view, the anterior ventral process (prv1, Fig. 15B) is small and situated at the level of the lateral corners, like the tergal angle. Behind it, there is a shallow median ventral groove (grm, Fig. 15B) which diminishes posteriorly. No structure is developed in front of the anterior ventral process. The overlap relationship with adjoining plates is typical of the Yunnanolepidoidei.

The PMD plate is not found in the Xishancun Formation. The re-examination of the plesiotype of Z. *aspratilis* (V4427.3, Fig. 15C), that is a PMD plate found in the Xitun Formation, shows that the *crista transversalis interna posterior* (cr.tp, Fig. 15C) lies lateral to the posterior ventral process and pit (prv2, pt2, Fig. 15C), as in *Chuchinolepis*.

The ADL plate (Fig. 15E) has the same shape as that of Z. *aspratilis* from the Xitun Formation (G.-R. ZHANG 1978). The plate is subdivided into the dorsal and lateral laminae by the dorsolateral ridge (dlr, Fig. 15E). The dorsal lamina has the broad anterior margin, below which there is the transverse articular fossa. Along its dorsal margin is the area overlapped by the AMD plate (oa.AMD, Fig. 15E). The lateral lamina descends posteriorly. The main lateral-line groove runs just below the dorsolateral ridge.

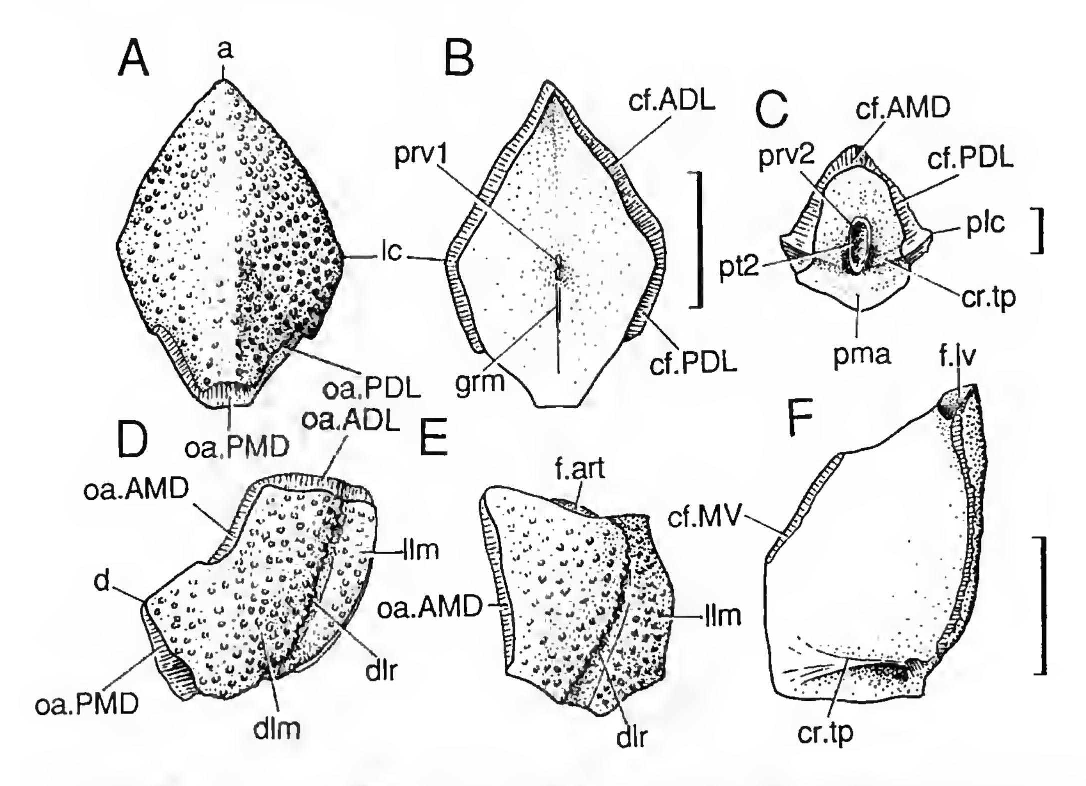


FIG. 15. — *Zhanjilepis aspratilis* G.-R. Zhang, Xishancun Formation (A-B, D-E) and Xitun Formation (C), Qujing. A-B, AMD plate in dorsal (A) and visceral (B) views (elastomer casts), V10501.1; C, PMD plate in visceral view, V4427.3; D, right PDL plate in dorsal view (elastomer cast), V10501.7; E, right ADL plate in dorsal view (elastomer cast), V10501.6; F, right PVL plate in visceral view (elastomer cast), V10501.5. (Scale bar 5 mm.)

The PDL plate (Fig. 15 D, pl. III, 9) also has dorsal and lateral laminae. The dorsal lamina (dlm, Fig. 15D) is relatively long and narrow, with a dorsal corner (d, Fig. 15D) which separates the dorsal margin into two portions. Along the anterior portion of the dorsal margin, the plate is overlapped by the AMD plate anteriorly (oa.AMD, Fig. 15D) and overlaps the AMD plate posteriorly. The plate is overlapped by the PMD plate (oa.PMD, Fig. 15D) behind the dorsal corner. The lateral lamina is fairly long and low, with the main lateral-line groove running below the dorsolateral ridge (dlr, Fig. 15D). Along its ventral margin, there is an area which is overlapped by the PL plate. This overlap area is less developed in its anterior part. Along its anterior margin, the PDL plate is overlapped by the ADL plate.

The lateral lamina of the PVL plate (Fig. 15F, pl. IV, 10) is partly observed in the specimen, showing a granular ornamentation. The ventral lamina has its anterior margin extending anterolaterally. In visceral view, the overlap area for the MV plate (cf.MV, Fig. 15F) is relatively short. At the anterior end of the ventrolateral ridge, the plate has a depression which is part of the ventrolateral fossa of the trunk-shield (f.lv, Fig. 15F). The *crista transversalis interna posterior* (cr.tp, Fig. 15F) lies close to the posterior extremity of the plate and becomes higher laterally.

Genus **HETEROYUNNANOLEPIS** Z.-S. Wang, 1994

Heteroyunnanolepis Z.-S. Wang, 1994: 21, fig. 1, pls I, II.

Emended diagnosis. — Yunnanolepidoidei in which the head-shield has a large semicircular preorbital recess instead of the preorbital depression; infraorbital sensory canal passing through the postmarginal plate; ADL plates of both sides with a short suture in front of the AMD plate; large MV plate with the anterior portion shorter than the posterior portion; trunk-shield fairly broad and low.

Type species. — *Heteroyunnanolepis qujingensis* Wang, 1994.

Remarks. — *Heteroyunnanolepis* differs from the Yunnanolepididae in its large semicircular preorbital recess, the absence of the preorbital depression, the path of the infraorbital sensory canal through the postmarginal plate, and the position of the *crista transversalis interna posterior*, which is lateral to the posterior ventral process and pit. The diagnostic character of the Yunnanolepididae is that the *crista transversalis interna posterior* bends anteriorly on the visceral surface of the PMD plate, and passes clearly in front of the posterior ventral process and pit. As to the relative size of the MV plate, *Heteroyunnanolepis* resembles *Y. chii*. However, a large MV plate is most likely to be plesiomorphic. Moreover, the MV plate of *Heteroyunnanolepis* has the posterolateral margin longer than the anterolateral margin, whereas the MV plate of the Yunnanolepididae, including *Y. chii*, is generally rhombic in shape. *Heteroyunnanolepis* resembles *Y. deprati* and *Zhanjilepis* by the lack of crests, ridges or humps usually seen in the external surface of the PMD plate in other yunnanolepidoids. *Heteroyunnanolepis* is suggestive of *Vanchienolepis* (Tong-Dzuy & Janvier 1990) by the joining of the ADL plates of both sides in front of the AMD plate. However, these two genera differ definitely in many other characters. *Vanchienolepis* lacks the MV plate and has a derived pectoral joint structure. The AMD plate of *Heteroyunnanolepis* is similar to that of the Yunnanolepididae and *Zhanjilepis* in shape, whereas the AMD plate of *Vanchienolepis* has a relatively short anterolateral margin and its tergal angle is anteriorly placed.

Heteroyunnanolepis qujingensis Z.-S. Wang, 1994
(Figs 16-17, pls VI, VII)

Diagnosis. — *Heteroyunnanolepis* in which the dorsolateral ridge of the trunk-shield is less developed; a round pit is present on the surface of the PMD plate; the posterior dorsal sensory-line groove extends from the PDL plate to the PMD plate.

HOLOTYPE. — External mould of a head-shield, V10113 (Z.-S. WANG 1994, pl. 1A).

NEW MATERIAL. — A complete trunk-shield, V10502.1 (Fig. 16A, pls VI, 1-2, VII, 1-2), an AMD (V10502.2), an AVL (V10502.3), a PVL (V10502.4) and a MV (V10502.5) plates.

LOCALITY AND HORIZON. — Qujing, Yunnan, Xishancun Formation, Early Devonian.

REMARKS. — It is likely that *Yunnanolepis meemannae* (TONG-DZUY & JANVIER 1994) should be referred to *Heteroyunnanolepis*. This antiarch (the only specimen) was found from the lower part of the Bac Bun Formation of Vietnam (Pragian in age). It resembles *H. qujingensis* in the relatively low and broad trunk-shield and the PMD plate which is devoid of crests, ridges and humps. Both species have the posterior margin of the trunk-shield moderately curved and lack the pronounced posterior dorsal angle. According to personal observations, the PMD plate of *Yunnanolepis meemannae* has the *crista transversalis interna posterior* situated lateral to the posterior ventral process, as in *H. qujingensis* and *Zhanjilepis*, that is quite different from the condition in the Yunnanolepididae. As far as the available information, *Yunnanolepis meemannae* differs from *H. qujingensis* in the following characters :

1) *Y. meemannae* has a conspicuous dorsolateral ridge whereas *H. qujingensis* lacks this ridge, like *Y. deprati*;

2) the posterodorsal sensory-line groove in *Y. meemannae* is a short groove restricted to the PDL plate as in *Yunnanolepis* and *Chuchinolepis* (TONG-DZUY & JANVIER 1990), whereas that of *H. qujingensis* extends dorsally to the PMD plate;

3) *H. qujingensis* has a rounded pit on the surface of the PMD plate.

DESCRIPTION

V10502.1 (Figs 16A, 17) is a medium-sized trunk-shield, almost completely preserved as an internal mould (pl. VII, 2). The external mould shows only the dorsal and lateral walls (pl. VII, 1), from which the bone fragments have been removed for latexing (pl. VI, 1). The specimen was flattened during fossilization, however, the low trunk-shield can be inferred from the positions of the dorsolateral and ventrolateral ridges. The dorsal wall of the trunk-shield is gently arched, more or less square-shaped, with both the length and width of about 5 cm. There is no median dorsal ridge. The ADL plates of both sides join in front of the AMD plate, which is situated about 5 mm behind the anterior margin of the dorsal wall. The posterior margin of the dorsal wall does not form a conspicuous posterior process as in *Yunnanolepis chii*, resembling somewhat *Y. deprati* (TONG-DZUY & JANVIER 1990, Fig. 10). The flat ventral wall is just a little longer than the dorsal wall. The MV plate occupies a fairly large area. The ornamentation consists of densely distributed, small tubercles.

The AMD plate of *H. qujingensis* (Fig. 16A) is similar to that of *Y. chii* (G.R. ZHANG 1978) in shape and size. The AMD plate of V10501 has a length/width index of about 124, whereas the isolated AMD plate (V10502.2, Fig. 16B) is a little smaller and has a length/width index of about 150, as the AMD plate of *Y. chii*. The plate has a very narrow anterior margin. The lateral corners are conspicuous, and the anterolateral and posterolateral margins are of about same length. The overlap relationships with the adjoining plates are just the same as those of the Yunnanolepididae. The posterior margin is straight and not as narrow as that of the Yunnanolepididae. In external view, the plate is gently arched and does not show the median dorsal ridge or the median elevation as in *Y. chii*. The arched point is at the level of the lateral corners, resembling those of the Yunnanolepididae and *Zhanjilepis*. In visceral view, the anterior ventral process (prv1, Fig. 16A) and pit (pt1, Fig. 16B) are situated just beneath the arched point of the plate. In front of the anterior ventral process, a conspicuous median ventral ridge (mvr, Fig. 16A, B) extends forwards to the anterior margin of the plate. In V10501.1 (Fig. 16A), the less pronounced median ventral ridge, as in *Y. chii*, extends from the anterior ventral process

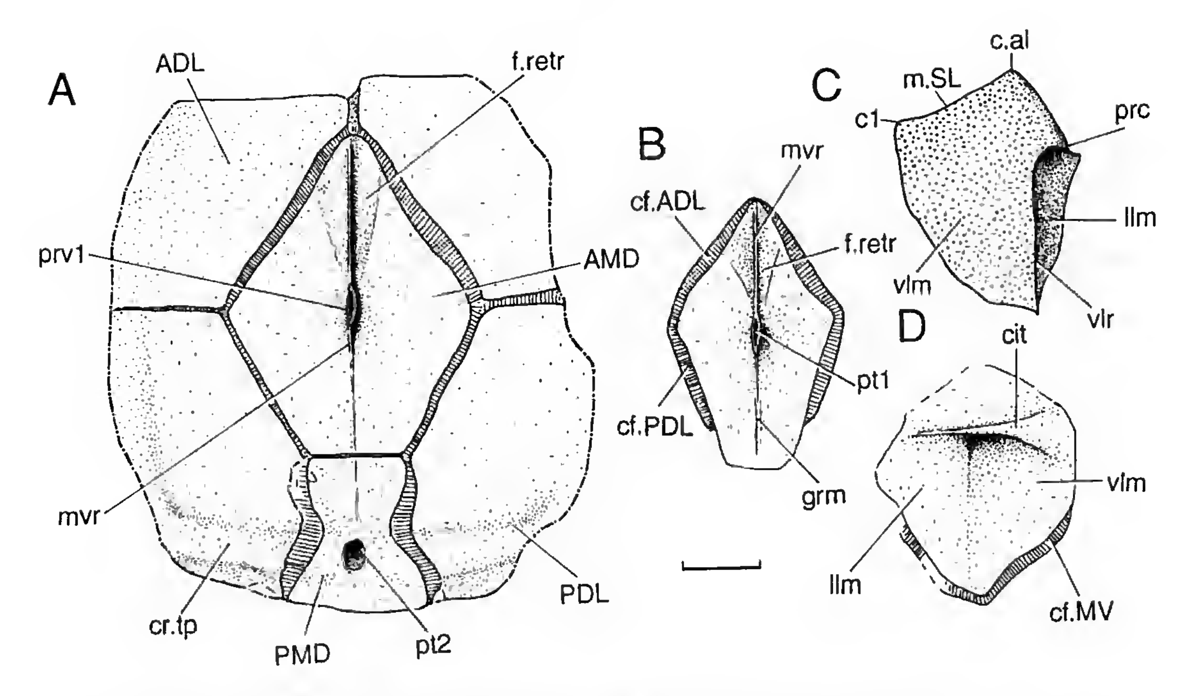


FIG. 16. — *Heteroyunnanolepis qujingensis* Z.-S. Wang, Xishancun Formation, Qujing. A, dorsal and lateral walls of the trunk-shield (holotype, V10502.1) in visceral view (elastomer cast); B, AMD plate in visceral view (elastomer cast), V10502.2; C-D, left AVL plate in external (C) and visceral (D) views (elastomer casts), V10502.3. (Scale bar 10 mm.)

to the posterior ventral process of the PMD plate. However, individual variation exists in V10502.2. In this AMD plate, the median ventral ridge behind the anterior ventral process is very short, and behind the ventral ridge is a long median ventral groove (grm, Fig. 16B), as in *Bothriolepis*. In the anterior portion of the plate, the levator fossa (f.retr, Fig. 16B) is subdivided into two parts by the median ventral ridge. Behind the levator fossa are the postlevator thickenings. The levator fossa and postlevator thickenings are widely distributed in euantiarchs, however, they are generally less developed in yunnanolepidoids (G.-R. ZHANG 1978).

The PMD plate (Figs 16A, 17) is more or less trapezoid in shape since its posterior margin does not project posteriorly to form a prominent posterior corner. The plate is relatively broad, and has a length/breadth index smaller than 100. The anterior margin, overlapping the AMD plate, is slightly convex. The lateral margin is slightly concave and overlaps the ADL plate. On its external surface, there is no ridge or elevation, but instead, a pit (p.PMD, Fig. 17A, C) is seen in the mid-line, corresponding to the position of the posterior ventral process. Behind this pit there is a pair of sensory-line grooves (pdg, Fig. 17A, C) extending laterally to the PDL plates. The groove is parallel to the posterior margin of the dorsal wall. In visceral view, the posterior ventral process and pit (pt2, Fig. 16A) are relatively large and occupy a fairly posterior position. In front, there is a low median ventral ridge (mvr, Fig. 16A). The *crista transversalis*

interna posterior (cr.tp, Fig. 16A) is lateral to the posterior ventral process and pit, as in *Zhanjilepis* and *Chuchinolepis*.

The much flattened ADL plates of the holotype is relatively short and broad, similar to that of *Y. bacboensis* (TONG-DZUY & JANVIER 1990). The main lateral-line groove (lcg, Fig. 17A) runs through the plate rostrocaudally, but disappears in the posterior portion of the plate. The dorsolateral ridge is invisible, and its approximate position could be inferred from the main lateral-line groove (lcg, Fig. 17A), which generally lies close to the ridge. The plate has a relatively broad dorsal lamina and a low lateral lamina, as inferred from the relatively low position of the groove. In *Yunnanolepis*, the dorsolateral ridge of the ADL plate, as well as the main lateral-line groove, has a dorsal or middle position, corresponding to the comparatively high trunk-shield. A short pit-line groove (adg, Fig. 17A) diverges from the lateral-line groove in the anterior part of the plate, as in *Y. porifera*.

The dorsal lamina of the ADL plate has a fairly broad anterior margin. The articular fossa and *crista transversalis interna anterior* are not preserved in the specimen. Since the ADL plates of both sides join in front of the AMD plate by a short suture, the plate has an additional anteromesial margin which was also seen in *Vanchienolepis* (TONG-DZUY & JANVIER 1990). The ADL plate is overlapped by the AMD plate, and overlaps the PDL and PL plates. The ventral margin of the low lateral lamina is more or less parallel to the main lateral-line groove.

The PDL plate is as flattened as the ADL plate. The faint dorsolateral ridge is seen in the posterior portion of the plate. As in *Yunnanolepis*, its dorsal lamina is fairly broad and its lateral lamina very low. The main lateral-line groove (lcg, Fig. 17A, C) reappears in the posterior portion of the plate, and lies closely below the faded dorsolateral ridge. Immediately in front of the posterior margin of the plate, an additional sensory-line groove (pdg, Fig. 17A, C) extends from the main sensory-line groove to the PMD plate. The dorsal lamina has a distinct dorsal corner, where the plate gets its maximum breadth. The anterior margin of the plate is somewhat concave and the area overlapped by the ADL plate is clearly visible in the holotype. The anterodorsal margin in contact with the AMD plate is slightly longer than the posterodorsal margin, where the plate is overlapped by the PMD plate. The plate is overlapped by the PL plate along its ventral lamina, which bears a shallow notch close to the posterior extremity, as in *Y. chii* (G.-R. ZHANG 1978). The *crista transversalis interna posterior* (cr.tp, Fig. 16A) is as in other yunnanolepidoids.

The PL plate (Fig. 17A) is a very low and long plate. The area overlapping the PDL plate is clearly observed in the holotype, whereas the other contact margins are invisible.

The AVL plate has ventral and lateral laminae separated by the ventrolateral ridge. V10502.3 (Fig. 16C-D) is an almost complete detached AVL plate, and with the aid of the mould, its detailed morphology can be studied. As in the Yunnanolepididae, the plate has a conspicuous prepectoral corner (prc, Figs 16C, 17A). The simple pectoral fenestra can be observed in the external mould of V10502.3 (Fig. 16C). The prepectoral corner is situated at the same level as the corner between the anterior and middle divisions of the mesial margin of the ventral lamina (c_1, Fig. 16C). At the anterior extremity of the plate is the anterolateral corner (c.al, Fig. 16C). From c.al to c_1 extends a long, oblique margin in contact with the semilunar plate (m.SL, Fig. 16C). Even though the semilunar plate is not preserved in the collection, its general shape can be estimated from the AVL plate to be triangular, as in *Y. porifera*, and quite different from

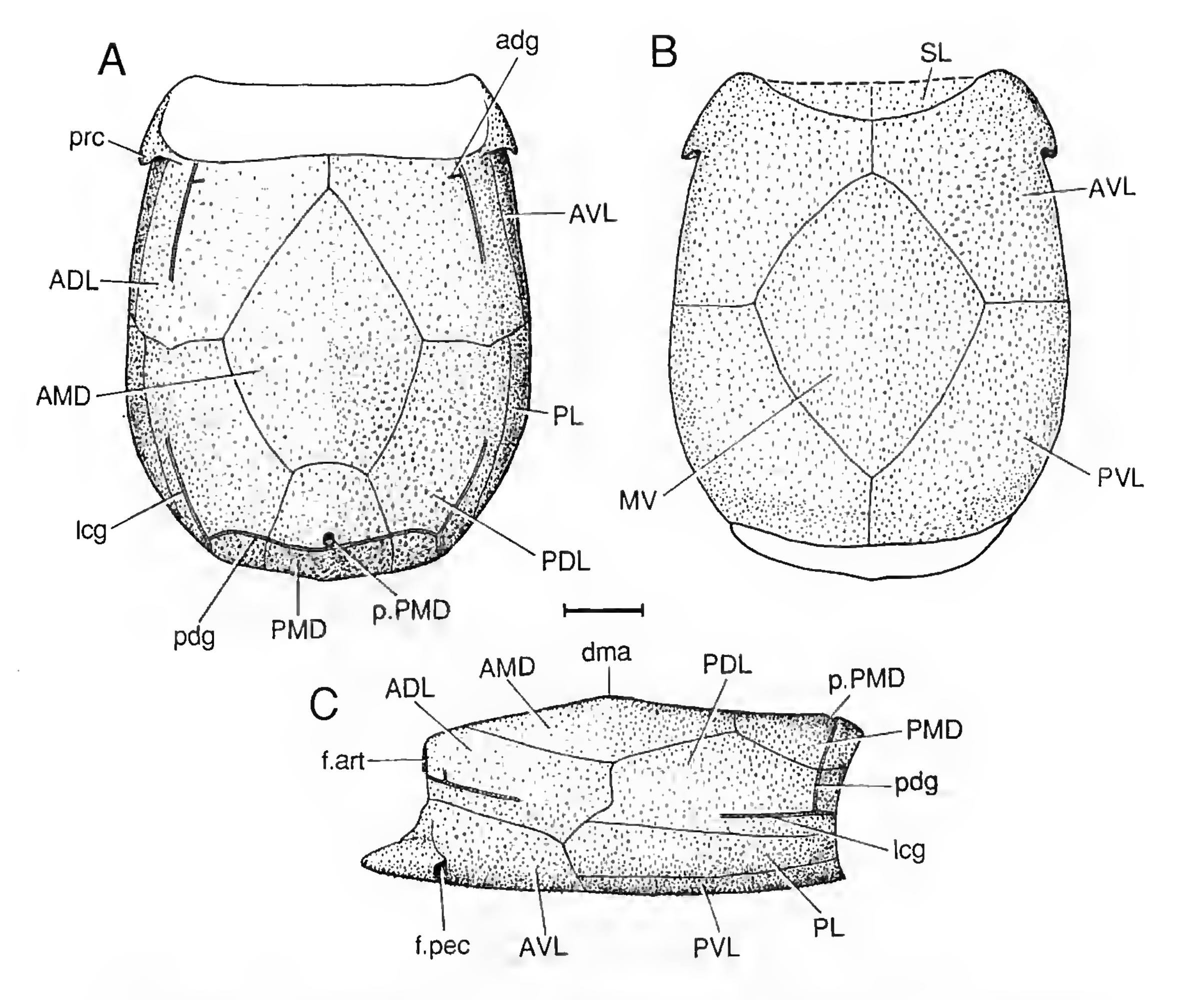


FIG. 17. — *Heteroyunnanolepis qujingensis* Z.-S. Wang, Xishancun Formation, Qujing. Restorations of the trunk-shield (mainly after the holotype, V10501.1) in dorsal (A), ventral (B) and lateral (C) views. (Scale bar 10 mm.)

the rectangular semilunar plate of *Y. chii*. The mesial margin in contact with the AVL plate of the opposite side is relatively short, about two thirds of the length of the whole plate. From V10502.3 is inferred that the right AVL plate overlaps the left one, like in most antiarchs except for *Y. chii* (G.-R. ZHANG, 1978, Fig. 6). The mesial margin in contact with the MV plate is very long, and extends laterally almost to the ventrolateral ridge, as in *Y. chii*. Along this margin, the area overlapping the MV plate is visible (cf.MV, Fig. 16D). The lateral lamina (llm, Fig. 16C, D) is relatively low. Anteriorly, the margin overlapping the ADL plate forms a corner, behind which the margin descends posteriorly. Internally, the *crista transversalis interna anterior* (cit, Fig. 16C) is at the same level as the prepectoral corner. There is no ventrolateral fossa of the trunk-shield along the posterior margin of the plate, unlike in *Yunnanolepis*.

The PVL plate (Fig. 17B, C) is longer than the AVL plate, and also comprises two laminae. The lateral lamina is low, as in the Yunnanolepididae. The ventral lamina has a very long margin in contact with the MV plate, which occupies nearly the two thirds of the plate length. The PVL plates of both sides meet on a relatively short suture. The *crista transversalis interna posterior* lies close to the posterior margin of the plate.

The MV plate (Fig. 17B) is a fairly large plate, like that of *Y. chii*. It occupies about three fifth of the trunk-shield breadth and about two third of the ventral wall length. The plate is overlapped by the AVL plates anteriorly and the PVL plates posteriorly. Since its anterolateral margin is obviously shorter than its posterolateral margin, the MV plate of *Heteroyunnanolepis qujingensis* is not rhombic in shape, which is typical for the MV plate of *Yunnanolepis*.

Family CHUCHINOLEPIDIDAE K.-J. Chang, 1978

[= Qujingolepidae G.-R. Zhang, 1978; Procondylolepidae G.-R. Zhang, 1978]

EMENDED DIAGNOSIS. — Yunnanolepidoidei in which the trilobate, perichondrally ossified scapulocoracoid is exposed in the bottom of the pectoral fenestra; three foramina for the neurovascular canals around the scapulocoracoid; single dermal articulation (parabrachial condyle and ventral articular fossa) between the unjointed pectoral fin and the trunk-shield; pectoral fin triangular in transverse section; two fossae for the abductor and adductor muscles of the fin on the trunk-shield; anterior median dorsal plate long and narrow, B/L index about 50-65, with the anteriorly placed tergal angle and anterior ventral process; no anterior ventral pit.

REMARKS. — This definition is modified from K.-J. CHANG (1978) and G.-R. ZHANG (1984). As stated below, *Procondylolepis* and *Qujinolepis*, are in fact junior synonyms of *Chuchinolepis*. Therefore, both the Procondylolepidae and Qujinolepidae are the junior synonyms of the Chuchinolepidae. According to the International Code of Zoological Nomenclature (RIDE *et al.* 1985, Art 29a), the Chuchinolepidae is revised as the Chuchinolepididae.

Genus **CHUCHINOLEPIS** K.-J. Chang, 1978

Chuchinolepis K.-J. Chang, 1978: 296, pl. 26.

Synonyms:
Orientolepis P'an & Wang, 1978: 322, pl. 28, 2.
Qujinolepis G.-R. Zhang, 1978: 173, figs 1317, pl. VII.
Procondylolepis G.-R. Zhang, 1984: 82, figs 14, pls III.

Others references:
Chuchinolepis TONG-DZUY & JANVIER 1990: 176, figs 18-22, pls V, VI, 1-3.
Qujinolepis TONG-DZUY & JANVIER 1987: 12, figs 6A-C, 7A, pl. I, 3-4. — S.-F. LIU, 1992: 214, pl. II, 1-7.
Procondylolepis YOUNG & ZHANG 1992: 445, figs 2F-G, 3B-D, 4-6. — F. ZHU, WANG & FAN 1994: 4, fig. 2, pl. I, 4-7.

EMENDED DIAGNOSIS. — As for the family (monogeneric).

TYPE SPECIES. — *Chuchinolepis gracilis* K.-J. Chang, 1978.

REMARKS. — K.-J. CHANG (1978) and TONG-DZUY & JANVIER (1990) defined *Chuchinolepis* as "chuchinolepid with very fine tubercular ornamentation, which is largely invisible to the naked eye". As seen below,

Procondylolepis qujingensis (G.-R. Zhang 1984) is quite similar to *C. gracilis*, except for the size of tubercles, and it seems better to place *P. qujingensis* in the genus *Chuchinolepis* to make the classification more simple. This problem is also related to the assignment of two other chuchinolepids from Qujing, Yunnan, the type locality of *C. gracilis* and *P. qujingensis*. One is a chuchinolepid with fairly large tubercles (*C. robusta* n. sp.). With regard to the pectoral fin articulation, *P. qujingensis* and *C. gracilis* are more similar than either is to *C. robusta*. If *Procondylolepis* was retained as an independent genus, *C. robusta* should be referred to as a new genus, thereby making the classification unnecessarily complicated. The other is a chuchinolepid (*C. sulcata* n. sp.) in which the fine-grained tubercles (of the same relative size as in *P. qujingensis*) are arranged in regular ridges on the pectoral fin plates and the dorsal wall of the trunk-shield, and very fine-grained tubercles (of the same relative size as in *C. gracilis*) are densely distributed between the ridges. Its assignment is greatly dependent of the character polarity of the tubercles. Therefore, for simplicity, we propose a more general defintion of *Chuchinolepis* to include *P. qujingensis*, *C. robusta* and *C. sulcata*.

Chuchinolepis gracilis K.-J. Chang, 1978
(Figs 18-20, pls VIII, 1-5; IX, 4-5)

Chuchinolepis gracilis K.-J. Chang, 1978: 296, pl. 26.

Synonyms:

Orientolepis neokwangsiensis P'an & Wang, 1978: 322, pl. 28-2.

Qujinolepis gracilis G.-R. Zhang, 1978: 173, figs 13-17, pl. VII.

Others references:

Qujinolepis gracilis S.-F. Liu 1992: 214, pl. II, 1-7.

Emended diagnosis. — *Chuchinolepis* in which the length/width index of the PMD plate is about 110.

Holotype. — A detached AMD plate, V4426.15.

Plesiotype. — A detached PMD plate, V4426.6.

New material. — V10510.1-12, material from the Xitun Formation; V10503.1-5, material from the Xishancun Formation.

Remarks. — This species is the type species of *Chuchinolepis* (K.-J. Chang 1978), and was assumed to bear a simple pectoral fin articulation, like the Yunnanolepididae (G.-R. Zhang 1978). This had not been questioned until 1990 when Tong-Dzuy & Janvier regarded it as a procondylolepiform. However, the proposal of Tong-Dzuy & Janvier (1990) still awaits confirmation by finding the AVL plate of *C. gracilis* in the original locality and horizon (the Xitun Formation in Qujing, Yunnan), where "*Procondylolepis*" *qujingensis* was found together. The diagnostic feature of *C. gracilis* is its very fine-grained ornamentation, by which K.-J. Chang (1978) and G.R. Zhang (1978) attributed the detached skull-roof and trunk-shield plates to this species. In this work, several AVL plates, which could be definitely referred to *C. gracilis*, are described from the Xitun Formation of Qujing, and it is shown that *C. gracilis* is indeed a procondylolepiform.

The discovery of *C. gracilis* in the Xishancun Formation shows that *Chuchinolepis* has an earlier distribution which might have a bearing on the biostratigraphic correlation.

This species shares the very fine-grained ornamentation (invisible to the naked eye) with *C. dongmoensis* (Tong-Dzuy & Janvier 1990). They differ in the length/width index of PMD plate, that of *C. dongmoensis* being about 150.

Description

Material from the Xitun Formation (Fig. 18, pls VIII, 5; IX, 4-6)

C. gracilis was originally described from this horizon, and all of the specimens were detached plates, including the Nu, L, AMD, PMD, ADL and PVL plates. Later, it was recorded

from the Lianhuashan Formation of Liujing, Guangxi, but no further anatomical character has been added (S.-F. LIU 1992).

The AVL plate of *C. gracilis* bears a brachial articulation, and has the very fine-grained tubercular ornamentation, like the other plates referred to *C. gracilis* which were found in the same locality and horizon (K.-J. CHANG 1978; G.-R. ZHANG 1978). As in *C. dongmoensis* (TONG-DZUY & JANVIER 1990), the tubercles on the area anterolateral to the parabrachial process (ppbr, Fig. 18A) and on the oblique ridges of the trunk-shield (r.obl, Fig. 18A) are slightly larger than those on the rest of the plate.

The ventrolateral ridge (vlr, Fig. 18C) divides the plate into ventral and lateral laminae (llm, vlm, Fig. 18), which meet at an almost right angle. The lateral lamina is relatively short and high, as in *C. dongmoensis* (TONG-DZUY & JANVIER 1990). Considering the lateral lamina of the PVL plate (G.-R. ZHANG 1978), which is very long and low, it could be inferred that

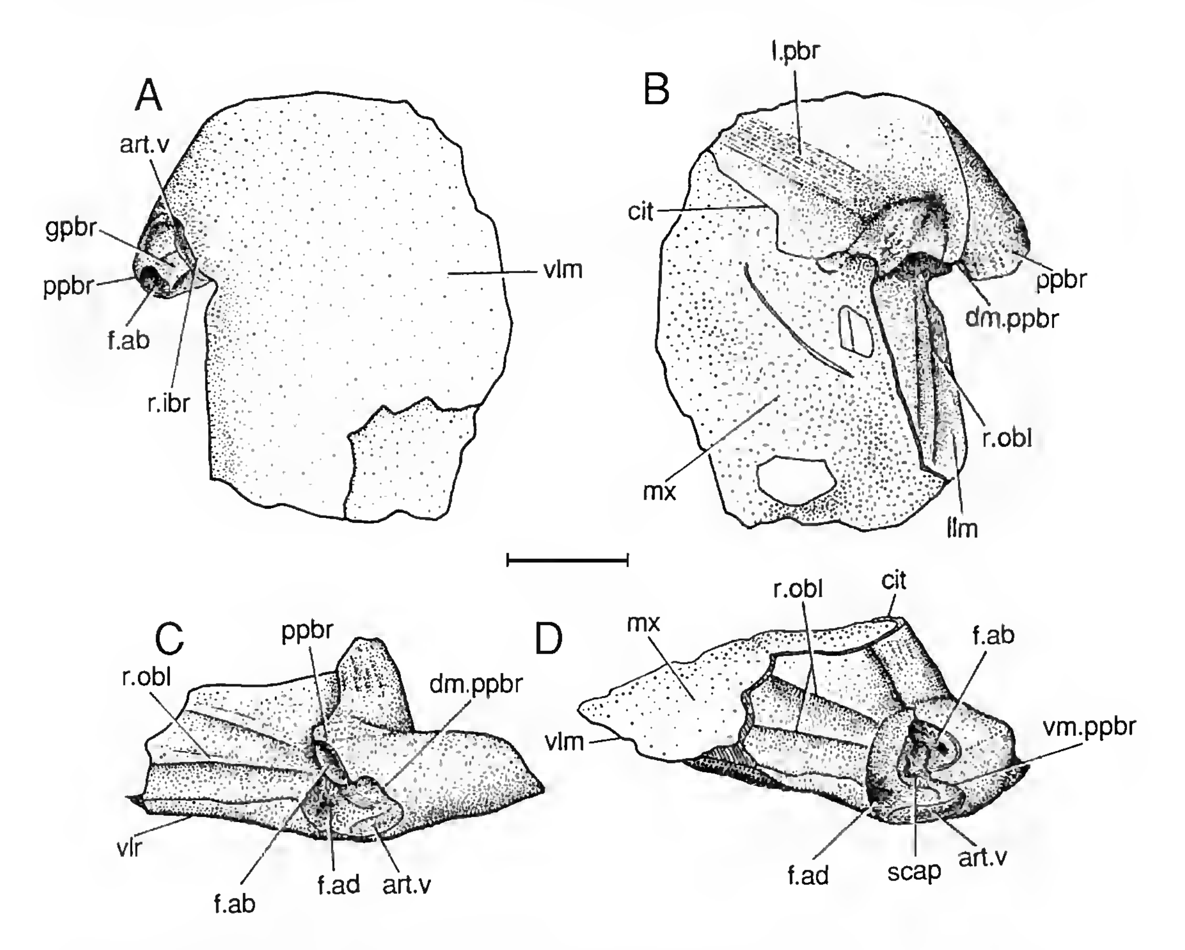


FIG. 18. — *Chuchinolepis gracilis* K.-J. Chang, Xitun Formation, Qujing. Right AVL plate in ventral (A), dorsal (B), lateral (C) and posterolateral (D) views. (Scale bar 5 mm.)

the PVL plate of *C. gracilis* is as elongated as in *C. dongmoensis* (TONG-DZUY & JANVIER 1990, Fig. 18). The AVL plate overlaps the ADL plate along its posteriorly slanting dorsal margin. The overlap area is very narrow. In *C. dongmoensis*, the lateral lamina of the AVL plate seems to ascend posteriorly. The posterior margin of the lateral lamina, which overlaps the PL and PVL plates, is not embayed, as in *C. dongmoensis*. On the external surface of the lateral lamina, there are two oblique ridges (r.obl, Fig. 18C, D), as in *C. dongmoensis* and *C. qujingensis*.

The slightly posteriorly extended parabrachial process (ppbr, Fig. 18) is anterolateral to the lateral lamina. Since the dorsal margin of the parabrachial process (dm.ppbr, Fig. 18B) forms an acute angle with the lateral lamina, the brachial depression between them is more or less closed. The ventral margin of this process (vm.ppbr, Fig. 18D) prolongs towards the ventrolateral ridge by a gently curved ridge. On the tip of the parabrachial process, there is an oval fossa for the attachment of the abductor muscle of fin (f.ab, Fig. 18A, C, D). On the inner surface of the parabrachial process, there is a groove (gpbr, Fig. 18A) which was termed by YOUNG & ZHANG (1992) as the "funnel groove". The perichondrally ossified scapulocoracoid (scap, Fig. 18D) extends outwards from the bottom of the pectoral fenestra. The distal end of the scapulocoracoid is trilobate, as in *C. qujingensis*. In the brachial depression, two other depressions or fossae are visible. One is the ventral articular depression for the dermal process of the pectoral fin (art.v, Fig. 18A, C, D), which lies ventrally to the pectoral fenestra. In many specimens, the *siebknochen* texture is visible on the surface of this ventral articular depression. The other is the depression for the attachment of the adductor muscle of the fin (f.ad, Fig. 18C, D), which lies mesiodorsally to the pectoral fenestra.

Anterior median dorsal plates from the Xishancun Formation (Fig. 19, pl. VIII, 1-4)

The AMD plate resembles very much that of *C. gracilis* from the Xitun Formation (K.-J. CHANG 1978; G.-R. ZHANG 1978). Only one external mould of the AMD plate (V10503.4) was discovered, and its ornamentation is found to be made up of very fine tubercles. The specimens of *C. gracilis* from the Xishancun Formation are smaller than those from the Xitun Formation. The largest one (V10503.2, Fig. 19C) is about 12 mm long. Some specimens should belong to juvenile individuals; however, it is possible that in the earlier period, *C. gracilis* is represented by a smaller form.

In general, the AMD plate is long and narrow, with a length/width index ranging from 149 to 176. Both the anterior and posterior margins are narrow. The overlap relationships with the adjoining plates are constant in all specimens. In visceral view, the anterior ventral process (prvl, Fig. 19A-C, E-F) lies far in front of the level of the lateral corners. This process is more or less elongated in shape, and seems to be devoid of the anterior ventral pit. Behind this process, there develops a median ventral groove (grm, Fig. 19A-C, E-F), which is prolonged to the posterior margin of the plate by a faint median ventral ridge (mvr, Fig. 19B). The same is found in the holotype of *C. gracilis* and in *C. dongmoensis* (TONG-DZUY & JANVIER 1990). K.-J. CHANG (1978) and G.-R. ZHANG (1978, Fig. 14) assumed that there is a short median ventral ridge immediately behind the anterior median ventral process. However, our examination of the type specimen shows that there is not such a subdivision between the process and supposed median ventral ridge, and the elongated process is followed posteriorly by the median ventral groove.

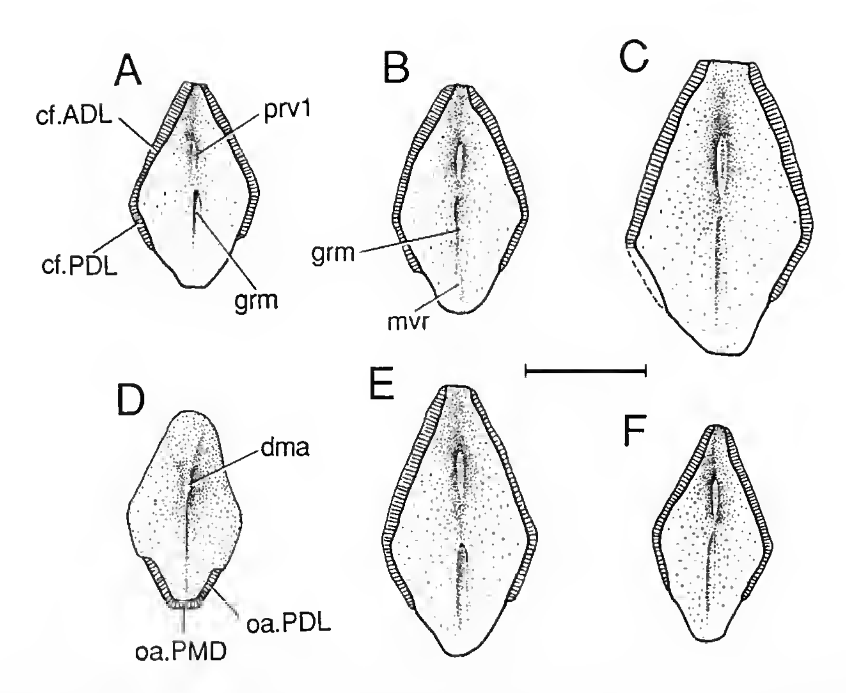


FIG. 19. — *Chuchinolepis gracilis* K.-J. Chang, Xishancun Formation, Qujing. All specimens figured are elastomer casts. A, AMD plate in visceral view, V10503.3; B, AMD plate in visceral view, V10503.5; C, AMD plate in visceral view, V10503.2; D, AMD plate in external view, V10503.3; E, AMD plate in visceral view, V10503.6; F, AMD plate in visceral view, V10503.4. (Scale bar 5 mm.)

Juvenile specimen of Chuchinolepis gracilis from the Xishancun Formation (Fig. 20, pl. VIII, 1).

This specimen belongs to a juvenile individual, and consists of a small, articulated skull-roof and trunk-shield, preserved as an internal mould.

The skull-roof is incompletely preserved, and the premedian, left lateral, postmarginal and paranuchal plates are missing. When restored, the juvenile skull-roof of *C. gracilis* appears as relatively long and narrow, like that of *Minicrania antiqua* (ZHU & JANVIER 1996). If we assume that the skull-roof of the adult *C. gracilis* had the similar morphology as that of *C. dongmoensis* (TONG-DZUY & JANVIER 1990), it can be inferred that, during the growth, the skull-roof was expanding laterally. Therefore, it is reasonable to regard the short and broad skull-roof as apomorphic for antiarchs. The lateral plate (L, Fig. 20) is poorly preserved, with its anterior extremity missing. The orbital notch, the margin for the postpineal plate, and the groove for the infraorbital canal are visible. This plate has the same shape as that of the adult (G.-R. ZHANG 1978). The postpineal plate (Pp, Fig. 20) is roughly oval and transverse in shape, and excludes the nuchal plate (Nu, Fig. 20) from the orbital fenestra (fe.orb, Fig. 20). Its anterior margin is fairly curved. As to the relative proportions, the juvenile postpineal plate seems shorter than that of the adult. The nuchal plate (Nu, Fig. 20) is long and narrow with a shallow anterior notch for the postpineal plate, similar to that of *C. dongmoensis*. Proportionally, the juvenile nuchal plate is even longer

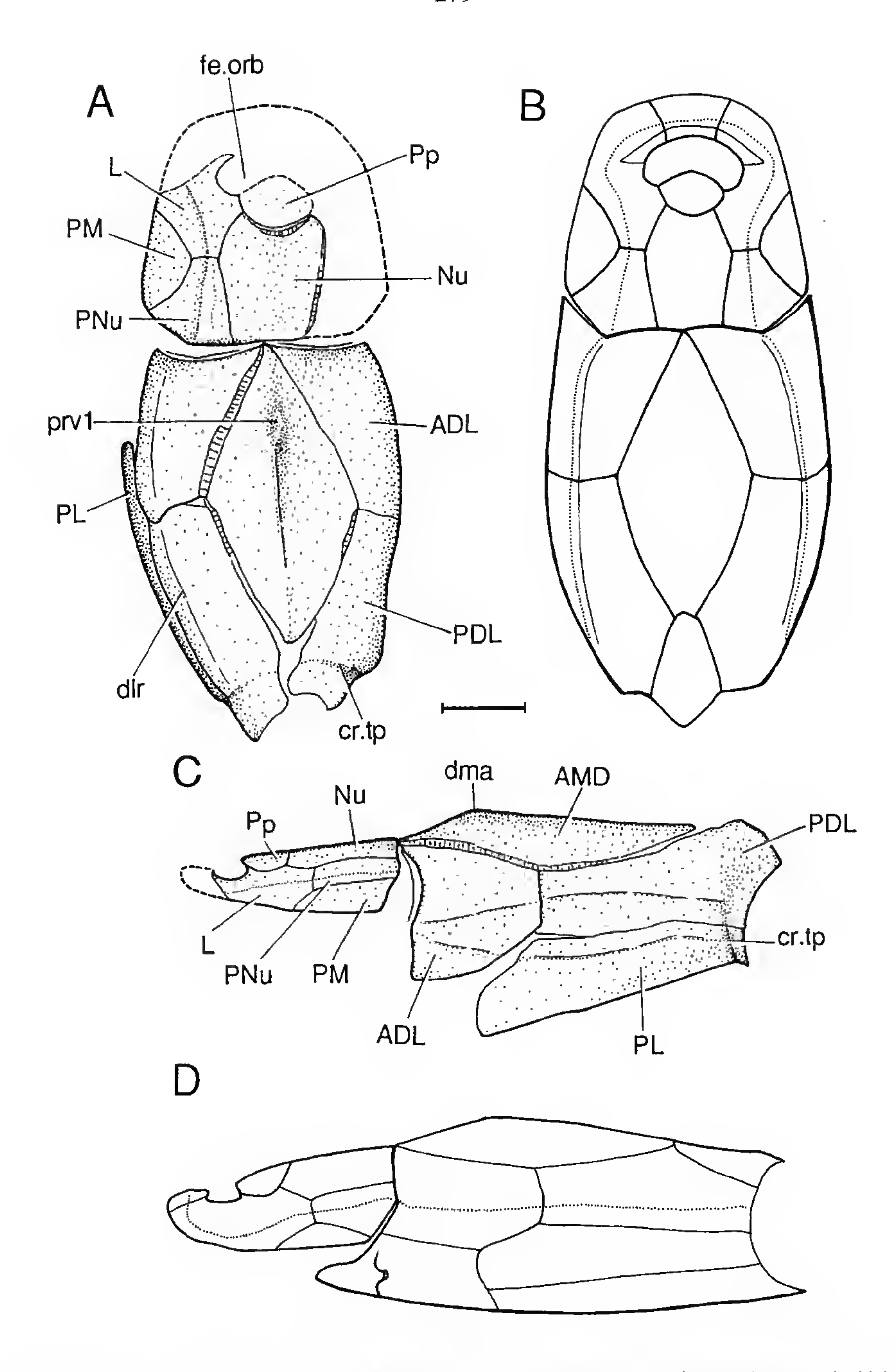


FIG. 20. — *Chuchinolepis gracilis* K.-J. Chang, Xishancun Formation, Qujing. Juvenile skull-roof and trunk-shield (V10503.1) in dorsal (A) and lateral (C) views, and its restorations in dorsal (B) and lateral (D) views. (Scale bar 2 mm.)

and narrower than that of the adult, and its lateral corner is less conspicuous. The postmarginal plate (PM, Fig. 20) is relatively large. However, contrary to the adult one, it does not extend laterally to form a distinct angle. Therefore, it has a triangular shape, unlike the rhombic shape of the postmarginal plate of the adult. The paranuchal plate (PNu, Fig. 20) is relatively small, and its anterior portion is narrow. The infraorbital groove passes through the plate lengthwise and, as in the nuchal plate, the obtected nuchal zone extends along its posterior margin. The obstantic margin is slightly inclined anteriorly, whereas in the adult of both *Yunnanolepis* and *Chuchinolepis*, it has a more anterior oblique orientation.

The trunk-shield is fairly long and narrow, as in *C. dongmoensis* (TONG-DZUY & JANVIER 1990). The AMD plate (AMD, Fig. 20), with much narrowed anterior and posterior margins, is similar to the isolated ones described above. The PMD plate is not preserved. However, from the short posterior dorsal margin of the PDL plate, it is inferred that the juvenile PMD plate of *C. gracilis* is not as long as that of *C. dongmoensis*. The ADL plate (ADL, Fig. 20) is relatively short, with a dorsolateral ridge. In dorsal view, its anterior margin is fairly broad, and the plate is overlapped by the AMD plate. Posteriorly, it overlaps the PDL and PL plates. On the lateral lamina of the ADL plate, there is another faint oblique ridge which stretches posteriorly to the PL plate. The PDL plate (PDL, Fig. 20) is much elongated, as in *C. dongmoensis* (TONG-DZUY & JANVIER 1990). Its dorsal corner is posteriorly placed, with a long contact margin with the AMD plate. Its lateral lamina is comparatively low. The groove corresponding to the *crista transversalis interna posterior* (cr.tp, Fig. 20A, C) appears in the posterior portion of the plate. The PL plate (PL, Fig. 20) is very similar to that of *C. dongmoensis*. It is low and long, extending anteriorly as far as below the posterior part of the ADL plate, and bears a faint longitudinal ridge. Along its posterior margin, there is a shallow groove corresponding to the *crista transversalis interna posterior* in the internal mould.

Chuchinolepis qujingensis G.-R. Zhang, 1984
(Figs 21-22, pls VIII, 6-12; X, 8-13)

Procondylolepis qujingensis G.R. Zhang, 1984: 82, figs 1-4, pls I-II.

Synonym:
Procondylolepis YOUNG & ZHANG 1992: 445, figs 2F-G, 3B-D, 4-6.

Others references:
Procondylolepis qujingensis ZHU, WANG & FAN 1994: 4, fig. 2, pl. I, 4-7.

DIAGNOSIS. — *Chuchinolepis* in which the ornamentation is composed of fine-grained tubercles.

HOLOTYPE. — An incomplete AVL plate (V6941.1).

NEW MATERIAL. — V10504.1-3 from the Xishancun Formation : V10511.1-20 from the Xitun Formation.

REMARKS. — This species differs from *C. gracilis* and *C. dongmoensis* mainly by its tubercles, which are much larger than those of *C. gracilis* and *C. dongmoensis*. *C. qujingensis* is more suggestive of *C. dongmoensis* than of *C. gracilis* in the lateral lamina of the ADL plate, which decreases in height posteriorly. Since the ornamentation of *C. qujingensis* is similar to that of *Yunnanolepis* and *Phymolepis* from the same locality, it is difficult to determine detached plates except the AVL plate with the fin articulation structures, the AMD plate and pectoral fin plates. Other plates which can be assigned to *C. qujingensis* with little doubt include three PMD plates from the Xitun Formation and two ADL plates from the Xishancun Formation. These PMD plates have

the same ornamentation as the AVL plate of *C. qujingensis*, as well as those of *Yunnanolepis* and *Phymolepis*. However, their *crista transversalis interna posterior* is situated lateral to the posterior ventral process and pit, in contrast, the PMD plate of *Yunnanolepis* and *Phymolepis* is specialized, with the *crista transversalis interna posterior* passing clearly in front of the posterior ventral process and pit. Another possibility, as to the assignment of these PMD plates, is *Zhanjilepis* (G.-R. Zhang 1978). However, the tubercles of *Zhanjilepis* are coarser, and its PMD plate seems to be devoid of the median ventral ridge. Therefore, it is most likely that these PMD plates from the Xitun Formation belong to *C. qujingensis*. Two ADL plates from the Xishancun Formation are specialized by the shape of their lateral lamina. As far as we know, the ventral margin of lateral lamina of ADL plate in antiarchs, except for *C. dongmoensis*, descends posteriorly or is at least parallel to the dorsolateral ridge. The ADL plates from the Xishancun Formation have the matching size and same ornamentation as the AMD plate of *C. qujingensis* from the same site. Moreover, they possess the ascending ventral margin of the lateral lamina as in *C. dongmoensis*. With reference to *C. dongmoensis*, the only species of *Chuchinolepis* in which the ADL plate is described, these two ADL plates from the Xishancun Formation, which have the same kind of ventral margin as that of *C. dongmoensis*, might be assigned to *Chuchinolepis*. By the ornamentation, they are referred to *C. qujingensis*.

Description

Material from the Xishancun Formation (Fig. 21, pl. VIII, 6-12)

The AMD plate (V10504.1, Fig. 21) is roughly rhombic and elongated in shape, as in *C. gracilis* and *C. dongmoensis*. It has the length of 24.9 mm and width of 14.7 mm, and a length/width index of about 170. The plate has very narrow anterior and posterior margins. The

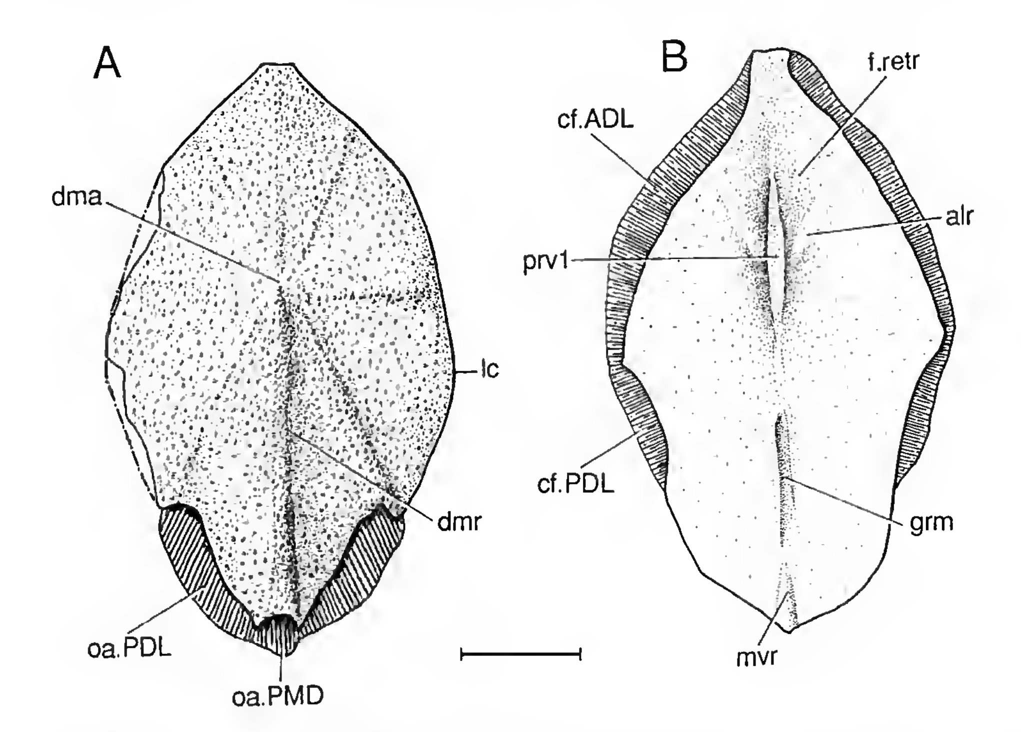


Fig. 21. — *Chuchinolepis qujingensis* (K.-J. Chang), Xishancun Formation, Qujing. AMD plate (V10504.1) in dorsal (A) and visceral (B) views (elastomer casts). (Scale bar 5 mm.)

anterolateral and posterolateral margins are relatively long and more or less convex. In external view, the plate is considerably arched with an anteriorly placed tergal angle (dma, Fig. 21A). The mid-line length in front of the tergal angle is about 38.4% of the plate length. The median dorsal ridge (dmr, Fig. 21A) is situated behind the tergal angle and extends backwards to the posterior margin of the plate. The tubercles are fine-grained, and densely distributed, but clearly visible to the naked eye, unlike *C. gracilis* and *C. dongmoensis* where a hand lens or microscope is needed to see the tubercle ornament. In visceral view, the elongated anterior median ventral process (prv1, Fig. 21B) lies beneath the tergal angle, and is prolonged posteriorly by a median ventral groove (grm, Fig. 21B), and a faint median ventral ridge (mvr, Fig. 21B). The levator fossa (f.retr, Fig. 21B) and postlevator thickenings (alr, Fig. 21B) lie on each side of the elongated anterior ventral process. The overlap relationships with the adjoining plates are like those in other *Chuchinolepis* species.

The ADL plate (pl. VIII, 9-12) has its dorsal lamina relatively long and narrow, and with a broad anterior margin. Its mesial margin is overlapped by the AMD plate. The lateral lamina is remarkable by its posteriorly ascending ventral margin. The deepest position of the lamina is at its anterior end. The main lateral-line groove lies just below the dorsolateral ridge and traverses the plate. Along the ventral and posterior margins, the plate overlaps the AVL and PDL plates. The *crista transversalis interna anterior* is visible in the anterior edge of the plate.

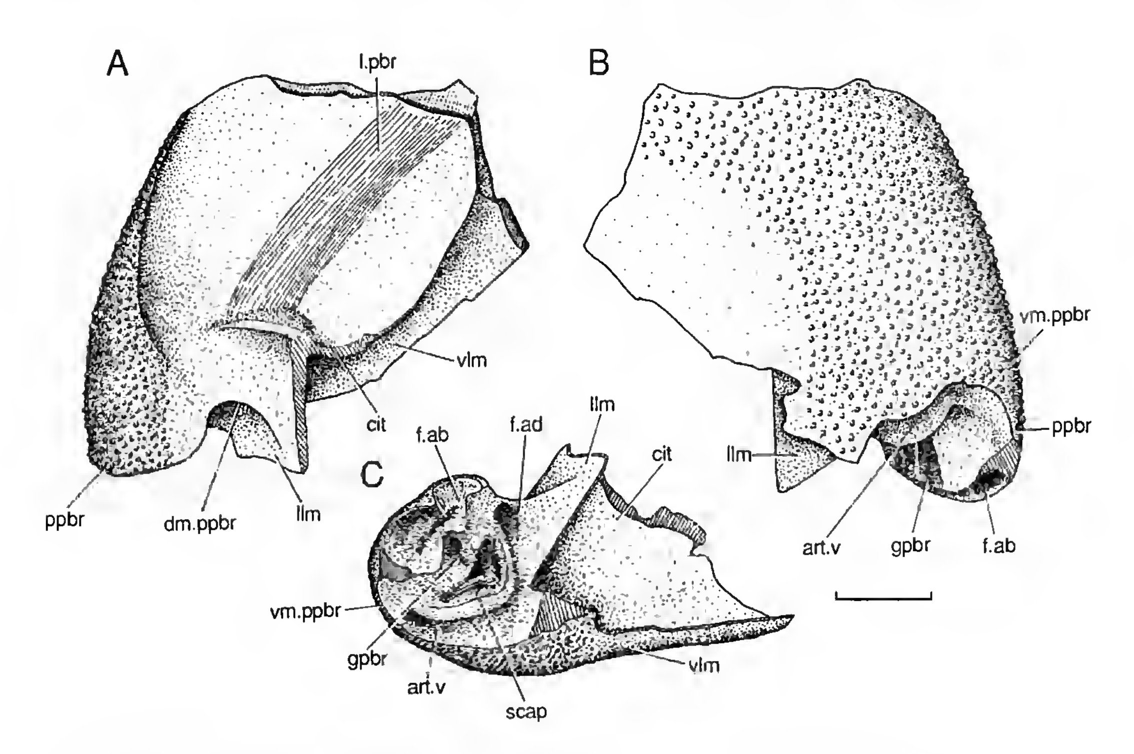


FIG. 22. — *Chuchinolepis qujingensis* (K.-J. Chang), Xitun Formation, Qujing. Incomplete left AVL plate in dorsal (A), ventral (B) and posterior (B) views, V10511.1. (Scale bar 5 mm.)

Material from the Xitun Formation (Fig. 22, pl. X, 8-13)

The AVL plates of *C. qujingensis* from the Xitun Formation were described in detail by G.-R. ZHANG (1984) and YOUNG & ZHANG (1992). More material was collected and prepared for the serial grinding study (ZHU in prep.). V10511.1 shows that the postbranchial lamina (l.pbr, Fig. 22A) is similar to that of *C. gracilis* and *Yunnanolepis*, which extends anteromesially and lies horizontally onto the floor of the plate. The *crista transversalis interna anterior* (cit, Fig. 22A, C) is fairly high and clearly behind the postbranchial lamina. The fossa (f.ab, Fig. 22B, C) on the parabrachial process (ppbr, Fig. 22) is kidney-shaped and fairly deep. A low ridge is sometimes visible on the dorsolateral surface of the fossa.

The PMD plates described here have the same ornamentation as the AVL plates of *C. qujingensis*. In external view (pl. X, 13), the plate is gently arched and is devoid of any ridge and process, as in *C. gracilis* (K.-J. CHANG 1978; G.-R. ZHANG 1978). The plate has its maximum breadth at the level of the lateral corners. In visceral view (pl. X, 12), the median ventral ridge extends from the anterior end of the plate to the posterior ventral process and pit, which are conspicuous and have a relatively posterior position. The *crista transversalis interna posterior* lies laterally to the posterior ventral process and pit, as in *C. gracilis* (G.-R. ZHANG 1978, pl. VII, 3).

Chuchinolepis robusta n. sp.
(Fig. 23, pl. IX, 1-3)

DIAGNOSIS. — *Chuchinolepis* in which the ornamentation consists of coarse tubercles; pectoral fin articulation region of the AVL plate fairly open.

ETYMOLOGY. — From *robustus* (Lat.), "robust", by reference to the coarse tubercles of the new species.

HOLOTYPE. — V10512, a detached AVL plate (the only material).

LOCALITY AND HORIZON. — Xitun Formation, Cuifengshan Group, Early Devonian, Qujing, Yunnan, China.

REMARKS. — This specimen could be assigned to *Chuchinolepis* by its unique pectoral fin articulation structure. It differs from other species of *Chuchinolepis* by its fairly open pectoral fin articulation area of the AVL plate and coarse ornamentation.

DESCRIPTION

This specimen is a medium-sized AVL plate with a length of 38 mm. The plate is similar to that of *C. gracilis*, *C. qujingensis* and *C. dongmoensis* with its typical pectoral fin articulation structures, *i.e.*, the trilobate, perichondrally ossified scapulocoracoid (scap, Fig. 23B, C) extending from the bottom of the pectoral fenestra, and the parabrachial process (ppbr, Fig. 23) with a fossa for the attachment of the fin muscle.

The AVL plate is divided into two perpendicular lateral and ventral laminae, by the ventrolateral ridge. On the lateral lamina, the tubercles are fairly coarse and loosely distributed, whereas on the ventral lamina, the tubercles are somewhat smaller. On the area anterior to the parabrachial process, the tubercles are a little larger than those on the ventral lamina, however, they are clearly smaller than those on the lateral lamina.

In dorsal view, the lateral lamina (llm, Fig. 23A) extends anteriorly far beyond the dorsal margin of the parabrachial process (dm.ppbr, Fig. 23A). At the level of the parabrachial process,

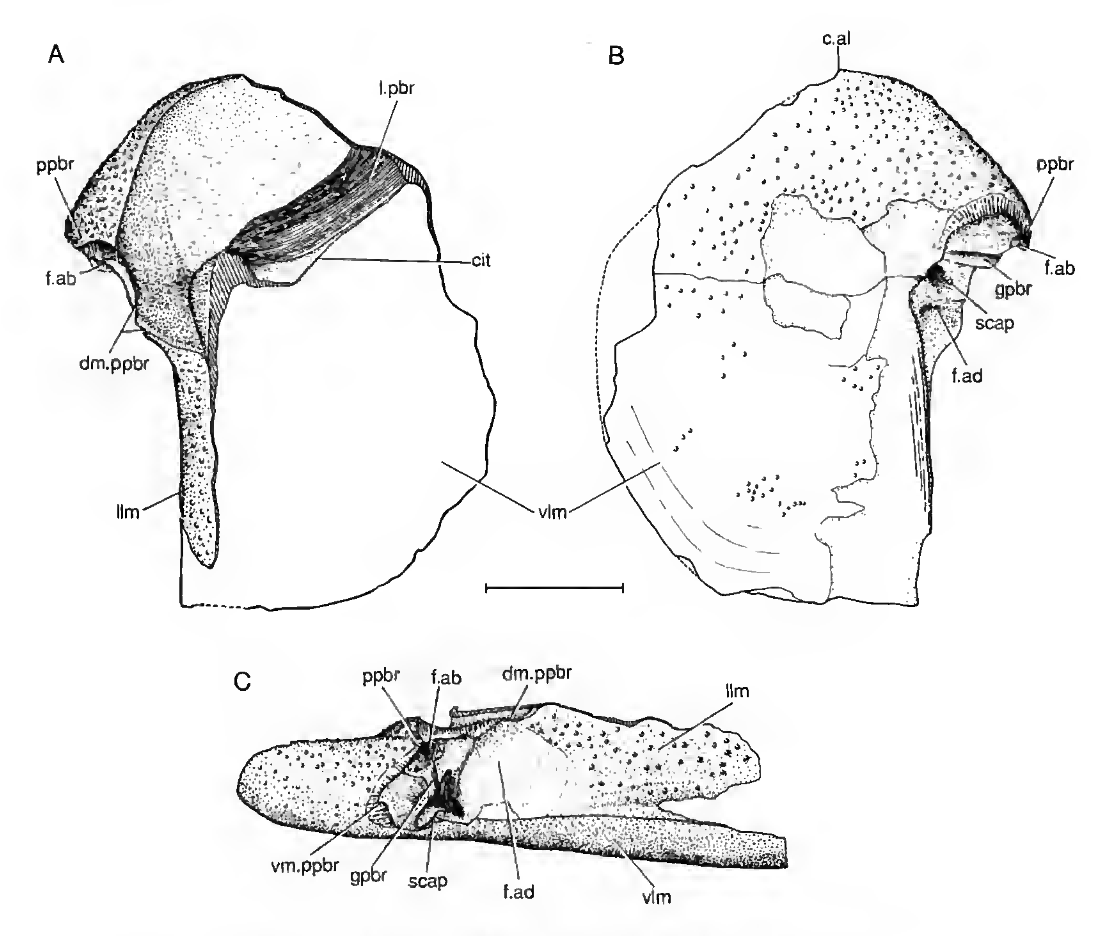


FIG. 23. — *Chuchinolepis robusta* n. sp., Xitun Formation, Qujing. Left AVL plate in dorsal (A), ventral (B) and lateral (C) views, Vf0512. (Scale bar 10 mm.)

it turns mesially to form the *crista transversalis interna anterior* (cit, Fig. 23A) which extends to the mesial margin of the plate and becomes lower mesially. The postbranchial lamina (l.pbr, Fig. 23A) has a ridged ornamentation, as in other yunnanolepidoids, and attaches on the anterior face of the *crista transversalis interna anterior*. In *C. gracilis* and *C. qujingensis*, the postbranchial lamina is situated in front of the *crista transversalis interna anterior*, and has a more oblique direction. Unlike that of *C. qujingensis* and *C. gracilis*, the parabrachial process of this new species has a more anterior and lateral position. The dorsal margin of the parabrachial process (dm.ppbr, Fig. 23A, C) extends more or less posteriorly and forms an oblique angle with the lateral lamina.

In lateral view, the fin articulation structures are clearly visible. Due to the anterior and lateral position of the parabrachial process, the articulation area of the plate is fairly open. On

the tip of the parabrachial process, there is a small, oval fossa for the attachment of the abductor muscle of fin (f.ab, Fig. 23). As in the other *Chuchinolepis* species, a groove (gpbr, Fig. 23B-C) descends from the parabrachial process toward the pectoral fenestra. The trilobate, perichondrally-lined scapulocoracoid (scap, Fig. 23C) is relatively large and extends outwards from the bottom of the pectoral fenestra. Since the ventral and middle lobes are very close to the ventral lamina of the plate, the infrabrachial ridge and ventral articular depression for the dermal process of the pectoral fin, which are present in the other *Chuchinolepis* species, are not preserved in the specimen. Dorsally to the middle lobe of the scapulocoracoid, there is a relatively large foramen for the nerves and vessels of the fin. The fossa for the adductor fin muscle (f.ad, Fig. 23B,-C) is large and shallow, and situated behind the postbrachial ridge. Behind the fossa is the ornamented lateral lamina of the plate, which descends backwards. The lamina has a sinuous posterior margin, due to the anteriorly intruding PL plate, as in *C. dongmoensis* (Tong-Dzuy & Janvier 1990).

In ventral view, only the mesial margin of the plate is somewhat damaged. The plate is broadest at the level of the parabrachial process, and the estimated breadth is more than 30 mm. Behind the parabrachial process, the plate is about 23 mm in breadth. The ventral margin of the parabrachial process (vm.ppbr, Fig. 23B, C) forms an obtuse angle with the ventrolateral ridge. The contact margin for the semilunar plate extends posteriorly in a straight oblique line, and does not form a notch, as in *Yunnanolepis* (G.-R. Zhang 1978, Fig. 6). The contact margin with the MV plate indicates that the MV plate of *C. robusta* is relatively small, as in *Y. porifera*. Two or three growth lines are visible near the plate margins.

Chuchinolepis sulcata n. sp.
(Figs 24-25, pl. X, 1-7)

Procondylolepis qujingensis G.-R. Zhang, 1984 (in part): V6941.5, fig. 2a-c, pl. I, 3.

Diagnosis. — *Chuchinolepis* in which the fine-grained tubercles are arranged into the regular ridges on the dorsal wall of the trunk-shield and the pectoral fin plates; very fine-grained tubercles distributed between the ridges.

Etymology. — From *sulcus* (Lat.), groove, by reference to the shallow grooves between the ridges on the dorsal wall of the trunk-shield.

Holotype. — V10513.1, a trunkshield (pl. X, 1-7).

Other material. — Three PMD plates (V10513.2-4), an incomplete pectoral fin (V10513.5), and a fragment of AMD plate (V0513.6).

Locality and horizon. — Xitun Formation, Cuifengshan Group, Early Devonian, Qujing, Yunnan, China.

Remarks. — This new species could be assigned to *Chuchinolepis* by its typical long and narrow AMD plate, which has its anterior ventral process far anterior to the level of the lateral corners. The difference between *C. sulcata* and the other *Chuchinolepis* species lies mainly in the ornamentation, the latter having tubercles, either fine or coarse, deprived of any ridges. By the very tiny and densely distributed tubercles between the ridges, the new species is more similar to *C. gracilis* and *C. dongmoensis* than to *C. qujingensis* and *C. robusta*.

The detached incomplete pectoral fin V6941.5 had been assigned to be the paratype of *C. (Procondylolepis) qujingensis* (G.-R. Zhang 1984). However, this pectoral fin was definitely different from the holotype and other pectoral fins of *C. qujingensis* by its regular ridges. Since the same kind of the regular ridges are found in the trunk-shield of *C. sulcata*, this ridged pectoral fin should be removed from the species which are devoid of the ridges.

DESCRIPTION

Trunk-shield (Figs 24, 25C-E; pl. X, 1-6)

This is a small to medium-sized antiarch. As in the other *Chuchinolepis* species, the trunk-shield of *C. sulcata* (Fig. 24) is relatively long and low, with a less developed median dorsal ridge. Its diagnostic character is the regular ridges formed by the tubercles on the dorsal wall of the trunk-shield.

The AMD plate (Figs 24, 25C) is very similar to that of the other *Chuchinolepis* species (G.-R. ZHANG 1978; TONG-DZUY & JANVIER 1990) except for the ridged ornamentation. It is long and narrow, with narrow anterior and posterior margins. The breadth/length index is about 57, just as that of *C. gracilis* (G.-R. ZHANG 1978). The lateral corner is less conspicuous, subdividing the lateral margin into two portions, which are roughly equivalent in length. Along the anterolateral margin, the AMD plate overlaps the ADL plate over the entire suture. The overlap relationship between the AMD and PDL plates (fig. 25C) is the same as that of other

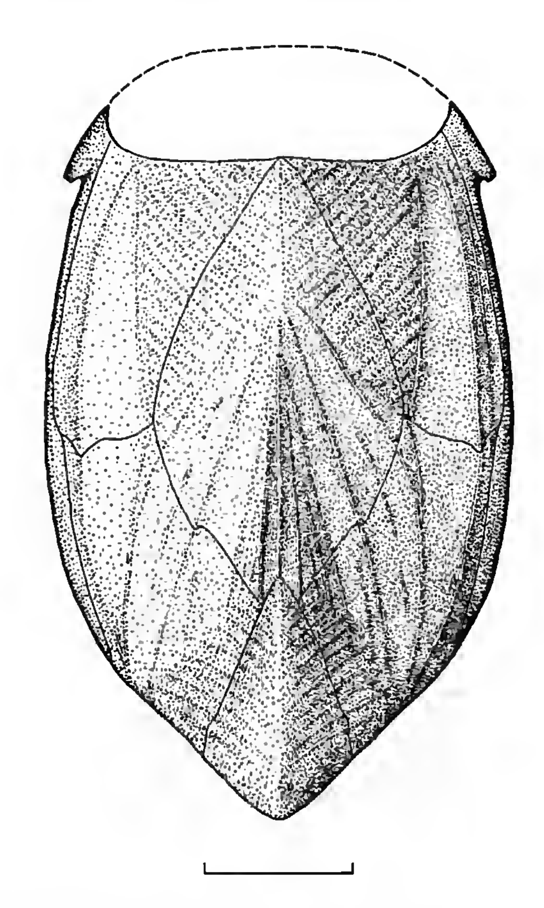


FIG. 24 — *Chuchinolepis sulcata* n. sp., Xitun Formation, Qujing. Restoration of the trunk-shield in dorsal view, based on the holotype (V10513.1). (Scale bar 10 mm.)

yunnanolepidoids. The area overlapped by the PMD plate is rather narrow. In dorsal view, the tergal angle has a fairly anterior position, about 1/51/6 of the mid-line length from the anterior extremity (fig. 24). Behind the tergal angle, the median dorsal ridge is less developed. The small tubercles turn to form the regular ridges, in a pattern similar to that of *Hunanolepis* (J.-Q. WANG 1991, fig. 13). All ridges intersect the corresponding plate margins. Between the ridges, the tubercles are tiny and densely distributed, and are invisible to the bare eyes, as in *C. gracilis*. In visceral view, the plate exhibits a shallow fossa for the levator muscle in front of the level of the tergal angle, as in *C. dongmoensis* (TONG-DZUY & JANVIER 1990, fig. 19). Immediately behind the fossa, the plate bears a relatively elongated anterior ventral process (prv1, fig. 25C), which is prolonged posteriorly by a long median ventral ridge (mvr, fig. 25C).

Three detached PMD plates are known, in addition to the PMD plate of the holotype. The plate has the same shape as that of other *Chuchinolepis* species, among which the new form is more suggestive of *C. dongmoensis* (TONG-DZUY & JANVIER 1990) than of *C. gracilis* as to the length/breadth index (about 150 in *C. sulcata* and *C. dongmoensis*, about 110 in *C. gracilis*). In external view (Fig. 24), the plate is more or less arched, forming a faint median dorsal ridge and a low posterior dorsal angle. Along the median dorsal ridge and the posterior margin of the plate, the small tubercles are closely set and do not form the ridges. However, laterally to the

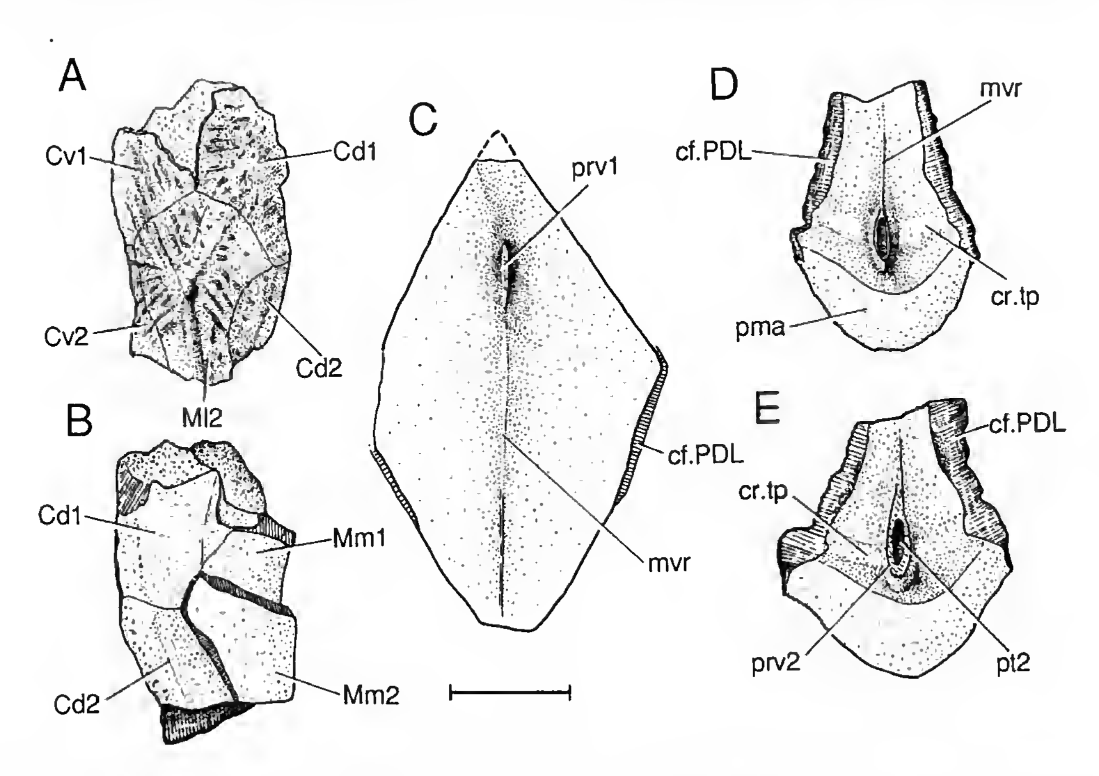


FIG. 25. — *Chuchinolepis sulcata* n. sp., Xitun Formation, Qujing. A-B, incomplete pectoral fin in lateral (A) and mesial (B) views, V10513.5; C, AMD plate of the holotype (V10513.1) in visceral view (elastomer cast); D, PMD plate in visceral view, V10513.2; E, PMD plate in visceral view, V10513.3. (Scale bar 5 mm.)

median dorsal ridge, the small tubercles form the ridges, which are more or less perpendicular to the lateral margins. Between the ridges, tiny tubercles could be observed under the microscope. In visceral view (Fig. 25D-E), the plate resembles very much that of *C. gracilis* (G.-R. ZHANG 1978). The *crista transversalis interna posterior* (cr.tp, Fig. 25D-E) lies laterally to the well-developed posterior ventral process and pit (prv2, pt2, Fig. 25D-E). Laterally, the plate overlaps the ADL plates (cf.PDL, Fig. 25D-E).

The ADL plate is preserved in the holotype, however, its lateral lamina and posterior extremity are damaged. Externally, the same ridged ornamentation as the AMD and PMD plates, and the area overlapped by the AMD plate are visible. As in the other *Chuchinolepis* species, the ADL plate is long and narrow. The dorsal lamina has a relatively broad anterior margin, ventrally to which extend the articular fossa and *crista transversalis interna anterior.*

The PDL plate is relatively long and narrow. As in other yunnanolepidoids, its lateral lamina is very low, indicating the presence of an independent PL plate. The dorsal corner of the dorsal margin is conspicuous. On the dorsal lamina, the ridges continue from the AMD and PMD plates in external view, whereas on the lateral lamina there are three longitudinal ridges parallel to the ventral margin. The overlapped areas by the PL, ADL, AMD and PMD plates are very clearly seen in the holotype. In visceral view, the overlap area for the AMD plate is observed.

Pectoral fin (Fig. 25A; pl. X, 7)

The pectoral fin of *C. sulcata* is very suggestive of that of *C. qujingensis* (G.-R. ZHANG 1984) except for its ornamentation. As in the trunk-shield, the ornamentation of the pectoral fin plates is composed of two types: one consists of small tubercles tending to form the regular ridges on the lateral surface, the other consists of very tiny tubercles between the ridges and on the mesial and ventral surfaces.

Unnamed antiarch

(Fig. 26A, pl. IV, 12)

?*Xichonelepis* sp. Janvier, 1995: 153, MNHN-CHD02, Fig. 7.

NEW MATERIAL. — V10515 from the Xitun Formation of Qujing, Yunnan.

REMARKS. — An AVL plate (MNHN-CHD02) from the Xitun Formation (Early Devonian) of Qujing, Yunnan was referred to *Xichonolepis* with a question mark by JANVIER (1995). That specimen bears definitely the same large ventral fenestra of the trunk-shield as in the Sinolepididae (RITCHIE *et al.* 1992) and *Vanchienolepis* (TONG-DZUY & JANVIER 1990), however, it retains the simple pectoral fin articulation as the Yunnanolepididae and should represent a new form of the Antiarcha. A detached PVL plate (V.10515) which could be referred to this new form was found by the author from the same locality and horizon, and its description is given below.

DESCRIPTION

V10515 has a length of 5.4 cm with a very low lateral lamina. Along its dorsal margin is the area overlapping the PL plate (cf. PL, Fig. 26A). The ventral lamina is rim-like as in the Sinolepididae. Its mesial natural margin shows neither the overlapped area nor the overlapping area, indicating the presence of a large fenestra of the ventral wall. In visceral view, the *crista transversalis interna posterior* (cr.tp, Fig. 26A) lies close to the posterior end of the plate.

Suborder YUNNANOLEPIDOIDEI gen. et sp. indet.
(Fig. 26B, pl. IV, 11)

MATERIAL. — V10506 from the Xishancun Formation of Qujing, Yunnan.

DESCRIPTION

This PDL plate (V10506) is characterized by its ornamentation, the tubercles forming many nodes (n, Fig. 26B) on the surface. The nodes are either rounded or elongated, and fairly developed on the anterior part of the plate and along the dorsolateral ridge (dlr, Fig. 26B). When compared to the PDL plate of other yunnanolepidoids, this plate looks relatively large, with a length of 4.2 cm. The dorsal lamina has a posteriorly placed dorsal corner (d, Fig. 26B), behind which is the area overlapped by the PMD plate (oa.PMD, Fig. 26B). Anteriorly, the plate is overlapped by the ADL plate. The lateral lamina forms a more or less blunt angle with the dorsal lamina. Its ventral lamina is overlapped by the PL plate (oa.PL, Fig. 26B).

PECTORAL FIN ARTICULATION OF THE CHUCHINOLEPIDIDAE

Since the pectoral fin articulation of the Chuchinolepididae (= Procondylolepiformes of G.-R. ZHANG) had been described and analyzed by G.-R. ZHANG (1984), this puzzling problem was discussed at length by TONG-DZUY & JANVIER (1990), YOUNG & ZHANG (1992) and JANVIER (1995). However, no consensus of opinion has been reached. Since knowledge will gain by the refutation or corroboration of the hypotheses, another hypothesis on the basis of new observations is proposed here. The review of the previous hypotheses about the brachial articulation of the Chuchinolepididae will be helpful to illustrate our hypothesis.

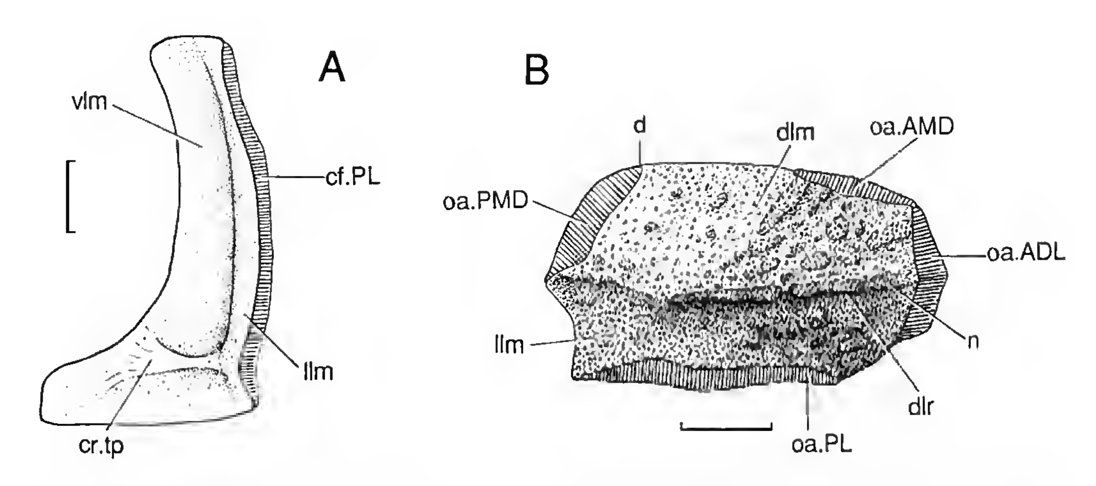


FIG. 26. — A, unnamed antiarch : right PVL plate in visceral view (elastomer cast), V10515, Xitun Formation, Qujing; B, Yunnanolepidoidei gen. et sp. indet. : right PDL plate in external view (elastomer cast), V10506, Xishancun Formation. (Scale bar 10 mm.)

Hypothesis of G.-R. ZHANG (1984)

This hypothesis suggested that the trilobate, perichondrally ossified scapulocoracoid exposed in the bottom of the pectoral fenestra was a primitive brachial process which later evolved into the brachial process of euantiarchs (including the Sinolepididae at that time). With regard to the dermal brachial articulations between the AVL plate and pectoral fin, three joints were proposed between the f.ab (Fig. 22C) and ar3v (Fig. 27), between the f.ad (Fig. 22C) and a restored process of his mm1 plate (Cd1, Fig. 27), and between the art.v (Fig. 22A, C) and a restored process of his Cv1 plate (Mm1, Fig. 27).

The first question raised by this hypothesis is the orientation of the pectoral fin. Since the available pectoral fins of the Chuchinolepididae are disarticulated, all reconstructions of the fin orientation are hypothetical. For the moment, we should decide which one is the most acceptable, since it affects directly the interpretation of pectoral fin plates of the Chuchinolepididae. As in

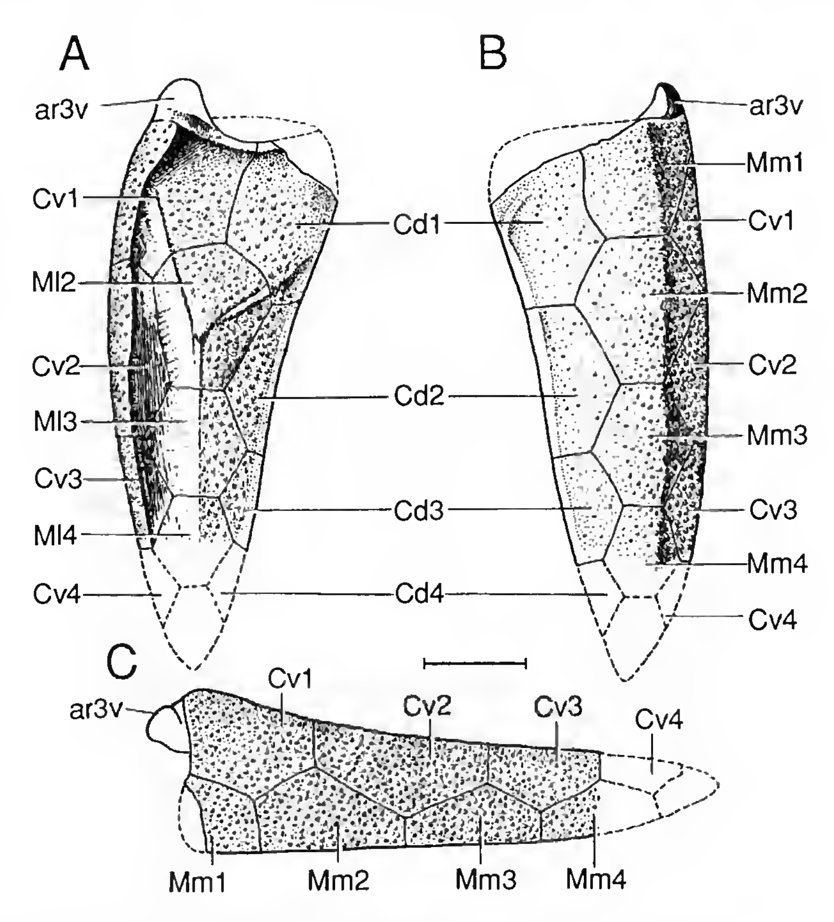


FIG. 27. — The left pectoral fin of *Chuchinolepis qujingensis* restored in lateral (A), mesial (B) and ventral (C) views (modified after G.-R. ZHANG 1984, fig. 4). (Scale bar 5 mm.)

the Euantiarcha and Sinolepididae, the pectoral fin of the Chuchinolepididae is covered by four series of dermal plates and is roughly triangular in transverse section. G.-R. ZHANG (1984) referred the three walls of the fin to the dorsal, lateral and ventral walls. His main argument was that the tubercles of the dorsal surface were coarser and more regular than those of the ventral surface. However, this kind of fin orientation is just contrary to what happens in euantiarchs, *e.g. Remigolepis*. Functionally, the orientation proposed by G.-R. ZHANG (1984) seems unreasonable since the lateral wall would be higher than the mesial wall, and this would hinder the movement. Moreover, this hypothesis was correct in supposing that the tubercles of the dorsal surface were coarser than those of the ventral surface, when compared with the trunk-shield. But what about the ornamentation of the lateral surface? If we take the trunk-shield as a reference, in general the ornaments of its lateral wall, are like those of its dorsal wall, coarser than those of the ventral wall. The finer ornamentation of the ventral wall was probably due to its frequent contacts with the substrate. The mesial wall of the fin in the Euantiarcha and Sinolepididae has a fine ornamentation because it faces the lateral wall of the trunk-shield. In the Chuchinolepididae, if we accepted the explanation of G.-R. ZHANG (1984), the ornamentation of the lateral wall was as fine as that of the ventral wall (G.-R. ZHANG 1984, fig. 2), that is contrary to the trunk-shield. However, if we interpret the fin orientation of the Chuchinolepididae like that of the Euantiarcha and Sinolepididae, we meet difficulties in the explanation of the dermal brachial articulation, as will be discussed below.

The second question is about the the dermal brachial articulation. As stated by G.-R. ZHANG (1984), there were three dermal joints, among which the joint between the f.ab and ar3v functioned as a fulcrum whereas the others rotated with in a very limited angle. However, among all of the pectoral fin specimens, only one kind of dermal articular process has been found. Moreover, the fossa on the parabrachial process, which was regarded by G.-R. ZHANG (1984) as the articular depression receiving the articular process of the fin, seems unsuitable for the articulation, even only as a pivot for the rotation of the fin. Our examinations of the parabrachial fossa (f.ab of this work) show that the fossa lacks the *siebknochen* texture, typical of the dermal brachial articulation, and its shape and size make obstacles to the explanation of its function as an articulation. The parabrachial fossa is peariform and variable in size, sometimes being fairly deep. We suggest that the parabrachial fossa is more likely to be a muscle insertion area, as for the adductor fossa (YOUNG & ZHANG 1992).

Hypothesis of YOUNG & ZHANG (1992)

YOUNG & ZHANG (1992) suggested that there are only two (not three) proximal dermal brachial articulations in the Chuchinolepididae, and the brachial articulation of chuchinolepids is transitional between that of yunnanolepids and that of sinolepids and euantiarchs. They tried to locate homologies in the structural components of the brachial articulation between the Chuchinolepididae on the one hand and the Sinolepididae + Euantiarcha on the other.

The first problem concerns the axillary foramen. As to the function of this structure, there had been many divergent opinions. STENSIÖ (1931, 1959) and GROSS (1933) regarded it as a passage for the adductor muscle for the pectoral fin. In the same time they supposed that the axillary foramen transmitted also nerves and vessels. WATSON (1961) noted the small size of the axillary foramen in *Pterichthyodes* compared to that of *Bothriolepis*, and suggested that it was too small for a muscle to pass, and must have been a passage only for the nerves and

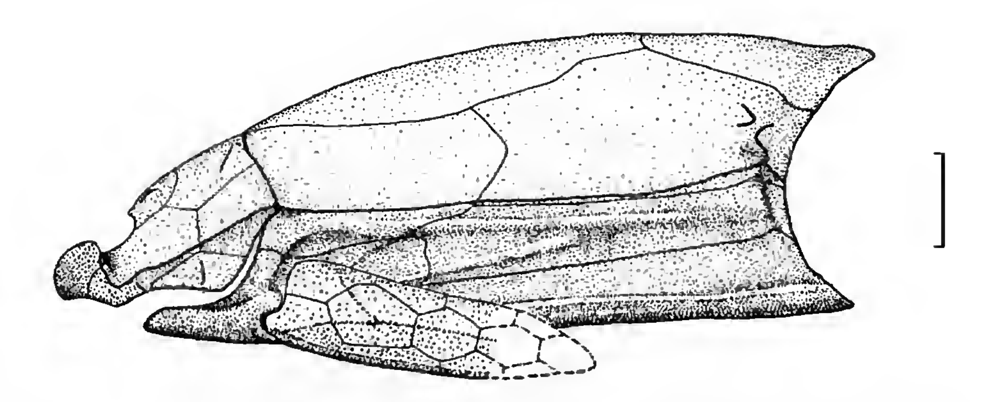


FIG. 28. — Restoration of *Chuchinolepis* in left lateral view. Trunk-shield and skull-roof after TONG-DZUY & JANVIER (1991, fig. 18), pectoral fin after G.-R. ZHANG (1984, fig. 4). (Scale bar 10 mm.)

vessels. This idea has been developed by YOUNG & ZHANG (1992), who considered that the axillary foramen was homologous to the small foramina piercing or encircling the scapulocoracoid in the Chuchinolepididae and other placoderms. However, considering the differences in size between the axillary foramen and the foramina of the Chuchinolepididae, it is difficult to understand this correlation. If the axillary foramen was a passage only for the nerves and vessels, it would be too large in many euantiarchs. I suggest here that the axillary foramen of Sinolepididae and Euantiarcha is homologous to the pectoral fenestra of the Yunnanolepididae, Chuchinolepididae and other placoderms. They have the same position relatively to the *crista transversalis interna anterior*. In addition to a passage for the vessels and nerves, the axillary foramen might have contained the cartilaginous scapulocoracoid, as in the Yunnanolepididae, where it forms an endoskeletal joint with the fin. Since the Sinolepididae and Euantiarcha have developed the brachial process and funnel pit (an apomorphy), and the cartilaginous scapulocoracoid in the funnel pit has formed a new endoskeletal joint with the fin, the part of the scapulocoracoid through the axillary foramen might have degenerated in some euantiarchs, *e.g. Pterichthyodes*.

Another problem is the insertion area for the abductor muscle of the fin in chuchinolepids. It is reasonable to assume that the posterolateral pit (f.ad) on the AVL plate is the insertion area for the adductor muscle as reinterpreted by YOUNG & ZHANG (1992). Since the parabrachial fossa was considered as the dorsal articular depression, YOUNG & ZHANG (1992) assumed the region between the f.ab and art.v to be the area for the attachment of the abductor muscle of fin. However, like G.-R. ZHANG (1984), we cannot find any definite depression for this attachment. Moreover, this position seems to be too ventral for the abductor muscle of fin.

Hypothesis in this work

Since the brachial articulations of the Chuchinolepididae and Sinolepididae + Euantiarcha are quite different in structure, I suggest that they have evolved independently from the primitive one, which is retained by some yunnanolepidoids. The trilobate, perichondrally ossified scapulocoracoid exposed in the bottom of the pectoral fenestra, as well as the parabrachial process and

fossa, is the synapomorphy of the Chuchinolepididae, whereas the brachial process and funnel pit are the synapomorphies of the Sinolepididae + Euantiarcha. The axillary foramen is homologous to the pectoral fenestra. In the Chuchinolepididae there is only one proximal dermal brachial articulation, that is between the art.v of the AVL plate and the ar3v of the pectoral fin. The fossa on the parabrachial process is the depression for the abductor muscle of fin.

As discussed above, the fin orientation of the Chuchinolepididae in G.-R. ZHANG's (1984) hypothesis is flawed with some inconsistencies. For example, the lateral surface of the fin has the same fine ornamentation as the ventral surface. However, if we accept a fin orientation similar to that of euantiarchs, *i.e.* the lateral surface of the fin *sensu* G.-R. ZHANG (1984) becoming the mesial (inner) surface of the fin, then we cannot make it compatible with the dermal brachial joint, since the articular process of the fin is at the mesioventral margin, whereas the articular depression on the AVL plate would be in a ventrolateral position. Here we propose another possibility, *i.e.* the pectoral fin in the Chuchinolepididae has a laterally compressed shape, with lateral, mesial and ventral surfaces (Figs 27, 28). In this new model, the ornamentation of the mesial and ventral surfaces is finer than that of the lateral surface. The only dermal brachial articulation, more or less ventral in position, is between the art.v and ar3v. This model is supported by the two following facts: the preserved dermal plates of the pectoral fin in *Phymolepis* (G.-R. ZHANG 1978; M.-M. ZHANG 1980; YOUNG & ZHANG 1992), which suggest a laterally compressed fin in this primitive antiarch, and the dorsoventrally extending scapulocoracoid in the Chuchinolepididae (G.-R. ZHANG 1984; YOUNG & ZHANG 1992).

Consequently, the dermal plates of the pectoral fin in the Chuchinolepididae are renamed (Table 1, Fig. 27). Like the Sinolepididae and Euantiarcha, the Chuchinolepididae have four series of dermal fin plates, and the first lateral marginal plate is missing from the proximal plate ring of the fin.

TABLEAU 1. — The terminology (in abbreviations) proposed by the various authors about the dermal plates of the pectoral fin in the Chuchinolepididae.

This work	YOUNG & ZHANG (1992)	G.-R. ZHANG (1994)	TONG-DZUY & JANVIER (1990)
Cd1-4	Mm1-4	Mm1-4	MM
Cv1	Cdl	M11	m1
Cv2-4	M12-4	M12-4	—
Mml-4	Cv1-4	Cv1-4	C
Ml2-4	Cd2-4	Cdl-3	—
ar3v	ar3d	adp	cdpbr
—	ar3v	avp	—
art.v	art.v	f.aPv	f.ibr
f.ab	art.d	f.aPd	fpbr
—	f.ab	—	—
f.ad	f.ad	s.art	—
gpbr	fgr	—	—
ppbr	prc	—	ppbr
scap	scap	p.pb	—

CLADISTIC ANALYSIS OF THE ANTIARCHA

Historical background

The study of antiarchs can be traced back to EICHWALD (1840) who erected two antiarch genera (*Bothriolepis* and *Asterolepis*). When the name Placodermi was proposed by M'COY (1848) for an extinct jawed fish group among the "ganoids", three genera of antiarchs (*Bothriolepis*, *Asterolepis* and *Pterichthys* [*now Pterichthyodes*]) were included in the group; the other three genera were an arthrodire *Coccosteus*, a ptyctodontid *Chelyophorus* and a heterostracan agnathan *Psammosteus*. COPE (1885) coined the name Antiarcha to distinguish the fishes such as *Bothriolepis* and *Asterolepis* from the other early vertebrates. The other researchers on antiarchs in the last century include MILLER (1841), AGASSIZ (1843, 1844, see also ANDREWS 1982), PANDER (1856, 1857), TRAQUAIR (1888, 1893) and WOODWARD (1891).

As to the affinity of antiarchs, COPE (1889) and WOODWARD (1891) rejected the homogeneity of placoderms, and suggested that antiarchs were closely related with "ostracoderm" agnathans, whereas they generally united ptyctodontids to holocephalans, and arthrodires to dipnoans. This opinion was followed by a majority of authors until STENSIÖ (1931) and GROSS (1931), who returned antiarchs to placoderms. However, the status of antiarchs among placoderms still remained unsettled (see GOUJET 1984a), and their classification and interrelationships has undergone great changes (see MILES 1968).

STENSIÖ (1931, 1948, 1959) subdivided antiarchs into two main groups, one for *Remigolepis* whose pectoral fin was unjointed, and one for the remaining genera which possessed the distal joint of the pectoral fin. This proposition had strong influence on the antiarch research and has been adopted for a fairly long time (BERG 1940; OBRUCHEV 1964; STENSIÖ 1969; G.-R. ZHANG 1984; PANTELEYEV 1992).

GROSS (1965) proposed that, as the whole exoskeleton is concerned, major subgroups of antiarchs should be the asterolepidoids, represented by *Asterolepis*, and bothriolepidoids, exemplified by *Bothriolepis*. *Remigolepis* was regarded as closely related to *Asterolepis*, and the absence of the distal joint was assumed to be secondary. At that time, the yunnanolepidoids from the Early Devonian of China (Y.-H. LIU 1963; M.-M. CHANG 1966), which turned out to be early representatives of antiarchs, began to raise interest, and a new suborder of antiarchs, the Yunnanolepidoidei, was erected by MILES (1968; see also GROSS 1965) to distinguish *Yunnanolepis* from the Bothriolepidoidei and Asterolepidoidei. However, since the detailed works about Early Devonian antiarchs of China had not been published, this rank of yunnanolepidoids was not adopted by DENISON (1978), who referred *Yunnanolepis* to the Bothriolepidae (= Bothriolepidoidei Miles 1968). In contrast, DENISON (1978) had acknowledged the Sinolepididae (LIU & P'AN 1958), which was originally assigned to asterolepidoids, as the third major antiarch group, the other two groups being the Bothriolepidae and Asteolepidae (= Asterolepidoidei Miles 1968). HEMMINGS (1978) removed the family Microbrachiidae from the Asterolepidoidei to the Bothriolepidoidei.

Important works on the anatomy and taxonomy of Early Devonian antiarchs from South China were undertaken by G.-R. ZHANG (1978), P'AN & WANG (1978) and M.-M. CHANG (1980), and confirmed that the yunnanolepidoids were the most primitive known forms of antiarchs, which provided links between the advanced antiarchs and other placoderms. However, until then,

these inquiries into the antiarch phylogeny were mainly within the framework of the evolutionary systematics.

The first cladistic analysis of antiarchs was that of JANVIER & PAN (1982). This cladogram suggested explicitly four major groups [Yunnanolepiformes (= Yunnanolepidoidei Miles, 1968), *Sinolepis* (the only genus of the Sinolepididae then known), Asterolepida (= Asterolepidoidei) and Bothriolepida (= Bothriolepidoidei)] within antiarchs, although the monophyly of the Yunnanolepiformes was uncertain. It was first proposed that *Sinolepis* is the sister-group of the asterolepidoid + bothriolepidoid pair, and the Sinolepididae was removed from the Asterolepidoidei. Following HEMMINGS (1978), *Microbrachius*, as well as *Wudinolepis*, was placed among the Bothriolepida. However, this cladogram was incomplete since many antiarch taxa were not included in the analysis.

LONG (1983) proposed a modified classification of MILES (1968). In this grouping, the Microbrachiidae was still placed within the Asterolepidoidei, and the Sinolepididae were removed from the Asterolepidoidei.

Important contributions to antiarch phylogeny, as well as to paleobiogeography, have been made by YOUNG (1984c, 1988) who provided us with a fairly complete cladogram of antiarchs, which is the basis of the present study. In YOUNG's cladogram, four major monophyletic groups of antiarchs were recognized, as in JANVIER & PAN (1982), and yunnanolepidoids were placed at the root of the cladogram. However, sinolepids were ranked as the sister-group of bothriolepidoids which included the Microbrachiidae, and the pair of sinolepids + bothriolepidoids formed the sister-group of asterolepidoids (*cf.* JANVIER & PAN 1982; RITCHIE *et al.* 1992). In his biogeographic analysis, YOUNG (1984c) pointed out that South China was the area of origin (or part of the area of the origin) of all major antiarch groups except for asterolepidoids. However, in my opinion, a fact should be taken into consideration, *i.e.* the Asterolepidoidei has a relatively younger distribution than the other antiarchs.

YOUNG (1990) found some features of *Nawagiaspis* suggestive of the Asterolepidoidei whereas others are suggestive of bothriolepid affinity, and the placement of this genus within his cladogram is rather difficult. In fact, when the range of the Bothriolepidoidei is expanded to include the Microbrachiidae and *Dianolepis* in addition to the Bothriolepididae *sensu stricto*, the boundary between the Asterolepidoidei and Bothriolepidoidei becomes more and more obscure. Another example is *Jiangxilepis* (ZHANG & LIU 1991), which was originally referred to the Bothriolepidoidei. However, it has many characters of the Asterolepidoidei, *e.g.*, the narrow anterior margin of the AMD plate, the loss of the anterior ventral process, and the mesially placed tergal angle. The same problem was encountered in *Luquanolepis* (ZHANG & YOUNG 1992), an Early Devonian bothriolepidoid from South China. This antiarch has the independent PL plate as in *Nawagiaspis* and some asterolepidoids, and the anterior margin of its AMD plate is supposed to be narrow. In my opinion, all these problems are related with the problem of the monophyly of the Bothriolepidoidei, which should in turn be resolved within the framework of the entire antiarch phylogeny.

ZHANG & YOUNG (1992) made the phylogenetic analysis of the Bothriolepidoidei using the Hennig86 program. This was the first phylogenetic work for antiarchs based on detailed character analysis with a parsimony program. However, the results are not so successful as desirable. The

source of the problem, in my opinion, is the presumed monophyly of the Bothriolepidoidei, which will be examined below on the basis of the phylogenetic analysis of 40 antiarch genera.

MATERIALS AND METHODS

Data

By now, there are 44 antiarch genera (154 species) described in the literature and an unnamed genus (JANVIER 1995; this work). Five of them (*Yunlongolepis, Chuanbeiolepis, Taeniolepis, Shimenolepis* and *Hyrcanaspis*) are not included in the present analysis because they are too poorly known.

Taeniolepis (GROSS 1932), from the Upper Devonian (Frasnian) of Latvia, is represented by nuchal and postpineal plates. Its nuchal plate is excluded from the orbital fenestra, and bears no sensory-line groove, thereby resembling more or less sinolepids and some asterolepidoids.

Hyrcanaspis (JANVIER & PAN 1982) is known from the Early Devonian (Emsian, JANVIER pers. comm.) of Iran. The described specimens include some disarticulated trunk-shield plates and a central plate of the pectoral fin. Its AVL plate bears a relatively large axillary foramen, somewhat similar to that of *Microbrachius*, and the dermal plates are ornamented with very thin, almost parallel ridges. It is distinguished from other euantiarchs by its almost ventral position of the precondylar ridge of the brachial process. *Hyracanaspis*, as well as *Microbrachius*, was provisionally regarded as a bothriolepidoid by JANVIER & PAN (1982).

Both *Yunlongolepis* and *Chuanbeiolepis* are found from the Early Devonian of Longmenshan, Sichuan, China (S.-T. WANG *in* HOU *et al.* 1988a). The AMD plate of *Yunlongolepis*, the only specimen of this genus, looks like that of *Yunnanolepis*, however it lacks the anterior ventral process and median ventral ridge. *Chuanbeiolepis*, a poorly preserved internal mould of the trunk-shield, is suggestive of *Chuchinolepis* by its anteriorly placed anterior ventral process, and the *crista transversalis interna posterior* lying laterally to the posterior ventral process.

Shimenolepis, the earliest representative of antiarchs (J.-Q. WANG 1991b), is known from the Early Silurian (late Landoverian) of Lixian, Hunan, China. However, the information about this genus is quite scarce, since only an internal mould of the PVL plate (the type specimen) was referred to it. This PVL plate has the *crista transversalis interna posterior* lying very close to the posterior extremity of the trunk-shield, as in yunnanolepidoids, and this may be plesiomorphic for antiarchs. Its lateral lamina has a fairly constant height, as in *Zhanjilepis* (G.-R. ZHANG 1978), and therefore, it was suggested to be a Yunnanolepidoidei by J.-Q. WANG (1991b). There is no impression for the ventrolateral fossa of the trunk-shield, which occurs in *Yunnanolepis* and *Phymolepis*. Noteworthy is an internal mould of the AMD plate from the same level, which was referred to as an undetermined form of the Chuchinolepididae by J.-Q. WANG (1991b). However, this specimen could also belong to *Shimenolepis*, since its size and ornament are compatible with those of the holotype. Like the AMD plate of *Chuchinolepis*, this plate is fairly long and narrow, and has the elongated, anteriorly placed anterior ventral process. The Chuchinolepididae (*Chuchinolepis*) is rather derived considering its pectoral fin articulation, but whether this early Silurian antiarch shares this derived feature of the Chuchinolepididae or just retains the simple fin articulation as in the Yunnanolepididae is unknown. It is probable that the anterior ventral process of the AMD plate, which is anteriorly placed, as in *Chuchinolepis* and this Silurian antiarch, is plesiomorphic for antiarchs. More material is needed to clarify this problem.

Ten genera among the rest of antiarchs have a poorly known skull-roof [*Vietnamaspis* (premedian plate), *Briagalepis* (lateral plate), and *Monarolepis* (nuchal plate)] or completely unknown skull-roof (*Zhanjilepis*, unnamed antiarch, *Vanchienolepis*, *Luquanolepis*, *Grossaspis*, *Lepadolepis* and *Wurungulepis*). However, since they have been well established by other diagnostic characters, they are included in the phylogenetic analysis in order to minimize the subjectivity in selecting the OTU's.

Among the analyzed antiarch taxa (40 genera, including the unnamed antiarch which is indeed a new genus), 22 of them are monospecific. For the other genera, we supposed *a priori*, that all of them are monophyletic and can be used as terminal taxa in the phylogenetic analysis.

Characters and character codings

Sixty-six characters were selected for the character analysis. Since the selection of the characters is the first level of a hypothesis, the character independence is taken into consideration and all characters are treated as unweighted in order to avoid biases as much as possible.

As to the multiple-state characters, the character analysis is done to construct the character cladogram. For the branching transformation series, the mixed coding (WILEY *et al.* 1991) is adopted and one character may be subdivided into several characters. Therefore, each character used below is a linear transformation series and is treated as additive.

As to the missing data, two situations may occur : one is the logical impossibility (coded in the data matrix as –), and the other is the unavailable information (coded in the data matrix as ?) due to either poor preservation or absence of fossils. However, because of the constraints of fossil preservation, there is a large number of missing data in the data matrix, that makes the results of the phylogenetic analysis nearly uninformative. Two options have been suggested to overcome this difficulty. One is to exclude the least known characters or/and the poorly known taxa from the data set, thereby making the analysis more informative. However, since many taxa are excluded from consideration, this kind of analysis has its limits. In order to overcome this default in the phylogenetic analyses of Paleozoic actinistians, CLOUTIER (1991) has adopted the complementary analyses on the basis of the main analysis to include the poorly known taxa. However, if the results of the main analysis are largely influenced by the subsequent complementary analyses, the interpretation of the cladograms is very ambiguous. The other option, used by ZHANG & YOUNG (1992) in the phylogenetic analysis of bothriolepidoids, is to fill in for some unknown data to give a much more complete data matrix. This has been adopted in the present study.

The filling in for the missing data has been selective and is made for a particular character of a particular taxon (coded in the data matrix in italics), using the criterion that, among its supposed closely related forms (according to the previous studies), the character state is well defined and uniform. This procedure involves more assumptions, but, it is compensated for by the less ambiguous and more informative results obtained from the analysis. Moreover, the phylogenetic inference itself is hypothetic deductive (NELSON & PLATNICK 1984), and these inferred states for unknown characters are consistent with the philosophical background of Cladistics. As defended by ZHANG & YOUNG (1992), no data set can be completely objective. The data matrix obtained here may provides us with a framework for further research; those inferred states can be either corroborated or refuted, and the gaps can be filled in by new material or more detailed observations. The results of the phylogenetic analysis are just hypotheses at the

TABLE 2. — Data matrix of 66 characters for 40 antiarch genera. *Kujdanowiaspis* (arthrodire) and *Romundina* (acanthothoracid) are used as the outgroups of antiarchs. – = logical impossibility coding; ? = unavailable information. X = intraspecific variations. Inferred states for unknown characters are shown in italics. Description of the characters and character states are in the text.

TAXA	CHARACTERS						
	1	1111111112	2222222223	3333333334	4444444445	5555555556	666666
	1234567890	1234567890	1234567890	1234567890	1234567890	1234567890	123456
Kujdanowiaspis	00-------0	00--------	0000000000	0000000000	0000---0--	-----0-000	0-0100
Romundina	00-------1	00--------	00000000-1	0000000000	00010-000-	000000001?	00??0?
Yunnanolepis	11000000-0	1300000000	001111000X	X100?01000	0011000101	0000100000	00???0
Mizia	11000000-0	1300000000	0010010000	1100?01110	0011000101	0000000000	000000
Phymolepis	11000000-0	1300000000	0010110000	1100?01100	0011000101	0000000000	00???0
Zhanjilepis	11000000-0	1300000000	0001010000	1100?01000	00111-2101	0000000000	00????
Heteroyunnanolepis	11000000-0	1300000000	0001000000	110000????	??11???10?	?00??????0	00????
Minicrania	11000000-0	1001000000	0001000000	1100?01011	0111001100	0000000000	00???0
Chuchinolepis	11000000-0	1301000000	0001000000	1100?01000	0011000101	0000100000	00????
Unnamed antiarch	11000000-0	1???0?0000	???1000?01	1100?0????	??11???10?	?00??????0	00????
Vanchienolepis	1101?0?0?0	1301000100	???1000001	1100?0????	??11???10?	?00??????0	00????
Xichonolepis	111010?000	1211010000	0101000101	1100?01111	001101?101	0001110000	00????
Grenfellaspis	111010?000	1121010001	0101000101	1100?01111	0011011101	0001100000	00????
Dayaoshania	1110100000	1211010000	0??1000101	1100?01111	001101?101	0001101000	00????
Liujiangolepis	1110101000	1001010000	0??1000101	1100001111	001100?101	0001121000	00????
Sinolepis	111010?000	1021010001	0??1000101	1100?01111	001101?100	0001100000	00????
Luquanolepis	11201?01?0	11010??000	1001000010	1100?0?1??	??11???10?	?00???????	??????
Wudinolepis	11211?01?0	1001001000	1001000110	1101?00111	011100?101	1000030?0?	00????
Hohsienolepis	112?1?0??0	1001001000	1001000110	1102?00111	0?1100?101	100003000?	?0????
Microbrachius	11211?00?0	1001001000	1001000110	1102?00111	0111000101	1000030001	00????
Vietnamaspis	11211????0	1101001001	1001000110	1100?0?1??	??111-?10?	10000?????	??????
Dianolepis	1120100??0	1101001000	1001000110	1100?00111	00111-2101	1000021001	00????
Jiangxilepis	11211011?0	1101001110	1001000110	1110?01111	00111-2100	100002100?	00????
Tenizolepis	112?1??1?0	1001101000	1001000110	1100?011?1	0?111-2101	100002100?	??????
Nawagiaspis	11201????1	1101???000	1001000010	1100?011??	00111-?100	1000031??1	000010
Briagalepis	112?1????0	1001101000	1001000110	1100?01110	0?11?-?10?	?00????1?1	??????
Monarolepis	112011???0	1001101000	1001000110	1100?0011?	??11?-?10?	?00???????	??????
Grossilepis	1121111110	1001010000	1001000110	1100?00100	10111-2101	1000121101	10011?
Bothriolepis	1121111110	1001001000	1001000110	1110000100	10111-2101	1000121101	100110
Grossaspis	11201000?1	1100001100	100100?0?0	1100?1?1??	??11?-?10?	??0???????	??????
Lepadolepis	11201000?1	1100001100	100100?0?0	1100?1?1??	??11?-?10?	??0???????	??????
Gerdalepis	1120100001	1100001100	1001001010	1100?11111	01111-1100	000000001?	??1???
Wurungulepis	11201000?1	1?00001?00	1001000000	110010?1??	??11?-?10?	??0???????	??????
Sherbonaspis	1120100001	1200001100	1001001000	1100?0111?	?1111-1100	01000?1010	001???
Stegolepis	11201000?1	1200000110	1001000000	110X?01111	01111-1100	110001101?	??1???
Byssacanthus	1120100011	1100000110	100100X000	1100?01111	11111-1100	1000020010	001???
Kirgisolepis	11201????1	1100????10	10010010?0	1100?00100	11111-1100	100002101?	??1???
Pterichthyodes	1120100001	1100001100	1001001000	1100101101	01111-1100	1000021010	001??1
Hunanolepis	1120100111	1100001100	1001001000	1100?01111	01111-1100	1000031010	001???
Asterolepis	1120100010	1300010100	1001001000	1100101111	01111-1110	0110011010	001??1
Pambulaspis	1120?000?0	1300001100	1001000000	1100?01111	01111-1110	011001101?	011???
Remigolepis	11200000-0	1300000100	1001000000	1100?01111	01111-1110	0110011010	011??1

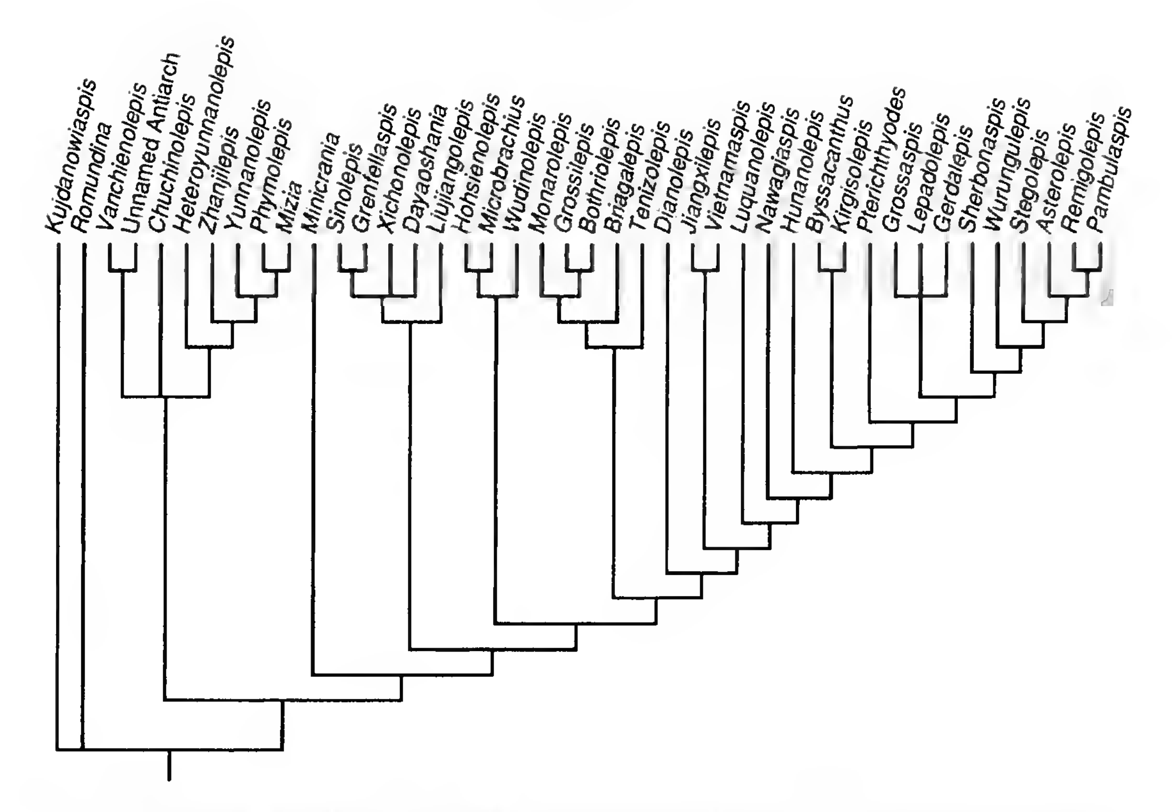


FIG. 29. — Strict consensus tree of antiarchs phylogeny constructed from 12 MP trees (L = 155, CI = 48) obtained with mhennig*+bb* analysis (Hennig86) of the character matrix in Table 2.

present stage, which await falsification. As stated by POPPER (1965 : 36) "[e]very genuine test of a theory is an attempt to falsify it, or to refute it. Testability is falsifiability."

In some cases, the interspecific variation for a particular genus is also coded as the unavailable information (X in the data matrix), which can be optimized later. In my opinion, this treatment is more rational.

Outgroups

Since either arthrodires or acanthothoracids have ever been considered as the sister-group of antiarchs (DENISON 1975, 1978, 1983; MILES & YOUNG 1977; YOUNG 1980, 1986; GARDINER 1984; LONG 1984; FOREY & GARDINER 1986; GOUJET 1984a), two genera of these two groups are selected as the outgroups in our analysis. One is the actinolepid *Kujdanowiaspis* (STENSIÖ 1945, 1963), the other is the acanthothoracid *Romundina* (ØRVIG 1975).

Tree calculations

In the first run, the data set was analyzed with the algorithms hennig* + bb of Hennig86. All the characters were treated as additive (ordered). This generated 100 most parsimonious (MP) trees (L = 157, CI = 47, RI = 80). By not specifying the * option for the bb algorithm,

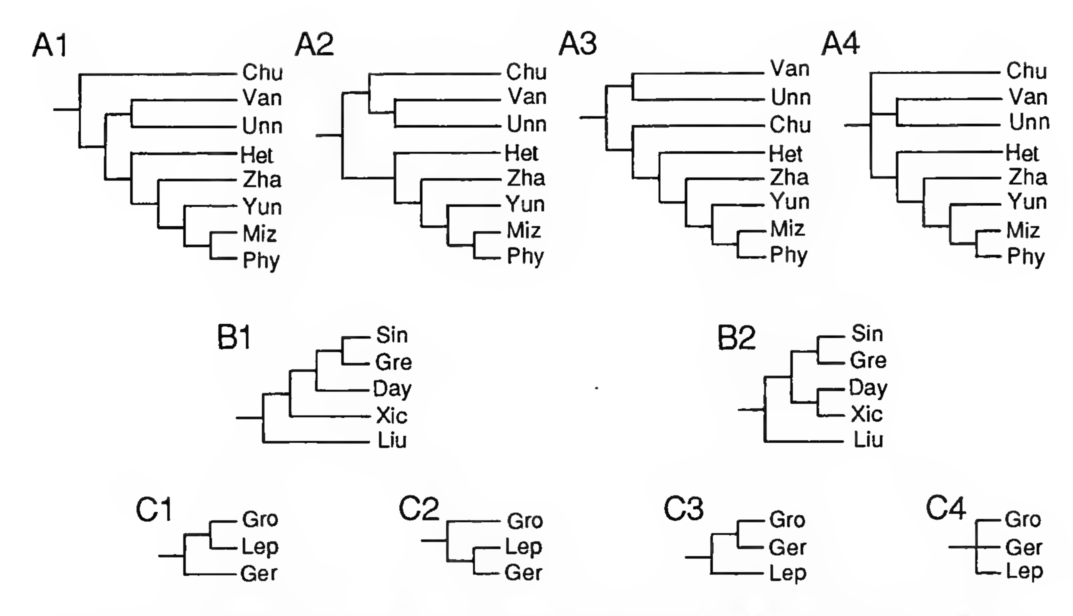


FIG. 30. — Three sets of unresolved nodes within yunnanolepidoids (A), sinolepids (B) and asterolepidoids (C) (all combinations = 32 MP solutions). Chu – *Chuchinolepis*, Day – *Dayaoshania*, Ger – *Gerdalepis*, Gre – *Grenfellaspis*, Gro – *Grossaspis*, Het – *Heteroyunnanolepis*, Lep – *Lepadolepis*, Liu – *Liujiangolepis*, Miz – *Mizia*, Phy – *Phymolepis*, Sin – *Sinolepis*, Unn – unnamed antiarch, Van – *Vanchienolepis*, Xic – *Xichonolepis*, Yun – *Yunnanolepis*, Zha – *Zhanjilepis*.

only 100 MP trees found at certain stage are saved. Therefore, the author performed a second run of the data set using the combination hennig* + bb* followed by the nelsen command. In this way, 12 MP trees (L = 155, CI = 48, RI = 81, Fig. 31) and the strict consensus tree of Fig. 29 are obtained. The same data were reanalyzed with the heuristic algorithms of PAUP (version 3.1), which yielded 18 MP trees with the same length as found with Hennig86. This data set is too large to use the branch and bound algorithm. The strict consensus tree is the same as in Fig. 29. In fact, there exists 32 MP trees as inferred from the combination of the trichotomies (Fig. 30). The MP trees were confirmed with MacClade (version 3.0), and the synapomorphies at each node were easily found with this software.

Character analysis of Antiarchs

1. Pectoral fin scale-covered (0) or modified into a slender appendage covered with small dermal plates (1).

The pectoral fin of antiarchs is modified into a slender appendage covered with small dermal plates, and is very specialized in comparison with the pectoral fin of other fishes which is scale-covered. The evidence from *Phymolepis* (G.-R. ZHANG 1978; M.-M. ZHANG 1980) confirms the slender appendage to be present in the Yunnanolepidoidei although it might be not completely developed (JANVIER 1995). A slender pectoral appendage is assumed to be present in all antiarchs, since it can be inferred from the small pectoral fenestra and the articulation structure of the AVL plate when the pectoral fin itself is unavailable.

2. Pectoral fenestra encircled by more than two plates (0) or by a single plate (1).

The pectoral fenestra of antiarchs is typically developed in *Minicrania* (ZHU & JANVIER 1996) and the Yunnanolepididae, although it is fairly small in comparison with that of other placoderms. The pectoral fenestra is assumed here to be modified into the axillary foramen of the advanced antiarchs. In general, the pectoral fenestra of placoderms is encircled by the anterior lateral, anterior ventrolateral or even posterior ventrolateral plates. In antiarchs, the pectoral fenestra or the axillary foramen is restricted within the AVL plate, which should be regarded as apomorphic.

3. Pectoral fin articulation simple (0), sinolepid type (1) and euantiarch type (2).

The simple pectoral fin articulation without any dermal articulation, exemplified by *Yunnanolepis* (G.-R. ZHANG 1978; M.-M. ZHANG 1980), is generally regarded as plesiomorphic for antiarchs by outgroup comparison. The pectoral fenestra of the Yunnanolepididae can be directly compared to that of other placoderms. The advanced types of pectoral articulation include those of *Chuchinolepis* (G.-R. ZHANG 1984; YOUNG & ZHANG 1992), *Vanchienolepis* (TONG-DZUY & JANVIER 1990), the Sinolepididae (YOUNG & ZHANG 1992; RITCHIE *et al.* 1992) and the Euantiarcha.

Turning to the evolution of the pectoral joint in antiarchs, G.-R. ZHANG (1984) proposed a transformation series from the Yunnanolepididae to the Chuchinolepididae, then to the Asterolepidoidei and Bothriolepidoidei including the Sinolepididae. This proposal was developed by YOUNG & ZHANG (1992), who suggested four hypothetical stages in the evolution of the pectoral fin articulation of antiarchs, *i.e.* those of the Yunnanolepididae, *Chuchinolepis* (*Procondylolepis*), the Sinolepididae and finally the Euantiarcha. However, there is no clear homology of the pectoral articulations in *Chuchinolepis* and the Sinolepididae + Euantiarcha. It is probable that the pectoral fin articulation of *Chuchinolepis* is derived independently from that of the Sinolepididae + Euantiarcha. The same applies to *Vanchienolepis*. Therefore, as to the polarity of pectoral fin articulation of antiarchs, a branching transformation series is proposed here. From the simple pectoral fin articulation derived independently three patterns : those of *Chuchinolepis*, *Vanchienolepis*, and the Sinolepididae leading to that of the Euantiarcha. Since either the articulation of *Chuchinolepis* or that of *Vanchienolepis* is only represented by one genus among antiarchs, these two types of pectoral fin articulation is useless for the phylogenetic analysis of antiarchs at the generic level. Only the third evolutionary path remains here for the analysis. With the mixed coding method, the articulation of the Yunnanolepididae, *Chuchinolepis* and *Vanchienolepis* is coded as "0", that of the Sinolepididae exemplified by *Grenfellaspis* (RITCHIE *et al.* 1992) as "1", and that of the Euantiarcha as "2". The fin articulations of *Dayaoshania* (RITCHIE *et al.* 1992) and *Liujiangolepis* (S.-T. WANG 1987) cannot be observed in the available material, and that of *Sinolepis* was only represented by an incomplete brachial process. However, their pectoral fins are relatively advanced, and their articulations are inferred to be the same as that of *Grenfellaspis*.

4. Axillary foramen small (0) or large (1).

The enlarged axillary foramen had been considered as one of the synapomorphies of the Bothriolepididae by YOUNG (1984c, 1988). LONG *et al.* (1990) quantified the size of the axillary foramen in terms of the ratio (height of the foramen to height of the lateral lamina of the AVL

plate) and it was suggested that the foramen exceeding 30% is "large" (ZHANG & YOUNG 1992), a criterion which is followed in this work. As to its phylogenetic significance, ZHANG & YOUNG (1992) found that it was difficult to be explained because of its scattered distribution and suggested that it may be correlated with the length of the proximal fin segment. The alternative explanation is that, if the axillary foramen gives a passage to the adductor muscle of the pectoral fin, as suggested by STENSIÖ (1959, 1969), enlarged foramen suggests a strong muscle and improved movement capacity of fin. Since the axillary foramen is homologous to the small pectoral fenestra of primitive antiarchs represented by the Yunnanolepididae, the enlarged axillary foramen is apomorphic whatever its function. A large axillary foramen is recorded in *Vanchienolepis* (TONG-DZUY & JANVIER 1990), *Wudinolepis*, *Microbrachius*, *Vietnamaspis*, *Jiangxilepis*, *Bothriolepis*, *Grossilepis* (ZHANG & YOUNG 1992) and *Hyrcanaspis* (JANVIER & PAN 1982). The axillary foramen of *Pambulaspis* (YOUNG 1983) is assumed to be small, as in other asterolepidoids.

5. Pectoral fin unjointed (0) or jointed (1).

No complete pectoral fin has yet been found in the Yunnanolepididae and Chuchinolepididae. However, the available material indicates that the pectoral fin of the Yunnanolepididae (G.-R. ZHANG 1978; M.-M. ZHANG 1980) and Chuchinolepididae (Procondylolepidae, G.-R. ZHANG 1984) is probably unjointed as in *Remigolepis* (STENSIÖ 1931; PAN *et al.* 1987). Thus, the Chuchinolepididae and those primitive antiarchs retaining a simple pectoral fin articulation are inferred to have unjointed pectoral fins. In contrast, those with more advanced fin articulation are presumed to have the jointed pectoral fin when fossil evidence is unavailable, except for *Pambulaspis* (YOUNG 1983). YOUNG (1983) suggested a closer relation between *Pambulaspis* and *Remigolepis* than either has with *Asterolepis*, and whether or not a distal joint is present in *Pambulaspis* is important for the analysis. Another genus which is scored as missing data is *Vanchienolepis*, which has a more complicated fin articulation structure than the Yunnanolepididae.

6. Cd1 and Cd2 plates in contact (0) or separated (1).

The reduction of the Cd2 plate, which is separated from the Cd1 plate by the Ml2 and MM2 plates, has a limited distribution in antiarchs (ZHANG & YOUNG 1992), and occurs only in some bothriolepidoids. The plesiomorphic state is that the Cd2 plate is in contact with the Cd1 plate (YOUNG 1983, 1984a; ZHANG & YOUNG 1992), and is common in other antiarchs, including the Yunnanolepididae and Chuchinolepididae. Sinolepids were proved to retain the primitive condition (RITCHIE *et al.* 1992).

7. Pectoral fin short (0) or elongated (1).

The pectoral fin extending backwards beyond the trunk-shield is defined here as the elongated fin, and is assessed as apomorphic. The primitive antiarchs such as the Yunnanolepididae probably have the short, unjointed fins, as in *Remigolepis*. In antiarchs, the elongated fin is present in *Jiangxilepis*, *Bothriolepis* (STENSIÖ 1963, 1969), *Grossilepis* and *Liujiangolepis* (S.-T. WANG 1987). The fin length has no clear correlation with the size of the axillary foramen. The antiarchs with a large axillary foramen, such as *Microbrachius*, may have the short pectoral fin. PAN *et al.* (1987) described a fairly elongated pectoral fin of *Sinolepis* associated with part of the AVL and PVL plates. However, RITCHIE *et al.* (1992) suggested that the specimen may belong to a bothriolepid antiarch. New material is needed to clarify this problem because the Sinolepid-

idae may possess a elongated pectoral fin, *e.g. Liujiangolepis* (S.-T. WANG 1987). Therefore, the coding of *Sinolepis* as "unknown" is preferable.

8. Ml2 plate relative to the trunk-shield short (0) or elongated (1).

The length of the Ml2 plate of the jointed pectoral fin roughly corresponds to the length of the proximal segment and its posterior end represents the extremity of the proximal segment. In *Remigolepis* and the Yunnanolepidoidei whose pectoral fin probably possesses only one segment, the Ml2 plate is generally short and broad; which is, the primitive condition for antiarchs. In some bothriolepidoids, such as *Bothriolepis* and *Grossilepis*, the Ml2 plate is much elongated with its posterior end situated behind the level of the posterior end of the MV plate, which should be interpreted as apomorphic. However, how to assess these two states remains a problem. ZHANG & YOUNG (1992) defined a similar character, *i.e.* the proximal segment of pectoral fin shorter or longer than the level of the posterior end of the MV plate. However, it was easily biased by the relative size of the MV plate or the space corresponding to the MV plate, especially when used in the Sinolepididae which have no MV plate. We suggest that the centre of the MV plate is more constant and thus more suitable for the reference. Moreover, the proximal segment is replaced here by the Ml2 plate, which can be used for the unjointed fins as well.

9. Three (0) or two (1) Ml plates of the distal segment.

The plate arrangement of the pectoral fin in the Yunnanolepididae and Chuchinolepididae suggests that 3 lateral marginal plates in the distal segment, as in *Dayaoshania, Liujiangolepis, Sherbonaspis, Gerdalepis* and *Pterichthyodes*, should be plesiomorphic. This character is unavailable in those antiarchs which are assumed to have unjointed fins.

10. Low and elongated (0) or high and short (1) trunk-shield.

JANVIER & PAN (1982) suggested that the very large and elongated trunk-shield was one of the asterolepid (*Remigolepis* and *Asterolepis*) synapomorphies. Alternatively, YOUNG (1984c, 1990) proposed that the high and short trunk-shield was apomorphic amongst asterolepidoids, as judged from the condition in the Yunnanolepidoidei.

11. One (0) or two (1) median dorsal plates.

Two median dorsal plates are present exclusively in antiarchs.

12. Index between width of anterior margin and maximum width of the AMD plate, > 55 (0), 35-55 (1), 15-35 (2), or < 15 (3).

The width of the anterior margin of the AMD plate is a very significant character in antiarchs. But how to define its relative narrowness is ambiguous. ZHANG & YOUNG (1992) compared the anterior margin width with the posterior margin width and proposed that the anterior margin broader than the posterior one was apomorphic. In our opinion, it is more appropriate to use the index between the anterior margin width and maximum width of the AMD plate. In general, a narrow anterior margin may correspond to a narrow posterior margin, as exemplified by *Yunnanolepis, Chuchinolepis, Remigolepis* and *Asterolepis*. The index proposed here, however, could reflect the relative narrowness of the anterior margin of the AMD plate. Then, the problem is to decide the polarity of this character.

ZHANG & YOUNG (1992) regarded the anterior pointed AMD plate of Early Devonian yunnanolepids and most asterolepidoids as primitive. The broad anterior margin of the AMD plate

was considered derived in comparison to that in *Yunnanolepis*. However, this polarity is contradicted by outgroup comparison. The median dorsal plate of other placoderms, if it is homologous to the AMD plate of antiarchs, has a broad anterior margin. [If we accept the proposition of Y.-H. LIU (1991), *i.e.* the AMD plate of antiarchs is homologous to the extrascapular plate of other placoderms, the conclusion will be same, by outgroup comparison.] Growth series in antiarchs provide further evidence. In *Bothriolepis canadensis* (WERDELIN & LONG 1986), the index between the anterior margin width and maximum width of the AMD plate of the juvenile individuals is much larger than that of the adults. The juvenile *Asterolepis ornata* (UPENIECE & UPENIEKS 1992) has a relatively broad anterior margin of the AMD plate whereas the adult *Asterolepis* has an anteriorly pointed AMD plate. Therefore, it is considered here that the narrow anterior margin of the AMD plate is apomorphic. In order to code the character, the subdivision of the morphological continuum is needed. In this work, we code the index above 55 as primitive (0), 35-55 as 1, 15-35 as 2, and below 15 as 3.

13. Index between anterior and posterior divisions of the AMD plate, < 300 (0), 300-500 (1), > 500 (2).

The AMD plate could be subdivided into two portions by the lateral corner, which corresponds to the suture between the ADL and PDL (or MxL) plates. The index indicates the relative position of the PDL plate with reference to the AMD plate. When the index becomes larger, the PDL (or MxL) plate has a more posterior position. The growth series in *Sinolepis* (LIU & P'AN 1958: 38) shows that the anterior division of the AMD plate in the juvenile individual is proportionally shorter than that in the adult, thus suggesting a polarity. As for the character 12, we code the index below 300 as plesiomorphic (0), 300-500 as 1, above 500 as 2.

14. Tergal angle of AMD plate centrally (0) or anteriorly (1) placed.

The position of the tergal angle of the AMD plate generally corresponds to that of the anterior ventral process whenever the process is present. The outgroup comparison is directly related with the homologue of the AMD plate in other placoderms, which is more or less controversial. If the median dorsal plate is homologous to the AMD plate of antiarchs, then the outgroup comparison suggests the posteriorly or centrally placed tergal angle is plesiomorphic. However, there is another possibility that the extrascapular plate is homologous to the AMD plate. If this be true, then we cannot determine the polarity by means of outgroup comparison. Amongst antiarchs, both states are found in the Yunnanolepidoidei. The anteriorly placed tergal angle is present in bothriolepidoids, sinolepids, chuchinolepids and *Minicrania* (ZHU & JANVIER 1996).

15. AMD plate completely (0) or partly (1) overlapping the ADL plate.

That the AMD plate overlaps the ADL plate along the entire contact margin in the Yunnanolepidoidei indicates that the very short overlap margin of the AMD plate for the ADL plate in *Briagalepis, Tenizolepis* (MALINOVSKAYA 1992) and *Monarolepis* is a derived feature (LONG *et al.* 1990).

16. AMD plate underlapping or partly (0) or completely (1) overlapping the PDL (or MxL) plate.

There are three types of the overlap relationship between the AMD and PDL (or MxL) plates in antiarchs. The first one is that the AMD plate overlaps the PDL or MxL plate over the anterior half of their common suture, whereas it is the reverse for the posterior half, as in *Yunnanolepis* and *Remigolepis*. The second one is that the AMD plate overlaps the PDL or MxL plate over the entire length of their common suture, as in *Sinolepis*, *Liujiangolepis* (S.-T. WANG 1987), *Xichonolepis*, and *Asterolepis* (KARATAJUTE-TALIMAA 1963). The third one is that the AMD plate is overlapped by the PDL or MxL plate over most of their common suture, as in *Bothriolepis*, *Jiangxilepis* (ZHANG & LIU 1991) and *Hunanolepis* (J.-Q. WANG 1991a). Since no outgroup comparison could be used to determine the polarity, the state in the Yunnanolepidoidei is regarded here as primitive. The second and the third states reflect the two different evolutionary directions. As the mixed coding (WILEY *et al.* 1991) is used here for the branching transformation series, the evolution regarding the overlap relationship between the AMD and PDL (or MxL) plate is treated as two characters (characters 16 and 17).

The AMD plate of *Vanchienolepis* (TONG-DZUY & JANVIER 1990) is poorly preserved in its posterior part, however, the type of its overlap relationship can be inferred from the information of the PDL plate, which is same as that of *Yunnanolepis*.

17. AMD plate partly or completely overlapping (0) or underlapping the PDL (or MxL) plate (1) (see character 16 for comments).

18. Anterior ventral process and pit on the AMD plate present (0) or absent (1).

The presence of the anterior ventral process and pit in primitive antiarchs, exemplified by *Yunnanolepis* and *Minicrania* (ZHU & JANVIER 1996), indicates that the loss of the anterior ventral pit and process in *Vanchienolepis*, *Jiangxilepis* and asterolepidoids is a derived feature for antiarchs. The anterior ventral process in *Microbrachius* was confirmed by PAN (1984; *cf.* HEMMINGS 1978).

19. AMD plate without (0) or with (1) the dorsal spine.

The dorsal spine of the AMD plate is present in *Byssacanthus*, *Kirgisolepis*, *Stegolepis* and *Jiangxilepis*.

20. Lateral process of the PMD plate conspicuous (0) or reduced (1).

A lateral process of the PMD plate is conspicuous in most antiarchs. A reduced lateral process is found in *Vietnamaspis* (LONG *et al.* 1990), *Sinolepis* and *Grenfellaspis* (RITCHIE *et al.* 1992), and makes the PMD plate somewhat rectangular in shape.

21. *Crista transversalis interna posterior* lying laterally to (0) or behind (1) the posterior ventral pit and process of the PMD plate.

In antiarchs, the position of the posterior ventral pit and process relatively to the *crista transversalis interna posterior* is a diagnostic character. The *crista transversalis interna posterior* of antiarchs should be regarded as the homologue to the posterior annular crest of other placoderms, such as arthrodires (GOUJET 1984b), where it is lateral to the median ventral process of the median dorsal plate. This is another evidence for Y.-H. LIU (1991)'s proposition, *i.e.* the PMD plate of antiarchs is homologous to the median dorsal plate of other placoderms. Therefore, by outgroup comparison, it is reasonable to assume that the *crista transversalis interna posterior* lying laterally to the posterior ventral pit and process is plesiomorphic, as exemplified by

Zhanjilepis, *Minicrania* and *Chuchinolepis*. Apart from this primitive state, three derived states are found in antiarchs. One is the posterior ventral pit and process lying in front of the *crista transversalis interna posterior* as in the Euantiarcha. The others are the posterior ventral pit and process lying behind the *crista transversalis interna posterior*, which is represented by two quite different conditions. In the Sinolepididae such as *Grenfellaspis* and *Xichonolepis*, the *crista transversalis interna posterior* extends dorsally with the same direction as that in the Euantiarcha, *Minicrania* (ZHU & JANVIER 1996) and *Chuchinolepis*. It is the posterior migration of the posterior ventral process, which lies near the posterior end of the plate, that results in the process behind the crista. In *Yunnanolepis*, *Phymolepis* and *Mizia*, the position of the posterior ventral process and pit behind the *crista transversalis interna posterior* is definitely due to the anteriorly bending of the *crista* on the visceral surface of the PMD plate. These three states represent three different evolutionary trends and form a branching transformation series together with the plesiomorphy, which is subdivided into three characters by the mixed coding method (characters 21-23).

The *crista transversalis interna posterior* lying behind the posterior ventral process and pit is widely seen in the Euantiarcha. It is supposed to be also present in those euantiarchs where this character is unavailable.

22. Posterior ventral pit and process on the *crista transversalis interna posterior* (0) or posteriorly migrated behind it (1).

The posteriorly migrated posterior ventral process and pit is seen in *Xichonolepis* (G.-R. ZHANG 1980; RITCHIE *et al.* 1992). The condition of *Grenfellaspis* is slightly different since its posterior ventral process and pit are separated. Its posterior ventral pit lies on the posterior part of the crista, and immediately in front of the posterior ventral process (RITCHIE *et al.* 1992). This may be caused by the robustness of the *crista* in *Grenfellaspis*. The posterior ventral process and pit are poorly preserved in the other presumable sinolepids, *i.e. Dayaoshania*, *Sinolepis* and *Liujiangolepis*. But they are clearly different from the state occuring in *Yunnanolepis*.

23. *Crista transversalis interna posterior* lying laterally to (0) or turning anteriorly and in front of (1) the posterior ventral process and pit.

In *Yunnanolepis*, *Phymolepis* and *Mizia*, the development of the *crista transversalis interna posterior* is rather specialized. On the visceral surface of the PMD plate, it becomes fairly strong and turns anteriorly, close to the anterior end of the plate. As stated above, this state should be regarded as apomorphic.

24. Presence (0) or loss (1) of the AL plate.

The anterior lateral plate is present in *Phymolepis* and *Mizia*. However, since the anterior lateral plate of *Phymolepis* and *Mizia* is extremely small, it is uncertain whether it is homologous to the anterior lateral plate of other placoderms.

25. Absence (0) or presence (1) of the CHANG's apparatus.

The CHANG's apparatus is exclusively found in *Yunnanolepis* and *Phymolepis*. Whatever its function is, by outgroup comparison it is an apomorphy in antiarchs.

26. Absence (0) or presence (1) of the ventrolateral fossa of the trunk-shield.

The ventrolateral fossa of the trunk-shield is observed in some yunnanolepidoids, which is assumed to be derived because of its limited distribution in antiarchs.

27. PDL and PL plates independent (0) or fused to form a MxL plate (1).

JANVIER & PAN (1982) commented upon the plate previously referred to as the mixilateral plate in bothriolepidoids and some asterolepidoids, and concluded that the plate in some asterolepidoids was a true mixilateral plate whereas that in bothriolepidoids was not a mixilateral plate, but a PDL plate as in *Yunnanolepis*. In the former case, the lateral lamina of PVL plate is lower than the lateral lamina of AVL plate. The mixilateral plate was found in *Pterichthyodes*, *Hunanolepis* (J.-Q. WANG 1991a), *Asterolepis* (TRAQUAIR 1914; STENSIÖ 1931), *Gerdalepis* (GROSS 1941), and is variable in *Byssacanthus* (KARATAJUTE-TALIMAA 1960).

28. PVL and PL plates independent (0) or fused to form (or replaced by) a single plate (1).

It was suggested that in bothriolepidoids the PL plate had been fused to the PVL plate (JANVIER & PAN 1982). In this case, the lateral lamina of the PVL plate is higher than, or at least equal to, the lateral lamina of the AVL plate. JANVIER & PAN's assumption has been corroborated by the condition in sinolepids. In *Grenfellaspis* and *Dayaoshania* (RITCHIE *et al.* 1992), the main lateral-line groove traverses the PDL plate almost next to the suture between the PDL and PVL plates, which rules out the possibility that the PDL plate of the Sinolepididae incorporated the PL plate. The PVL plate of sinolepids may include the element of the PL plate, as in bothriolepidoids (JANVIER & PAN 1982). The alternative explanation is that the PL plate is lost in sinolepids and most bothriolepidoids. *Nawagiaspis* (YOUNG 1990) and *Luquanolepis* (ZHANG & YOUNG 1992) were considered to be bothriolepidoids with an independent PL plate.

29. Semilunar plate paired (0) or unpaired (1).

The semilunar plate of antiarchs is likely to be homologous to the interolateral plate of other placoderms, which is typically a rod-like plate possessing a postbranchial lamina. In antiarchs, since the postbranchial lamina becomes a rather internal structure and is less developed, the postbranchial lamina of the semilunar plate, if the latter is homologous to the interolateral plate, is largely or entirely lost. The postbranchial lamina of *Phymolepis guoruii* extends onto the semilunar plate, thereby supporting the homology. The position of the scapulocoracoid relatively to the postbranchial lamina of the interolateral plate could not be used as a reference, since the postbranchial lamina of antiarchs is rather evenly attached to the ventral wall of the trunk-shield, and a derived *crista transversalis interna anterior* is formed to conceal the scapulocoracoid. The outgroup comparison and the condition in the Yunnanolepidoidei suggests that the paired semilunar plate is plesiomorphic for antiarchs.

30. Absence (0) or presence (1) of a large rectangular aperture on the ventral wall of trunk-shield.

This character is also stated as "the median ventral plate absent", and has been considered as one of the most important synapomorphies defining the Sinolepididae (RITCHIE *et al*, 1992). In the outgroups of antiarchs, both the presence and absence of the median ventral plate could be found.

31. Presence (0) or absence (1) of the spinal plate.

The spinal plate is commonly absent in antiarchs, and is only present in one species of *Yunnanolepis* (*Y. porifera*). Since the absence of the spinal plate is recorded in the other species of *Yunnanolepis*, this genus is coded as X in the data matrix.

32. Postbranchial lamina external and upright (0) or internal and horizontal (1).

The postbranchial lamina of antiarchs is modified into a rod-shaped structure lying horizontally on the visceral surface of the ventral wall of the trunk-shield and having a fairly internal position. This apomorphy is partly due to the anterior extension of the subcephalic portion of the trunk-shield.

33. Adult ornamentation tubercular (0) or reticular (1).

The outgroup comparison indicates that the tubercular ornamentation in antiarchs is primitive. The two derived states are as follows: 1) reticular in *Bothriolepis* (YOUNG 1988) and *Jiangxilepis* (ZHANG & LIU 1991); 2) ridged in *Wudinolepis* (K.-J. CHANG 1965), *Hohsienolepis* (P'AN & WANG 1978), *Microbrachius* (HEMMINGS 1978; PAN 1984). Both the tubercular and ridged ornaments are present in *Stegolepis* (MALINOVSKAYA 1973). This is a branching transformation series and is coded in two characters (characters 33 and 34).

34. Adult ornamentation tubercular (0), ridged (1) or subparallel ridges on the dorsal wall of trunk-shield (2).

Among the antiarchs which bear the ridged ornamentation, the ridges on the dorsal wall of the trunk-shield are subparallel in *Microbrachius* (PAN 1984) and *Hohsienolepis* (P'AN & WANG 1978). and should be regarded as more derived.

35. Absence (0) or presence (1) of ridged scales.

The outgroup comparison indicates that the scales ornamented with tubercles is plesiomorphic. To date, ridged scales have been found in *Asterolepis* (LYARSKAYA 1977), *Wurungulepis* (YOUNG 1990) and *Pterichthyodes* (HEMMINGS 1978).

36. Absence (0) or presence (1) of a dorsal spongy layer in dermal bone of trunk-shield.

A dorsal spongy layer in the dermal bone of trunk-shield is restricted to *Lepadolepis*, *Grossaspis* and *Gerdalepis* and has been used to distinguish them from other asterolepidoids by GROSS (1965) and YOUNG (1984c).

37. Presence (0) or absence (1) of the central sensory-line groove.

The central sensory-line groove is also termed as the posterior oblique cephalic line groove in antiarchs. The outgroup comparison indicates that the absence of the central sensory-line is a derived feature. The presence of the central sensory-line groove has long been considered as one of the synapomorphies defining bothriolepidoids by YOUNG (1984c, character 24). Since it is absent in *Jiangxilepis* (ZHANG & LIU 1991), *Nawagiaspis* (YOUNG 1990) and *Briagalepis* (LONG & WERDELIN 1986), ZHANG & YOUNG (1992) regarded the development of this groove as an apomorphy among the bothriolepidoids. We suggest that the development of this groove in some bothriolepidoids might be due to reversion as indicated by outgroup comparison.

As to the distribution of the central sensory-line groove among antiarchs, the homology of the X-shaped pit lines on the nuchal plate in *Yunnanolepis* and *Chuchinolepis* (TONG-DZUY & JANVIER 1990) should be incorporated. G.-R. ZHANG (1978) suggested that in *Yunnanolepis* the X-shaped grooves were just the posterior pit lines and that there was no central sensory-line groove. But the case is that the X-shaped grooves consist of two pairs of grooves. M.-M. ZHANG (1980) assigned the anterior pair to the central sensory-line groove, and the posterior pair to

the posterior pit-line groove. TONG-DZUY & JANVIER (1990) proposed another interpretation : the anterior one as the central sensory-line groove and the posterior one as the supraoccipital commissure. However, the fact that entire X-shaped pit lines are lying in front of the openings of endolymphatic ducts, suggests that the posterior pair cannot be assigned to the supraoccipital commissure. In placoderms, the supraoccipital commissure is the canal or groove behind the openings of endolymphatic ducts (DENISON 1978). The posterior pair should be the posterior pit line. In the outgroups of antiarchs, such as arthrodires, petalichthyids and acanthothoracids, there are two pairs of pit lines (middle and posterior pit lines) on the central plates, which in general lie on the endocranial ridges caused by semicircular canals. In antiarchs, there is no central plate. However, the endocranial ridges caused by semicircular canals could be inferred in *Yunnanolepis* and *Chuchinolepis*, just below the X-shaped pit lines of the skull-roof as in the outgroups. It is suggested here that in antiarchs, since the semicircular ridges of both sides migrated next to the midline, the pairs of pit lines of both sides converged toward each other to form the X-shaped pit lines. The same X-shaped pit lines are also seen in *Pterichthyodes milleri* and had been assigned to the middle and posterior pit lines respectively by HEMMINGS (1978). In *P. milleri*, sometimes the anterior pair of X-shaped pit line grooves is in connection with the central sensory-line groove, which extends from the infraorbital groove (HEMMINGS 1978, Fig. 1B). As analyzed above, we conclude that in *Yunnanolepis* and *Chuchinolepis* there is no central sensory-line groove and that the X-shaped pit-line grooves were the middle and posterior pit-line grooves respectively.

38. Presence (0) or absence (1) of the supraorbital groove.

In antiarchs, the supraorbital groove has been defined as the groove on the premedian plate between the infraorbital grooves of both sides (MILES, 1968; G.-R. ZHANG 1978; HEMMINGS 1978; YOUNG & GORTER 1981; LONG & WERDELIN 1986; YOUNG 1988; TONG-DZUY & JANVIER 1990; RITCHIE *et al.* 1992). However, it is difficult to understand the homology between this groove and the supraorbital canal in other placoderms, especially that of acanthothoracids. In *Yunnanolepis* (TONG-DZUY & JANVIER 1990), *Heteroyunnanolepis* (Z.-S. WANG 1994) and *Minicrania* (ZHU & JANVIER 1996), an additional pair of V-shaped sensory-line grooves are found on the postpineal plate and can be compared to the supraorbital groove of *Romundina* (ØRVIG 1975), which is also situated behind the nasal openings and pineal plate. Therefore, the supraorbital groove in antiarchs is redefined here as the V-shaped grooves on the postpineal plate, whereas that on the premedian plate, which was defined before as a supraorbital groove, is better referred to STENSIÖ's (1969) original terminology, that is, the commissure between the infraorbital sensory lines. The absence of the supraorbital groove is coded as "1" by outgroup comparison.

39. Presence (0) or absence (1) of X-shaped pit-line grooves.

X-shaped pit-line grooves are composed of the middle and posterior pit-line grooves, and are typically developed in *Yunnanolepis*, *Chuchinolepis* and *Pterichthyodes*. In *Bothriolepis* and *Grossilepis* in which central sensory-line grooves are developed, the middle pit-line groove is continuous to the central sensory-line groove. The outgroup comparison suggests that the presence of X-shaped pit-line grooves is plesiomorphic.

40. Presence (0) or absence (1) of the branch of the infraorbital groove diverging on lateral plate.

This sensory-line groove is equivalent to the postorbital branch of the infraorbital sensory line in arthrodires and petalichthyids. The absence of this branch of the infraorbital sensory-line groove in antiarchs is apomorphic by outgroup comparison.

41. Absence (0) or presence (1) of the semicircular pit-line groove.

This pit-line groove is a derived structure in antiarchs. No homologous pit line could be found in outgroups.

42. Middle pit-line groove issued from the infraorbital groove absent or short (0), or long and extending onto the nuchal plate (1).

By outgroup comparison. the long middle pit-line groove extending from the infraorbital groove onto the nuchal plate is apomorphic in antiarchs. In *Sherbonaspis*. the nuchal plate held a transverse groove which was assigned as the "occipital cross-commissural pit-line groove" by YOUNG & GORTER (1981). In comparison with other asterolepidoids, this groove should be the transverse middle pit-line groove.

43. Absence (0) or presence (1) of the lateral plate.

The lateral plate, a large plate of the skull-roof taking the place of preorbital, postorbital, marginal and central plates, is unique to antiarchs.

44. Absence (0) or presence (1) of the premedian plate.

The premedian plate is a skull-roof plate covering the anterior part of the head in front of the rostral plate, and is present in antiarchs, rhenanids and acanthothoracids (DENISON 1978; GOUJET 1984a).

45. Preorbital depression present (0) or absent (1).

The homology problem between the preorbital depression and preorbital recess in antiarchs had been discussed by JANVIER & PAN (1982), LONG (1983), YOUNG (1984b, c, 1988), LONG & WERDELIN (1986). ZHU & JANVIER (1996) have made the detailed analysis on this question on the basis of new information on *Minicrania*. It was concluded that the preorbital depression and preorbital recess are not homologous. The preorbital depression is not the suitable place for the rhinocapsular cartilage. Because the preorbital depression of antiarchs could be traced back to the depression on the "median prerostral plate" in *Romundina* (ØRVIG 1975), the preorbital depression is regarded as plesiomorphic for antiarchs.

46. Preorbital depression extending laterally onto the lateral plates (0) or restricted to the premedian plate (1).

Since the primitive antiarchs – the Yunnanolepidoidei and *Minicrania* (ZHU & JANVIER 1996) – possess the depression crossing the premedian and lateral plates, the depression restricted to the premedian plate, as in the Sinolepididae (RITCHIE *et al.* 1992) and *Wudinolepis* (K.-J. CHANG 1965), is assumed to be a derived character.

47. Preorbital recess absent (0), restricted to the premedian plate (1), or extending laterally to the lateral plates (2).

The preorbital recess is an internal space which houses the rhinocapsular cartilage and is roofed by dermal plates. Since no similar structure was found in outgroups, the preorbital recess is unique to antiarchs. In antiarchs, there exist two types of preorbital recess. In bothriolepidoids, the preorbital recess lies in the premedian and lateral plates, whereas in asterolepidoids, sinolepids and *Minicrania*, it is restricted to the posterior part of the premedian plate. Since the preorbital recess in the yunnanolepidoid-like antiarch *Minicrania* (ZHU & JANVIER 1996) is small and restricted to the premedian plate, we propose that the recess in asterolepidoids was less derived than that in bothriolepidoids.

48. Orbital opening open (0) or enclosed by dermal skull-roof plates (1).

The orbital openings of antiarchs are dorsally placed and enclosed by the dermal skull-roof plates, *i.e.*, the premedian, lateral, rostral, pineal, postpineal plates. In some cases, the nuchal plate takes part in the orbital margin.

49. Nasal opening at the anterolateral corners of the rostral plate (0) or at the anterior margin of the rostral plate (1).

In antiarchs, the position of the nasal openings display two states. In most cases, the nasal openings are at the anterolateral corners of the rostral plate, whereas in *Asterolepis* and *Remigolepis*, the nasal openings are at the anterior margin of the broad rostral plate. By outgroup comparison, one may assess the former state as plesiomorphic.

50. Narrow (0) or broad (1) lateral plate.

JANVIER & PAN (1982) suggested that during the evolution of asterolepidoids the lateral plate was becoming narrower and narrower. *Stegolepis jugata* was regarded as the least derived asterolepidoid, since it retained a relatively broad lateral plate (JANVIER & PAN 1982: 383; PAN *et al.* 1987). Their argument was that the broad lateral plate is present in yunnanolepidoids, bothriolepidoids and *Sinolepis*. The shape of the lateral plate has a direct bearing on the shape of the skull roof. In asterolepidoids, the skull roof is more or less narrow and elongated, whereas in bothriolepidoids, yunnanolepidoids and *Sinolepis* which possess the broad lateral plate, the skull roof is relatively broad and short.

In fact, the shape of the skull-roof and lateral plate in yunnanolepidoids, which was previously regarded as plesiomorphic because they were the most primitive antiarchs known at that time, is most likely to be apomorphic (ZHU & JANVIER 1996). When we compare antiarchs with its outgroups, it is quite clear that the long and narrow skull-roof should be regarded as plesiomorphy, which was corroborated by *Minicrania* (ZHU & JANVIER 1996). *Minicrania* has a relatively long, narrow skull-roof and narrow lateral plate, however it possesses a simple pectoral fin articulation, like the Yunnanolepididae. Therefore, in our character data matrix, the narrow lateral plate is coded as plesiomorphic.

51. Premedian plate short and broad (0) or long and narrow (1).

The growth series in antiarchs (WERDELIN & LONG 1986; ZHU & JANVIER 1996) indicates that the short and broad premedian plate is a primitive character. In the growth series of *Bothriolepis canadensis* and *Minicrania* (ZHU & JANVIER 1996), the premedian plate in the juvenile

individuals is proportionally shorter than in the adult, suggesting that the short premedian plate is a plesiomorphic character for antiarchs.

52. Anterior margin of premedian plate convex (0) or slightly concave.

The slightly concave anterior margin of the premedian plate is present in *Remigolepis*, *Pambulaspis*, *Asterolepis* (YOUNG 1984c), *Stegolepis* (MALINOVSKAYA 1977) and *Sherbonaspis* (YOUNG & GORTER 1981).

53. Absence (0) or presence (1) of an unornamented shelf and rostrocaudal groove on the premedian plate.

In antiarchs, only *Asterolepis*, *Pambulaspis* and *Remigolepis* (YOUNG 1984c) bear the unornamented shelf and rostrocaudal groove on the premedian plate, which should be regarded as apomorphic since it is present neither in primitive antiarchs nor in outgroups.

54. Rostral width/orbital width index of premedian plate smaller (0) or larger (1) than 200.

It has been shown that in the growth series the rostral margin of the premedian plate grows more rapidly than its orbital margin (WERDELIN & LONG 1986; ZHU & JANVIER 1996). In the Sinolepididae, *e.g. Sinolepis* and *Grenfellaspis*, the rostral margin of the premedian plate extends much laterally, which is considered as an apomorphy. In the data matrix, the rostral width/orbital width index superior to 200 is coded as 1.

55. Orbital fenestra large (0) or small (1).

The orbital fenestra incorporates orbital openings, sclerotic plates, nasal openings, rostral and pineal plates. The size of the orbital fenestra is mainly affected by the size of orbital openings and the breadth of the rostral and pineal plates. Compared with other placoderms, it is suggested here that large-sized orbital fenestra is plesiomorphic, as supported by the condition in one of the primitive antiarchs *Minicrania* (ZHU & JANVIER 1996).

56. Relative position of the orbital fenestra anterior (0), slightly anterior (1), slightly posterior (2) or posterior (3).

The relative position of the orbital fenestra could be indicated by the index between the length of the postpineal and nuchal plates and the length of the premedian plate. But this index has its defaults. The large-sized orbital fenestra as in *Asterolepis* and *Minicrania* (ZHU & JANVIER 1996) will bias the index. In order to overcome this bias, we subdivide the skull-roof length into two portions by the centre of the orbital fenestra and adopt the index between the length of the posterior portion and the length of the anterior one. The outgroup comparison indicates that the posteriorly placed orbital fenestra is apomorphic. For convenience, we code the index larger than 200 (anterior) as 0, between 200 and 140 (slightly anterior) as 1, between 140 and 90 (slightly posterior) as 2, smaller than 90 (posterior) as 3.

57. Postpineal and nuchal plate long and narrow (0) or short and broad (1).

By outgroup comparison, we assume that the long and narrow postpineal and nuchal plates are plesiomorphic. In order to quantify this character, the length/width index of the postpineal and nuchal plate is used here. It is proposed that the index higher than 90 is coded as 0 whereas that below 90 is coded as 1.

58. Nuchal plate without (0) or with (1) orbital facets.

This character could be expressed in another way: the postpineal plate excluded from the lateral plate or not. The out-group comparison indicates that the nuchal plate with orbital facets is apomorphic. The orbital facet of the nuchal plate in *Briagalepis* could be inferred from the shape of the lateral plate (LONG & WERDELIN 1986).

59. Long (0) or short (1) obstantic margin.

In asterolepidoids, the postmarginal plate extends posterolaterally and forms a short obstantic margin facing posteriorly. The out-group comparison suggests that the relatively long obstantic margin is plesiomorphic.

60. Absence (0) or presence (1) of the submarginal articulation.

In placoderms, the dermal articulation between the submarginal plate and skull-roof was first recorded in *Bothriolepis* by YOUNG (1984b). Later, this articular process was described in *Nawagiaspis* (YOUNG 1990). It is suggested to be present in *Grossilepis*, *Dianolepis* and *Briagalepis*, as inferred from the structure of the lateral plate (ZHANG & YOUNG 1992). This articular process is absent in the Yunnanolepidoidei (Y.-H. LIU 1963; G.-R. ZHANG 1978), *Minicrania* (ZHU & JANVIER 1996), the Sinolepididae (PAN *et al.* 1987; RITCHIE *et al.* 1992), and Asterolepidoidei (STENSIÖ 1969; HEMMINGS 1978; YOUNG 1984b). Its presence in *Microbrachius*, as assumed by ZHANG & YOUNG (1992), is admitted in this work.

61. Endocranial postorbital process short (0) or extending in front of the orbital notch (1).

The long endocranial postorbital process extending in front of the orbital notch on the lateral plate is present only in *Bothriolepis* and *Grossilepis* (ZHANG & YOUNG 1992).

62. Absence (0) or presence (1) of the pronounced postpineal thickening.

It is known only in *Remigolepis* and *Pambulaspis* (YOUNG 1984c).

63. Presence (0) or loss (1) of the prelateral plate.

The prelateral plate of antiarchs is homologous to the postsuborbital plate of other placoderms (YOUNG 1984b). By outgroup comparison, the loss of the plate is a secondary feature.

In antiarchs, the prelateral plate has only been described in *Bothriolepis*, *Grossilepis* and *Nawagiaspis*. In *Mizia (Yunnanolepis) parvus* (V4424.3), M.-M. ZHANG (1980: pls I-2, III-1) identified a suture in the dermal bones of the cheek which was referred to as the suture between the suborbital and postsuborbital plates, and at the same time she considered that the postsuborbital and submarginal plates had fused to some extent and the suture between them was fairly vague. Since the dermal cheek bone complex of *M. parvus* fits in the notch on the lateral margin of the skull-roof and behind the infraorbital groove, this suture is most likely to be between the postsuborbital and submarginal plates, by comparison with the cheek plates in other placoderms. The suborbital plate occupies a more anterior position and bears the infraorbital groove. This is confirmed by the detached suborbital plate of *Yunnanolepis* (TONG-DZUY & JANVIER 1990) which bears the sensory-line grooves very similar to those found in other placoderms. In asterolepidoids, the entire submarginal plate occupies the notch in the lateral margin of the skull-roof, and the postsuborbital plate is lost secondarily, as in *Asterolepis*, *Remigolepis*, *Pterichthyodes* (HEMMINGS 1978) and *Hunanolepis* (J.-Q. WANG 1991a). However, the condition in other antiarchs is unknown and coded as missing data.

64. Prelateral plate with a long anterior process (0) or equilateral, triangular in shape (1).

The prelateral plate of *Bothriolepis* and *Grossilepis* is somewhat equilateral, triangular in shape. The long anterior process in *Nawagiaspis* (YOUNG 1990) is assumed to be primitive, as suggested by the state in *Mizia parvus*.

65. Prelateral plate behind (0) or above (1) the mental plate.

In *Bothriolepis*, *Grossilepis* and *Nawagiaspis* (YOUNG 1990), the prelateral (= postsuborbital) plate is between the skull-roof and the mental (= suborbital) plate and the infraorbital groove traverses through the prelateral plate. By outgroup comparison, this is shown to be a derived character for antiarchs.

66. Mental plates of both sides separated (0) or meeting in the mid line (1).

Since the mental plate is homologous to the suborbital plate of other placoderms (YOUNG 1984b), the separated mental plates of both sides, as in *Bothriolepis* (YOUNG 1984b) and *Nawagiaspis* (YOUNG 1990), are plesiomorphic. The same applies to the Yunnanolepidoidei and *Minicrania* (ZHU & JANVIER 1996), as inferred from the visceral surface of the skull-roof. In *Asterolepis, Remigolepis* (NILSSON 1941; LYARSKAYA 1981) and *Pterichthyodes* (HEMMINGS 1978), the mental plates of both sides contact each other and form a complete upper biting margin of the jaw.

RESULTS

The tree calculating algorithm of Hennig 86 (h*, bb*) gives 12 equally most parsimonious (MP) trees with length of 155, consistency index of 48 and retention index of 81. A strict consensus tree with the nelsen option (Fig. 29) shows three trichotomies. The same data set has been calculated using the heuristic algorithm of PAUP (version 3.1), and 18 minimum-length trees with a length of 155 are found (consistency index = 0.477, homoplasy index = 0.523, retention index = 0.810, rescaled consistency index = 0.387). The strict consensus tree is same as that found with Hennig86. All of the equally shortest trees obtained from Hennig86 are not included among those from PAUP. In fact, three sets of unresolved nodes (Fig. 30), have 32 combinations, indicating 32 equally parsimonious trees, that are confirmed by means of MacClade (version 3.0) (all having the length of 155). One of the most parsimonious cladograms (Fig. 31) is selected for the analysis.

The antiarchs form a clade (Node 1), supported by nine synapomorphies:

– the pectoral fin modified into a slender appendage covered by small dermal plates (character 1);

– the pectoral fenestra encircled by a single plate (character 2), two median dorsal plates (character 11);

– the loss of the anterior lateral plate (character 24);

– the absence of the spinal plate (character 31);

– the postbranchial lamina internal and horizontal in position (character 32);

– the absence of the central sensory-line groove (character 37);

– the presence of the lateral plate (character 43);

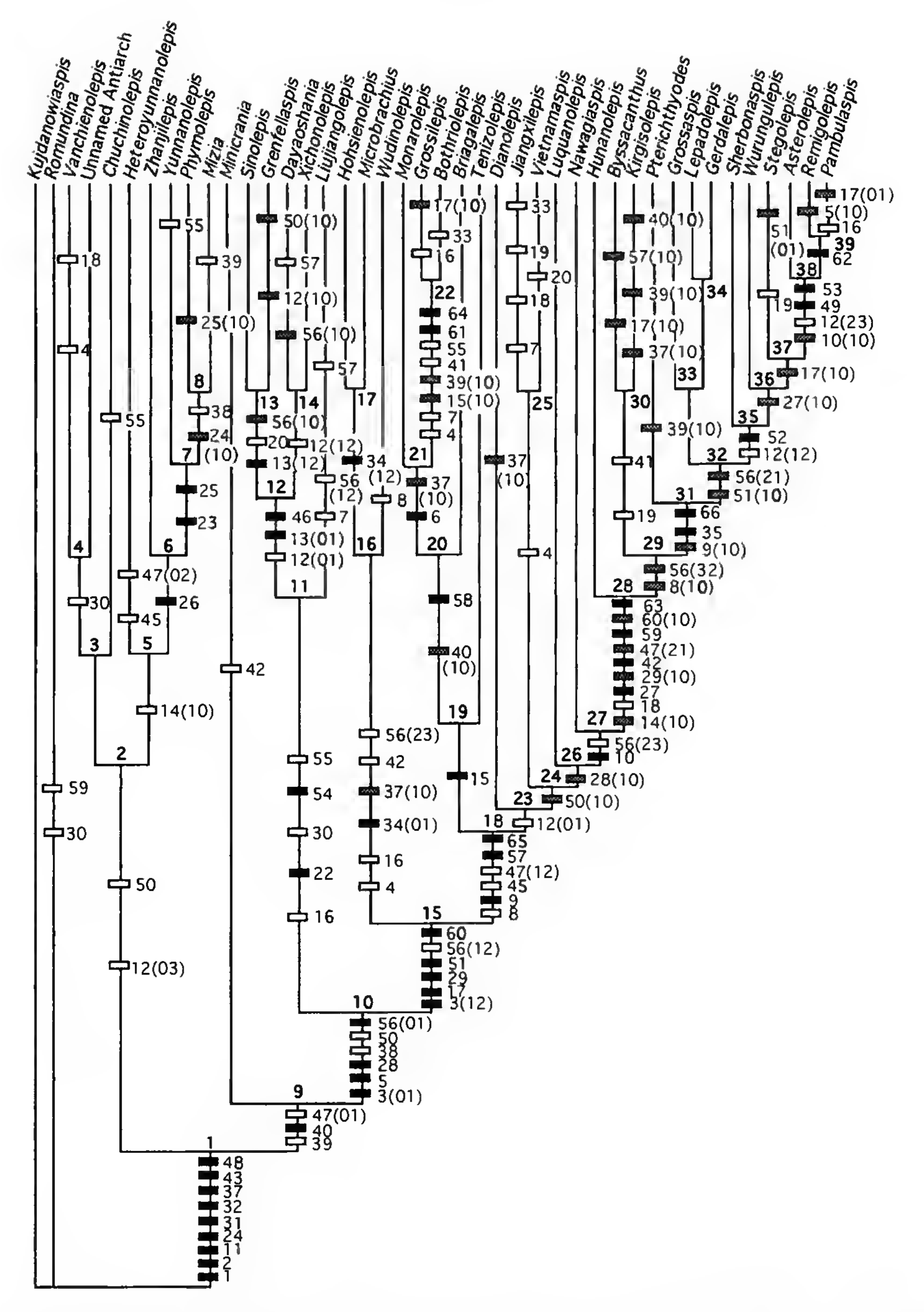


FIG. 31. — One of the equally parsimonious solutions showing one possible set of character distributions with character change in brackets. Where character changes are not shown, the transformation is 0 to 1. Black squares represent a uniquely derived feature, squares with dots represent reversals, and squares represent parallelisms.

– orbital openings enclosed by the dermal skull-roof plates (character 48);
– the anterior lateral plate reappears at Node 8 (*Mizia* and *Phymolepis*).

The presence of the spinal plate in *Yunnanolepis porifera* is also a reversion as indicated by the cladogram. The central sensory-line groove shows three independent reversions in antiarchs. The presence of the premedian plate (character 44) indicates the closer affinity between *Romundina* and the Antiarcha than either with *Kujdanowiaspis* (GOUJET 1984a), and it is retained in the analysis, although it does not provide any additional phylogenetic information in this work.

Five major monophyletic groups are clearly shown in the cladogram, *i.e.* the Yunnanolepidoidei (Node 2), Sinolepididae (Node 11), Microbrachiidae (Node 16), Bothriolepididae (Node 19) and Asterolepidoidei (Node 28). The Bothriolepidoidei as previously defined (MILES 1968; LONG 1983; DENISON 1978; JANVIER & PAN 1982; YOUNG 1984c, 1988, 1990; ZHANG & YOUNG 1992) turns out to be paraphyletic.

The Yunnanolepidoidei is redefined to include *Vanchienolepis*, the Chuchinolepididae, the Yunnanolepididae, *Zhanjilepis*, *Heteroyunnanolepis* and an unnamed antiarch, and its monophyly is supported by the anteriorly pointed AMD plate (character 12 [3]) and broad lateral plate (character 50). The broad lateral plate corresponds to the broad and short skull-roof, and has a parallelism at Node 10, which reverses later (Node 24). Among the Yunnanolepidoidei, three groups are found (Nodes 4, 5, *Chuchinolepis*) and their interrelationships cannot be resolved with the available information (none of the synapomorphies to support Node 3). *Vanchienolepis* and the unnamed antiarch are grouped together (Node 4) by the large rectangular aperture on the ventral wall of the trunk-shield (character 30). This state of the character 30 has once been considered as the synapomorphy of the Sinolepididae (YOUNG 1984c; RITCHIE *et al.* 1992). According to our cladogram, this large ventral trunk-shield aperture must be developed independently three times (Nodes 4, 11 and an undetermined species of *Yunnanolepis*).

Node 5 is supported by the centrally placed tergal angle of the AMD plate (character 14). The cladogram assumes that the anteriorly placed tergal angle, as in *Chuchinolepis*, *Vanchienolepis*, *Minicrania* (ZHU & JANVIER 1996) and *Bothriolepis*, is plesiomorphic for antiarchs, and the centrally placed tergal angle develops independently at Node 28.

Node 6 corresponds to the branching between *Zhanjilepis* and the Yunnanolepididae. It is characterized by the ventrolateral fossa of the trunk-shield (character 26).

Node 7 represents the Yunnanolepididae, which is defined by the *crista transversalis interna posterior* turning anteriorly and in front of the posterior ventral process and pit (character 23) and CHANG's apparatus (character 25, a reversal in *Mizia*).

Among the Yunnanolepididae, *Mizia* and *Phymolepis* are closely related at Node 8 by the lack of the supraorbital sensory-line groove (character 38) and a reversal (appearance of the anterior lateral plate, character 24[0]).

Node 9 corresponds to the branching between *Minicrania* (ZHU & JANVIER 1996) and other advanced antiarchs possessing the brachial process and funnel pit. It is characterized by the preorbital recess (character 47), the loss of X-shaped pit-line grooves (character 39) and absence of the branch of the infraorbital groove diverging on the lateral plate (character 40). The

preorbital recess is independently derived in *Heteroyunnanolepis* and secondarily lost in the Microbrachiidae (Node 16), and its presence in the Sinolepididae is confirmed by *Grenfellaspis* (RITCHIE *et al.* 1992). Character 39 is a highly homoplastic character, and shows a parallelism in *Phymolepis* and three reversals in *Kirgisolepis, Pterichthyodes* and at Node 39. Character 40 shows two reversals in *Kirgisolepis* and at Node 20.

Node 10 represents the branching between the Sinolepididae and Euantiarcha, supported by six synapomorphies, *i.e.* the sinolepid type pectoral fin articulation (character 3[1]), the jointed pectoral fin (character 5, a reversal in *Remigolepis*), the PVL and PL plate fused to form a single plate (character 28), the absence of the supraorbital groove (character 38), the broad lateral plate (character 50, two reversals respectively at Node 24 and in *Sinolepis*) and the slightly anterior position of the orbital fenestra (character 56[1]). The distribution of character 28 in the cladogram suggests that the independent PVL and PL plates in the Euantiarcha are due to secondary separation. In combination with character 27, the mixilateral plate of some asterolepidoids is formed by the PDL and PL plates after this secondary separation.

Node 11 defines the Sinolepididae and corresponds to the branching between *Liujiangolepis* and the other sinolepids. This node is characterized by the AMD plate completely overlapping the PDL plate (character 16), the posterior ventral pit and process posteriorly migrated behind the *crista transversalis interna posterior* (character 22, unknown in *Liujiangolepis*), the presence of the large rectangular aperture in the ventral wall of the trunk-shield (character 30), the rostral width/orbital width index of the premedian plate larger than 200 (character 54) and the small orbital fenestra (character 55). Character 16 has two parallelisms in *Grossilepis* and *Asterolepis*, and character 55 shows three parallelism's in *Chuchinolepis, Yunnanolepis* and the *Bothriolepis* + *Grossilepis* pair.

Node 12 represents an unsolved trichotomy in the Sinolepididae, *Dayaoshania* and *Xichonolepis* being either monophyletic as shown in Fig. 31 (also Fig. 30B2) or paraphyletic as shown in Fig. 30B1. This node is supported by two uniquely shared derived characters, the index between anterior and posterior divisions of the AMD plate higher than 300 (character 13[1]) and the preorbital depression restricted to the premedian plate (character 46), and a homoplastic character, the index between the width of the anterior margin and the maximum width of the AMD plate smaller than 55 (character 12[1], with a reversal in *Sinolepis*).

Node 13 is the branching point between *Grenfellaspis* and *Sinolepis*, supported by the index between anterior and posterior divisions of the AMD plate higher than 500 (character 13[2]), the reduced lateral process of the PMD plate (character 20), and a reversal (anterior position of the orbital fenestra, character 56[0].

The *Dayaoshania-Xichonolepis* relationship (Node 14) is supported by the index between the width of the anterior margin and the maximum width of the AMD plate below 35 (character 12[2]).

Node 15 corresponds to the branching between the Microbrachiidae and the other euantiarchs. This node is characterized by six synapomorphies:
- the euantiarch type pectoral fin articulation (character 3[2]);
- the AMD plate underlapping the PDL or MxL plate (character 17);

– the *crista transversalis interna posterior* situated behind the posterior ventral process and pit (character 21);

– the unpaired semilunar plate (character 29);

– the long and narrow premedian plate (character 51);

– the slightly posterior orbital fenestra (character 56[2]), and the submarginal articulation (character 60).

Character 17 is a homoplastic character and reverses three times in *Grossilepis*, *Byssacanthus* and at Node 37 (reversal once again in *Pambulaspis*). Character 29 has a reversal at Node 28 and again in *Gerdalepis*. Character 51 has a reversal at Node 32 and again in *Stegolepis*. The loss of the submarginal articulation (a reversal) occurs at Node 28 or 29. Character 56 is a highly homoplastic character and shows two parallelisms in the lineage of the Sinolepididae (*Xichonolepis* and *Liujiangolepis*). In the lineage of the Euantiarcha, the orbital fenestra has a more posterior position (character 56[3]) respectively at Nodes 16 and 27 (or 26, since it is unknown in *Luquanolepis*). Above Node 29, a reversal pattern of character 56 is found in the cladogram.

Node 16 represents the branching between *Wudinolepis* and *Microbrachius* + *Hohsienolepis*, and defines the Microbrachiidae. This lineage is united by one uniquely derived character, the ridged adult ornamentation (character 34[1]), and five homoplastic characters:

– the enlarged axillary foramen (character 4);

– the presence of the central sensory-line groove (character 37[0]);

– the middle pit-line groove issued from the infraorbital groove long and extending onto the nuchal plate (character 42, a parallelism at Node 28);

– the loss of the preorbital recess (character 47[0]);

– the posterior position of the orbital fenestra (character 56[3]).

According to the cladogram the axillary foramen is enlarged four times, in:

1) *Vanchienolepis*;

2) *Bothriolepis* and *Grossilepis* (Node 22);

3) *Wudinolepis* and *Microbrachius*;

4) *Vietnamaspis* and *Jiangxilepis* (Node 25).

The enlarged foramen is predicted in *Hohsienolepis*.

Node 17 indicates the sister-group relationship between *Microbrachius* and *Hohsienolepis*, supported by the subparallel ridges on the dorsal wall of the trunk-shield (character 34[2]).

Node 18 corresponds to the branching between the Bothriolepididae + *Tenizolepis* and all other euantiarch genera excluding the Microbrachiidae. This node is supported by:

– the Ml2 plate elongated relatively to the trunk-shield (character 8, a reversal at Node 29);

– two Ml plates in the distal segment (character 9, unknown in the Microbrachiidae and a reversal at Node 31);

– the absence of the preorbital depression (character 45);

– the preorbital recess extending laterally onto the lateral plates (character 47[2]);

– the postpineal and nuchal plates short and broad (character 57);

– the prelateral plate dorsal to the mental plate (character 65, unknown in the Sinolepididae, Microbrachiidae and *Minicrania*).

Character 8 shows also a parallelism in *Wudinolepis*. The alternative explanation is the derived state of character 8 at Node 15, and later two reversals, respectively at Nodes 17 and 29). Characters 45 and 47 have parallelisms in *Heteroyunnanolepis* (Z.-S. WANG 1994).

Node 19 represents the branching between the Bothriolepididae and *Tenizolepis*, and is characterized by the AMD plate overlapping the ADL plate anteriorly and being overlapped by the ADL plate posteriorly (character 15). It has a reversal at Node 22.

Node 20 defines the Bothriolepididae, and corresponds to the branching between *Briagalepis* and all other bothriolepids. It is defined by one uniquely derived character: the nuchal plate with orbital facets (character 58);

and one reversal: the presence of the branch of the infraorbital groove diverging on the lateral plate (character 40[0]).

Node 21 is the branching between *Monarolepis* and *Grossilepis* + *Bothriolepis*, and is supported by the separated Cd1 and Cd2 plates (character 6, unknown in *Briagalepis* and *Tenizolepis*) and a reversal, the presence of the central sensory-line groove (character 37[0]).

Node 22 characterizes the sister-group relationship between *Bothriolepis* and *Grossilepis*. The eight synapomorphies are:

– the large axillary foramen (character 4);
– the long pectoral fin (character 7, unknown in other bothriolepidoids and *Tenizolepis*);
– the AMD plate completely overlapping ADL plate (character 15[0]);
– the presence of the X-shaped sensory-line grooves (character 39[0]);
– the presence of the semicircular pit-line groove (character 41, unknown in *Monarolepis* and a parallelism at Node 30);
– small orbital fenestra (character 55, unknown in *Monarolepis* and *Briagalepis*);
– the endocranial postorbital process extending in front of the orbital notch (character 61);
– the prelateral plate equilateral triangular in shape (character 64).

Among them, characters 15 and 39 are reversals, and character 64 is quite ambiguous because of the large number of missing data.

Node 23 represents another larger diversification among the Euantiarcha, and *Dianolepis* is at the base of this lineage. It is supported by the narrowed anterior margin of the AMD plate (character 12[1]).

Node 24 corresponds to the branching between *Jiangxilepis* + *Vietnamaspis* and *Luquanolepis* + *Nawagiaspis* + Asterolepidoidei. It is supported by a reversal, the narrow lateral plate (character 50[0]).

Node 25 suggests that *Jiangxilepis* is the sister-group of *Vietnamaspis*, with an enlarged axillary foramen (character 4).

Node 26 is the branching between *Luquanolepis* and *Nawagiaspis* + Asterolepidoidei. It is characterized by a reversal, the PVL and PL plates being independent (character 28[0]).

Node 27 indicates that *Nawagiaspis* is the closest sister-group to the Asterolepidoidei. This node is supported by the high and short trunk-shield (character 10, with a reversal later at Node 38) and the posterior orbital fenestra (character 56[3], unknown in *Luquanolepis*).

Node 28 defines the Asterolepidoidei and corresponds to the branching between *Hunanolepis* and all other asterolepidoids. It is characterized by nine synapomorphies:

– the tergal angle of the AMD plate mesially placed (character 14[0]);
– the anterior ventral process and pit lost (character 18);
– the PDL and PL plates fused to form a mixilateral plate (character 27);
– the semilunar plates paired (character 29[0]; unknown in *Nawagiaspis*);
– the middle pit-line groove issued from the infraorbital groove long and extending onto the nuchal plate (character 42);
– the preorbital recess restricted to the premedian plate (character 47[1]);
– the short obstantic margin (character 59);
– the loss of the submarginal articulation (character 60);
– the loss of the prelateral plate (character 63).

The cladogram suggests that the centrally set tergal angle is apomorphic for antiarchs, and it shows a parallelism at Node 5. The short obstantic margin is possibly present in *Nawagiaspis* according to YOUNG (1990: 47), if so, character 59 is an uniquely derived character at Node 27.

Node 29 represents the branching between *Kirgisolepis* + *Byssacanthus* and the other asterolepidoids excluding *Hunanolepis*. It is supported by two reversals: the Ml2 plate short relatively to the trunk-shield (character 8[0]); and the slightly posterior orbital fenestra (character 56[2]).

Node 30 indicates a sister-group relationship between *Kirgisolepis* and *Byssacanthus*, and is defined by two slightly homoplastic characters: the dorsal spine of the AMD plate (character 19); and the presence of the semicircular pit-line groove (character 41).

Node 31 corresponds to the branching of *Pterichthyodes* and the other asterolepidoids excluding *Hunanolepis*, *Kirgisolepis* and *Byssacanthus*. It is characterized by a reversal: three Ml plates of the distal segment (character 9[0]), a less informative character because of many missing data (the ridged scale, character 35), and a uniquely derived character, the mental plates of both sides meeting in the mid-line (character 66, unknown in *Hunanolepis*, *Byssacanthus* and *Kirgisolepis*).

Node 32 is the branching between the Gerdalepididae and *Sherbonaspis* + *Wurungulepis* + *Stegolepis* + Asterolepididae. It is characterized by two reversals:

the short and broad premedian plate (character 51[0]);
the slightly anterior orbital fenestra (character 56[1]).

Node 33 defines the Gerdalepididae and is characterized by the similar dorsal spongy layer in the dermal bone of the trunk-shield (character 36). It represents one of the unresolved trichotomies in this cladogram since no derived character is found at Node 34.

Node 35 represents the branching between *Sherbonaspis* and *Wurungulepis* + *Stegolepis* + Asterolepididae. It is united by the fairly narrow anterior margin of the AMD plate, its index between the width of the anterior margin and the maximum width below 35 (character 12[2]), and the anterior margin of the premedian plate slightly concave (character 52).

Node 36 shows *Wurungulepis* as the sister-group of *Stegolepis* + Asterolepididae. It is characterized by the independent PDL and PL plates (character 27[0]).

However, since the independent PDL and PL plates of *Wurungulepis* is an inferred character, its position at this node is provisional. If the mixilateral plate of *Wurungulepis* is evidenced, it will result in an additional trichotomy at Node 35. This cladogram indicates that, among the advanced antiarchs which possess the brachial process, the fusion and separation of the PDL, PL and PVL plates occurred twice. The first time is at Node 10, where the PVL and PL plates are fused to form a composite plate, which is separated as in *Luquanolepis* and *Nawagiaspis*, then a second fusion took place between the PDL and PL plates to form the mixilateral plate. The independent PL and PDL plates at Node 36 are due to the secondary separation.

Node 37 corresponds to the branching between *Stegolepis* and the Asterolepididae, and is supported by one reversal, the AMD plate partly overlapping the PDL (or MxL) plate (character 17[0]).

Node 38 defines the Asterolepididae, and is the branching between *Asterolepis* and *Remigolepis* + *Pambulaspis*. It is characterized by four synapomorphies:
– the low and elongated trunk-shield (character 10[0]);
– the index between the width of the anterior margin and the maximum width of the AMD plate below 15 (character 12[3]);
– the nasal openings at anterior margin of the rostral plate (character 49);
– the unornamented shelf and rostrocaudal groove on the premedian plate (character 53).

Character 10 is a reversal. Node 39 suggests a sister-group relationship between *Remigolepis* and *Pambulaspis* with an uniquely derived character: the pronounced postpineal thickening (character 60).

COMMENTS ABOUT ANTIARCH PHYLOGENY

1) The monophyly of the Yunnanolepidoidei is corroborated in the cladogram, although, with an emended definition. The simple pectoral fin articulation and large triangular or oval preorbital depression are plesiomorphic for antiarchs, and cannot be used to define the Yunnanolepidoidei. This order is characterized by the anteriorly pointed AMD plate and broad lateral plate, and is expanded to include the Chuchinolepididae, *Vanchienolepis* and an unnamed antiarch. However, *Minicrania* (Zhu & Janvier 1996), which retains the simple pectoral fin articulation and large preorbital depression, is excluded from the Yunnanolepidoidei. The Yunnanolepidoidei are found exclusively in the Early Silurian-Early Devonian deposits of South China block, including North Vietnam.

2) The Chuchinolepididae have closer affinity with the Yunnanolepididae than either has with the Sinolepididae + Euantiarcha. They represent an unsuccessful attempt at developing a dermal pectoral fin articulation. The same applies to *Vanchienolepis*.

3) The large rectangular aperture on the ventral wall of the trunk-shield is apomorphic for antiarchs, and occurs independently in the Sinolepididae and a lineage of the Yunnanolepidoidei.

4) The brachial process and related structures are the successful attempt of antiarchs as to the pectoral fin articulation. The antiarchs with these advanced structures dominated during the Middle and Late Devonian.

5) A yunnanolepidoid-like antiarch *Minicrania* (ZHU & JANVIER 1996) is the sister-group of the advanced antiarchs, sharing with the latter a preorbital recess.

6) The monophyly of the Sinolepididae is confirmed. *Vanchienolepis* and the unnamed antiarch cannot be referred to sinolepids. As proposed by YOUNG & ZHANG (1992), the brachial process of the Sinolepididae is rather primitive compared to that of the Euantiarcha. The Sinolepididae is the sister-group of the Euantiarcha, as suggested by JANVIER & PAN (1982), and RITCHIE *et al.* (1992).

7) The Microbrachiidae is at the base of the Euantiarcha. It cannot be referred to the Asterolepidoidei as proposed by MILES (1968), LONG (1983) and J.-Q. WANG (1991a).

8) The Bothriolepidoidei, as previously defined, turns out to be paraphyletic. In contrast, the Bothriolepididae are still valid as a monophyletic group defined by the orbital facet of the nuchal plate.

9) *Nawagiaspis*, which possesses both asterolepidoid and bothriolepidoid features and was referred to the Bothriolepidoidei (YOUNG 1990), comes out as the closest sister-group of the Asterolepidoidei.

10) The monophyly of the Asterolepidoidei is well supported in the cladogram. *Hunanolepis* from the Middle Devonian of South China is placed at the base of the Asterolepidoidei.

11) The Pterichthyodidae as defined earlier (STENSIÖ 1948; HEMMINGS 1978; YOUNG 1984c, 1988; J.-Q. WANG 1991a) fail to be monophyletic. JANVIER & PAN (1982) regarded *Stegolepis*, *Byssacanthus*, and *Pterichthyodes* as a paraphyletic group, and this is partly corroborated here. In our cladogram, the Pterichthyodidae turns out to be polyphyletic.

12) *Stegolepis* is the sister-group of the Asterolepididae, however, this is only supported by a reversal. The Asterolepididae is well supported in the cladogram, as in YOUNG (1984c, 1988), and the unjointed fin of *Remigolepis* is a secondary condition (YOUNG 1984c). G.-R. ZHANG (1984) considered that the unjointed fin of *Remigolepis* is a primitive antiarch condition, from which derived the jointed fin of the other euantiarchs. This is the most parsimonious treatment as regard to the fin evolution, however it is fairly less parsimonious as to other characters. G.-R. ZHANG's view is partly followed by PAN in PAN *et al.* (1987), who thought that *Remigolepis* was the only representative among euantiarchs retaining the unjointed fin. However, if his preferred cladogram (PAN *et al.* 1987, Fig. 51) is taken into consideration, the jointed fin originated independently at least four times, which is very unlikely.

Acknowledgements

The research was carried out under the supervision of Dr Ph. JANVIER during my stay at the Laboratoire de Paléontologie, Muséum national d'Histoire naturelle, URA 12 CNRS, Paris in 1993-94, which is thanked for the provision of working facilities. The stay was financed by grants of the Chinese Academy of Sciences. I express my special thanks to Dr Ph. JANVIER for his valuable comments and suggestions throughout this project and his help in improving the manuscript of this work. For the sponsorship of this project, I am very much indebted to Pr. M.-M CHANG (IVPP, Beijing), who is also deeply thanked for her gifts of many valuable specimens and continuous encouragement. I am most grateful to Drs Ph. JANVIER, D. GOUJET, H. LELIÈVRE (Paris) and Pr TONG-DZUY Thanh (Hanoi University, Vietnam) for the fruitful discussions and their generosity in providing the specimens in their care. I am much indebted to Dr D. GOUJET for his help and permission in running the Hennig86, PAUP and MacClade programs in his care. I also thank

Dr L. MARCUS (American Museum of Natural History) who introduced me to use the Hennig86 program in 1989. I wish to express my gratitude to Dr Gavin YOUNG (Bureau of Mineral Resources, Camberra) for reading and commenting on the manuscript and improving it stylistically. Thanks are also due to Pr Ph. TAQUET (Paris) for the invitation to his laboratory, and to Mr D. SERRETTE (Paris), who took the photographs.

Manuscript submitted for publication on 17 June 1994; accepted on 22 September 1995.

REFERENCES

AGASSIZ J. L. R. 1843. — *Recherches sur les poissons fossiles.* 5 vols, Imprimerie Petitpierre, Neuchâtel.

— 1844. — *Monographie des poissons fossiles des Vieux Grès Rouges ou Système Dévonien (Old Red Sandstone) des Iles britanniques et de Russie.* Jent & Gassmann, Neuchâtel.

ANDREWS S. M. 1982. — *The discovery of fossil fishes in Scotland up to 1845.* Royal Scottish Museum, Edinburgh.

ANONYMOUS 1985. — *International Code of Zoological Nomenclature.* Third edition. London, International Trust for zoological Nomenclature, University of California Press, Berkeley & Los Angeles: 1-338.

BERG L. S. 1940. — Classification of fishes, both recent and fossil. *Trudy zool. Inst., Leningrad,* **5**: 85-517 [in Russian and English].

CHANG K.-J. 1965. — New antiarchs from the Middle Devonian of Yunnan. *Vertebrata PalAsiatica* **9**: 114 [in Chinese with English summary].

— 1978. — Early Devonian antiarchs from Chuifengshan, Yunnan. *In* : *Symposium on the Devonian System of South China 1974.* Geological Press, Beijing: 292-293 [in Chinese].

CHANG M.-M. 1966. — Notes on some vertebrates from the Early Devonian of Yunnan, China. *Preprint : Colloque international Centre national de la Recherche scientifique* **163**.

CHI Y.-S. 1940. — On the discovery of *Bothriolepis* in the Devonian of central Hunan. *Bulletin of the Geological Society of China* **20**: 57-72.

— 1942. — Upper Devonian *Bothriolepis* beds of Yunnan. *Scientific Record. of the Academia sinica* **1**: 1-2.

CLOUTIER R. 1991. — Interrelationships of Palaeozoic actinistians : patterns and trends. *In* M.-M. CHANG, Y.-H. LIU & G.-R. ZHANG (eds). *Early Vertebrates and related problems of evolutionary biology,* Science Press, Beijing: 379-428.

COPE E. D. 1885. — The position of *Pterichthys* in the system. *American Naturalist* **19**: 289-291.

DENISON R. H. 1975. — Evolution and classification of placoderm fishes. *Breviora* **432**: 1-24.

— 1978. — Placodermi. *In* H.-P. SCHULTZE (ed.). *Handbook of Paleoichthyology,* Gustav Fischer Verlag, Stuttgart **2**: 1-128.

— 1983. — Further consideration of placoderm evolution. *Journal of Vertebrate Paleontology* **3**: 69-83.

EICHWALD E. I. VON 1840 — Die Thier-und Pflanzenreste des alten rothen Sandsteins und Bergkalks im Novgorodschen Gouvernement. *Bulletin de l'Académie des Sciences de Saint-Petersbourg* **7**: 78-91.

FANG R.-S., JIANG N.-R., FAN J.-C., CAO R.-G., LI D.-Y. 1985. — *The Middle Silurian and Early Devonian Stratigraphy and Palaeontology in Qujing District, Yunnan.* The People's Publishing House of Yunnan, Kunming, China: 1-171 [in Chinese with English abstract].

FARRIS J. S. 1988. — *Hennig 86, Version 1.5.* Port Jefferson Station, New York.

FOREY P. L. & GARDINER B. G. 1986. — Observation on *Ctenurella* (Ptyctodontida) and the classification of placoderm fishes. *Zoological Journal of the Linnean Society* **86**: 43-74.

GARDINER B. G. 1984. — The relationships of placoderms. *Journal of Vertebrate Paleontology* **4**: 379-395.

GOUJET D. 1984a — Placoderm interrelationships : a new interpretation, with a short review of placoderm classifications. *Proceedings of the Linnean Society of New South Wales* **107**: 211-243.

— 1984b. — Les Poissons Placodermes du Spitsberg. Arthrodires Dolichothoraci de la Formation de Wood Bay (Dévonien Inférieur). *Cahiers de Paléontologie* Éd. CNRS Paris : 1-284.

GROSS W. 1931. — *Asterolepis ornata* Eichw. und das AntiarchiProblem. *Palaeontographica A* **75**: 162.

— 1932. — Fossilium Catalogues I : Animalia. Pars 57: Antiarchi. *W. Junk, Berlin*: 1-40.

— 1933. — Die Fische des baltischen Devons. *Palaeontographica* A **79**: 1-74.

— 1941. — Die *Bothriolepis*-Arten der cellulosa-Mergel Lettlands. *Kungliga svenska Vetenskapsakademiens Handlingar* ser. 3 **19**: 1-79.

— 1965. — Uber die Placodermen-Gattungen *Asterolepis* und *Tiaraspis* aus dem Devon Belgiens und einen fraglichen *Tiaraspis* -Rest aus dem Devon Spitzbergens. *Bulletin de l'Institut Royal des Sciences naturelles de Belgique* **41**: 119.

HEMMINGS S.K. 1978. — The Old Red Sandstone antiarchs of Scotland: *Pterichthyodes* and *Microbrachius*. *Palaeontographical Society Monographs, London* **131**: 164.

HENNIG W. 1966. — *Phylogenetic Systematics*. University of Illinois Press, Urbana.

HOU H-F. 1988a. — *The Devonian Stratigraphy and Sedimentary Facies of Longmenshan, Sichuan Province*. Geological Publishing House, Beijing [in Chinese].

— 1988b. — *The Devonion System of China, Stratigraphy of China, N° 7*. Geological Publishing House, Beijing [in Chinese].

JANVIER Ph. 1995. — The brachial articulation and pectoral fin in Antiarchs (Placodermi). *In*: M. ARSENAULT, H. LELIEVRE & Ph. JANVIER (eds). Studies on Early Vertebrates (VIIth International Symposium, 1991, Miguasha Parc, Quebec). *Bulletin du Muséum national d'Histoire naturelle, Paris 4ᵉ série, section C* **17**(1-4) : 143-162.

JANVIER P. & PAN J. 1982. — *Hyrcanaspis bliecki* n. g., n. sp., a new primitive euantiarch (Antiarcha, Placodermi) from the Eifelian of northeastern Iran, with a discussion on antiarch phylogeny. *Neues Jahrbuch für Geologie und Paläontologie Abhandlung* **64**: 364-392.

KARATAJUTE-TALIMAA V. N. 1960. — *Byssacanthus dilatatus* (Eichw.) from the Middle Devonian of the USSR. *Collection of the Acta Geologica Lithuanica*, Vilnius: 293-305.

— 1963. — Genus *Asterolepis* from the Devonian of the Russian Platform. *In* A. GRIGELIS & V.N. KARATAJUTE-TALIMAA (eds). *The data of geology of Lithuania. Geological and Geographical Institute of the Academy of Science of Lithuania SSR*, Vilnius: 65-223 [in Russian with English summary].

LIU S.-F. 1974. — Discovery of *Yunnanolepis* fauna in Kwangsi and its stratigraphical significance. *Vertebrata PalAsiatica* **12**: 243-248 [in Chinese].

— 1992. — On the Lower Devonian antiarchians of Guangxi, China. *Vertebrata PalAsiatica* **30**: 210-220 [in Chinese with English summary].

LIU T.-S. & P'AN K. 1958. — Devonian fishes from the Wutung Series near Nanking, China. *Palaeontologica Sinica* **141**: 1-41 [in Chinese with English summary].

LIU Y.-H. 1963. — On the Antiarchi from Chutsing. *Vertebrata PalAsiatica* **7**: 39-46 [in Chinese with English summary].

— 1973. — On the new forms of Polybranchiaspiformes and Petalichthyida from Devonian of Southwest China. *Vertebrata PalAsiatica* **11**: 132-143 [in Chinese].

— 1991. — On a new petalichthyid, *Eurycaraspis incilis* gen. et sp. nov. (Placodermi, Pisces) from the Middle Devonian of Zhanyi, Yunnan. *In* M.-M. CHANG, Y.-H. LIU & G.-R. ZHANG (eds). *Early Vertebrates and related problems of evolutionary biology*. Science Press, Beijing: 139-178.

LIU Y.-H. & WANG J.-Q. 1981. — On three new arthrodires from Middle Devonian of Yunnan. *Vertebrata PalAsiatica* **19**: 295-304 [in Chinese with English summary].

LONG J. A. 1983. — New bothriolepid fish from the Late Devonian of Victoria, Australia. *Palaeontology* **26**: 295-320.

— 1984. — New phyllolepids from Victoria and the relationships of the group. *Proceedings of the Linnean Society of New South Wales* **107**: 263-308.

LONG J. A., BURETT C. F., NGAN P. K., & JANVIER Ph. 1990. — A new bothriolepid antiarch (Pisces, Placodermi) from the Devonian of Do Son Peninsula, northern Vietnam. *Alcheringa* **14**: 181-194.

LONG J. A. & WERDELIN L. 1986. — A new Late Devonian bothriolepid (Placodermi, Antiarcha) from Victoria, with description of other species from the state. *Alcheringa* **10**: 355-399.

LYARSKAYA L. A. 1977. — New data on *Asterolepis ornata* from the early Frasnian deposits of the Baltic region. *In*: V. V. MENNER (ed.). *Essays on phylogeny and systematics of fossil fishes and agnathan*. Nauka, Moscow: 36-45 [in Russian].

— 1981. — Baltic Devonian Placodermi. Asterolepidae. Zinatne, Riga, 152 p.

MALINOVSKAYA S. P. 1973. — *Stegolepis* (Antiarchi, Placodermi), a new Middle Devonian genus from Central Kazakhstan. *Paleontologicheskii Zhurnal* **7**: 189-199 [in Russian].

— 1977. — Systematic position of antiarchs of Central Kazakhstan. *In* V. V. MENNER (ed.). *Essays on phylogeny and systematics of fossil fishes and agnathan.* Nauka, Moscow: 29-35 [in Russian].

— 1992. — New Middle Devonian antiarchs (Placodermi) of Central Kazakhstan. *In* E. MARK-KURIK (ed.) *Fossil fishes as living animals.* Academy of Sciences of Estonia, Tallinn: 177-184.

MANSUY H. 1907. — Résultats paléontologiques. *In* M. H. LANTENOIS (ed.). *Résultats de la mission géologique et minière du Yunnan méridional (Septembre 1903-Janvier 1904).* Dunod & Pinat, Paris : 150-177.

— 1912. — Étude géologique du Yun-Nan oriental, 2ᵉ partie. Paléontologie. *Mémoire du Service géologique d'Indochine* **1** : 1-146.

— 1915. — Contribution à l'étude des faunes de l'Ordovicien et du Gothlandien du Tonkin. *Mémoire du Service géologique d'Indochine* **4** : 1-7.

M'COY F. 1848. — On some new fossil fish of the Carboniferous Period. *Annales Magazine of natural History* Ser. 2, **2**: 1-10.

MILES R. 1968. — The Old Red Sandstone antiarchs of Scotland. Family Bothriolepididae. *Palaeontographical Society Monographs* **122**: 1-130.

MILES R. S. & YOUNG G. C. 1977. — Placoderm interrelationships reconsidered in the light of new ptyctodontids from Gogo, Western Australia. *In* S. M. ANDREWS, R. S. MILES & A. D. WALKER (eds). *Problems in vertebrate evolution.* Academic Press, London: 123-198.

MILLER H. 1841. — *The Old Red Sandstone.* 1st ed., Adam & Charles, Edinburgh.

NELSON G. & PLATNICK N. I. 1984. — Systematics and evolution. *In* M.-W. HO & P.T. SAUNDERS (eds). *Beyond Neo-Darwinism.* Academic Press, New York: 143-158.

NILSSON T. 1941. — The Downtonian and Devonian vertebrates of Spitsbergen. 7. Order Antiarchi. *Skrifter Svalbard Ishavet* **82**: 1-54

ORUCHEV D. V. 1964. — Class Placodermi. *In* ORLOV (ed.). *Fundamentals of Paleontology* 11, Agnatha, Pisces. Nauka, Moscow: 118-171 [in Russian].

ØRVIG T. 1975. — Description, with special reference to the dermal skeleton, of a new radontinid arthrodire from the Gedinnian of Arctic Canada. *In* J.P. LEHMAN (ed.). *Problèmes Actuels de Paléontologie – Évolution des Vertébrés* CNRS Colloques Internationaux **218**: 41-71.

P'AN K. 1964. — Some Devonian and Carboniferous fishes from south China. *Acta palaeontologica sinica* **12** : 139-168.

— 1973. — New material of Devonian fish fossils from Central South China. *In The collected papers of Stratigraphy and Paleontology, Symposium on the atlas of Paleontology of Central South China*: 35-44 [in Chinese].

— 1981. — Devonian antiarch biostratigraphy of China. *Geological Magazine* **118**: 6975.

— 1984. — A new species of *Microbrachius* from Middle Devonian of Yunnan. *Vertebrata PalAsiatica* **22**: 8-13.

PAN J. & DINELEY D. L. 1988. — A review of early (Silurian and Devonian) vertebrate biogeography and biostratigraphy of China. *Proceedings of the Royal Society of London B* **235**: 29-61.

P'AN K. & WANG S.-T.1978. — Devonian Agnatha and Pisces of South China. *In Symposium on the Devonian System of South China 1974.* Geological Press, Beijing: 298-333 [in Chinese].

— 1981. — New discoveries of Polybranchiaspida from Yunnan Province. *Vertebrata PalAsiotica* **19**: 113-121.

P'AN K., WANG S.-T., KAO L.-D. & HOU J.-P. 1978. — Devonian continental sedimentary formations of China. *In Symposium on the Devonian System of South China 1974.* Geological Press, Beijing: 240-269 [in Chinese].

P'AN K., WANG S.-T. & Y.-P. LIU 1975. — The Lower Devonian Agnatha and Pisces from South China. *Professional Paper in Stratigraphy and Palaeontology* **1**: 153-169 [in Chinese].

PAN J., HUO F.-C., CAO J.-X., GU Q.-C., LIU S.-Y., WANG J.-Q., GAO L.-D. & LIU C. 1987. — *Continental Devonian System of Ningxia and its Biotas.* Geological Publishing House, Beijing [in Chinese with English summary].

PANDER C. H. 1856. — Monographie der fossilen Fische des Silurischen Systems der Russich-Baltischen Gouvernements. *Königliche Akademie der Wissenschaften* St Petersburg.

— 1857. — Ueber die Placodermen des devonischen Systems. *Königliche Akademie der Wissenschaften* St. Petersburg.

PANTELEYEV N. 1992. — New remigolepids and high armoured antiarchs of Kirgizia. *In* E. MARK-KURIK (ed.) *Fossil fishes as living animals.* Academy of Sciences of Estonia, Tallinn: 185-191.

PIEN C.-S. 1948. — Note on the occurrence of *Bothriolepis* in northern Kwangtung. *Scientific Journal of the Sun Yat-Sen University* (N. S.) University of Kansas, Lawrence **1**: 1.

POPPER K. 1965. — *Conjecture and Refutations: the Growth of Scientific Knowledge.* Harper & Row, New York.

RITCHIE A., WANG S.-T., YOUNG G. C. & ZHANG G.-R., 1992. — The Sinolepidae, a family of antiarchs (placoderm fishes) from the Devonian of South China and Eastern Australia. *Australasian Museum Records* **44**: 319-370.

STENSIÖ E. A. 1931. — Upper Devonian vertebrates from East Greenland, collected by the Danish Greenland Expedition in 1929 and 1930. *Meddellesler om Grønland* **86**: 1-212.

— 1945. — On the head of certain arthrodires : II. On the cranium and cervical joint of the Dolichothoraci (Acanthaspidae). *Kungliga svenska Vetenskapsakademiens Handlingar* **22** (3): 170.

— 1948. — On the Placodermi of the Upper Devonian of East Greenland. 2. Antiarchi: subfamily Bothriolepinae. With an attempt at a revision of the previously described species of that family. *Meddellesler om Grønland* **139**: 1622.

— 1959. — On the pectoral fin and shoulder girdle of the arthrodires. *Kungliga svenska Vetenskapsakademiens Handlingar* **8** (4): 1-229.

— 1963. — Anatomical studies on the arthrodiran head. Part 1. Preface, geological and geographical distribution, the organization of the head in the Dolichothoraci, Coccosteomorphi and Pachyosteomorphi. Taxonimic appendix. *Kungliga svenska Vetenskapsakademiens Handlingar* **9** (4): 1-419.

— 1969. — Placodermata. *In* J. PIVETEAU (ed.), *Traité de Paléontologie*, Masson, Paris **4** (2) : 71-692.

TONG-DZUY T. & JANVIER Ph. 1987. — Les Vertébrés Dévoniens du Viêt Nam. *Annales de Paléontologie (Vertébrés Invertébrés)* **73** : 165-194.

— 1990. — Les Vertébrés du Dévonien inférieur du Bac Bo oriental (provinces de Bac Thaï et Lang Son, Viêt Nam). *Bulletin du Muséum national d'Histoire naturelle, Paris 4e série section C* **12** : 143-223.

— 1994. — New Early Devonian vertebrates from Trang Xa (Bac Thai, Vietnam), with remarks on the distribution of the vertebrates in the Song Cau Group. *Journal of Southeast Asian Earth Science* **10**: 235-243.

TRAQUAIR R. H. 1888. — On the structure and classification of the Asterolepidae. *Annales Magazine of natural History* **2** (6): 485-504.

— 1893. — On the British species of Asterolepidae. *Proceedings of the Royal physical Society of Edinburg* **10**: 283-286.

— 1914. — A monograph of the fishes of the Old Red Sandstone of Britain. Pt.2. — The Asterolepidae. *Palaeontographical Society Monographs* **1-4**: 63-134.

UPENIECE I. & UPENIEKS J. 1992. — Young Upper Devonian antiarch (*Asterolepis*) individuals from the Lode quarry, Latvia. *In* E. MARK-KURIK (ed.). *Fossil fishes as living animals.* Academy of Sciences of Estonia, Tallinn: 167-176.

WANG H.-C. 1942. — The stratigraphical position of Devonian fish-bearing series of E. Yunnan with a special discussion on the Tiaomachien Formation of central Hunan. *Bulletin of the Geological Society of China* **12**: 217-225.

WANG J.-Q. 1979. — A new family of Arthrodira from Yunnan, China. *Vertebrata PalAsiatica* **17**: 179-188 [in Chinese with English summary].

— 1982. — New materials of Dinichthyidae. *Vertebrata PalAsiatica* **20**: 181-186 [in Chinese with English summary].

— 1991a. — New material of *Hunanolepis* from the Middle Devonian of Hunan. *In* M.-M. CHANG, Y.-H. LIU & G.-R. ZHANG (eds). *Early Vertebrates and related problems of evolutionary biology.* Science Press, Beijing: 213-247.

— 1991b. — The Antiarchi from Early Silurian of Hunan. *Vertebrata PalAsiatica* **29**: 240-244 [in Chinese with English summary].

— 1991c. — A fossil Arthrodira from Panxi, Yunnan. *Vertebrata PalAsiatica* **29**: 1-7 [in Chinese with English summary].

WANG J.-Q. & WANG N.-Z. 1983. — A new genus of Coccosteidae. *Vertebrata PalAsiatica* **21**: 1-8 [in Chinese with English summary].

— 1984. — New material of Arthrodira from the Wuding Region. *Vertebrata PalAsiatica* **22**: 1-7 [in Chinese with English summary].

WANG J.-Q. & ZHU M. 1995. — On the age of the Jiucheng Formation of Wuding, Yunnan. *Acta Stratigraphica Sinica.*

WANG S.-T. 1987. — A new Antiarchi from the Early Devonian of Guangxi. *Vertebrata PalAsiatica* **25**: 81-90 [in Chinese with English abstract].

WATSON D. M. S. 1961. — Some additions to our knowledge of Antiarchi. *Palaeontology* **4**: 210-220.

WERDELIN L. & LONG J. A. 1986. — Allometry in the placoderm fish *Bathriolepis canadensis* Whiteaves and its evolutionary significance. *Lethaia* **19**: 161-169.

WILEY E. O., SIEGEL-CAUSEY D., BROOKS D. R. & FUNK V. A. 1991. — *The compleat cladist: a primer of phylogenetic procedures.* Special publication No. 19, The University of Kansas. Museum of Natural History, Lawrence.

WOODWARD A. S. 1891. — *Catalogue of the fossil fishes in the British Museum of Natural History. Pt. II.* British Museum (Natural History), London, 567 p.

YOUNG G. C. 1980. — A new Early Devonian placoderm from New South Wales, Australia, with a discussion of placoderm phylogeny. *Palaeontographica A* **167**: 10-76.

— 1983. — A new antiarchan fish (Placodermi) from the late Devonian of Southeastern Australia. *BMR Journal of Australasian Geology and Geophysics* **8**: 71-81.

— 1984a. — An asterolepidoid antiarch (placoderm fish) from the Early Devonian of the Georgina Basin, central Australia. *Alcheringa* **8**: 65-80.

— 1984b. — Reconstruction of the jaws and braincase in the Devonian placoderm fish *Bothriolepis. Palaeontology* **27**: 635-661.

— 1984c. — Comments on the phylogeny and biogeography of antiarchs (Devonian placoderm fishes) and the use of fossils in biogeography. *Proceedings of the Linnean Society of New South Wales* **107**: 443-473.

— 1986. — The relationships of placoderm fishes. *Zoological Journal of the Linnean Society London* **88**: 1-57.

— 1988. — Antiarchs (Placoderm fishes) from the Devonian Aztec Siltstone, Southern Victoria Land, Antarctica. *Palaeontographica A* **202**: 1-125.

— 1990. — New antiarchs (Devonian placoderm fishes) from Queensland, with comments on placoderm phylogeny and biogeography. *Memoirs of the Queensland Museum* **28**: 35-50.

YOUNG G. C. & GORTER J. D. 1981. — A new fish fauna of Middle Devonian age from the Taemas/Wee Jasper region of New South Wales. *Bureau of Mineral Resources of Australia, Bulletin* **209**: 83-147.

YOUNG G. C. & ZHANG G.-R. 1992. — Structure and function of the pectoral joint and operculum in antiarchs, Devonian placoderm fishes. *Palaeontology* **35**: 443-464.

ZHANG G.-R. 1978. — The antiarchs from the Early Devonian of Yunnan. *Vertebrata PalAsiatica* [in Chinese with english abstract] **16**: 148-186.

— 1979. — Some opinions on the description of antiarchs in "Devonian Agnatha and Pisces of South China". *Vertebrata PalAsiatica* **17**: 85-89 [in Chinese].

— 1980. — New material of *Xichonolepis qujingensis* and discussion on some of its morphological characteristics. *Vertebrata PalAsiatica* **18**: 272-280 [in Chinese with English abstract].

— 1984. — New form of the Antiarchi with primitive brachial process from Early Devonian of Yunnan. *Vertebrata PalAsiatica* **22**: 82-91 [in Chinese with English abstract].

ZHANG G.-R. & LIU Y.-G. 1991. — A new antiarch from the Upper Devonian of Jiangxi, China. *In M.-M.* CHANG, Y.-H. LIU & G.-R. ZHANG (eds). *Early Vertebrates and related problems of evolutionary biology.* Science Press, Beijing: 195-212.

ZHANG G.-R. & YOUNG G. C. 1992. — A new antiarch (placoderm fish) from the Early Devonian of South China. *Alcheringa* **16**: 219-240.

ZHANG M.-M. 1980. — Preliminary note on a Lower Devonian antiarch from Yunnan, China. *Vertebrata PalAsiatica* **28**: 179-190 [in Chinese with English abstract].

ZHU M. & JANVIER Ph. 1994. — Un Onychodontide (Sarcopterygii) du Dévonien inférieur de Chine. *Comptes Rendus de l'Académie des Sciences Paris, Série II* **319**: 951-956.

— 1996. — A small antiarch, *Minicrania lirouyii* n. g., n. sp., from the Early Devonian of Qujing, Yunnan (China), with remarks on antiarch phylogeny. *Journal of Vertebrate Paleontology* **16** (1): 1-15.

ZHU M. & WANG J.-Q. in press. — On the Early-Middle Devonian boundary in Qujing, Yunnan. *Acta Stratigraphica Sinica.*

ZHU M., J.-Q. WANG & FAN J.-H. 1994. — Early Devonian fishes from Guijiatun and Xujiachong Formations of Qujing, Yunnan, and related biostratigraphic problems. *Vertebrata PalAsiatica* **32**: 1-20 [in Chinese with English summary].

PLATE 1

Antiarcha, Xitun Formation, Early Devonian, Qujing, Yunnan, China.

Yunnanolepis porifera n. sp.

1, 2 – Trunk-shield in dorsal (1) and ventral (2) views, V10507.3, ×2.

3, 4 – Trunk-shield in dorsal (3) and lateral (4) views, V10507.1, ×2.

5 – Trunk-shield in dorsal view, V10507.2, ×2.

6, 7 – Left AVL plate in lateral (6, × 3) and posterolateral (7, × 8, showing the scapulocoracoid in the pectoral fenestra) views, V10507.4.

Phymolepis cuifengshanensis K.-J. Chang

8, 9 – PMD plate in dorsal (8) and visceral (9) views, V10508.3, ×2.

10 – PMD plate in dorsal view, V10508.2, ×2.

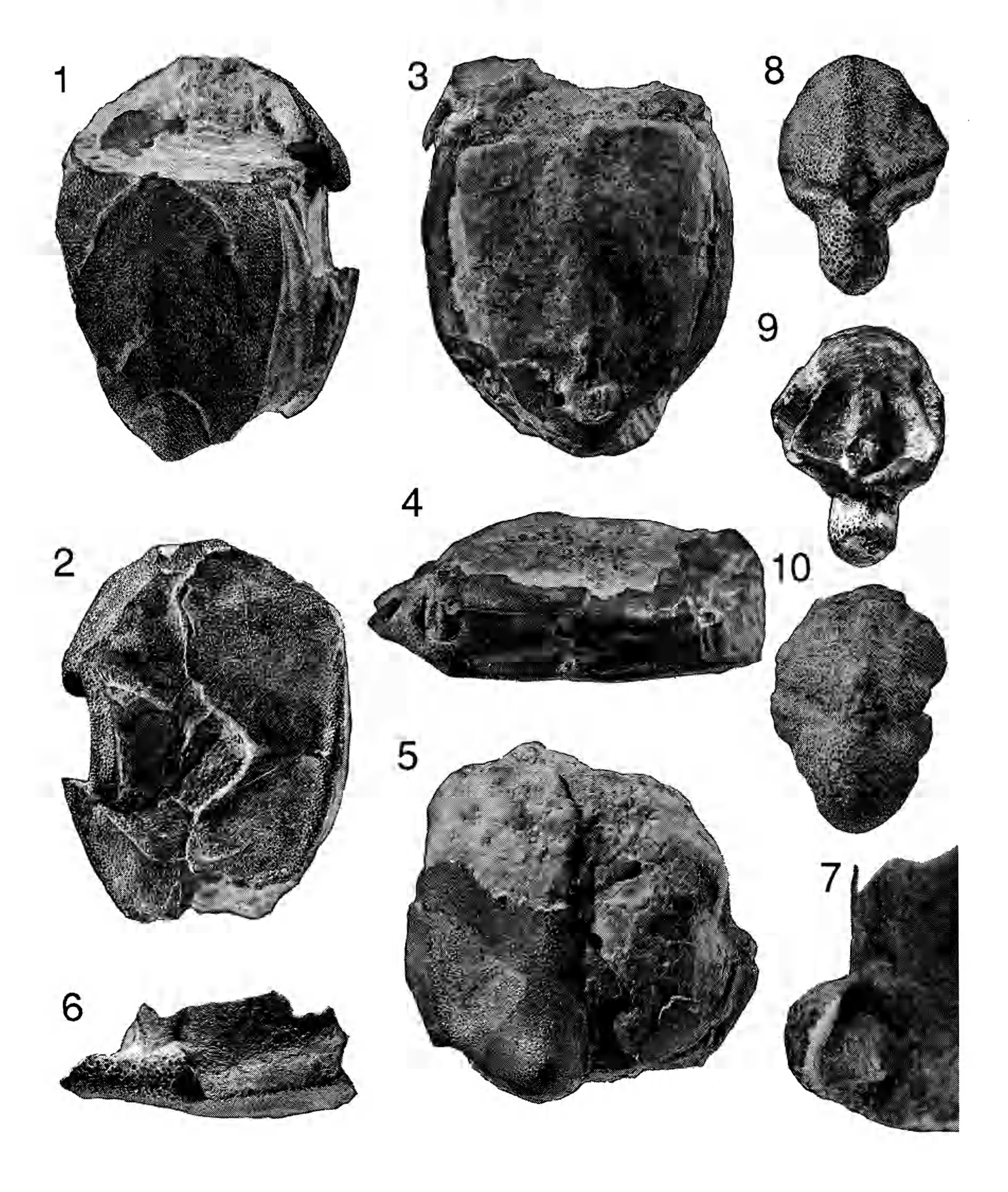

1
3
8
9
4
2
10
5
7
6

PLATE 11

Antiarcha, Xishancun, Xitun and Xujiachong Formations, Early Devonian, Qujing, Yunnan, China.

Yunnanolepis porifera n. sp.

1 – AMD plate in external view (elastomer cast), V10499.16, Xishancun Formation, × 3.
2 – PMD plate in visceral view (elastomer cast), V10499.23, Xishancun Formation, × 3.
3 – Left AVL and Sp plates (elastomer cast), V10499.37, Xishancun Formation, × 3.
4 – External mould of left AVL and Sp plates, V10499.36, Xishancun Formation, × 3.
5 – Incomplete AMD and ADL plates in visceral view, V10507.7, Xitun Formation, × 3.
6 – Incomplete right ADL and AVL plates in dorsal view, V10507.5, Xitun Formation, × 3.
7 – Incomplete right AVL plate in dorsal view, V10507.6, Xitun Formation, × 3.

Mizia longhuaensis n. g., n. sp.

8, 9, 10 – Trunk-shield (holotype) in dorsal (8), ventral (9) and lateral (10) views, V10515, Xujiachong Formation, × 3.

Yunnanolepis sp.

11 – Incomplete trunk-shield and skull-roof in dorsal view, V10514, Xitun Formation, × 3.

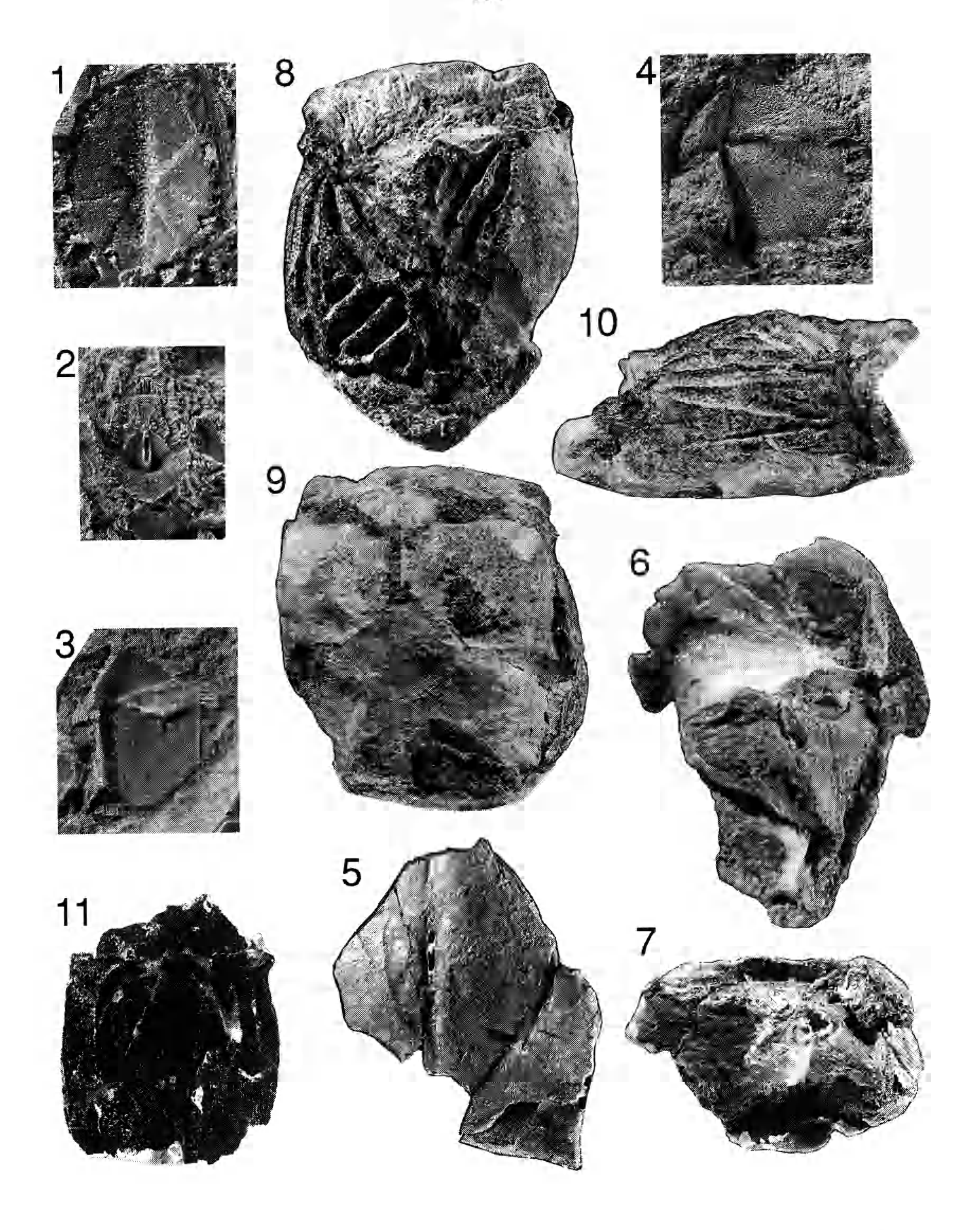

1
8
4
10
2
9
6
3
5
11
7

PLATE III

Antiarcha, Xishancun Formation, Early Devonian, Qujing, Yunnan, China.

Yunnanolepis porifera n. sp.

1 – Trunk-shield in ventral view (internal mould of the ventral and lateral walls and external mould of the dorsal wall), V10499.1, × 3.

2 – Trunk-shield in dorsal view (internal mould of the dorsal and lateral walls, and external mould of the ventral wall), V10499.3, × 4.

3 – Internal mould of an AMD plate, V10499.9, × 3.

4 – Two ADL plates in external view (elastomer casts), V10499.24-25, × 3.

5 – PDL plate in external view (elastomer cast), V10499.36, × 3.

6 – External mould of a trunk-shield (ventral and lateral walls), V10499.2, × 3.

7 – Trunk-shield in ventral view (internal mould of ventral and lateral walls), V10499.2, × 3.

8 – AMD plate in visceral view (elastomer cast), V10499.11, × 3.

Zhanjilepis aspratilis G.-R. Zhang

9 – Internal mould of a right PDL plate, V10501.7, × 3.

10,11 – AMD plate in dorsal (10) and visceral (11) views (elastomer casts), V10501.1, × 3.

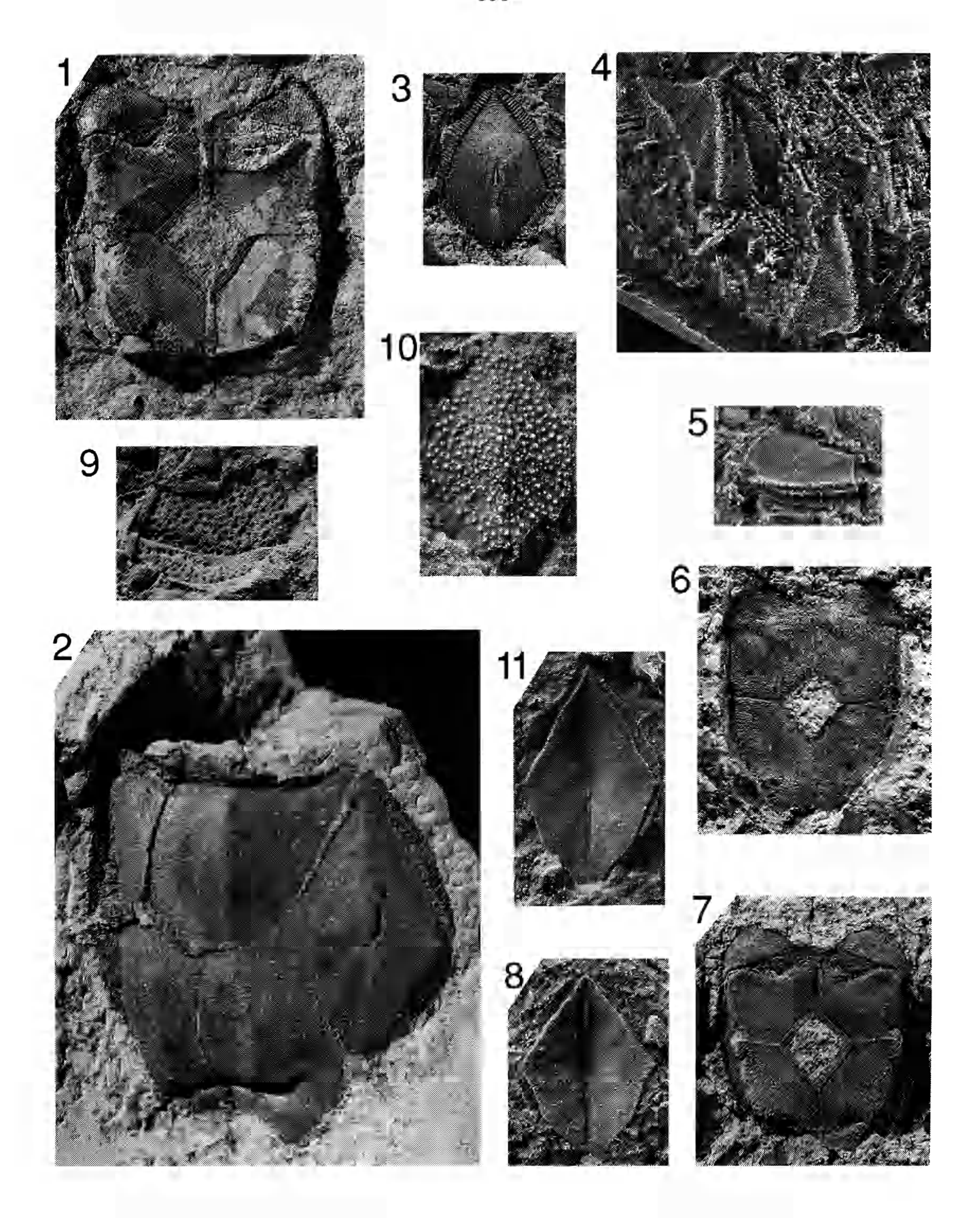

1
3
4
10
5
9
6
2
11
7
8

PLATE IV

Antiarcha, Xishancun Formation (1-11) and Xitun Formation (12), Early Devonian, Qujing, Yunnan, China.

Phymolepis cuifengshanensis K.-J. Chang

1 – Left ADL plate in dorsolateral view (elastomer cast), V10500.2, × 2.
2 – PMD plate in dorsal view (elastomer cast), V10500.1, × 2.
3 – Internal mould of a PMD plate, V10500.1, × 2.
4 – PMD plate in visceral view (elastomer cast), V10500.1, × 2.
5 – Left PDL plate in visceral view (elastomer cast), V10500.3, × 2.
6 – External mould of a right PL plate, V10500.4, × 2.
7 – Internal mould of a left AVL plate, V10500.5, × 2.
8 – Left AVL plate in visceral view (elastomer cast), V10500.5, × 2.
9 – Right PVL plate in visceral view (elastomer cast), V.10500.6, × 2.

Zhanjilepis aspratilis G.-R. Zhang

10 – Right PVL plate in visceral view (elastomer cast), V10501.5, × 3.

Yunnanolepidoidei gen. et sp. indet.

11 – Left PDL plate in external view (elastomer cast), V10506, × 1.5.

Unnamed antiarch

12 – Internal mould of PVL plate in ventral view, V10515, × 1.5.

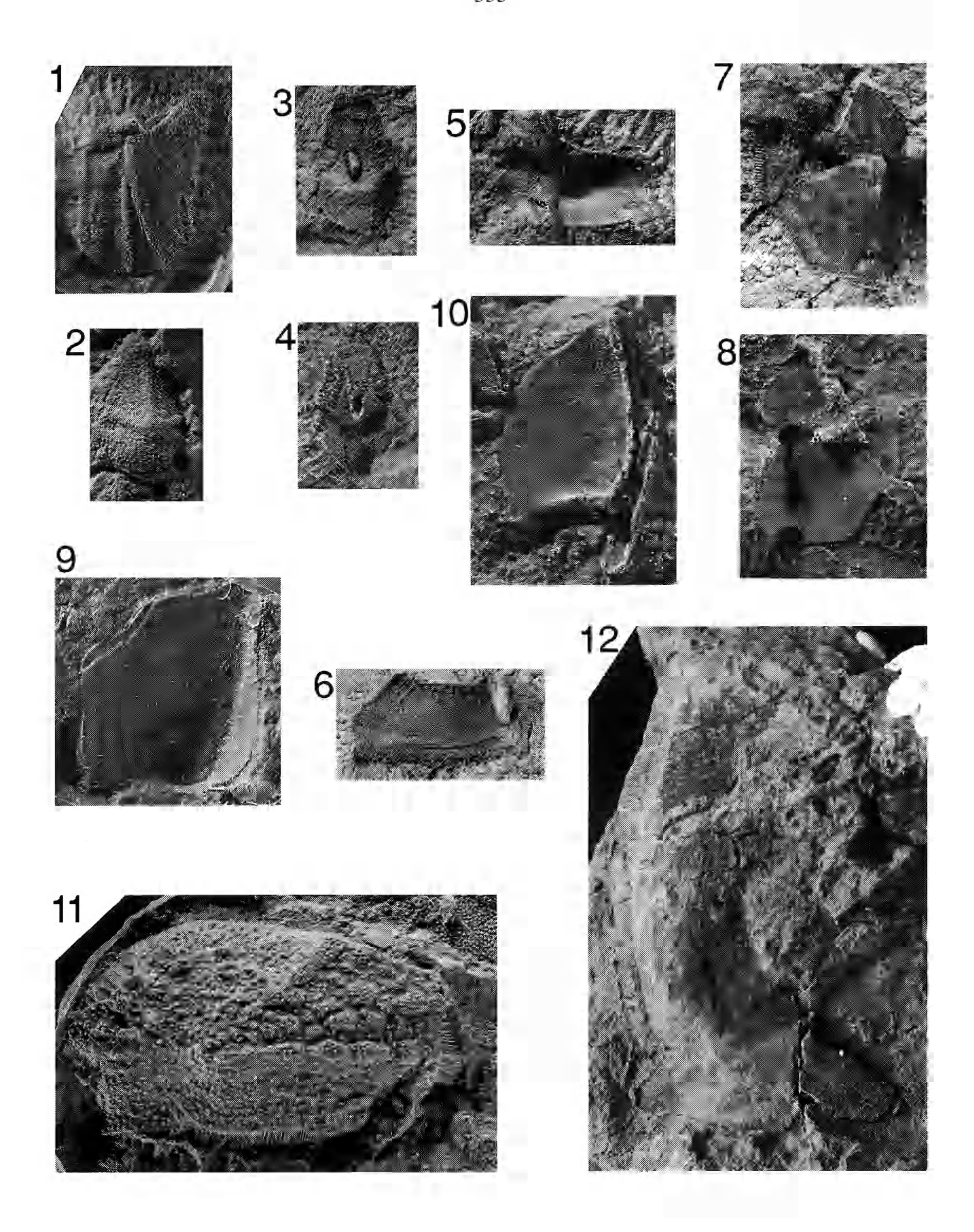

1
2
3
4
5
6
7
8
9
10
11
12

Plate V

Antiarcha, Xitun Formation, Early Devonian, Qujing, Yunnan, China.

Phymolepis guoruii n. sp.

1, 2, 3 – Trunk-shield (holotype, V10509.1) in dorsal (1), ventral (2) and lateral (3) views, × 1.5.
4 – Trunk-shield in dorsal view, V10509.2, × 1.5.
5, 6 – Incomplete AMD plate in dorsal (5) and visceral (6) views, V10509.3, × 2.
7 – PMD plate in dorsal view, V10509.5, × 2.
8, 9 – PMD plate in dorsal (8) and visceral (9) views, V10509.6, × 2.

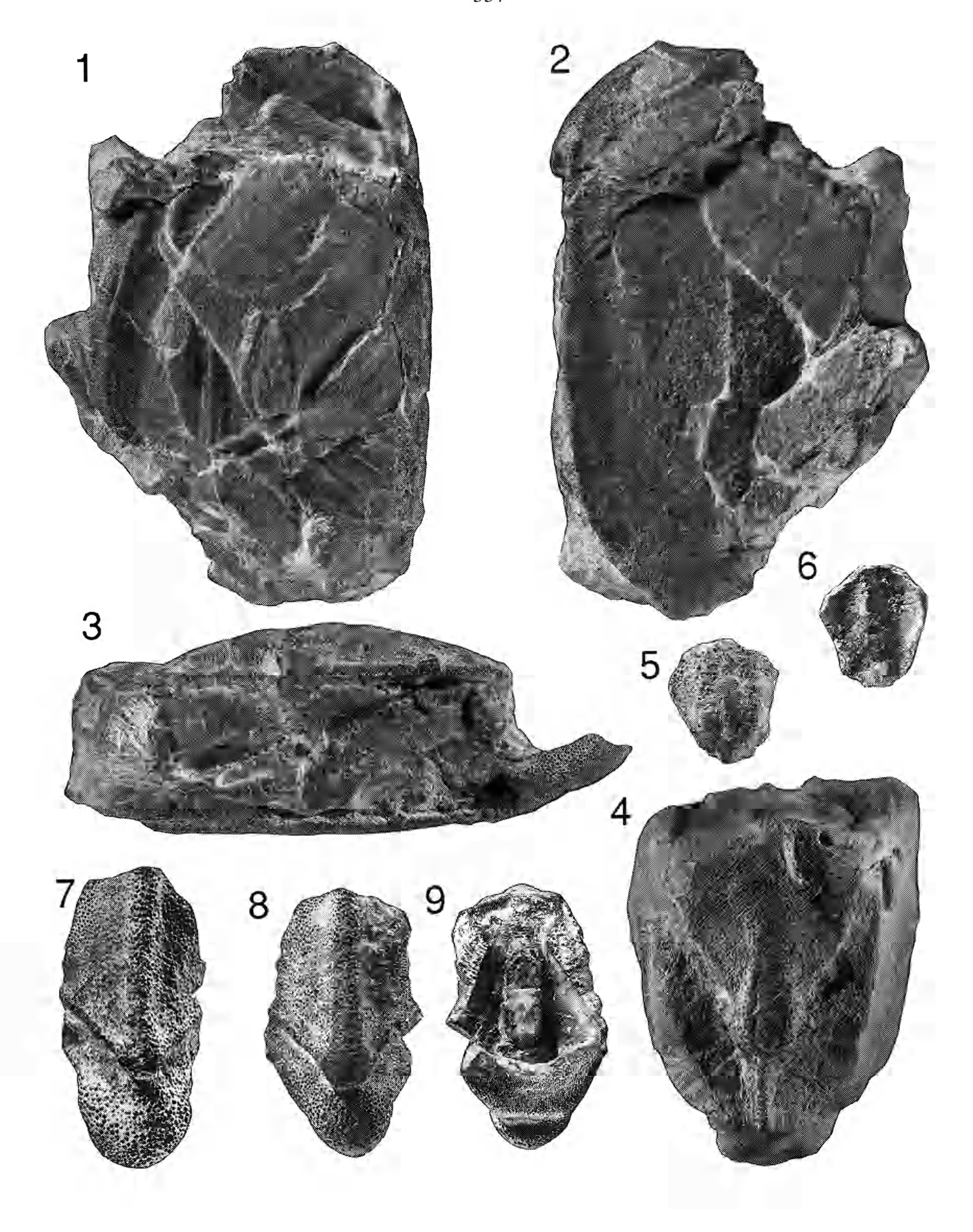

1
2
6
3
5
4
7
8
9

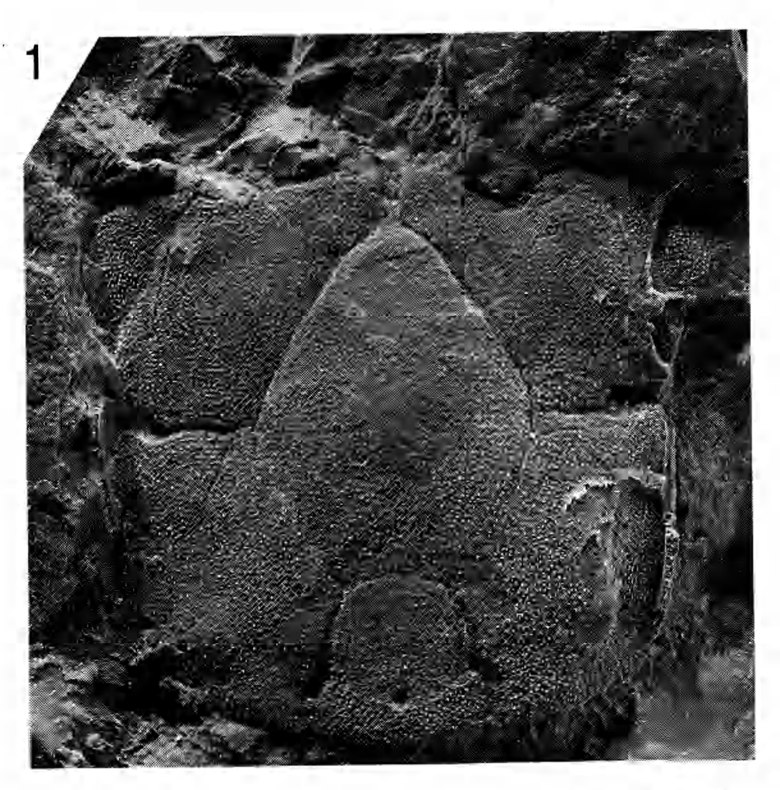
PLATE VI

Antiarcha, Xishancun Formation, Early Devonian, Qujing, Yunnan, China.

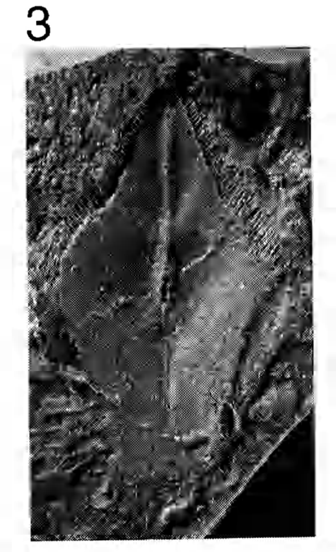
Heteroyunnanolepis qujingensis Z.-S. Wang

1 – Trunk-shield (V10502.1) in dorsal view (elastomer cast), × 1.5.
2 – Dorsal and lateral walls of the trunk-shield (V10502.1) in visceral view (elastomer cast), × 1.5.
3 – AMD plate in visceral view (elastomer cast), V10502.2, × 2.
4 – Internal mould of a left AVL plate, V10502.3, × 2.

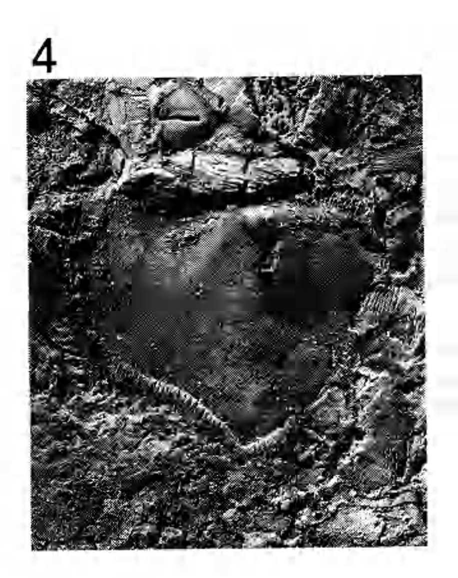
1



3



4



2

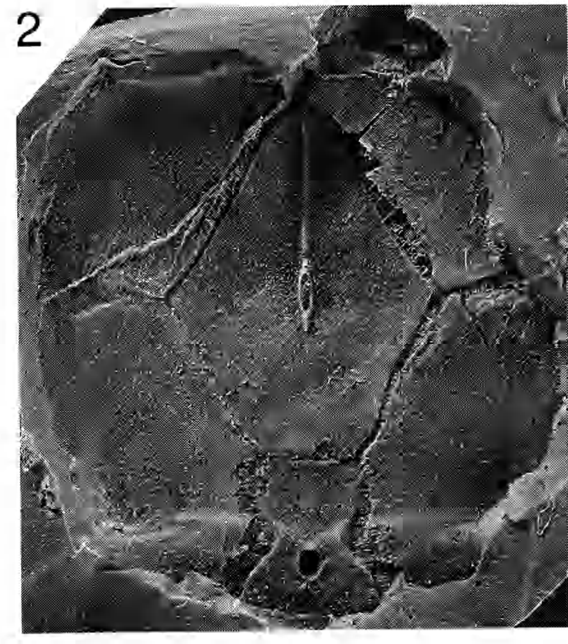


PLATE VII

Antiarcha, Xishancun Formation, Early Devonian, Qujing, Yunnan, China.

Heteroyunnanolepis qujingensis Z.-S. Wang

1 – External mould of dorsal part of a trunk-shield (V10502.1), × 1.5.

2 – Internal mould of a trunk-shield (V10502.1) in ventral view, × 1.5.

3, 4 – Left AVL plate in external (3) and visceral (4) views (elastomer casts), V10502.3, × 2.

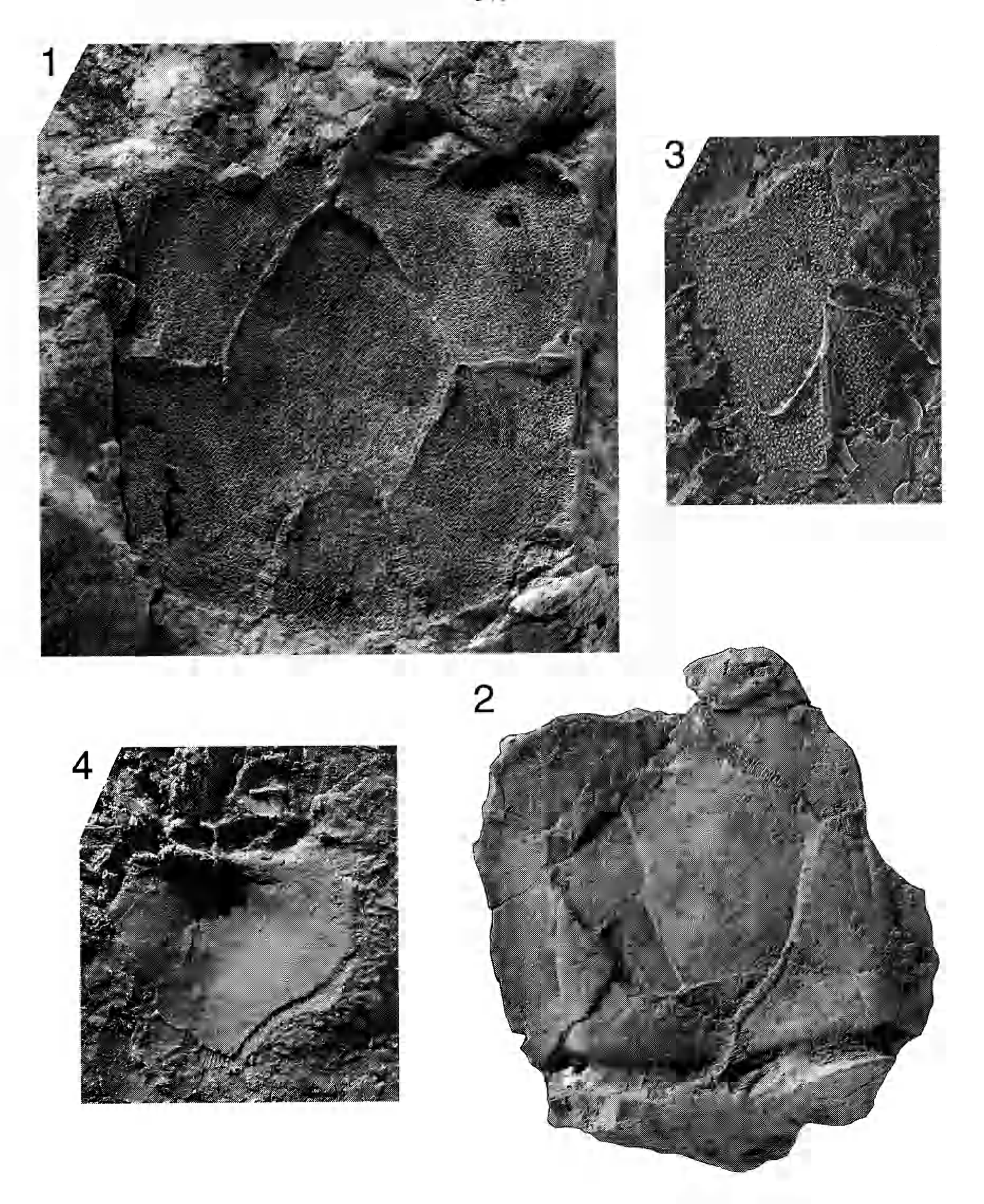

1
3
2
4

PLATE VIII

Antiarcha, Xishancun (1-4, 6-12) Formation and Xitun (5) Formation, Early Devonian, Qujing, Yunnan, China.

Chuchinolepis gracilis K.-J. Chang

1 – Internal mould of a juvenile skull-roof and trunk-shield in dorsal view, V10503.1, × 5.
2 – AMD plate in visceral view (elastomer cast), V10503.5, × 3.
3 – Internal mould of an AMD plate, V10503.4, × 3.
4 – AMD plate in external view (elastomer cast), V10503.3, × 3.
5 – Right AVL plate in dorsal view, V10510.2, × 3.

Chuchinolepis qujingensis (K.-J. Chang)

6 – Internal mould of an AMD plate, V10504.1, × 2.
7, 8 – AMD plate in visceral (7) and dorsal (8) views (elastomer casts), V10504.1, × 2.
9 – Internal mould of a left ADL plate, V10504.2, × 2.
10 – Left ADL plate in visceral view (elastomer cast), V10504.2, × 2.
11 – Left ADL plate in external view (elastomer cast), V10504.3, × 2.
12 – External mould of a left ADL plate, V10504.3, × 2.

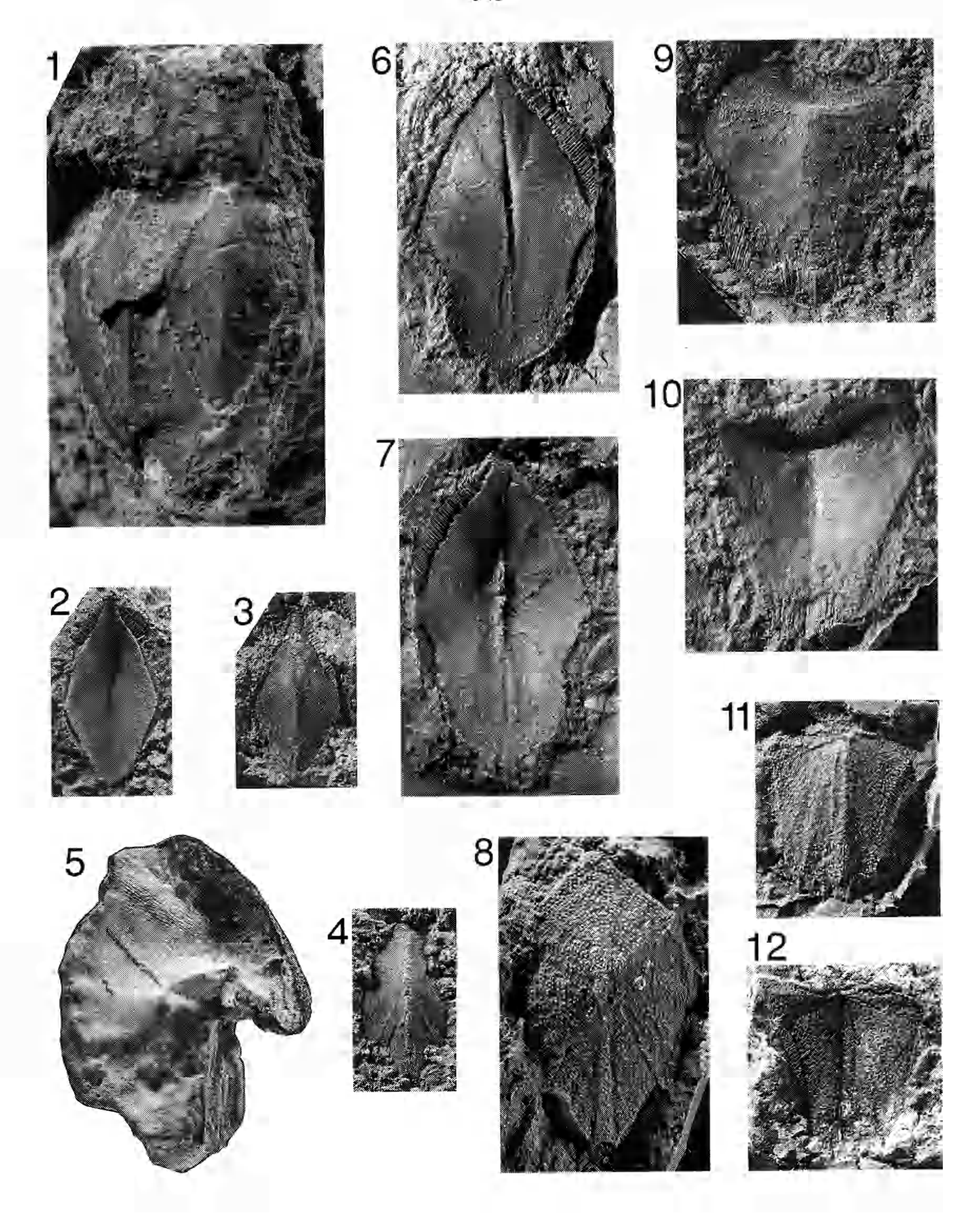

1
2
3
4
5
6
7
8
9
10
11
12

PLATE IX

Antiarcha, Xitun Formation, Early Devonian, Qujing, Yunnan, China.

Chuchinolepis robusta n. sp.
1, 2, 3 – Left AVL plate in dorsal (1), ventral (2) and lateral (3) views, V10512, × 2.

Chuchinolepis gracilis K.-J. Chang
4, 5, 6 – Right AVL plate in dorsal (4), ventral (5) and posterolateral (6) views, V10510.1, × 3.

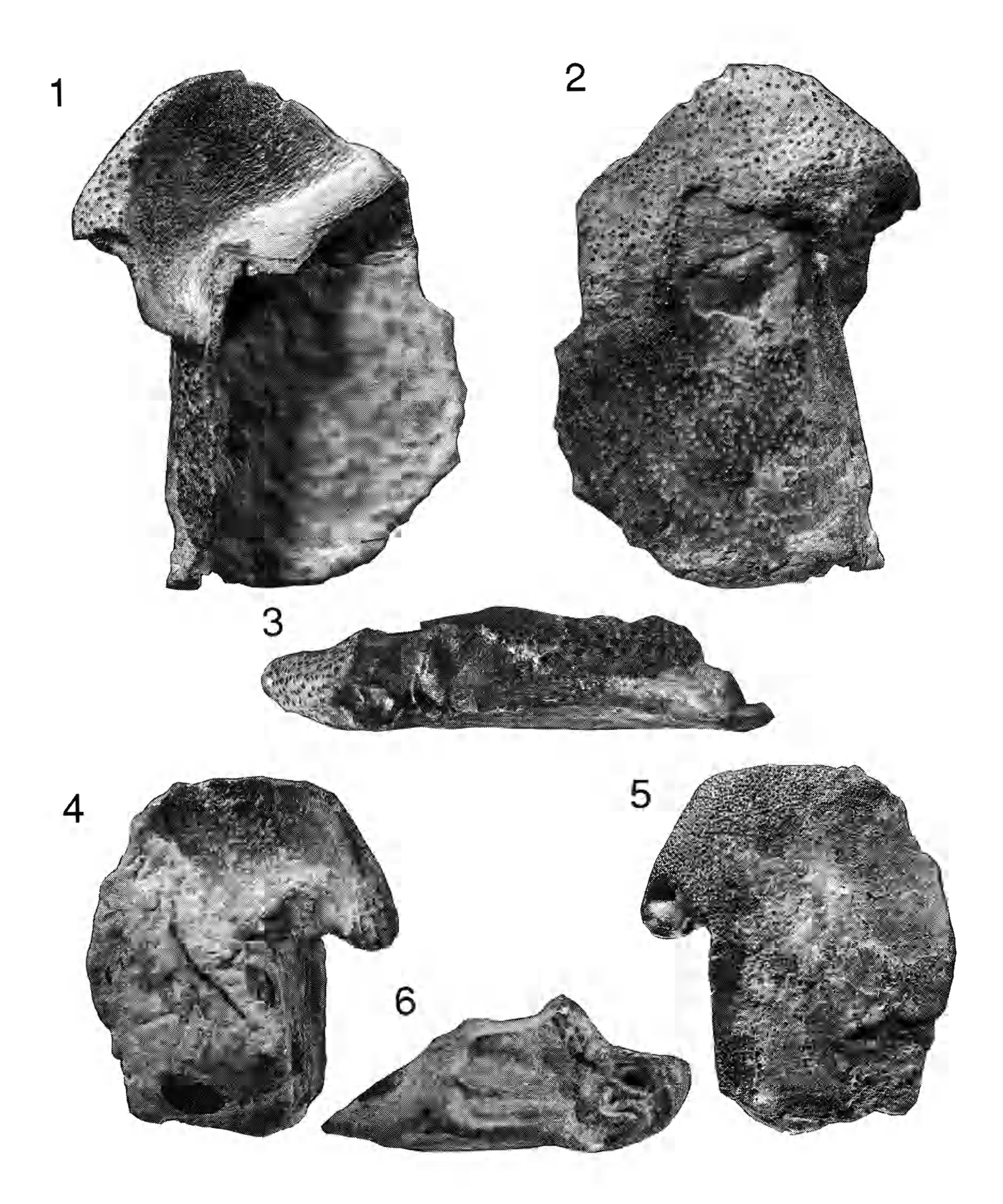

1
2
3
4
5
6

PLATE X

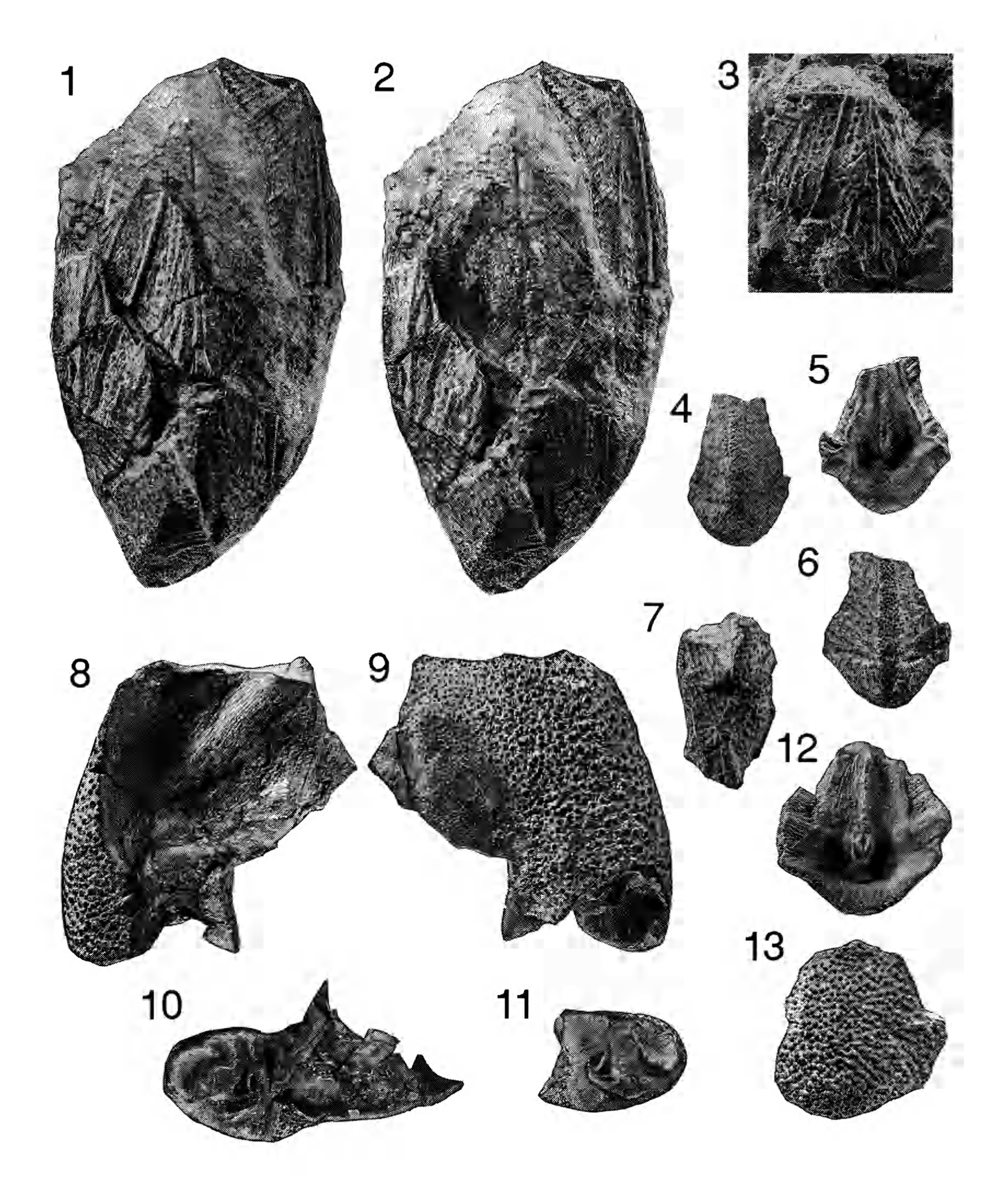
Antiarcha, Xitun Formation, Early Devonian, Qujing, Yunnan, China.

Chuchinolepis sulcata **n. sp.**

1 – Trunk-shield (holotype, V10513.1) in dorsal view, × 2.
2 – Trunk-shield (holotype, V10513.1) in dorsal view, with the fragment of AMD plate removed, × 2.
3 – Incomplete AMD plate in dorsal view, V10513.6, × 2.
4 – PMD plate in dorsal view, V10513.2, × 2.
5, 6 – PMD plate in visceral (5) and dorsal (6) views, V10513.3, × 2.
7 – Incomplete pectoral fin in lateral view, V10513.5, × 2.

Chuchinolepis qujingensis (K.-J. Chang)

8, 9, 10 – Fragment of left AVL plate in dorsal (8), ventral (9) and posterior (10) views, V10511.1, × 2.
11 – Incomplete right AVL plate in posterior view, V10511.2, × 2.
12, 13 – PMD plate in visceral (12) and dorsal (13) views, V10511.9, × 2.


1
2
3
4
5
6
7
8
9
10
11
12
13

Bulletin du Muséum national d'Histoire naturelle, Paris, 4e sér., **18**, 1996
Section C, nos 2-3 : 349-402

Isolated Dinosaur bones from the Middle Cretaceous of the Tafilalt, Morocco

by Dale A. RUSSELL

Abstract. — The "Grès rouges infracénomaniens" of southern Morocco, possibly of Albian age, contain evidence of one of the most diversified dinosaur assemblages known from Africa, including a relatively long-necked species of *Spinosaurus* and abundant but isolated bones of a peculiar theropod ("*Spinosaurus* B" of STROMER 1934). Also preserved are the oldest records of abelisaurids and among the oldest records of titanosaurids in Africa. Theropods are most abundantly represented, followed by sauropods; ornithischian remains were not identified. Bones of infantile dinosaurs are present, one of which was derived from an individual weighing less than 4 kg. The assemblage resembles that of the Bahariya Formation more than that of Gadoufaoua, possibly because of a trophic dependence upon large, freshwater fishes. It was more closely linked zoogeographically to South America than to North America.

Key-words. — Dinosaurs, Middle Cretaceous, Morocco, biogeography.

Os isolés de Dinosaures du Crétacé moyen du Tafilalt, Maroc

Résumé. — Les Grès rouges infracénomaniens du Maroc méridional, supposés d'âge Albien, ont fourni l'un des ensembles de dinosaures les plus diversifiés d'Afrique, avec en particulier une espèce de *Spinosaurus* à cou relativement long, et des os abondants mais isolés d'un théropode singulier (« *Spinosaurus* B » de STROMER 1934). Sont également conservés les plus vieux restes connus d'abelisaurides et parmi les plus vieux de tinosaurides en Afrique. Les théropodes sont les formes les plus abondamment représentées, suivis par les sauropodes; aucun reste d'ornithischien n'a été identifié. Des os de dinosaures juvéniles sont aussi présents, l'un d'eux provenant d'un individu d'un poids inférieur à quatre kilogrammes. L'ensemble évoque davantage celui de la Formation Bahariya que celui de Gadoufaoua, peut-être en raison d'une dépendance trophique envers de grands poissons d'eau douce. D'un point de vue zoogéographique, cet assemblage se relie de plus près, à l'Amérique du Sud qu'à l'Amérique du Nord.

Mots-clés. — Dinosaures, Crétacé moyen, Maroc, Biogéographie.

D. A. RUSSELL, *North Carolina State Museum of Natural Sciences, and North Carolina State University, Raleigh, USA; formerly of the Canadian Museum of Nature, Ottawa, Canada.*

INTRODUCTION

Fed by melting snows in the High Atlas, the Rheriss and Ziz rivers descend to an alluvial plain (the Tafilalt) surrounding the oases of Erfoud and Taouz in the Moroccan Presahara. The plain lies within a terrain dominated by ranges of folded Paleozoic strata (the Anti-Atlas). At the southern edge of the Tafilalt, the two stream courses merge to form the Oued Daoura, which continues through a broad tableland (hamada) called the Kem Kem into Algeria. Continental

strata of middle Cretaceous age are exposed along both the plateau bordering the Tafilalt to the north and the base of the escarpment of the Kem Kem (Figs 1, 2).

Fossil vertebrate remains were collected from these strata by René LAVOCAT, in the course of four winter expeditions (often in the company of Fernand JOLY and Georges CHOUBERT; LAVOCAT 1954a) to the Tafilalt between 1947 and 1952. These included sawfish and rare lungfish teeth, cranial parts of a giant coelacanth, a fragment of a skull possibly referrable to *Libycosuchus* (H. D. SUES, pers. comm. 1994), and teeth and an anterior portion of the skull of a very large crocodile. Several varieties of theropod teeth were also recovered, as well as isolated bones compared to skeletal parts of *Elaphrosaurus*, *Carcharodontosaurus* and *Spinosaurus* (see Table 1). LAVOCAT's outstanding discovery was the incomplete but partially articulated sauropod skeleton constituting the type of *Rebbachisaurus garasbae* (LAVOCAT 1952, 1954b), which he excavated during the winters of 1949-50 and 1951-52 with the assistance of the Service géologique du Maroc.

In 1971, collections were made near Taouz by a party from the Institut und Museum für Geologie und Paläontologie of the Georg-August-Universität in Göttingen, led by H. ALBERTI.

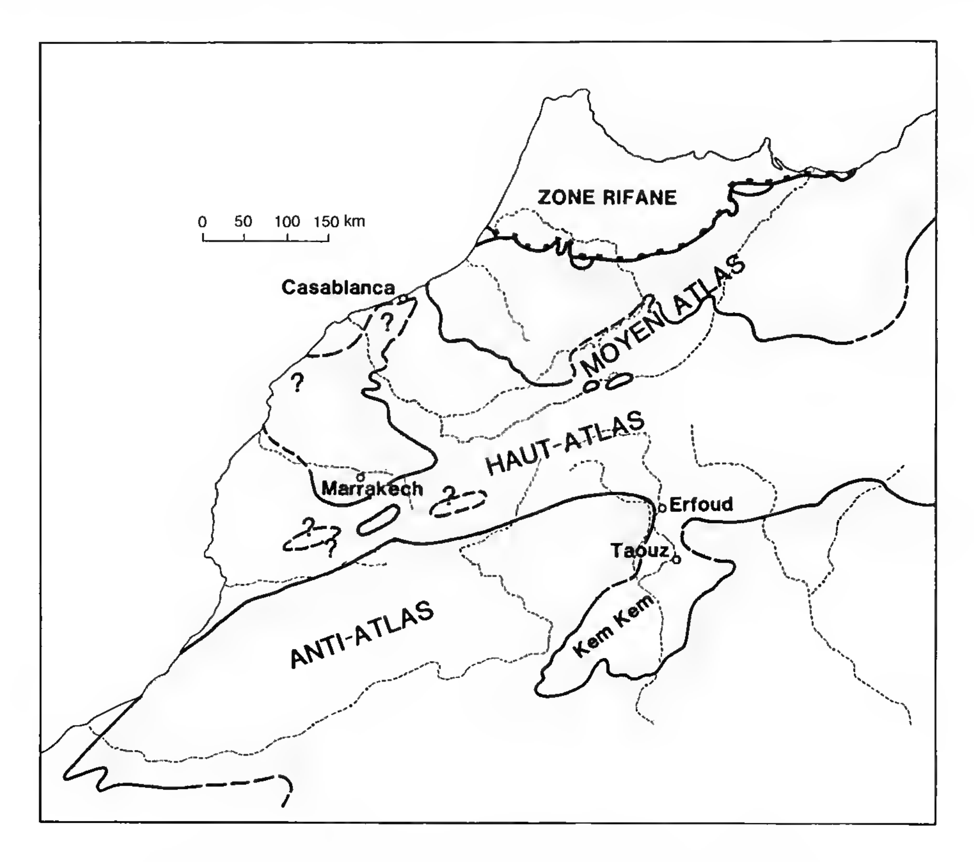


FIG. 1. — Cenomanian-Turonian transgression in Morocco (after CHOUBERT 1952).

TABLE 1. — Fossil vertebrate taxa previously recorded in the "Grès rouges infracénomaniens" of the Tafilalt.

Hybodontidae
Hybodus sp. (TABASTE 1963)
Sclerorhynchidae
Onchopristis numidus, isolated teeth very common (LAVOCAT 1948, 1954a, 1955b: 20; TABASTE 1963; CAPPETTA 1980: 155-6; WENZ 1980)
Semionotidae
Lepidotes sp. (LAVOCAT 1954a: 102; TABASTE 1963)
Gigantodontidae
Stromerichthys aethiopicus? (TABASTE 1963)
Eotrigonodontidae
Eotrigonodon tabroumiti (TABASTE 1963)
Ceratodontidae
Ceratodus africanus, isolated tooth plates rare (LAVOCAT 1948, 1954; CHOUBERT 1952; TABASTE 1963; WENZ 1980)
Ceratodus humei (TABASTE 1963)
Ceratodus sp. (LAVOCAT 1948, 1954a, 102; TABASTE 1963)
Coelacanthidae
Mawsonia lavocati (TABASTE 1963; WENZ 1980, 1981)
Podocnemididae
Gen. indet. (DE BROIN 1988)
Araripemydidae
Araripemys sp. (DE BROIN 1988)
Libycosuchidae
Libycosuchus sp. (BUFFETAUT 1976, 1994)
cf. Trematochampsidae
Hamadasuchus rebouli (BUFFETAUT 1994)
Crocodilia, fam. indet.
"*Thoracosaurus*" *cherifiensis* (LAVOCAT 1955b); large, long-snouted form (LAVOCAT 1954a: 102; not *Sarcosuchus*, DE BROIN in TAQUET 1976: 50; BUFFETAUT 1989a; may be a pholidosaurid, BUFFETAUT *in* BENTON 1993: 698).
Theropoda, fam. indet.
cf. *Elaphrosaurus* sp. (LAVOCAT 1954a: 102; 1954b; 1955b: 56)
Spinosauridae
Spinosaurus sp. (BUFFETAUT 1989a, 1989b)
Theropoda, fam. indet.
Carcharodontosaurus sp., isolated teeth numerous (LAVOCAT 1954b; TAQUET 1976: 39; BUFFETAUT 1989a)
Diplodocidae
Rebbachisaurus garasbae (LAVOCAT 1951, 1954a, 1954b, 1955c: 20, 56)
cf. Ornithischia
Gen. indet. (LAVOCAT 1954b, 1955c: 20)

Additional sawfish, lungfish and giant coelacanth remains were recovered (WENZ 1980), as well as those of a trematochampsid and a large, presumably long-snouted crocodile (BUFFETAUT 1989a). Among the dinosaurian remains were teeth of *Carcharodontosaurus* and a maxilla referred to *Spinosaurus* (BUFFETAUT 1989a, 1989b).

More recently, the inhabitants of the Tafilalt have been encouraged by a growing international market for extinct vertebrates to search adjacent escarpments for fossil teeth and bones. Most of the materials now in private ownership probably consist of crocodile and *Carcharodontosaurus* teeth. Many specimens have been obtained from local sources in the Tafilalt by Brian

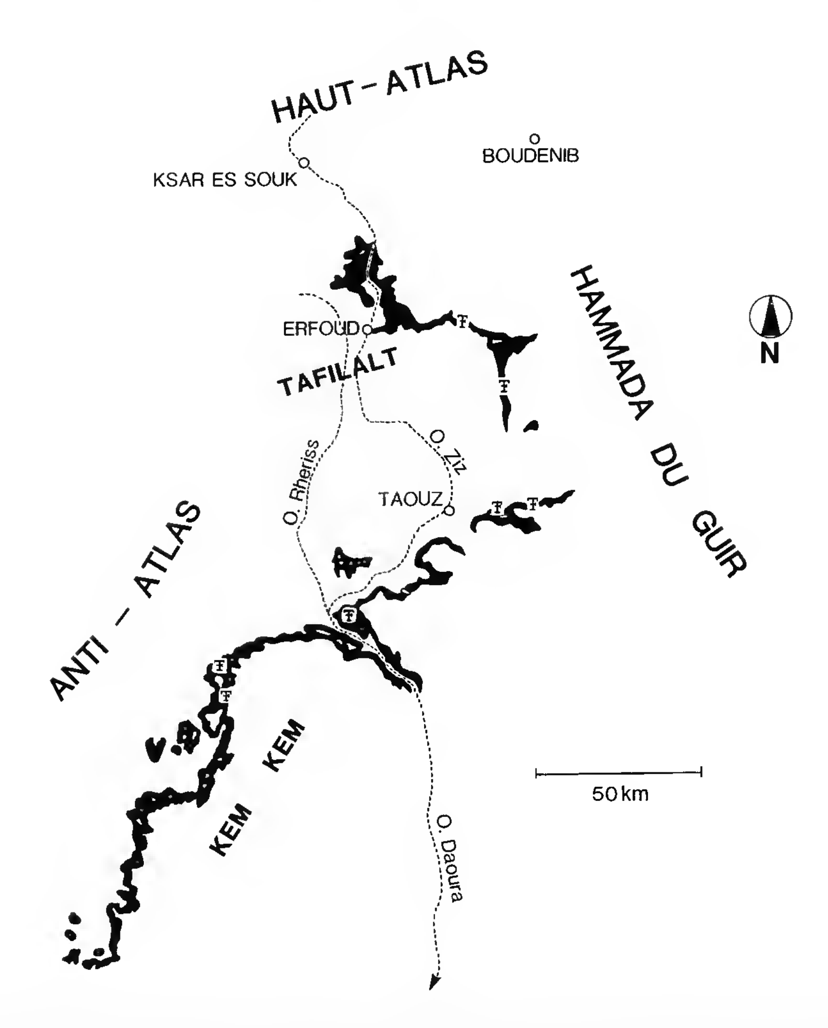


FIG. 2. — Area of outcrop (in black) of the "Grès rouges infracénomaniens" near the Tafilalt (after LAVOCAT 1954a). Dotted lines represent drainage ("O." – oued), "F" indicates a fossil occurrence (after LAVOCAT 1954a, EBERHARDE, pers. comm. 1994).

EBERHARDE (of Moussa Direct, Cambridge, U.K.), some of which were in turn deposited in the Natural History Museum in London, and a larger proportion of which was acquired by the Canadian Museum of Nature. Of the materials deposited in the latter institution, those of fishes will be described by Stephen CUMBAA of the Canadian Museum of Nature, of chelonians by France DE BROIN of the Muséum national d'Histoire naturelle, Paris, and of crocodiles by Hans-Dieter SUES of the Royal Ontario Museum. Dinosaurian materials are described below.

Because the teeth and bones were collected by non-specialists, only general locality information could be provided by Mr. EBERHARDE. The new materials do provide morphological

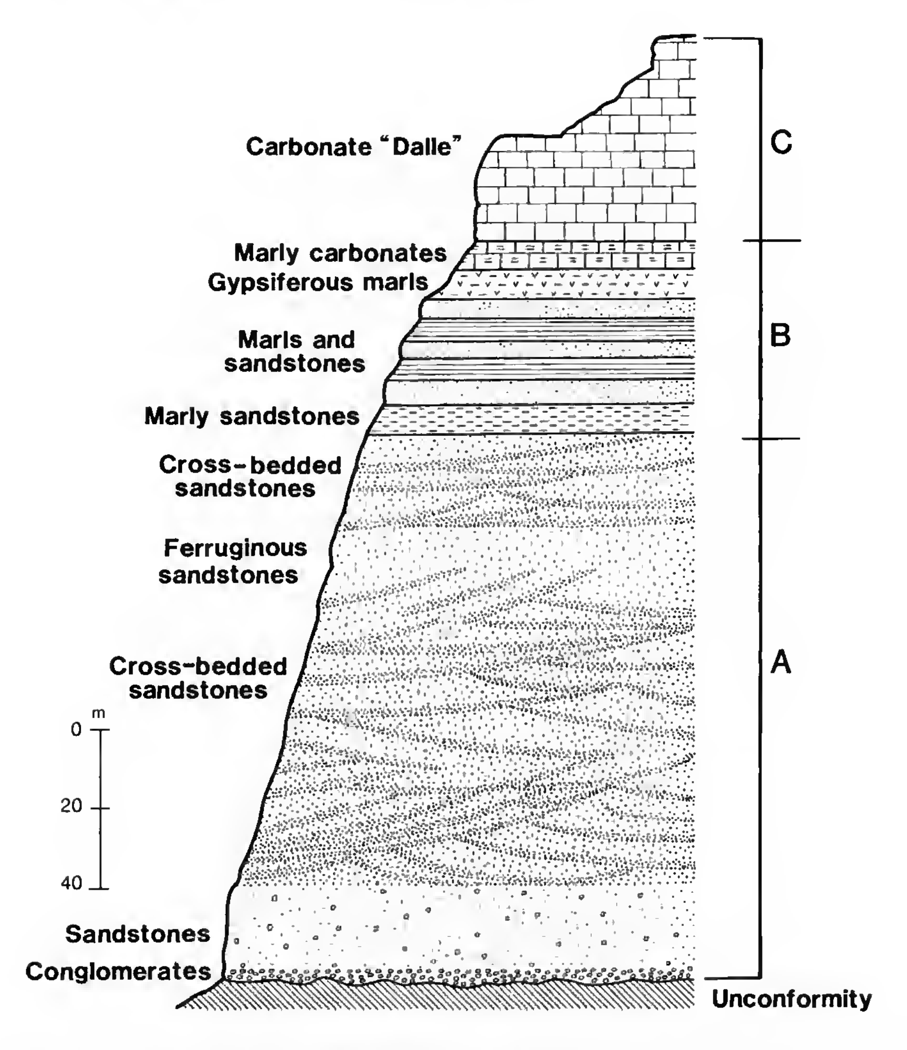


FIG. 3. — Representative section of the "Trilogie mésocrétacée" in the region of the Tafilalt (after JOLY 1962). A, "Grès rouges infracénomaniens"; B, "Marnes versicolores à gypse"; C, "Calcaire cénomano-turonien".

information which would otherwise be lost were the specimens to be excluded from paleontological consideration. Hopefully, inadequacies regarding the provenance of specimens will partly be offset by a fuller appreciation of the character of vertebrate assemblage inhabiting the Tafilalt during Middle Cretaceous time.

STRATIGRAPHY AND CORRELATION

The "Trilogie mésocrétacée" which borders the Anti-Atlas region to the east and south has been separated into three lithologic entities (CHOUBERT 1952). The sequence (Fig. 3) was summarily described by JOLY (1962: 60-62):

*"1. Des **grès inférieurs**, rouges, détritiques, alluviaux et continentaux. Leur épaisseur moyenne est de l'ordre de 100 à 150 m ; mais elle peut varier, surtout lorsque les grès recouvrent une surface accidentée dont ils ennoient les irrégularités ; en outre, elle s'amincit sur le bord des bassins de sédimentation. Le faciès présente aussi de légères variations selon les lieux et surtout selon les niveaux.*

À la base, et particulièrement dans les creux des reliefs ennoyés, ils sont grossiers et hétérogènes. Ils recouvrent souvent le Primaire par l'intermédiaire d'un lit discontinu de quelques dm, tantôt de cailloutis anguleux qui évoquent le revêtement des glacis d'érosion, tantôt de galets roulés comme ceux des fonds d'oueds. Ils se composent de passées de graviers ou de sables en forte proportion émoussés et luisants, intercalés dans des grès rouges mal cimentés, à gros grains souvent mats ou au moins picotés, avec parfois des traces de calcaire ou de gypse, ou, plus communément, des bancs de conglomérats à éléments de Primaire.

Plus haut, les grès sont plus fins, plus uniformes aussi dans leur composition minéralogique essentiellement quartzeuse, et mieux calibrés. Ils sont de teinte plus claire, voire même franchement jaunes ; les grains luisants abondent ; les stratifications entrecroisées sont plus fréquentes et plus nettes ; les dragées de quartz sont plus nombreuses. On y rencontre souvent des passées argileuses, des traces de plantes et des ossements plus ou moins roulés d'animaux de lagunes ou de marigots (poissons, crocodiliens, dinosauriens).

Enfin, vers le sommet, s'affirment et se multiplient les entrelits marneux et argileux qui annoncent des conditions nouvelles.

*2. Des **couches de passage** marneuses, rouges, blanches ou bigarrées, parfois gypseuses, passant à des marno-calcaires ou des calcaires gréseux. Elles peuvent atteindre plusieurs dizaines de mètres d'épaisseur. Elles annoncent le retour de la mer et le début de la grande transgression cénomanienne. Cette formation évoque un régime de lagunes où s'accumulaient encore des dépôts détritiques, en bordure d'une mer transgressive.*

*3. Un puissant complexe calcaire, la **dalle**, formation franchement marine, épaisse de 40 à 75 m, qui marque le maximum d'extension de la mer."*

The three divisions are more generally known, respectively, as the "Grès rouges infracénomaniens" (locally exceeding 200 m in thickness), "Marnes versicolores à gypse" (100-200 m), and "Calcaire cénomano-turonien" (100-150 m; CHOUBERT 1952; BASSE & CHOUBERT 1959). The ammonite *Neolobites vibrayeanus* occurs at the base of the "Calcaire cénomano-

turonien" in the Anti-Atlas region (CHOUBERT 1952: 145-146), and more particularly in the western Kem Kem (BASSE & CHOUBERT 1959: 72). The *Vibrayeanus* Zone is considered by MEISTER *et al.* (1991) to represent the lower part of the upper Cenomanian, which accordingly represents the younger limit for the age of the Tafilalt fossil vertebrate assemblage.

The older limit for the age of the assemblage is very poorly constrained. The mineralogy of the "Grès infracénomaniens" corresponds to that of "séquence B" of the "Couches rouges" in the High Atlas, which apparently was deposited during Upper Jurassic and Lower Cretaceous time (MONBARON *et al.* 1990). Near Anoual, some 150 km north-east of the Tafilalt, "séquence B" contains a mammal-bearing horizon which may be of Berriasian-Valanginian age (SIGOGNEAU-RUSSELL *et al.* 1990; DUFFIN & SIGOGNEAU-RUSSELL 1993). A Barremian detritic episode is widely developed across north-western Africa (BUSSON & CORNÉE 1989, 1991). Whether or not this detritic episode is related to pre- or intra-Barremian tectonic movements in the Middle Atlas (CHARRIÈRE 1992), a "faible discordance" above the mammal-bearing horizon in the section near Anoual (SIGOGNEAU-RUSSELL *et al.* 1990: 474) and the Paleozoic erosional surface buried beneath the "Grès infracénomaniens" in the Tafilalt (JOLY 1962) is an unresolved question. Possibly in part due to their successional continuity with the overlying Cenomanian carbonates, the "Grès infracénomaniens" are usually considered to be of Albian to Cenomanian age (*cf.* de BROIN 1988; BUFFETAUT 1994; CAPPETTA 1980; WENZ 1980).

Exposures of the "Grès infracénomaniens" extend for 250 km, curving east and south from Erfoud, and then southwest along the northern escarpment of the Kem Kem (Fig. 2). Fossil occurrences are rare and usually consist of isolated teeth or a few fragments of abraded bone (LAVOCAT 1949, 1954a). Occasionally, large concentrations of water-worn fossils occur, including *Onchopristis* and crocodile teeth, and ganoid scales. Teeth of *Carcharodontosaurus* are about half as abundant as those of crocodiles, and sauropod teeth are less than half as abundant as those of *Carcharodontosaurus*. Shark teeth are rare and apparently limited to outcrops near Erfoud (Brian EBERHARDE, pers. comm. 1994). Occurrences of associated skeletal parts of large dinosaurs include the type of *Rebbachisaurus garasbae*, cited above, and unconfirmed reports of two specimens, which were allegedly discovered by local people recently and partly destroyed.

SYSTEMATIC PALEONTOLOGY

Super-order SAURISCHIA Seeley, 1888
Order THEROPODA Marsh, 1881
Family SPINOSAURIDAE Stromer, 1915

Spinosaurus maroccanus n. sp.

TYPE. — Median cervical vertebra NMC 50791 (Fig. 4a-c, NMC is the acronym for a specimen in the collections of the Canadian Museum of Nature), acquired by the Museum through the courtesy of Mr. Raymond MEYER.

REFERRED SPECIMENS. — Dentary fragments NMC 50832 (Fig. 5), 50833 (Fig. 6); median cervical vertebrae NMC 41768 (Fig. 4d), 50790 (Fig. 7), dorsal neural arch NMC 50813 (Fig. 8).

Diagnosis. — Ratio between length of *centrum* (excluding anterior articular condyle) and height of posterior articular facet of *centrum* approximately 1.5 in mid-cervical vertebrae.

Etymology. — The species is named for the "royaume du Maroc" (kingdom of Morocco).

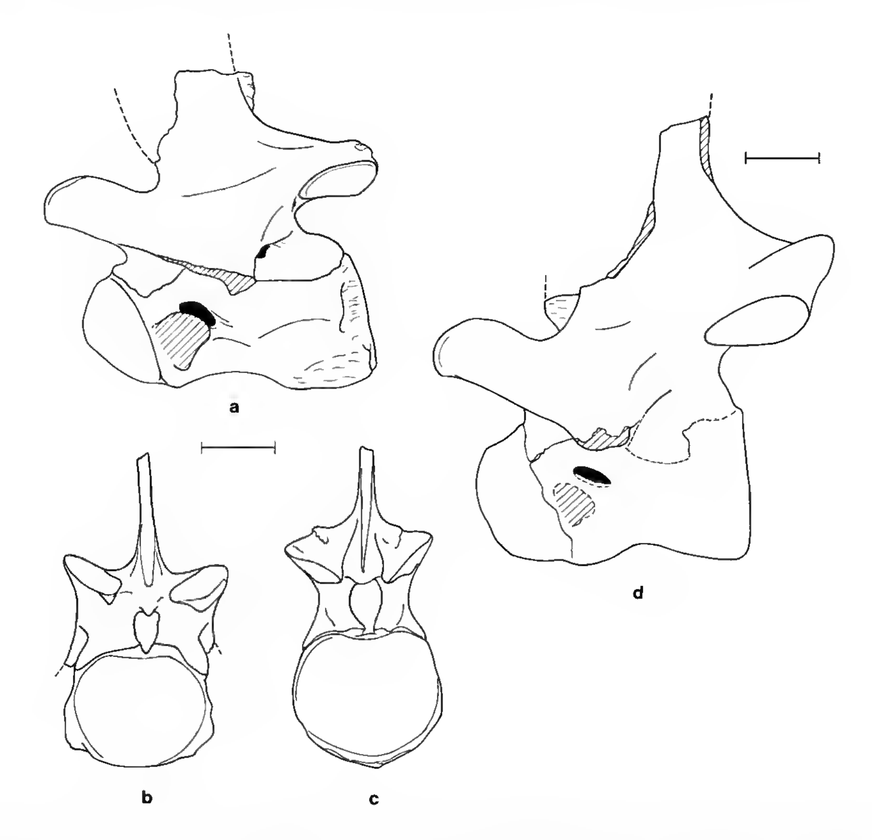


Fig. 4. — *Spinosaurus marocannus* sp. nov., median cervical vertebrae of NMC 50791 (type) in (a) left lateral, (b) anterior and (c) posterior aspect; (d) NMC 41768 in left lateral aspect. Unless otherwise indicated, scale bar in this and following figures represents 5 cm; cross-hatching indicates broken surfaces.

Description and discussion

In *S. aegyptiacus* the ratio between length of *centrum* and height of posterior articular facet approaches 1.1, suggesting that the cervical centra were more slender and the neck was longer in the Moroccan species (see Fig. 9, Table 2A). The pedicles of the neural arch are also elongated, but the vertebrae are otherwise very similar in the two forms. The cervical vertebrae strikingly differ from those of "*Spinosaurus* B" in the greater height of the vertebral spines, and in that the neck was bowed dorsally, in the manner usual for large theropods.

Two dentary fragments (NMC 50832, 50832: Figs 5, 6) are essentially indistinguishable from the dentary in the type of *S. aegyptiacus* (*cf.* Stromer 1915, pl. 1, figs 6, 12a-b), if only

TABLE 2A. — *Spinosaurus maroccanus* n. sp., measurements of vertebrae: Hc and Wc measured from the posterior articular facet, L represents total length, Lc does not include the anterior hemispherical surface, @ means "approximately". LZ represents total length between anterior rim of anterior zygapophysis and posterior rim of posterior zygapophysis, LNA represents minimum length of neural arch pedicles, HV represents height of vertebra from posteroventral edge of *centrum* to top of neural spine. Measurements of the type of *S. aegyptiacus* are from STROMER (1915: 24; those preceded by an asterisk were taken from pl. 2).

	L	Lc	Hc	Wc	LZ	LNA	HV
Anterior							
NMC 41768	183	143	103	—	242	126	—
NMC 50790	—	@ 152	95	99	233	120	289
NMC 50791	195	146	91	100	328	115	—
Posterior							
Type of *S. aegyptiacus*							
vert a	?190				*195	*100	
vert b	185	*140	*133			*108	

slightly more than three quarters the linear dimensions of the Egyptian specimen. They were derived from opposite dentaries of similar size, and the alveoli are here arranged into an anteroposterior series (Table 2B) in the assumption that NMC 50832 contains the anterior two pairs of small, mid-mandibular alveoli present in *S. aegyptiacus* (STROMER 1915, pl. 1, fig. 12b), and NMC 50833 contains the posterior two pairs (for a total of four pairs). There are no indications of interdental plates. An unerupted tooth was present in the second alveolus from the front of the dentary in NMC 50832. It consists of an enamel shell measuring 45 mm in height, and 18 mm anteroposteriorly and 17 mm transversely at the base. The carinae are smooth, and bordered by a smooth longitudinal sulcus approximately 2 mm wide. The remainder of the surface of the crown is covered with small, 1 mm wide longitudinal ridges which become finer and converge toward the apex of the tooth.

TABLE 2B. — *Spinosaurus maroccanus* n. sp., measurements of length of alveolar openings in dentary, from front to back.

NMC 50832		NMC 50833	
1	27	8	14
2	32	third pair	
3	28	9	11
4	34	10	12
first pair		fourth pair	
5	16	11	11
6	14	12	12
second pair		13	11
7	16	14	20
8	incomplete	15	21
		16	27
		17	incomplete



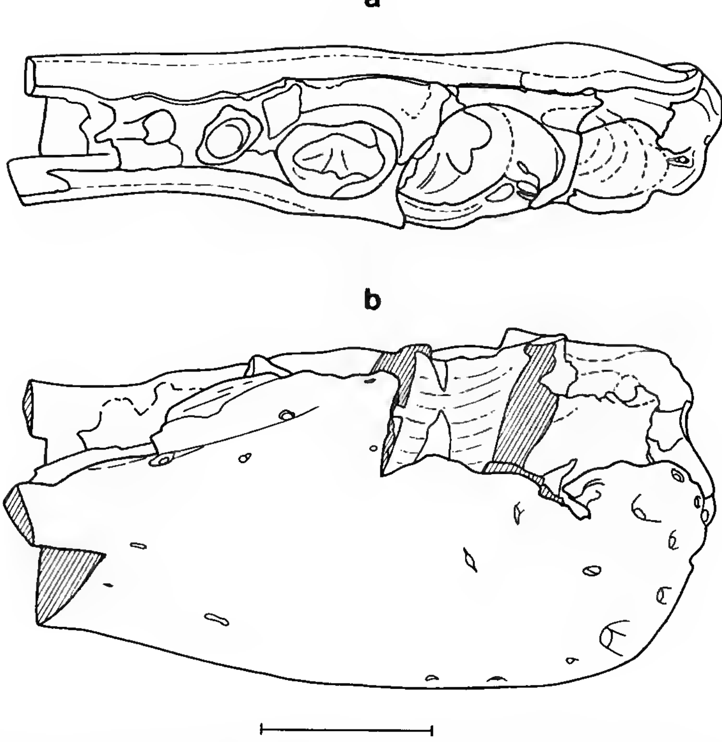


FIG. 5. — *Spinosaurus maroccanus* n. sp., NMC 50832, anterior end of right dentary in (a) dorsal and (b) lateral aspect. Scale bar: 5 cm.

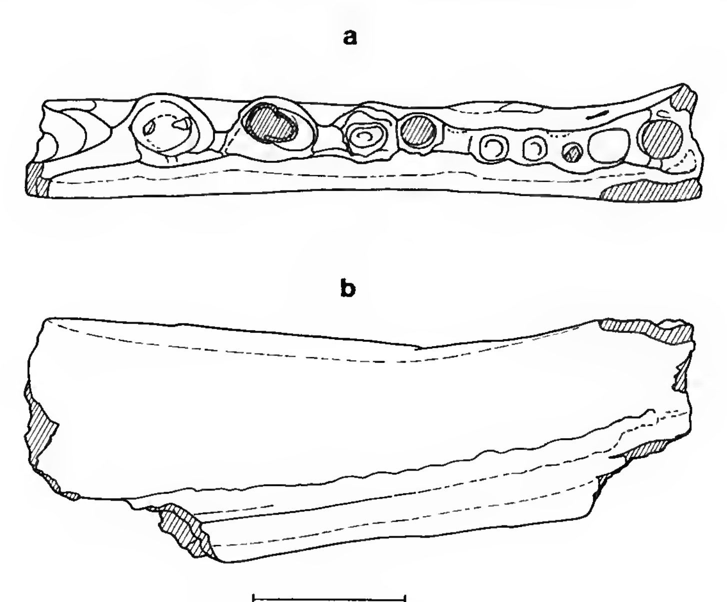


FIG. 6. — *Spinosaurus maroccanus* n. sp., NMC 50833, central part of left dentary in (a) dorsal and (b) medial aspect. Scale bar: 5 cm.

Of the cervical vertebrae, NMC 41768 is larger than NMC 50791 but its morphology reflects a more anterior position in the neck. The postzygapophyseal epipophyses are relatively larger in NMC 41768, the diapophysis are less robust and there is no elevated area for insertion of flexor musculature on the posteroventral edge of the *centrum*, as there is in NMC 50791. The epipophyses are approximately intermediate in development in NMC 50790. Found in association with the latter vertebra were two long and slender cervical ribs, the more complete of which (NMC 50790B) measures 493 mm in length and 10 to 12 mm in mid-shaft diameter. The base of the tuberculum is 36 mm broad anteroposteriorly and of the correct proportions to articulate smoothly with a cervical diapophysis; the abraded *capitulum* was apparently subcircular in outline. Although the distal end of the rib is missing, the shaft exceeded the length of the *centrum* by a factor of at least 3.2. By comparison, in *Carnotaurus* the length of the fourth cervical rib exceeds that of the *centrum* by a factor of about 5 (BONAPARTE *et al.* 1990). Isolated fragments of cervical ribs could easily be mistaken for ornithopod ossified tendons.



FIG. 7. — *Spinosaurus maroccanus* n. sp., NMC 50790, median cervical vertebra in lateral aspect. Scale bar: 5 cm.

A neural arch (NMC 50813) is referred to *Spinosaurus* because of an exceedingly robust and buttressed neural spine base (Fig. 8, see also STROMER 1915, pl. 1, fig. 19). It was derived from the anterior portion of the dorsal column, as indicated by the capitular facet being shared between the *centrum* and the neural arch. The spine base is much more massive than in a vertebra similar to those of "*Spinosaurus* B" (NMC 41850) from the same region of the vertebral column. The anterior pedicles of the neural arches broadly diverge anteriorly.

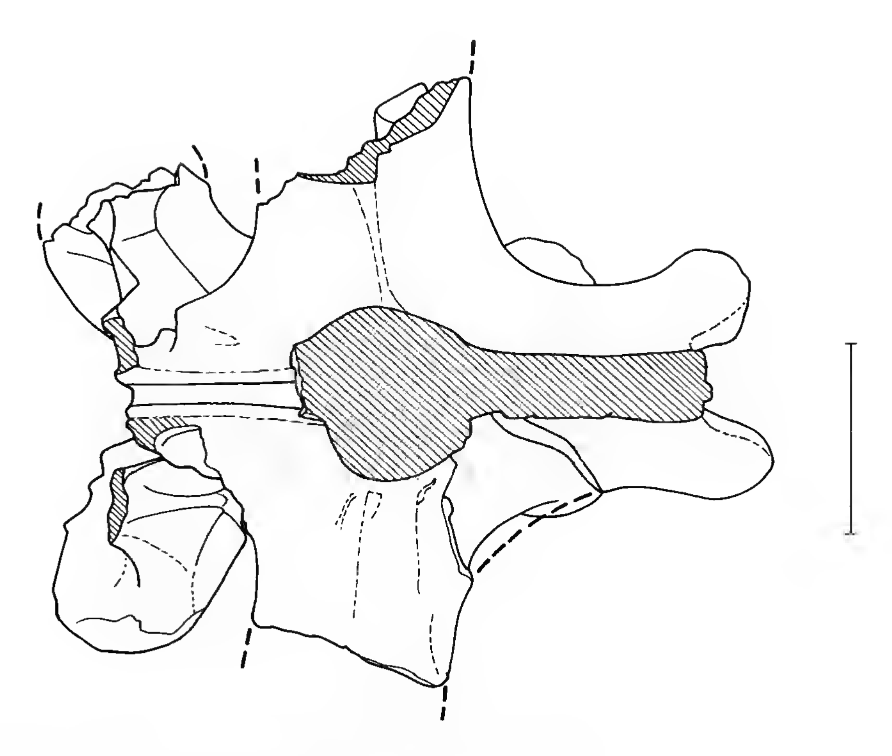


FIG. 8. — *Spinosaurus marocannus* n. sp., NMC 50813, neural arch and broken spine of dorsal vertebra in superior aspect (anterior base of neural arches to left, posterior zygapophyses to right).

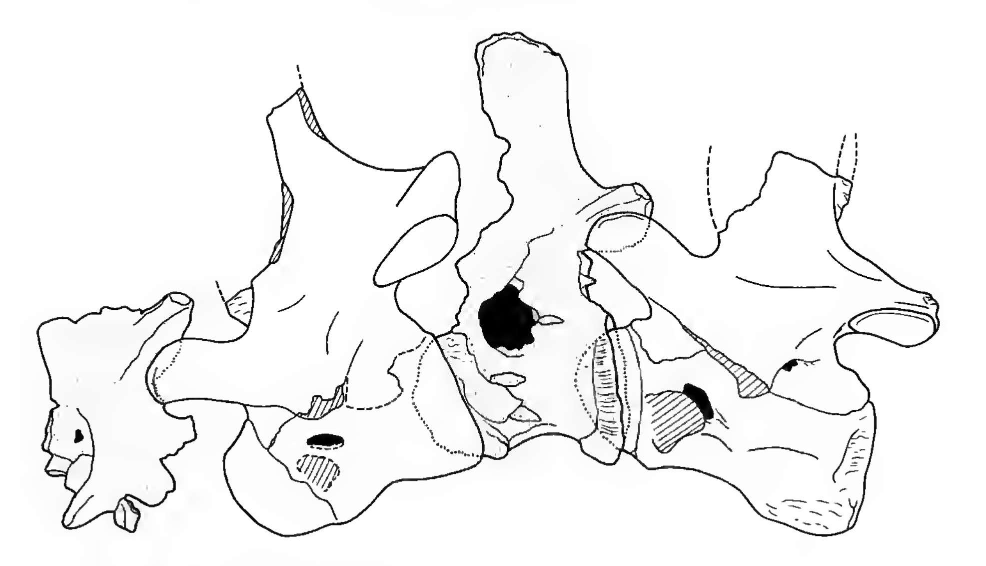


FIG. 9. — Cervical vertebrae of *Spinosaurus maroccanus* and *S. aegyptiacus* (dotted, after STROMER 1915) drawn to equal central height in order to show relatively greater central and neural arch length in *S. maroccanus*.

SIGILMASSASAURIDAE, fam. nov.

SIGILMASSASAURUS, n. g.

DIAGNOSIS. — Apomorphies in the cervical vertebrae for the genus and family include: spines short, wider transversely than long; intercentral articulations wider than high, exceeding length of *centrum* in width; transverse planes through anterior and posterior intercentral articulations converge dorsally, indicating cervical series "U"-shaped in lateral aspect; parapophyses project ventrolaterally beyond rim of intercentral articulations; hypapophyses more powerfully developed in middle of cervical series than in region of cervico-dorsal transition.

ETYMOLOGY. — The generic name is derived from the ancient city of Sigilmassa, former capital of the Tafilalt and a former centre of commerce in the western Sahara.

STROMER (1934) designated theropod skeletal elements collected from a single site in the Bahariya Oasis of Egypt as "*Spinosaurus* B," noting that two individuals were represented. He doubted that the limb elements, which belonged to an animal weighing on the order of 400 kg (*cf.* ANDERSON *et al.* 1985), could be referred to *Spinosaurus*. However, the vertebrae, which were derived from an animal the size of *Allosaurus* or *Carnotaurus* (about 1,400 kg, *cf.* ANDERSON *et al.* 1985; BONAPARTE *et al.* 1990: 30), apart from the shortness of their spines, were considered to resemble those in the type of *Spinosaurus aegyptiacus*. BUFFETAUT (1989a, 1989b) also noted that the short spines in the vertebrae of "*Spinosaurus* B" distinguished them from those of *S. aegyptiacus*. Indeed, the cervical vertebrae of *Sigilmassasaurus* differ so greatly from those of *S. aegyptiacus* in the relative length and breadth of the *centra*, the angle between the plane of the intercentral articulations and the longitudinal axis of the *centrum*, and the height of the spines (see above) that the two forms are here held to be distinct on a family-group level. Vertebrae are here identified as *Sigilmassasaurus* because of their fundamental similarity to vertebrae from the cervical, dorsal and caudal regions of the larger specimen described and figured by STROMER (1934: 8-11, pl. figs 2-6).

These vertebrae also differ from those of other Bahariya theropod taxa. A mid-cervical ("Halswirbel b") in the major specimen STROMER (1931: 11) referred to *Carcharodontosaurus* differs in that the width of the anterior central facet is less than the length of the *centrum* and the median ventral keel thickens posteriorly, the reverse of conditions in "*Spinosaurus* B." Proximal caudals referred by STROMER (1931, pl. 1 fig. 10; 1934, pl. 2 fig. 5) to *Carcharodontosaurus* and *Bahariasaurus* bear pleurocoels, unlike in "*Spinosaurus* B." The chevrons are not bridged in "*Spinosaurus* B," as they are in *Carcharodontosaurus* (STROMER 1934: 12).

Sigilmassasaurus brevicollis n. sp.

TYPE. — Cervical vertebra NMC 41857 (Fig. 10).

DIAGNOSIS. — As for genus; for species-level characters see under "Description" and "Discussion", *Sigilmassasaurus* sp., below.

ETYMOLOGY. — The species name alludes to the shortness of the cervical *centra*.

REFERRED SPECIMENS. — (Listed in a morphologically anteroposterior sequence, although none are known to have been associated): cervical vertebrae NMC 41790, 41774, 41856, 41857 (type); dorsal vertebrae NMC 41858 (Fig. 11a-b), 41850 (Fig. 11c-d), 50428, 50402, 41776, 50407, 50800, 41772, 41851; caudal vertebrae NMC 41854 (Fig. 12a), 41775, 41853 (Fig. 12b-d), 41855 (Fig. 12e-g).

DESCRIPTION

The difference in the proportions of the smallest (NMC 41774) and largest (NMC 41856) cervical *centrum* in the collection (see Table 3) suggests an order of magnitude difference in weight between the animals which produced them. Although it has not been possible to observe sequential variation within an articulated series of anterior presacral vertebrae, the vertebrae can

TABLE 3. — *Sigilmassasaurus brevicollis*, measurements of vertebrae: Hc and Wp measured from the posterior articular facet, Wa measured from the anterior articular facet, L represents total length. @ means "approximately". Lc excludes the anterior hemispherical surface, Dw measured across the ends of the diapophyses. The vertebrae are arranged morphologically in an anterior-posterior sequence. All except NMC 41629 (*S.* sp.) have been assigned to *S. brevicollis*.

	L	Lc	Hc	Wa	Wp	Dw
			CERVICALS			
Anterior						
NMC 41790	@ 127	90	—	—	115	—
NMC 41774	67	56	44	66	69	130
NMC 41856	146	113	95	145	150	—
NMC 41857	121	102	94	147	149	@ 336
NMC 41629	150	113	—	@ 115	124	— (*S.* sp.)
Posterior						
			DORSALS			
Anterior						
NMC 41858	—	103	101	@ 141	142	
NMC 41850	152	122	110	115	110	
NMC 50428	—	—	—	25	—	
NMC 50402	195	168	119	—	120	
NMC 41776	@ 150	134	116	—	—	
NMC 50407	98	84	64	@ 63	@ 69	
NMC 50800	88	78	59	@ 56	@ 59	
NMC 41772	162	138	109	@ 81	@ 93	
NMC 41851	157	134	101	@ 88	—	
Posterior						
			CAUDALS			
Anterior						
NMC 41854	110	110	90	80	—	
NMC 41775	94	94	81	64	66	
NMC 41853	110	110	87	81	75	
NMC 41855	59	59	49	42	38	
NMC 41862	58	58	46	41	38	
Posterior						

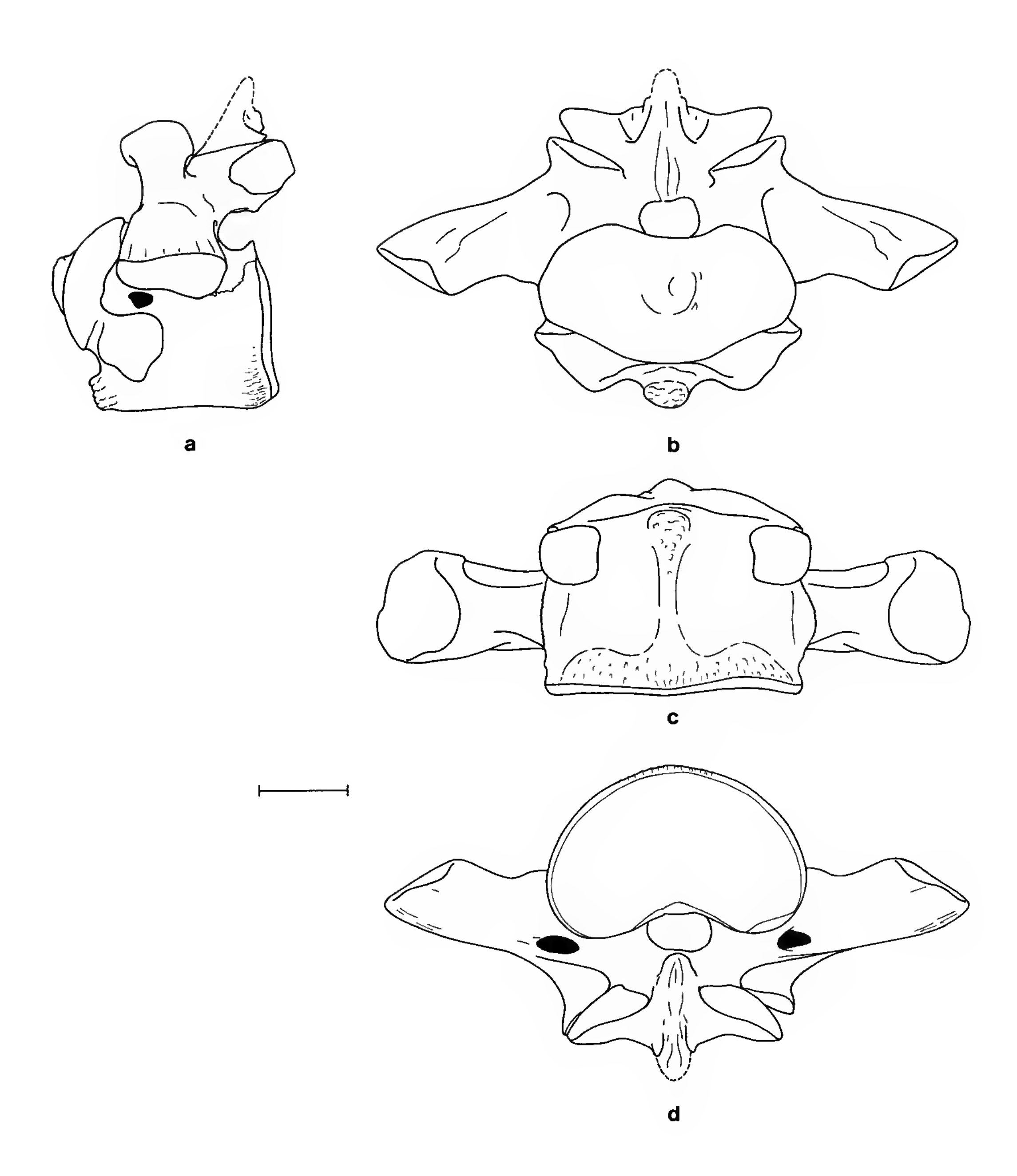


FIG. 10. — *Sigilmassasaurus brevicollis* n. g. et n. sp., NMC 41857 (type), cervical vertebra in (a) left lateral, (b) anterior, (c) ventral and (d) posterior (inverted) aspect. Scale bar: 5 cm.

easily be assembled into a morphological series. In theropods, the posteriormost cervical vertebra may be separated from the anteriormost dorsal by the change in the associated rib from a slender element lying subparallel to the vertebral column to an angled structure with its long axis nearly perpendicular to the vertebral column. This change occurs between the 9th and 10th postcranial segments in *Allosaurus* and *Monolophosaurus*, and the 10th and 11th postcranial segments in *Carnotaurus* and *Tyrannosaurus*. In each of these genera, the transverse process becomes horizontal, or nearly so, on the anteriormost dorsal vertebra (OSBORN 1917, pl. 27; MADSEN 1976; BONAPARTE *et al.* 1990; ZHAO & CURRIE 1993). By virtue of the fact that the transverse process is horizontal on NMC 41858, this vertebra will be considered as an anterior dorsal.

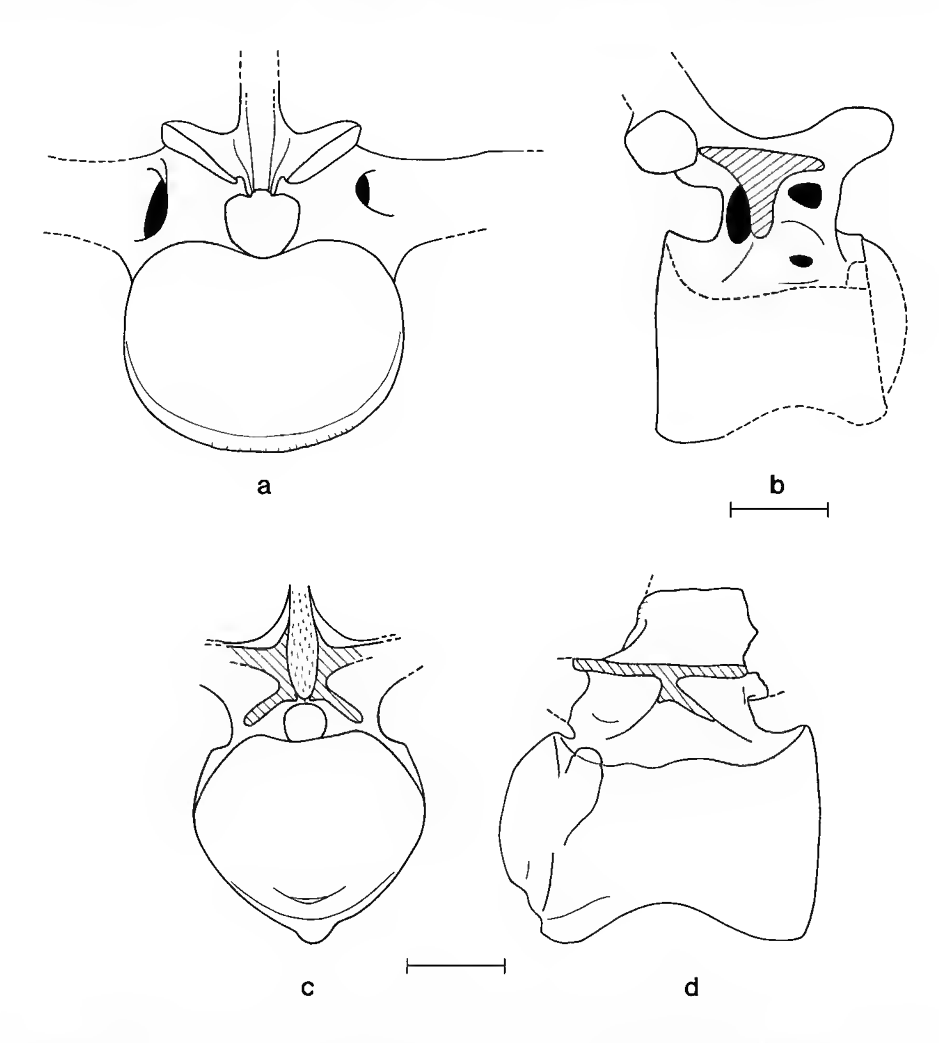


FIG. 11. — *Sigilmassasaurus brevicollis* n. g. et n. sp., referred dorsal vertebrae; NMC 41858, postulated anteriormost dorsal in (a) posterior and (b) right lateral aspect; NMC 41850, anterior dorsal in (c) anterior and (d) right lateral aspect. Scale bar: 5 cm.

The spines are short, anteroposteriorly narrow and wide transversely through much of the cervical sequence (NMC 41790, 41774, 41856, 41857), unlike in *Spinosaurus* where the spines are elongated (STROMER 1915). They broaden anteroposteriorly in the anterior dorsal region (NMC 41858, 41850) where they apparently remain short but slope posterodorsally. The articular surfaces of the anterior and posterior zygapophyses are, respectively, gently convex and concave. The superior surfaces of the posterior zygapophyses are smooth in the cervical region, with no indications of the epipophyseal tuberosities which occur in *Spinosaurus* (STROMER 1915). The diapophyses are short, straight and project ventrolaterally in an anterior cervical (NMC 41790), become recurved and elevated in median cervicals (NMC 41774, 41856, 41857), are straight, and posterolaterally directed in an anterior dorsal (NMC 41858), and slightly elevated and anterolaterally directed in an anterior dorsal (NMC 41850) which occupied a morphologic position posterior to the preceding vertebra. Pneumatic foramina on the anterior and posterior surfaces

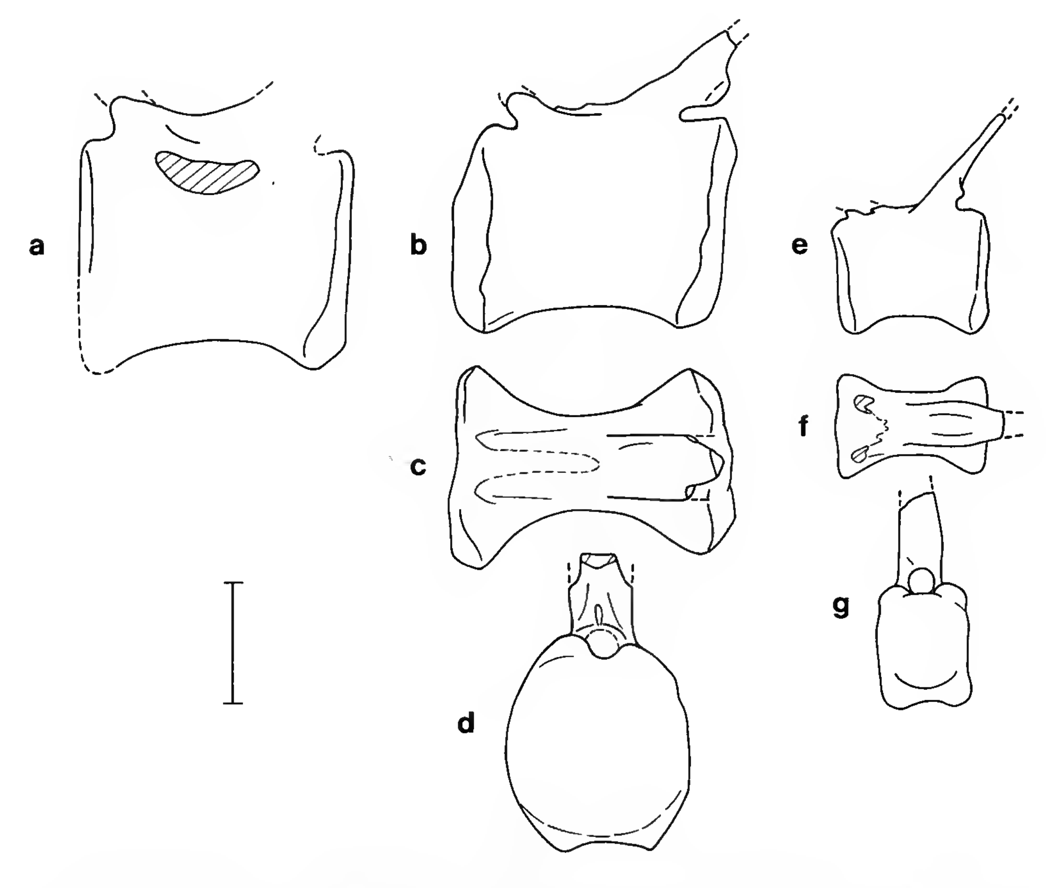


FIG. 12. — *Sigilmassasaurus brevicollis* gen. et sp. nov., referred caudal vertebrae; (a) NMC 41854, mid-caudal in left lateral aspect; NMC 41853, mid-caudal in (b) left lateral, (c) dorsal and (d) posterior aspect; NMC 41855, posterior caudal in (e) left lateral, (f) dorsal and (g) posterior aspect. Scale bar: 5 cm.

of the diapophysis in the cervical vertebrae disappear posteriorly within the anterior dorsal region, and an infradiapophyseal lamina, which appears in the posterior cervical sequence, becomes divided into anterior and posterior branches in the anterior dorsal region.

The cross-sectional area of the neural canal remains relatively constant in the morphological sequence including cervicals NMC 41856, 41857 and dorsal NMC 41858, averaging 8.6% of the area of the intercentral articulations. However, in the anterior dorsal (NMC 41850) located morphologically behind NMC 41858 it is only 4.6% of that of the intercentral articulations. These circumstances suggest that the forelimbs were rudimentary in this form, for the neural canal is proportionately larger in those with large forelimbs (GIFFIN 1990). A very shallow emargination for the neural canal is present within the dorsal margin of the posterior central articular surface in several cervicals (NMC 41790, 41774 and 41856). The emargination is deeper in a posterior cervical (NMC 41857) and an anterior dorsal (NMC 41858, in which the posterior end of the right neural arch is necrotic). The emargination is no longer present in a more posteriorly situated anterior dorsal (NMC 41850).

Relative to those of other theropods, the cervical *centra* are exceedingly broad, and the width of the posterior articular surface exceeds its height by a factor of about 1.5. In *Allosaurus* (MADSEN 1976), *Carnotaurus* (BONAPARTE *et al.* 1990) and *Spinosaurus* (see above) the ratio is about 1.25, and in *Deinonychus* (OSTROM 1969) and tyrannosaurs (RUSSELL 1970a) it is about 1.00. Behind the anterior end of the dorsal column (NMC 41858), the intercentral articulations narrow and begin to deepen (NMC 41850), becoming vertically oval (NMC 41776, 41772, 41851). The width/length ratio increases (see Table 3) from the anterior (NMC 41774, 41856) to the posterior cervical region (NMC 41857), after which it diminishes through the anterior dorsal sequence. All preserved dorsal vertebrae are strongly opisthocoelous.

The parapophysis is low in anterior cervicals (NMC 41790, 41856, 41774) but occurs at *mid-centrum* height in a posterior cervical (NMC 41857). It straddles the *centrum*-neural arch suture in two anterior dorsals (NMC 41858, 41850). In *Allosaurus* and *Tyrannosaurus* the parapophysis is confined to the *centrum* on all of the anterior presacral vertebrae back to and including the second dorsal, and it straddles the *centrum*-neural arch suture on several more segments posteriorly (MADSEN 1976; OSBORN 1917, pl. 27). A small, posteriorly sloping neural spine would place the first Moroccan dorsal toward the front of the anterior dorsal series, and the broad neural spine would place the second several segments behind. A pleurocoel situated above the parapophysis in cervical *centra* diminishes posteriorly in the sequence as it is apparently displaced to a position above the suture for the neural arch (NMC 41858); there are no pleurocoels on available dorsal *centra* (the *centrum* is incompletely preserved in NMC 41858).

The angle between the plane of the intercentral articulations and the longitudinal axis of the cervical *centra* indicates that the neck was strongly arched into a "U"-shaped curve (Fig. 13), a condition apparently unknown in any other theropod. Measurements of available vertebrae suggest that the surface area of the intercentral articulations may not have increased greatly posteriorly in the cervical series, although it typically doubles in other large carnivorous theropods (*cf.* measurements in *Allosaurus* Gilmore, 1920; *Monolophosaurus* Zhao & Currie, 1993; *Carnotaurus* Bonaparte *et al.*, 1990; and *Albertosaurus* and *Daspletosaurus* Russell, 1970a). In hadrosaurs, where the neck is also "U"-shaped in lateral profile, the intercentral articulations do not increase greatly in area from front to back (pers. obs.). Perhaps the neck in *Sigilmassasaurus*

was composed of a relatively large number of vertebral segments, as in hadrosaurs (WEISHAMPEL & HORNER 1990). It is probable that it was more flexible and capable of a much greater variety of movements than the back.

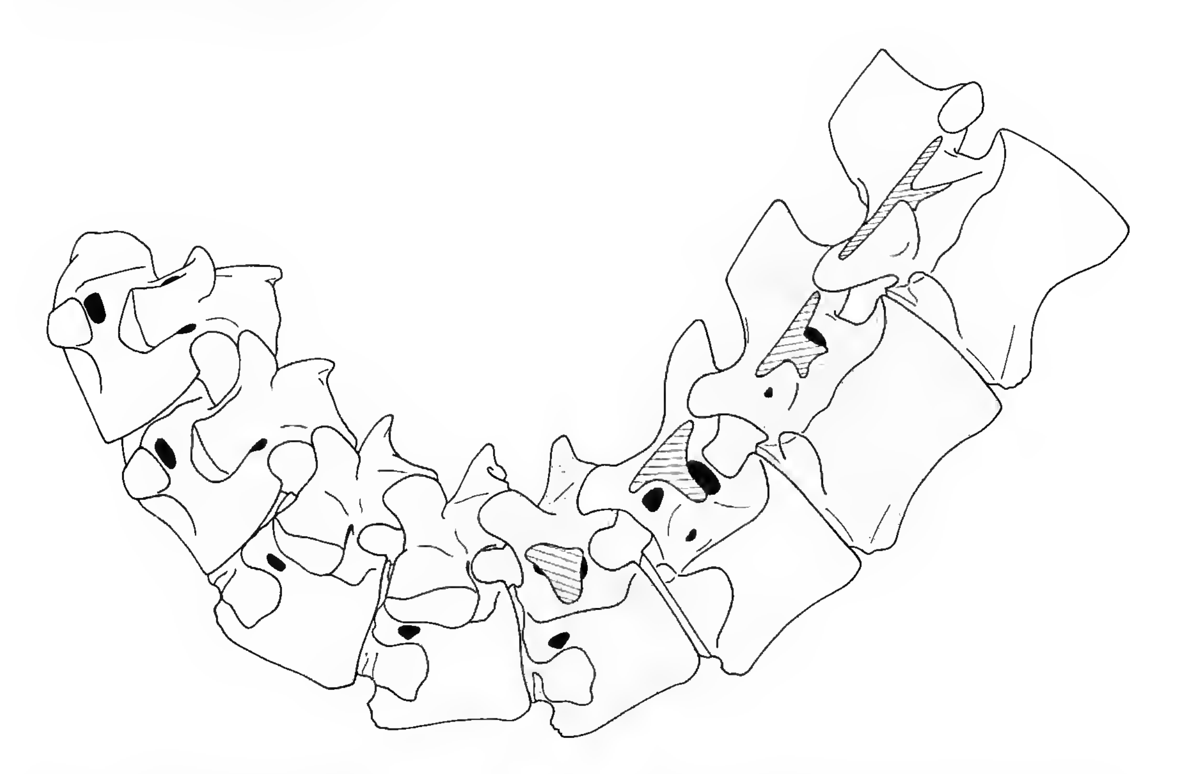


FIG. 13. — *Sigilmassasaurus brevicollis* n. g. et n. sp., reconstructed anterior presacral vertebral column; vertebrae, from left to right, are reconstructed and scaled after NMC 41790, 41774, 41856, 41857 (dotted, interpolated), 41858 (dotted, interpolated) and 41850.

Although a longitudinal keel is present, a hypapophyseal tuberosity is not developed on an anterior cervical from a juvenile (NMC 41774). It is small in the mid-cervical region (NMC 41856), enormously developed on a posterior cervical (NMC 41857) and diminishes in size within the anterior dorsal region (NMC 41850, 41776). In *Deinonychus* (OSTROM 1969) and *Sinornithoides* (RUSSELL & DONG 1993) the hypapophyses are most strongly developed behind the posterior cervical region, within the cervico-dorsal transition.

In a dorsal in the specimen originally designated as "*Spinosaurus* B" the parapophysis is situated entirely on the neural arch, and the vertebra must have occupied a morphological position posterior to NMC 41850. As in the latter vertebra, however, the transverse process is anterolaterally directed. The Egyptian vertebra evidently lacks a hypapophysis, but does bear a longitudinal ridge ventrally (STROMER 1934: 8, pl. 1 fig. 4). Of three median dorsal *centra* from Morocco, one (NMC 41776) bears a small longitudinal keel anteroventrally, the second (NMC 41772) bears a slightly elevated longitudinal rugosity, the third (NMC 41851) bears a

diffuse swelling in this region marked by longitudinal striae. The dorsal vertebrae are arranged in a hypothetical anteroposterior series in Table 3 on the basis of the narrowing intercentral facets which more closely approximate an orientation at right angles to the long axis of the *centrum*, and diminishing hypophyseal keel. The dorsal *centra* are very similar to those of *Spinosaurus*, and some may here mistakenly be assigned to *Sigilmassasaurus*. Two dorsal *centra* from similar anatomical positions represent extremes of a possible growth series; one (NMC 50402) is about 5.3 times the linear dimensions of the other (NMC 50428), which cubed yields a volume (weight) difference on the order of 150 times. The neural arch suture is open in both vertebrae.

Several caudal vertebrae also appear to form a morphological series (NMC 41854, 41775, 41853, 41855) consistent with caudals belonging to "*Spinosaurus* B." In the rectangular shape of the *centra*, the vertebrae also generally resemble median and distal caudals of *Ouranosaurus* (TAQUET 1976). This resemblance is enhanced by tall, posterodorsally projecting spines. However, STROMER (1934: 10), because of the divided nature of the spine in a distal caudal, interpreted the structure as representing the anterior zygapophyses. None of the Moroccan caudals described here possess a divided spine, but NMC 41854 and 41855 otherwise closely resemble those figured by STROMER (1934, pl. 1 figs 4, 6). The "anterior zygapophyses" articulate with nothing in the Egyptian vertebra, and would represent a zygapophyseal adaptation unique among the distal caudals of dinosaurs. It would be more conservative to interpret the structure as either a divided or a pathologic spine; the latter alternative is provisionally adopted here.

In all of the available caudals, the spine rises from the posterior half of the neural arches, and is wider than long. Anteriorly, the smooth lamina of bone roofing the neural canal is very thin, and broken away between the bases of the anterior zyagapophyses. The latter are broken off, but probably lacked articular surfaces in the more distal caudals (NMC 41853, 41855). Broken but well-developed transverse processes are present in NMC 41854, and a low, longitudinal ridge is present in this region of the *centrum* in NMC 41775.

DISCUSSION

The cervical vertebrae superficially resemble those of *Ouranosaurus* (TAQUET 1976) in lacking a well-developed neural spine, but differ greatly in possessing pneumatic foramina on the *centrum* and neural arches, very broad central articular facets, powerfully developed diapophyses and abbreviated postzygapophyses. The cervical *centra* also superficially resemble those of titanosaurs in possessing pneumatic foramina, but are much shorter than in these sauropods (*cf.* BONAPARTE & POWELL 1980; POWELL 1987; JACOBS *et al.* 1993). In the extreme reduction of the neural spine, the recurving diapophyses and the emplacement of the pneumatic foramen on their anterior surfaces, and the broad intercentral articulations, the cervicals closely resemble an anterior dorsal from Tendaguru referred by JANENSCH (1929a, fig. 11) to the sauropod "*Gigantosaurus*." The latter vertebra is reconstructed to measure over 1 m across the diapophyses, whereas the largest Moroccan vertebra possessing well-preserved diapophyses probably measured but 34 cm in this dimension. The position of the parapophysis indicates that the East African vertebra is from the anterior dorsal region. Yet it lacks a spine, which is well developed in the anterior dorsals of the Moroccan theropod. It also lacks a hypapophyseal peduncle. The resem-

blance is nonetheless striking. The morphological transition from cervical into normal theropod dorsal vertebrae, however, supports the theropod affinities of *Sigilmassasaurus*.

From the enormous size of the hypapophyses in the posterior cervical region, it could be inferred that the muscles attached to them would have powerfully and rapidly projected the neck downwards. As noted above, the cervical segments become more robust posteriorly in theropods with large skulls. If the skull of *Sigilmassasaurus* was small (relative to conditions in large theropods), and comparable in size to the skull in most hadrosaurs with cervical vertebrae of approximately equal size and comparable morphology, one is left with the image of a theropod weighing well over a tonne, with rudimentary forelimbs, a neck adapted for pecking and a skull of avian proportions relative to the size of the body. Superficially, the tail may have resembled that of an ornithopod more closely than that of a theropod. It is evident that *Sigilmassasaurus* may represent a truly unusual group of theropod dinosaurs.

Sigilmassasaurus sp.

REFERRED SPECIMEN. — Posterior cervical *centrum* NMC 41629 (Fig. 14c, f, g), and distal caudal vertebra NMC 41862.

DESCRIPTION AND DISCUSSION

The cervical *centrum* belonged to a large vertebra, but the sutures were insufficiently closed to prevent the separation and loss of the neural arch. The colour of preservation is a deep, reddish brown, and quite distinct from the white to light orange colour of other bones in the NMC collection. Its dark colour is consistent with the darker colour of sediments at the base of the "Grès rouges," and suggests that the bone was derived from the base of the sequence. It could be older than the other specimens by tens of million of years (late Barremian through early Cenomanian time spans nearly 35 million years, HARLAND *et al.*, 1990).

The parapophysis in NMC 41629 is located at mid-height on the anterior edge of the lateral wall of the *centrum*. It is also located at this level in a cervical vertebra figured by STROMER (1934, pl. 1 fig. 2) from Egypt, as well as in NMC 41857, described above. Thus, all three vertebrae were from the base of the neck. They can nevertheless be arranged in a regular morphologic sequence from relatively plesiomorphous to relatively derived:

Sigilmassasaurus sp. (NMC 41629, Fig. 14c, f, g):
Centrum narrow, posterior width: length ratio 1.10;
Intercentral articulations indicate neck flexed slightly (Fig. 15);
Lateral wall of *centrum* planar above pleurocoel;
Pleurocoel large;
Parapophyseal articulation faces laterally;
Hypapophyseal peduncle small.

"*Spinosaurus* B" of STROMER (1934, pl. 1 fig. 2; here Fig. 14b, e, h, stippled):
Centrum intermediate, posterior width: length ratio 1.24;
Orientation of intercentral articulations uncertain;
Lateral wall of *centrum* swollen above pleurocoel;

Pleurocoel intermediate in size;
Parapophyseal articulation faces lateroventrally;
Hypapophyseal peduncle enlarged.

Sigilmassasaurus brevicollis (NMC 41857, Fig. 14a, d, i):
Centrum broad, posterior width: length ratio 1.46;

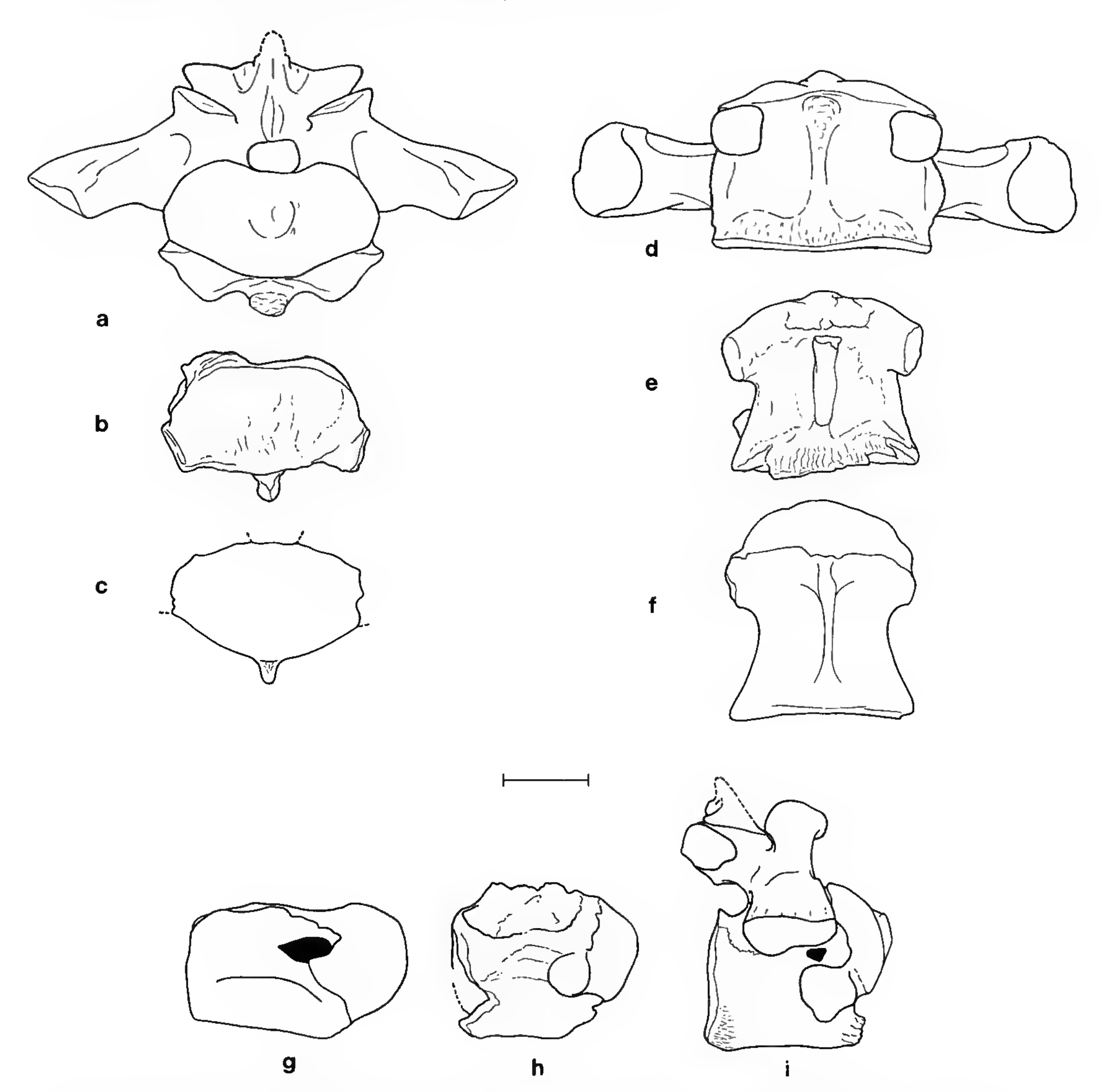


FIG. 14. — *Sigilmassasaurus* sp., posterior cervical vertebrae; NMC 41857 *S. brevicollis* (type) in (a) anterior, (d) ventral and (i) left lateral (reversed) aspect; "*Spinosaurus* B" (dotted, after STROMER 1934) in (b) anterior, (e) ventral and (h) right lateral aspect; NMC 41629 *S.* sp. in (c) anterior, (f) ventral and (g) left lateral (reversed) aspect. Scale bar: 5 cm.

Intercentral articulations indicate strongly flexed neck (Fig. 13);
Lateral wall of *centrum* greatly swollen above pleurocoel;
Pleurocoel small;
Parapophyseal articulation faces ventrolaterally;
Hypapophyseal peduncle greatly enlarged.

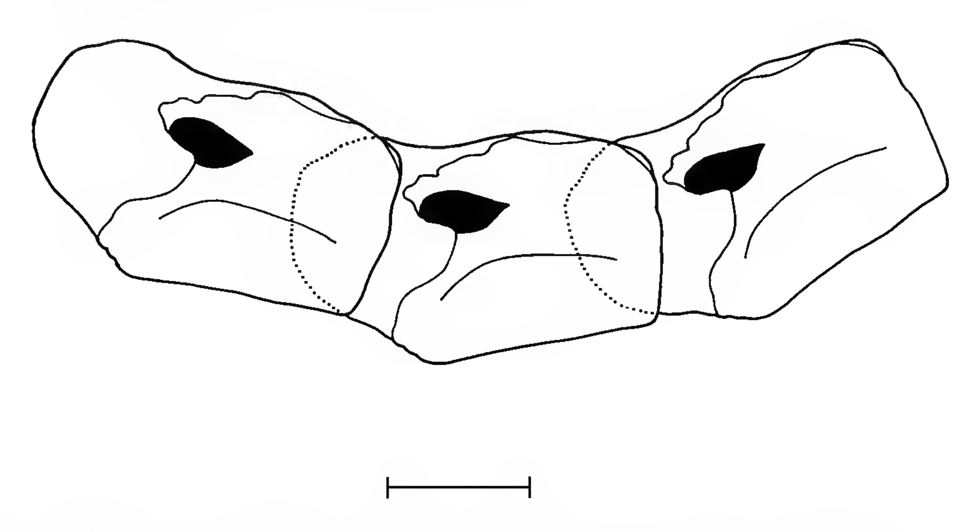


FIG. 15. — *Sigilmassasaurus* sp.; suggested curvature of cervical series, fitting three outlines of NMC 41629 in left lateral aspect. Scale bar: 5 cm.

The sequence, however, may not represent a single phylogenetic clade; see "Paleoenvironmental and Paleobiogeographical Comparisons" below.

Although the *centrum* of a distal caudal (NMC 41862) is of the same proportions as a similar element referred to *S. brevicollis* (NMC 41855), it is less constricted medially and much more robust in appearance. The diameter of the neural canal is much greater than in NMC 41855 (19 mm vs 11 mm). It may belong to a distinct, but closely related form, and, as in NMC 41629, is more darkly coloured.

Family CARCHARODONTOSAURIDAE Stromer, 1931

Carcharodontosaurus saharicus (Depéret & Savornin, 1927)

REFERRED SPECIMENS. — Maxilla fragment NMC 41859; isolated teeth NMC 41908, 41910, 41817, 41818, 41819; cervical vertebra NMC 50792 (Fig. 16).

DESCRIPTION AND DISCUSSION

DEPÉRET & SAVORNIN (1927) established *Megalosaurus saharicus* on two teeth collected from coarse clastics of late Barremian age near Timimoun in central Algeria, 460 km south-east of the Tafilalt (DE LAPPARENT 1960: 15; LEFRANC 1983). The species was in turn designated

as the type species of *Carcharodontosaurus* by STROMER (1931). The denticles of the posterior carina in teeth here referred to *C. saharicus* are consistently smaller than in most theropods, as has been reported in *Carcharodontosaurus* by FARLOW *et al.* (1991: 175 and equation on 174) and as in the complete crown in the type of *Megalosaurus saharicus* figured by DEPÉRET & SAVORNIN (1927, pl. 12 fig. 1, 1A). The denticles are approximately the same size in a well-preserved replacement tooth in the maxilla of the skeletal specimen described by STROMER. However, the apex of the crown in this tooth is symmetrical (STROMER 1931, pl. 1 fig. 2), not posteriorly recurved as it is in other teeth referred to this species (*cf.* DEPÉRET & SAVORNIN 1927, pl. 12 figs 1-2; STROMER 1931, pl. 1 fig. 1; teeth referred to the *C. saharicus* herein). Measurements of the teeth from the Tafilalt are given in Table 4A.

TABLE 4A. — *Carcharodontosaurus saharicus*, measurements of teeth.

	Basal W	Basal L	Crown H	Denticles/5 mm
NMC 41908	11	24	30	14
NMC 41910	6	19	23	14
NMC 41817	12	27	54	11
NMC 41818	22	36	67	10
NMC 41819	16	34	69	10

A fragment of a left maxilla (NMC 41859) bears impressions of four alveoli (two in anteroposterior sequence measure 39 and 35 mm in longitudinal diameter), separated by three *septa* measuring between 7 and 11 mm thick ventrally. These dimensions are similar to those near the centre of the left *maxilla* described by STROMER (1931: 7). The subrectangular outline of the *alveoli* differs greatly from circular *alveoli* in the *maxilla* from Morocco referred by BUFFETAUT (1989a) to *Spinosaurus*. The lateral surface of the fragment is slightly concave; the lateral surface of the nearly complete maxilla described by STROMER is flat.

A single cervical vertebra (NMC 50792, Fig. 16, Table 4B) is similar to "Halswirbel b" in the series of large vertebrae of the specimen referred to *Carcharodontosaurus* by STROMER (1931: 11-12, pl. 1 fig. 9). However, the parapophysis is located in a more elevated position than in the Egyptian element, near the middle of the lateral surface of the *centrum*. Furthermore, a large, conical excavation is also developed between the anterior zygapophysis and the neural canal, which was not described by STROMER in the Egyptian specimen. Both characters are typical of vertebrae occupying a more posterior position within the cervical series than the Egyptian vertebra (*cf.* MADSEN 1976). The absence of a powerfully developed ventral keel in the Moroccan vertebra may also be due to its position within the cervical column.

TABLE 4B. — *Carcharodontosaurus saharicus*, measurements of cervical vertebra (NMC 50792, for abbreviations, see table 3).

	L	Lc	Hc	Wa	Wp
NMC 50792	148	96	101	107	101

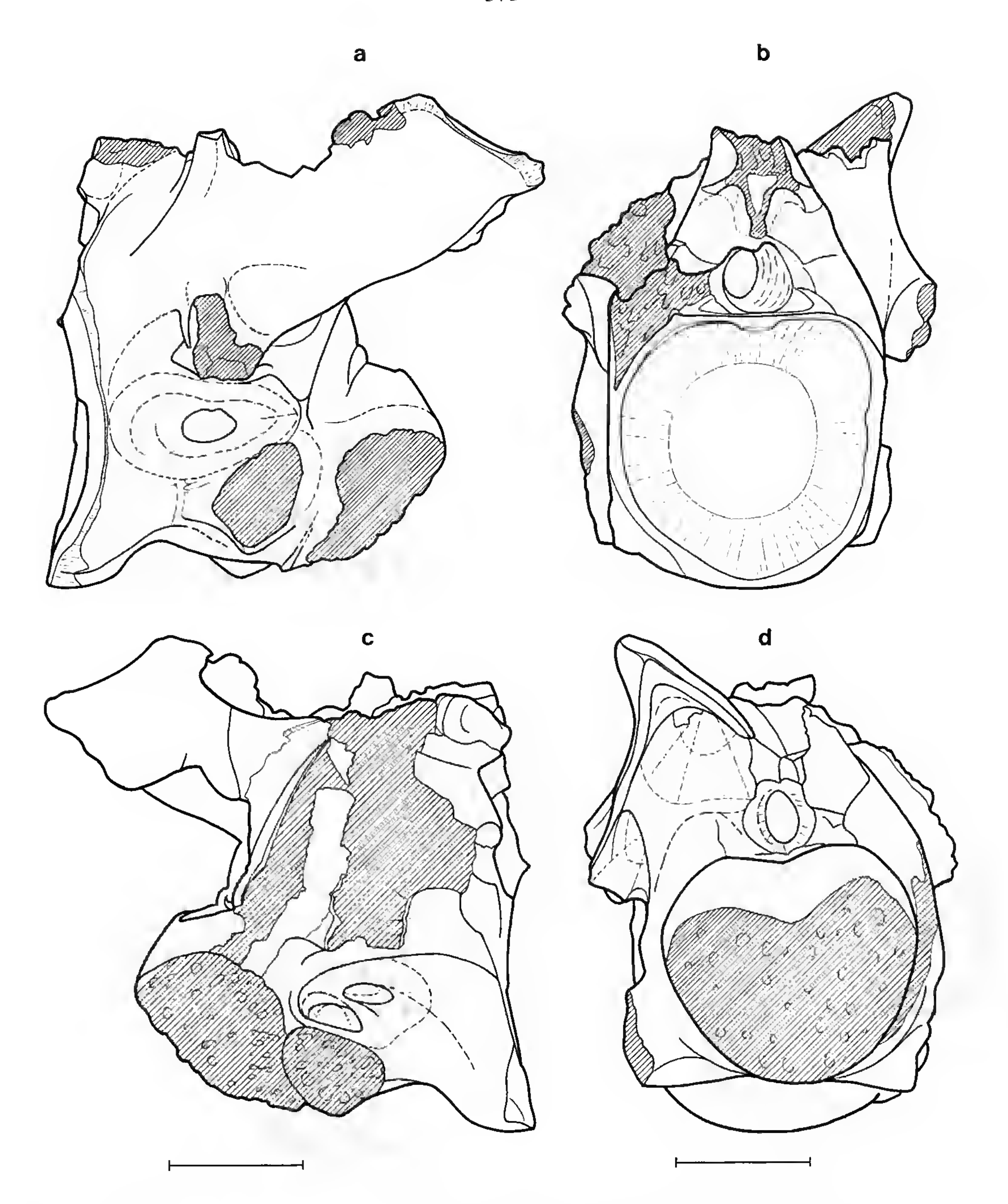


FIG. 16. — *Carcharodontosaurus saharicus*, NMC 50792, cervical vertebra in (a) right lateral, (b) posterior, (c) left lateral and (d) anterior aspect. Scale bar: 5 cm.

The vertebra differs strikingly from cervicals of *Spinosaurus* and *Sigilmassasaurus* in that the neural spine appears to have been entirely or nearly entirely replaced by a shallow groove extending along the mid-line of the element, above the neural canal. The zygapophyses are located dorsolateral to the groove, similar to their elevated position in cervical vertebrae of *Carnotaurus* (in which, however, a small neural spine is present, *cf.* BONAPARTE *et al.* 1990). The dorsal mid-line of the Egyptian vertebra (STROMER 1931: 11) is not preserved, so that its morphology could not be described. The angle (15°) between the planes of the anterior and posterior inter-central articulations of the Moroccan vertebra indicates that the neck was strongly arched dorsally adjacent to it. Anteriorly, the neural canal measures 34 mm in height and 25 mm in width; posteriorly the measurements are 24 and 29 mm, respectively. For other measurements, see Table 4B. The vertebra is strongly opisthocoelous.

Family ABELISAURIDAE Bonaparte & Novas, 1985
cf. ***Majungasaurus*** sp.

REFERRED SPECIMEN. — Fragment, median portion of ramus of right dentary NMC 41861 (Fig. 17d).

DESCRIPTION AND DISCUSSION

The element is badly abraded. As preserved, it measures 35 mm in depth and 134 mm in length, and was originally probably slightly smaller than the dentary referred to *Majungasaurus crenatissimus* by LAVOCAT (1955b). It contains portions of nine empty alveoli, the close spacing of which suggests that there may have been as many dentary teeth (17) as in the dentary from Madagascar. Unlike in *Majungasaurus*, the alveoli increase in length posteriorly (from 6 to 14 mm) but remain similar (rectangular) in dorsal outline. The eroded lateral surface of the bone appears to have been massively constructed. It is peculiar in that it is marked by indistinct vertical ridges which parallel, but do not coincide with the anterior and posterior limits of the alveoli. No Meckelian groove is present on the medial surface of the bone; perhaps the fragment was separated from a now-missing ventral half before it was buried.

ABELISAURIDAE, gen. et sp. indet.

REFERRED SPECIMEN. — Fragment, median portion of ramus of right dentary NMC 41859 (Fig. 17a-c).

DESCRIPTION AND DISCUSSION

The fragment is approximately 20 cm long and contains empty alveoli for four teeth. It measures 93 mm in depth below the anteriormost, and 98 mm below the posteriormost alveolus. In dorsal view, the alveolar margin curves anteromedially, as in a Lameta "allosaurid" dentary (VON HUENE & MATLEY 1933, pl. 12 fig. 1), *Majungasaurus* (LAVOCAT 1955a) and *Carnotaurus* (BONAPARTE *et al.* 1990). The central two alveoli are essentially complete, measuring 26 mm in length, 10 mm in width and at least 32 mm in depth. They are slightly constricted medially. An interdental lamination appears to have been present rather than separate interdental plates

(as is apparently also the case in the dentary of *Majungasaurus* Lavocat, 1955a). Unlike in the forms cited above, the external surface of the dentary does not appear to be divided into a wider, convex lower half and a narrower, flat upper half. There is no evidence preserved of a posterior emargination in the dentary. Sutures are present posteroventrally on the medial surface for contact with a splenial.

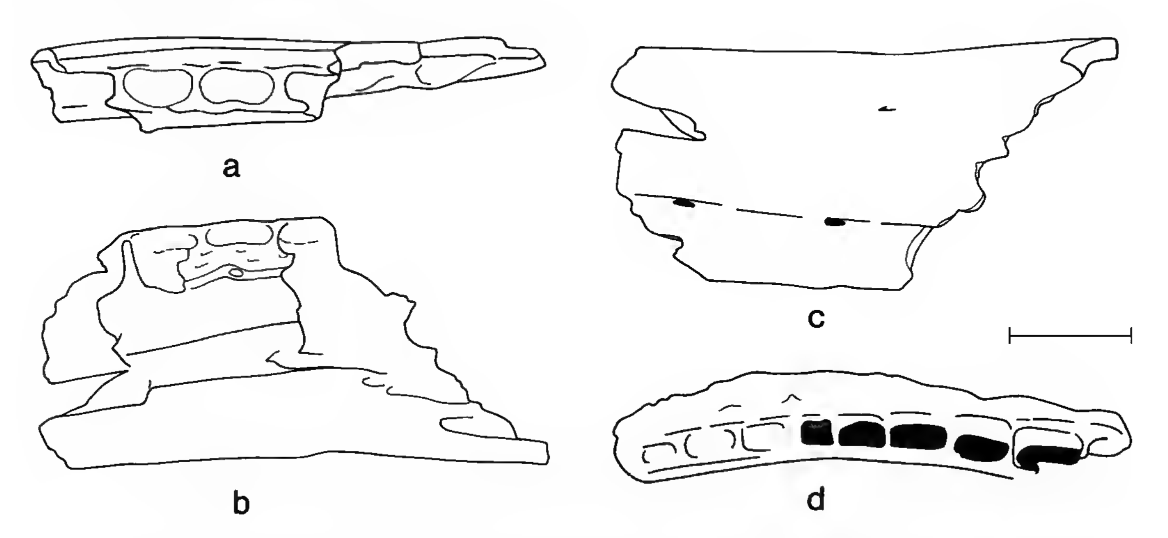


Fig. 17. — Abelisauridae, gen. et sp. indet., NMC 41859, fragment of right dentary in (a) dorsal, (b) medial and (c) lateral (inverted) aspect; (d) cf. *Majungasaurus* sp., NMC 41861, fragment of right dentary in dorsal aspect. Scale bar: 5 cm.

The elongated alveoli preclude the specimen's referral to *Spinosaurus*, and their relatively small size is incompatible with tooth dimensions in *Carcharodontosaurus*. The dentary is also much smaller than in these two taxa.

THEROPODA indet.

The following bones are sufficiently characteristic to suggest that they will be recognized in materials obtained in the future. Some anatomically similar elements differ morphologically to the extent that they appear to belong to separate species. All are separated into informal bone "taxa" designated by letters so they can be easily cited. How they could be grouped together into skeletons of distinct species is purely speculative at present. Theropod humeri were separated from those of crocodiles through the presence of thick cortical bone at mid-shaft, presumably an adaptation to withstand stresses generated by a massive body upon a relatively small forelimb. In NMC 41865 and 41873 cortical bone is very thick in this region (see also in *Allosaurus* Gilmore 1920, pl. 6, fig. 7; an unusually large proportion of tyrannosaur humeri sustained injury in life; Russell 1970a: 18).

BONE "TAXON" A (CRANIAL ROOF)

Two interorbital fragments (NMC 50807 and 50808 (Fig. 18) apparently represent the same small to medium sized form. They do not resemble the skull roof in any known southern hemisphere theropod (*cf.* VON HUENE & MATLEY 1933; BONAPARTE & NOVAS 1985; BONAPARTE *et al.* 1990). The co-ossified frontals are powerfully constructed, as are sutural contacts for adjacent ossifications. A transverse flexure occurs anterior to the centre of the orbits, so that the anterior portion of the frontals descends at an angle of 25° to the posterior half of the bone. Longitudinal striations marking the posterior limits of the nasal alae extend back to the point of flexure; they become stronger anterolaterally in the area of contact with the prefrontal and lacrimal. In NMC 50808, the frontals extend 50 mm along the cranial mid-line from the flexure to their posterior limit. This measurement is 65 mm in NMC 50807. The parietals, which are preserved in the latter specimen, form a saggital crest rather than a flattened surface along the cranial mid-line.

On the ventral surface of the skull roof, the horizontal diameter of the orbit is approximately 50 mm in NMC 50808, and a perpendicular drawn through its centre meets the cranial mid-line at an angle of 55°. Anteriorly, the shallow cavity containing the olfactory bulbs is 18 mm wide; well-marked twin cavities for the cerebral hemispheres total 27 mm in width near the posterior limit of the frontals.

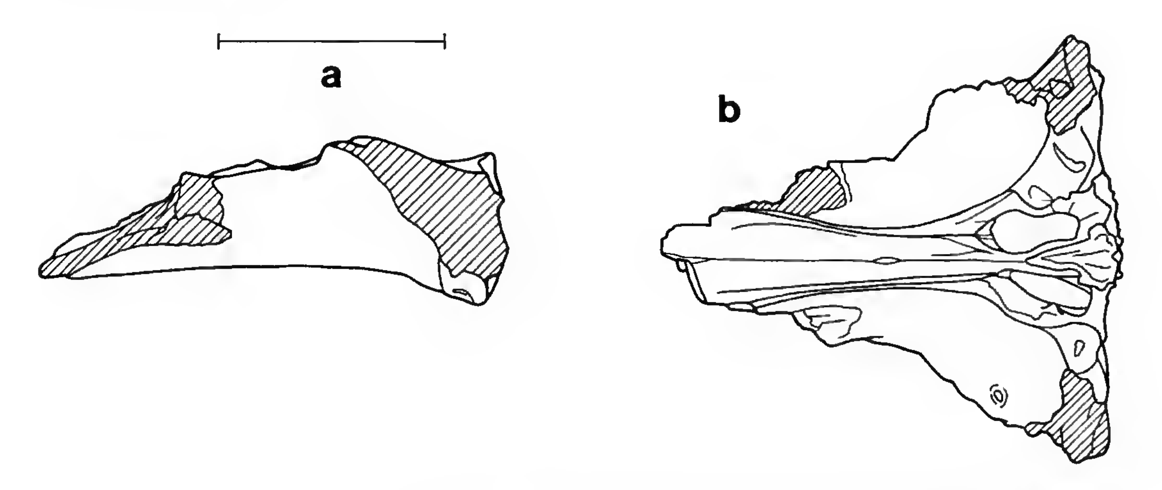


FIG. 18. — Theropoda, indet. (bone "taxon" A), NMC 50808, co-ossified frontals in (a) left lateral and (b) ventral aspect. Scale bar: 5 cm.

BONE "TAXON" B (CERVICAL VERTEBRAE)

An axis vertebra (NMC 50810, Fig. 19) with closed *centrum*-neural arch sutures documents the presence of a small theropod within the assemblage. It differs from a cervical described by DE LAPPARENT (1960: 31, pl. 11, fig. 5) from In Tedreft, Niger, in that the *centrum* is rounded rather than square in ventral cross-section, the pleurocoel is located posterior to rather than above the capitular facet, and in that the two small excavations situated above the posterior exit of neural canal in the specimen from Niger are not present. The slender *centrum* (45 mm long and

18 mm wide posteriorly) is suggestive of an elongated neck. A *centrum* from the mid-cervical region (NMC 50810) is similar in size but more robustly constructed (34 mm long and 27 mm wide posteriorly). A small pleurocoel is located above and behind the capitular facet; another small opening is present at the same level, centred within the posterior half of the left side.



FIG. 19. — Theropoda, indet. (bone "taxon" B), NMC 50810, axis vertebra in right lateral aspect. Scale bar: 5 cm.

BONE "TAXON" C (POSTERIOR DORSAL VERTEBRA)

NMC 50403 (Fig. 20, Table 4C) is a relatively large vertebra. The posterior central facet is marked by shallow, radiating suture-like grooves, suggesting proximity to the sacrum. Longitudinally striated tuberosities occur between the posterior (but not anterior) zygapophyses, indicating the existence of tendinous links to the vertebra behind. The bone thus probably represents the last dorsal vertebra. It differs markedly from vertebrae in the anterior dorsal region of *Spinosaurus* and *Sigilmassasaurus* in its amphiplatyan nature and in the exceedingly weak, anteriorly inclined base of the neural spine. Nor is an assignment to *Carcharodontosaurus* likely because

TABLE 4C. — *Theropoda* indet., measurements (in mm) of posterior dorsal vertebra (NMC 50403).

Length of centrum	158
Width of anterior zygapophyses	35
Width of centrum anteriorly	37
Width of centrum posteriorly	122
Height of centrum posteriorly	120
Height of centrum anteriorly	141
Width of neural canal (between neural arch pedicils)	33
Width of neural canal (within centrum)	9
Depth of neural canal (between neural arch pedicils)	42
Depth of neural canal (within centrum)	13

it lacks pleurocoels, which are present posteriorly into the caudal series of the latter genus (STROMER 1931, pl. 1, fig. 10).

Other attributes of the vertebra include an anterior zygapophyseal facet that faces nearly directly upwards, and a relatively large neural canal. The dorsal margin of the canal is separated into two halves by a low, longitudinal ridge; ventrally the canal is incised deeply into the dorsal part of the *centrum*. The bases of the transverse processes indicate that the structures were only slightly elevated distally. Another central fragment (NMC 50404) closely resembles the anterior half of the *centrum* in NMC 50403.

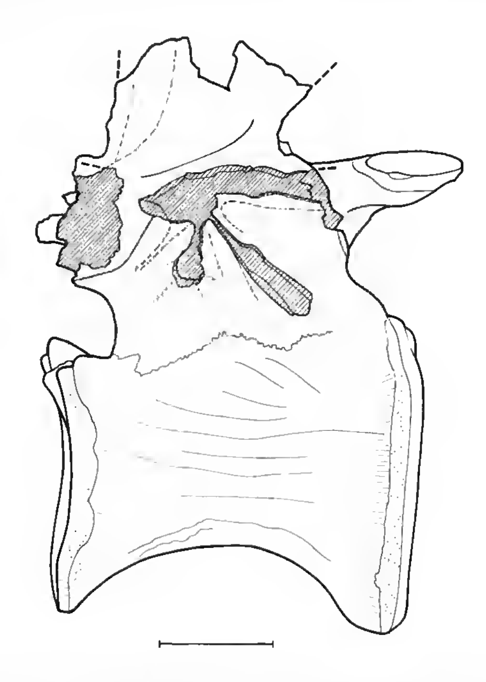


FIG. 20. — Theropoda, indet. (bone "taxon" C), NMC 50403, posterior dorsal vertebra in right lateral aspect. Scale bar: 5 cm.

BONE "TAXON" D (CAUDAL VERTEBRAE)

A vertebra (NMC 41863, Fig. 21) from the anterior portion of the distal half of the tail differs from those assigned above to *Sigilmassasaurus* in its more cylindrical form and in the presence of strongly developed bases for the anterior zygapophyses. A bony ridge along the dorsolateral surface of the *centrum* implies that the element was originally located immediately behind vertebrae bearing transverse processes. The anterior border of the much-abraded neural spine is vertical, suggesting that the spine might also have been nearly vertical. In median caudals referred by STROMER (1934: 34, pl. 2, fig. 11) to *Bahariasaurus* the spine is posterodorsally inclined. The *centrum* is less elongated than in median caudals referred by DE LAPPARENT (1960) to *Elaphrosaurus*. Its length is 86 mm, and the posterior central articulation is 51 mm wide and 50 mm high.

Another caudal (NMC 50797) is smaller and lacks any trace of transverse processes. The shape of the *centrum* and vertical anterior base of the neural spine suggests that it was derived from the same taxon as the previous vertebra. However, although the *centrum* is smaller (with a length of 65 mm, and a posterior central articulation measuring 34 mm wide and 30 mm high), the bases of the anterior zygapophyses are much more robustly developed. This could be a consequence of a more distal position in the caudal series.

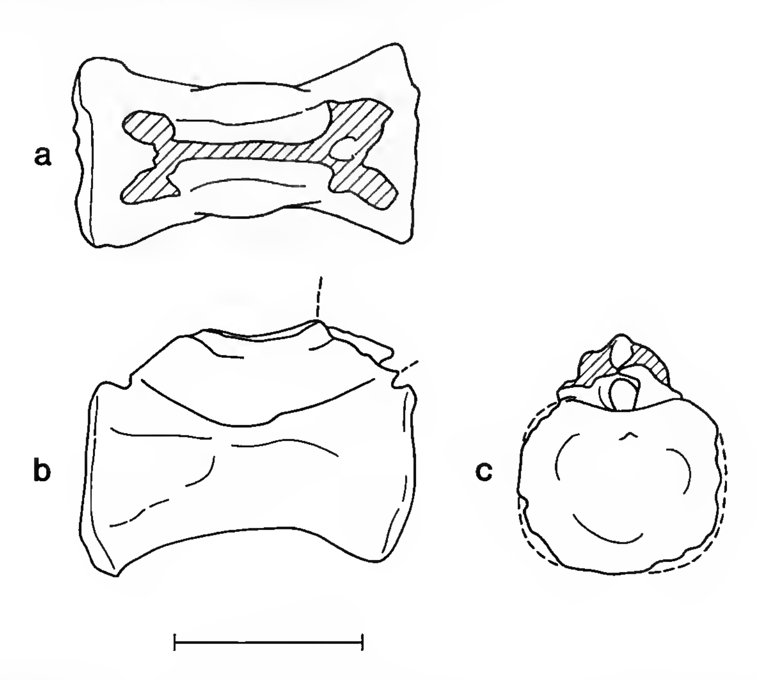


FIG. 21. — Theropoda, indet. (bone "taxon" D), NMC 41863, distal caudal vertebra in (a) dorsal, (b) right lateral and (c) anterior aspect. Scale bar: 5 cm.

BONE "TAXON" E (CORACOID)

NMC 41806 is a fragment of a coracoid, apparently derived from the left side, which contains the coracoid foramen. There is no sutural surface preserved for contact with the scapula. The greatest proximal width of the element is 44 mm; it was probably about as large as the coracoid of *Albertosaurus libratus* (NMC 2196). The coracoid foramen is, however, much larger (30 mm vs 17 mm in the vertical diameter of external opening), and is also larger than in the coracoid questionably referred by STROMER (1934: 33, pl. 3, fig. 14) to *Carcharodontosaurus*. There is no channel from the foramen toward the medial surface of the scapula, as there is in *Allosaurus* (MADSEN 1976, pl. 41).

BONE "TAXON" F (HUMERUS)

The distal end of left humerus (NMC 41865, Fig. 22a) measures 156 mm in width. At mid-shaft, the horizontal and vertical diameters are 69 and 55 mm, respectively, and the cortical

wall is approximately 19 mm thick. Because the distal end of NMC 41865 resembles that of the humerus in *Baryonyx* (CHARIG & MILNER 1990, fig. 9.5) in a manner analogous to similarities between cervical vertebrae of *Spinosaurus maroccanus* and *Baryonyx* (compare NMC 41768, and NORMAN & MILNER 1989: figure on p. 55), it might pertain to *Spinosaurus*.

BONE "TAXON" G (HUMERUS)

A large left humerus (NMC 41852, Fig. 22b-c) can be distinguished from NMC 41865 on the basis of a much more robust mid-shaft region, and the absence of a large, moderately deep concavity situated proximal to the radial condyle. Its shaft is very straight, and the long axis

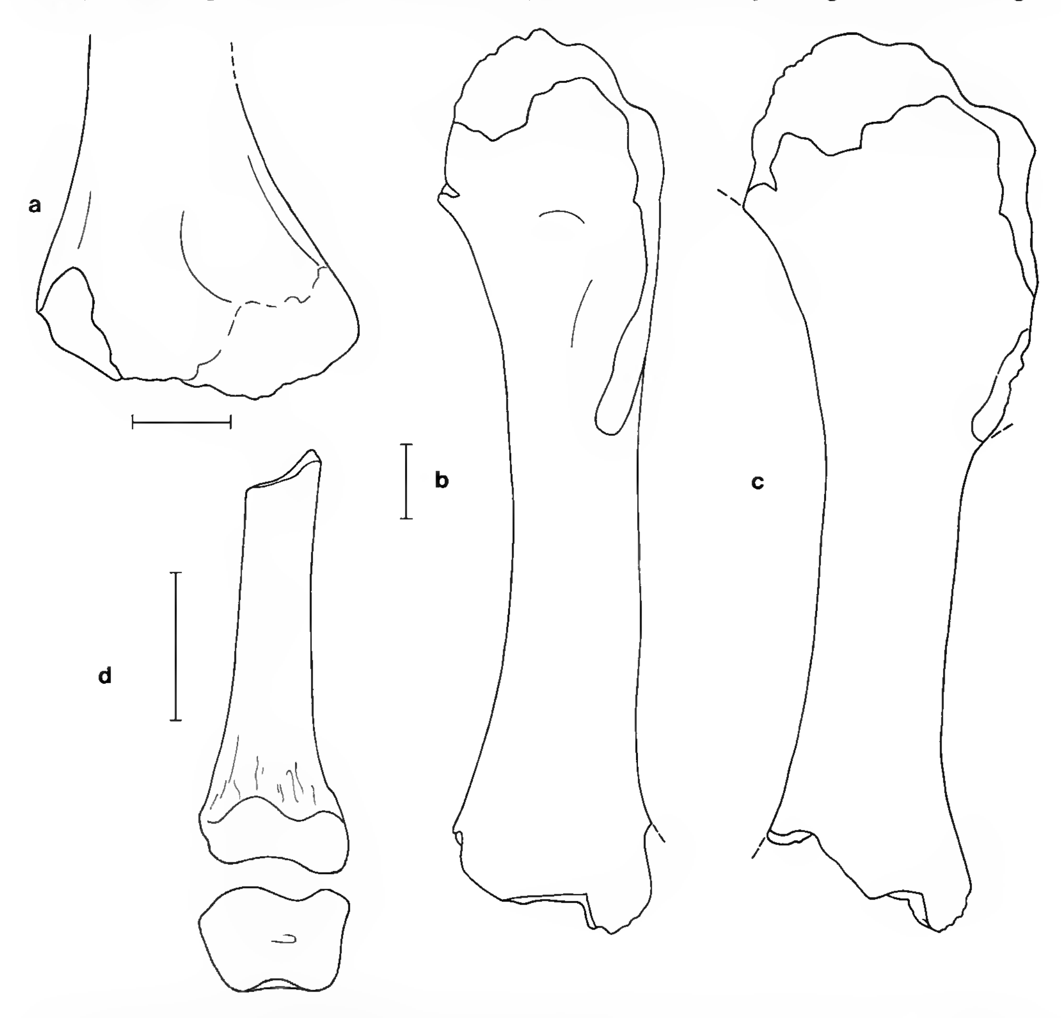


FIG. 22. — Theropoda, indet.; (a) NMC 41865 (bone "taxon" F), distal end of left humerus in flexor aspect; NMC 41852 (bone "taxon" G), left humerus in (b) ventral aspect and (c) with the distal end in flexor aspect; (d) NMC 41873 (bone "taxon" H), distal end of C right humerus in flexor aspect. Scale bar: 5 cm.

of the articulation for the antebrachium is rotated clockwise (when viewed distally) about 45° with respect to the long axis of the proximal articular surface. The latissimus scar on the proximodorsal surface is weak. The element measures but 150 mm in distal width, with robust horizontal and vertical mid-shaft diameters of 89 and 78 mm, respectively (the mid-shaft circumference is 271 mm).

The humerus is unusually long for that of a theropod, measuring 60 cm as preserved, and probably about 65 cm long when entire. It is thus longer than recorded in *Daspletosaurus* (35.7 cm; RUSSELL 1970a), *Tyrannosaurus* (36 cm; OSBORN 1906), *Allosaurus* (38.6 cm, MADSEN 1976), *Torvosaurus* (42.4 cm; GALTON & JENSEN 1979), *Baryonyx* (46.3 cm; CHARIG & MILNER 1990), *Gallimimus* (53 cm; OSMOLSKA *et al.* 1972), *Segnosaurus* (56 cm; PERLE 1979) and *Chilantaisaurus* (58 cm; HU 1964). The humerus is known to be longer only in *Therizinosaurus* (76 cm), where the shaft is more sigmoid, and the ends more expanded (BARSBOLD 1976), and in *Deinocheirus* (93.8 cm), in which it is much more slender (OSMOLSKA & RONIEWICZ 1970).

BONE "TAXON" H (HUMERUS)

NMC 41873 (Fig. 22d) is the distal end of a right humerus. The bone is about the size and general proportions of the humerus of *Deinonychus* (OSTROM 1969, figs 55-56). It is unusual in that the radial condyle is very large and smooth, suggesting a well-developed capacity for pronation and supination. The element measures 48 mm in distal width, with horizontal and vertical mid-shaft diameters of 23 and 21 mm, respectively; at mid-shaft, its circumference is 72 mm, and the cortical wall is approximately 8 mm thick.

The humerus, as well as the tibia from the Kem Kem escarpment which was compared to that of *Elaphrosaurus* by LAVOCAT (1954b), were both derived from a theropod approximately equal in size to the type of *Elaphrosaurus bambergi* (JANENSCH 1925). No special affinity to the Late Jurassic *Elaphrosaurus* is thereby implied.

BONE "TAXON" I (MANAL PHALANGES)

Three large manal phalanges were probably all derived from the same species, and are reminiscent of, but slightly smaller than a large phalanx from Afrar near the Libyan frontier of Algeria described by DE LAPPARENT (1960, "métatarsien": 29, pl. 9, fig. 1). NMC 50794 (Fig. 23) is probably from the first digit, and measures 250 mm in interarticular length, 45 and 50 mm, respectively, in the height and width of the distal articular surface, and 65 mm in the height of the proximal articular surface. A fragment of a distal articulation (NMC 41800) is essentially

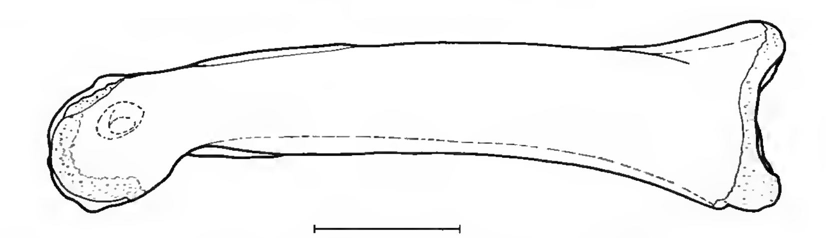


FIG. 23. — Theropoda, indet. (bone "taxon" I), NMC 50794, manal phalanx in lateral (?) aspect. Scale bar: 5 cm.

indistinguishable from that of NMC 50794. NMC 50805 is probably from the second digit, and measures 111 mm in interarticular length, 29 and 42 mm, respectively, in the height and width of the distal articular surface, and 43 mm in the height of the proximal articular surface.

BONE "TAXON" J (MANAL UNGUALS)

NMC 41820 (Fig. 24a) generally resembles a manal ungual from the Tinrhert, Algeria, described and figured by DE LAPPARENT (1960: 29, pl. 6, fig. 11). An extensor tuberosity above the articular facet is reminiscent of, but broader than in oviraptorosaurs; the flexor tuberosity is less prominent (*cf.* CURRIE & RUSSELL 1988, fig. 4). It measures (as preserved) 91 mm along the dorsal curve, 81 mm from the articular facet to apex of the claw, and its articular facet is 28 mm high and 21 mm wide. A cast (NMC 41977, fig. 24b) of a larger, but otherwise similar claw in the personal collections of Brian EBERHARDE measures 232, 189, 64 and 37 mm in the same dimensions. This claw is of a suitable size to be supported by the large manal phalanges described above (bone "taxon" I). When articulated with NMC 50794, a digit length of 435 mm is suggested. This is approximately 90% of the length of the first digit in the giant hand of *Deinocheirus*, from the Upper Cretaceous of Mongolia (OSMOLSKA & RONIEWICZ 1970, fig. 2). The linear differences between the Moroccan unguals suggest a weight difference in excess of an order of magnitude between the two animals which produced them.

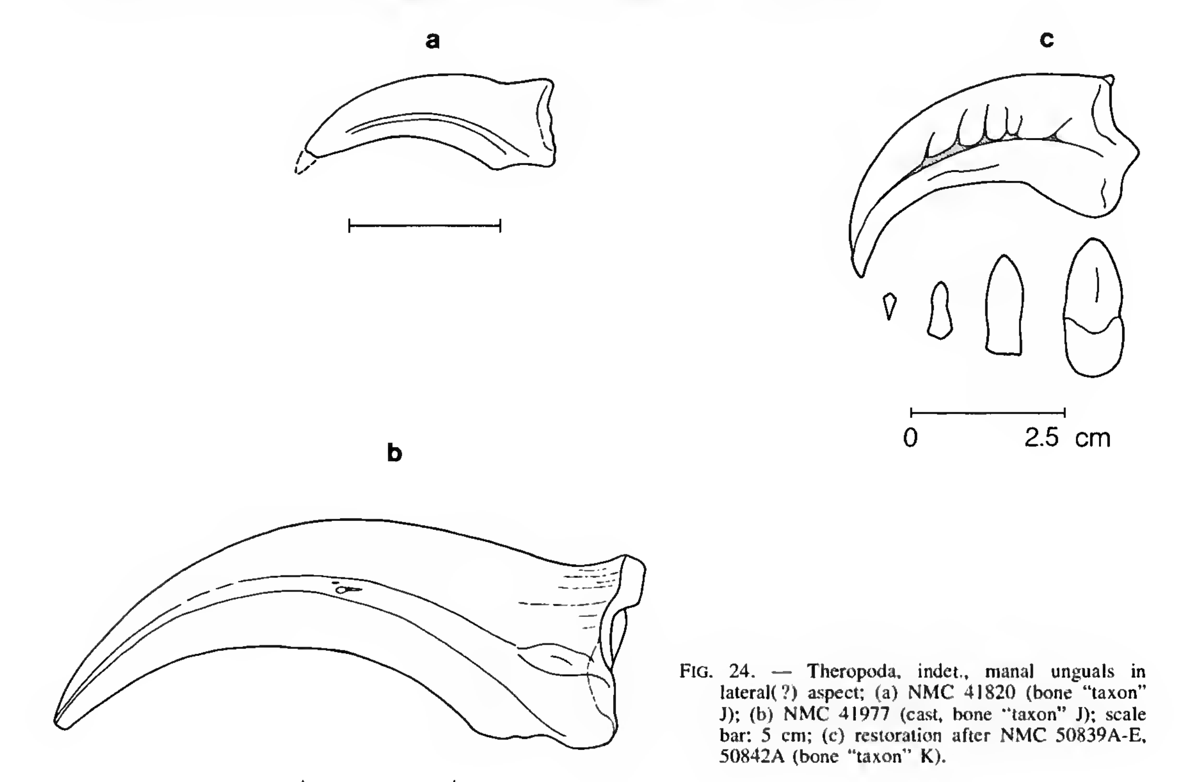


FIG. 24. — Theropoda, indet., manal unguals in lateral(?) aspect; (a) NMC 41820 (bone "taxon" J); (b) NMC 41977 (cast, bone "taxon" J); scale bar: 5 cm; (c) restoration after NMC 50839A-E, 50842A (bone "taxon" K).

BONE "TAXON" K (MANAL UNGUALS)

NMC 50839a-e, 50842a (the form of the unguals is restored in Fig. 24c to the scale of the largest fragment) are characterized by a proximally squared but distally trenchant ventral edge of the claw, and by a rounded dorsal margin which is invaded by what appear to be vascular channels spreading from the curved longitudinal grooves present on both surfaces of the claw. A relatively prominent flexor tuberosity is present.

The relative extent of lateral surface exposed below the longitudinal grooves varies between specimens; whether this is due to interdigital or taxonomic effects is unknown. The unguals are small and incomplete, but are estimated to have measured 20 to 50 mm in straight line from the proximal articulation to the distal point.

BONE "TAXON" L (MANUS UNGUAL)

NMC 50842B lacks the proximal articulation. It resembles the second manus ungual in *Deinonychus* (OSTROM 1969, fig. 63), but is less recurved. The fragment measures 30 mm from the broken proximal surface to the distal point.

BONE "TAXON" M (FEMORA)

The proximal end of a right femur (NMC 41869, Fig. 25a-c) differs from the large but slender femur referred by STROMER (1934: 36, pl. 3, fig. 5) to *Bahariasaurus* in the exceptionally heavy development of both the fourth trochanter and the scar for the insertion of pubischiofemoralis musculature. A similarly powerfully constructed lesser trochanter lies well below the head of the femur, unlike in the latter femur and that of *Carcharodontosaurus* (STROMER 1931, pl. 1, fig. 14).

Although both fragments appear to be from femora of similar size, NMC 41869 cannot directly be compared to the distal fragment that STROMER (1934: 39) compared to the femur of *Erectopus sauvagei*. Near the base of the fourth trochanter, the circumference of the femur is approximately 310 mm, suggesting that the weight of the animal from which it was derived probably did not exceed one metric tonne (*cf.* ANDERSON *et al.* 1985).

A small, but nearly complete right femur (NMC 50382, Fig. 25d) closely resembles NMC 41869 in the morphology of its proximal end and is generally congruent with that of the distal femoral fragment referred to *Erectopus* by STROMER (1934, pl. 3, figs 9a-b).

If these bones belong to the same taxon, the larger femur was probably very short and massive, implying a hind limb which was similarly short and massive. The element thus appears to be built for power rather than speed (*cf.* robust femora from the Lameta Group of India; VON HUENE & MATLEY 1933: 54), and it is tempting to speculate that the hind limb was very short relative to the size of the animal's body.

The external surface of the smaller bone is rather smooth and slightly porous, which, together with the poorly ossified distal end, suggests immaturity. The bone is 118 mm long, and is about 13% of the linear dimensions of the Egyptian specimen. A mid-shaft circumference of approximately 40 mm suggests a body weight (3.78 kg) which is smaller than that indicated for NMC 41869 by a factor of about 270.

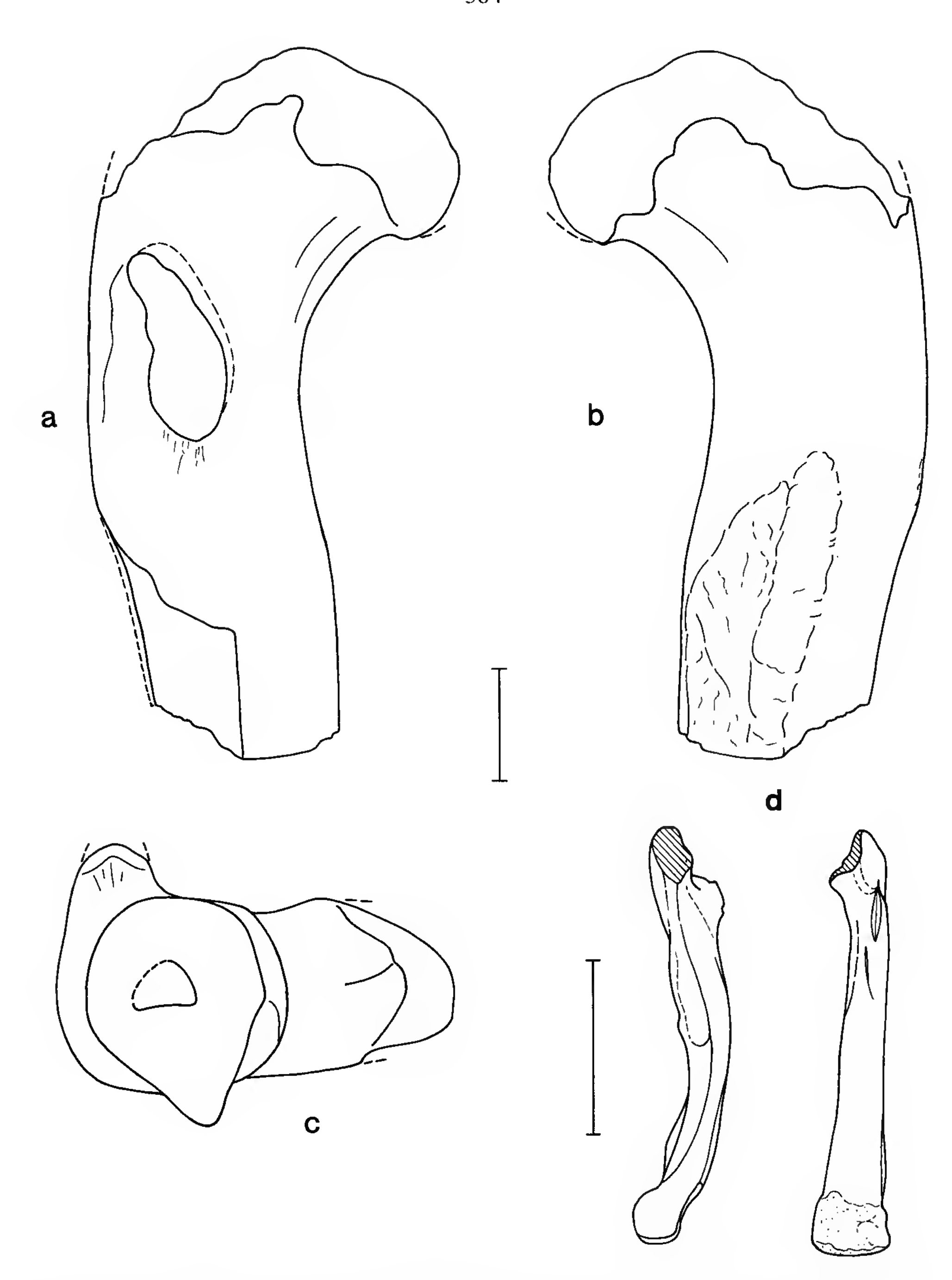


FIG. 25. — Theropoda, indet. (bone "taxon" M); NMC 41869, right femur in (a) anterior, (b) posterior and (c) distal aspect; NMC 50382, right femur in medial (left) and anterior (right) aspect. Scale bar: 5 cm.

BONE "TAXON" N (METATARSAL IV)

A right metatarsal IV (NMC 41770, Fig. 26) is approximately the same length (430 mm) as an element so identified by STROMER (1934: 56), but its shaft curves markedly distolaterally. It resembles the metatarsal IV in *Allosaurus* (MADSEN 1976, pls 54-55), although the Moroccan bone is more robust. Areas of insertion for flexor musculature are particularly prominent, and the bone is compressed in the mid-shaft region (anteroposterior diameter 67 mm, transverse diameter 82 mm). In its robustness, the metatarsal resembles the femur described above. However, according to the ratios of the mid-shaft diameters of the femur and metatarsal IV in *Allosaurus* (*cf.* GILMORE 1920: 69, 75), the femur would have been derived from an animal linearly about half the size of the animal from which the metatarsal was derived.

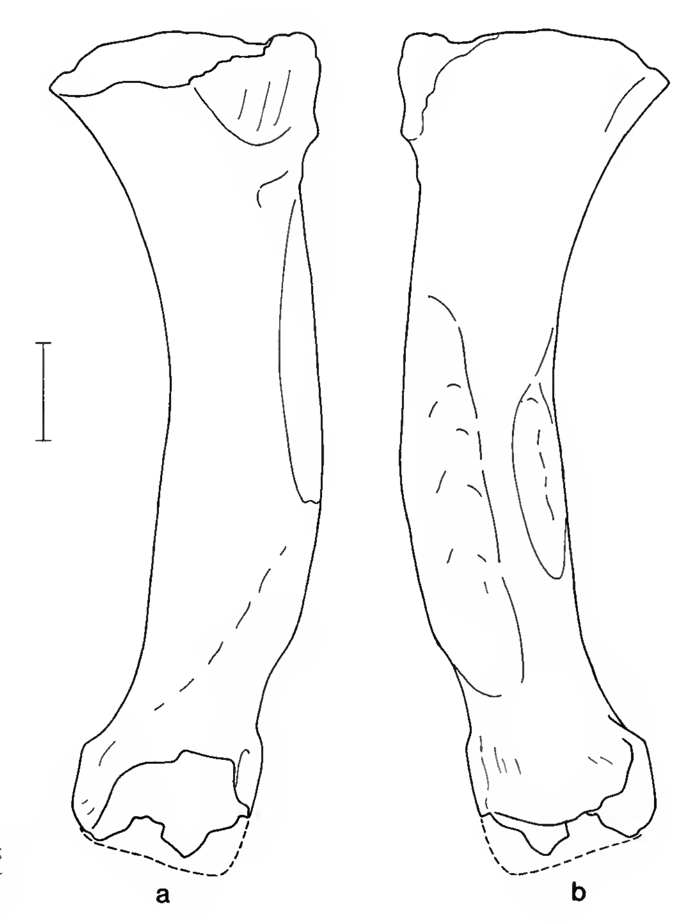


FIG. 26. — Theropoda, indet. (bone "taxon" N); NMC 41770, right metatarsal IV in (a) extensor and (b) flexor aspect. Scale bar: 5 cm.

BONE "TAXON" O (METATARSAL V)

A left metatarsal V (NMC 50830, Fig. 27) measuring 187 mm in length is much more massively constructed and more recurved than in *Allosaurus* (*cf.* MADSEN 1976, pl. 53). It is interesting that vertebrae of *Sigilmassasaurus* appear to be relatively common and morphologically very peculiar, and the robust limb elements (bone "taxa" M-O) are also relatively common and morphologically peculiar. It is conceivable, but not demonstrable, that all of these could be derived from the same taxon.

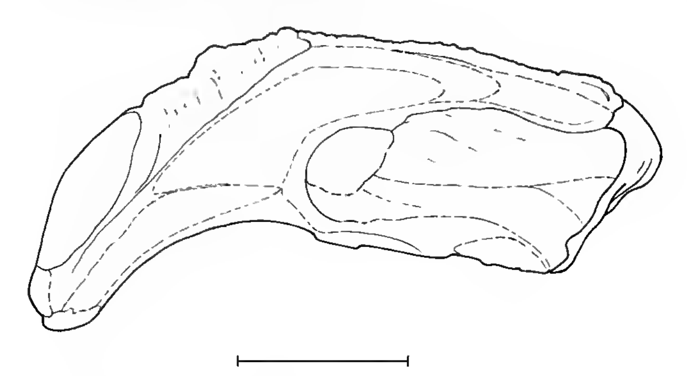


FIG. 27. — Theropoda, indet. (bone "taxon" O); NMC 50830, left metatarsal V in medial aspect. Scale bar: 5 cm.

BONE "TAXON" P (PEDAL UNGUAL)

A cast of a pedal ungual fragment (NMC 50987, Fig. 28a), presented through the courtesy of Mr Kirk LEAVESLEY of New Prague, Minnesota, generally resembles a pedal ungual from In Abangarit, Niger, described and figured by DE LAPPARENT (1960: 29, pl. 6, fig. 10). The fragment is characterized by a flat flexor surface which is inclined at an angle of about 20° to its transverse axis. It was derived from a claw about the same size as the specimen from Niger. A second, somewhat smaller ungual (NMC 50826, Fig. 28b) is morphologically indistinguishable from the preceding specimens.

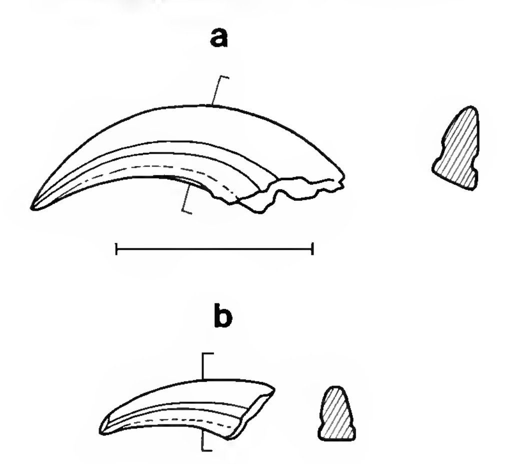


FIG. 28. — Theropoda, indet. (bone "taxon" P), pedal unguals in lateral (?) aspect; (a) NMC 50987 (cast) and (b) NMC 50826. Scale bar: 5 cm.

Order SAUROPODA Marsh, 1878
Family DIPLODOCIDAE Marsh, 1884
Subfamily DICRAEOSAURINAE Janensch, 1929

Rebbachisaurus garasbae Lavocat, 1954

REFERRED SPECIMENS. — Isolated teeth NMC 41808, 41810, 41812; questionably referred teeth: NMC 41809, 41811; cervical spine NMC 41872 (Fig. 29); anterior dorsal vertebra NMC 50844 (Fig. 30).

DESCRIPTION AND DISCUSSION

Rebbachisaurus garasbae is provisionally referred to the Diplodocidae, although new South American materials warrant a review of its affinities (BONAPARTE, pers. comm. 1994). General diplodocoid relationships are suggested by the reduced suprazygapophyseal laminae and presence of a vertical ridge on the lateral surface of the dorsal spine in the type specimen (pers. obs.; see RUSSELL & ZHENG 1993: 2094, character 16, state 2).

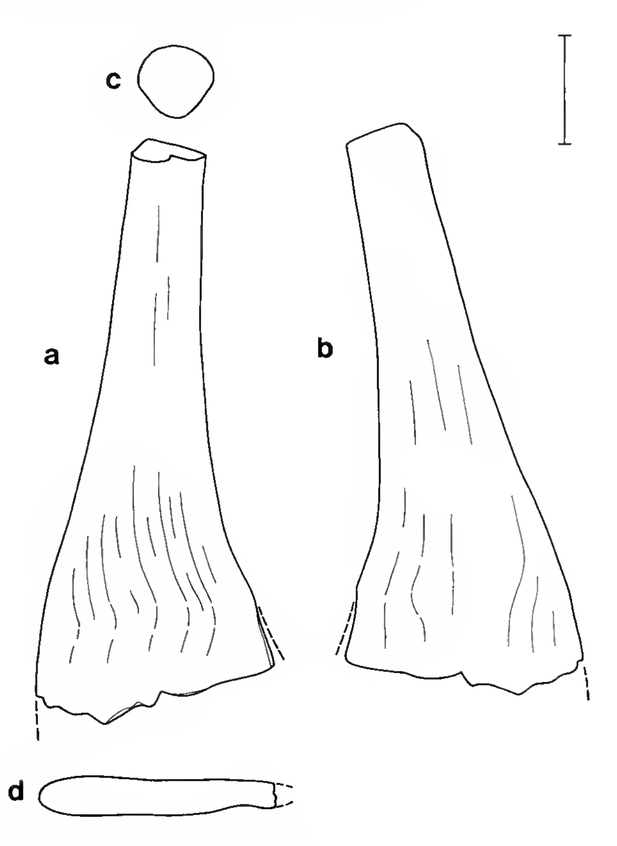


FIG. 29. — *Rebbachisaurus garasbae*, NMC 41872, cervical spine in (a) lateral (?), (b) medial (?), (c) distal and (d) proximal aspect. Scale bar: 5 cm.

Three pencil-shaped teeth are accordingly referred to *R. garasbae*. Two of them (NMC 41810, 41812) are slightly curved, relatively large and resemble each other in colour and preservation. Both are approximately 9 by 13 mm wide at the base of the enamel crown, and 35 mm high from the enamel base to the apex of a chisel-shaped, lingually inclined wear facet. The enamel surface is slightly crinkled ventrally and becomes smooth toward the apex; there are no indications of carinae or vertical striations. Another tooth (NMC 41808) is similar but badly abraded. Similar teeth also occur in the Albian of Tunisia (BOUAZIZ *et al.* 1988).

A peculiar bone fragment (NMC 41872, Fig. 29) is flattened at one end (where it measures 107 mm in width and 17 mm in thickness) and tapers to the opposite end 270 mm distant (where it is nearly circular in cross-section and measures 34 mm in diameter). The fragment closely resembles the longitudinally expanded base of a single ramus of a deeply divided cervical spine in *Amargasaurus cazaui* (SALGADO & BONAPARTE 1991; cast of the type specimen in CMN collections). In view of resemblances between dorsal vertebrae of *Amargasaurus*, *Dicraeosaurus* and *Rebbachisaurus* (see below) the element is tentatively referred to *R. garasbae*.

The contour of the pleurocoels and absence of zygosphene-zygantrum articulations, as well as the dimensions of the *centrum* clearly suggest affinities between an isolated dorsal vertebra (NMC 50844, Fig. 30, Table 5A) and a posterior dorsal in the type of *Rebbachisaurus garasbae* (LAVOCAT 1954B; Table 5B, pers. obs.). The greater length of the *centrum* relative to the height and width of the intercentral articulations and less steeply projecting transverse processes imply that the vertebra occupied a more anterior position in the column. Only the basal portion of a delicately constructed neural spine is preserved, but because the bone is thicker laterally, the spine may have been divided dorsally into two transversely broadened alae. Among dorsal vertebrae of diplodocoid sauropods, it would appear that those of *Dicraeosaurus* (JANENSCH 1929b), *Amargasaurus* (SALGADO & BONAPARTE 1991) and *Rebbachisaurus* resemble each other in the shape of the posterior dorsal spines and the dorsolateral inclination of the transverse processes. Dorsals of *Rebbachisaurus*, however, are easily separated from those of the other two genera in the presence of a large pleurocoel, a smoothly continuous articular surface linking the left and right zygapophyses and absence of zygosphene-zygantral articulations.

TABLE 5A. — *Rebbachisaurus garasbae*, measurements of anterior dorsal vertebra (NMC 50844).

Length of centrum	190
Width of anterior zygapophyses	160
Width of centrum anteriorly	171
Width of centrum posteriorly	212
Height of centrum posteriorly	227
Height of centrum anteriorly to base of neural canal	200
Height of centrum posteriorly to base of neural canal	219
Base of centrum anteriorly to anterior zygapophyses on mid-line	450
Diameter of neural canal	45
Right pleurocoel, length	78
height	79

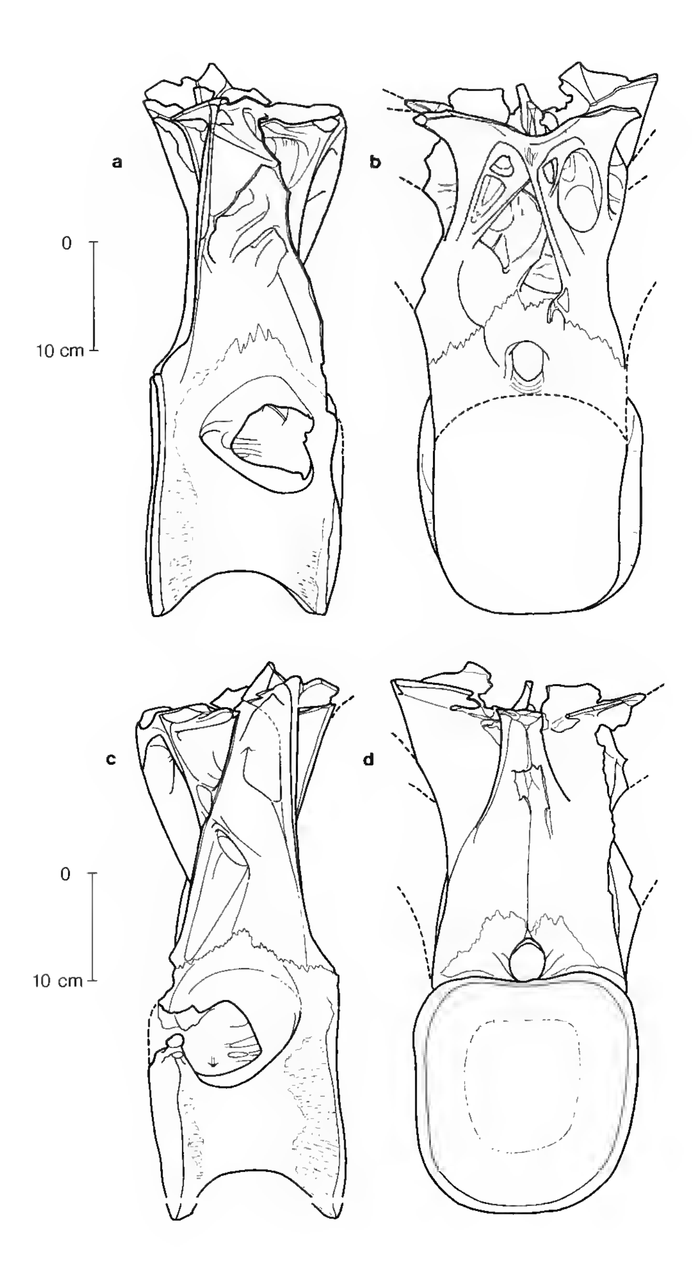


FIG. 30. — *Rebbachisaurus garasbae*, NMC 50844, dorsal vertebra in (a) right lateral, (b) anterior, (c) left lateral and (d) posterior aspect.

TABLE 5B. — *Rebbachisaurus garasbae*, measurements of posterior dorsal vertebra in type specimen (Muséum national d'Histoire naturelle, Paris).

Length of centrum	195
Width of centrum posteriorly	230
Height of centrum posteriorly	236
Maximum transverse width of spine, as preserved	240
Base of centrum posteriorly to base of posterior zygapophyses on mid-line	456
Diameter of neural canal	34
Base of posterior zygapophyses on mid-line to top of neural spine, as preserved	887
Height of vertebra, as preserved	1 343

cf. ***Rebbachisaurus*** sp.

REFERRED SPECIMEN. — Juvenile anterior dorsal *centrum* NMC 50809 (Fig. 31).

A vertebral *centrum* (NMC 50809, Table 5C) from the anterior region of the dorsal column is smaller than that of most previously described sauropod specimens (*cf.* CARPENTER & MCINTOSH 1994, Table 17.1), but is about 1.3 times longer than a diminutive and relatively more slender sauropod *centrum* from the Albian of Sudan (WERNER 1994, pl. 5, fig. 2). Both of these tiny African *centra* differ from the above-described *Rebbachisaurus* dorsals in that the pleurocoels are lenticular and extend across most of the dorsolateral surface of the *centrum*. As pointed out by MCINTOSH (1990: 394), a dorsal from the Late Cretaceous of northern Patagonia described by NOPCSA (1902) resembles those of *Rebbachisaurus*. However, the spine is shorter and, as in the juvenile *centra*, the pleurocoel is lenticular and relatively elongated.

In the Patagonian vertebra, the lower position of the anterior zygapophyses relative to that of the posterior zygapophyses suggests that it is from a position morphologically anterior to that of the Moroccan vertebra here referred to *R. garasbae* (compare NOPCSA 1902, fig. 2, and

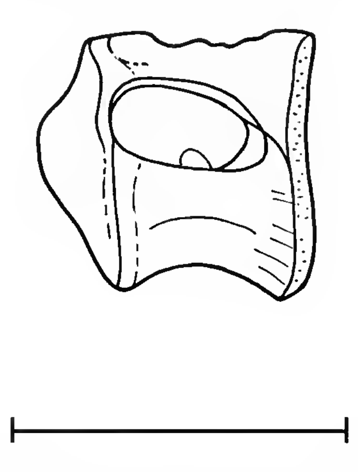


FIG. 31. — cf. *Rebbachisaurus* sp., NMC 50809, dorsal *centrum* in left lateral aspect. Scale bar: 5 cm.

fig. 30). Yet its spine is not divided, as was apparently the case in the Moroccan vertebra. The Patagonian vertebra is not large; the dimensions of its *centrum* apparently exceed those of the juvenile *centrum* by factors of two to three. It would thus appear that both a large and a small rebbachisauroid sauropod were present in the Tafilalt assemblage.

TABLE 5C. — cf. *Rebbachisaurus* sp., measurements of juvenile anterior dorsal *centrum* (NMC 50809).

Length of centrum	28
Length of centrum including anterior cotylus	39
Width of centrum anteriorly	44
Width of centrum posteriorly	48
Height of centrum anteriorly to base of neural canal	36
Height of centrum posteriorly to base of neural canal	38
Right pleurocoel, length	25
height	9

Family TITANOSAURIDAE Lydekker, 1885
Subfamily ANDESAURINAE Calvo and Bonaparte, 1991
gen. et sp. indet.

REFERRED SPECIMENS. — Isolated teeth NMC 41799, 41801; caudal centra NMC 41773 (Fig. 32), 50793 (Fig. 33); astragalus NMC 41868 (Fig. 34).

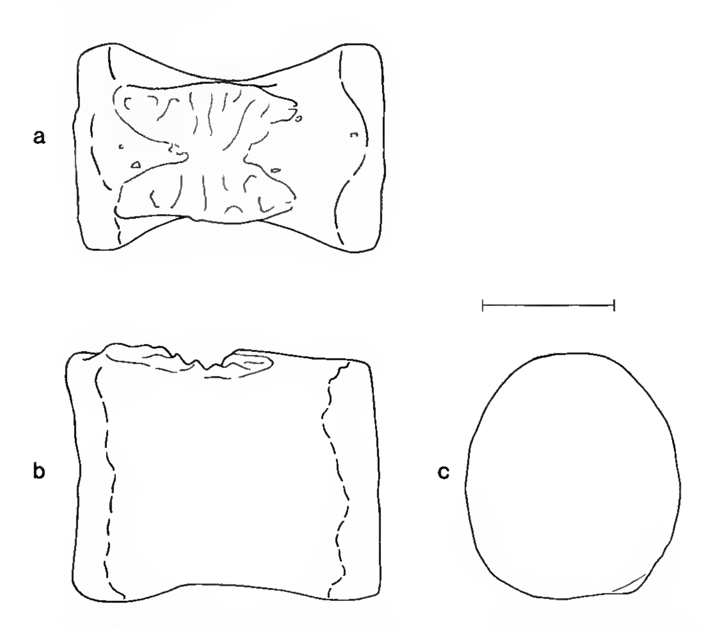


FIG. 32. — Andesaurinae, gen. indet., NMC 41773, median caudal *centrum* in (a) dorsal, (b) left lateral and (c) posterior aspect. Scale bar: 5 cm.

DESCRIPTION AND DISCUSSION

Two small, eroded teeth resemble those referred to *Malawisaurus* by JACOBS *et al.* (1993). They measure about 5 by 8 mm in diameter at the base and approximately 30 mm in height, as preserved. Smooth carinae are surely present on NMC 41799, and the abrasion pattern suggests they were probably also present on NMC 41801. In the latter tooth, the maximum expansion of the crown is closer to the tip than to the base.

NMC 41773 is a gently amphicoelous median caudal *centrum* in which the sutures for the neural arches are located over the anterior two thirds of the element, and the proportions of the *centrum* (length 113 mm, height 91 mm, posterior width 80 mm) are similar to those of a median caudal referred by JACOBS *et al.* (1993: 527, fig. 2D) to *Malawisaurus dixeyi*. These authors consider the non-procoelous nature of median caudals in *Malawisaurus* as primitive for titanosaurids, citing conditions in *Andesaurus* (CALVO & BONAPARTE 1991) from the Albian-Cenomanian of Argentina. NMC 50793 (Fig. 33) is an eroded distal caudal vertebra in which the neural arch is also anteriorly placed and the intercentral articulations were probably amphiplatyan. The length of the *centrum* is 134 mm.

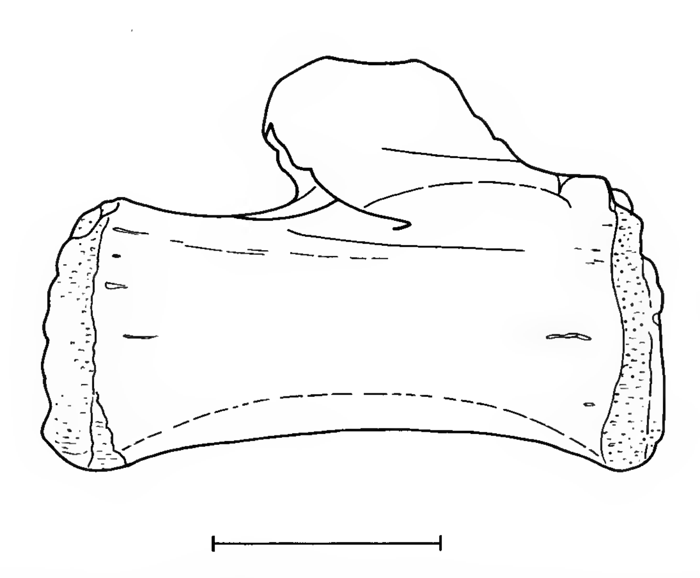


FIG. 33. — Andesaurinae, gen. indet., NMC 50793, distal caudal vertebra in right lateral aspect. Scale bar: 5 cm.

NMC 41868 (Fig. 34) is a right astragalus which is similar to that of *Neuquensaurus australis* (VON HUENE 1929: 43, pl. 17, fig. 1, for taxonomy see POWELL 1992) from the Late Cretaceous of Argentina, but is less derived in that the element is more oblong in shape and the dorsal crest linking the articular surfaces is more narrow posteriorly. The bone is 178 mm wide and measures 127 mm anteroposteriorly and 106 mm vertically.

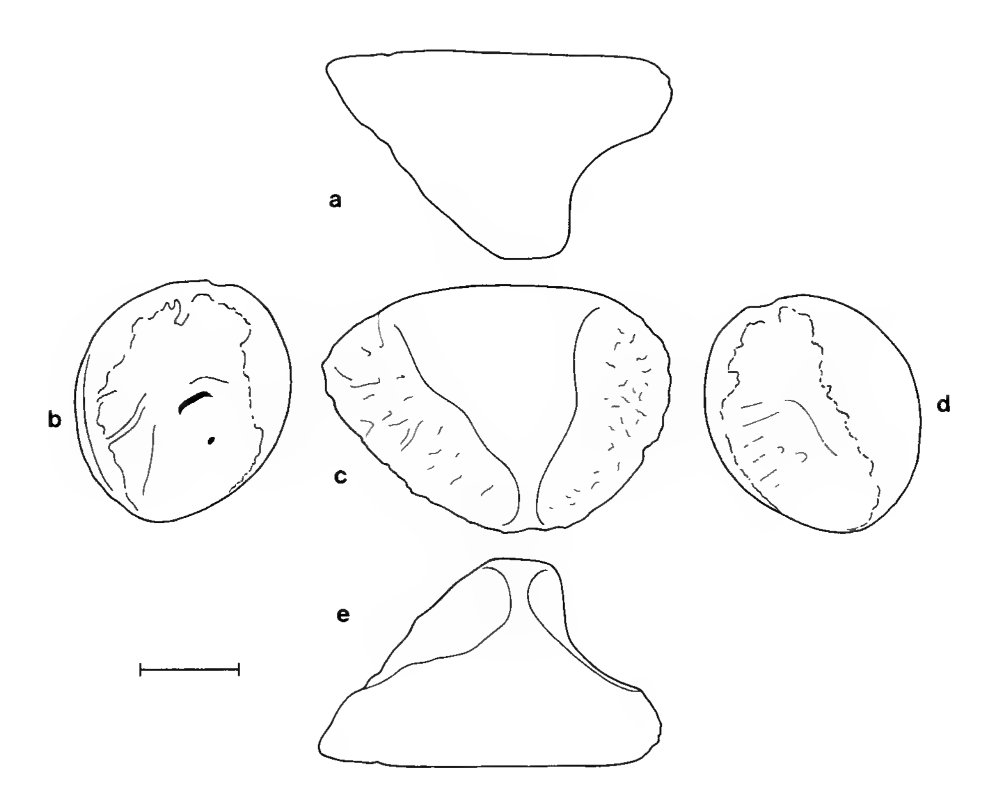


FIG. 34. — Andesaurinae gen. indet., NMC 41868, right astragalus in (a) anterior, (b) internal, (c) dorsal, (d) external and (e) posterior aspect. Scale bar: 5 cm.

SAUROPODA indet.

REFERRED SPECIMENS. — Isolated teeth NMC 41809, 41811.

DESCRIPTION AND DISCUSSION

Two sauropod teeth (NMC 4180, 41811) resemble each other in preservation, and differ both preservationally and morphologically from those referred to *Rebbachisaurus*. One (NMC 41810) is small (9 by 11 mm at the base, 41 mm long); the other (NMC 41809) is large (9 by 14 mm at the base, 48 mm long). The long axis of the teeth is nearly straight, and their surfaces bear indistinct longitudinal grooves and ridges. The apex is acuminate and lacks an oblique wear facet, which is present on the teeth referred to *Rebbachisaurus*. The teeth differ from those referred to the Titanosauridae in their larger size and in the absence of carinae.

PALEOENVIRONMENTAL AND PALEOBIOGEOGRAPHICAL CONSIDERATIONS

Within the Tafilalt, the "Grès infracénomaniens" blanketed an erosional surface developed on metamorphosed Paleozoic strata with as much as 100 m of relief locally (JOLY 1962: 157-164). To the East or North-East was an advancing marine gulf (FERRANDINI *et al.* 1985). All three units of the "Trilogie mésocrétacée" diminish in thickness toward the West, the "Marnes versicolores à gypse" progressively becoming more sandy, and the "Calcaire cénomano-turonien" less fossiliferous (CHOUBERT 1952: 146, pl. 12; LAVOCAT 1954a; FERRANDINI *et al.* 1985).

Drainage through the Tafilalt was evidently toward the east, and the semi-articulated (non-transported) condition of the type skeleton of *Rebacchisaurus* suggests that these animals frequented the surrounding fluvial plain. However, most bones are isolated and abraded (LAVOCAT 1949; JOLY 1962: 60), indicating substantial transport. The presence of fresh-water coelacanth remains derived from fish 3.5 m or more in length (WENZ 1980; see SCHWIMMER *et al.* 1994 for an Upper Cretaceous marine coelacanth of similar dimensions) implies the existence of substantial fresh water bodies upstream, either within the plain or possibly even beyond it to the west. The state of preservation of large theropod bones is similar to those of giant crocodiles. Perhaps carnivorous animals were attracted to the margins of stream courses (skeletal remains of tyrannosaurs are also very abundant in fluviatile environments of deposition in the Nemegt Formation in Mongolia; RUSSELL 1970b; OSMOLSKA 1980), or perhaps they were linked to the food chain within large bodies of water. The latter possibility tends to be supported by speculation on the piscivorous habits of baryonychids (TAQUET 1984; BUFFETAUT 1989a), which may have been related to *Spinosaurus* (BUFFETAUT 1989a, 1989b). Rare lungfish teeth (LAVOCAT 1948) imply only seasonal water abundance in more distal communities.

With the onset of deposition of the "Marnes versicolores à gypse" sediment transport greatly slowed, and insufficient fresh water entered the basin to prevent the formation of evaporites. Lungfish teeth have been recovered near the base of the unit (CHOUBERT 1952: 145). The coastal plain fell below sea level during deposition of the "Calcaire cénomano-turonien," which has yielded well-preserved skeletal material of marine dyrosaurian crocodiles north of Erfoud (EBERHARDE, pers. comm. 1994). As noted above, the ammonite *Neolobites vibrayeanus* occurs at the base of the "Calcaire cénomano-turonien" (CHOUBERT 1952; FERRANDINI *et al.* 1985).

A transgression culminating in marine strata with the *Vibrayeanus* Zone at their base gradually brought terrestrial deposition ("Continental Intercalaire") to an end over broad areas of North Africa (BUSSON & CORNÉ 1989, 1991). In most cases, dinosaurian materials in underlying Cretaceous strata are limited to scattered bones the biostratigraphic implications of which are uncertain (DE LAPPARENT 1960; LEFRANC & GUIRAUD 1990: 56, Table 8). At only three other localities have associated dinosaurian remains of Cretaceous age been found in a horizon which occurs below strata containing the *Vibrayeanus* Zone.

In one of these, from the Tiourarén Formation within the Iullemmeden Basin in Niger, the few specimens which have been collected show no special affinity to dinosaurian materials from the Tafilalt, perhaps due to the likelihood that they were derived from a much older level (MOODY & SUTCLIFFE 1990, 1991; SERENO *et al.* 1994). Some 300 km to the east in the same basin, spectacularly abundant fossil vertebrate remains occur near the middle of the 680 m thick "Série de Tégama" at Gadoufaoua (TAQUET 1976, 1994). This sequence is overlain successively by

deltaic and marine clastics (the latter containing *Neolobites vibrayeanus* MEISTER *et al.* 1991; MOODY & SUTCLIFFE 1991). Fish remains in the underlying "Argile de l'Irhazer" are suggestive of a late Early Cretaceous age (MOODY & SUTCLIFFE 1991), and the Gadoufaoua dinosaur assemblage has generally been considered to be of Aptian age (TAQUET 1976).

A similar transition from fluviatile to neritic and marine sedimentation occurs in the Bahariya Oasis, in the Western Desert of Egypt. There, *Neolobites* cf. *vibrayeanus* occurs within estuarine strata immediately overlying dinosaur-bearing sediments, and the ammonite species occurs in marine carbonates which may have been deposited contemporaneously in the southern part of the basin. The Bahariya assemblage is accordingly considered to be of Cenomanian (ALLAM 1986) or early Late Cenomanian age (DOMINIK 1985; WERNER 1990). Thus, three assemblages of middle Cretaceous dinosaurs from the Sahara (Gadoufaoua, Tafilalt, Bahariya) were probably situated in general proximity to each other in time. However, fish remains from these localities have been assigned to different species, often represent forms of differing sizes, and generally support successively younger ages for the three assemblages (MARTIN 1981, 1982; TAQUET, pers. comm. 1996).

These circumstances suggest that the apparently derived *Spinosaurus maroccanus* from the Tafilalt, and the apparently plesiomorphous *S. aegypliacus* from the Bahariya Oasis may not belong to a single phylogenetic clade. Similarly, the continuous morphologic sequence represented by the *Sigilmassasaurus* sp., "*Spinosaurus* B" and *Sigilmassaurus brevicollis* could mask an underlying phylogenetic complexity. Because the age of the three dinosaurian assemblages predates the deposition of marine strata containing the *Vibrayeanus* Zone, any vicariance events could not have been the result of an isolation of terrestrial faunas in the western Sahara from their counterparts on the remainder of the continent by a trans-Saharan seaway. Furthermore, the Cenomanian-Turonian seaway was very shallow (20-30 m, REYMENT 1980: 317) and a complete trans-Saharan isthmus linking the North African and Iullemmeden basins is postulated to have been of short duration (only a few tens to hundreds of thousands of years, *cf.* REYMENT & DINGLE 1987; MEISTER *et al.* 1991: 94). Effects on terrestrial vertebrate distributions would have been minimal.

Reptilian abundances in the three assemblages can be ranked as follows (an ornithischian occurrence in the Tafilalt by LAVOCAT 1954b, 1955b, is based on an ilium of probable theropod affinities, TAQUET, pers. comm. 1996; for Gadoufaoua, see TAQUET 1976; for Bahariya, see STROMER 1936; SCHAAL 1984; isolated fragments of turtle armour are relatively abundant at Bahariya: SCHAAL 1984: 31):

Tafilalt (Morocco)	Gadoufaoua (Niger)	Bahariya (Egypt)
Crocodilia	Crocodilia	Theropoda
Theropoda	Ornithopoda	Crocodilia
Sauropoda	Chelonia	Sauropoda
Chelonia	Sauropoda	Chelonia
(Ornithopoda absent)	Theropoda	(Ornithopoda absent)

The assemblage from the Tafilalt closely resembles that of the Bahariya. The similarity is reinforced by the abundance of giant fresh water fishes in both assemblages (*e.g. Hybodus, Lepidotes, Ceratodus, Mawsonia*; see Table 1; STROMER 1936: 75-76). However, *Onchopristis* is relatively more abundant in the Tafilalt, as is *Ceratodus* in the Bahariya (SCHAAL 1984).

Another, more continental environment was apparently sampled at Gadoufaoua, which has produced the only known major Gondwana assemblage where ornithopods outnumber all other groups of dinosaurs (*cf.* VON HUENE 1929; VON HUENE & MATLEY 1933; TAQUET 1976). No teeth of *Onchopristis* or *Carcharodontosaurus* were recovered at Gadoufaoua, although they occur in relative abundance in the other two assemblages. Their absence has been suggested to be due to a greater age for the "Série de Tégama" (TAQUET 1976), but ecological effects cannot be excluded (the type teeth of *C. saharicus* were collected from strata inferred by LEFRANC 1983 to be of late Barremian age). The dinosaurian assemblage from the underlying "Série de Irhazer" (Tiourarén Formation) is dominated by skeletons of camarasauroid sauropods, although the fish assemblage is similar to that in higher levels of the Saharan middle Cretaceous (MOODY & SUTCLIFFE 1990, 1991; SERENO *et al.* 1994).

A mammalian microfaunal assemblage, recently discovered in older Early Cretaceous strata (see "Stratigraphy and Correlation," above), shows Laurasian as well as Southern Hemispheric zoogeographic affinities (SIGOGNEAU-RUSSELL *et al.* 1990, SIGOGNEAU-RUSSELL 1991). Interchange between Europe and Africa during Early Cretaceous time is also suggested by the dinosaurian record on both continents (RUSSELL 1993, 1995; SERENO *et al.* 1994). By the time of deposition of the "Grès rouges infracénomaniens" in the Tafilalt, terrestrial vertebrates in West Africa remained linked by a continuous land surface to those of South America (REYMENT & DINGLE 1987). This is confirmed by the identification of similar fresh water fish, turtle and crocodilian taxa in what have since become separate continents (*e.g.* BUFFETAUT & TAQUET 1977; WENZ 1980; DE BROIN 1988; MAISEY 1991; BUFFETAUT & RAGE 1993), as well as by a record of a *Rebbachisaurus*-like dinosaur in Argentina (MCINTOSH 1990: 394). The identification of abelisaurid and titanosaur remains in the Albian of southern Morocco is also consistent with Albian-Cenomanian records of the two groups in Argentina (BONAPARTE *et al.* 1990; CALVO & BONAPARTE 1991). In contrast, the absence of diagnostic remains of abelisaurids, diplodocoids and titanosaurs in Aptian-Albian assemblages in North America (OSTROM 1970) suggests that faunal relationships between Africa-South America ("Gondwana") and North America were more remote, in keeping with plate tectonic evidence. The post-Cenomanian record of dinosaurs in Africa is much too incomplete to serve as a basis for biogeographic speculation (RUSSELL 1995).

CONCLUSIONS

The "Grès rouges infracénomaniens" of the Tafilalt have yielded abundant, if usually isolated and often water-worn remains of dinosaurs, possibly of Albian age. Discrete forms so far identified include:

Theropoda, small, sp.
Spinosaurus maroccanus n. sp.
Sigilmassasaurus brevicollis n. g. et n. sp.
Carcharodontosaurus saharicus cf. *Majungasaurus* sp.
Abelisauridae, sp. indet.
Rebbachisaurus garasbae cf. *Rebbachisaurus* sp.
Titanosauridae, sp. indet.

To these may possibly be added a stegosaur-like femur (EBERHARDE, pers. comm. 1994). In the case of *Spinosaurus* and *Sigilmassasaurus*, differences of a species-level magnitude separate them from their counterparts in the Bahariya Formation of Egypt. Vertebrae assignable to *Sigilmassasaurus* dominate dinosaurian vertebrae from the Tafilalt, and include a range of sizes consistent with body weight differences of a factor of approximately 150. Undetermined femora indicate the presence in the assemblage of infantile individuals of large theropods weighing less than 4 kg. Remains of at least three taxa of sauropods have been identified, but those of ornithischian dinosaurs, if present, are not abundant. Variation in the preservation and morphology of *Sigilmassasaurus centra* pose the question how much of middle Cretaceous time is represented by the deposition of the "Grès rouges infracénomaniens."

The number of different varieties of dinosaurs, represented by isolated elements found within a relatively small region, document one of the most diverse dinosaurian assemblages known from Africa. Faunal resemblances are closest to the Bahariya assemblage from deltaic-lagoonal strata of Cenomanian age in Egypt, as was originally noted by LAVOCAT (1954a: 102). The abundance of theropod dinosaurs in both assemblages may be the result of their linkage to fresh water ecosystems containing giant fishes. This coastal community evidently differed greatly from an ornithopod-dominated assemblage at Gadoufaoua, which was separated by over 1000 km from the nearest contemporary coastline (*cf.* REYMENT & DINGLE 1987, figs 3, 4; MOODY & SUTCLIFFE 1991, figs 1, 2). The dinosaurian assemblage of the Tafilalt exhibits closer zoogeographic affinities to those from the Early Cretaceous of South America than to those in North America.

Acknowledgements

Mr William PINCH, of Rochester, New York, recognized the importance of fossil vertebrate remains from the Tafilalt displayed at the Tucson Gem and Mineral Show between 1992 and 1994. It is through his enthusiasm and initiative that some of these fossils were acquired by the CMN. Mr Brian EBERHARDE, of Moussa Direct, Cambridge, England, generously supplied information on the occurrence and condition of preservation of specimens he consigned to the Museum. Specimens were also acquired from Mr Raymond MEYER, of Buffalo, New York, and Mr Horst BURKARD, of Mineralien und Fossilien, Bonn, Germany. Colleagues from the Muséum national d'Histoire naturelle, Paris, generously provided guidance to the stratigraphy of the Sahara, as well as to Saharan dinosaur collections under their care; special thanks are due to France DE BROIN, Denise SIGOGNEAU-RUSSELL and Philippe TAQUET. Georges BUSSON graciously reviewed the stratigraphic portions of the manuscript in detail, and provided suggestions to clarify the regional relationships of the Cretaceous record in the Tafilalt. Valuable counsel of a geological nature was provided by André CHARRIÈRE (Université Paul-Sabatier, Toulouse), René GUIRAUD (Institut des Sciences de la Terre, de l'Eau et de l'Espace de Montpellier) and Michel MONBARON (Université de Fribourg). José BONAPARTE (Museo Argentino de Ciencias Naturales) and Hans-Dieter SUES (Royal Ontario Museum) also freely contributed of their paleontological expertise. It is particularly gratifying to acknowledge the interest of His Excellency, Dr Tajeddine BADDOU, Ambassador to Canada from the kingdom of Morocco. Philip CURRIE (Royal Tyrrell Museum of Paleontology) and Philippe TAQUET carefully reviewed the final manuscript and made numerous suggestions which clarified both meaning and content. The support of this international group of scholars has been deeply appreciated.

Manuscript submitted for publication on 27 June 1995; accepted on 13 February 1996.

REFERENCES

ALLAM A. M. 1986. — A regional and paleoenvironmental study on the Upper Cretaceous deposits of the Bahariya Oasis, Libyan Desert, Egypt. *Journal of African Earth Sciences* **5**: 407-412.

ANDERSON J. F., HALL-MARTIN A. & RUSSELL D. A. 1985. — Long-bone circumference and weight in mammals, birds and dinosaurs. *Journal of Zoology* **207**: 53-61.

BARSBOLD R. 1976. — New data on *Therizinosaurus* (Therizinosauridae, Theropoda). *Trudy Sovmestnoi Soviet-sko-Mongol'skoi Paleontologicheskoi Ekspeditsii* **3**: 76-92 [in Russian].

BASSE E. & CHOUBERT G. 1959. — Les faunes d'ammonites du "Cénomano-Turonien" de la partie orientale du domaine atlasique marocain et de ses annexes sahariennes. C. R. 20th International Geological Congress, 1959, *in* L. B. KELLUM (ed.). *El Sistema Cretacico* **2** : 59-81.

BENTON M. J. (editor) 1993. — *The fossil record 2*. Chapman & Hall, London. xvii + 845 p.

BONAPARTE J. F. & NOVAS F. E. 1985. — *Abelisaurus comahuensis*, n.g., n.sp., carnosauria del Cretacico tardio de Patagonia. *Ameghiniana* **21**: 259-267.

BONAPARTE J. F. & POWELL J. E. 1980. — A continental assemblage of tetrapods from the Upper Cretaceous of Argentina (Sauropoda-Coelurosauria-Carnosauria-Aves). *Mémoires de la Société géologique de France* Nouvelle Série **139** : 19-28.

BONAPARTE J. F., NOVAS F. E. & CORIA R. A. 1990. — *Carnotaurus sastrei* Bonaparte, the horned, lightly built carnosaur from the Middle Cretaceous of Patagonia. *Contribution in Science* **416**: 1-41.

BOUAZIZ S., BUFFETAUT E., GHANMI M., JAEGER J. J., MARTIN M., MAZIN J. M. & LONG H. 1988. — Nouvelles découvertes de vertébrés fossiles dans l'Albien du Sud tunisien. *Bulletin de la Société géologique de France* Série 8, **4** : 335-339.

BROIN F. DE 1988. — Les tortues et le Gondwana. Examen des rapports entre le fractionnement du Gondwana et la dispersion géographique des tortues pleurodires à partir du Crétacé. *Studia Geologica Salmanticensia, Studia Palaeocheloniologica* **2** : 103-142.

BUFFETAUT E. 1976. — Der Land-Krokodilier *Libycosuchus* Stromer und die Familie Libycosuchidae (Crocodylia, Mesosuchia) aus der Kreide Afrikas. *Mitteilungen Bayerischen Staatssammlung fuer Paläontologie Historische Geologie* **16** : 17-28.

— 1989a. — New remains of the enigmatic dinosaur *Spinosaurus* from the Cretaceous of Morocco and the affinities between *Spinosaurus* and *Baryonyx*. *Neues Jahrburch fuer Geologie und Paläontologie Monatsheffe* 1989 **2**: 79-87.

— 1989b. — New remains of *Spinosaurus* from the Cretaceous of Morocco. *Archosaurian Articulations* **1** (9): 65-68.

— 1994. — A new crocodilian from the Cretaceous of southern Morocco. *Comptes Rendus de l'Académie des Sciences* Paris Série 2 **319** : 1563-1568.

BUFFETAUT E. & RAGE J.-C. 1993. — Fossil amphibians and reptiles and the Africa-South America connection. *In* W. GEORGE & R. LAVOCAT (eds). *The Africa-South America connection*. Clarendon Press, Oxford: 87-99.

BUFFETAUT E. & TAQUET P. 1977. — The giant crocodilian *Sarchosuchus* in the early Cretaceous of Brazil and Niger. *Palaeontology* **20**: 203-208.

BUSSON G. & CORNÉE A. 1989. — Données sur les paléoclimats déduites de la sédimentation continentale du Mésozoïque saharien. *Centre International de Formation et d'Échanges en géologie* Publication occasionnelle **18**, 87 p.

— 1991. — The Sahara from the Middle Jurassic to the Middle Cretaceous: data on environments and climates based on outcrops in the Algerian Sahara. *Journal of African Sciences* **12**: 85-105.

CALVO J. O. & BONAPARTE J. F. 1991. — *Andesaurus delgadoi* gen. et sp. nov. (Saurischia-Sauropoda). dinosaurio Titanosauridae de la Formacion Rio Limay (Albiano-Cenomaniano), Neuquen, Argentina. *Ameghiniana* **28**: 303-310.

CAPPETTA H. 1980. — Les sélaciens du Crétacé supérieur du Liban II Batoïdes. *Palaeontographica Abteilung* A **168** : 149-229.

CARPENTER K. & MCINTOSH J. 1994. — Upper Jurassic sauropod babies from the Morrison Formation. *In* K. CARPENTER, K. F. HIRSCH & J. R. HORNER (eds). *Dinosaur Eggs and Babies*. Cambridge University Press, Cambridge: 265-278.

CHARIG A. J. & MILNER A. C. 1990. — The systematic position of *Baryonyx walkeri*, in the light of Gauthier's classification of the Theropoda. *In* K. CARPENTER & P. J. CURRIE (eds). *Dinosaur Systematics*. Cambridge University Press, Cambridge: 127-140.

CHARRIÈRE A. 1992. — Discontinuités entre les "Couches rouges" du Jurassique moyen et du Crétacé inférieur dans le Moyen Atlas (Maroc). *Comptes Rendus de l'Académie des Sciences* Paris Série 2 **315** : 1389-1396.

CHOUBERT G. 1952. — Histoire géologique du domaine de l'Anti-Atlas. Notes *Mémoires du Service géologique* (Maroc) **100** : 75-194.

CURRIE P. & RUSSELL D. A. 1988. — Osteology and relationships of *Chirostenotes pergracilis* (Saurischia, Theropoda) from the Judith River (Oldman) Formation of Alberta, Canada. *Canadian Journal of Earth Sciences* **25**: 103-115.

DEPÉRET C. & SAVORNIN J. 1927. — La faune de reptiles et de poissons albiens de Timimoun (Sahara algérien). *Bulletin de la Société géologique de France* Série 4 **27** : 257-265.

DOMINIK W. 1985. — Stratigraphie und Sedimentologie (Geochemie, Schwermineralanalyse) der Oberkreide von Bahariya und ihre Korrelation zum Dakhla-Becken (Western Desert, Ägypten). *Berliner geowissenschaften Abhandlungen* Reihe A, **62** : 1-173.

DUFFIN C. J. & SIGOGNEAU-RUSSELL D. 1993. — Fossil shark teeth from the Early Cretaceous of Anoual, Morocco. Professionnal Paper, *Belgium Geological Survey* **264**: 175-190.

FARLOW J. O., BRINKMAN D. L., ABLER W. L. & CURRIE P. J. 1991. — Size, shape, and serration density of theropod dinosaur lateral teeth. *Modern Geology* **16**: 161-198.

FERRANDINI M., PHILIP J., BABINOT J.-F., FERRANDINI J. & TRONCHETTI G. 1985. — La plate-forme carbonatée du Cénomano-Turonien de la région d'Erfoud-Errachidia (Sud-Est marocain): stratigraphie et paléo environnements. *Bulletin de la Société géologique de France* Série 8 1985 **1** : 559-564.

GIFFIN E. 1990. — Gross spinal anatomy and limb use in living and fossil reptiles. *Paleobiology* **16**: 448-458.

GALTON P. M. & JENSEN J. A. 1979. — A new large theropod dinosaur from the Upper Jurassic of Colorado. Brigham Young Univ., *Geological Studies* **26** (2): 1-12.

GILMORE C. W. 1920. — Osteology of the carnivorous dinosauria in the United States National Museum, with special reference to *Antrodemus* (*Allosaurus*) and *Ceratosaurus*. *Bulletin of the U.S. National Museum* **110**, xi + 154 p.

HARLAND W. B., ARMSTRONG R. L., COX A. V., CRAIG L. E., SMITH A. G. & SMITH D. G. 1990. — *A geologic time scale 1989*. Cambridge University Press, Cambridge, p. xv + 263.

HU S. Y. 1964. — Carnosaurian remains from Alashan, Inner Mongolia. *Vertebrata PalAsiatica* **8**: 43-63 [in Chinese, English abstract].

HUENE F. VON 1929. — Los saurisquios y ornitisquios de Cretácio Argentino. *Anales del Museo La Plata* Ser. 2 **3**: viii + 196 p.

HUENE F. VON & MATLEY C. A. 1933. — The Cretaceous Saurischia and Ornithischia of the central provinces of India. *Memoir of Geological Survey India* **21**: 1-74.

JACOBS L. L., WINKLER D. A., DOWNS W. R. & GOMANI E. M. 1993. — New material of an Early Cretaceous titanosaurid sauropod dinosaur from Malawi. *Palaeontology* **36**: 523-534.

JANENSCH W. 1925. — Die Coelurosaurier und Theropoden aus der Tendaguru-Schichten Deutsch-Ostafricas. *Palaeontographica* Suppl. 7 Erste Reihe **1** : 1-99.

— 1929a. — Material und Formengehalt der Sauropoden in der Ausbeute der Tendaguru-Expedition. *Palaeontographica* Suppl. 7 Erste Reihe **2** : 1-34.

— 1929b. — Die Wirbelsäule der Gattung *Dicraeosaurus*. *Palaeontographica* Suppl. 7 Erste Reihe **2** : 35-133.

JOLY F. 1962. — Études sur le relief du sud-est marocain. *Travaux de l'Institut des Sciences chérifien* Série Géologie, Géographie Physique **10** : 578 p.

LAPPARENT A. F. DE 1960. — Les dinosauriens du "Continental intercalaire" du Sahara central. *Mémoire de la Société géologique de France* **88**A : 1-57.

LAVOCAT R. 1948. — Découverte de Crétacé à vertébrés dans le soubassement de la hammada du Guir (sud marocain). *Comptes Rendus de l'Académie des Sciences* Paris Série 2 **226** : 1291-1292.

— 1949. — Les gisements de vertébrés crétacés du sud Marocain. *Comptes Rendus Sommaires de la Société géologique de France* 1949 **7** : 125-126.

— 1951. — Découverte de restes d'un grand dinosaurien sauropode dans le Crétacé du sud marocain. *Comptes Rendus de l'Académie des Sciences* Paris Série 2 **232** : 169-170.

— 1952. — Les gisements de dinosauriens du Crétacé du sud marocain. *Comptes Rendus Sommaires de la Société géologique de France* 1952 **2** : 12-13

— 1954a. — Reconnaissance géologique dans les hammadas des confins algéro-marocains du sud. Notes *Mémoires du Service géologique* (Maroc) **116** : 147 p.

— 1954b. — Sur les dinosauriens du Continental Intercalaire des Kem-Kem de la Daoura. *Comptes Rendus 19th International Geological Congress* 1952 part **15**: 65-68.

— 1955a. — Sur une portion de mandibule de théropode provenant du Crétacé supérieur de Madagascar. *Bulletin du Muséum national d'Histoire naturelle* Paris Série 2 **27** : 256-259.

— 1955b. — Découverte d'un crocodilien du genre *Thoracosaurus* dans le Crétacé supérieur d'Afrique. *Bulletin du Muséum national d'Histoire naturelle* Paris Série 2 **27** : 338-340.

— 1955c. — *Titres et travaux scientifique de M. René Lavocat*. Imprimerie Centrale, Romorantin, France, 95 p.

LEFRANC J.-P. 1983. — Corrélation vers le nord et description stratigraphique détaillée du Continental intercalaire (Mésozoïque continental) de la sebkha de Timimoun, Gourara, Sahara algérien. *Comptes Rendus de l'Académie des Sciences* Paris Série 2 **296** : 193-196.

LEFRANC J.-P. & GUIRAUD R. 1990. — The Continental Intercalaire of northwestern Sahara and its equivalents in the neighbouring regions. *Journal of African Earth Sciences* **10**: 27-77.

MADSEN J. H. 1976. — *Allosaurus fragilis*: a revised osteology. *Bulletin of Utah Geological and Mineral Survey* **109** xii + 163 p.

MAISEY J. G. 1991. — Concluding remarks. *In* J. G. MAISEY (ed.). *Santana fossils: an illustrated atlas*. Neptune City, New Jersey: 422-433.

MARTIN M. 1981. — Über drei Zahnplatten von *Ceratodus* aus der ägyptischen Kreide. *Mitteilungen der Bayerischen Staatssammlung Paläontologie und Historische Geologie* **21** : 73-80.

— 1982. — Nouvelles données sur la phylogénie et la systématique des dipneustes postpaléozoiques. *Géobios* Mémoire **6** : 53-64.

MCINTOSH J. A. 1990. — Sauropoda. *In* D. B. WEISHAMPEL, P. DODSON & H. OSMOLSKA (eds). *The Dinosauria*. University of California Press, Berkeley: 345-401.

MEISTER C., ALZOUMA K., LANG J. & MATHEY B. 1991. — Les ammonites du Niger et la transgression transsaharienne au cours du Cénomanien-Turonien. *Géobios* **25** : 55-100.

MONBARON M., KUBLER B. & ZWEIDLER D. 1990. — Detrital rubified sedimentation in the High Atlas trough in the Mesozoic: attempt at lateral correlations using correspondence factor analysis. *Journal of African Earth Sciences* **10**: 369-384.

MOODY R. T. J. & SUTCLIFFE P. J. C. 1990. — Cretaceous-Tertiary crossroads of migration in the Sahel. *Geology Today* **6**: 19-23.

— 1991. — The Cretaceous deposits of the Iullemmeden Basin of Niger, central West Africa. *Cretaceous Research* **12**: 137-157.

NOPCSA F. 1902. — Wirbel eines südamerikanischen Sauropoden. Sitzungsber. *Kaiserl. Akad. Wiss., Math.-Naturwiss. Klasse* **111** : 108-114.

NORMAN D. & MILNER A. C. 1989. — *Eyewitness Books: Dinosaur*. Stoddart, Toronto, 64 p.

OSBORN H. F. 1906. — *Tyrannosaurus*. Upper Cretaceous carnivorous dinosaur (second communication). *Bulletin of the American Museum of Natural History* **22**: 281-296.

— 1917. — Skeletal adaptations of *Ornitholestes, Struthiomimus, Tyrannosaurus*. *Bulletin of the American Museum of Natural History* **35**: 733-771.

OSMOLSKA H. 1980. — The late Cretaceous vertebrate assemblages of the Gobi Desert, Mongolia. *Mémoires de la Société géologique de France* **139** : 145-150.

OSMOLSKA H. & RONIEWICZ E. 1970. — Deinocheiridae, a new family of theropod dinosaurs. *Paloeontologica Polonica* **21**: 5-19.

OSMOLSKA H., RONIEWICZ E. & BARSBOLD R. 1972. — A new dinosaur, *Gallimimus bullotus* n. gen., n. sp. (Ornithomimidae) from the Upper Cretaceous of Mongolia. *Palaeontologica Polonica* **27**: 103-143.

OSTROM J. H. 1969. — Osteology of *Deinonychus antirrhopus*, an unusual theropod from the Lower Cretaceous of Montana. *Bulletin of the Peabody Museum of Natural History* Yale Univ. **30**: 165 p.

— 1970. — Stratigraphy and paleontology of the Cloverly Formation (Lower Cretaceous) of the Bighorn Basin area, Wyoming and Montana. *Bulletin of the Peabody Museum of Natural History* Yale University **35**: 234 p.

PERLE A. 1979. — Segnosauridae, a new family of theropods from the Late Cretaceous of Mongolia. *Trudy Sovmestnoi Sovietsko-Mongol'skoi Paleontologicheskoi Ekspeditsii* **8**: 45-55 [in Russian].

POWELL J. E. 1987. — Morfologia del esqueleto axial de los dinosaurios titanosauridos (Saurischia, Sauropoda) del estado de Minas Gerais, Brasil. *Anales X Congresso Brasil Paleontologia*: 155-171.

— 1992. — Osteologia de *Saltasaurus loricatus* (Sauropoda-Titanosauridae) de Cretácico Superior del Noroeste argentino. *In* J. L. SANZ & A. D. BUSCALIONI (eds), *Los dinosaurios y su entorno biotico, Actas del Segundo Curso de Paleontologia en Cuenca*. Instituto Juan de Valdes, Ser. Act. Acad. **4**: 165-230.

REYMENT R. A. 1980. — Biogeography of the Saharan Cretaceous and Paleocene transgressions. *Cretaceous Research* **1**: 299-327.

REYMENT R. A. & DINGLE R. V. 1987. — Palaeogeography of Africa during the Cretaceous Period. *Palaeogeography, Palaeoclimatology, Palaeoecology* **59**: 93-116.

RUSSELL D. A. 1970a. — Tyrannosaurs from the Late Cretaceous of western Canada. *Canadian National Museum Publication in Paleontologie* **1**, 34 p.

— 1970B. — The dinosaurs of Central Asia. *Canadian Geographer Journal* **81** (6): 208-215.

— 1993. — The role of Central Asia in dinosaurian biogeography. *Canadian Journal of Earth Sciences* **30**: 2002-2012.

— 1995. — China and the lost worlds of the dinosaurian era. *Historical Biology* **10**: 3-12.

RUSSELL D. A. & DONG Z. M. 1993. — A nearly complete skeleton of a new troodontid dinosaur from the Early Cretaceous of the Ordos Basin, Inner Mongolia, People's Republic of China. *Canadian Journal of Earth Sciences* **30**: 2163-2173.

RUSSELL D. A. & ZHENG Z. 1993. — A large mamenchisaurid from the Junggar Basin, Xinjiang, People's Republic of China. *Canadian Journal of Earth Sciences* **30**: 2082-2095.

SALGADO L. & BONAPARTE J. F. 1991. — Un nuevo Dicraeosauridae, *Amargasaurus cazaui* gen. et sp. nov., de la Formación La Amarga, Neocomiano de la Provincia del Neuquén, Argentina. *Ameghiniana* **28**: 333-346.

SCHAAL S. 1984. — Oberkretazische Osteichthyes (Knochenfische) aus dem Bereich von Bahariya and Kharga, Ägypten, und ihere Aussagen zur Palökologie und Stratigraphie. *Berliner geowissenschaften Abhandlingen* Riehe A **53**: 1-79.

SCHWIMMER D. R., STEWART J. D. & WILLIAMS G. D. 1994. — Giant fossil coelacanths of the Late Cretaceous in the eastern United States. *Geology* **22**: 503-506.

SERENO P. C., WILSON J. A., LARSSON H. C. E., DUTHEIL D. B. & SUES H. D. 1994. — Early Cretaceous dinosaurs from the Sahara. *Science* **266**: 267-271.

SIGOGNEAU-RUSSELL D. 1991. — Nouveaux mammifères thériens du Crétacé inférieur du Maroc. *Comptes Rendus de l'Académie des Sciences* Paris Série 2 **313**: 279-285.

SIGOGNEAU-RUSSELL D., MONBARON M. & KAENEL E. DE 1990. — Nouvelles données sur le gisement à mammifères Mésozoïques du Haut-Atlas marocain. *Geobios* **23**: 461-483.

STROMER E. 1915. — Ergebnisse der Forschungsreisen Prof. E. Stromers in den Wüsten Ägyptens II. Wirbeltier-Reste der Bajarîjestufe (unterstes Cenoman). 3. Das Original des Theropoden *Spinosaurus aegyptiacus* nov. gen., nov. spec. *Abhandlungen und Bayerische Akademie der Wissenschaften Mathematik-Naturwissenschaften* Kl. **3**: 1-32.

— 1931. — Ergebnisse der Forschungsreisen Prof. E. Stromers in den Wüsten Ägyptens II. Wirbeltier-Reste der Bajarijestufe (unterstes Cenoman). 10. Ein Skelett-Rest von *Carcharodontosaurus* nov. gen. *Abhandlungen und Bayerische Akademie der Wissenschaften Mathematik-Naturwissenschaften Kl.* **9**: 1-23.

— 1934. — Ergebnisse der Forschungsreisen Prof. E. Stromers in den Wüsten Ägyptens II. Wirbeltier-Reste der Bajarîjestufe (unterstes Cenoman). 13. Dinosauria. *Abhandlungen und Bayerische Akademie der Wissenschaften Mathematik-Naturwissenschaften Kl.* **22**: 1-79.

— 1936. — Ergebnisse der Forschungsreisen Prof. E. Stromers in den Wüsten Ägyptens VII. Baharîje-Kessel und – Stufe mit deren Fauna und Flora – Eine ergänzende Zusammenfassung. *Abhandlungen und Bayerische Akademie der Wissenschaften Mathematik-Naturwissenschaften Kl.* **33**: 1-102.

TABASTE N. 1963. — Étude des restes de Poissons du Crétacé saharien. *Mémoire de l'Institut Français d'Afrique noire* **68**: 437-485.

TAQUET P. 1976. — Géologie et paléontologie du gisement de Gadoufaoua (Aptien du Niger). *Cahiers de Paléontologie C.N.R.S.*: 191 p.

— 1984. — Une curieuse spécialisation du crâne de certains dinosaures carnivores du Crétacé: le museau long et étroit des Spinosauridés. *Comptes Rendus de l'Académie des Sciences* Paris Série 2 **299** : 217-222.

— 1994. — *L'Empreinte des dinosaures*. Odile JACOB (ed.), Paris. 363 p.

WEISHAMPEL D. B. & HORNER J. R. 1990. — Hadrosauridae. *In* D. B. WEISHAMPEL, P. DODSON & H. OSMOLSKA (eds). *The Dinosauria.* University of California Press, Berkeley: 534-561.

WENZ S. 1980. — À propos du genre *Mawsonia*, coelacanthe géant du Crétacé inférieur d'Afrique et du Brésil. *Mémoires de la Société géologique de France* **139** : 187-190.

— 1981. — Un cœlacanthe géant *Mawsonia-lavocati* Tabste, de l'Albien-base du Cénomanien du sud marocain. *Annales de Paléontologie, Vertébrés* **67** : 1-20.

WERNER C. 1990. — Biostratigraphical results of investigations on the Cenomanian elasmobranchian fauna of Bahariya Oasis, Egypt. *Berliner geowissenschaften Abhandlungen Reihe A* **120** : 943-956.

— 1994. — Die kontinentale Wirbeltierfauna aus der unteren Oberkreide des Sudan (Wadi Milk Formation). *Berliner geowissenschaften Abhandlungen B Krebs Festschrift*: 221-246.

ZHAO X. J. & CURRIE P. J. 1993. — A large crested theropod from the Jurassic of Xinjiang, People's Republic of China. *Canadian Journal of Earth Sciences* **30**: 2027-2036.

Bulletin du Muséum national d'Histoire naturelle, Paris, 4[e] sér., **18**, 1996
Section C, n[os] 2-3 : 403-415

Conservation de sucres dans les phases organiques d'os de bovidés fossiles

par Hélène DAVID, Yannicke DAUPHIN, Martin PICKFORD & Brigitte SENUT

Résumé. — Les observations au MEB et les analyses à la microsonde électronique ont montré que la microstructure et la composition chimique élémentaire d'un os de bovidé fossile (Plio-pléistocène d'Angola – plateau d'Humpata) étaient bien conservées. Cependant, la spectroscopie infrarouge (DRIFT) montre une diminution des bandes organiques, une augmentation du taux de cristallinité et du rapport CO_3/PO_4 dans l'os fossile par rapport à l'os actuel. Les spectres obtenus sur les phases organiques extraites confirment la présence de protéines et de sucres chez le fossile, tout en mettant en évidence leur altération par les processus diagénétiques.

Mots-clés. — Angola, Bovidae, spectroscopie infrarouge, sucres.

Sugar preservation in the organic matter in fossil bovid bones

Abstract. — SEM observations and electron microprobe analyses have shown that the microstructure and chemical composition of a Plio-pleistocene bovid bone (Humpata Plateau, Angola) are well preserved. However, infrared spectroscopy spectra exhibit clear differences between Recent and fossil samples. Organic bands weaken relatively to mineral ones in the fossil, whereas cristallinity rate and CO_3/PO_4 ratio increase. DRIFT spectra carried on the extracted organic matrices demonstrate the presence of proteic and sugar contents in the fossil bone, but the composition of the fossil organic matrices are modified by diagenetic processes.

Key-words. — Angola, Bovidae, infrared spectroscopy, sugar.

H. DAVID, Y. DAUPHIN, *Laboratoire de paléontologie, URA 723, bât. 504, Université Paris XI-Orsay.*
M. PICKFORD, *chaire de paléoanthropologie et préhistoire du Collège de France et Laboratoire de paléontologie du Muséum national d'Histoire naturelle, 8 rue de Buffon, F-75231 Paris cedex 05.*
B. SENUT, *Laboratoire de paléontologie du Muséum national d'Histoire naturelle, 8 rue de Buffon, F-75231 Paris cedex 05.*

INTRODUCTION

L'os est un complexe organo-minéral dont la structure et la composition sont relativement bien connus. Toutefois, les divers composants de ce tissu ont été inégalement analysés et la majeure partie des données disponibles sur la phase organique concerne les protéines et surtout le collagène. Collagéniques ou non, les protéines de l'os sont associées à d'autres constituants : les sucres. Par exemple, le galactose et le glucose permettent d'établir des liens entre les molécules de tropocollagène. Les protéoglycannes sont formées par un cœur protéique sur lequel se fixent des chaînes de glycosaminoglycannes, chaînes principalement composées de

chondroïtine sulfate. Les sialoprotéines et les phosphoprotéines sont des glycoprotéines acides impliquées notamment dans la fixation du Ca^{2+}, l'initiation et la régulation de la calcification.

Le comportement des sucres de l'os au cours de la fossilisation et des phases diagénétiques postérieures est encore mal connu. En outre, la composition des phases organiques fossiles est rarement corrélée avec l'état de conservation de la phase minérale et celui des autres composants de la phase organique. Actuellement, aucun critère (sédimentologie, âge...) ne permet une sélection rationnelle d'un site favorable à la conservation de la phase organique. Le choix effectué repose donc sur des indices tels que la bonne conservation de la microstructure osseuse et de la composition chimique globale. Une étude préliminaire a montré que certains fragments osseux de bovidés provenant de remplissages plio-pléistocènes du plateau d'Humpata (Angola) répondaient à ces conditions (David 1994); de plus, la recherche des taxons actuels de comparaison dont la position systématique était proche ne constituait pas de difficultés. Un protocole permettant de détecter rapidement la présence et la diagenèse de sucres dans les phases organiques de l'os fossile a été mis au point.

TRAVAUX ANTÉRIEURS

L'os frais contient environ 70 % de matériel inorganique, 18 % de matériel organique, et 12 % d'eau. La phase organique est composée d'environ 85 % de collagène de type I insoluble, et de 5 % d'autres collagènes, des divergences subsistant sur la présence de certains types. À celà s'ajoutent environ 10 % de protéines non collagéniques.

Spectrométrie infrarouge

L'os total

Les données sur les apatites de synthèse sont très abondantes, celles sur les os sont plus ponctuelles. L'os des bovidés aurait le même comportement que la dahllite (Herman & Dallemagne 1964). Les spectres DRIFT (Diffuse Reflectance using Infrared Fourier Transform) de l'os humain présentent des bandes d'intensité variable vers 560-600 cm^{-1}, 1000 cm^{-1}, 1500 cm^{-1} et 3500 cm^{-1} (Suzuki 1975). Une bande carbonate a été également détectée vers 850 cm^{-1}. Les bandes des groupes phosphates et de la phase organique (amides I et II) sont présentes. Le taux de cristallinité de l'os en cours de croissance serait voisin de 23 %. Lorsque le degré de calcification augmente, les bandes organiques deviennent plus faibles, alors que la bande à 600 cm^{-1} (PO_4) et les bandes carbonates deviennent plus intenses. Les sites de substitution de CO_3 dans l'apatite de l'os ont été localisés par spectrométrie infrarouge (El Feki *et al.* 1991; Rey *et al.* 1989, 1991a, 1991b). Rey *et al.* (1990, 1991c) ont également mis en évidence des changements structuraux dans le domaine ν3 PO_4 et ν4 PO_4 lors de la maturation d'apatites biologiques et minérales actuelles.

Outre les données fournies par les spectres sur la présence d'un composé, diverses méthodes basées sur les rapports d'intensité des bandes permettent d'accéder à d'autres types d'informations.

TERMINE & POSNER (1966) ont ainsi mis au point une méthode de calcul du taux de cristallinité (SF) à partir de la bande ν4 PO_4 située vers 600 cm^{-1} et établi une corrélation entre le taux de cristallinité et le rapport Ca/P de l'apatite. Le pourcentage en matière organique peut également être estimé grâce à divers rapports basés sur les intensités des bandes minérales et organiques (DAUPHIN 1993a, b). Les bandes minérales sont situées vers 1 030 cm^{-1} et 1 430 cm^{-1}. Celles associées à la phase organique sont vers 3 300 cm^{-1} ou 1 654 cm^{-1}. Quatre rapports peuvent être calculés d'après les intensités de ces bandes. Si les valeurs chiffrées dépendent naturellement des bandes choisies, sur une série d'échantillons donnés, les courbes obtenues sont parallèles (DAUPHIN 1993a, b). L'absence de certaines bandes sur les fossiles ne constitue donc pas un inconvénient majeur pour l'estimation de la quantité de phase organique selon cette méthode.

La désintégration de l'os de restes humains historiques a été reconnue par NEWESELY (1989), la présence de collagène (vers 3 300 cm^{-1}) n'apparaissant pas clairement dans ces spécimens.

La phase organique

Les données bibliographiques sur les bandes du collagène, détectées par diverses méthodes, dans une gamme d'ondes allant de 400 à 2 000 cm^{-1} ont été résumées par FUREDI & WALTON (1968). Généralement, la bande amide A du collagène est légèrement plus élevée que celle des autres protéines : 3 330 cm^{-1}. Toutefois, le degré d'humidité fait varier sa fréquence. Il en est de même pour les bandes amide B, amide I, II et V (SUSI *et al.* 1971). FRASER & MACRAE (1973) ont signalé en outre une faible bande vers 2 940 cm^{-1}.

WEINER & BAR-YOSEF (1990) ont constaté la conservation des protéines non collagéniques sur divers os fossiles provenant de seize sites préhistoriques. De plus, les spectres infrarouges montrent la présence d'argiles et parfois d'une phase organique semblable aux acides humiques.

CARACTÉRISATION DES SUCRES

Les données concernant la caractérisation et les quantités des poly- et monosaccharides associés aux protéines osseuses actuelles sont à la fois nombreuses et limitées. En effet, elles sont établies sur du matériel fractionné, et aucune donnée globale sur la composition en sucres élémentaires n'est fournie dans ces travaux spécialisés.

Les fractionnements chromatographiques des résidus de digestion de la phase organique par des protéases ont montré que les mucopolysaccharides acides contenaient de la chondroïtine sulfate, mais aussi du galactose, du mannose, du fucose et du xylose (HERRING 1972). Les glycoprotéines contiennent une grande variété de sucres, parmi lesquels la glucosamine, la galactosamine, le galactose, le mannose, le glucose, le fucose et des acides sialiques ont été identifiés. Deux types principaux d'hétéropolysaccharides seraient associés au collagène. En outre, la molécule de collagène elle-même est une glycoprotéine contenant des hexoses (WOODHEAD-GALLOWAY 1980).

En ce qui concerne l'os fossile, des colorations spécifiques de mucopolysaccharides ont été positives sur les coupes d'un dinosaure : *Tarbosaurus* du Crétacé supérieur du Gobi (PAWLICKI 1977), mais la composition élémentaire n'est pas précisée.

MATÉRIEL ET MÉTHODES D'ÉTUDE

MATÉRIEL

Le fragment d'astragale de bovidé fossile a été récolté lors d'une campagne de l'Angola Palaeontology Expedition (PICKFORD *et al.* 1992, 1994) dans des remplissages de fissures (plateau d'Humpata, sud de l'Angola). Il provient de la carrière de Cangalongue III, sur la rive occidentale de la vallée de Cangalongue. Le sédiment est composé de brèches grossières, contenant de nombreux fragments de stalagmites recimentées par des travertins. La présence de *Serengetilagus*, de *Gigantohyrax*, et surtout de *Metridiochoerus andrewsi* permet de dater ces gisements du Plio-pléistocène.

Le matériel de comparaison est constitué par un tibia de bœuf actuel provenant d'un élevage; il s'agit donc d'un animal assez jeune. Cet os ayant été conservé au congélateur pendant plusieurs années, il est relativement sec. Une référence supplémentaire a été utilisée : un os d'un cheval contenant encore la matrice organique non liée à l'os, incluant les cellules osseuses.

MÉTHODES D'ÉTUDE

Contrôle de la conservation de la structure osseuse

L'étude de l'état de la structure osseuse a été effectuée au microscope électronique à balayage. Des cassures brutes ou traitées avec des solutions enzymatiques ont été observées au microscope électronique à balayage (Philips SEM 505) après une métallisation à l'or palladium.

Extraction des phases organiques

Après une décontamination à l'hypochlorite de soude pendant 24 heures, les fragments osseux actuels et fossiles ont été rincés à l'eau distillée et déionisée (qualité Milli-Q), puis séchés. Ils ont ensuite été broyés afin d'obtenir une poudre de granulométrie régulière. Une partie de ces poudres a été décalcifiée à l'acide acétique à pH constant de 4. Les phases solubles et insolubles ont été séparées par centrifugation. La phase soluble a été dessalée par ultrafiltration sur une membrane Filtron de 3kDa, puis concentrée et lyophilisée. La phase insoluble est dessalée par centrifugations successives dans de l'eau (qualité Milli-Q) avant d'être lyophilisée.

La préparation de l'os fossile à l'acide acétique s'est révélée être inefficace (*cf.* « Résultats », « Phase organique insoluble »). Les poudres ont donc été décalcifiées à HCl, à un pH constant de 2. Les opérations suivantes (centrifugations, rinçages, etc.) ont été identiques à celles menées sur les spécimens actuels.

Spectrométrie infrarouge

Les poudres et les lyophilisats sont mélangés à du KBr de même granulométrie. Le mélange contenant environ 5% d'échantillon est séché dans une étuve (35 °C) pendant une nuit.

Le spectrophotomètre infrarouge à transformée de Fourier (FTIR) Perkin Elmer modèle 1600 est équipé de fenêtres en KBr et d'un accessoire à réflexion diffuse : DRIFT ou DRIFTS (Diffuse Reflectance using Infrared Fourier Transform) qui permet de travailler sur des poudres. Les modifications de la phase organique provoquées par les élévations de température et les fortes

pressions nécessaires à la confection de pastilles pour les acquisitions classiques en mode transmission sont ainsi évitées.

Le mode d'utilisation préconisé par PERKIN ELMER permet d'obtenir des spectres dont la qualité atteint celle des spectres établis par transmission. Le temps d'analyse supérieur à 4 mn correspond à 64 balayages, dans une gamme d'onde de 500 à 4000 cm^{-1}, avec une résolution nominale de 4 cm^{-1}. Le système élimine automatiquement les bandes dues à la présence de CO_2 et H_2O. Afin de rendre les spectres satisfaisant à la loi de Beer-Lambert, il est nécessaire de procéder à la conversion de Kubelka-Munk, proposée en routine par le système.

RÉSULTATS

MICROSTRUCTURES ET COMPOSITION CHIMIQUE ÉLÉMENTAIRE (Fig. 1)

La première étape dans le contrôle de l'état de conservation repose sur l'analyse microstructurale et la composition chimique élémentaire des spécimens.

L'os actuel montre la structure classique de l'os lamellaire, du système haversien et des zones à structure de type « lamellaire croisé » ou en « contreplaqué » (Fig. 1a-c). La microstructure de l'astragale fossile de Cangalongue est assez bien conservée : la disposition en lamelles (Fig. 1d, e) et des zones de résorption différentielle sont identifiables. Les cavités osseuses naturelles sont généralement dépourvues de sédiment, et aucune trace pouvant être attribuée à des micro-organismes n'a été observée (Fig. 1f). Les risques de contamination par du matériel allogène semblent réduits. La composition chimique élémentaire (microsonde électronique EDS) montre également des modifications modérées par rapport à l'os actuel : augmentation du Ca, P et Fe, légère diminution du Mg (DAVID 1994).

OS TOTAL (Tableau 1, Fig. 2)

Les spectres infrarouges des poudres d'os total actuel montrent les bandes minérales et organiques signalées dans la littérature. Les bandes minérales attribuées à PO_4 et à CO_3 sont nettement visibles (Tableau 1). Certaines bandes organiques sont présentes, mais elles ne sont pas spécifiques des protéines ou des sucres ; amide A, amide I (deux bandes), amide II (trois bandes), et amide III. Sur les poudres d'os total, certaines bandes se chevauchent. Par exemple, la présence éventuelle de sucres (1 050-1 150 cm^{-1}) est masquée par la bande minérale $\nu 3$ de PO_4 qui est toujours beaucoup plus intense.

Les spectres réalisés sur le fossile ont le même profil général que l'actuel (Fig. 2). Néanmoins, la phase minérale y semble plus abondante et plus cristalline ; ceci est particulièrement net pour les bandes CO_3. La matrice organique est également présente : les amides A, I et II sont conservés, mais avec des pics plus faibles que dans les os actuels ; la bande de protéines située à 1 474 cm^{-1} disparaît. D'après les critères de STUTMAN *et al.* (1965), aucun enrichissement en F n'est décelable dans l'os fossile.

Une déconvolution du domaine $\nu 3$ PO_4 fait apparaître différentes bandes chez le bœuf actuel. D'après REY *et al.* (1991a), les bandes vers 1 125, 1 110 et 1 020 cm^{-1} caractérisent plutôt les apatites nouvellement formées ; la bande 1 145 cm^{-1}, quant à elle, indiquerait la présence de

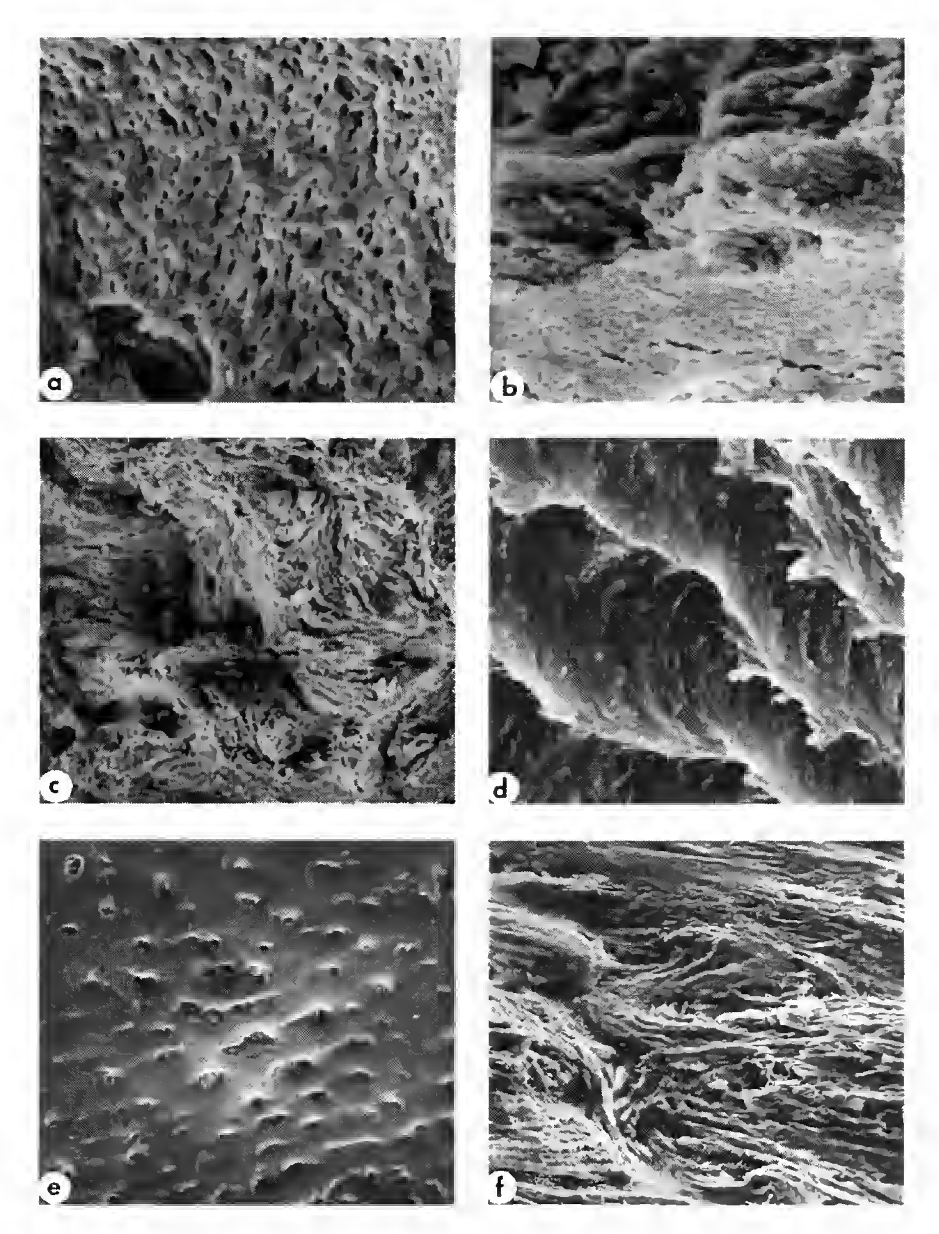


FIG. 1. — Comparaison des microstructures de l'os de bœuf actuel (a-c) et du bovidé fossile du Plio-pléistocène d'Angola (d-f) ; a, cassure oblique montrant une structure lamellaire. La phase organique a été partiellement éliminée par une solution de trypsine, dans un tampon H_2O + Hepes à pH 7,15, pendant 8 heures à 37 °C. × 302 ; b, détail de la surface de l'endéoste. Trypsine, dans un tampon H_2O + Hepes à pH 7,15, pendant 4 heures à 37 °C. × 2 400 ; c, cassure oblique montrant les changements d'orientation des fibres dans l'os lamellaire. Même préparation que b. × 2 112 ; d, cassure montrant l'organisation lamellaire, avec de nombreuses cavités. Comparer avec a. Préparation non traitée. × 273 ; e, cassure oblique montant la conservation de la disposition lamellaire de l'os, et les micropores sur la surface. Préparation non traitée. × 1 060 ; f, surface interne d'un vaisseau sanguin. La disparition partielle de la phase organique pendant la fossilisation rend distincts les micropores. Préparation non traitée. × 1 260.

TABLEAU I. — Bandes infrarouges présentes dans l'os frais (d'après FUREDI & WALTON 1968), dans le collagène, et les os actuels et fossiles de bovidés. OS : os non décalcifié, MOI : matrice organique insoluble, MOS : matrice organique soluble.

			ACTUEL			FOSSILE	
ATTRIBUTION	**LITTERA-TURE**	**COLLAGENE TYPE I**	**OS**	**MOI**	**MOS**	**OS**	**MOI**
amide A	3330	3290	3300	3290	3306	3347	3304
amide B	3060-3085	3070			3076		
COOH	1743-1734	1742					
	1680			1684		1684	
amide I	1659	1661	1654		1655	1654	1660
	1649	1641	1647	1648		1647	1653
	1632					1636	
	1559			1559	1550	1560	1558
amide II	1547	1550	1540	1540		1541	1540
		1532		1532			
	1515			1507		1507	1505
protéines	1480						
	1470						
CH2, CH3 déformations	1447-1464	1443		1457	1457		1457
CO3	*1450*		*1446*			*1457*	
	1410					*1424*	
COO	1400-1410	1402-1411			1400		1418
CH2 déformation	1378-1388						1374
protéines	1344	1343		1350	1339		
protéines	1276					1281	1280
amide III /SO4	1238	1241	1242		1240		
	1233			1225			
protéines	1204						
PO4	**1250**						
	910		**1047**			**1043**	
	1150			1128			
sucres	à						1120
	1050	1083		1061	1082		
	1028	1033			1033		1035
PO4	**960**		**960**			**963**	
CO3	*878*		*873*			*874*	
	871						
PO4	**600**		**604**			**602**	
	560		**567**			**575**	

groupements HPO_4^{2-}. Chez le fossile, les bandes 1 145, 1 125 et 1 110 cm^{-1} n'apparaissent plus; or d'après REY *et al.* (1991a), ces bandes sont les plus sensibles aux changements structuraux. Toutefois la bande 1 100 cm^{-1} également susceptible de disparaître aisément, est conservée. Selon ces auteurs, les bandes 1 125 et 1 110 cm^{-1} diminuent jusqu'à disparaître en cas d'augmentation de la cristallinité de l'apatite, ou de dissolution.

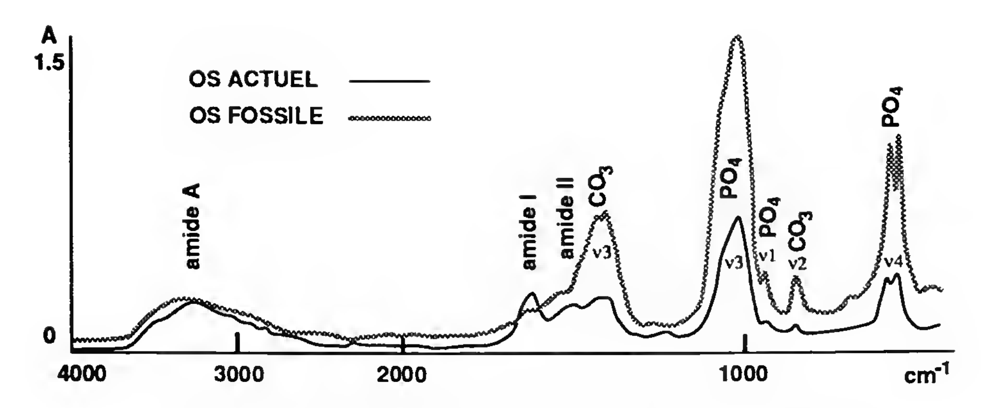


FIG. 2. — Spectres infrarouges des os de bovidés actuel et fossile non décalcifiés.

L'examen des spectres DRIFT sur poudre totale indique donc l'existence de modifications modérées dans la structure et la composition du spécimen fossile.

Les taux de cristallinité calculés d'après la méthode de TERMINE & POSNER (1966) sur l'os de bœuf actuel varient, bien que les prélèvements n'aient pas été localisés dans des zones particulières. Toutefois, la moyenne est égale à 0,10, ce qui est similaire à la moyenne obtenue sur les os de rongeurs actuels (DAUPHIN 1993a, b). Le taux de cristallinité moyen du bovidé fossile est supérieur à 0.14.

Le rapport A/CO_3 (phase organique : amide A, bande vers 3300 cm^{-1}/phase minérale, bande vers 1450 cm^{-1}) dans l'os actuel : 0,82 est similaire à la moyenne établie sur divers rongeurs. Par contre, le rapport A/PO_4 (amide A vers 3300 cm^{-1}/phase minérale vers 1030 cm^{-1}) est plus faible que chez les rongeurs, puisqu' il ne dépasse pas 0,33. Les rapports basés sur l'intensité de la bande de l'amide I (vers 1654 cm^{-1}) sont, comme chez les rongeurs actuels, plus élevés que ceux basés sur l'amide A. Ces rapports phase organique/phase minérale chez le bovidé fossile indiquent tous une diminution relative importante de la quantité de matière organique, sans que l'on puisse préciser s'il s'agit de la phase soluble ou insoluble (Fig. 3).

L'analyse DRIFT confirme les résultats des observations microstructurales et de la composition chimique élémentaire : les modifications induites par la diagenèse augmentent l'importance relative de la phase minérale par rapport à la phase organique. Toutefois, si la phase organique est présente, elle semble modifiée.

PHASE ORGANIQUE SOLUBLE (Figs 4, 5 ; Tableau 1)

La phase soluble de l'os actuel montre de nombreuses bandes : amide A vers 3305 cm^{-1}, amide B vers 3076 cm^{-1}, amide I vers 1655 cm^{-1}, amide II vers 1550 cm^{-1}, amide III vers 1240 cm^{-1}. Sont également présentes les bandes à 1457 cm^{-1}, 1400 cm^{-1} (COO^{-}), 1339 cm^{-1}, 1083 cm^{-1} (sucres), 1033 cm^{-1}, fréquement signalées dans la littérature pour les protéines. Les différences observées dans les deux spectres du bœuf et du cheval actuels, notamment la plus forte intensité des bandes de la phase organique dans le cheval, sont probablement dues à la différence de fraîcheur du matériel. Rappelons en effet que le cheval contenait la presque totalité

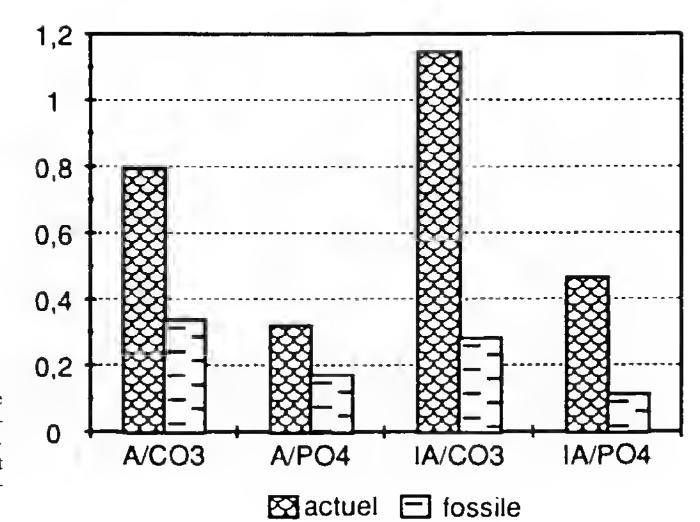


FIG. 3. — Estimation de la quantité de matière organique contenue dans les os actuel et fossile d'après les intensités des bandes organiques (A : amide A, IA : amide I) et minérales (CO_3 et PO_4) des spectres infarouges.

de la phase organique non liée à l'os. Les faibles quantités de matrice soluble extraites du bœuf fossile n'ont pas permis l'analyse par spectrométrie infrarouge.

PHASE ORGANIQUE INSOLUBLE (Figs 4, 5; Tableau 1)

La phase insoluble, majoritairement collagénique, est abondante dans les os de bœuf et de cheval actuels (Tableau 1, Fig. 4). Les différences entre le cheval et le bœuf sont moins importantes dans la phase insoluble que dans la phase soluble. La bande de l'amide A apparaît à 3 290 cm^{-1}. La bande amide B, située à 3 071 cm^{-1} sur le collagène de type I, n'est pas identifiée sur ces spectres. Deux bandes représentent l'amide I, tandis que l'amide II en montre trois. La bande à 1 457 cm^{-1} due aux déformations de CH_2 et CH_3 est généralement reconnue dans le collagène. L'amide III montre une bande vers 1 225 cm^{-1}, déjà visible dans les spectres d'os total. Dans la zone habituellement considérée comme indiquant la présence de sucres, trois bandes sont clairement apparentes : 1 128 cm^{-1}, 1 061 cm^{-1}, 1 055 cm^{-1}. Toutefois, l'attribution exacte de la bande à 1 128 cm^{-1} reste incertaine, car elle est parfois interprétée comme caractéristique des liaisons SO_4 (SUZUKI 1975). L'une des molécules contenant de telles liaisons, abondante dans les tissus osseux, est la chondroitine sulfate, mais celle-ci devrait apparaître dans la phase soluble de l'os. Ces bandes n'ont pas été mises en évidence dans le collagène de type I, seule une bande vers 1 084 cm^{-1} étant susceptible de représenter les sucres.

Le spectre de la « phase organique insoluble » obtenue par décalcification à l'acide acétique du bœuf fossile est pratiquement identique à celui des poudres totales. Les bandes de la phase minérale sont toutes présentes et très intenses. Par contre, les spectres de la matrice insoluble fossile résultant de la seconde décalcification (HCl) offrent la même allure générale que ceux

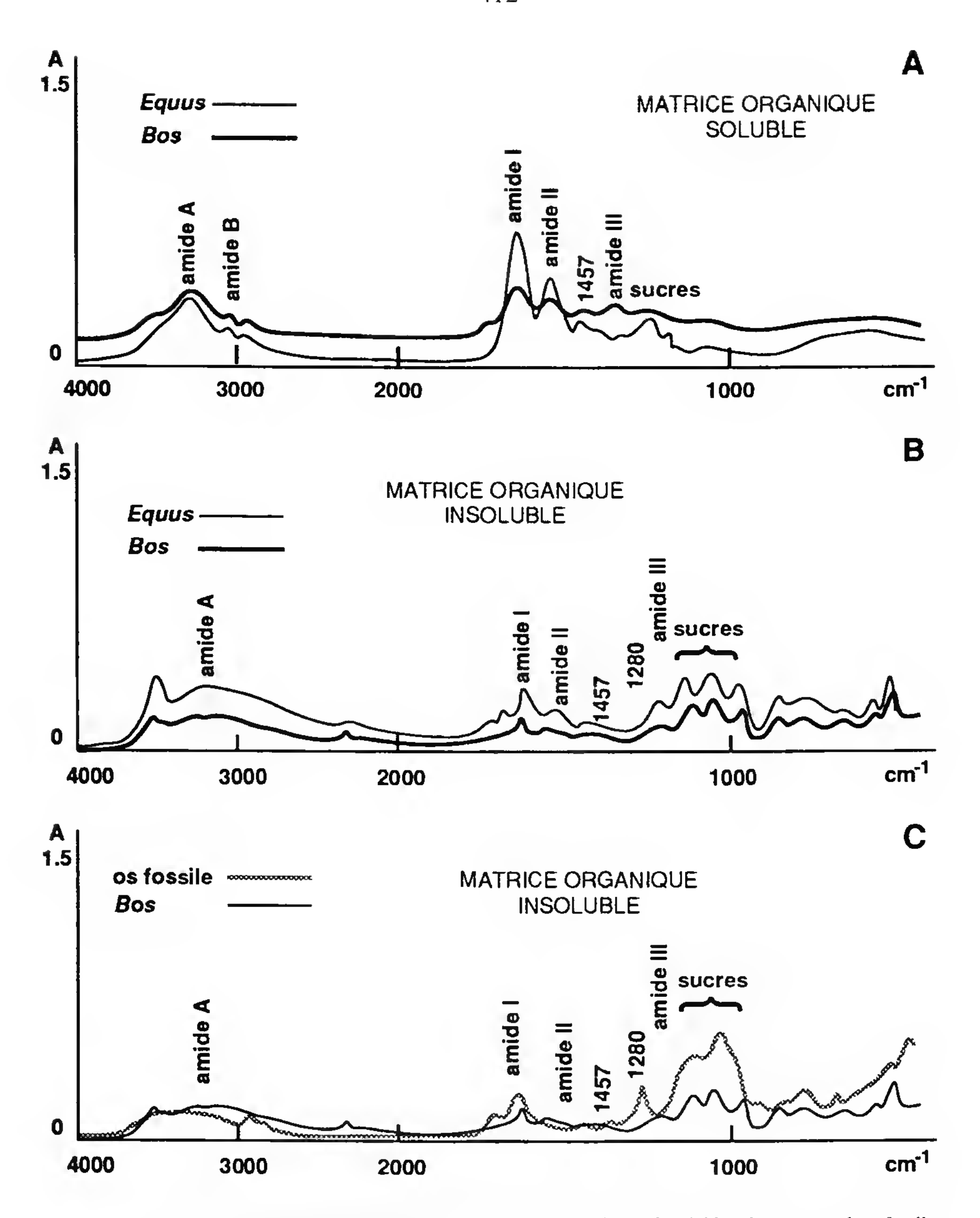


FIG. 4. — Spectres infrarouges des phases organiques solubles et insolubles des os actuel et fossiles.

des spécimens actuels (Fig. 4); ils se caractérisent néanmoins par une bande amide I (vers 1 651 cm^{-1}) et une bande amide III (vers 1 280 cm^{-1}) plus fortes. Une très légère fraction minérale persiste cependant dans les domaines ν4 PO_4 et donc peut-être au niveau de la zone d'apparition des sucres (ν4 PO_4).

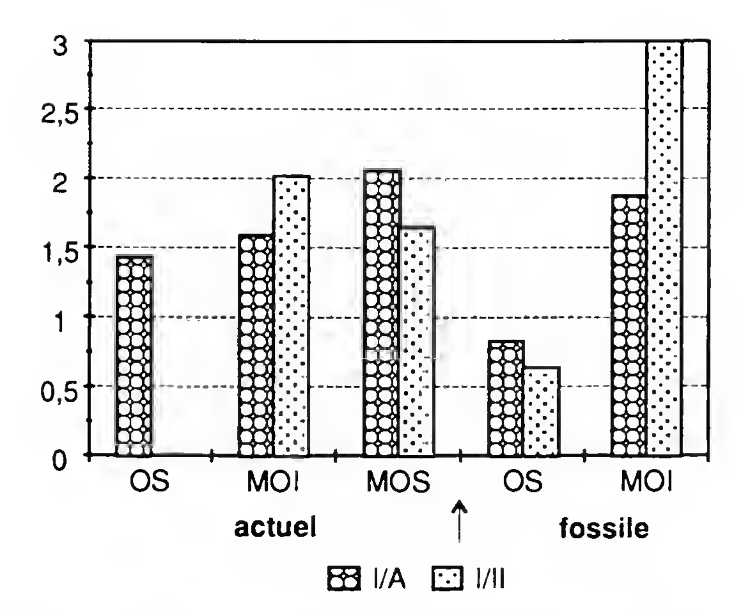


FIG. 5. — Estimation de la composition des phases organiques des os actuels et fossiles d'après les intensités des bandes organiques. OS : os non décalcifié ; MOI : matrice organique insoluble ; MOS : matrice organique soluble ; I : amide I ; A : amide A ; II : amide II.

CONCLUSION

D'un point de vue méthodologique, l'utilisation de l'analyse DRIFT permet une estimation rapide et assez complète de l'état de conservation d'un os fossile. Effectuée sur une simple poudre, sans autre préparation qu'une décontamination préalable, cette méthode permet d'apprécier les modifications de composition aussi bien de la phase minérale que de la phase organique. Elle nécessite très peu de matériel, et celui-ci peut être réutilisé par élimination du KBr, soluble dans l'eau. Il est donc possible, sur des os de grande taille, d'effectuer des prélèvements ponctuels localisés afin d'établir une cartographie de la diagenèse et/ou un choix des zones à étudier de façon plus détaillée.

Du point de vue des résultats, les spectres DRIFT ont tout d'abord permis de mettre en évidence que la méthode de décalcification utilisée pour l'os actuel ne convenait pas aux spécimens fossiles, malgré les indices de bonne conservation fournis par l'analyse microstructurale et la composition chimique élementaire : la phase « organique insoluble » du fossile est pratiquement identique à la poudre non décalcifiée. Dès cette phase de l'analyse, des altérations sont ainsi mises en évidence. Des résultats similaires ont été obtenus sur d'autres os fossiles provenant de sites d'âge et de sédimentologie très variés.

Dans le bovidé fossile, la présence de protéines indiquée par les bandes amides détectées sur les spectres a été confirmée par la fluorescence UV et les analyses en acides aminés (DAVID 1994). Par ailleurs, les modifications de la composition de la phase organique décelée par les

rapports amide I/amide A et amide I/amide II dans les spectres DRIFT des phases organiques isolées (Figs 4, 5) peuvent être mises en rapport avec les altérations des teneurs en acides aminés par rapport aux phases organiques du bœuf actuel. En ce qui concerne plus particulièrement les sucres, leur présence est généralement masquée par les larges bandes intenses du PO_4 entre 910 et 1 250 cm^{-1}. Il est donc nécessaire, pour détecter leur présence, de décalcifier les poudres. Là encore, les spectres DRIFT ont mis en évidence la présence de sucres chez le fossile, tout en indiquant des modifications par rapport au bœuf actuel.

En ce qui concerne le fossile, les phases organiques sont nettement modifiées par rapport à l'actuel. Ceci est en accord avec les résultats obtenus sur la composition en acides aminés des mêmes spécimens, montrant que les modifications des phases solubles et insolubles n'étaient pas identiques (DAVID 1994).

Remerciements

Les auteurs tiennent à remercier les nombreuses personnes qui ont permis la réalisation de la campagne de terrain en Angola en 1990. En France : Prof. Y. COPPENS et Prof. P. TAQUET ; en Angola : Dr S. AÇO (co-directeur de l'expédition) et J. FERREIRA (directeur du Museu Regional da Huila), ainsi que A. M. OLIVEIRA, M. BATALHA, V. COELHO, E. FREIRE, P. BONDO, R. GOMES, R. DA SOUZA, J. EDOUARDO, A. SAKATENGO, S. TCHIHONGA, J. KATCHATCHA et T. M. GOMES, et Son Excellence l'ambassadeur de France à Luanda, M. S. FILLIOL et M. E. ROLAND, conseiller à la Coopération, ainsi que toute son équipe ; Son Excellence l'ambassadeur de la République populaire d'Angola à Paris et son équipe ; M. J. BLACKSHEAR, directeur de CONOCO ANGOLA et son équipe.

Manuscrit soumis pour publication le 21 mars 1995 ; accepté le du 29 novembre 1995.

RÉFÉRENCES

DAUPHIN Y. 1993a. — Spectrométrie infrarouge (DRIFT) des os de rongeurs fossiles de Tighenif (Pléistocène, Algérie). *Paläontologische Zeitschrift* **67** (3-4) : 377-395.

— 1993b. — Potential of the Diffuse Reflectance Infrared Fourier Transform (DRIFT) method in paleontological studies of bones. *Applied Spectroscopy* **47** (1): 52-55.

DAVID H. 1994. — État diagénétique des os de quelques mammifères fossiles du plateau d'Humpata (Plio-pléistocène, Angola). Mémoire de D.E.A., Université de Montpellier 2, 59 p. inédit.

EL FEKI H., REY C. & VIGNOLES M. 1991. — Carbonate ions in apatites : infrared investigations in the v_4 CO_3 domain. *Calcified Tissue International* **49**: 269-274.

FRASER R. D. B. & MACRAE T. P. 1973. — Conformation in fibrous proteins and related synthetic polypeptides. *In* B. HORECKER, N. O. KAPLAN, J. MARMUR & H. A. SCHERAGA (eds). *Molecular Biology*, Academic Press, London, 628 p.

FUREDI H. & WALTON A. G. 1968. — Transmission and attenuated total reflection (ATR) infrared spectra of bone and collagen. *Applied Spectroscopy* **22**: 23-26.

HERMAN H. & DALLEMAGNE M. J. 1964. — Les carbonato-hydroxylapatites et le carbonate des os et des dents étudiés par la spectrophotométrie infrarouge. *Bulletin de la Société de chimie biologique* **46** (2-3) : 371-383.

HERRING G. M. 1972. — The organic matrix of bone. *In* G. H. BOURNE (ed). *The Biochemistry and Physiology of Bone*, Academic Press, New York **1**: 127-189.

NEWESELY H. 1989. — Fossil bone apatite. *Applied Geochemistry* **4**: 233-245.

PAWLICKI R. 1977. — Histochemical reactions for mucopolysaccharides in the Dinosaur bone. Studies on epon- and methacrylate-embedded semithin sections as well as on isolated osteocytes and ground sections of bones. *Acta histochemica* **58**: 75-78.

PICKFORD M., MEIN P. & SENUT B. 1992. — Primate bearing Plio-Pleistocene cave deposits of Humpata, Southern Angola. *Human Evolution* **7** (1): 17-33.

— 1994. — Fossiliferous Neogene karst fillings in Angola, Botswana and Namibia. *Southern African Journal of Sciences* **90**: 227-230.

REY C., COLLINS B., GOEHL T., DICKSON I. R. & GLIMCHER M. J. 1989. — The carbonate environment in bone mineral : A resolution-enhanced Fourier Transform infrared spectroscopy study. *Calcified Tissue International* **45**: 157-164.

REY C., SHIMIZU M., COLLINS B. & GLIMCHER M. J. 1990. — Resolution-enhanced Fourier Transform infrared spectroscopy study of the environment of phosphate ions in the early deposits of a solid phase of calcium-phosphate in bone and enamel, and their evolution with age. 1. Investigations in the v_4 PO_4 domain. *Calcified Tissue International* **46**: 384-394.

REY C., RENUGOPALAKRISHNAN V., SHIMIZU M., COLLINS B. & GLIMCHER M. J. 1991a. — A resolution-enhanced Fourier Transform infrared spectroscopic study of the environment of the CO_3^{2-} ion in the mineral phase of enamel during its formation and maturation. *Calcified Tissue International* **49**: 259-268.

— 1991b. — Fourier Transform infrared spectroscopic study of the carbonate ions in bone mineral during aging. *Calcified Tissue International* **49**: 251-258.

REY C., SHIMIZU M., COLLINS B. & GLIMCHER M. J. 1991c. — Resolution-enhanced Fourier Transform infrared spectroscopic study of the environment of the phosphate ion in the early deposits of a solid phase of calcium phosphate in bone and enamel and their evolution with age : 2. Investigations in the v_3 PO_4 domain. *Calcified Tissue Int*ernational **49**: 383-388.

STUTMAN J. M., TERMINE J. D. & POSNER A. S. 1965. — Vibrational spectra and structure of the phosphate ion in some calcium phosphates. *Transaction of the New York Academy of Science*, ser. II, **27** (6): 669-675.

SUSI H., ARD J. S. & CARROLL R. J. 1971. — The infrared spectrum and water binding of collagen as a function of relative humidity. *Biopolymers* **10**: 1597-1604.

SUZUKI M. 1975. — Studies on the physicochemical nature of hard tissues. Infrared, N.M.R., X-ray diffraction investigation of hydroxyl-radical, crystalline water and carbonate substitution in biological apatites. *In Physico-chimie et cristallographie des apatites d'intérêt biologique*, Colloques Intern. C.N.R.S., n° 230, Paris : 77-83.

TERMINE J. D. & POSNER A. S. 1966. — Infrared analysis of rat bone : age dependency of amorphous and crystalline mineral fractions. *Science* **153**: 1523-1525.

WEINER S. & BAR-YOSEF O. 1990. — States of preservation of bones from prehistoric sites in the Near East : a survey. *Journal of Archaeological Science* **17**: 187-196.

WOODHEAD-GALLOWAY J. 1980. — *Collagen: the anatomy of a protein*. Institute of Biology's Studies in Biology **117**: 60 p.

Bulletin du Muséum national d'Histoire naturelle, Paris, 4e sér., **18**, 1996
Section C, nos 2-3 : 417-450

Rooting ungulates within placental mammals : Late Cretaceous/Paleocene fossil record and upper molar morphological trends

by Leandro O. SALLES

Abstract. — Basal ungulate interrelationships (Cretaceous/Paleocene condylarths) are seen here in a broader placental mammal phylogenetic context and based on a cladistic scrutiny of the upper molar morphology. After running the ie* option of the Hennig86 software and applying the successive weighting algorithm for a sample of 19 taxa and 23 characters, a fully resolved branching diagram came out as result with 18 components. Under parenthetical notation the relationships obtained are the following : (*Pappotherium* (*Prokennalestes* (*Bobolestes* (*Kennalestes* (*Cimolestes* (*Prototomus* (*Miacis* (*Proviverra* (*Zalambdalestes* (*Leptictis* (*Scenopagus* ((*Paramys* and *Eosigale*) (*Purgatorius* and *Palaechthon*)) (*Oxyprimus* (*Dysnoetodon* (*Protungulatum* and *Mimatuta*))))))))))))))). Although it is questionable whether some very basal condylarths are indeed exclusive stem groups of ungulates, the results of this study support the monophyly of ungulates. Ungulata is viewed as a member of a large clade, named Magnorder Herbotheria, and comprising Anagalida (*sensu* STUCKY & MCKENNA 1993 and here represented by rodents and anagalids), Archonta (represented by plesiadapiformes), and Ungulata (exclusively represented by four basal condylarths).

Key-words. — Cretaceous/Paleocene, placentals, basal ungulates, upper molar morphology and parsimony analysis.

L'enracinement des ongulés dans les mammifères placentaires : les données fossiles du Crétacé supérieur et du Paléocène et les tendances morphologiques des molaires supérieures

Résumé. — Une analyse cladistique fondée sur la morphologie des molaires supérieures est proposée. Il s'agit des relations basales des ongulés (condylarthres du Crétacé Supérieur/Paléocène) vues dans le contexte phylogénétique plus large des placentaires. Après avoir utilisé l'option ie* du logiciel Hennig86 et appliqué la pondération successive pour un échantillon de 19 taxons et 23 caractères, un arbre complètement résolu avec 18 composants émerge comme résultat. Sous annotation parenthétiques les relations phylogénétiques obtenues sont les suivantes: (*Pappotherium* (*Prokennalestes* (*Bobolestes* (*Kennalestes* (*Cimolestes* (*Prototomus* (*Miacis* (*Proviverra* (*Zalambdalestes* (*Leptictis* (*Scenopagus* ((*Paramys* and *Eosigale*) (*Purgatorius* and *Palaechthon*)) (*Oxyprimus* (*Dysnoetodon* (*Protungulatum* and *Mimatuta*))))))))))))))). Bien qu'il soit discutable que certains condylarthres basaux apparaissent comme groupes souches propres aux ongulés, les résultats de cette étude appuient la monophylie des ongulés. Le taxon Ungulata est compris comme membre d'un grand clade, ici nommé Mégaordre Herbotheria qui comprend les Anagalida (*sensu* STUCKY & MCKENNA 1993 et représenté par les rongeurs et anagalidés), les Archonta (représentés par les plésiadapiformes) et les Ungulata (représentés par quatre condylarthres basaux). Une série d'autres analyses de parcimonie sont également présentées, mais aucun des résultats obtenus n'est en contradiction avec celui représenté dans l'annotation parenthétique.

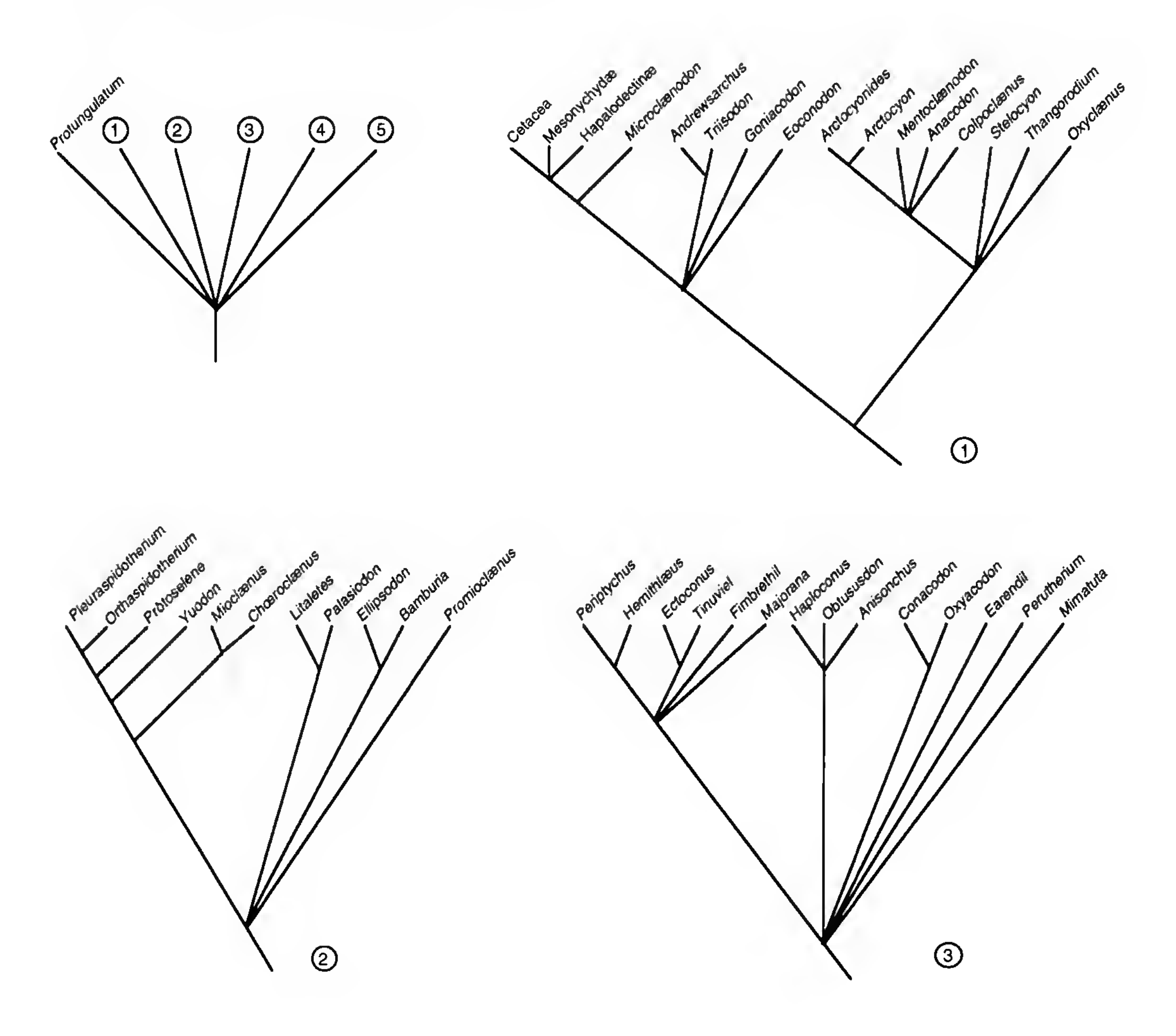
Mots-clés. — Crétacé/Paleocène, placentaires, ongulés et morphologie des molaires supérieures, analyse de parcimonie.

L. O. SALLES, *Muséum national d'Histoire naturelle, Laboratoire de paléontologie, 8 rue de Buffon, F-75231 Paris cedex 05.*

SCOPE

The monophyly of ungulates is one of the ongoing debates regarding high interrelationships of placental mammals. Available evidence supporting the monophyly of ungulates was characterized by NOVACEK *et al.* (1988) as "embarrassingly poor", and since then not much has been achieved. Nevertheless, after the first attempt to examine the mammalian phylogenetic relationships under a cladistic framework (MCKENNA 1975), approximately the same large ungulate groups have been lumped together in a monophyletic group. The latest two broad phylogenetic analysis on ungulate relationships are proposed by PROTHERO *et al.* (1988) and ARCHIBALD (1994).

In this essay, basal ungulate interrelationships are approached taking into account late Cretaceous/Paleocene condylarths as well as a set of basal placental mammals as a mean of



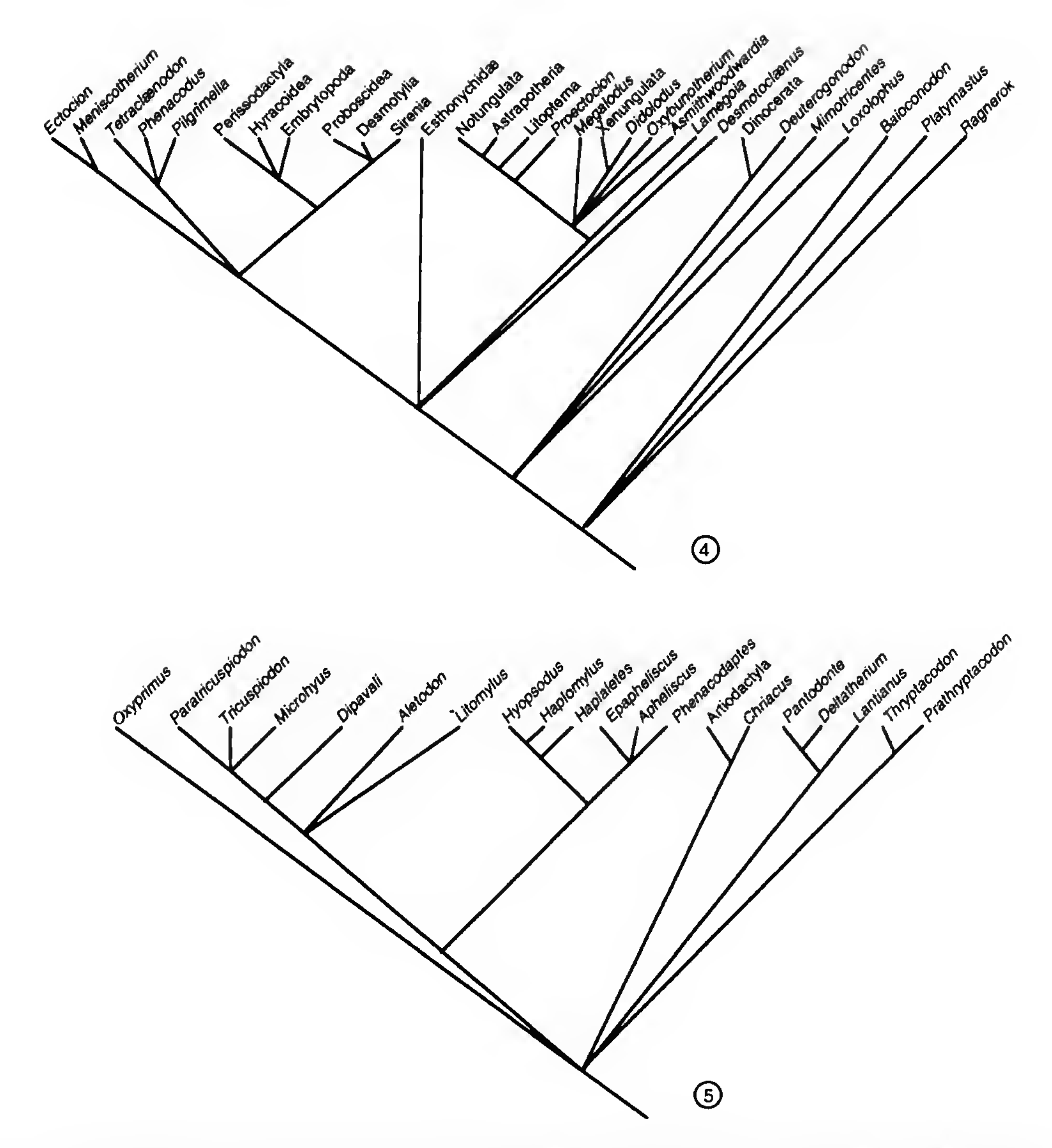


FIG. 1. — Branching diagram derived from the evolutionary schemes of VAN VALEN (1978) for ungulate interrelationships. Five major groups are recognized and all of them are directly rooted at the basal node numbered 0 together with the Late Cretaceous genus *Protungulatum*. This is the major overall analysis of ungulates centered on condylarths preceding that of PROTHERO *et al.* (1988).

placing ungulates in a broader phylogenetic context. The identity of condylarths has for decades been a controversial subject, and it is nowadays widely cited as an example of a mammalian "waste basket". Condylarths as conceived by VAN VALEN (1978) comprise an assemblage of highly diverse taxa distributed within the boundaries of the Ungulata (see Fig. 1 for a cladistic

synthesis of the evolutionary schemes proposed by VAN VALEN). In this synthesis five major clades are assigned and all of them are rooted at the basal node together with the genus *Protungulatum*. It is to be noted that Pantodonta is placed within the large clade (5) where *Oxyprimus* is assumed to be the basal taxon. Here, we indeed support the traditional view of condylarths as a paraphyletic complex placed as stem group to a number of high rank ungulate taxa. This point of view agrees with PROTHERO *et al.* (1988) and ARCHIBALD (1994). A detailed discussion of condylarth interrelationships is the subject of a monograph in preparation.

This paper is focused on the upper molar morphology of the condylarths considered to be basal with respect to the entire clade Ungulata. The justification for selecting the dental morphology is simply because a great majority of the late Cretaceous/Paleocene fossil records are fundamentally known from fragments of maxilla and lower jaw. Therefore, the idea here is to put forward a preliminary phylogenetic hypothesis of these basal condylarths in a broader placental mammal context, avoiding problems of missing data. Moreover, this note is conceived as a cladistic test to whether molar morphology (internal congruence) can yield somewhat well resolved trees with significant consistency and retention indices.

By considering just the upper molars, this phylogenetic analysis is also free from assumptions of morpho-functional independence between the upper an lower teeth. Generalizations regarding the upper molar morphology are based on the invariable mophology (the basal topographical pattern) among the three upper molars and focus on the second upper molar tooth.

The terminology applied follows BROWN & KRAUS (1979), CROMPTON & KIELAN-JAWOROWSKA (1978), HERSHKOVITZ (1971), and MINGZHEN *et al.* (1975) (Fig. 2). The notion of upper and lower levels are inverted in order to facilitate the normal tendency with dental fragments: the base of the maxilla is read as the lower level and the crown shearing surfaces as the upper level. In this research for molar homologies within placentals, no morpho-functional analysis is performed and therefore shearing surfaces are not considered.

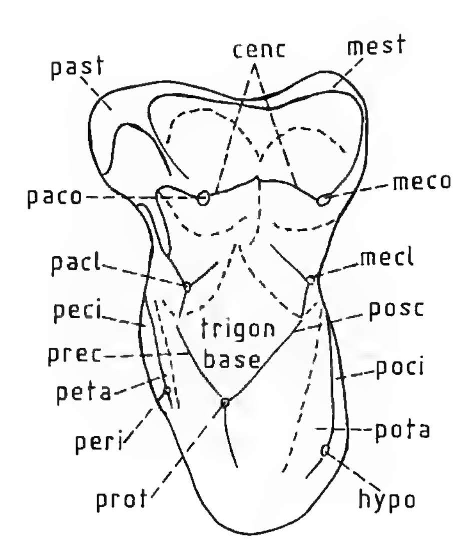


FIG. 2. — Placental upper molar dental nomenclature partially based on BOWN & KRAUS (1979). The abbreviations used here are applied throughout this article, and they are the following: cenc = centrocrista; past = parastyle; mest = mesostyle; paco = paracone; meco = metacone; pacl = paraconule; mecl = metaconule; peci = precingulum; poci = postcingulum; prec = preprotocrista; posc = postprotocrista; peta = pretalon; pota = post-talon; peri = pericone; hypo = hypocone; prot = protocone.

An assemblage of basal placentals is selected in order to allow different hierarchical levels of comparison within Placentalia. The classification of STUCKY & MCKENNA (1993, Fig. 3) is then utilized for sampling the following selection of placental mammals, taken as representative of the major placental clades and considered as terminal taxa: *Pappotherium* (the only non-placental, a lower Cretaceous metatherian); four leptictids – *Prokennalestes*, *Bobolestes*, *Kennalestes*, and *Leptictis*; four basal feraeans *Cimolestes*, *Prototomus*, *Proviverra*, and *Miacis*; one lipotyphlan – *Scenopagus*; three anagalids – *Zalambdalestes*, *Eosigale*, and *Paramys*; and two basal archontans (plesiadapiformes) – *Purgatorius* and *Palaechthon*. *Pappotherium* considered to be representing the Metatheria and therefore assumed to be the sister group of the assemblage of placental mammals listed. The character polarizations performed here are often supported by comparisons with the genus *Sulestes*, assumed to be rooted at the same basal trichotomy from which *Pappotherium* and placentals are branching off. Therefore, *Sulestes* serves in this analysis as an another outgroup.

In the data matrix analyzed, only *Pappotherium* is included, because the notion here applied of a basal metatherian are mostly driven from detailed examinations of the *Pappotherium* molar morphology. The reason for including a metatherian in the analysis of parsimony here performed is simply to have means to appreciate the bearing of the upper molar morphology on the matters concerning the monophyly of placental mammals. The character polarity is based on the study

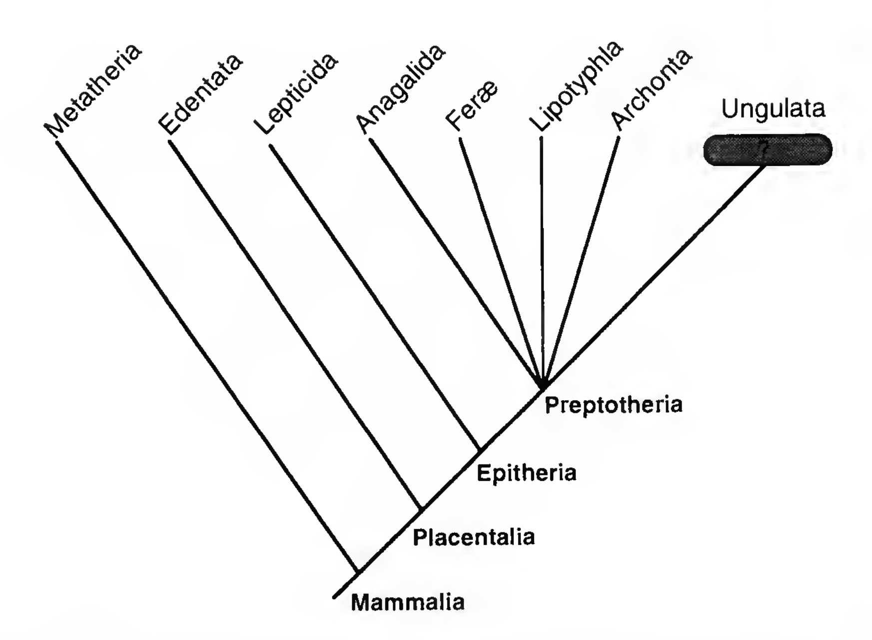


FIG. 3. — Branching diagram derived from the classification of STUCKY & MCKENNA (1993). The question mark over the Ungulata clade emphasizes problems regarding ungulate monophyly and interrelationships. In fact, STUCKY & MCKENNA's classification does indeed question the frequently accepted notion of Ungulata. But, the polytomy for the component Preptotheria does reflect the broad controversy that has taken place in the last ten years regarding high placental interrelationships. In the results section these matters are addressed.

of non-therian mammals, *Pappotherium* being only minimally different from the postulated morphology of the ancestral morphotype of therian mammals.

Based on preliminary evidence concerning ratios of parallelisms and convergences of the dental morphology between ungulates and other placentals, it is decided here to limit the number of ungulates to be studied to just a few genera that seems really to represent basal ungulate forms. Thus at this preliminary stage of our research programme on ungulate basal interrelationships, just four basal condylarths are examined: *Protungulatum* Sloan & Van Valen, 1965; *Mimatuta* Van Valen, 1978; *Oxyprimus* Van Valen, 1978; and *Dysnoëtodon* Zhang, 1980 (the taxonomic status of this genus is addressed below). Hence, the rooting context of ungulates is here addressed in the light of these four genera.

There follows a discussion of all upper molar attributes considered to be phylogenetically informative at the basal placental mammal level; and the assignments regarding their taxonomic ranges are of course limited to the very sample of taxa described above.

CHARACTER ANALYSIS

The morphological complex scrutinized in this cladistic analysis is the upper molar morphology and mainly focused on patterns of change preceding and related to the emergence of the ungulates. The character state distributions of the terminal taxa are shown in the data matrix (Table 1), and are only partially referred in this section. The character polarizations are based on the comparison between tribosphenic and non-tribosphenic mammals (*sensu* CIFELLI 1993). The "ancestral morphotype" of tribosphenic mammals is doubled in data matrix, this is due to the fact that the program Hennig86 roots networks with outgroups on the initial hypothesis that the basal node is a trichotomy. Referring of non-placental mammals, the character polarizations are more accurately determined when using *Pappotherium* rather than *Sulestes* as outgroup, because the former has been studied in more detail. In a few cases, it was not possible to establish the homologous condition in the outgroups. This is generally due to the fact that the outgroups lack or have the structure(s) evolved in the particular character formulation in a rudimentary stage of development. For a few features described, it is uncertain whether or not they are aspects of the same character. But, as far as their variation is concerned, it is argued that although some clear functional correlations can be observed they seem to vary as independent phylogenetic units.

Given the preliminary scope of this article and the complex literature regarding the dental patterns of placental mammals, the characters listed below are not formally referred to previous discussions. Thus, for a number of features, a series of previous interpretations have been proposed. The originality of some of those attributes relies on the way they have been formalized, or on the manner the character state partition has been formulated. Nevertheless, the pertinent literature is followed as much as possible. A few of the characters listed below seem to represent new topographical relationships, for instance characters 9 and 21. It is important to bear in mind that some of the qualitative multistate characters proposed below might be better formulated in

the context of a set of specific measures. However, only small samples of each terminal taxa have been available, making it spurious to attempt a detailed quantitative study.

TABLE 1. — Data matrix for 23 of the 26 characters formulated for placental mammals. Note therefore that the three autapomorphies referent to characters 16, 20, and 25 are excluded from this matrix. The numbered characters are described in the text.

```
Data Matrix
Characters :      00000000011111111122222
                  12345678901234578912346
-----------------------------------------
Hyp. anc. 1       00000000000000000000000
Hyp. anc. 2       00000000000000000000000
Pappotherium      00001000000000000000000
Prokennalestes    11002100000000010100000
Bobolestes        21001100100000011200000
Kennalestes       21003210210000011100000
Leptictis         32123210320100111200000
Scenopagus        21224221320100111200000
Cimolestes        21013210200000011301000
Prototomus        21013210210100111201200
Proviverra        22123211210101011301100
Miacis            22111111220201111200100
Purgatorius       22224222320210211200011
Palaechthon       22224222320210211200011
Zalambdalestes    33224211200000001200001
Eosigale          4212422242222020?300002
Paramys           42333223422220212200003
Protungulatum     32224222320200113110001
Dysnoetodon       22223222320201213110001
Oxyprimus         32224222320200221210002
Mimatuta          32224221321210113210001
```

1. Stylar shelf, labial extension (Fig. 4).

The stylar shelf is characterized by the crown expansion labially to the paracone and metacone. The contraction of this shelf is widely considered to be related to the early evolutionary history of placental mammals. The reduction of the stylar shelf is thus hypothesized as a derived unique feature for the Placentalia. Here, this reduction trend is interpreted as comprising a transformation series of five character states.

They are the following: (0) – well-developed, considerably labially expanded; (1) – partially contracted; (2) – reduced, all along its sagittal extension; (3) – residual or very narrow, displaying like a thin border labially to the two cones; (4) – nearly absent, the labial walls of the paracone and metacone forming the very labial portion of the crown. The extremes of this trend are clearly illustrated by the configuration found in *Pappotherium*, representing the primitive state 0, and by *Paramys* for the extremely derived one.

2. Paracone and metacone, height.

It is considered that a trend towards reduction in height of the paracone and metacone takes place within placentals. Therefore, this feature is formulated to stand for the paracone and metacone patterns of height above the basal plane of the crown.

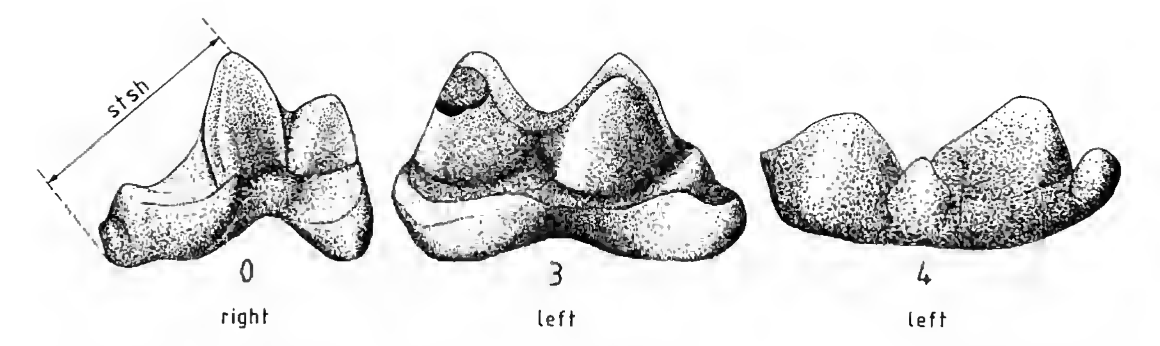


FIG. 4. — Stylar shelf, development (character 1): state 0, *Pappotherium* (anterior toward right); state 3, *Protungulatum* (anterior toward left); state 4, *Paramys* (anterior toward left); stsh = stylar shelf lateral dimension. This dimension permits a lateral perception of the labial projection of the stylar shelf. Labial view.

Three character states are hypothesized: (0) – paracone and metacone very high; (1) – high; (2) – low, or simply not characteristically high; (3) – considerably reduced in height.

The condition found in *Pappotherium* (Fig. 6) is a good example of that interpreted as state 0 and *Protungulatum* (Fig. 6) of that viewed as state 2.

3. Paracone and metacone, relative positions (Fig. 5).

The character state distributions observed here seem to covary with those of character 2. The degree of contact between the internal walls of these two cups ranges from a full contact where the two parts merge with one another to a condition where they are completely apart; the latter is present in *Paramys*.

Hence, four states are formulated: (0) – the two internal walls in full contact, with their base portions somewhat emersed in one another; (1) – clearly in contact to one another; (2) – closely placed, maintaining some contact only at the extremities of their basal portions; (3) – completely apart from one another.

4. Centrocrista, development.

This crista is located in between the paracone and metacone, and connects the upper surfaces of these two cusps. The development of this crista includes its width and height.

Four character states are formalized: (0) – well-developed; (1) – developed; (2) – not conspicuously developed or simply poorly developed; (3) – absent. The state 3 is uniquely displayed by the considered rodent, *Paramys*.

In principle, the fact that in *Paramys* these two cusps are widely apart does not prevent the existence of a centrocrista. There seems to exist a topographical dependence between this feature and the one numbered 3, which turns the judgment of the degree of development of the centrocrista quite complex sometimes.

5. Protocone, overall size (Fig. 6).

In order to have a better understanding of the spectrum of variation regarding the evolution of the hypocone, the polarization of this character makes reference to non-tribosphenic mammals

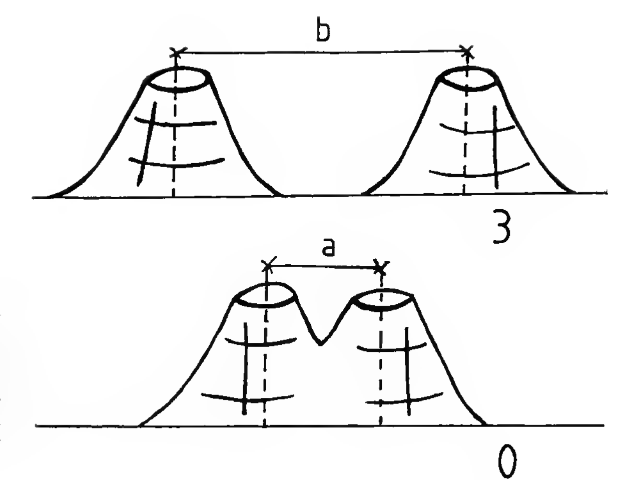


FIG. 5. — This scheme illustrates trends regarding the paracone metacone relative positions (character 3): state 0, the distance *a* reflects a condition where the two cones are very close to one another having full contact between their internal walls; state 3, represents a condition where the two cones are away a part with the distance *b* reflecting it. The scheme under state 3 is derived from the genus *Paramys*.

(this is the only case where the character polarity is determined referring to basal mammals other than *Pappotherium* and *Sulestes*).

Therefore the primitive character state (0) is considered to be the absence of the protocone, as represented by non-tribosphenic mammals. The degrees of development of the protocone are

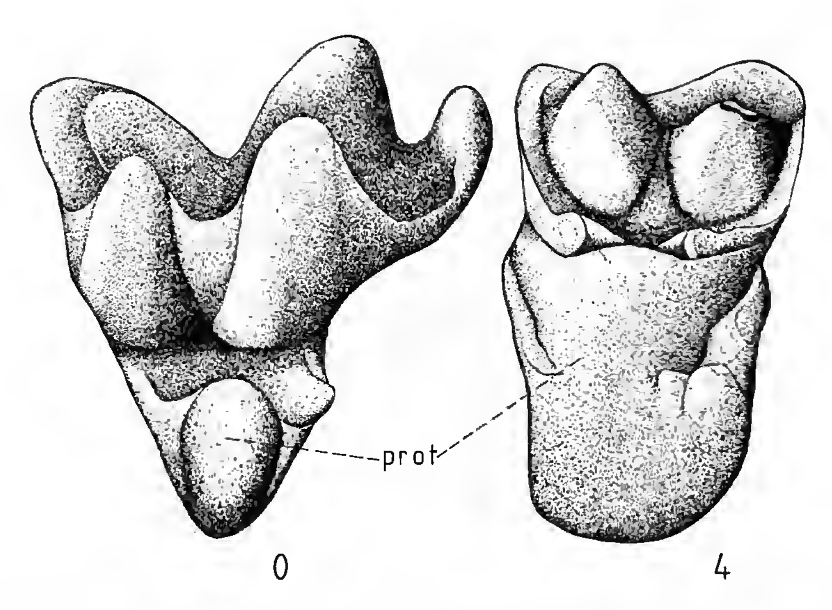


FIG. 6. — Protocone, overall development (character 5): state 0, poorly developed, *Pappotherium* (anterior toward right); state 4, well-developed, considerably larger than the paracone and metacone, *Protungulatum* (anterior toward left). Linguo-occlusal view.

formulated in reference to the size of the paracone and metacone, and the condition found in *Pappotherium*, where the protocone is very reduced in relation to either one of the two cusps represents the derived character state, coded as (1). There, the protocone displays more like an accessory cusp rather than a major cusp encompassing a significant part of the crown area. State (2) is an intermediate condition where the protocone emerges as a main cusp but not as developed as the paracone or the metacone. The other states demarcate a shift in these cusp size relationships, where the protocone is larger (3) or considerably larger (4) than the paracone and metacone. State 4 is widely distributed within ungulates.

6. Protocone, transverse expansion.

This is a feature broadly discussed in the literature (*e.g.* CIFELLI 1993), here divided into three states: (0) – protocone poorly expanded transversely, more like an accessory than a major lingual cusp of the crown, and so relatively poorly developed in relation to the paracone and metacone; (1) – protocone transversely expanded; and (2) – protocone with a well-developed transverse expansion. The formalization of this character is not simple, given the myriad of possible intermediate degrees of expansions and reductions due to the well-known plasticity of this dental region in placentals. Nevertheless, it seems clear that a major transverse expansion is related to the evolution of basal placentals. However, until better phylogenetic hypotheses become available regarding the sister-group relationship of placentals, it is doubtful whether or not the transverse expansion of the protocone is homologous with that found in some metatherians. MARSHALL & KIELAN-JAWOROWSKA (1992) and CIFELLI (1993) discussed metatherian-eutherian interrelationships and arrived at contradictory results. Briefly, CIFELLI presented the metatherians as paraphyletic whereas MARSHALL & KIELAN-JAWOROWSKA viewed metatherians as monophyletic.

7. The mesiodistal dimension of the crown, where the protocone labial face meets the crown margin (Fig. 7).

In order to better visualize this morpho-change, it is important to understand that the antero-posterior expansion of the mesiodistal dimension might be the result of two independent

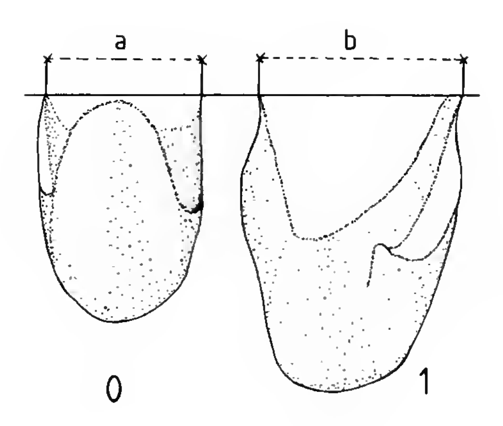


FIG. 7. — Schematic drawings for the mesiodistal dimension of the crown (character 7): state 0, poorly expanded; state 1, expanded. The two drawings are derived respectively from *Kennalestes* (distance *a*) and *Leptictis* (distance *b*), and *b* is to be read larger than *a*. Lingo-occlusal view.

events. Here, the first one is represented by the character 7 and the other by the next one numbered 8, which accounts for the antero-posterior enlargement of the lingual portion of the protocone. These events are normally read as composing one single character as formulated by CIFELLI (1993).

At this stage, it seems that three states are distinguishable: (0) – poorly expanded, condition found in *Pappotherium* and *Sulestes*; (1) – expanded, condition widespread among placentals; (2) – greatly expanded.

8. Protocone, antero-posterior expansion of the very lingual portion relative to the mesiodistal dimension of the crown (Fig. 8).

As previously discussed in character 7, the antero-posterior enlargement includes two independent expansion events. Here, the transformation series is composed of four states: 0 – extremely poorly expanded; (1) – slightly expanded; (2) – well-expanded; (3) – greatly expanded. The development of the hypocone and pericone are not placed as part of this protocone expansion. Figure 9 exemplifies the problems of interpretation that may result when the development of these cones are added to account for the protocone expansion. The lingual portion of the crown changes when these cones are present, however, they should be examined independently.

9. Protocone, labial wall and the trigon base (Fig. 10).

This feature accounts for the development of the protocone labial portion, and the paracone and metacone are used as topological reference points.

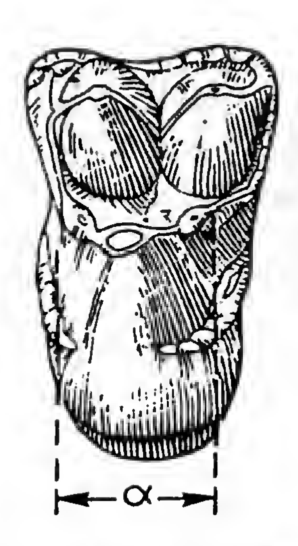


FIG. 8. — Protocone, antero-posterior expansion of the very lingual portion (character 8): the distance α represents the derived state 2 and is illustrated by the condition found in genus *Protungulatum* (anterior toward left).

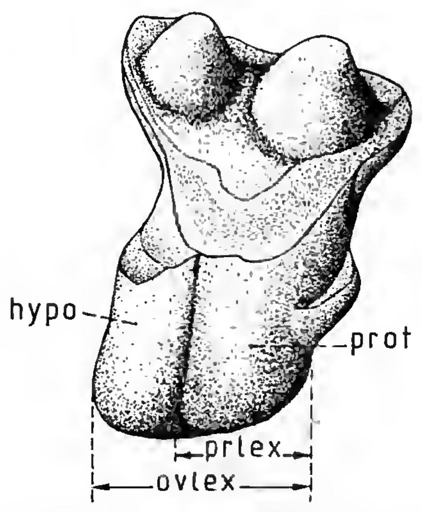


FIG. 9. — This is the case found in the genus *Leptictis* (anterior toward right) showing that the hypocone development can mislead an attempt to measure the protocone antero-posterior expansion of the very lingual portion (abbreviated by prlex). Here the overall expansion of the very labial portion of the crown (abbreviated by ovlex) is the sum of the protocone and hypocone expansions.

The character state (0) is represented by the cylindrical-like shape of the labial wall of the protocone ending in a closed angle at the base of the crown, and away from the lingual portion of the paracone and metacone. The protocone displays a cone-like shape with a poorly expanded basal diameter lingually. In state (1), the labial portion displays in a more open angle regarding that one of state 0, and forms together with the mesiodistal portion of the crown a surface that could be viewed as part of the trigon base, but this surface ends labially also away from the paracone and metacone (lingual surface). In state (2), a trigon base is also formed but it is more labially expanded reaching the very portion below the basal level of the paracone and metacone. In state (3), it ends in an even more open angle, forming a "true" trigon base and reaching the basal portion of the paracone and metacone; in state (4,) this surface (trigon base) merges with

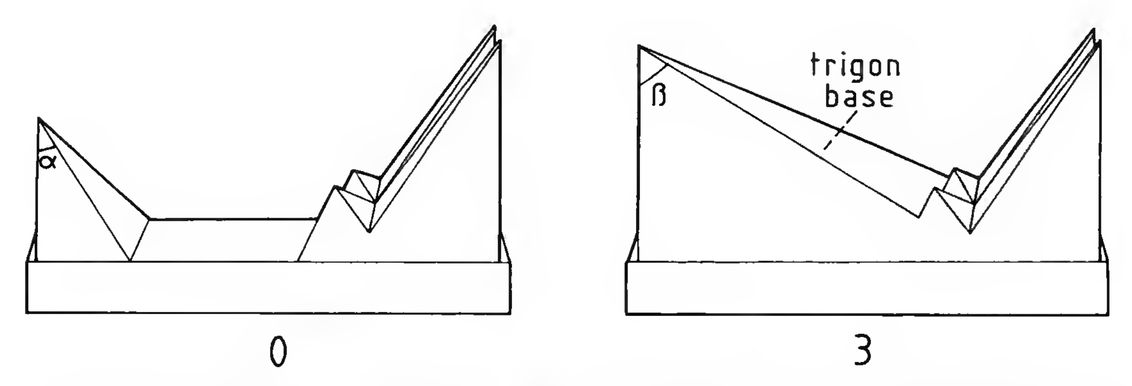


FIG. 10. — Schematic drawings representing two extremities of the development of the protocone labial portion (character 9): state 0, the protocone labial wall ends on the base crown surface in close angle (α) and away from the paracone and metacone; in the derived state 3, it is well-developed ending on the crown surface in a more open angle (β) reaching both paracone and metacone connecting the paraconule and metaconule, hence forming a recognizable trigon base.

the crown in a very open angle, nearly in parallel to the basal plane and reaching the paracone and metacone (a typical bunodont pattern of low cusp relief). When the conules are present, they seem to be independent of these character states: the conules apparently do not demarcate the labial extremity of the trigon base.

10. Post-talon basin, development (Fig. 11).

The post-talon basin is displayed as a sort of a flat upper surface or more like a crista or even as a fossa at the upper portion of the post-cingulum, which frequently connects the hypocone when it occurs. In cases of "crista shape" – a narrow fossa is also present between the posterior wall of the protocone and the internal one of the crista. The shapes of the post-talon basin are not considered here to be phylogenetically informative. However, the overall development of the talon seems to be phylogenetically relevant at the basal placental branching level.

This character is interpreted as having three states: the primitive state coded as (0) is the absence of the talon, or the absence of the post-cingulum; the derived state (1) – presence of

the talon in a very rudimentary stage of development; and state (2) referring to a clearly developed or well-developed post-talon basin.



Fig. 11. — Development of the post-talon, or of the upper portion of the posterior cingulum (character 10): state 0, absence or vestigial stage of development, illustrated by *Cimolestes*; state 1, developed, illustrated by *Oxyprimus*. Both anterior toward right.

11. Position of the labial portion of the post-talon basin (Fig. 12).

The labial portion of the post-talon basin is also named pre-talon basin by some other authors. Here, we named pre-talon basin the anterior portion of the crown where this basin is placed at the upper portion of the pre-cingulum. But, in this context this attribute refers to the extent that the post-cingulum grows labially over the upper surface of the crown, interpreted as the trigon basal level.

Three character states are then proposed to approach this topographical pattern: (0) – the labial extremity of the post-talon clearly away from the upper crown surface; (1) – near the level of the crown surface, but not there; (2) – reaching the crown upper surface, composing this way a condition where the labial growth of the post-cingulum go in the meta-cingulum bypassing the post-metaconule crista.

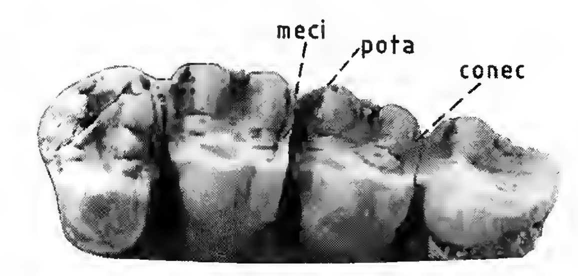


Fig. 12. — Position of the labial portion of the post-talon basin (character 11): *Paramys* (anterior toward left) illustrates condition 2 where the meta-cingulum (meci) meets the post-talon (pota). the point of connection is represented by the abbreviation conec.

12. Pre-talon basin, development.

Here, the character states are formalized pretty much the same way as indicated for character 10. The development pre-talon basin is examined in order to interpret the extent of its emerge over the anterior side of the protocone.

When it is present in a sort of rudimentary stage, it is coded as state (1); and state (2) goes for the developed or well-developed stage of the talon; the primitive state (0) refers to the absence of the pre-cingulum and this way to the absence pre-talon.

13. Position of the labial portion of the pre-talon basin.

This is a very similar morphological situation with that of character 11, where three character states are formulated to account to the position of the labial extremity of the pre-talon basin relative to the upper crown surface: (0) – away from the upper crown surface; (1) – near the level of the upper surface; (2) – reaching the upper surface and connecting the para-cingulum; characterizing this way a case where the labial growth of the pre-cingulum go in the meta-cingulum bypassing the pre-metaconule.

14. Post-cingulum and pre-cingulum (Fig. 13).

In some taxa the post-cingulum and pre-cingulum are developed in such a way that they meet lingually, encircling the crown, state (1). The primitive state (0) refers just to the absence of this condition.

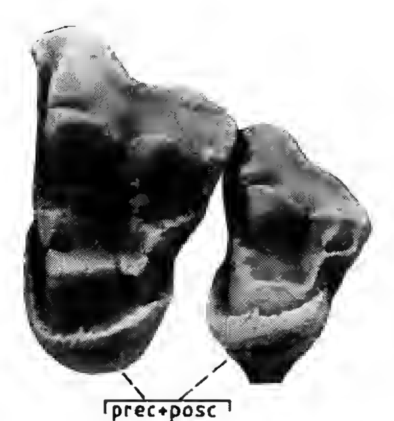
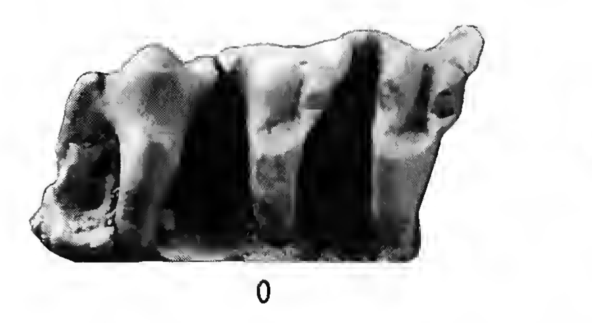


FIG. 13. — *Miacis* (anterior toward left) illustrating a derived condition 1 where the pre-cingulum and post-cingulum encircle the lingual portion of the crown.

15. Hypocone, development (Fig. 14).

The hypocone is frequently placed at the very lingual edge, composing therefore the lingual wall of the crown with the protocone. This feature refers to the degree of the development of the hypocone, and, to avoid problems due to the complex variation of this character, just four states are proposed: (0) – absent; (1) – rudimentary or very small; (2) – developed and well-developed; (3) – extremely enlarged.

These size coding problems are stated in reference to the overall size of the crown taking into account basically the height and width of the hypocone. The reason for not using the pro-



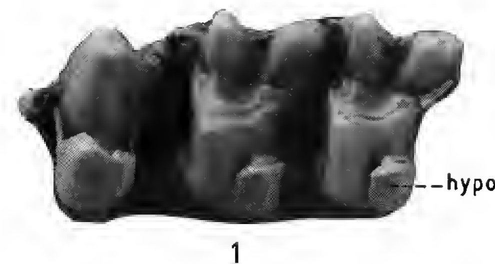


FIG. 14. — Hypocone, development (character 15): state 0, absent (*Cimolestes*); state 1, developed (*Scenopagus*). Both anterior toward left.

tocone size as a reference is simply to avoid problems of possible independent reductions of the protocone which would necessarily change the hypocone protoeone size relationships. There seems to be a certain ambiguity related to the overall size of development of the hypocone, given that there are cases where *e.g.* a distinct enlargement of the hypocone diameter is not followed by a proportional growth in height. This is the case of *Scenopagus*, which is questionably coded as 1, and is illustrated in figure 14. Both *Pappotherium* and *Sulestes* lack the hypocone; however, it is relevant to note that some other metatherians do have the hypocone, or hypocone-like cusps.

16. Pericone, development.

The pericone is placed at the opposite side to the hypocone on the antero-lingual wall of the protocone. The development of the pericone is formulated as a binary character: state (0) absence, and (1) presence.

A point to bear in mind is that one may easily misidentify of similarly placed accessory cusps by that named pericone.

17. Conules, development (Fig. 15).

This feature stands for the different degrees of development of the conules. Three character states are formulated: (0) – very poorly developed or nearly absent; (1) – developed; (2) – a further derived condition where the conules are considerably well-developed, a condition well illustrated in *Paramys*.

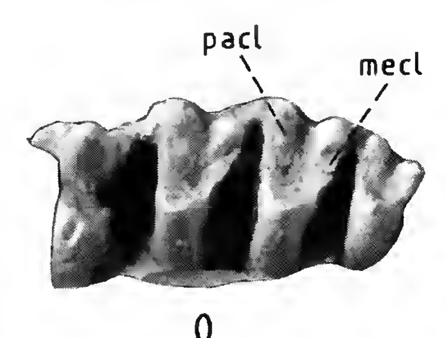


FIG. 15. — Development of the conules (character 17): state 0, poor development or vestigial; the genus *Zalambdalestes* (anterior toward left) seems to represent a case of this primitive condition.

18. Conules, shape (Fig. 16).

Four types of conules are recognized but of unclear topographical relationships. They are the following: (0) – pointed cone-like shape; (1) – wing-like shape; (2) – flat cylindrical-like; (3) – rounded, bunodont-like.

Given that no logical topographical sequence of changes is justifiable for these conule shapes, this character is considered unordered.

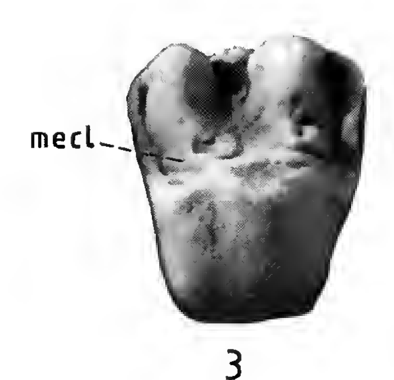


FIG. 16. — Conules, shape (character 18): state 3, cylindrical-like shape, it pictures the condition observed in *Paramys* (anterior toward right).

19. Conules, position relative to the paracone and metacone.

This character accounts for the extent that the conules are approximated to the paracone and metacone, basically the distance between the conules and those two cusps.

Three derived conditions are proposed, and when the conules are away from the two cited cones, it is coded as (0). State (1) represents the case where the conules are close to the cones but have no contact. In the other two derived states the conules are placed in contact with the paracone and metacone: the state (2) is good for a partial contact, and state (3) for full contact between those cusps.

20. Conules, placement in relation to the anterior and posterior crest of the protocone.

This is a binary character, where state (0) stands for the placement of the conules on both protocone crests. The derived state (1) is a case of displacement of the conules with respect to the crests of the protocone. This feature is indeed an autapomorphy for *Paramys*.

21. Conules, lingual portion (Fig. 17).

This feature describes the relationships of the lingual portion of the conules with the protocone. Two conditions are assigned, one where the lingual wall of the conules are free from contact with the protocone state (0), of course not referring to its basal portion. The derived state (1) is characterized by a sort of torsion towards the protocone, resulting therefore in a considerable contact of the lingual wall of the conules with that of the protocone. This derived condition seems to be widespread among basal ungulates.

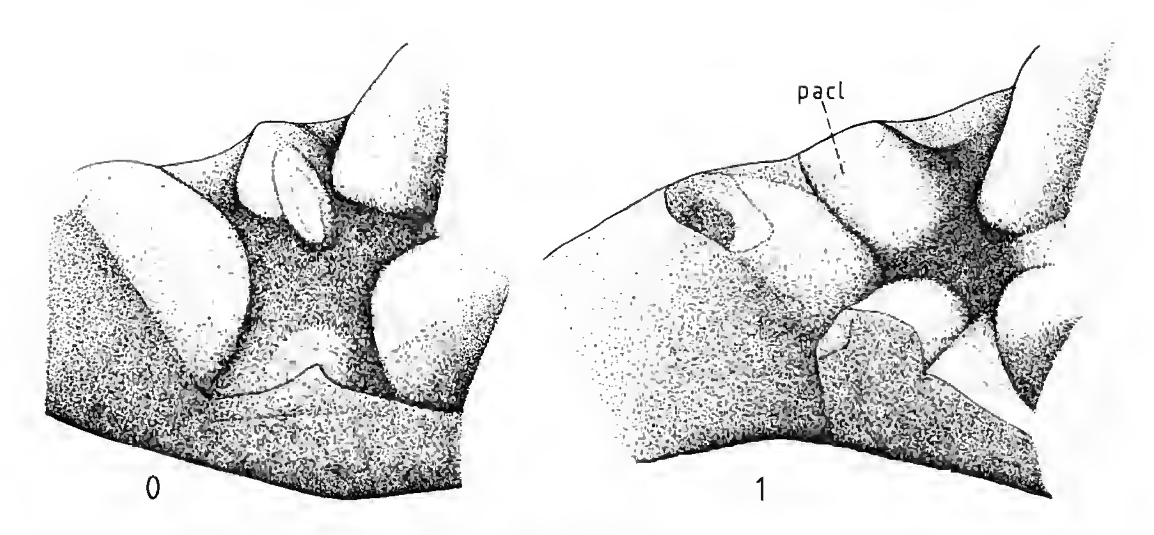


Fig. 17. — Conules projection towards the protocone having a large portion of each conule lingual wall lying over the labial surface of the protocone (character 21): state 0, absence of such a trend (*Prototomus*); state 1, presence of this derived projection, here illustrated by the condition found in the genus *Protungulatum*. Postero-occlusal view.

22. Metacone and metastyle, shearing surface (Fig. 18).

This attribute characterizes a case of carnassial evolution where the metastyle is placed labially to the metacone forming a carnassial shearing surface, condition coded as state (1). This condition is reported for *Cimolestes* as well as other feraeans examined. The primitive state is the absence of this condition (0).

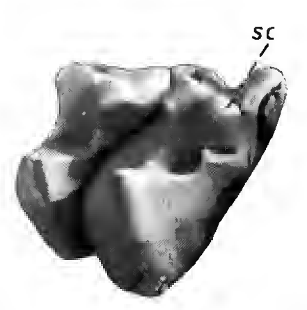


Fig. 18. — Metacone and metastyle, shearing surface (= sc; character 22): state 1, the derived condition where such shearing surface is present, here illustrated by the condition found in the genus *Cimolestes* (anterior toward left).

23. Paracone and parastyle, shearing surface.

The paracone and parastyle also form a carnassial shearing surface (1), similar to that of character 22, but its distribution among the taxa examined is slightly different. The primitive state (0) is the absence of this carnassial surface.

24. Relative position of the labial portion of the crown (Fig. 19).

This region of the crown is viewed as fundamentally composed by the paracone and metacone, and englobing the stylar shelf. In the two plesiadapiformes examined, a posteriorly orientated torsion of the labial portion of the crown is observed. Viewing from antero-lateral angle, this torsion seems to permit the paraconule wing to reach the pre-paracrista without having contact with the pre-cingulum.

The presence of this condition is considered derived (1), and the absence primitive (0).



FIG. 19. — Position of the paracone-metacone portion on the crown (character 24): state 1, posteriorly oriented torsion displacing the paracone and metacone from a central position on the crown (*Palaechthon*). In this scheme the arrows show the estimated points of torsion, and *x* is a projection of the medial line of the protocone demarcated here by its tip and serving then as reference for the displacement of paracone-metacone region. Anterior toward right.

25. Paracone and metacone, lingual expansion.

This character stands for the lingual expansion of the paracone and metacone over the paraconule and metaconule respectively.

The presence of this condition is considered derived (1) and the absence primitive (0). This is another character that comes out as an autapomorphy for *Paramys*.

26. Protocone, shapes.

This character regards the shapes of the protocone upper portion exposed on the crown surface. It is not viewed as a general trend for the three main cusps because the shapes of the paracone and the metacone seem to covary only to a certain extent with that of the protocone: for example, there seems to be no cases where a very high pointed paracone and metacone coexist with a characteristically shallow protocone, but no further morphological cohesion among these cusps can be formulated as a rule of variation.

Four general patterns are proposed to account for the variability observed: (0) – cone-like shape with somewhat high pointed cusps; (1) – slightly rounded, but not representing a typical bunodont pattern; (2) – definitely rounded, displaying a typical bunodont like cusp; (3) – somewhat flattened, composing a very shallow lingual crown upper surface. This character state relationships are unclear, in the sense that no consistent argument can be made in order to advocate that the transformation between one state into another requires more than one step. Hence, this

character is treated as unordered. Notice that this feature is not applicable to the taxa displaying the protocone in a rudimentary stage of development.

Among the 26 characters formulated, characters 9, 17, 18, and 26 are considered to be unordered. Table 1 summarizes all the character information discussed above and gives the distribution assigned to each. It is clear that in order to achieve more accuracy in the character partition for the type of qualitative characters discussed above, a biometrical study followed by a gap coding system is needed. But, whatever the improvements might be, while limited to the upper molar cusp topographical interrelationships, they will be confined to the tribosphenic placental "ground-plan": a mosaic of three basal elements composed by the paracone, metacone and protocone varying in size, shape and their relative positions along with a series of accessory cusps and crests that also vary in size and shape, greatly modifying the basal tribosphenic system.

ANALYSIS OF PARSIMONY

In this attempt to contribute to a better understanding of the phylogenetic information content in the placental dental morphology 26 characters are proposed, the majority being multistate characters with 4 of them read as unordered. Three characters (16, 20, and 25) are autapomorphies and are then disregarded in the parsimony analysis performed here to prevent the consistency index from getting inflated (CARPENTER 1988).

After running the ie* exact algorithm that generates trees by implicit enumeration of the Hennig86 software (FARRIS 1988), and applying two hypothetical ancestors in order to bring about the monophyly of the ingroup, 30 most parsimonious trees came out as result with a length of 93 steps, consistency index (ci) of 59 and retention index (ri) of 80. The outcomes of exact algorithms are considered to be certain minimal length trees (DARLU & TASSY 1993). The strict consensus of these 30 trees (appendix 1) has 17 components (excluding the basal node 39, where the two hypothetical ancestor are rooted).

Successive approximations weighting (FARRIS 1969, CARPENTER 1988) was then applied, and it is stabilized after the third weighting with one tree of length 395, ci of 72 and ri of 88 (Fig. 20). Characters 14 and 22 became of no value. As discussed by SALLES (1992: 41), FARRIS stated that the point made by CARPENTER (1988) about the necessity of recoding multistate characters to binary, when applying the successive weighting option, is not applicable to the Hennig86 software. Nevertheless, an article that is in press in *Cladistics* by FARRIS, KLUGE & CARPENTER may present different thoughts on this matter. But, at least, the four characters considered to be unordered are not cases of totally inapplicable "additivity", and on LIPSCOMB's manual of the Hennig86 software there is no reference for the need of having multistate characters change into binary ones.

The final tree (Fig. 20) obtained after weighting is later compared with the one obtained after running the ie* option with all characters unordered, which first resulted in 205 most parsimonious trees with length of 88, ci of 62 and ri of 75, and then the same weighting procedure is applied – ending up with 12 trees with length of 412, ci of 74 and ri 84 (see appendix 2 for the strict consensus of these 12 trees as well as directly from the 205 trees obtained before weighting).

It is important to understand the nature of the diagram of Figure 20, in the sense that this branching pattern is an expression of the congruences among attributes of a single morphological complex. Therefore, the relationships advocated by this diagram might be better read as patterns of upper molar evolution rather than a phylogenetic hypothesis among the 18 taxa considered. These relationships should be simply viewed as statements of overall congruence among the 22 dental traits, and concerning then morphological complex mostly studied by paleo- and neo-mammalogists in order to interprete the evolutionary history of mammals.

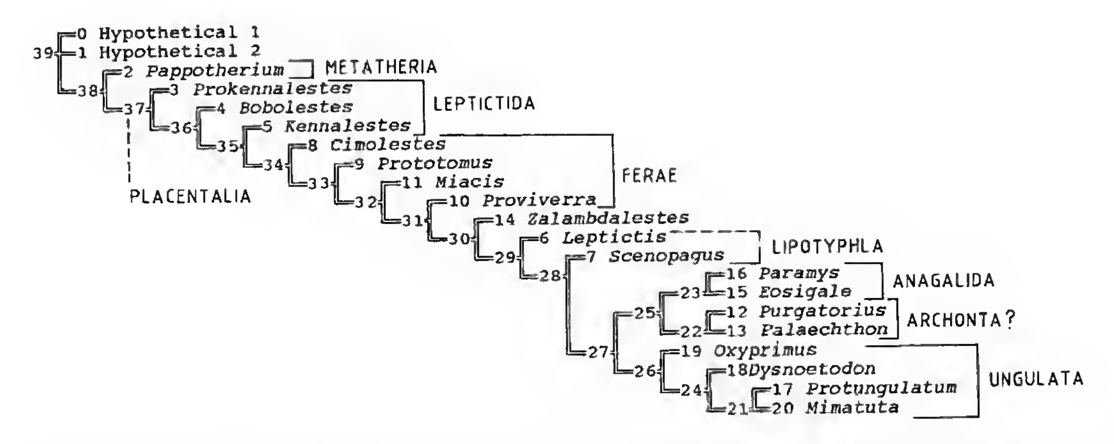


FIG. 20. — Branching diagram for placental mammals obtained after applying the ie* option of the Hennig86 software and making use of the successive weighting algorithm. The interpretation of the component 22 as Archonta is very weak in the sense that it may be simply delineating Plesiadapiformes. However, if these are assumed to be basal primates, and primates are accepted as members of the Archonta, the interpretation that these two genera represents Archonta would be plausible. Lipotyphla may be either represented by *Scenopagus* alone or it may include the genus *Leptictis*. The position of the genus *Zalambdalestes* is questionable: STUCKY & MCKENNA (1993) have classified it as a basal lagomorphan. The stated placental interrelationships are discussed in the text.

Character optimizations of features 3, 5, 9, 10, 14, 15, 19, 22 and 26 have assigned more than one character state for one or more nodes, representing therefore a set of quite complex alternative paths of evolutionary change. To build a table of nodes and corresponding characters, somewhat arbitrary decisions have been made, in order to simplify the optimization of their character state distributions. The rationale applied is later discussed under the transformation series analyzed. But, briefly, it is to choose the possible basal position of the further derived character state – a procedure that would be more like the ACCTRAN optimization (SWOFFORD & MADDISON 1987). In some cases this rule could not be applied. A simplified version of the character state distributions on the 17 components in Figure 20 are summarized in Table 2.

TABLE 2. — Character distributions on the branching diagram of figure 20, and the * symbol identifies homoplasies, character states placed at more than one node.

Node 38:	5(1)*.	Node 29:	9(3)*, 10(2).
Node 37:	1(1), 2(1), 5(2)*, 6(1), 17(1), and 19(1)*.	Node 28:	7(2).
Node 36:	1(2)*, 9(2)*, 18(1), and 19(2)*.	Node 27:	8(2), 12(2), and 15(2)*.
Node 35:	5(3)*, 6(2), 7(1), 9(2), and 10(1)*.	Node 26:	21(1).
Node 34:	4(1) and 22(1)*.	Node 25:	13(1).
Node 33:	12(1), 15(1)*, and 23(1)*.	Node 24:	18(3).
Node 32:	2(1), 3(1)*, 8(1), 11(2), and 14(1)*.	Node 23:	1(4), 9(4), 13(2).
Node 31:	4(2).	Node 22:	24(1)
Node 30:	1(3)*, 3(2)*, 5(4)*.	Node 21:	15(1)*.

INTERRELATIONSHIPS OF PLACENTAL MAMMALS (UPPER MOLAR MORPHOLOGY, INTERNAL CONGRUENCE)

In the latest matrix revised by NOVACEK (1992) regarding extant and fossil mammals, the crown morphology of upper molars was stated to be informative at three branching levels: the placental level (narrow stylar shelves of the upper molars); the ungulate basal node (general bunodont transformation including the considerable development in size of the hypocone) and the third level expressed by the bilophodonty of tethytherians. These dental informations are here readdressed as discussed in the "Character Analysis" section, but generally the partitions of the molar mosaic are refined and the character states expanded, frequently resulting in multistate characters. The following discussion refers to character distributions on the branching pattern of Figure 20.

The first somewhat surprising result involves the overall phylogeny of placental mammals, here examined from a late Cretaceous/Paleocene fossil record perspective, which emerges fully resolved. As expected, *Pappotherium* is placed at the base, and is followed by a paraphyletic sequence of leptictids *Prokennalestes*, *Bobolestes* and *Kennalestes*. *Cimolestes* branches off after this last leptictid and it is succeeded by the other three feraeans, *Protoiomus*, *Miacis* and *Proviverra*. Hence, the monophyly of Ferae is not supported. However, if Ferae is assumed to become monophyletic at some point in this branching area, basally demarcated by *Cimolestes*, feraeans would be rooted at a relatively basal position within placentals which is an intriguing possibility. This would support an uncommon interpretation of the phylogenetic status of Ferae.

Zalambdalestes, *Leptictis* and *Scenopagus* formed another paraphyletic sequence where the last is sister group of clade 27. *Zalambdalestes* is a late Cretaceous placental frequently interpreted as closely related to anagalids, and recently proposed as a basal lagomorphan (STUCKY & MCKENNA 1993). Assuming that rodents (here represented by *Paramys*) and lagomorphans are indeed sister groups, the topology of the placental branching diagram (Fig. 20) does not support the placement of *Zalambdalestes* as a lagomorphan. *Leptictis* is here placed apart from

the "closely related" basal paraphyletic assemblage of leptictids, and *Scenopagus* represents the "true insectivorans", the Lipotyphla. Hence, leptictids are indicated to be paraphyletic and lipotyphlans to be sister group of clade 27.

The monophyly of clade 27 is a subject apart but it is striking that another set of different features seems to indicate a similar scheme of relationship (now under study by a team of paleontologists); the main difference is that basal ungulates had not been considered.

Ungulata is here represented by four basal condylarths and it is hypothesized to be a member of this clade 27. Therefore, ungulates are suggested to be closely related to the plesiadapiformes (clade 22) and anagalids plus rodents (clade 23). The four condylarths came out rooted at node 26, with *Oxyprimus* at the base and the others three forming a clade numbered 24, in which *Dysnoetodon* branches off from the base and *Protungulatum* and *Mimatuta* are sister groups, clade 21. The genus *Dysnoetodon* is here identified as a condylarth-like placental, but ZHANG (1980) suggested that it could be a tillodont. We can assert that at least it is not a typical tillodont. But, if one assumes that it might indeed represent a basal form of tillodont, our results would then corroborate the old hypothesis that Tillodontia is derived from a condylarth basal form (see *e.g.* GINGERICH & GUNNELL 1979).

Those relationships discussed above are not really incongruent with any of the other results obtained after applying different algorithm combinations for that same matrix illustrated in Table 2, except for a single component comprising two terminal taxa. First, the relationships summarized in Figure 20 are partially supported by the Nelson consensus tree (appendix 1) derived directly from the 30 most parsimonious trees from the ie* algorithm. The components that are identical are the following (the numbers on the left correspond to the components of the branching diagram of Figure 20 and the ones on the right to the components of appendix 1): 37 = 28; 37 = 27; 36 = 26; 35 = 25; 32 = 24; 27 = 23; 23 = 22; 22 = 21. None of the components of the branching diagram of appendix 1 are incompatible with the ones observed in Figure 20; it is simply a less resolved branching diagram. We want to point out that component 27 emerges without successive weighting.

Comparing the placental tree in Figure 20 with that of appendix 2, in which all characters are read as unordered and obtained after applying the ie* and successive weighting options, a list of the identical components between those two diagrams follows (components of Fig. 20 on the left): 38 = 33; 37 = 32; 36 = 31; 35 = 30; 32 = 29; 28 = 28; 27 = 26; 26 = 25; 24 = 22; 23 = 24; 22 = 23; 21 = 21. In fact there is one component from this unordered tree that is not found in that one in Figure 20; namely component 27, which places *Proviverra* and *Miacis* as sister groups. Finally, the option of having the characters unordered and not applying the successive weighting results in a poorly resolved branching diagram. The relevant point is that it displays one component which is identical to the component 32 of Figure 20, to the component 24 of the tree in appendix 1, and to the component 29 of the tree in appendix 2. What is intriguing is that these components have *Proviverra* and *Miacis* as members, having then the two other feraeans out of their assemblages. Hence, these results definitely question the monophyletic status of Ferae. Nevertheless, at this point we still understand these results as very preliminary and possibly simply reflecting the absence of enough character information to bring about the monophyly of Ferae.

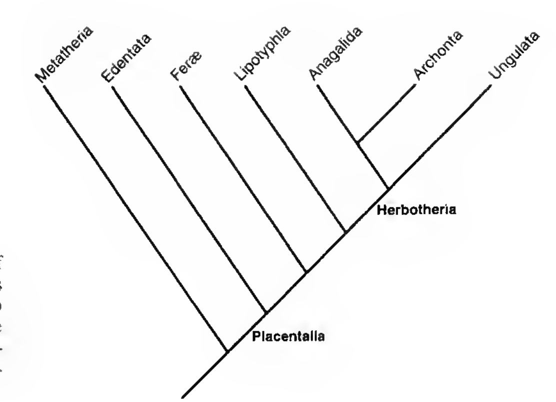
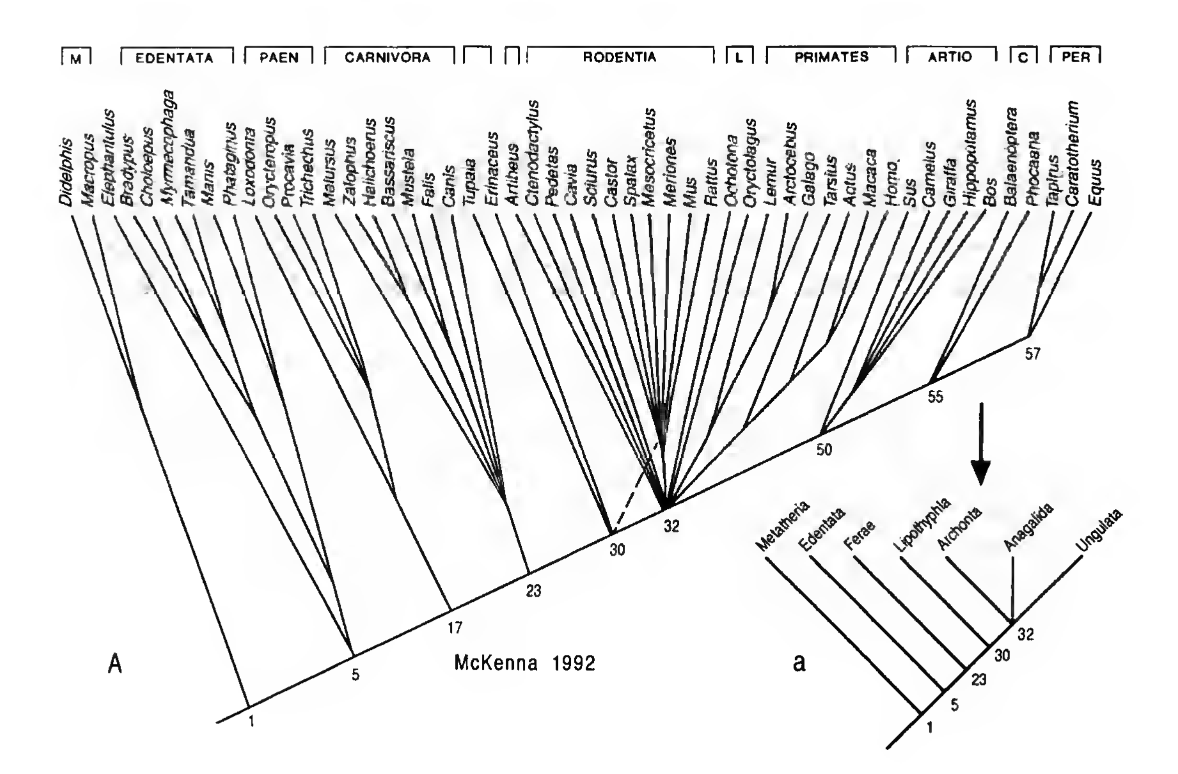


FIG. 21. — Simplified branching diagram derived from that of Figure 20; the assumptions made to produce this synthesis are the following: the three basal leptictids are assumed to be monophyletic; the same goes for the four feraeans; the two plesiadapiformes could well represent Archonta. Herbotheria is the name given to component 27 of the tree illustrated in Figure 20.

Now, comparing the assemblage of placental interrelationships here advocated (Figs 20, 21 for a comparable high level synthesis) with the ones supported by MCKENNA (1992: 351; here illustrated in Figs 22A, 22a for a comparable synthesis), and based on the amino acid sequences for the alpha crystallin A chain, the number of nearly identical components between these two trees is striking. First, component 37 of the dental-based branching diagram (Figs 20, 21) is identical to numbered 1 of the alpha crystallin one (Fig. 22). This is to say that Metatheria is read as the sister group of Placentalia in both branching diagrams. To our knowledge all assigned basal edentates have their dental pattern extremely differentiated, hence they are not considered in this study. Therefore, component 5 of Figure 22A having edentates as basal placental cannot be a test against the branching pattern of Figure 20. A similar but opposite argument goes for the phylogenetic position of the first three basal placentals of the dental-based tree, which are only known as fossils from the late Cretaceous. However, it is very curious that component 23 which has Carnivora branching off from the base is identical to component 34 if we consider *Cimolestes* as the basal Ferae: and it may also be that their paraphyletic distribution between nodes 33 to 30 is due to absence of information. Alternatively, their dental attributes may be insufficiently informative in this character survey to express the monophyly of the feraeans, or perhaps a series of dental parallelisms exist between feraeans and their relatives. Now, we could well read component 29 of the dental-based branching pattern as identical to that numbered 30 in MCKENNA's scheme. For this we take *Scenopagus* and *Leptictis* as lipotyphlans and (if *Leptictis* is not considered, component 28 would be identical to 30) and branching off from the base. Component 27, which is named Herbotheria (and later discussed), is identical to 32 of the molecular-based cladogram formulated by MCKENNA. For this we understand Plesiadapiformes as basal archontans, component 23 (Fig. 20) standing for Anagalida (*sensu* STUCKY & MCKENNA 1993), and of course component 26 with the four basal condylarths representing Ungulata. Summarizing, a total of four nearly identical high rank taxa are reported with the comparison of these two phylogenetic schemes. This way, both morphological and molecular data support a very similar scheme of placental mammal interrelationships.

Examining the phylogenetic scheme of MACPHEE & NOVACEK (1993: 25), here illustrated in Figure 22b, which is derived from that of NOVACEK (1989) after a manipulation of its major basal polytomy in order to achieve the best optimisation for a series of entotympanic characters, it is clear that the only real incongruence between this branching pattern for placental mammals and that of MCKENNA's (Fig. 22a) is that Lipotyphla is placed as the sister group of Ferae (component 7) instead of sister group to the clade composed of Anagalida, Archonta and Ungulata. As previously discussed, this component 30 of MCKENNA's scheme (Fig. 22a), where Lipotyphla branches off from the basal node, is identical to our phylogenetic scheme (Fig. 21). In that sense we also do not support component 7 (Fig. 22b) proposed by MACPHEE & NOVACEK. Another incongruence between our dental-based branching pattern and the one of MACPHEE & NOVACEK (Fig. 22b) is that, for them Anagalida is the sister group to Ungulata whereas Anagalida is sister group to Archonta. Given the scope of this article, it is most relevant to note that our component 27 is identical to the 32 of MCKENNA's scheme (Fig. 22a) and to component 3 of MACPHEE & NOVACEK (Fig. 22b). It follows from these comparisons that we might be indeed accumulating independent evidence supporting the phylogenetic identity of a new high rank placental clade, named Herbotheria.

Placental mammal phylogeny is quite a complex subject which awaits better fossil sampling across the late Cretaceous/Paleocene boundary. This complexity becomes evident by examining the number of contradictory phylogenetic statements that have been published in the last eight



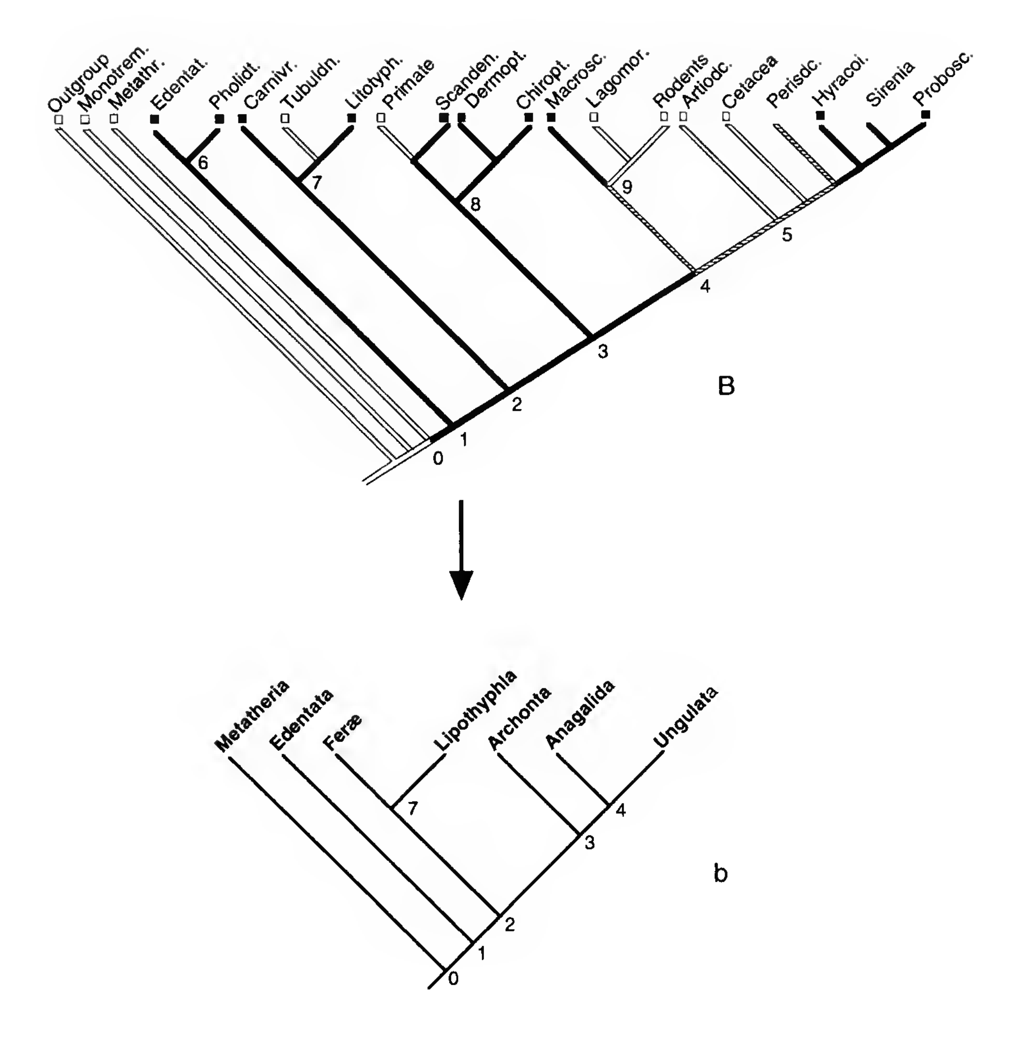
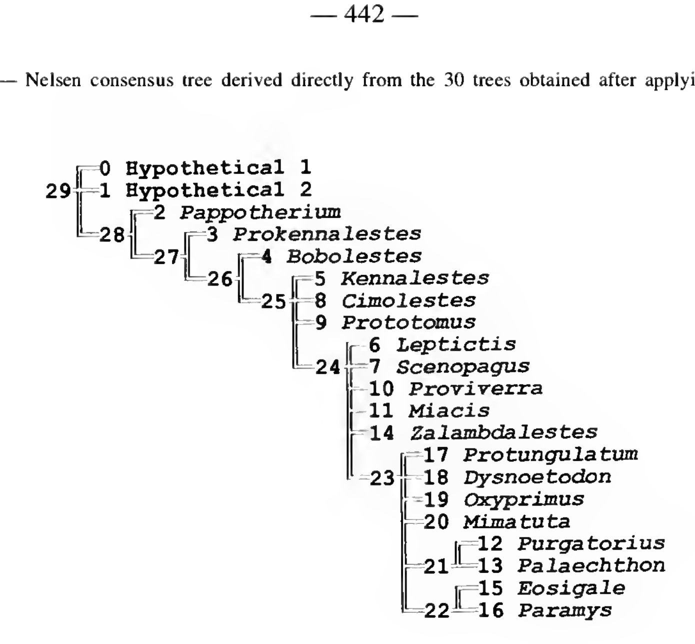
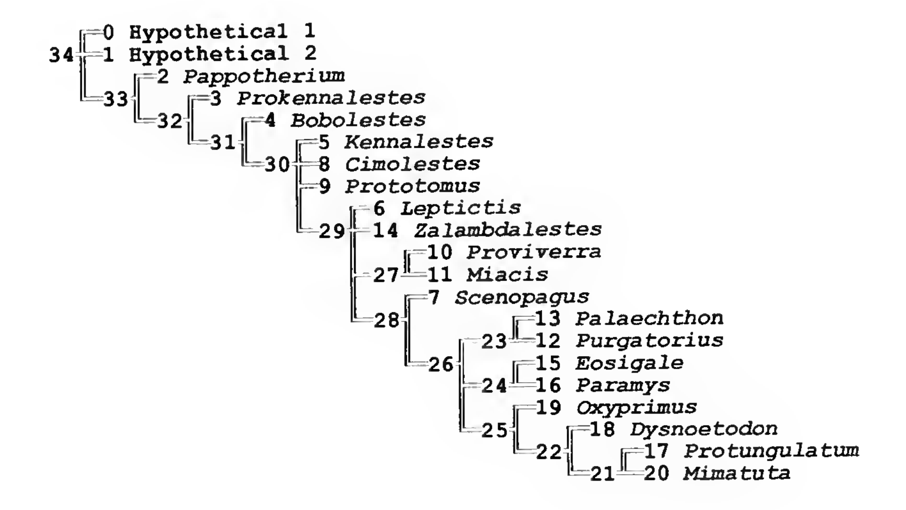


FIG. 22. — The upper two branching diagrams refer to the alpha crystallin A chain based cladogram of MCKENNA (1992): A, is directly redrawn from MCKENNA's cladogram, it adds only letter L (in bold) for demarcating the lipotyphlans and the letter H (also in bold) for demarcating the Chiroptera; a, is a simplified version of A. The lower two cladograms refer to the phylogenetic scheme of MACPHEE & NOVACEK (1993); b, is a simplified version of the original B. To facilitate the understanding of the component differences among MCKENNA's phylogenetic scheme and the MACPHEE & NOVACEK's one with that of Figure 20, their respective simplified derived versions (22a, 22b, and 21) may well be used in the comparison of these three branching diagrams.

APPENDIX 1. — Nelsen consensus tree derived directly from the 30 trees obtained after applying the ie* option.



APPENDIX 2. — Nelsen consensus tree derived from the 12 trees obtained after applying the ie* and successive weighting options having all characters unordered.



years (after the publication of NOVACEK & WYSS 1986), *e.g.* see articles in BENTON (1988) and SZALAY *et al.* (1993). This progress report advances some hypotheses of dental trends within placental mammals, and their alternative paths of evolutionary change are discussed below based on the branching pattern shown in Figure 20.

DENTAL TRENDS AND THEIR PATHS OF EVOLUTIONARY CHANGE

In this section character state distributions on the branching diagram of Figure 20 are presented with a discussion of their alternative pathways of evolutionary change. Given the scope and size of this essay, the transformation series are generally briefly discussed but all attributes are considered.

1. (7 steps, ci 57 – ri 75).

It first appears at node 37, with the placement of character state 1. Therefore, the partial contraction of the stylar shelf supports, as expected, the monophyly of Placentalia, represented by component 37. At next node 36, state 2 composes a set of four synapomorphies that places *Prokennalestes* as the basal placental and all the other taxa forming a large monophyletic clade. The third appearance of the further derived state 3 is placed at component 30 having *Zalambdalestes* as sister group of clade 29 (anagalids, including the rodent *Paramys*, ungulates, plesiadapiformes, plus *Leptictis*, and the true insectivora – *Scenopagus*). The furthest derived state 4, where the stylar shelf is considered to be nearly absent, is interpreted to be a synapomorphy for clade 23, possibly representing the broad notion of anagalids of STUCKY & MCKENNA (1993). At node 22, there is a reversal from state 3 to state 2, and it comes to support the monophyly of Plesiadapiformes or of Archonta if one wishes so: Plesiadapiformes may well be read as a sort of stem-group of the whole clade Archonta (a matter lately discussed with Malcolm MCKENNA). Another reversal takes place from state 3 to 2 and results in autapomorphy for *Scenopagus*.

2. (4 steps, ci 75 – ri 90).

The first trend towards the reduction in height of the cusp complex formed by the paracone and the metacone appears at the basal node 37, state 1. Therefore, it is here supported as another trend of the upper molar morphology related to the emergence of placental mammals. The transformation to state 2 is placed at node 32. The furthest reduction is placed as an autapomorphy for *Zalambdalestes*. *Scenopagus* is victim of another reversal, from state 2 to state 1.

3. (5 steps, ci 60 – ri 86).

The derived state 1 is placed at node 32, marking the first trace of the displacement of the paracone and the metacone from a full contact, where they are somewhat laterally emersed in one another. At node 30, the further derived state 2 becomes a possible synapomorphy (the above arbitrarily selected placement), however this state becomes unambiguous only at node 28. Nodes 30 and 29 can be either represented by states 1 or 2. The character state 3 is placed as an autapomorphy for *Paramys*.

4. (3 steps, ci and ri 100).

It is assigned a trace of reduction of the centrocrista (state 1) at clade 34, where *Cimolestes* is rooted at the base. At the lower level 31, a transformation from state 1 to state 2 takes place. Again, in *Paramys*, the furthest derived condition (3) is read as an autapomorphy, characterized by the absence of growth of the centrocrista.

5. (10 steps, ci 40 – ri 64).

This transformation series concerns the overall development of the protocone. As expected, character state 5 (1) is placed at node 38, and indeed refers to a basal tribosphenic hierarchical level, where *Pappotherium* (the objective outgroup referential included in the matrix) is directly rooted at this node. At the next nodes 36 and 37, states 1 and 2 are competing hypotheses for this character evolution, and at node 35 state 3 is unambiguously placed representing the stage of growth of the protocone where it becomes larger than the paracone. At a lowest level, where *Zalambdalestes* is rooted at the basal node (30), the furthest derived state 4 is a potential synapomorphy. However, state 4 becomes unambiguous at node 28, and at nodes 29 and 30, states 3 and 4 are equally parsimonious optimizations. A reversal takes place in *Miacis* (3 → 1) and another in *Paramys* (4 → 3).

6. (3 steps, ci 66 – ri 85).

Character state 1, evidence of the transverse expansion of the protocone here supports the monophyly of Placentalia (clade 37). State 2 emerges at clade 35 characterizing a further developed stage of this transverse expansion. A reversal from state 2 towards the less expanded condition 1 occurs in *Miacis*.

7. (2 steps, ci and ri 100).

The derived state 1 assigned for the antero-posterior expansion of the labial portion of the protocone is supporting the monophyly of clade 35, and a transformation to state 2 is determined to have occurred at clade 28, where the insectivora *Scenopagus* is placed as sister group of clade 27.

8. (5 steps, ci 60 – ri 85).

The first derived condition of the antero-posterior expansion of the lingual portion of the protocone is placed at node 32, and the further derived state 2 is supporting the monophyly of clade 27. Within this clade a reversal towards the less derived state 1 is recorded for *Mimatuta* and the differentiation for the furthest derived state 3 occurs in *Paramys*.

9. (4 steps, ci and ri 100).

The various stages of development of the labial portion of the protocone are determined to be unordered. Despite the complexity of this character it presents just one ambiguity at node 36, where states 0, 1, and 2 are equal optimizations. In Table 2, state 1 is selected on the basis that the previous node 37 maintains the plesiomorphic condition and the next lower level, clade 35, state 2 is fixed. This way state 1 would be placed as an intermediate condition between 0 and 2. The transformation to state 3 occurs in clade 29, and the anagalid component 23 is supported by the furthest derived state 4.

10. (5 steps, ci 40 – ri 80).

The basal possible placement of the derived state 1, regarding the development of the post-talon basin, is at node 35. However, it is at node 33 that this condition becomes unambiguously determined. Despite this ambiguity for the 0 → 1 transformation, there is no problem with the optimization for the following change from states 1 to 2, being assigned to take place at the hypothetical ancestor represented by node 33.

11. (3 steps, ci and ri 66).

State 1 is not assigned to any hypothetical ancestor position and the stage where the labial portion of the post-talon basin reaches the crown upper surface state 2, is determined to be a synapomorphy for clade 23. This transformation counted two steps given that it has transformed directly from the plesiomorphic state 0. State 1 stands as an autapomorphy for *Mimatuta*.

12. (4 steps, ci 50 – ri 86).

This character optimization assigns for the 0 → 1 character change (appearance of the pre-talon basin) at the hypothetical ancestor 33, and the transformation from state 1 to state 2 supports the monophyly of clade 27. A reversal to the plesiomorphic condition occurs in *Zalambdalestes*.

13. (3 steps, ci 66 – ri 80).

The evolutionary pathways of this character are limited to clade 25, where the derived state 1 regarding the position of the labial portion of the pre-talon basin is indicated to be supporting the monophyly of this whole clade. The further derived transformation state 2 is assigned to be placed at hypothetical ancestor 23. State 1 is homoplastic for the appearance in *Mimatuta*, resulting therefore in an autapomorphy for this genus.

14. (3 steps, ci 33 – ri 0).

The distribution of this character results in ambiguities regarding nodes 31 and 32. There are two equally parsimonious hypotheses for this character optimization: one that places state 1 as a synapomorphy of clade 32 and consequently with a reversal to the plesiomorphic state at node 30; and the other interpreting two independent appearances of state 1, one in *Miacis* and another in *Proviverra*. A character step is also counted for the derived condition (autapomorphy) of *Mimatuta*.

15. (8 steps, ci 40 – ri 76).

This feature concerns the hypocone development and its distribution. The basal possible placement for the first derived condition 1 is at node 33, but it is an ambiguous position since state 0 is an alternative hypothesis. It becomes unequivocal at node 29 and the further derived state 2 appears as a synapomorphy for clade 27. Within this clade a reversal to the less derived state 1 takes place at node 21, the one indicating the sister-group relationship between *Protungulatum* and *Mimatuta*.

16. The development of the pericone stands here as an autapomorphy for *Scenopagus*, and therefore it is excluded from the data matrix here analyzed.

17. (4 steps, ci and ri 50).

The first stage of development of the conules is considered as a synapomorphy of clade 37, state 1. This is one of the cases where better refined knowledge of the Placentalia sister-group

relationships could change completely the interpretation of this character state optimizations. The main remaining question is whether the dental similarities between metatherians and eutherians are due to convergence or common inheritance. The derived state 2 comes out as an autapomorphy for the condylarth *Oxyprimus*. *Zalambdalestes* and *Eosigale* seem to have independently lost the conules, but it is questionable wether they do not have the conules in very rudimentary stage of development.

18. (3 steps, ci and ri 100).

This transformation series concerns the evolution of the shape of the conules. The shape coded as 1 is indicated to be a synapomorphy for clade 36 (from where *Bobolestes* is rooted at the base) and the one coded as 3 is placed at clade 24, with a reversal to condition 1 in *Oxyprimus*. There are two alternative paths of evolutionary change regarding the character state 2, one where it would be placed at node 23 and therefore read as a synapomorphy for the anagalid clade, or as an autopomorphy for *Paramys*. This is because *Eosigale* is coded as missing data (?).

19. (8 steps, ci 37 – ri 50).

The position of the conules relative to the paracone and metacone allows a diverse number of competing hypotheses of character optimizations. Therefore, the analysis of this character is limited to the following relevant points. First state 1 is unambiguously placed at node 37, therefore having the status of synapomorphy for all taxa considered. But at the next nodes 36 and 35 states 1 and 2 are competing hypothesis, and at the node 34 state 2 becomes unequivocal. Character state 1 reappears at node 24 as an alternative path of evolutionary change, or as a potential shared derived character for the monophyly of the clade that places *Dysnoetodon*, *Protungulatum* and *Mimatuta*. Character state 3 is an homoplastic character appearing as autapomorphies for *Cimolestes*, *Proviverra* and *Eosigale*.

20. The displacement of the conules of the post-protocrista and pre-protocrista is interpreted as a uniquely derived character state for *Paramys*, and therefore this is another character excluded from the performed analysis of parsimony.

21. (1 step, ci and ri 100).

The full contact of the very lingual portion of the paraconule and metaconule with the protocone comes out in this analysis as the only synapomorphy for ungulates (clade 26).

22. (3 steps, ci 33 – ri 0).

This is another case where the monophyly of the feraeans would better accommodate this character distribution. At nodes 34 to 31, both the derived shearing carnassial surface and the primitive one are assigned as possible alternatives. With this scenario it is not worth analyzing all the equally parsimonious character state arrangements. It is to if the monophyly of feraeans is assumed then the optimization of this character would be quite different, possibly having the derived state at the basal position within Ferae.

23. (3 steps, ci 66 – ri 50).

This is another trend for the carnassial shearing surface, and it is placed as a synapomorphy for component 33, with a reversal to the primitive condition at node 30. The further derived state 2 comes out as an autapomorphy for *Prototomus*.

24. (1 step, ci and ri 100).

The derived torsion of the paracone-metacone region, state 1, is a synapomorphy for the plesiadapiformes (clade 22).

25. The derived character state 1 is an autapomorphy for *Paramys* and therefore is not taken into consideration in the analysis of parsimony performed.

26. (5 steps, ci 60 – ri 66).

This is another feature considered to be unordered, and its state distributions are complex. The really interesting information is that all the derived states range within clade 27. This suggests that a general bunodont trend may be homologous throughout those taxa of clade 27. This would be the case if states 1 and 2 were considered as one single condition, it would then result in another synapomorphy for clade 27.

ROOTING THE UNGULATES

The Grandorder Ungulata, represented by the four basal condylarths, is as a monophyletic clade (26). The single upper molar character that is a synapomorphy for ungulates is the torsion of the very lingual portion of the conules resulting in full contact with the protocone labial wall (character 21, Fig. 17). However, SALLES (1994) discussing an earlier version of the data matrix here analyzed, pointed out that *Oxyprimus* might be a sister-taxon of anagalids (including rodents) plus plesiadapiformes, an assemblage equivalent to clade 25. The general similarity of the upper molar of *Oxyprimus* and *Purgatorius*, especially in wear pattern on the paracone and metacone is striking. This might indicate that not necessarily all upper Cretaceous/Paleocene condylarths are distributed within Ungulata. Or even, that basal condylarths might not be strictly related to the emergence of ungulates but also to other large groups of placental mammals. Following this view it is not surprising that *Oxyprimus* is placed at the basal node as sister-taxon of the other three condylarths (clade 24). The synapomorphy of this clade 24 is state 3 of the character 18, which concerns the bunodont shape of the conules.

The dental features frequently referred to as characteristic of ungulates, their general bunodont squarish shape, are here indicated to be in fact related to more basal level relationships within clade 27. Clade 27 supports the broad notion of anagalids (STUCKY & MCKENNA 1993) plus the plesiadapiformes composing a monophyletic group with the ungulates. The three character states supporting the monophyly of clade 27 [8(2), 12(2), and 27(1)] are related to a general bunodont dental pattern. The resemblance of the molar morphology between early rodents and primates with basal condylarths is an old subject in the mammal literature, extending back at least to the late nineteenth century (*e.g.* COPE 1883; MATTHEW 1897) and the early decades of this century (*e.g.* OSBORN 1902). More recently, SZALAY (1963) and CARTMILL (1974) have recognized these affinities but assumed that they were all due to adaptive convergences, and, as earlier discussed, MCKENNA (1992) and MACPHEE & NOVACEK (1993) published phylogenetic schemes placing ungulates together with anagalids (*sensu lato*) and archontans (primates). As mentioned above, other ongoing research, also concerning the masticatory apparatus, have as their preliminary phylogenetic conclusions the plesiadapiformes as sister group of the rodents

plus anagalids. In the light of the general placental dental patterns represented in Figure 20 it seems an attractive idea to see the plesiadapiformes representing basal archontans rather than just primates. This would be then corroborating the idea of reading component 27 as an assemblage comprising Archonta, Anagalida and Ungulata. But, the underlying question is whether the similarities observed are indeed homologies, or due to convergences for a herbivorous diet. This question is widely answered based on a common view that places insectivore-like placentals as basal to nearly all major placental clades. Therefore, this question is *a priori* answered as due to cases of parallel evolution. It seems that it is frequently taken for granted that clearly environmentally correlated characters are generally the results of independent evolutionary histories, and so the possibility of these type of characters are representative cases of "adaptative synapomorphies" is discarded without proper examination.

Based on the hypothesis of monophyly of clade 27, including the interrelationships there proposed, and also on the placement of an additional placental mammal, the genus *Tribosphenomys*, MENG *et al.* 1994, is a sister-group of *Paramys* (this result is obtained after applying the combined option of branching swapping mhennig* bb* of the Hennig86 based on the same data matrix and adding a new character). We argue that the very basal history of clade 27 is characterized by primitive bunodont (condylarth-like) transformations. In an ontological interpretation, it is hypothesized that some sort of placental "herbivores" may have indeed their very early history unfolding as part of a monophyletic plexus of phylogenetically related organisms, therefore supporting the view that cases of "herbivore-like" parallel evolution do indeed happen but at more advanced stages of bunodonty in already differentiated branches of clade 27. In other words, the very first steps towards the bunodont transformation characterizing a condylarth-like dental pattern are considered to be evidence for the monophyly of an assemblage of placental mammals here represented by clade 27, and named Magnorder Herbotheria, and that later, more differentiated bunodont features come to be often homoplastic among members of this high taxon. The clade Herbotheria is discussed also in another article in preparation. But, shortly, it could be provisionally placed in a classification derived from that one of STUCKY & MCKENNA (1993) and based on the phylogenetic scheme of Figure 20 (and not taking into consideration node 24), as follows:

Supercohort	PLACENTALIA Owen, 1837
Cohort	EPITHERIA McKenna, 1975
Subcohort	PREPTOTHERIA McKenna, 1975 new rank
Magnorder	HERBOTHERIA new taxon
Grandorder	ANAGALIDA Szalay & McKenna, 1971
Grandorder	ARCHONTA Gregory, 1910
Grandorder	UNGULATA Linnaeus, 1766

We are fully aware of the preliminary nature of this classification, specially concerning the fact that not all major groups of Archonta are considered and also that only one morphological complex is examined. However, we have reasons to advance that the new Magnorder Herbotheria seems to be an idea that indeed carries potential phylogenetic information content.

CONCLUDING REMARKS

First, in order to better understand placental interrelationships, it is clearly necessary to add new recently described fossil taxa finds across the Late Cretaceous/Tertiary boundary. Regarding our basal ungulate research programme, it is also evident that for achieving progress it will be necessary to cover a broader spectrum of the condylarth phase morphology. In that sense, a more complete detailed cladistic character analysis of the whole masticatory apparatus for these basal placental mammals is an enterprise waiting to be accomplished.

Readdressing the earlier question regarding whether or not the molar morphology is a good source of phylogenetic information, it is clear that the fully resolved hierarchical pattern here encountered for a set of considerably diverse placentals speaks for itself, thus giving a full yes to this question.

To conclude, the phylogenetic relationships of the placental mammal branching diagram (Fig. 20) put forward are generally supported by the different options of parsimony analysis other than the one performed. Hence, despite the preliminary nature of these results, it seems that the phylogenetic patterns proposed might be indeed representing some historical aspects of the placental mammal evolution, and we understand that the clade Herbotheria is possibly the most interesting outcome of this study.

Acknowledgements

During my last trip to the American Museum of Natural History (AMNH), in the winter of 1994, this study began as part of my Ph.D project regarding basal ungulate interrelationships. Motivated by discussions with Malcolm McKenna and Jin Meng, it became clear to me that an attempt to reexamine phylogenetic matters concerning the molar morphology of placental mammal would be worth doing. First, I would like to thank Richard Tedford for allowing me to study the fossil mammal collections of the AMNH and the two researchers mentioned from this same institution for kindly exchanging their ideas with me. As a formal doctoral student of the Université de Paris VII (Formation doctorale A. de Ricqlès), I am also very grateful to Philippe Taquet for having opened to me the opportunity of developing research programs on mammal systematics at the Laboratoire de Paléontologie of the Muséum national d'Histoire naturelle (MNHN). I specially acknowledge the time and suggestions of Daniel Goujet and Donald Russell, who together with Denise Sigogneau-Russell permitted me to have access to their fossil mammal cast collection. This manuscript was greatly improved by discussions with my adviser Pascal Tassy, and critical reviews by Jerry Hooker to whom I am especialy indebted, Malcolm McKenna, Pascal Tassy, Anwar Janoo, and Mario de Pinna. Financial support was provided by the Conselho Nacional de Desenvolvimento Cietífico e Tecnológico (CNPq), Brazilian Federal Government, and an auxiliary funding was received from the Laboratoire de Paléontologie (URA 12, CNRS) of the MNHN and by the Université de Paris VII.

Manuscript submitted for publication on 27 July 1994; accepted on 22 October 1995.

REFERENCES

ARCHIBALD D. in press. — Archaic ungulates ("Condylarthra") (85 p. ms.). *In* C. JANIS, L. JACOBS & K. SCOTT (eds). *Tertiary Mammals of North America*. Cambridge University Press.

BENTON M. J. 1988. — *The Phylogeny and Classification of the Tetrapods*, Volume 2. Mammals. Clarendon Press, Oxford, England, 329 p.

CARPENTER J. M. 1988. — Choosing among multistate equally parsimonious cladograms. *Cladistics* **4** (3): 291-296.

CIFELLI R. 1993. — Theria of Metatherian-Eutherian Grade and the origin of Marsupials. *In* F. SZALAY, M. NOVACEK & M. MCKENNA (eds.). *Mammal Phylogeny, Placentals*. Springer-Verlag Press, **2**: 205-215.

DARLU P. & TASSY P. 1993. — *La reconstruction phylogénétique : concepts et méthodes*. Masson, Paris, 245 p.

FARRIS J. S. 1988. — Hennig86 (version 1.5) software. Distributed by the author. New York: 41 Admiral Street, Port Jefferson Station 11776.

GINGERICH P. D. & GUNNELL G. F. 1979. — Systematics and evolution of the genus *Esthonyx* (Mammalia, Tillodontia) in the early Eocene of North America. *University of Michigan Museum of Paleontology Contributions* **25**: 125-153.

MCKENNA M. C. 1975. — Toward a phylogenetic classification of the Mammalia. *In* W. P. LUCKETT & F. S. SZALAY (eds.). *Phylogeny of the Primates: a Multidisciplinary Approach*. Plenum Press, New York.

— 1992. — The alpha crystallin A chain of the eye lens and mammalian phylogeny. *Annales Zoologici Fennici* **28**: 349-360.

MACPHEE R. D. E. & NOVACEK M. J. 1993. — Definition and relationships of Lipotyphla. *In* F. SZALAY, M. NOVACEK & M. MCKENNA (eds.). *Mammal Phylogeny, Placentals*. Springer-Verlag Press, **2**: 13-31.

MARSHALL L. G. & KIELAN-JAWOROWSKA Z. 1992. — Relationships of the dog-like marsupials, deltatheroidans and early tribosphenic mammals. *Lethaia* **25** (4): 353-460.

MARSHALL L. G. & DE MUIZON C. 1992. — Atlas photographique (MEB) de Metatheria et de quelque Eutheria du Paléocène inférieur de la Formation Santa Lucia à Tiupampa (Bolivie). *Bulletin du Muséum national d'Histoire naturelle*, Paris, 4[e] série, 14, C **1**: 63-91.

NOVACEK M. J. 1992. — Fossils, topologies, missing data, and the higher level phylogeny of eutherian mammals. *Systematic Biology* **41** (1): 58-73.

NOVACEK M. J., WYSS A. & MCKENNA. M. C. 1988. — The major groups of eutherian mammals. *In* M. J. BENTON (ed.). *The Phylogeny and Classification of the Tetrapods*, *Mammals*. Claredon Press, Oxford, England **2**: 31-72.

PROTHERO D., MANNING E. & FISCHER. M. 1988. — The phylogeny of ungulates. *In* M. J. BENTON (ed.). *The Phylogeny and Classification of the Tetrapods*, *Mammals*. Claredon Press, Oxford, England **2**: 201-234.

SALLES L. O. 1992. — Felid phylogenetics: extant taxa and skull morphology (Felidae, Aeluroidea). *American Museum Novitates* **3047**, 67 p.

— 1994. — Rooting ungulates within placental mammals: Upper Cretaceous/Paleocene fossil record. *Progress report in the "III Simpósio sobre o Cretáceo do Brasil"*, Rio Claro, Brazil: 109-111.

STUCKY & MCKENNA. M. C. 1993. — Mammalia. *In* M. J. BENTON (ed.). *The Fossil Record II*. Chapman & Hall, London: 739-771.

SWOFFORD D. L. & MADDISON W. P. 1987. — Reconstructing ancestral character under Wagner parsimony. *Mathematical Biosciences* **87**: 199-229.

SZALAY F., NOVACEK M. & MCKENNA M. 1993. — *Mammal Phylogeny, Placentals*. Springer-Verlag Press, **1**, 321 p.

VAN VALEN L. 1978. — The beginning of age mammals. *Evolutionary Theory* **4**: 45-80.

ZHANG Y. 1980. — A new tillodont-like mammal from the Paleocene of Nanxiong Basin, Guangdong. *Vertebrata PalAsiatica* **18** (2): 126-130.

Bulletin du Muséum national d'Histoire naturelle, Paris, 4e sér., **18**, 1996
Section C, nos 2-3 : 451-516

Earth Expansion, Plate Tectonics and Gaia's Pulse

by Martin PICKFORD

"Great spirits have always encountered violent opposition from mediocre minds."

Albert EINSTEIN

"Plate Tectonics on the globe is essentially the same as on a plane."

A. COX & R. HART 1986

"Because the Earth is a near-spherical body and a map is projected on a flat sheet of paper, distortion is inevitable."

H. OWEN 1983

"Uniformitarianism today: Plate Tectonics is the key to the past."

B. F. WINDLEY 1993

"Plate Tectonics (PT) includes many points of contrary evidence that have been bypassed or ignored."

M. L. KEITH 1993

Abstract. — There are four possibilities concerning the size of the Earth, which impinge on all theories of its global-scale tectonic evolution – a) its radius has remained constant through geologic time (the constant "r" hypothesis underpins much past and current thought in the Theory of Plate Tectonics); b) its radius has increased with the passage of geologic time (the increasing "r" hypothesis is the main proposition of the Expanding Earth Theory); its radius has decreased with the passage of geological time (an early idea put forward to explain the existence of the world's fold mountain belts); and d) its radius has fluctuated over geological time, sometimes increasing, sometimes decreasing (an idea put forward to explain the existence of both compressional and tensional structures in the Earth's crust).

The first two parts of this paper deal with two of the above competing theories of global tectonics – a) the Plate Tectonics Theory in a globe of constant "r", and b) the Expanding Earth Theory in which "r" has increased over geologic time. Examination of these theories indicates that there are serious difficulties in reconciling the available geological data with the Plate Tectonics paradigm in which it is almost universally assumed that the globe has remained constant in size and the oceans constant in volume through geological time. Many of the inconsistencies disappear if the same data are viewed within a model of an expanding Earth, as long as appropriately sized globes are used for plotting up the data.

The third section of the paper examines the periodicity of events in the lithosphere, hydrosphere, atmosphere and biosphere and relates these to episodic changes in the orientation of the axis of rotation of Earth which induce changes in the Sun/Earth relationship and the development of tremendous stresses and strains in the fabric of the globe, as well as other effects. The causes of such changes are themselves related to alterations of the Earth's fabric during Earth Expansion, principally due to unevenly distributed generation of oceanic crust at spreading ridges, which induces imbalance in the global gyroscope. The third part also looks at some of the secular changes that have occurred in various Earth systems, including the biosphere, hydrosphere and atmosphere.

The paper ends with several major conclusions which attempt to explain the evidently close relationship that existed between events in the lithosphere, hydrosphere, atmosphere and biosphere.

Key-words. — Global tectonics, Plate Tectonics, Earth Expansion, Endogenetic energy. Exogenetic energy.

L'Expansion terrestre, la Tectonique des plaques et les pulsations de Gaïa

Résumé. — Plusieurs géologues ont déclaré s'interroger à propos de la théorie de la Tectonique des plaques sur une Terre à rayon constant. Ils formulent une série de questions sur les sources d'énergie et les mécanismes de déplacement des plaques qui leur paraissent rester sans réponses. Les cellules de convexion du manteau terrestre animées par l'énergie géothermique, mécanisme retenu par les tenants de la théorie de la Tectonique globale, ne constituent pas, à leurs yeux, un mécanisme convaincant pour expliquer le mouvement des plaques. En effet, l'énergie géothermique est beaucoup trop faible pour accomplir les mouvements envisagés. Il existe, de plus, beaucoup de faits de divers ordres qui réfutent cette théorie. Ainsi, des problèmes de cartographie, des solutions parochiales dans deux dimensions de l'espace, enfin des solutions contradictoires émises sur le mouvement des plaques. D'autres géologues ont envisagé des mécanismes différents (la tectonique de membranes et le flux de liquides) pour expliquer la Tectonique globale, mais leurs propositions sont faites dans le cadre d'une Terre à rayon constant. Un nombre croissant de géologues considère la possibilité d'une Terre en expansion au cours des temps géologiques, et envisage qu'elle ait joué un rôle majeur dans la Tectonique globale.

L'Expansion de la Terre n'a pas eu une expression uniforme à sa surface comme le montre la largeur et la répartition des rides d'expansion océanique. Ainsi, seuls 17 % de ces rides d'expansion sont répartis au nord du Grand Cercle constitué par les chaînes téthysiennes, tandis que 83 % le sont au sein et au sud de ce cercle. Cela signifie que l'expansion de l'hémisphère sud a été plus forte que celle de l'hémisphère nord, et que si la gravité avait été nulle, alors la terre aurait dû se gonfler inégalement. Mais l'action de la gravité, source d'énergie terrestre la plus puissante, a maintenu la forme sphérique du globe terrestre, en conséquence de quoi, elle a donné naissance aux chaînes orogéniques et aux fosses océaniques qui sont alignées plus ou moins selon un grand cercle. Cela serait dû au fait que l'aire d'un hémisphère croît pendant que son périmètre décroît, engendrant ainsi une compression le long de la zone de contact entre les hémisphères (le Grand Cercle). Une Expansion terrestre qui n'est pas uniforme rendrait compte, d'une part, des anomalies dont la Tectonique des plaques est incapable d'expliquer l'origine et, d'autre part, des données géologiques telles que : 1) le rapport isotopique d'hélium dit « cosmic » des rides médio-océaniques, 2) la baisse des paléotempératures des océans, 3) la contemporanéité des phases tectogéniques et celle de l'activité des rifts, les flux de basaltes, les irrégularités du déplacement des points chauds, l'existence des rides d'Expansion océanique abandonnées et d'autres faits encore. Dans le cadre de l'hypothèse de l'Expansion terrestre, la Tectonique globale résulterait de l'effet réciproque de l'énergie, de l'expansion et de la gravité.

Deux des mécanismes possibles de l'Expansion terrestre sont discutés : 1) un noyau terrestre aux propriétés d'un plasma, 2) une Terre hydrique (des protons disséminés dans des lattices métalliques). Ces deux mécanismes peuvent rendre compte de l'Expansion terrestre sans qu'il y ait eu une augmentation de la masse de la Terre. Le mécanisme envisagé est le suivant : le plasma (ou la Terre hydrique) s'altère progressivement en libérant des protons qui se lient avec des électrons pour constituer des atomes, un processus qui s'accompagne d'un fort accroissement du volume sans changement de masse globale.

La troisième partie de notre article traite du comportement par à-coups de la planète ainsi que des changements séculaires. Au sein du premier d'entre eux, on dénombre les phases tectogéniques, les pulsations des rifts et les éruptions sporadiques de flux basaltiques ; tous semblent être liés au cours des temps géologiques et avoir été engendrés par les mêmes causes. Au même moment se déroulent dans la biosphère, des événements majeurs comme les extinctions globales. Parmi les changements séculaires envisagés, ceux de l'obliquité de la planète et de la position de son axe de rotation ont dû joué chacun un rôle important en modifiant la périodicité des saisons et le climat mondial, ce qui s'est traduit par des changements majeurs sur la biosphère.

Des conclusions, qui tentent d'expliquer les relations étroites qui unissent les événements de la lithosphère, de l'hydrosphère, de l'atmosphère et de la biosphère, sont tirées.

Mots-clés. — Expansion terrestre, Tectonique des plaques, phases tectogéniques, sources d'énergies endogènes, ceintures orogéniques, Grand Cercle, réorientation de l'axe de rotation terrestre, paléotempératures océaniques, ceintures écoclimatiques, obliquité de l'axe de rotation terrestre.

M. Pickford, *Muséum national d'Histoire naturelle, Laboratoire de paléontologie, 8 rue de Buffon, F-75231 Paris; Collège de France, 11 Place Marcellin Berthelot, F-75005 Paris cedex 05; Geological Survey of Namibia, P.O. Box 2168, Windhoek, 9000 Namibia.*

AIM

The aim of this paper is to examine the history of various Earth systems (lithosphere, hydrosphere, atmosphere, biosphere) for evidence concerning the rhythms, modes and trends of change that they have undergone since the Cretaceous. An understanding of these systems may throw some light on the evolution of the Earth's lithosphere and biosphere during the Cainozoic, which may thereby lead to a better understanding of the close historical relationship that existed between the Earth's crust and the biosphere.

INTRODUCTION

For the past three decades, Plate Tectonics has been the predominant theory in global geotectonics. The Theory of Plate Tectonics rest on several basic assumptions, the validity of which have been questioned. One of these assumptions is that the Earth has remained the same size since the Proterozoic. This assumption has been called into question on several occasions but the majority of geotechnicians have refused to respond to the challenges. A second is that the plates are tortionally rigid, an assumption that has been succesfully challenged to the extend that many geotechnicians no longer consider it valid. A third assumption is that the volume of the hydrosphere has remained constant since the Proterozoic. And there are several more which are seldom questioned such as the ideas that obliquity has not changed and the pole of rotation has been "fixed" throughout geological time. A further assumption is that plates are driven by convection cells in the mantle, of which ridge push, slab pull, deviatoric tensional stresses and other forces are considered to be manifestations.

This paper examines several of these assumptions in detail. It also looks at many of the contentious aspects of Plate Tectonics, including the apparent lack of sufficient energy to power the plate tectonic "motor". This and many anomalies that have been noted by researchers indicate that something is seriously wrong with the basic assumptions of Plate Tectonics. It is concluded that most of these are invalid. In particular, the assumption that the Earth has remained constant in size is seriously challenged by a variety of data which indicate that the radius of the Earth has increased during the Phanerozoic. This conclusion has led to the proposition of a theory of global geotectonics called "Expanding Earth Hypothesis". There are two versions of the latter hypothesis – "fast expansion" and "low expansion". The trajectory of continental masses as envisaged in the Plate Tectonics and Earth Expansion hypotheses are summarized in Figure 1.

FRAMES OF REFERENCE

A troubling problem in global geotectonics, and one that is not often addressed adequately, is the definition of frames of reference which apply over geological time scales. In fact there do not seem to exist any "absolute" long term frames of reference.

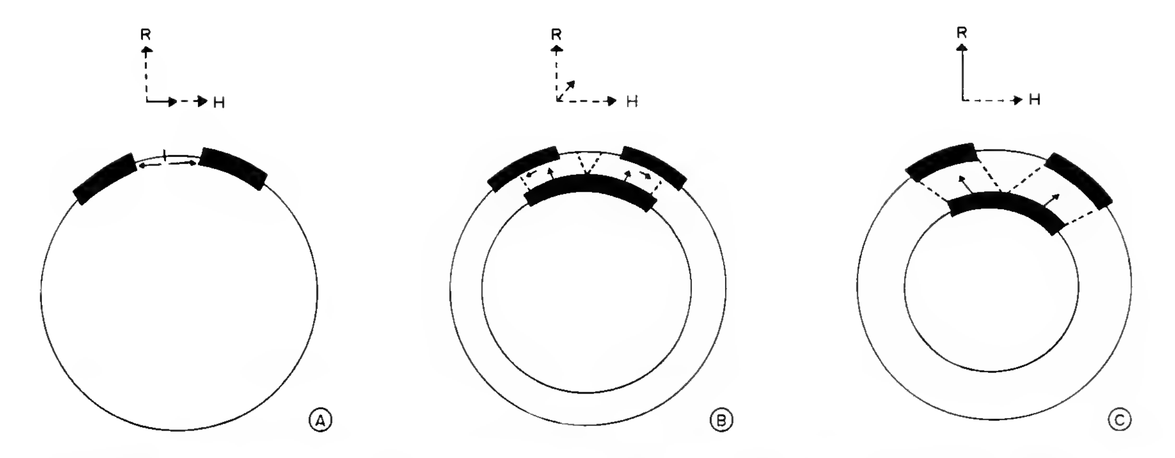


FIG. 1. — Comparison of three theories of global tectonics. A. Plate Tectonics in a globe of constant "r"; B. Slow Earth Expansion (triassic globe 80% of modern globe; C, fast Earth Expansion (Cambrian globe 60% of modern globe). In A, all movements of continents (arrows below dark masses) are horizontal (small cartoon above globe shows no radial vector of movement). B, movement of continents is mainly radial away from the centre of the Earth but there is room for some horizontal vectors of movement (arrows below dark masses representing contiments)(small cartoons above globe shows that a combinaison of radial and horizontal movements has occured). C, all movements of continents is considered to be radial (arrows below dark masses) (cartoon above globe shows no horizontal vector of movement).

In Plate Tectonics analyses, a common practice has been to select one or other of the continents, often Africa or South America, as a reference, and to relate other plate movements to it. But since the break-up of Pangaea, Africa has moved northwards with respect to the present day South Pole, so such solutions are not "accurate" with respect to any global frame of reference such as the present day latitude/longitude graticule. Inspection of any series of palaeogeographic maps, including cartographically accurate ones, such as those of OWEN (1983a), will highlight the problem.

The magnetic dipole changes position on a daily basis, but is often assumed to average out over geological time to provide a notion of where "true north" and "true south" were located at any desired period in the past. This is despite the fact that at present magnetic north is inclined at some 14° from the rotational North Pole.

The hot-spot (and wet-spot) frame of reference has been in use for more than a decade, but the crustal hot-spot tracks related to this system show kinks and dog-legs in them, indicating that the outer layers of the Earth seem to have been moving independently of the inner layers, at least during some geological periods. Furthermore two of the prime examples of hot-spots – the Cook-Austral chain and the Marquesas chain – show gross violations of the simple age-distance relationship which is supposed to characterize hot-spot tracks (KEITH 1993).

All this means that the search for an absolute long term frame of reference for the entire globe and its contents is probably a futile one.

LAMBECK (1979) discussed the question of frames of reference in some detail and showed that tectonic motions of the continents or plates cannot be separated from any drift of the axial dipole. The marine magnetic anomalies, which permit the relative motion of the plates to be

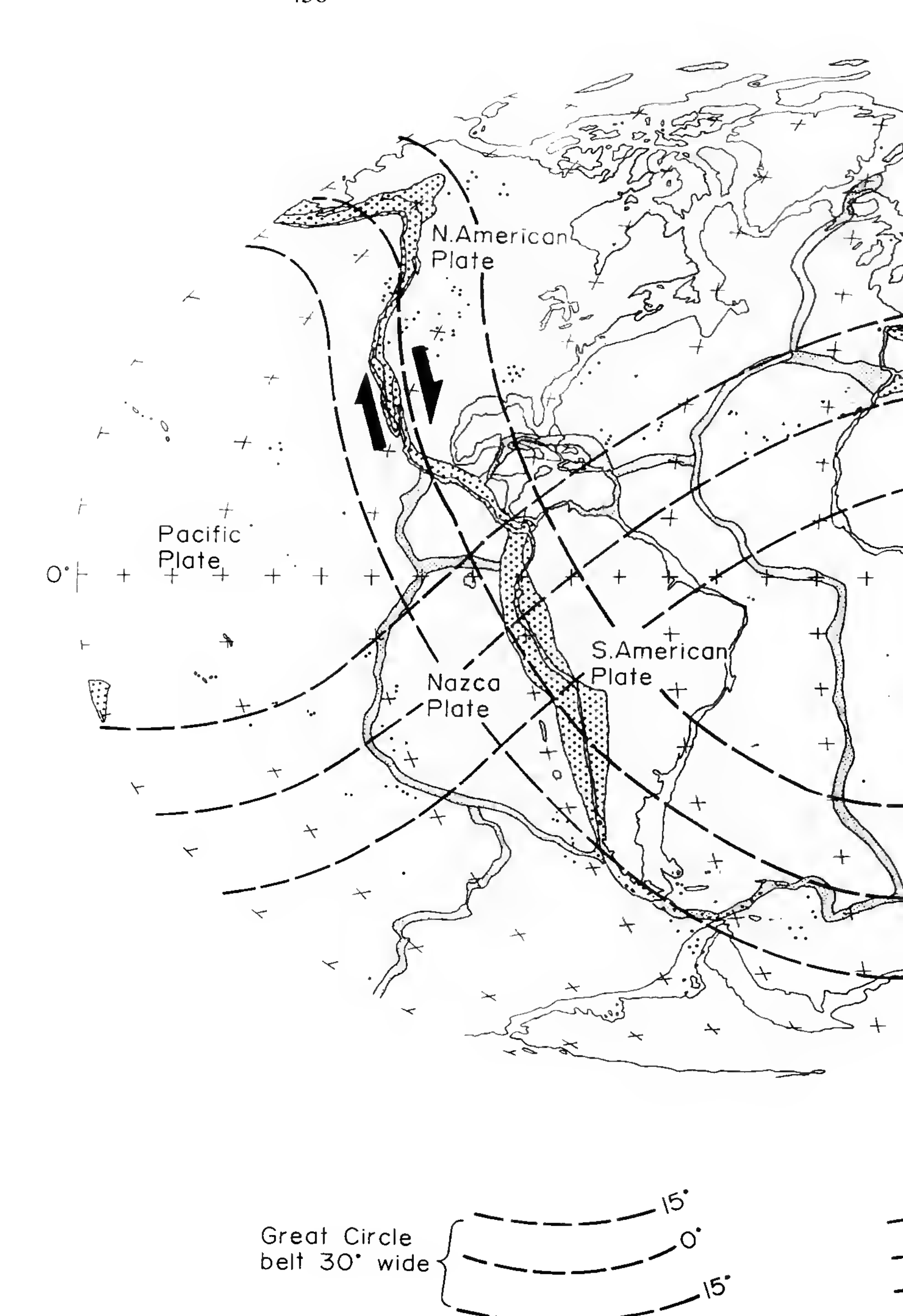
determined throughout the Cainozoic and Mesozoic do not solve the problem, even if one adopts an additional frame of reference such as the hot-spot frame, or by minimizing the motions of plate margins. The reason is that "to fix any one plate requires three parameters and, if there are N moving plates and a wandering pole, there will be a total of (3N-1)+2 unknowns (if one longitude is arbitrarily fixed) for any one geological epoch. As independent observations we have the relative motions between the plates and the position of the apparent pole relative to one plate, or a total of 2+3(N-1). Thus the number of unknowns always exceeds the number of observations. A unique solution is impossible." (LAMBECK 1979: 76)

Under these circumstances, it appears to be absurd to claim that, over geological time periods, it is impossible for the Earth's axis of rotation to experience reorientation, either within the Earth or with respect to the Universe. The Earth's axis of rotation is not fixed with respect to all the matter comprising the crust, nor is it fixed with respect to all the matter making up the mantle, and it would be surprising if it were found to be fixed with respect to the core. Even more surprising would it be to find that it is fixed with respect to an external frame of reference such as the plane of the ecliptic or any other celestial reference, if only because the entire universe has itself been evolving along with all the matter in it (LASKER *et al.* 1993, LASKER & ROBUTEL 1993; VERMEERSEN & VLAAR 1993; WILLIAMS 1993). However, the "belief" that the axis of rotation of Earth cannot change appears to be remarkably deeply ingrained into the conscience of many geoscientists.

In the final analysis, there is no ideal solution to the question of frames of reference, but we should not be straight-jacketed into thinking that any frame of reference, including the axis of rotation of the Earth, is fixed. The Earth is not a school globe fixed to a set of gymbols. It has no gymbols at all, except those imaginary ones that we give it for mathematical and geophysical purposes. A fixed or permanent axis of rotation is as imaginary as Euler poles are.

METHODS

CAREY (1983) and OWEN (1983a, b) have highlighted some of the pitfalls of working on flat sheets of paper when dealing with structures that are disposed over the surface of a globe. For example, on a globe, pi, the ratio between the radius of a circle and its circumference, is not a constant. On a flat sheet of paper it is. On curved and enclosed surfaces, this gives rise to some peculiar, even counter-intuitive geometry, which has fooled more than one geotectonician during the past thirty years. On flat surfaces, the angles of a triangle always add up to 180°. On a sphere they can add up to any value between 180° and 540°. Draw a circle on a globe, and then try to represent it on a flat sheet of paper. Depending upon the projection used and the position of the circle on the projection, a circle on a globe can take on a formidable array of forms on a sheet of paper ranging from a circle through an entire family of ellipses and other closed shapes to a straight line. Distortion of shape, size (or scale) and relationships between neighbouring entities is the usual result of depicting on a flat sheet of paper the forms seen on a globe. A scale bar which can be used anywhere on a globe is almost worthless on a flat plan of the globe. On a globe the north arrow of a compass always points directly towards the North


N.American
Plate
Pacific
Plate
0°
Nazca
Plate
S.American
Plate
Great Circle
belt 30° wide
15°
0°
15°

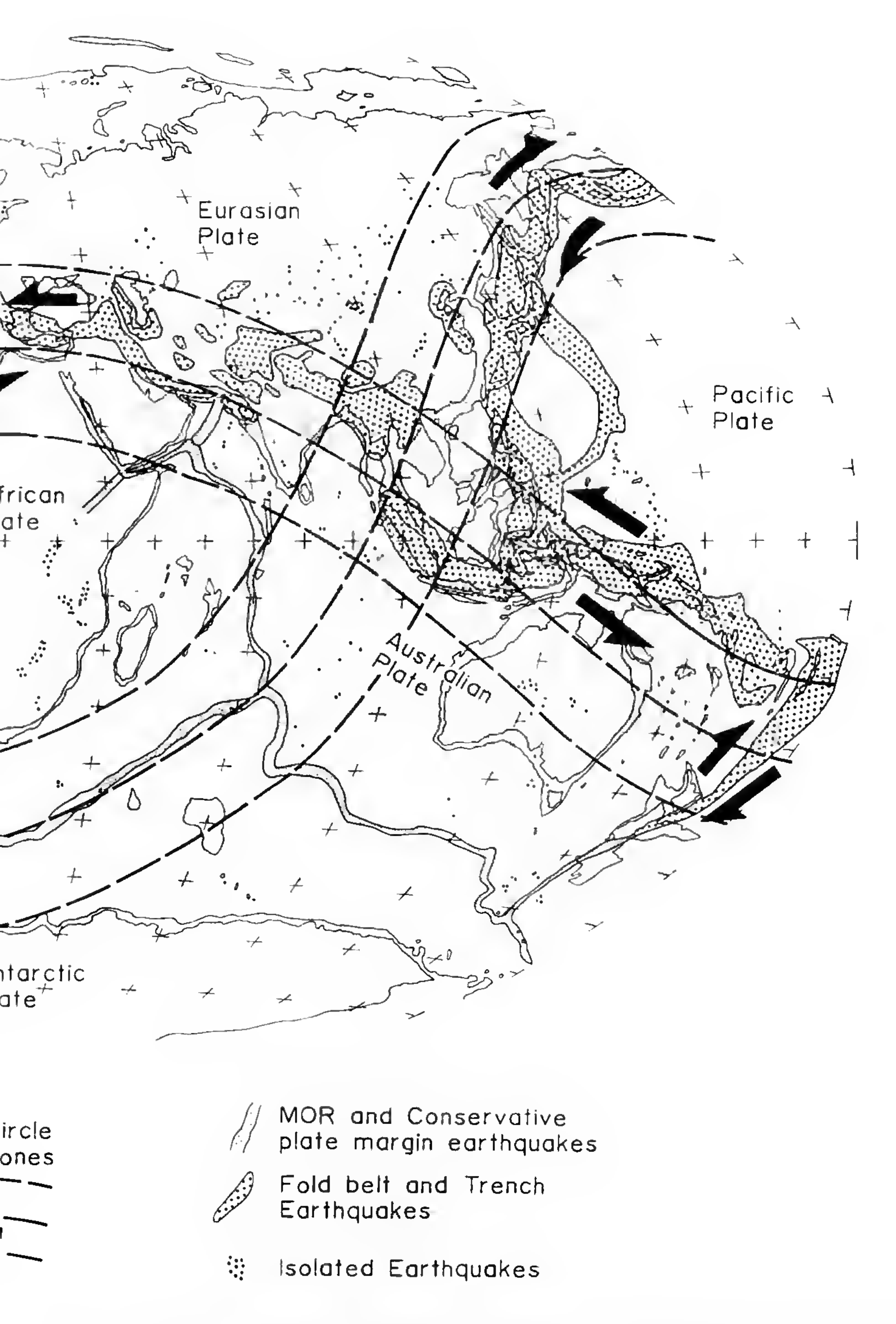


FIG. 2. — Modern globe[21] showing epicentres of earthquakes of magnitude greater than 4.5 in the period 1963-1977[12], the major plates and the two great circle belts (30° wide) in which occur the world's fold mountain belts, most of the Earth's subduction zones, and most of its compressional earthquakes and volcanoes. The Tethyan Great Cercle belt contains the Atlas, Pyrenees and Alpine-Himalayan fold mountain belt and the Sumatra-Soloman subduction zone and is characterized hy sinistral torsion. The Cordilleran Great Cercle belt contains the Rockies and Andes fold mountains belt, and most of the circum-Pacific subduction zones. It has dextral torsion.

magnetic Pole. On a flat map of the world it seldom points directly at the magnetic North Pole but at various angles from it, the "direct" line being depicted by a curved line.

There are many other "surprises" for scientists who study global problems by working on flat sheets of paper. For example, we take an ordinary pair of compasses and a globe. We fix one of the points of the compass at a point on the surface of the globe (for instance at the North Pole) and start to draw concentric circles on its surface, beginning with the points of the compass close together and ending with its points far apart. Initially the circumference of the circles being drawn and the parts of the globe's surface enclosed by them both increase in size, but we will soon reach a stage – called a great circle – beyond which the circumference of the circles being drawn begins to get smaller, even though the part of the globe's surface enclosed by the circles continues to increase. We will eventually reach a stage of the exercise where the circumference of the circle being drawn becomes zero – the drawing point of the compass has arrived at the South Pole – but the entire globe's surface area is enclosed by it. Continue to increase the distance between the fixed point of the compass and its drawing point, and you will fail to make any mark on the globe.

This "thought experiment" might at first glance appear to have little practical use, but consider the Pacific Ocean, the surface area of which is still increasing. Its rim already approximates a great circle. What will happen if the surface area of the Pacific Ocean continues to augment by addition of crust at spreading ridges, as it surely will? On a constant diameter Earth, its perimeter will decrease in length, and this will have many geotectonic implications.

On a globe, the two areas on either side of a closed perimeter add up to a constant. This remains true no matter what the size and shape of the perimeterare. The Pacific Rim has increased in length by about a third of a great circle since the days of Pangaea at the onset of the Jurassic. On a globe of constant dimensions this would only be possible if the Pacific Rim was shorter than a great circle at the time of Pangaea. There are two possibilities on such a globe: either Pangaea occupied an area less than a hemisphere while the proto-Pacific covered an area greater than a hemisphere, or Pangaea was greater than a hemisphere while the proto-Pacific was smaller than a hemisphere. All reconstructions of Pangaea show that it covered slightly more than a hemisphere of a globe of today's dimensions (CAREY 1988, fig. 29). Thus, on a globe of constant dimensions, the Pacific Rim could only get longer if the proto-Pacific (or Eopacific as it is sometimes called) increased in size at the expense of Pangaea. The proto-Pacific has indeed got larger since the days of Pangaea – the ocean floor palaeomagnetic data shows this amply. But the proto-Pacific did not get larger at the expense of Pangaea. During the same period the Pangaea side of the Earth has also greatly increased in area by the insertion of the Atlantic, Indian, Arctic and Southern Oceans between its various continental fragments. Something must be amiss with the assumption of constant "r".

METHODOLOGICAL PROBLEMS

Two further very real methodological problems have been the tendency for geotectonicians to work 1) on planar maps of the world rather than on globes and 2) on restricted parts of the world, rather than examining the globe as a whole. One result has been that solutions to

geotectonic problems proposed for a particular area often contradict solutions proposed for a neighbouring area or for areas on the far side of the globe. The "gap artefact" is a classic example of this cartographic problem – see, for example, the paper by BIJU-DUVAL *et al.* (1976, fig. 5) for an erroneously wide Tethys in the vicinity of Europe. If we begin reconstructing Gondwanaland on a globe of constant dimensions, starting in the west, by the time we reach the eastern edge of the reconstruction there is an enormous gap between Asia and Australia (OWEN 1983a, b). There is much geological and palaeobiological evidence to indicate that this gap did not exist, and that, in reality, during the Mesozoic, Australia and Asia were not as far apart as the "gap artefact" suggests. If we now try a reconstruction of Gondwana but this time starting in the east, with Asia and Australia near each other, then by the time we reach the west, there is an unacceptably wide gap between Africa and Europe. The only realistic way to close the gap or gore while maintaining cartographic and geological integrity, is to decrease the dimensions of the globe by a suitable amount. No amount of pulling and tugging will get a small waistcoat to button neatly onto an oversized waist.

As geologists, we are trained to think in three dimensions – four are better – and even parochial geotectonic studies are usually carried out in three dimensions. However, the vast majority of such studies consist of the three dimensions of a tiny portion of the Earth's crust. So restricted are some portions studied, that at the scale of the globe they effectively represent two dimensional, unidimensional or even point studies, depending upon the size and shape of the areas examined. For example, at the scale of the globe, the Alpine Fold Belt is like a length of tape draped across a large globe. Its width – about 800 km if we are generous – is a mere 2% of the circumference of the Earth. Its length from Portugal to the Bay of Bengal is about 30% of the circumference of the Earth, while its thickness usually represented in cross sections is of the order of 0.5% of the diameter of the Earth. The average width of the Great Rift System of Africa is a mere 0.1% of the circumference of the globe and the relief between its shoulders and its floor is of the order of 0.025% of the Earth's circumference. At the scale of the globe, the Great Rift is basically a unidimensional feature – a line on a globe.

As OWEN (1983b) and CAREY (1988) have explained, many of the objections to the Expanding Earth Theory are invalid because the objector failed to consider the differences between planar and spherical geometry. Legion are the planar maps that have been published on plate tectonic themes which are cartographically inexact. As OWEN writes it, many of these maps are nothing more than "cartoons".

For example, POWELL (1979) reconstructed the history of the Indian plate during its journey from the southern hemisphere in the middle Cretaceous to its "docking" with the Eurasian landmass during the Oligocene. The successive outline maps of the Indian plate do not change in size or in shape during this voyage on the chosen projection, even though they should do so according to accepted cartographic procedures. It looks for all the world as though POWELL cut out a map of India and redrew the same map in various positions on the flat base map, forgetting that this is an invalid procedure from any cartographic point of view, except on a globe.

A further example of the pitfalls of working on planar maps of the globe concerns the difficulties of appreciating the three dimensional aspect of global tectonics from a planar rendition of the data, even if the latter are impeccably accurately plotted. DOGLIONI (1993, fig. 1) for example, provides a standard view of the world with the centre of the map occupied by the

western part of the Pacific Ocean with Africa to the left of the map and South America to the right. On this map he distinguishes "West"-dipping, and "East or NE"-dipping subduction zones. However, a plot of the subduction zones of the Pacific Ocean region on a globe rather than on a map, reveals that all these zones are dipping in the same way – away from the Pacific hemisphere. The Pacific hemisphere is in effect being overridden by the opposite hemisphere, and where the activity is taking place, a great circle zone of cordilleras and trenches has formed (Fig. 2). A similar great circle zone of cordilleras and trenches occurs along the alpine fold belt from Portugal to the Tonga Trench, where the southern hemisphere is dipping under the northern one.

Mutter & Mutter (1993) use another standard map (which only extends to 70° of latitude) in which the centre of the map is in the eastern Pacific, but in which South America and Africa are in the right hand half of the map. On this map, Mutter & Mutter have depicted the direction of plate movements by drawing arrows at right angles to spreading ridges and trenches. The Pacific plate is shown to be moving westwards with respect to the South American plate and the eastern part of Asian plate, yet northwards with respect to the northeastern part of Asia and the northwestern extremity of North America, at the same time it is undergoing dextral shift with respect to North America in the region of California. Is the Pacific plate moving westwards, northwards or is it rotating anticlockwise? On the planar map it is difficult to reconcile the conflicts.

On the same map, the depiction of movement vectors of the Antarctic plate indicate that all around its periphery, the edges of the Antarctic plate are moving southwards (an impossibility, even on a globe). In fact, what has happened is that the edges of the Antarctic plate, as defined by the spreading ridges which surround Antarctica, have accreted northwards with respect to the continent, which has been relatively immobile since the break-up of Gondwanaland. Thus, far from the Antarctic plate having a southwards plate motion as depicted on the map, it is the spreading ridge system which has increased in length and thereby shifted northwards with respect to the continent of Antarctic.

In effect, when working on global tectonic problems, there is no alternative but to work on globes and not on planar maps.

THE PLATE TECTONICS PARADIGM AND SOME PROBLEMS WITH IT

Definitions

A definition of Plate Tectonics given in the *Glossary of Geology* (Bates & Jackson 1990) is as follows:

"A theory of global tectonics in which the lithosphere is divided into a number of plates whose pattern of horizontal movement is that of torsionally rigid bodies that interact with one another at their boundaries, causing seismic and tectonic activity along these boundaries."

Naturally, there are many aspects to the Theory of Plate Tectonics, and each one of which can be considered a theory in its own right. These include the concepts of subduction and obduction, the notion that plates are driven by convection cells in the upper mantle and several others. One should add that most supporters of Plate Tectonics assume that the radius of the

Earth has not changed since at least the Mesozoic (ZIEGLER 1993, refers to it as the "finite" globe) itself a theory of the Earth about which there is not universal agreement.

There are a few researchers who accept the plate-like character of the lithosphere and some of the aspects of motion – such as lateral displacement of plates – implied in the Theory of Plate Tectonics, but who consider that, in addition, the Earth's radius has increased by some 20% since the Triassic. These scientists comprise the so-called "slow expansion" school of the Earth Expansion Theory (OWEN 1983). In this version of Earth Expansion, some of the continents have experienced lateral movement with respect to the underlying mantle, but all of them have in addition experienced radial movement outwards from the centre of the Earth.

An alternative group of geoscientists, the "fast expansion" school of the Earth Expansion Theory, holds that no lateral (or horizontal) movement of lithospheric plates has occurred, but that the whole separation of the continents has been achieved by a process by which the radius of the Earth has increased by 40% since the Triassic (CAREY 1978). In this version of Earth Expansion, the major movement vector of the continents has been radial, away from the centre of the Earth.

ORIGIN OF PLATE TECTONIC THEORY

The origin of the concept of Plate Tectonics is described by COX & HART (1986). They point out that while he was writing his paper to *Nature*, WILSON (1965) cut out some pieces of paper and moved them around the table top. COX and HART recommend that students do the same in order to understand the basic principles involved. Whilst such a procedure is very pedagogical, it is incomplete if not followed up by doing similar things on a globe. These flat pieces of paper moving about on a flat table top help to illustrate the concepts of ridges (or rises), trenches, polarity, transform faults and dextral and sinistral movements.

The concepts as described by COX & HART (1986) are essentially two-dimensional and of a parochial nature. Indeed, in the entire text amounting to 392 pages, there is not a single presentation of a whole-globe view of plate tectonic activity. Instead we find the statement that "plate tectonics on a globe is essentially the same as on a plane." The most complicated system discussed by these authors is the "three plate problem." Nowhere is there a warning to budding plate tectonicians that their solutions to parochial problems should be compatible with plate movements everywhere else in the globe.

FROM HYPOTHESIS BY WAY OF THEORY TO DOGMA

For three decades the Theory of Plate Tectonics in a globe of constant dimensions has dominated the thought processes of most of the world's geologists and many of its palaeontologists. This theory seeks to propose a mechanism – Plate Tectonics – which can explain the distribution of the continents and ocean floors and all the structures observed in them. Yet, since its inception, observations have been made which cast doubt upon its validity as a universal explanation of the evolution of the Earth's crust. Such is to be expected as a normal facet of scientific theory – what seems abnormal or contentious is the tendency for some geoscientists to ignore the criticisms as though they are trivial or of no consequence. In reality, many of the problems raised for the Theory of Plate Tectonics during the past three decades are serious and

should not merely be ignored. These difficulties certainly won't just "go away". Some of these observations are of a parochial nature and are usually not considered by many adherents to the theory to be problematic for it. Other criticisms, however, undermine the theory by aiming at its roots.

Since the early 1960s alternative explanations of the evolution of the Earth's lithosphere have generally been ignored, even in the rare event that they could be published in accessible scientific journals. Unfortunately, the tendency on the part of the scientific community to ignore or to suppress the publication of alternative points of view – by ridicule, by simply ignoring them, or by unscientific or undeontologic refereeing processes for example – has led to a situation in which Plate Tectonics Theory has for many scientists become a "dogma" rather than a scientific concept to be examined, questioned, modified and accepted or rejected on the merits of its evidential basis and its predictive and explanatory powers.

At its inception, the Theory of Plate Tectonics was treated by most scientists as a genuine scientific theory to be subjected to the usual scientific scrutiny. Consequently, it underwent modifications as new data and interpretations became available. As time passed however, in the minds of many people it has crossed the threshold which separates scientific theory from dogma, and for many researchers it has now become a matter of unquestioning belief. In a scientific domain, the latter is clearly an unacceptable state of affairs. There are numerous publications, for example in the domain of palaeobiogeography, in which Plate Tectonics has been invoked to explain biogeographic data without the authors having the slightest inkling of what Plate Tectonics means or how it is supposed to work. Even in the domain of geotectonics, there are those who perform incredible mental gymnastics in order to get their field observations to fit into the plate tectonic paradigm. For those who implicitly believe in Plate Tectonics as the principal mechanism behind global tectonics, alternative explanations of the evolution of the Earth's crust appear to be anathema – they are concepts to be rejected outright, generally even without their basis having been read and understood.

For the past three decades, many of the geographical aspects of the geological and biological changes which occurred during the Tertiary have been explained within a model of mobile continents whose movements relative to each other on a globe of constant dimensions, have been determined by "plate tectonics" (COX & HART 1986; CONDIE 1989). Indeed, it appears from the way they write, that for many researchers "plate tectonics" has become synonymous with "continental shift", which of course it is not. One is a theory of mechanism to explain an observation, the other is the observation itself.

PHILOSOPHY

In the belief that science best advances by the overthrow or modification of previously cherished theories, especially those that have tended to cross the threshold into dogmatism, I have been taking a look at some of the different ideas that have been proposed to explain past events in the Earth's lithosphere and biosphere. I do this because for the past two decades I have found that many of the palaeobiological and palaeoecological events of the Cainozoic Era are incompatible with plate movements as reconstructed on a globe of constant dimensions, or that they cannot be satisfactorily explained by it. As a result I have looked at some of the points

of dissatisfaction that other earth scientists and palaeontologists have expressed about the Theory – more properly "theories", since there are several variations on the basic theme – of Plate Tectonics. I have also looked at some of the alternative proposals to explain the history of the Earth's crust and its inhabitants, both animal and plant, and I pass some of these on to the reader in the hope that they will raise questions in his or her mind. I cannot pretend that any of the ideas are originally mine; most of them have been proposed at one time or another by my predecessors. The motive for writing this lengthy review of the matter is to highlight the varied aspects of the theories of global tectonics with a view to stimulating discussion.

Some of the ideas were considered worthy of research long before the Theory of Plate Tectonics came onto the scene. Most of them were never refuted or disproven in scientific debate, they were simply ignored or put to rest once Plate Tectonics "arrived", because it was considered by many – erroneously as it happens – that the Plate Tectonic Theory rendered all other geotectonic hypotheses redundant. What unites these alternative hypotheses is the fact that all of them are at present vigorously denied by the majority of supporters of the Theory of Plate Tectonics.

Focus of this paper

In this paper, I focus for the most part on African and European Cainozoic geology and palaeontology. I am fully aware of the dangers of adopting a parochial Old World focus – which I tend to do in this paper, because that is where I have experienced the Earth's Geology and Palaeontology – but since this region is so complex, there is much to learn from it. It is well to keep in mind that the area subjected to close scrutiny is a minor part of the entire lithosphere, and that any hypothesis about its evolution should accord with the evolution of the globe as a whole. There is no use in presenting a solution to the Mediterranean problem for example, if it only raises contradictions elsewhere in the globe. As Carey (1988) and Owen (1983b) have pointed out, parochial studies have long been the bane of geotectonics.

Problems for Plate Tectonics

Ever since its general acceptance by most western geologists and palaeontologists, the Theory of Plate Tectonics in a globe of constant dimensions has had its detractors, most of whom have been ignored despite the fact that they have posed serious questions (Carey 1988; Keith 1993; Steiner 1977; Owen 1976) based on clear observations, some of them apparently fatal to certain aspects of the theory (Table 1). There are enormous problems for Plate Tectonics regarding increases in the surface area of the globe (Steiner 1977). Subduction, obduction, folding and under-plating simply do not resolve these problems. Carey (1988) discusses several enigmas in which the horizontal motion of plates proposed by proponents of Plate Tectonics on a globe of constant "r" does not accord with the field evidence.

Keith (1993) has compiled an impressive list of paradoxes and puzzles which run counter to current Plate Tectonics (PT) dogma, including radioactivity in the continental crust and the upper mantle, the heat flow paradox, anomalous "hot-spot" tracks which are marked by gross violations of the simple age-distance relationship, and many others. He proposes an alternative model of global tectonics which he has called the Viscous Flow (VF) Model, that he believes is better supported by the observations. While having a great deal of sympathy for the VF model

TABLE 1. — Comparison of Early version of Plate Tectonic Theory and Fast Expansion Theory.

	PLATE TECTONICS	FAST EXPANDING EARTH
Substrate	Layered Planet with rigid crust	Layered Fluid Planet
Observations and evidence	Shapes of continents Sea-floor magnetics Mid-ocean ridges Transform faults Fracture zones Trenches & island arcs Mountain Fold belts Hot-spot tracks Earthquake distribution Volcano distribution Terranes	Shapes of continents Sea-floor magnetics Mid-ocean ridges Transform faults Fracture zones Separation of continents Continental magnetics Cartographic fits Earthquake distribution Volcano distribution Rotation of microplates
Mechanisms	Convection in mantle Accretion at ridges Subduction at trenches Collision shortening	Vertical tectonics Accretion at ridges Rock flow
Result	Plate movements Separation + convergence	Plate enlargement Separation of continents
Motion of plates	Lateral on surface of globe	Radial to surface of globe
Energy source	Geothermal Mantle drag force Ridge push force Slab pull force Slab drag force Suction force	Gravity (secular change?) Kinetic energy of rotation Mechanical energy of Earth
Reaction forces	Transform fault resistance Colliding resistance	
Rates	+/– constant (2-10 cm/a)	+/– constant
Assumptions	Constant "r" Constant ocean volume Pre-Jurassic ocean-floor Completely subducted Constant atmosphere volume Iron/nickel solid core Rigid plates Rotation axis fixed Obliquity fixed	No pre-Jurassic ocean Area of continents +/– constant
Implications		Ocean volume not constant Atmosphere volume changes Moment of inertia not fixed Rotation axis not fixed Obliquity not fixed Great Circle Torsion 60% Earth radius at Jurassic

Difficulties	Arctic Paradox Biogeography of Tethys Many cartographic problems Large palaeomag. error bar 2 Dimensional thought Pacific Rim Paradox Tethys Gape Artifact Insufficient energy Northwards vector paradox Palaepole overshoot paradox Pacific Paradox Indian Enigma Missing Archaean crust Africa enigma Antarctic enigma Peru-Chile Trench anomaly Kermadec Trench anomaly lapetus ocean Myth Zodiac Fan Anomaly 175 km deep continental keel Distribution of radioactive elements 10 km depth to brittleductile transition Overlapping spreading centres	No known mechanism of expansion Moment of inertia Lack of expansion on Moon, Mars, Mercury and Venus Palaeozoic Invertebrate biogeography "G" change less than 1% since 4.6 Ga Sea-levels Palaeomagnetic radius
Comparisons of Modified Plate Tectonic Theory and Slow Expansion Theory		
Main differences from early version of PTT and Fast EET	Plates deformable Rates of motion variable Deviatoric tensional stresses over mantle plumes Continental undertow Microplates Ridge jumps Overlapping spreading centres	Some lateral plate motion Rates of motion variable 80% Earth radius at Jurassic Some subduction and obduction Pulsed Tectogenesis

proposed by KEITH (1993) – especially when one considers the fact that over geographic scales of 10^2 km and time spans of 10^6 years, even solid rock behaves like a fluid – I consider that it suffers from some of the same problems as the PT model, in particular the assumption of constant "r" and inadequate sources of energy to account for the viscous flow.

The question of energy supply to power the plate tectonic motor has still not been successfully addressed by supporters of the theory, despite the fact that these questions have been posed from the very dawn of the era of plate tectonics (ALVAREZ 1990; WILSON 1993). As ALVAREZ (1990) points out, the lack of a mechanism for WEGENER's theory of continental displacement caused it to die, yet a similar lack of a mechanism has not prevented the modern version of the same theory – continental displacement by plate tectonics – from gaining widespread acceptance, even among those that previously rejected it on those very grounds. Currently proposed energy sources, such as geothermal energy (Table 2) appear to be much too feeble to drive the plate tectonic motor(s) (MARCHAL 1991). Apart from which, geothermal energy has been suggested as one of the major sources of energy that maintains the Earth's magnetic field (Table 2) and would apparently be unable to supply enough energy to drive both systems. Other proposed

TABLE 2. — Energy sources on Earth. For explanation of the number/p/number convention, see MARCHAL (1991): (*e.g.* 2.139p29 = 2.139 × 10^{29}).

Endogenetic (telluric) energy	
a) Kinetic energy of rotation of the Earth	2.139p29 joules
b) Gravitational energy of the Earth	– 2.44p32 joules
c) Mechanical energy of the Earth	p26 joules
d) Geothermal flux	3 to 4p13 watts
Exogenetic (extra-telluric) energy	
a) Tidal energy	p12 watts
b) Solar energy	61% of 1.8p17 watts
(39% of solar energy receipt is immediately re-radiated to space)	
Comparison	
A large earthquake may dissipate up to p19 joules of mechanical energy. (Data from MARCHAL 1991.) There are about 10^4 earthquakes every year.	
Over a period of 1 million years geothermal flux would release about 10^{27} joules of energy into the fabric of the Earth.	
The energy required to produce and maintain the Earth's magnetic field is between 10^{10} and 10^{11} watts; it is thought to derive from radioactive decay or from latent heat of solidification of the inner core.	
Heat loss from continents is about 12 × 10^{12} watts (= 55 mW/m^2), heat loss from the oceans is about 30 × 10^{12} watts (= 95 mW/m^2); of the latter, the average measured oceanic heat flow is 67 mW/m^2, the difference from 95 mW/m^2 being heat losses at ocean ridges by hydrothermal circulation. (Data from CONDIE 1989.)	

energy sources such as ridge push, slab pull and trench suction (COX & HART 1986), deviatoric tensional stresses (ZIEGLER 1993; WILSON 1993; DOGLIONI 1993; PAVONI 1993) and continental undertow (ALVAREZ 1990) have overtones of perpetual motion, and as such are unlikely to solve the problem of energy supply to make the plate tectonic motor work.

A further problem with mantle convection as a mechanism for plate motion, is that the convections cells are supposed to remain in relatively stable positions relative to ridges and trenches over geological time frames (PAVONI 1993), yet at the same time they have to change their volume, and therefore their geometry, as the plates expand or contract in size. The African plate, for example, is considerably larger now than it was during the Jurassic, and the same applies to the Australian plate, the Antarctic plate, the South American plate, the Eurasian plate, as inspection of a global map of plates and spreading ridges will show. For much of its history, even the Indian plate got larger with the passage of time, and it was only during the Late Cretaceous and Cainozoic that its northern parts began to decrease in area. There appears to be a fundamental contradiction here between the observation that oceanic crust is generated along a well-defined global system of spreading ridges – implying stability of the spreading system – and the observed enlargement of most of the plates in the globe – implying, in a globe of constant dimensions, a changing system of convection cells. The adoption of a two-layered mantle in

which only the deep layer is convecting (ALVAREZ 1990) does not solve the problem of what energy source is supposed to drive the convection cells.

Furthermore, calculations presented by STEINER (1977) have indicated that whilst individual spreading centres have generated new crust at varying rates, the overall global sea-floor spreading phenomenon is a co-ordinated global process, where at any given time, high-spreading rates in one ocean basin are compensated by low rates in another. If this is so, then a speed-up in crustal generation at one spreading ridge would have to be balanced out exactly by a slow-down in the others. What the overall control of such a mechanism is – especially if spreading is visualized as being related in some way to convection cells in the mantle – remains to be addressed by Plate Tectonics adherents.

In contrast, in the Expanding Earth paradigm, expansion is expected to occur preferentially along a global spreading system and to produce the enlargement of plates as a consequence of activity along this system. Furthermore, the localized expression of expansion could vary greatly, a speed-up in one area being naturally accompanied by a slow-down elsewhere.

ASSUMPTIONS ARE THEORIES

We need to keep in mind that "Continental Displacement" and "Plate Tectonics" are two quite separate theories. So is the theory that the Earth's dimensions have remained constant through Phanerozoic time – the finite globe concept of ZIEGLER (1993). The former is based on observations of the Earth's crust, both continental and oceanic, and proposes that continents today occupy positions which are different from those that they occupied in the past. The latter is a theory to explain how and why the continents come to occupy different positions during the passage of geological time. It seeks to present a mechanism (plate tectonics) to explain the observation (continental displacement). Foundering or modification of the Plate Tectonic Theory will not lead to automatic rejection of the Theory of Continental Displacement, although many of the details of continental displacement history might change if current mechanisms of plate tectonics should prove to be inappropriate models to account for it (KEITH 1993).

Plate Tectonic theory has "evolved" during the past two decades, to the extent that plates are no longer thought of as rigid slabs of rock floating on a liquid magma – in fact, as shown by KEITH (1993) there are many geotectonicians who still regard plates as being rigid. For example, KEAREY & VINE (1990) have published a textbook in which the following definition appears: "Within the basic Theory of Plate Tectonics, plates are considered to be internally rigid and to act as extremely efficient stress guides. A stress applied to one margin of a plate is transmitted to its opposite margin with no deformation of the plate interior." However, such extreme views are now considered to be far from mainstream plate tectonic theory.

Nowadays, plates are generally considered to be subject to deformation of various sorts (shear, transcurrent faulting, fragmentation, flow, folding, nappe activity and so on). What has not changed in Plate Tectonics Theory – indeed, any possibility that it has occurred is vigorously denied by the majority of geotectonicians – is that the dimensions of the Earth are assumed to have remained constant at least since the Jurassic period if not since the PreCambrian.

A subsidiary "belief" is that the volume of the world's oceans has remained constant through geological time. There are several other "fixist" (or "permanentist") notions which underlie much

current thought in geosciences, most if not all of which will prove to be incorrect once they are investigated more closely by scientists with uncluttered minds. This paper addresses several of these "fixist" ideas with a view to demonstrating their inherent weaknesses. I include among these the notion that the Earth's obliquity is fixed, that its axis of rotation is as firmly defined as it is in a school globe, that the volume of the atmosphere is more or less constant, that the Sun's output has been more or less constant over geological time, and that the Earth's core is like a solid iron-sulphur cannon-ball and has been so at least since the Jurassic.

Special pleading

A well-used tactic on the part of geotectonicians has been to keep the globe constant in dimensions but to make huge areas of ocean-floor disappear down subduction zones or to override continental crust at obduction zones, and to induce large areas of continental crust to crumple up into the world's fold belts or to slide underneath each other to produce "double-thickness" crust. So much so, that it has been said that this is a well-established fact of geotectonics. By this means, proponents of an Earth of constant dimensions endeavour to keep the total surface area of the globe constant while acknowledging that vast areas of oceanic crust have been generated at an exponential rate in the western, eastern, southern and northern hemispheres since the Jurassic Period (Steiner 1977).

In regard to subduction, the implication is that it would increase through geological time. Yet the history of Panthalassa (*i.e.* the Eo-Pacific on a modern dimensions Earth) is the reverse: fast subduction in the remote past to get rid of the Panthalassa crust (pre-Mesozoic) to allow the generation of the post-Mesozoic crust that we see now (Steiner 1977).

Case histories

The Mediterranean region

Earth scientists who work in the Mediterranean region experience perhaps the greatest difficulties. A referee of an early version of this paper even attested that this section was an "absolutely unacceptable assumption on the evolution of the Mediterranean" but he neglected to say why he thought so, or to provide any evidence to the contrary. A review of the literature on the region will show that barely two authors agree on the interpretation of the Mediterranean, yet some patterns of its history seem to be clear (Owen 1983a; Carey 1988).

According to many plate tectonicians, the entire region between Africa and Eurasia ought to be in compression, because according to these scientists, Africa is moving northwards across a broad front against a more or less immobile Europe (Berthelson & Sengor 1990). Yet many of the structures in the Mediterranean and in neighbouring land masses are extensional in origin (Doglioni 1993). Spain and Turkey, for example, are littered with "endorheic" basins which have filled with continental sediments containing rich fossil assemblages. Many of the islands and land masses in the Mediterranean region have been rotated sinistrally – *i.e.* the northern hemisphere has sheared clockwise relative to the southern hemisphere as observed from above the surface of the Earth – along its entire length. According to Carey (1988), this belt of sinistral shear extends right round the globe following a great circle known as the "Tethyan Shear". While there are some aspects of Carey's Tethyan Shear that appear to be controversial, there

is a great measure of truth in what he says, as a plot of the Alpine fold ranges and associated trench systems will show – many of these structures lie within 10° of a great circle.

In the Mediterranean region, this shear zone has caused fragmentation of the Earth's crust within a belt more than 700 km wide running from Spain in the west to Arabia in the east. It has resulted in an offset of some 1800 km between the northern and southern "hemispheres" in the longitudes of Africa and Europe. Instead of Africa moving northwards towards Europe, it actually appears to have increased its distance from it. Examination of the rotated "microcontinents" (Moesia, Rhodope, Iberia, Turkey, etc.) within the Mediterranean region indicate that the distance between Africa and Europe has increased during the Tertiary (CAREY 1988; OWEN 1983b). This contention is borne out by the tensional nature of the Red Sea Rift and its extensions southwards into mainland Africa, and of the extensional nature of several of the Mediterranean deep basins (OWEN 1983b). If CAREY's proposals concerning Tethyan Shear are valid, then all previous plate tectonic explanations of the evolution of the Mediterranean Basin can be discarded or will have to be greatly modified. Furthermore, if the radius of the planet has changed (OWEN 1983a, b), then all reconstructions of the history of the Mediterranean based on the assumption of a constant dimensions Earth, are false.

Adherents to Plate Tectonic Theory have identified numerous "microplates" in the Mediterranean region, but few can agree on how many plates there ought to be and in which direction they are supposed to have moved (compare for instance the figures in DEWEY *et al.* 1973; BERTHELSON & SENGOR 1990; BIJU-DUVAL *et al.* 1976; CAREY 1988). In fact, the results sometimes look like *ad hoc* science, a sort of patchwork quilt in which each investigator ignores or is unaware of what his neighbour has done. It is rare to see a convincing synthesis of the tectonic history of the entire region, nor to see how the evolution of the Earth's crust in the Mediterranean region relates to that of the rest of the lithosphere. CAREY (1988) is one of the few who regard the Mediterranean as part of a circum-global structure, the Tethyan Torsion. The only cartographically precise reconstruction of the history of the Mediterranean region is that by OWEN (1983a, b). All other efforts exhibit greater or lesser distortion of the outlines, sizes and positions of plates in order to produce a "likely" story or to illustrate a concept.

Orogenic Belts and Great Circles

It is no coincidence in my opinion, that today's orogenic belts lie along arcs of great circles or are not greatly removed from such arcs, as DU TOIT (1937) noticed. I have plotted out the Alpine fold belt and its associated trench systems, as well as the circum-Pacific cordillera and trench system, and it is evident that these immense systems are confined to a zone that is less than 10° either side of a great circle. Even though Proterozoic, Palaeozoic and Mesozoic orogenic belts have been fragmented and somewhat distorted, it is clear that they also originally lay along great circles. Without exception, the pre-Mesozoic fold belts were considerably shorter than the Cainozoic belts (ZIEGLER 1993), which I take to provide good evidence that the globe was smaller in pre-Mesozoic times than it is now. The Old World and New World Tertiary fold belts may owe their origin to the increase in area of one side of the globe at the expense of the other.

On a globe, a perimeter and the area enclosed on one side by it can both increase until the perimeter becomes a great circle – even if it is not precisely circular due to inhomogeneities in structure or in its history – after which any further increase in area can only induce a decrease in perimeter. Such is the Pacific rim (or perimeter). If however, the globe is expanding in volume

at an appropriate rate, the length of such a great circle – *e.g.* the Pacific rim – need not become shorter to accomodate the increase in surface area enclosed by it – the Pacific Ocean – depending upon the rate of increase in volume. The presence of the Cordilleran fold belt indicates that Earth Expansion has not been able to compensate entirely for inhomogeneous – *i.e.* one-sided (geotumors) – expansion of the globe, and the result has been a difference between the rate of increase in surface area of the Pacific and of the length of its rim, resulting in compression of the Pacific rim great circle relative to the area (on the Pacific side) that it encloses. Compression structures thus typify more than half the length of the Pacific rim great circle.

At right angles – a spherical right angle – to the Cordilleran fold belt, there is the Alpine fold belt. This also lies more or less along a great circle, although the Indian plate has distorted it since the Eocene, producing kinks in the arc. Folding, thrusting, nappe formation and other tectonic activity in the Alpine fold belt appears to be due to shortening or contraction of a great circle perimeter related to lopsided growth of the mantle: more in the southern hemisphere than the north. This has in effect led to greater production of oceanic crust in the circum-antarctic region and the Southern Atlantic, Indian and Pacific Oceans than in the Northern Oceans. This predominantly one-sided (*i.e.* single hemisphere) expansion has led to the apparent net northwards displacement of all continents (except Antarctica) and older oceanic crust relative to the present equator, recorded as the palaeomagnetic northward movement effect, a feature that has been observed and commented upon since the dawn of the "Plate Tectonic" Era, if not before. This net northwards displacement of the continents produced an effect which is well described by CAREY (1988) but which still confuses many "traditional" thinkers. As the northern continents were apparently displaced northwards, they carried their palaeomagnetic signatures with them. Thus the Mesozoic "equatorial" magnetic signature – *i.e.* the zone where magnetic declination was nearly zero, or horizontal, has been carried northwards, which gives the impression that Africa and South America have migrated northwards since the Jurassic. The Mesozoic mid-latitude magnetic signature, where the declination is about 45° (positive or negative doesn't matter), has also moved northwards, giving the impression that Eurasia and North America have also shifted northwards during and since the Mesozoic. Those scientists who assume that the dimensions of the globe have remained constant, are forced to conclude that all continents except Antarctica have been converging on the Arctic, the northern ones more slowly than the southern ones. The maps of SMITH *et al.* (1981) represent a classic example of this trend of thought – in the maps, the Arctic Ocean becomes smaller and smaller in extent as geological time passes, and as the continental palaeomagnetic signature tells the authors that the continents have shifted northwards. Yet, studies of the palaeomagnetic signature of the floor of the Arctic Ocean reveal that it has increased in area since the Cretaceous, not decreased. In other words, relative to the present North Pole, the continents have been shifting southwards since the Cretaceous. Yet, despite this insurmountable contradiction, most geotectonicians continue to maintain their faith in constant "r".

Palaeontology

Palaeontologists have often noted that some types of palaeobiological data seem to contradict reconstructions of plate movements on a constant dimensions globe, either in the details of movement directions or of timing of events or of past positions of plates (HALLAM 1981). For example, according to currently accepted versions of plate tectonic history, India was deep in the Indian

Ocean throughout the Cretaceous, Palaeocene and the first half of the Eocene (PATRIAT & ACHACHE 1984). Yet throughout this period India appears to have been much closer to Asia than the plate reconstructions suggest (SAHNI 1984), so much so that it failed to develop an endemic fauna – endemism, even in land mammals appears to have been weakly expressed, although the terrestrial fossil record is rather poor in the latter domain. During the Early Oligocene, India was inhabited by a few typically African faunal elements such as Hyracoidea (PICKFORD 1986a) suggesting that there may have been an interchange of terrestrial faunas between Africa and India at some stage during the Early Oligocene. At the same time, it also contained some typically European faunal elements, such as *Anthracotherium magnum*, which indicate faunal interchange with Europe before or during the Stampian Period (Middle Oligocene) (PICKFORD 1987). All this supports the observation by HALLAM (1981) that the palaeobiogeographic evidence reveals disparities with plate tectonic reconstructions in which India was well separated from Eurasia. He concluded that the width of the Tethyan barrier may have been overestimated by many researchers.

Climate

The climatic changes which took place at the onset of the Middle Miocene are sometimes explained in terms of plate tectonics. For example, the development of dryshod access across the Tethys Seaway would automatically have severed the oceanic circulation between the Indian and Atlantic Oceans (HALLAM 1981) thereby perturbing global climates. At the beginning of the Middle Miocene, Europe's climate became more tropical. But during the Upper Miocene, it became less tropical – the boundary zone between the Palaearctic and Ethiopian Realms began to shift southwards (PICKFORD 1986b) – with the result that almost all the Ethiopian lineages eventually died out in Europe. On its own, the northwards shift of Africa towards Eurasia can hardly account for the onset of tropical conditions in Europe and then for the subsequent undoing of these conditions. At least not without a certain amount of special pleading. As far as I am aware, no one has yet proposed that the Upper Miocene climatic changes resulted from plate tectonic activity between Africa and Europe, although uplift of the Himalayas has been proposed as a possible contender for the onset of monsoon climates during the latest Miocene (QUADE *et al.* 1989), contemporaneous with faunal changes in the Indian subcontinent. At the same time, the dessication of the Mediterranean during the Messinian Crises has been correlated (or mis-correlated) with faunal changes in Europe and North America (ALROY 1992).

ENERGY AND PLATE TECTONICS

Despite the title of their book (*Plate Tectonics – How it works*), the very pedagogical book by COX & HART (1986) only gets onto what drives the plates on page 339. In the following ten pages, the authors champion the idea that some kind of thermal convection is responsible for plate movement. Yet not a word is said about the quantities of energy available in the supposed convection cells, nor of the amount of energy required to cause the observed motions. The last four pages of the ten which are devoted to what drives the plates, are given over to a discussion of "Driving Forces". These are listed as Mantle Drag Force, Continental Drag Force, Ridge Push Force, Slab Pull Force, Slab Drag Force, Transform Fault Resistance, Colliding Resistance and Suction Force. Of these, Ridge Push and Slab Pull, if they occur, are gravity driven, while the

so-called drag forces and resistances would actually tend to impede plate movements. The amounts of energy required for plate movements are simply not addressed by COX & HART (1986).

Nor are they discussed by ZIEGLER (1993) who merely states that "Earth's mantle convection system... facilitates escape of thermal energy from the Earth's interior" or by DOGLIONI (1993), PAVONI (1993) and WILSON (1993). In a series of companion papers, these authors discuss the usual forces supposed to move the plates, such as ridge push, trench suction, deviatoric tensional stresses, slab drag and so on. It is evident from the papers that there is no consensus among these or any other authors concerning the mechanisms that move plates. None of them address the question of an energy source and its magnitude, except for invoking thermal energy in the mantle.

The situation is similar to the debate among non-mechanics concerning what moves a car. For one it is the frictional force between the rubber tyres and the road surface. For a second it is the turning of the propellor shaft, while for a third it is the up and down motion of the pistons in the cylinders of the engine. Without mentioning the source of the motive power, which is of course the fuel in the tank, the debates are rather futile, even though valid within the parochial view of each debater. As every mechanic knows, the fuel is the crucial factor, without which none of the rest would be possible.

In the plate tectonic model of evolution of the Earth's crust, the energy sources which are supposed to result in continental displacement have not yet been satisfactorily identified (MARCHAL 1991). Geothermal flux on its own appears to be insufficient to account for such activity, apart from the fact that the same energy has been said to produce and maintain the Earth's magnetic field (CONDIE 1989). In any case, as MARCHAL points out, the distribution of radioactive elements in the lithosphere and mantle would tend to impede the formation of convection cells. The rotation of the Earth may well also interfere with the formation of convection cells.

Exogenetic, or extra-telluric energy sources, such as astronomic (solar, tidal) supplies, are far too weak to drive the plate tectonic motor (Table 2), even if they were combined with geothermal energy. Endogenetic, or telluric energy sources, such as gravitational energy and kinetic energy of rotation, are the only known ones which are potentially powerful enough to supply the requisite amounts of energy for continental displacement. Of these two, the kinetic energy of rotation of the globe may be important in inducing lateral displacement of the continental crusts with respect to their underlying mantle and for inducing other effects such as "Tethyan Shear".

A third, hypothetical source of energy is encompassed by the idea that the core of the Earth is a proton plasma, rather than a solid iron-sulphur "cannon-ball". Capture of electrons by protons in the plasma would lead to the creation of enormous expansion energy, as well as of energy released by the fusion. The volume occupied by atoms is orders of magnitude greater than the volumes occupied by either protons or electrons on their own. A plasma core decaying progressively to an atomic state – the outer core – and the production of heavier elements to form the mantle would yield vast quantities of energy which might be sufficient to drive both Earth Expansion and some plate movements. Indeed, OWEN (1981, 1992) has espoused the idea of a plasma core for the Earth, and considers that the combined energy of a decaying plasma core, geothermal energy, Earth Expansion and the very slow rotational effect would be sufficient to produce the movements of continents.

ALLÈGRE *et al.* (1993) have reported that recent developments in rare gas geochemistry suggest that the terrestrial atmosphere was generated by degassing part of the Earth's mantle, but that neither Neon nor Helium fit the general picture. The ratio of $^{20}Ne/^{22}Ne$ ratios in MORB (between 10 and 13) and in air (9.8) are very different. The $^{20}Ne/^{22}Ne$ ratios of up to 13 in upper mantle derived basalts cannot be explained by any known nuclear reaction. ALLÈGRE *et al.* (1993) postulate that most of the ^{20}Ne is of cosmic origin, reaching the mantle basalts by subduction of micrometeorites. However, it is perhaps more likely that the "cosmic" signature of ^{20}Ne derives from the Earth's own cosmic-like core, which would tend to support the idea that the Earth's core is a proton plasma. Most of the ^{3}He in the atmosphere, also said to be of cosmic origin, could likewise be derived, not from the cosmos, but from the Earth's plasma core. Similarly, the hydrogen that is lost to space due to photo-dissociation in the upper atmosphere may well be replaced by juvenile hydrogen resulting from decay of protons in a proton plasma core to the atomic state by addition of electrons. If the source of ^{20}Ne and ^{3}He is the Earth's core, then it renders the hypothesis of cosmic origin followed by subduction reworking unlikely.

The mechanical energy of rotation could lead to slight differential movement between continental crust and oceanic crust (CAREY 1976, 1988) because the continents are on average 4.6 km further from the axis of rotation than are the oceans (mean altitude of continents: 870 metres above sea-level; mean depth of oceans: 3.740 metres below sea-level). These deformations would tend to be elongated in the north-south sense, and would either be compressive (along west coasts of continents) or extensional (on east sides of continents). The separation of Euro-Africa from the Americas may well be partly driven by such a mechanism, while the trench and cordillera systems of North and South America could be partly due to the same phenomenon. However, such powers probably play a minor role in the overall global geotectonic scheme. Nevertheless they should not be forgotten.

Lack of sufficient energy supply to drive its motors, suggests that plate tectonics driven by convection cells in the mantle is not a suitable model for explaining the evolution of the Earth's lithosphere, a conclusion already reached by a number of independent studies (CAREY 1976, 1983, 1988; MARCHAL 1991). If convection cells exist in the mantle, then they probably play a minor role in the evolution of the Earth's crust. Nor can slab pull, ridge push and trench suction solve the problem of motive power for plate movements, mainly because without a further source of energy powering some part of the cycle, the machine would grind to a halt very rapidly. As described by COX & HART (1986) the ridge push/slab pull model closely resembles a perpetual motion machine in which one force drives the other which provides power for the first one, and so on *ad infinitum*. Much more powerful forces, such as gravity or the kinetic energy of rotation of the Earth seem to be implicated.

THE EXPANDING EARTH HYPOTHESES

INTRODUCTION AND ORIGIN OF CONCEPT

A distinct possibility is that the assumption of a constant dimensions Earth is invalid, and that the Earth has expanded significantly since the Jurassic. Only in an expanding globe can the sum of the areas of two surfaces defined by a perimeter on its surface increase in value.

The hypothesis of expansion of the Earth has been seriously proposed (although the idea has often been vehemently rejected) as a way of resolving virtually all the problems encountered in reconstructing past continental configurations. Among those who have proposed Earth Expansion, there are two principal groups: those whose reconstructions of Pangaea at the beginning of the Jurassic cover the entire globe (*i.e.* there was no proto-Pacific Ocean) – called fast expanders – and those whose reconstructions of Pangaea at the beginning of the Jurassic cover a little more than a hemisphere, a large proto-Pacific Ocean (Panthalassa) covering the other half – the slow expanders. The fast expansion hypothesis, chiefly advanced by CAREY (1983, 1988) begins with a Jurassic globe about 60% of modern dimensions. The slow expansion hypothesis, whose principal advocate is OWEN (1983b) begins with a Jurassic globe about 80% of modern dimensions. In the slow expansion model, extrapolation backwards into geological time beyond the Jurassic results in a Pangaea which covers the entire surface of the globe sometime in the Late PreCambrian. Understandably, some scientists are reluctant to extrapolate backwards from the Jurassic, because the constraints provided by palaeomagnetic patterns of the ocean-floor are not available for pre-Jurassic periods. Nevertheless, the fact that orogenie belts appear to form along arcs of great circles, provides some information and the hope is that pre-Jurassic reconstructions of Pangaea may be forthcoming, along with details of crustal deformation during the Palaeozoic and Early Mesozoic due to Tethyan-type torsion, flow, folding, faulting and other surficial phenomena. If such reconstructions become available, various problems of Palaeozoic and Early Mesozoic biogeography – there are many for which there seem to be no solutions under the constant "r" hypothesis – may be resolved.

CONTEMPT, RIDICULE AND BIASED TREATMENT

The advancement of geological and palaeontological sciences was delayed and hampered for four decades by the rejection of WEGENER's theory of continental displacement on the grounds that he had proposed an unsatisfactory mechanism to account for it. In palaeontological circles, reluctance to accept continental displacement led to the proposal of numerous *ad hoc* explanations for palaeobiological observations, including the notorious transoceanic "land bridges," "floating islands" and other fanciful faunal dispersion mechanisms and pathways. DU TOIT (1937) wrote an eloquent commentary on various reactions of the scientific community to the concept of "Continental Drift." With minor rewording his comments would apply curiously closely to recent reactions to the Expanding Earth Theory. Current reluctance on the part of many geoscientists to accept Earth Expansion as a hypothesis to be tested on its own merits – that is, not to be rejected out of hand – uncannily resembles the resistance that WEGENER's concept of continental displacement experienced for forty years.

CONDIE (1989) for example, in his textbook on Plate Tectonics and Crustal Evolution, dismissed Earth Expansion in less than a page of text in an ill-informed and rather condescending way. He began by saying that "evidence for an expanding Earth are (*sic*) either ambiguous or are (*sic*) based on *ad hoc* assumptions." He then proceeded to cite as the chief evidence, the argument of ocean volumes put forward long ago by EGYED (1956) but which has not been used as support for Earth Expansion by its proponents for the past three decades. After dismissing this piece of evidence – which is a pyrrhic victory since it hasn't been taken seriously as support for Earth Expansion by expansionists themselves – he continues by stating that "other evidences

for an expanding Earth are even more tenuous," again citing examples that are not used by the majority of proponents of the theory, including the odd notion that the Earth is expanding according to HUBBLE's Law and the idea that significant Earth Expansion is related to decreases in the gravitational constant over time.

Consequently his ill-informed dismissal of Earth Expansion on the basis of false criteria is unfortunate, especially so because it gives students the incorrect impression at the outset of their careers that those in authority have thought deeply about the possibility of Earth Expansion, but that they consider it so feeble a hypothesis that it merits less than a page of discussion in a 288 page book. Invidious is the imparting to students of the idea that Earth Expansion rests solely on such weak evidence as ocean volume, HUBBLE's Law and changes in gravitational forces. Barely a word is mentioned about the wealth of other evidence for expansion which has been published in support of the theory. In effect, students have been denied access through their textbooks to ideas which could shape the way they view the world for the rest of their lives.

The textbook by COX & HART (1986) introduces and dismisses Earth Expansion in two sentences, referring to it as a pre-Plate Tectonic Theory offered in the late 1950s to explain the observation that mid-ocean ridges had rifts along their crests. Anyone reading COX & HART's book and not knowing the literature, including most students, would be forgiven for thinking that nothing has apparently been written about expansion since the 1950s. The alternative that these authors imply is that Plate Tectonics provides all the answers to global tectonic questions, which renders such old ideas as Earth Expansion unworthy of further consideration. No refutation is offered by these authors, they merely discard the idea with the words "this theory raised so many other questions that it never gained much credence." We are not informed by the authors of the nature of these "other questions" that were raised by Earth Expansion, many of which are discussed herein.

TETHYS AND TETHYAN SHEAR

For much of the Mesozoic and Cainozoic, the Old World consisted of two broad regions of continental crust separated from each other by the east-west oriented Tethys Seaway, most of which was floored by continental crust (OWEN 1983a, b). There was some genuine oceanic crust north of India, but not the incredible area required by proponents of the constant dimensions Earth. For details of a more credible history of the Tethys and of the extent of Tethyan oceanic floor, the reader is referred to OWEN's (1983b) maps. This relatively shallow water-filled depression proved to be an effective barrier to many groups of terrestrial vertebrates and invertebrates (HALLAM 1981), with the result that the evolutionary histories of northern and southern continental faunas tended to follow different trajectories. Yet from time to time, land-bound animals and plants managed to cross the Tethys Seaway. During the Palaeogene, numerous mammalian lineages crossed Tethys from north to south, while very few managed to cross in the opposite direction (PICKFORD 1990b), suggesting that the water flowing through the Tethys Seaway had a southerly drift component. During the Tertiary, however, the seaway ceased to be a continuous water body stretching from the Atlantic to the Indo-Pacific (ADAMS *et al.* 1983). There were points of dry land contact between India and Asia on the one hand, sometime during the Eocene and subsequently (PATRIAT & ACHACHE 1984), and between Africa and Europe on the other hand at the beginning of the Middle Miocene and in following periods (ADAMS *et al.* 1983).

The development of dryshod access between northern and southern continents led to greatly increased interchanges of their terrestrial faunas and floras. Some of these interchanges were impressive enough to be identified as first order faunal turnover pulses.

However, the development of dry land access between continents has not been the only cause of faunal turnover pulses. Since the Middle Miocene, Africa and Eurasia have been more or less in constant contact, yet during this period there have been several turnover pulses, about 12 to 13 m.y. ago, about 8 to 7 m.y. ago and during the Plio-Pleistocene. Some other factor or factors other than merely the development of dry-land contact between two land masses have played a role in driving these post-contact turnover pulses. The same applies to the India/Asia pair and to the North America/South America couplet, where faunal turnover pulses occurred closely in time with those that took place in Africa (ALROY 1992; BARRY *et al.* 1985, 1990). Palaeontologists usually talk about climatic forcing, or other environmental prime movers as the causes of such faunal turnover pulses (*e.g.* ALROY 1992) although what led to the climatic or environmental changes in the first place has seldom been specified.

The role that the Tethys Seaway has played in the evolution of Afro-Eurasian Tertiary faunas is crucial. The only way to understand its biological role is to appreciate the history of its lithic substrate (geotectonics) and that of the seawater that filled it (eustacy) (HALLAM 1979). For the former, three major classes of geotectonic behaviour need to be examined, all of which could be active concurrently:

a) Tethyan Torsion (or geotectonic movements oriented generally east-west);

b) Vertical tectonics (uplift of mountain chains, downthrow of basin-floors);

c) Continental Displacement (or geotectonic movements oriented generally north-south) (CAREY 1988).

As far as the Mediterranean region is concerned, there has been a long list of contradictory descriptions and a large variety of hypotheses proposed to explain its complex geology. For example, DEWEY *et al.* (1973) suggested that during the Cainozoic Era Africa had moved several hundred kilometres westwards relative to Europe. CAREY (1988) in diametric opposition to DEWEY and colleagues, observed that Africa has been offset several hundred kilometres eastwards relative to Europe. A third stance (BERTHELSON & SENGOR 1990) is that there was little if any longitudinal offset between the two continents. Many authors have suggested that Africa has moved northwards towards Europe during the Tertiary (*e.g.* DEWEY *et al.* 1973) whereas, CAREY (1988) considered that the opposite happened – the distance between Africa and Europe increased by 700 km during the Tertiary, a view which is supported by DOGLIONI (1993) and OWEN (1983b), but which is denied by many geotectonicians, including a referee to an early version of this paper. The latter merely stated that the idea was "false" without elaboration. With such a diversity of observations and opinions, it is necessary to re-examine all the available data with an open mind. In my opinion, the only reconstructions of the evolution of the Mediterranean which come near to representing its actual history are those by OWEN (1983b) which are closely constrained by cartographical, geological and palaeomagnetic data. Without exception, all the other versions that I have examined – perhaps have I missed some – are based on one or more "distortions", either cartographic or geological.

The eustatic history of the Tethyan Seaway is equally, if not more complex than that of its crust. Not only is there the complicated geotectonic history of the Earth's lithosphere to

consider because it changes the geometry of the basins holding the water (HALLAM 1979; HAQ *et al.* 1987), but there is also the contribution made by changes in the volume of the world's oceans (CAREY 1988), such as for example occur during glacial and interglacial cycles, or during long term eruptions of neonate waters from the mantle at mid-ocean ridges and other volcanic sources. Furthermore, the comet-like trail of hydrogen left by the Earth as it orbits round the Sun (OWEN 1992) suggests that photo-dissociation of water vapour in the upper atmosphere has been going on since the origin of the Earth, an observation that indicates that there are continual net losses of water from the planet. Without the more or less continuous eruption of immense quantities of water from the interior of the Earth, the planetary surface would long ago have gone bone dry. Variations in the rates of photo-dissociative losses of water in the atmosphere or in rates of eruption of neonate waters from the mantle may well have played a role in determining the volume of the oceans during the past. These would lead to global scale transgressions or to regressions, depending upon the photo-dissociation/neonate water eruption budget.

At first glance, it would seem that some of the geotectonic aspects of the globe cannot be explained by Earth Expansion, but they are in any case probably ultimately related to it, especially as expansion was not expressed evenly over the surface of the globe. Among these are the Tethyan Shear and its related structures which encircle the globe, noted early on by DU TOIT (1937) but confirmed by CAREY (1988). CAREY (1988: 285-286) proposes that "the Tethyan Torsion seems to be due to the interaction of gravity and rotational inertia." During the lifetime of the Tethys Sea, much more oceanic crust was generated south of Tethys than north of it, at the same time that all continents (except Antarctica) moved appreciably northwards. As a result, the moment of inertia of the northern hemisphere increased compared to that of the southern hemisphere. Because of this difference in inertial moment, a sinistral torsion began to operate along the Tethys Seaway, "with the northern side tending to lag in rotation with respect to the southern side." CAREY (1988, fig. 80) has calculated that in the vicinity of Africa and Europe, sinistral torsion has displaced Africa eastwards by some 700 km relative to Europe since the Cretaceous.

Whilst CAREY's explanation of the Tethyan Shear is contentious, the existence of the shear zone is less so, even though one referee of this paper stated that "the Tethyan Shear with sinistral component is unacceptable", but without stating why he thought so. There is little doubt that Africa has sheared eastwards relative to Europe by a distance of about 700 km. In the region of New Guinea to the Tonga Trench there has also been tremendous shear in a sinistral sense to a similar extent. South America has sheared eastwards relative to North America, thus forming part of the same global shear zone. Under these circumstances, I do not see why the concept of a sinistral Tethyan Shear zone is unacceptable. The idea may need modifying, and previous explanations may be incorrect, but declaring it "unacceptable" does not do away with the observed sinistral offsets between Africa and Europe, between New Guinea and South-East Asia, and between South America and North America.

Elsewhere in this paper, I link Tethyan Shear to the process by which the southern hemisphere is underriding the northern one with a clockwise component of movement. Similarly, the Pacific rim dextral shear zone is underriding the opposite hemisphere with an anticlockwise component of movement, seen on land as dextral shear in California.

EARTH EXPANSION, THE LITHOSPHERE AND THE PLANETARY GYROSCOPE

We should not reject the reality of continental displacement on the grounds that Plate Tectonics is not an entirely suitable or complete model to account for it. No one has yet satisfactorily explained how the Earth's magnetic field originated or is maintained, but this does not mean that it doesn't exist. We can't reject the plate tectonic concept or aspects of it without having determined an alternative explanation for continental displacement. The evidence that the distance between most continents has increased during the past 200 m.y. cannot be lightly denied (OWEN 1983a, b), the only exception being provided by India and Asia. But even in the case of India, from the break-up of Gondwana until the Cretaceous, it was distancing itself from its neighbours. It has only been during the latter third of its post-break-up history that it has closed the gap between itself and Asia.

As CAREY (1988) has pointed out, after the Jurassic Period the distance between each of the continents increased. Subduction of continental and/or oceanic crust on a globe of constant size does not account for this observation, which suggests that there must be another explanation. Furthermore, reconstructions of past continental positions based on cartographically accurate plotting of ocean floor magnetic anomalies on a globe of constant dimensions results in gaping gores or gaps (OWEN 1983b). Making reconstructions using the same data on globes that are smaller than the present day reference globe, eliminates all these cartographic anomalies, as long as globes of suitable sizes are selected (OWEN 1983b).

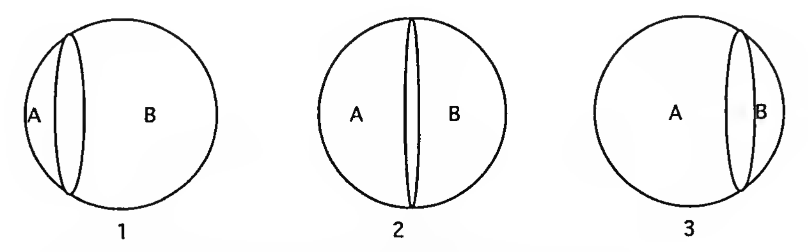
HALLAM (1981) concluded that the problem of excessive width of the Tethyan Ocean during the Cretaceous and Palaeogene "disappears if one accepts the novel reconstructions of OWEN because the Tethys Ocean is eliminated, but these are based on the assumption that the Earth has expanded by some 20% since the Triassic." HALLAM reported that he felt unable to promote the idea of Earth Expansion "because of the serious geophysical difficulties posed by such a rapidly expanding planet." He did not specify what the serious geophysical difficulties were.

There can be little doubt that the principal cause of the increase of the distance between continents is their movement radially outwards with respect to the centre of the globe: the proximate mechanism is ocean-floor spreading and the symmetrical generation of oceanic crust each side of the spreading axes. Crustal masses can shift laterally about the surface of the globe by a variety of mechanisms (flow, transform faults, nappes, folds, rifts, tethyan type torsion, differential rotation drag and so on) all of which can result in increased or decreased separation between two land masses.

The expansion of the Earth is not analogous to blowing up a balloon on which cutouts of the continents have been attached. In such a model, expansion would tend to be homogeneous, which is patently not the case for planet Earth. Instead, expansion is inhomogeneous: far more surface area has been added in the Pacific hemisphere than in the Atlantic/Indian hemisphere, and the southern hemisphere has increased its surface area greatly with respect to that of the northern hemisphere. The ocean-floor palaeomagnetic patterns confirm this amply. In such unevenly expanding masses, there would be a tendency for the expanding body to swell out of shape – the geotumor concept of CAREY (1988) – but the force of gravity in a planet as large and as dense as Earth, ensures that the geoid remains quasi-spherical. The adjustments between the tendency for the planet to swell out of shape, due to inhomogeneous expansion, and the

tendency for gravity to maintain a spherical form in it, lies at the heart of the global geotectonic system, the surface expressions of which are visible world-wide, but principally in the fold mountain belts and rift valley systems as well as the palaeomagnetic patterns that stripe the ocean floor.

The discovery of the palaeomagnetic pattern of the ocean-floor was early and correctly interpreted as providing evidence that the continents have indeed been moving around. The mechanism by which the magnetic stripes were generated at spreading ridges is not seriously



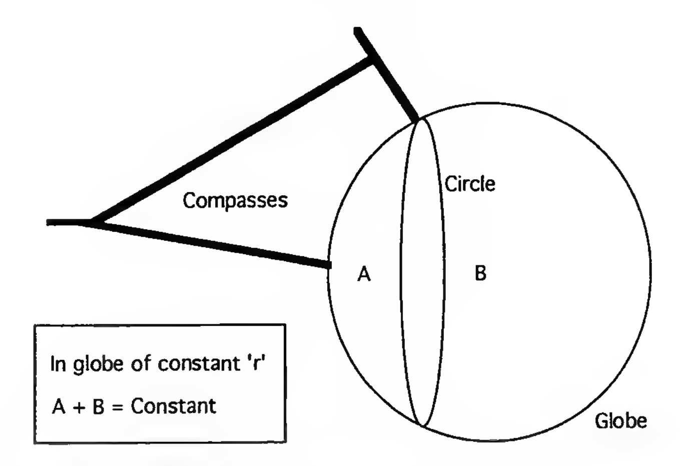


FIG. 3. — From left to right, the upper row shows the effect of drawing circles on a globe, in the way depicted in the second row. From "1" to "2" area A increases in size, as does the length of its perimeter: Area B decreases in size as its bounding perimeter increases in length. Beyond the great circle stage shown in "2" to "3", area A continues to increase in size, even though its perimeter decreases in length, while area B decreases in size. In a dynamic situation in which there is uneven expansion of one hemisphere of a sphere of constant dimensions – the sum of areas A and B is constant – such as is caused by uneven generation of crust at spreading axes, and a force such as gravity which maintains the spherical shape of the sphere, compressive forces will be generated along a great circle zone as the perimeter of the expanding hemisphere is forced to become shorter. Even in an expanding sphere – in which the sum of areas A and B increases – the combination of uneven expansion of one hemisphere and the force of gravity will lead to compression along a great circle zone. For this reason, the Earth's great fold belts and torsion zones occur along or close to arcs of great circles.

contended, although what it means in terms of Plate Tectonics or Earth Expansion has been. In fact, the spreading ridge evidence could as legitimately be considered the surface expression of Earth Expansion rather than of Plate Tectonics. It does not uniquely support the Plate Tectonic Theory as opposed to any other. The main problem with Earth Expansion which also applies to Plate Tectonics, is the question of what happens at depths greater than 15 km where we have so far been unable to "observe" or deduce satisfactorily what has been going on, even with high resolution seismicity. As COFFIN & ELDHOLM (1993) point out "all models of the internal structure of the Earth are built on inference."

Subduction of oceanic crust, principally near the Pacific rim, at first glance seems to provide evidence that refutes Earth Expansion, in the sense that no crust should be subducted if the generation of new crust is solely by expansion. However, uneven expansion on a globe, which is a feature of the Earth's spreading ridge systems, automatically leads to the genesis of cordillera and trench systems along Great Circle zones, along which limited subduction can take place. This is because gravity maintains the spherical shape of the globe against the tendency for spreading ridges to develop a non-spherical globe.

Expansion has indeed not been uniformly expressed over the surface of the globe (STEINER 1977). Steiner calculated that both sea-floor spreading rates and subduction rates increased with the passage of time, but that throughout the post-Jurassic period there appears to have been an excess of sea-floor spreading over subduction. His conclusion was that an expanding Earth is strongly indicated.

The generation of new crust has been highly uneven, with much greater quantities generated in the Pacific hemisphere than in the opposite one, and much more in the southern than in the northern hemisphere. Furthermore, generation of oceanic crust in the Pacific hemisphere appears to have been exponential (STEINER 1977), so that in the constant "r" plate tectonic paradigm, the subduction burden must also have been exponential. Such appears to have been the case, but global subduction rates seem to have been lower than global ocean-floor spreading rates throughout the post-Jurassic period.

These facts, together with the tendency for gravity to maintain the spherical form of the Earth are of the greatest importance. In our thought experiment above, we showed how on a globe of constant dimensions, the perimeter of an expanding area reaches a stage – the Great Circle – where the perimeter begins to shorten even though the area enclosed by it continues to increase. In an expanding globe, uneven expansion has a similar effect, although the mathematics is more complicated. If there were no gravitational force to maintain sphericity, the expanding globe would simply become distorted, much as a balloon with a weak patch becomes misshapen as it is blown up. However, the force of gravity – the most powerful source of energy in the globe – maintains the Earth's almost spherical form. The crust experiences and records the adjustments at so-called subduction zones and fold belts, usually expressed along arcs of Great Circles (see Fig. 4).

Continents such as Antarctica and South America, which are surrounded by mid-ocean ridges whose traces appear to be enlarged "caricatures" of the continents they encircle, have suffered little if any lateral shift over the surface of the Earth. Apart from its northern margin, the same can be said of Africa. These continents are said to have passive margins. Instead, the increase in distance between these continents has been principally due to radial movement away from the centre of the Earth by a mechanism of insertion of oceanic crust symmetrically on either

side of the mid-ocean ridge systems. Since the Cretaceous Period, about 5000 km of separation of such continents, measured along Great Circle traces, can be accounted for purely by Earth Expansion in the slow model of Earth Expansion (OWEN 1983b). In the fast model of Earth Expansion espoused by CAREY (1988), all the separation of continents would be due to Earth Expansion, and virtually none would be due to lateral movements about the surface of the globe.

In passive margined continents, the continental crust appears to be firmly welded onto its underlying mantle. It is difficult to imagine a system of convection cells with descending walls beneath Africa, Australia and Antarctica. In Africa, in particular, the evidence from diamondiferous intrusions into the crust, suggest that the diamond-bearing sub-cratonic rocks have not moved significantly since the Early PreCambrian. The diamonds themselves crystallized during the PreCambrian, yet they erupted to the surface at various times during the Palaeozoic and Mesozoic Eras (up to Cretaceous times). Under a convecting mantle system, such diamonds would probably long ago have been carried away from beneath the continents perhaps to be spewed up in mid-ocean ridge systems.

Lateral shift over the surface of the globe is less important for all continents except India, which is the only large land mass to have moved any appreciable distance laterally across the surface of the globe (there are many so-called microcontinents or terranes that have done so, principally in Tethyan type torsion zones). But even in the case of India, initial separation from its neighbouring continents from the Jurassic until the Turonian (Upper Cretaceous) was due largely to radial movement outwards from the centre of the Earth by the mechanism of symmetrical growth of oceanic crust at mid-ocean ridges, and it was only during the Late Cretaceous and Tertiary that India began its lateral movement across the surface of the globe (OWEN 1983b) and in so doing, decreased its distance from Asia. From the Jurassic until the Turonian its separation from Asia had increased in a similar way and by comparable distances to its separation from its other neighbours (Madagascar, Africa, Antarctica, Australia). As a result, until the Turonian, India used to be surrounded on all sides by a mid-ocean ridge system which looked like an enlarged caricature of the subcontinent. Today, all that remains of this "caricature" are the Carlsberg and mid-Indian Ocean ridges, the northern parts having been incorporated into the ophiolite belts of Oman, Afghanistan, Pakistan and India. Thus, India only became an exception to the usual expression of passive margined continents during the Upper Cretaceous – meaning that it conformed to the general pattern for more than half the time since the onset of the breakup of Pangaea.

In other words, from the Jurassic until the Turonian, every continent – including India – was distancing itself from all its neighbours. Only since the Turonian has India approached Asia, thereby producing an anomaly and a conundrum. The only way to increase the distance between all continents is to increase the size of the globe, and this means that Earth Expansion must have occurred.

ENERGY FOR EARTH EXPANSION

The primary factors controlling the geometry and physiology of Earth Expansion and lithospheric evolution is the interplay between three energy source:

a) gravitational energy, the most powerful known source of endogenetic energy in the globe (CAREY 1988; MARCHAL 1991);

b) the kinetic energy of rotation of the globe, the second most powerful source of energy in the globe;

c) expansion energy.

Two versions of expansion energy have been proposed (OWEN 1992; LARIN 1993), both of which involved the progressive decay of protons in a proton-rich core into an atomic state by escaping from the core after which they combine with electrons already present in abundance in the mantle than either protons or electrons. OWEN (1992) has proposed that the Earth has a plasma core which is progressively decaying to an atomic state, not only resulting in great expansion, but also in the generation of fusional heat, which contributes to the Earth's geothermal budget. OWEN (pers. comm.) has suggested that changes in gravitational forces may affect weak and strong forces, and thereby play a role in plasma decay.

LARIN (1993), in contrast, has suggested that the primordial Earth was hydrogen enriched, with most of the hydrogen locked up within metallic crystal lattices. The dissolved hydrogen in this situation is in the proton form, the atomic form being too large. With the passage of geological time, protons escape from the metallic crystal lattices, capture an electron and become hydrogen atoms which are considerably larger than proton. The long term result is expansion of the body of the globe as it adjusts to the increases volume of hydrogen so released. An attractive aspect of LARIN's hypothesis is that metallic hydrides can be produced in the laboratory at pressures of 2-3 megabars, and their behaviour studied.

In both OWEN's (1992) and LARIN's (1993) concepts. Earth Expansion is accomplished without an increase in mass of the globe. This is an important point to note, because it has often been assumed by plate tectonicians that expansion would automatically be accompanied by mass increase, for which there is no evidence. Indeed, the study of growth increment in corals, rhythms in varvites and other evidence concerning ancient orbital and rotational parameters of the Earth, indicate that no signifiant increase in the Earth's mass has occurred since the Proterozoic.

A second important aspect to emerge from OWEN's and LARIN's ideas, is that the changes in the Earth's radius would have positive polarity. Decrease of "r" would not be possible unless hydrogen was decomposed into protons and electrons and the protons once more inserted into a plasma or a metallic crystal lattice. At some stage in the early history of the planet, this probably happened, but since at least the Archaen, the process has been one of protons decaying to the atomic state.

LARIN discussed many of the implicatons of his concept of the hydridic Earth, one in particular of which is of pertinence to the present article. He suggested that the volume of the hydrosphere would have increased with the passage of geological time, as hydrogen released from atomic lattices reacted with oxygen to form water.

Also discussed by LARIN are the global tectonic implications of a hydridic Earth, in particular Earth Expansion, geosynclinal processes, flood basalt episodes, evolution of the oceans and many others. LARIN appears to fall into the category of "fast expanders" discussed in the present article, in which the notion of subduction is rejected as a mechanism of global tectonics. For him, the separation of the continental masses has been by radial movement away from the centre of the Earth, and none of it by lateral motion across or over the mantle. Needless to say, he discounts the idea of mantle convection as a source of energy to drive plates, and along, with it, the whole Theory of Plate Tectonics is considered untenable.

HUNT *et al.* (1992) also support the concept of Earth Expansion and consider that Plate Tectonics is obsolete and should be discarded because it has rendered geosciences torpid and stagnant for the past three and a half decades. The authors provide several lines of evidence in support of their contention that Plate Tectonics cannot possibly explain the distribution of the continents and the oceans. In their book *Expanding Geospheres* they enter into some detail about the Expanding Earth concept, although the book is not primilary concerned with this theory. In particular they discuss the importance of hydrides, carbides and silicides in modifying the planet's volume and its crustal and superficial features, and they discuss the origins of flood basalts, the origins of the hydrosphere, the nature of the Earth's core and a variety of other factors that have played important roles in the evolution of the Earth.

Geothermal energy within the mantle can only play a minor role in terms of overall global tectonics, although its localized expressions can appear to be dramatic (COFFIN & ELDHOLM 1993). The ultimate causes of Earth Expansion – such as could be produced by the capture of electrons by protons in a plasma core which thereby produce atoms, the volumes of which are considerably greater than the volume of either the original protons or the original electrons – are a matter for further research, but the reality of Earth Expansion should not be denied because for the time being we remain unsure of its ultimate cause. If we were to apply the same logic to glacial deposits, we would have to reject the former existence of glaciations because as yet we do not fully understand what causes them.

GREAT CIRCLE TECTONIC BELTS

The two great Tertiary fold belts lie approximately along arcs of great circles mutually at right angles to each other. Although the fold belts do not intersect, the great circle tectonic zones that they are part of do so, once in the region east of the Himalayas and once just west of the Isthmus of Panama. The Rockies and Andes lie along an arc of a great circle called the Counter-Tethyan Torsion by CAREY (1988), a Great Circle trend which continues through Antarctica, the Indian Ocean via the Ninety East Ridge, the Eastern Himalayas, China, Kamchatka to Alaska. The Alpine fold belt runs from Portugal and Morocco in the west to the Himalayas in the east, deviating from a great circle where India has contacted Asia and where the Alps have been distorted by the Tethyan Torsion system. This system continues round the globe via Malaya and Indonesia, across the Pacific to the Isthmus of Panama and thence across the Atlantic to the Mediterranean.

Reconstructions of ancient fold belts of the Mesozoic and Palaeozoic reveal that these also tended to develop along arcs of Great Circles (EYLES 1993, fig. 9.1).

Under the Theory of Plate Tectonics, there is no explanation for the observation that the Tertiary and prior fold belts tend to lie along arcs of great circles, or to deviate only slightly from such arcs, and that they are often parallelled by trench systems, thrust systems and torsion zones. The Tethyan system has sinistral torsion, the Cordilleran (Counter-Tethyan) one has dextral torsion, despite the bold statement of one of the referees of this paper who declared that the concept of torsion was "false", but without saying why he thought so. Where the Tethyan torsion zone emerge onto land, such as for example in New Guinea and between Africa and Europe, and between South and North America, the evidence for torsion is difficult to deny. Where the

Pacific rim torsion zone emerges onto land, such as in California and New Zealand, dextral torsion can be observed with the naked eye.

I consider it likely that the special relationship between great circles and fold belts is not merely coincidental or accidental, but is related to the way that the latter formed. I have already explained how circles drawn on a globe from a point (or pole) can increase in surface area and in perimeter length until they become great circles. Beyond this stage, the surface area within the circles continues to increase, but only if the perimeter of the circles decreases (Fig. 4).

The three following paragraphs have been criticized by a referee of this paper.

In a globe such as the Earth in which new crust is being generated preferentially in certain sectors of the surface (*i.e.* not uniformly distributed over the surface of the globe), a stage will soon be reached in which a great circle perimeter will be forced to shorten in order that the surface area in that hemisphere can increase. In a globe in which surface areas of widely separated sectors are increasing in size, shortening along one great circle trend is insufficient to accomodate all the increase. The result will be the tendency for shortening of a second great circle more or less at right angles to the first, which will produce a second fold belt and related structures at right angles to the first. Where these belts cross, there will be evidence of great tectonic activity producing complex fragmentation and mega-shearing of the crust. Shortening along a third great circle mutually at right angles to the first two might be necessary in some crust expansion configurations, but seems not to occur on Earth.

In the case of the Earth, major surface area increase has occurred in the Pacific region. Its related Great Circle fold belt is the Cordilleran system and its continuation round the Counter-Tethyan torsion zone. The second major area of expansion has occurred all round Antarctica and in the southern parts of the Atlantic, Indian and Pacific Oceans, its related Great Circle fold belt being the Alpine-Himalayan system and the Tethyan torsion zone.

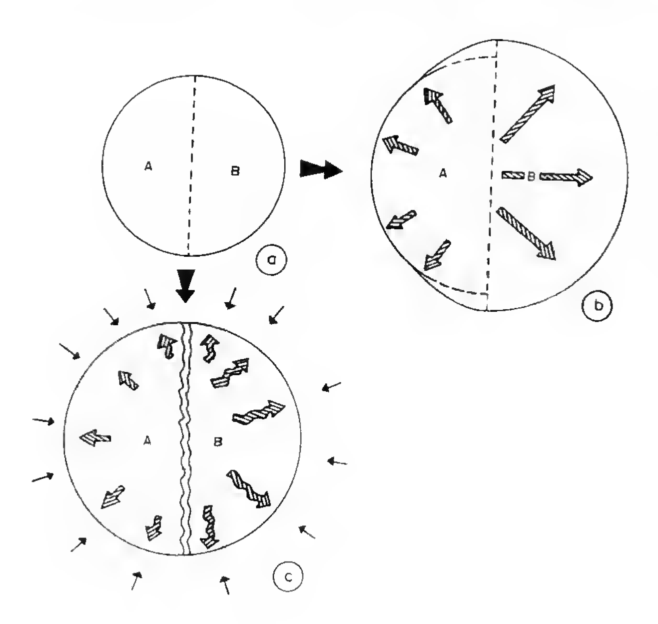


FIG. 4. — Generation of Great Circle fold belts in an expanding Earth. Frame A, the Triassic globe 80% of the size of the modern globe undergoes uneven expansion so that hemisphere A expands at a slower rate than hemisphere B. Frame B, represents the hypothetical shape of such an expanding globe if there were no gravitational force acting on the mass. The globe would expand out of shape, the A hemisphere would end up significantly smaller than the B hemisphere, even though both were larger than they were in a Triassic globe. Frame C, the force of gravity maintains the spherical shape of the unevenly expanding globe, causing crust in hemisphere B (the more rapidly expanding hemisphere) to converge towards that of hemisphere A, thereby forming a Great Circle compressional front (note the straight arrows of frame B are now compressed, producing a horizontal component of movement towards the Great Circle compression front). Figure 1 explains why the compression occurs along a Great Circle belt. These Great Circle compressive forces produce the world fold belts, subduction zones and island arcs (see Figure 4). Thin arrows: force of gravity; hollow arrows: expansion energy.

The crust on the opposite side of the Great Circle to the expanding hemisphere resists the tendency for shortening of the Great Circle. The result is that the edges of the expanding hemisphere override or underride the edges of the other hemisphere. It is this tendency, driven by hemisphere expansion (unevenly distributed Earth Expansion) and gravity, that gives rise to thrust fault systems, folding of the crust into fold belts, trench systems and other phenomena related with the Great Circle tectonic belts of the world. To a great extent strength inhomogeneities within the Earth's crust will determine where the shortening will begin, but once having started, shortening activity will tend to continue along the same trends. Furthermore, since it is unlikely that overriding or underriding of crust would occur in a perfectly vertical sense, there will be a tendency for some lateral displacement to take place, which would give rise to either sinistral or dextral shear components. Once sinistral or dextral shear was established in a Great Circle system, it would tend to continue shearing in the same sense. The Tethyan Shear has been sinistral throughout the Cainozoic, while the Cordilleran Shear has been dextral. Thus the southern hemisphere can be thought of as "screwing" itself under the northern hemisphere with a clockwise motion, while the western hemisphere is "screwing" itself under the eastern hemisphere with a counterclockwise motion.

CHANGING CURVATURE OF CONTINENTS

One of the objections to Earth Expansion is that the curvature of continental surfaces would have to change as "r" increased. DOOLEY (1983) for example, was unable to reconcile the required readjustment of curvature of Australia to the gravity data available for that continent. CAREY (1988) has responded to such criticisms, showing that DOOLEY'S gravity analysis was flawed, and in addition he has pointed out that the numerous joint systems that characterize almost all continental rocks are probably a result of millions of microscopic adjustments due to curvature change.

There may well be larger scale structures related to change in surface curvature of continents. For example, the regional tensional re-entrants from the Gulf of Guinea and on the opposite East African coast may represent "stretch marks" related to such curvature change in the continent of Africa. The continent-wide basin and swell structure of Africa (CAREY 1988) could also represent alternating compressional and tensional accomodations to changing curvature. As such, aspects of "membrane" tectonics may play a role in the development of some of the continental rifts and of their basin and swell structures.

One of the swells which has been studied is that of Namibia. It is represented by a north-east/south-west oriented domain of high topography, of which the Otavi Mountain Land is the north-east extremity. On its southern margin the elevated terrain is bordered by the Waterberg Thrust; which suggests that the swell is essentially compressional in origin. The Waterberg Thrust is a fault over 240 km long with at least 4 km of overthrusting of Damara Marbles (PreCambrian) over Mesozoic sediments of the Omingonde Basin (Post-Triassic at the top) (LÜDTKE 1970). The outcrop of the thrust is oriented north-east/south-west, with the marbles overthrusting younger rocks lying to the south of the fault. This thrust took place after initial breakup of Gondwanaland.

Since breakup of Gondwana, the western coast of Southern Africa has been in tension and has experienced uplift of over a thousand metres. Since the Mesozoic there has been little or

no laterally directed compressional forces in this region: many of the Mesozoic and Palaeozoic strata of Namibia still lie essentially untilted and unfolded on top of PreCambrian rocks. How then, can the existence of the Waterberg Thrust with its unmistakeable, even if localized, signs of compressive forces, be explained? One possibility is that it represents a localized crumpling of the crust due to change in curvature of the African continent as a result of Earth Expansion, the energy source being gravity. A second possibility is that it was a response on the part of the crust to forces set up during a period of axial reorientation, the energy being drawn from the kinetic energy of rotation of the Earth. What seems sure is that it does not have a ready explanation within the Plate Tectonics paradigm, since it occurs near a "passive margin" and is oriented at right angles to the mid-Atlantic spreading axis.

PHYSICAL GEOLOGY (GAIA'S PULSES AND SECULAR CHANGES)

INTRODUCTION

In Greek mythology, the Earth goddess was Gaia. LOVELOCK (1990) has suggested that the Earth behaves like a super-organism which he calls Gaia, and which is, among other attributes, able to fall ill and subsequently to heal itself. While LOVELOCK's thesis is highly contentious, and the subject of debate, there is general applause for his attempts to view the biosphere as a whole. While I do not ascribe to the Gaia cult which has emerged from LOVELOCK's work, I do maintain that the solution to many geological problems is only possible if one examines the Earth as an entity, and not as a series of disjointed sub-totals.

Being a goddess, Gaia did not have a pulse of human kind, but it is certain that she has experienced numerous exogenic and endogenic pulse-like behaviours during her long history. These range in scale from day and night (daily), phases of the moon (mensual), winter and summer (annual), the sunspot cycle (*c*.11 years), and glacial and interglacial cycles (0.5 m.y. +/–), to tectogenic phases (7 m.y. +/–) and many others at various scales of frequencies. All of these and more have left their mark, either in the geological record or in the fossil record of beings which have inhabited the biofriendly planet Earth.

TECTOGENIC PHASES

A second phenomenon that at first glance appears difficult to relate directly to Earth Expansion, is the pulsed nature of geotectonic processes (SCHERBA 1987; SCHWANN 1987; STILLE 1924; CAREY 1983). SCHERBA (1987) and SCHWANN (1987), following the researches of STILLE (1924), recently summarized the field evidence for tectonic activity and sedimentation in the part of the Alpine fold belt which runs from Portugal to the Pamirs. These authors have confirmed that the intensity of tectogenesis fluctuated in space and in time. Figure 5 extracts data concerning olistostrome formation during the Cainozoic in 27 areas within this belt (SCHERBA 1987). To the right of the figure is a histogram of the number of areas experiencing olistostrome activity at various times. According to SCHERBA's data, there were several periods during which no olistostrome activity is known to have occurred, and others during which up to 13 areas out of 27 experienced such activity. During the past 45 million years, for which there is sufficient data,

there were seven major periods during which olistostrome activity occurred. Because olistostromes are generally generated under conditions of high energy, usually, but not always due to uplift of source areas, and are often triggered by earthquakes, the pulsed nature of the olistostrome record suggests that orogenesis, to which most olistostromes owe their origin, was also pulsed. These pulses were called tectogenic "phases" (or "epochs") by STILLE (1924), although it is clear that they were not very regular in their timing. Pulsed tectogenesis suggests in turn that energy expended during tectogenesis was supplied in pulses (SCHWANN 1987), from which it seems probable that whatever causes orogenesis does not run at a steady rate.

During the Cainozoic Era, there were at least nine tectogenic "phases" (Laramide 1, Laramide 2, Illyrian, Pyrenean, Savic, Styrian, Attic, Rhodanian and Valachian) (Fig. 3, Tables 3-8) each of which lasted, on average, about 2.4 million years, and which were separated by relatively tectonically "quiet" periods ranging in duration from 4 to 11 million years. Similar pulsed tectogenic activity characterized the Mesozoic (SCHWANN 1987).

No convincing mechanism has yet been suggested to account for these phenomena, although short term fluctuation in the gravitational "constant" G has been proposed, partly because the implied rate of such geotectonic processes requires immense quantities of energy which only gravity can offer – in fact, the kinetic energy of rotation of the Earth offers enough energy to accomplish such activity. For the moment, to many geologists pulsed geotectonic activity remains an empirical observation although some scientists even doubt the validity of the observation that geotectonic processes can be pulsed in nature. Having seen some of the olistostromes in Oman and Italy sandwiched between undisturbed strata, I consider that the pulsed nature of tectogenic

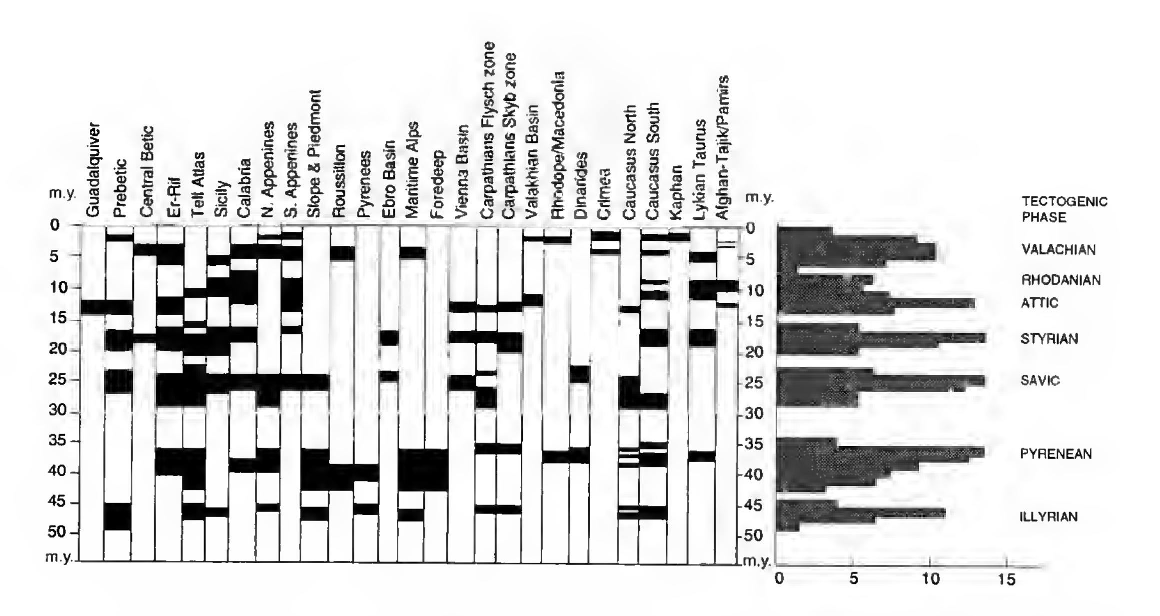


FIG. 5. — Tertiary olistostrome activity in 27 sectors of the Alpine fold belt and a histogram of the number of areas undergoing such activity in each period of 1.25 m.y. There were seven major peaks during the past 50 m.y. (Data from SCHERBA 1987.)

TABLE 3. — Tectogenic phases of the Cainozoic Era. Tectogenic activity took place during about 33% of the Tertiary, whilst about 66% of the era was tectogenically "quiet".

Tectogenic phase	Period of activity m.y.	Peak of activity m.y.	Stratigraphic correlation (/ = boundary)
VALACHIAN	6.3-2.5	3.7	Late Pliocene event
RHODANIAN	9-7.5	8	Late Miocene event
ATTIC	13-9	12	Mid-Late Miocene
STYRIAN	19-16	17	Early/Mid Miocene
SAVIC	28-23	24.2	Early/Late Oligocene
PYRENEA	41-34	35.5	Eocene/Oligocene
ILLYRIAN	47.5-44	45.2	Mid Eocene event
LARAMIDE 2	53-52	52.5	Palaeo/Eocene
LARAMIDE 1	66-64	65	Cretaceous/Tertiary

phases has been convincingly demonstrated by SCHERBA and his colleagues. The famous Neogene "nappes" of Daroca (Spain) and Perpignan (France) are of interest, because they moved into place during tectogenic phases, yet they are relatively far from high relief features. The forces that drove huge sheets of Cambrian limestones to override Neogene sediments (MN 04) at Daroca during the Styrian or Attic phase were essentially horizontal. This suggests that the energy supply was the kinetic energy of rotation of the globe, rather than gravitational energy, which has predominantly vertical components of action. However, the Daroca nappe has been interpreted to be probably extensional in origin, related to the gravitational collapse of the orogen (DOBLAS pers. comm.), in which case gravity would have been the main force involved in its emplacement.

RIFTING PULSES

My studies of the Gregory and Albertine Rifts of Africa reveal that rifting tended to occur in pulses. Further work has shown that the major rifting episodes coincide reasonably closely in time with tectogenic phases of Scherba (Table 5). For example, in Kenya, major tectonic activity took place about 17 to 16 m.y., about 12 to 13 m.y., about 8 to 7 m.y. and during the Plio-Pleistocene. In the Western Rift, Uganda there were major movements about 12 m.y., about 6 to 7 m.y., about 4 m.y., and during the Pleistocene. In view of the enormous amounts of energy required and the pulsed nature of the work done, I feel that such pulsed activities may be related to the second most powerful source of energy in the globe, the kinetic energy of rotation (Table 2).

CONTINENTAL (TRAPS) AND OCEANIC FLOOD BASALTS (PLATEAUX)

Orogenesis and its localized consequences such as olistostrome formation and nappe emplacements, represent only a part of the geotectonic activity that occurred during these phases. There are others, including rifting, mega-fissure eruptions and possibly the Tethyan Shear which encircles the globe. Major rifting episodes in the African Rift System generally occurred at the same time as tectogenic phases, as did major trap volcanism, including the Deccan Traps of

TABLE 4. — Tertiary Trap Eruptions.

Name of Trap Field	Period of activity m.y.	Correlation to tectogenic phases
Ethiopian Basalts (Afar)	1.5-4.5	Valachian
Plateau Phonolites (Kenya)	12-13	Attic
Ethiopian Basalts (Central)	9-13	Attic
Columbia River Basalts (USA)	15-17	Styrian
Ethiopian Basalts	21-32	Savic
Ethiopian Basalts	36-43	Pyrenean
North Atlantic Flood Basalts	36-43	Laramide 2
Deccan Traps (India)	54-56	Laramide 1
	65-67	

India at the same time as the Laramide 1 phase, The Ethiopian Traps during the Pyrenean Phase, the Columbia River Basalts of North America during the Styrian phase and the Plateau Phonolites of Kenya coincident with the Attic phase, even though the record is less complete (or less well-documented) for such activities (MACDOUGALL 1988; CARLSON 1992; WHITE, 1991).

COFFIN & ELDHOLM (1993) have reviewed the available information concerning "large igneous provinces" which consist essentially of vast fields of lava, principally basaltic, which erupted during relatively brief geological periods (ranging between 1.5 and 4.5 million years). The volumes erupted are indeed vast, the Ontong Java Plateau containing some 36 millions km^3 of basalt which erupted in less than 3 millions years. As COFFIN & ELDHOLM stress, this rate of eruption is equal to or greater than the rate of emplacement of new crust over the entire global spreading ridge system. These authors conclude that the eruption of continental and oceanic flood basalts was due to brief but powerful pulses of magmatic activity. Furthermore they discussed some of the effects that such pulsed igneous activity might have on the hydrosphere, lithosphere, atmosphere and biosphere. The formation of the Ontong Java Plateau would have caused a global sea-level rise of 10 metres unless there were isostatic adjustment of the crust below the plateau.

The eruption of basalts is usually accompanied by aqueous and gaseous phases, meaning that during flood basalt eruptions, immense volumes of water and gases would have been released into the hydrosphere and atmosphere, depending on whether the eruptions took place on land or under the ocean. These injections of water and gases were sufficiently voluminous that they would have altered seawater and atmospheric composition on a global scale. These in turn would plausibly have affected the biosphere, and COFFIN & ELDHOLM make several provocative cor-

TABLE 5 — Main Periods of Rifting Activity in East Africa.

Period of Rifting m.y.	Rift System	Correlation to tectogenic phases
5 to 4 and younger	Gregory and Albertine	Valachian
8 to 7	Gregory, Nyanza and Albertine	Rhodanian
13 to 12	Gregory, Nyanza and Albertine	Attic
17 to 16	Gregory and Nyanza	Styrian

relations between the formation of large igneous provinces and mass extinctions, including the extinction of the dinosaurs at the time of the eruption of the Deccan Traps, India, and the Early Miocene/Middle Miocene faunal turnover pulse.

KINKS IN HOT-SPOT TRACKS

VINK (1984) described numerous hot-spot tracks in various parts of the globe and proposed that hot-spots could be used as a frame of reference for determining relative plate motions through geological time. The classic example, the Hawaiian-Emperor chain has long straight sections with a simple age-distance relationship, Hawaii being at the young end of the chain. The proposal of a hot-spot frame of reference has been widely used in plate tectonic studies. COX & HART (1986) for example, illustrate the concept with a drawing of a ball with nails driven into it, the ball representing the core and the nails the hot-spot plumes. The purpose of this drawing is to reveal how solidly fixed the hot-spots are relative to the core. However, as has been pointed out by KEITH (1993) and others, there are hot-spot tracks whose behaviour does not conform to the nails in a ball model, including the Marquesas chain and the Cook-Austral chain which show important violations of the simple age-distance relationship which would be expected if the nails were indeed firmly hammered into a solid core. There are also serious petrologic and geochemical problems with the hot-spot model. The Azores "hot-spot" for example, is more likely to be a wet-spot related to a lowered solidus (due to the addition of CO_2 and H_2O to mantle peridotites), rather than a hot-spot due solely to elevated temperatures.

An important point about hot-spot tracks is that they are comprised of relatively straight sections interrupted by dog-leg kinks, called cusps. On a parochial scale, hot-spot kinks could be related to changes in direction of movement of plates. On a global scale, it could be due to a shift of the entire crust relative to the mantle. VINK (1984) reported that there was a dog-leg in the Iceland hot-spot at 36 m.y., which coincides closely in time with the "Grande Coupure" and the Pyrenean Tectogenic Phase. A further dog-leg occurred at the KT boundary, which was also a period of major faunal changes and tectogenesis, and a major one took place about 110-120 m.y. ago (Barremian-Aptian). It is perhaps not coincidental that major changes took place concurrently in the lithosphere (as recorded by dog-legs in hot-spot tracks) and the biosphere (as represented by the fossil record). Major tectogenic phases, first order biosphere changes and bends in hot-spot tracks may well be varied aspects of the same overall cause – an episodically shifting axis of rotation of the globe which would cause the Earth's crust to shift relative to the core and the mantle, thereby inducing stresses and strains over the entire globe, and altering the positions of biogeographic realms.

The Tristan hot-spot has an intriguing history. From its inception some 120 m.y. until 80 m.y. it was located precisely on the mid-Atlantic ridge system, and thus produced a bilaterally symmetrical pair of hot-spot tracks – the Walvis ridge on the African side and the Rio Grande Rise on the South America one. At 80 m.y. it shifted position relative to the mid-Atlantic ridge and intra-plate hot-spot, located within the African plate (MILNER *et al.* 1995; O'CONNOR & DUNCAN 1990; O'CONNOR & LE ROEX 1992). However, as far as the Walvis Ridge is concerned, its behaviour remained the same, whereas it stopped feeding material to the Rio Grande Rise which ends abruptly some distance from the mid-Atlantic ridge. This history suggest that there is no convection cell below the African plate, because, if there was such a cell, then the course of the

Tristan hot-spot should have been deviated by the convecting mantle through which it passes. If the convection cell was strong enough to move the African plate, then it follows that it should have moved the Tristan plume. But it did not, which indicates that below the African plate the convecting mantle model is incorrect.

In a recent publication, NORTON (1995) demonstrated that the 43 m.y. event in the Emperor-Hawaiian seamount chain, which has often been taken to prove a change in direction of plate movements at that time – the "43 m.y. events" – exhibits behaviour that is clearly delinked from that of the various plates that comprise the global geotectonic machine. Reconstructions of plate positions using the Hawaiian hot-spot as a reference are thus refuted.

It should be noted that the 43 m.y. event affected not only the lithosphere, but also the biosphere. The most important faunal change of the Palaeogene apart from the "Grande Coupure" occurred at this time (WOODBURNE & SWISHER 1995), providing yet another example of the close link between tectogenic events and biospheric changes.

EXTINCT SPREADING RIDGES

Several of the oceanic plates contain extinct spreading ridges (ESR). The most extensive system occurs on the Nazca plate between South America and the active Pacific spreading ridge. Others are smaller, but nevertheless provide evidence of shifting axes of crustal generation. Some extinct spreading ridges, or portions there of may have been subducted, for example in the Cocos Plate.

A plot of the age of abandonment of these ESRs reveals that most, if not all of them became extinct during periods of tectogenesis in the Alpine fold belt (Table 6). Since tectogenesis spanned approximately 33% of Cainozoic time, the correlations between abandonment of ESRs

TABLE 6. — Extinct spreading ridges and other anomalies in the ocean floor.

Extinct Spreading Ridge	Magnetic Anomaly	Tectogenic Phase	Period of abandonment (m.y. +/–)	Kink in hot-spot track	Flood basalt
Sea of Japan	5	Attic	12.5		Plateau Phonolite
Cocos	5	Attic	12.5		Plateau Phonolite
Nazca	5	Attic	12.5		Plateau Phonolite
Iceland	5	Attic	12.5		Plateau Phonolite
Cocos	6	Styrian	17-20		Columbia River
Marion	8	Savic	25-27		Ethiopian 2
Phillipines	16-17	Pyrenean	37-41	xxxx	Ethiopian 1
Iceland	20	Illyrian	45-47		
Greenland	21-22	Laramide 2	49-53		
SE Australia	23	Laramide 2	54-55		North Atlantic
Baffin	23	Laramide 2	54-55		
Coral Sea	24	Laramide 2	55-56		
Agulhas	31	Laramide 1	67	xxxx	Deccan/Mascarenes
Biscay	33	?	72-76		
Phoenix	M9	?	121	xxxx	
Wallaby	D	?	?		Ontong Java

and of tectogenic phases is not likely to be due to chance alone. It is more probable that there is a causal relationship between the two phenomena. It is noted that one of the ESRs correlates in age with the major kink in the Hawaii-Emperor hot-spot track and there seems to be a correlation between the age of ESRs and of flood basalt eruptions.

The simultaneity of these events suggest that there was a shift of the crust with respect to the mantle on a global scale, which caused increased tectogenesis, flood basalt activity, increased rifting, abandonment of parts of established spreading ridges and the birth of new ones and changes in the axes of some hot-spots.

Causes of pulsed activity in the lithosphere

Whatever the ultimate cause of tectogenic phases, rifting pulses and episodic trap eruptions, the contemporaneity of activity suggests that they were all responses to the same overall prime mover. This ultimate cause led to the generation of compressive forces in some sectors of the Earth's crust at the same time that it caused extensional ruptures and shears in other parts. Earth Expansion is a possible candidate although it is not specifically known to occur in pulses and it would be unlikely to produce contemporaneous pulsed activity in widely scattered parts of the globe. A more likely cause is the reorientation of the axis of rotation within the globe, something that would produce stresses and strains throughout the fabric of the globe and which would naturally tend to be pulsed, due to the gyroscopic properties of spinning objects.

In the literature on Plate Tectonics, one seldom sees references to pulse-like behaviour. Indeed, a basic assumption of the theory used to be that rates of spreading at any one mid-ocean ridge system were constant, although PATRIAT & ACHACHE (1984) concluded that the spreading rate of the ridge that "drove" the Indian plate into the Asian plate slowed down considerably once contact between the two continents had been made. Subsequent radioisotopic dating of DSDP borings has provided a geochronologic control on the characteristic palaeomagnetic signatures, which seems to confirm the constancy of rate of spreading at mid-ocean ridges. Such constancy of rate has been taken to provide support for the proposal that geothermal energy is the source of power for the plate tectonic motor.

Axial reorientation

It seems counter-intuitive to expect that a constant rate continental shift motor could produce pulsed mountain building activity in the Alpine and other fold belts of the world. Inhomogeneous expansion of the Earth, in which considerably more oceanic crust is generated in the southern hemisphere than in the north, together with gravity driven adjustments to restore the geoid to its quasi-spherical form, is unlikely to act in pulses. It is perhaps more likely that the imbalance induced in the rotating Earth by inhomogeneous expansion, would tend to throw the planetary gyroscope out of equilibrium, which would then have a tendency to adopt a new axis of rotation as the imbalance reached a critical value. Such readjustments of the axis of rotation would naturally be episodic rather than continuous.

Axial reorientation is not a new idea, its pedigree going back more than 110 years. GOLD (1955) considered that large-scale "polar wander" was inevitable if the long-term rheology of the Earth is inelastic. GOLDREICH & TOOMRE (1969) pointed out that in a quasi-rigid body such as the Earth, large-scale displacements of the pole can be readily explained by small relative

displacements of material in the mantle. Furthermore, they suggested that if mantle convection causes the inertia axis to shift, so will the rotation axis change. LAMBECK (1979) discussed the matter at some length.

Rotating bodies tend to rotate round a relatively stable spin axis, but if there is a change in the distribution of mass within a rotating body, the moments of inertia will change, which will lead to a shift in the orientation of the axis of rotation (VERMEERSEN & VLAAR 1993; LASKER & ROBUTEL 1993). In rotating bodies in which the distribution of mass changes, there is usually a threshold of imbalance to cross before the axis will actually change. The axis of rotation would tend to shift from one quasi-stable orientation to another, in which case the kinetic energy of rotation of the globe would be tapped in pulses. Since the kinetic energy of rotation of the Earth is the second most powerful source of endogenetic energy in the globe (Table 2), the work done during axial reorientation may be considerable. Orogenic belts, the Tethyan and Pacific rim shear, nappes, continental rifts, abandonment of spreading ridges – giving rise to extinct spreading ridges – and trap type fissure eruptions may represent diverse aspects of such work.

Earth Expansion does not occur uniformly over its surface. Most new crust is generated at the mid-ocean ridges which are not disposed equally over the Earth's crust. Vertical uplift of parts of the lithosphere also occurs at various scales up to epeirogenies and the entire globe, but gravity maintains the almost spherical shape of the globe. The result of this non-uniform style of expansion is that the global gyroscope can be rendered out of balance (partly due to the generation of geotumors due to unequally distributed insertion of new oceanic crust at spreading axes, crust whose density is greater than that of continental crust). This concept has been described in detail by CAREY (1988). With the progressive production of gyrosopic imbalance, the axis of the rotating Earth will eventually reach a threshold beyond which it will gradually change its orientation to a new position of maximum moment of inertia. This implies that the poles of rotation are not fixed, a phenomenon which has been known for nearly a century (CAREY 1988; LAVALLARD 1988).

EFFECTS OF AXIAL REORIENTATION

Repositioning of the Earth's axis of rotation will lead to the generation of stresses and strains in the fabric of the globe. TARLING & TARLING (1971), in an argument aimed against the concept of pole repositioning, considered that such a repositioning would lead to fragmentation of the globe, or at least that it would induce "major adjustments in the lithosphere", for which they said they could see no evidence. They were apparently implying that polar repositioning would release so much energy that it would cause fragmentation of the globe. However, if repositioning occurred over geological time scales rather than rapidly, then much of the stress and strain would be released non-destructively, mostly as heat (see section on ocean warming peaks) and as adjustments to the lithosphere such as nappe movements, fold mountains, rifting and shears. We must keep in mind that at the scale of hundreds of kilometres and of millions of years, the apparently rock solid lithosphere behaves like a fluid (MARCHAL 1968). In my opinion, much of the geological evidence currently interpreted within the framework of Plate Tectonics, such as fold mountain belts, nappes and rift valleys, represents the "major adjustments in the lithosphere" that TARLING & TARLING had so much difficulty envisaging while they were rejecting the concept of axial reorientation.

Lithosphere at the equator is rotating at a speed of 1670 km/h while that at the poles is rotating at 0 km/h. If the position of the equator were to change, then crust formerly at the equator would be rotating at a slower speed than previously, whereas crust underlying the re-positioned equator would be rotating at a higher speed. These differences would induce acceleration or deceleration forces in the Earth's crust. These forces would act tangentially to the radius of the Earth. In most places, the crust would absorb the forces so generated by folding, flowing, faulting and compression/relaxation, but occasionally the crust would rupture and sheets of rock would override nearby rock masses. Where these sheets come to overlie younger rocks, they are recognized as nappes, such as the well-exposed example of Precambrian (Damara) Marbles which overlie Jurassic quartzites along the 240 km long Waterberg Thrust in Namibia, and the Cambrian limestones lying on top of Middle Miocene terrigenous strata at Daroca, Spain, which dates from the Middle Miocene. Where they come to overlie older rocks or rocks of the same age, such sheets of rock tend not to be recognized as nappes, but are generally mapped as concordant rock units.

The orientation of the major transform traces in the Atlantic suggests at first glance that the spin axis of the Earth has changed little during the past 200 millions years. However, examination of the orientation of major transform traces in the other oceans indicates that these traces are not causally linked to the axis of rotation of the Earth – they are independent systems, just as the axis of rotation and the magnetic dipole axis are delinked. At present, for example, the magnetic axis is inclined at some 14° from the rotational axis, and it is not fixed in geographical position.

Axial repositioning – inducing a "graticule shift" – would have other consequences, including climatic and biospheric changes (CREBER & CHALONER 1984). One of these is related to the fact that the rotating Earth has an equatorial "bulge" (polar radius: 6357.774 km; equatorial radius: 6378.16 km). As the axis of rotation shifts, so would the position of the equatorial bulge, and this would induce stresses and strains in the Earth's crust, as well as other effects such as transgressions and regressions of water bodies due to differences in the fluidity of the lithosphere and the hydrosphere. This is because the equatorial Great Circle has a circumference of 40,075 km, whereas polar Great Circles have circumferences of about 39,945 km, a difference of 130 km. If the equator changes position, the crust ahead of it will become slightly "stretched" while that behind it will become slightly "compressed". Some of this stretching could be accomodated at spreading ridges, but in wide continents such as Africa, some localized effects such as rifting and tilting of joint blocks may be expected. Such membrane tectonics has support from a number of scientists (DOBLAS, pers. comm.).

As far as Africa is concerned, there has been a southwards propagation of rifting (Early Oligocene in Red Sea, Late Oligocene in Ethiopia, Lower Miocene in Northern Kenya, Upper Miocene in Southern Kenya and Western Uganda, Pliocene in Northern Tanzania and Pleistocene in Southern Tanzania and Malawi). East African volcanic rocks also tend to decrease in age from north to south, the onset of volcanism usually postdating the earliest signs of rifting by a million years or so (basal strata in the African Rift System are usually non-volcanic), also suggesting a southwards propagation through geological time of the tensional cracks up which magma flowed to reach the surface. Could this southerly propagation of rifting and volcanism be related to the proposed southerly movement of the equator during the late Cainozoic? Or is it more likely to be related to Coriolis forces acting over geological time periods?

Pole orientation and ecoclimatic zones

The graticule which geographers use as a reference for locating points on the surface of the globe (latitude and longitude) moves in phase with axial repositioning, because the graticule is defined by the poles, while East is defined by the sense of rotation of the globe. Thus if the poles shift, so would the equator, because the poles define the equator.

Because the poles of rotation of the Earth are oriented at a high angle to the ecliptic, the solar radiation arriving at the Earth's surface is not uniformly distributed (Williams 1993). With modern obliquity, averaged over the year, solar energy receipt is maximal at the equator and minimal at the poles (Collingbourne 1976). This non-uniform distribution of solar energy captured at the Earth's surface is responsible for generating the ecoclimatic zones which encircle the globe (tropical, subtropical, temperate, boreal, taiga and polar zones). Thus a change in orientation of the axis of rotation of the Earth with respect to its surface (graticule shift), would result in a comparable shift in the position of its ecoclimatic zones and this would in turn affect the biosphere (Creber & Chaloner 1984). The latitudinally arranged ecoclimatic zones would track changes in graticule position.

Pulsed energy expenditure

If the concordances highlighted in Figure 6 are indeed manifestations of a single underlying cause in five different systems (the solar system and four Earth systems), then we may conclude that whatever was driving the changes acted in pulses which usually lasted about 2 to 2.5 million years, and which were separated from each other by about 7 m.y. (ranges between 4 and 11 m.y.). The available evidence suggests that the most active periods of tectogenesis depended upon pulsed energy supply. It is less likely that the gravitational constant changed in a pulsed manner, or that Earth Expansion was itself pulsed (see Carey 1988, for a discussion about pulsed expansion at several time scales). The most likely mechanism that presents itself is that the axis of rotation of the globe changed periodically from one quasi-stable orientation to another, and that during the period of change (2 to 2.5 m.y.) the Earth's crust tapped into the kinetic energy of rotation, causing worldwide stresses and strains within the fabric of the globe, recognized by geologists as nappes, rift valleys and trap fields that characterize the lithosphere. Apart from gravity and the progressive decay of a plasma core to the atomic state, other endogenic and exogenetic energy sources are too feeble to result in the sort of lithospheric damage observed.

In a rotating, non-solid, expanding body, such as the Earth, the distribution of mass within the body is changing constantly. The Earth is a rotating fluid body, because, at the scales of 100 km and of geologic time, even "solid" rock behaves like a fluid (Marchal 1968). In the Earth, there are several categories of redistribution of mass: atmospheric, hydrospheric, lithospheric and probably also of the deeper layers of the Earth. Forces generated by the redistribution of atmospheric masses (winds) are already known to lead to perturbations in the orientation of the axis of rotation of the globe (Lavallard 1988) by distances of several metres in several years. Ocean circulation patterns may have played a role in determining pole position, especially following fundamental changes in ocean circulation patterns as the result of the opening and closing of seaways between neighbouring continental masses.

Redistribution of lithospheric mass, especially the uneven generation of oceanic crust at mid-ocean ridges (greater quantities of new crust have been generated in the western and southern hemispheres than in the eastern and northern ones) have induced imbalance in the planetary gyroscope in much the same way that redistribution of mass in a revolving car wheel (due to wear and tear, or to the addition or loss of extraneous mass to the rims) can lead to "wheel wobble". Such "wheel wobble" results from the rotation of unbalanced masses on a fixed axis of rotation, the "wobble" only becoming evident after an imbalance threshold has been crossed (in the case of car wheels, the threshold is related either to the amount of mass imbalance or to the speed of rotation, but in rotating planets, the speed of rotation does not change rapidly, in which case the threshold for "wobble" will relate primarily to mass imbalance).

The car tyre, spinning on its fixed axis is prevented by its axle fittings from adopting a more balanced spin axis, with the result that it wobbles. Correction of wheel wobble is achieved by adding suitable masses at appropriate locations on the rim to restore balance. The Earth's axis is not fixed, and it is therefore free to take up any convenient orientation that maximizes balance, but because of rotational inertia, an unbalanced spinning globe must cross a threshold of imbalance before it will take up a new axis of rotation. Having adopted an axis of maximal moment of inertia, the Earth will tend to continue rotating about this axis until imbalance grows sufficiently large that the imbalance threshold is crossed; thus changes will tend to be pulsed. If the internal forces generated by imbalance and axial reorientation are dissipated over geological time, then planetary disintegration need not occur. If the reorientation is too rapid, disintegration may take place (TARLING & TARLING 1971). That planetary disintegration has happened in the Solar System is suggested by the presence of the asteriod belt (a fragmented hypothetical planet called Aster) between the orbits of Mars and Jupiter.

It is therefore proposed that the orientation of the spin axis of the Earth (and of other planets and moons) has changed during geological history, and that stresses and strains induced within the fabric of the globe by such changes have resulted in tectogenesis, rifting and volcanic activity, as well as major changes in world climate (both by shift in the positions of ecoclimatic belts relative to the surface of the Earth and by changes in the degree of seasonality due to obliquity changes) and in the biosphere. Spin axis reorientation has occurred infrequently (9 times during the Cainozoic) and took place over significant spans of geological time (2 to 2.5 m.y.). At a rate of 1 metre per year (measured at the Earth's surface) the spin axis could migrate up to 23° of latitude in 2.5 m.y. if the movement was unidirectional. Spin axes would be quasi-stable, which means that reorientations would be episodic, leading to pulsed changes in Earth systems sensitive to such changes (lithosphere, biosphere, atmosphere, hydrosphere). They would also induce adjustments to the extra-terrestrial relationships of the Earth, due to gyroscopic effects (precession, tilting, nutation), which would alter the Earth/Sun relationship (graticule shift and obliquity shift), which would result in climatic changes on Earth.

THE HYDROSPHERE

Ocean Palaeotemperatures

Throughout the Cainozoic there has been an overall cooling trend in the world's oceans, interspersed by small warming peaks or by temperature "plateaux". Various explanations have been proposed to account for this global cooling trend (*e.g.* BARRON 1985). Most attempts are

based on changing the amount of Sun's energy reflected into space from the Earth by changing some parameter on the surface of the Earth or in its atmosphere. I consider it more likely that the trend towards global cooling is probably due to an increase in the total volume of seawater that accompanied Earth Expansion (CAREY 1988). As the volume of seawater increased over geological time, the solar energy that supplies most of the ocean's heat energy – over 99% of it, most of the rest being endogenic in origin – became dispersed through greater and greater volumes of seawater. The increase in surface area of the Earth compensated to some extent because the total solar energy captured by the Earth would increase as its surface area increased, even if the solar energy flux remained constant (mean solar flux at Earth's surface today is about 350 watts per square metre). The temperature of the oceans therefore decreased throughout the Tertiary, the cooling curve following approximately a slope of volume (L^3) over area (L^2). Endogenetic heat (geothermal flux) plays a role in warming the world's oceans, but its effects are considerably less (mean geothermal heat flux at the Earth's surface is about 0.818 watts per square metre). However, during tectogenic phases (see section on energy supplies) greater quantities of endogenetic heat energy may have been released into the environment, which could have contributed to short-lived (*c.*1-2 m.y.) ocean warming episodes. Alternatively, slight "pulse-like" activity of the Sun could account for these short-lived ocean warming peaks and temperature plateaux. A further possibility is that temporary slow-downs in the eruption of neonate waters from the mantle occurred from time to time, leading to a decrease in the volume of the world's oceans, and thus to an increase in its temperature as the incoming solar energy was absorbed by smaller quantities of water.

The MILLER & FAIRBANKS (1985) curve of $\delta^{18}O$ values obtained from benthic Foraminifera of the Pacific and Atlantic oceans shows that several short-lived warming events interrupted the overall tendency of global cooling that characterizes the Tertiary. Comparison of this curve with information about tectogenic phases reveals that 6 out of the 13 main warming peaks occurred closely in time with 6 of the 9 tectogenic phases (Laramide 2, Illyrian, Pyrenean, Savic, Rhodanian and Valachian Phases). From this we tentatively conclude that tectogenic phases tended to release great quantities of heat energy into the environment, including the world's oceans, which thereby experienced warming peaks.

Eustacy

It has been suggested that eustatic regressions (HAQ *et al.* 1987) of the sort identified by + symbols in Figure 6, were cold (VAN COUVERING 1988), that transgressions were warm, and that regressions coincide with major faunal turnovers (GINSBURG 1984, 1986). Examination of the data (Fig. 6) reveals that there is not an obvious close correlation between oceanic temperature and changes in sea-level, nor of regressions and faunal turnovers. On the contrary, most of the major faunal turnover pulses appear to have occurred during periods of high sea-level. This may suggest that the so-called eustatic transgressions and regressions may not have been worldwide events, but were more localized phenomena. In any case, the Vail Curve shows so much activity that one could propose almost any correlation and have a good chance of finding a match. The lack of correlation between the Vail Curve and the $\delta^{18}O$ curve is therefore probably significant. The two phenomena of global cooling and of eustacy are not related to the same overall cause. They appear to be varying completely independently of each other.

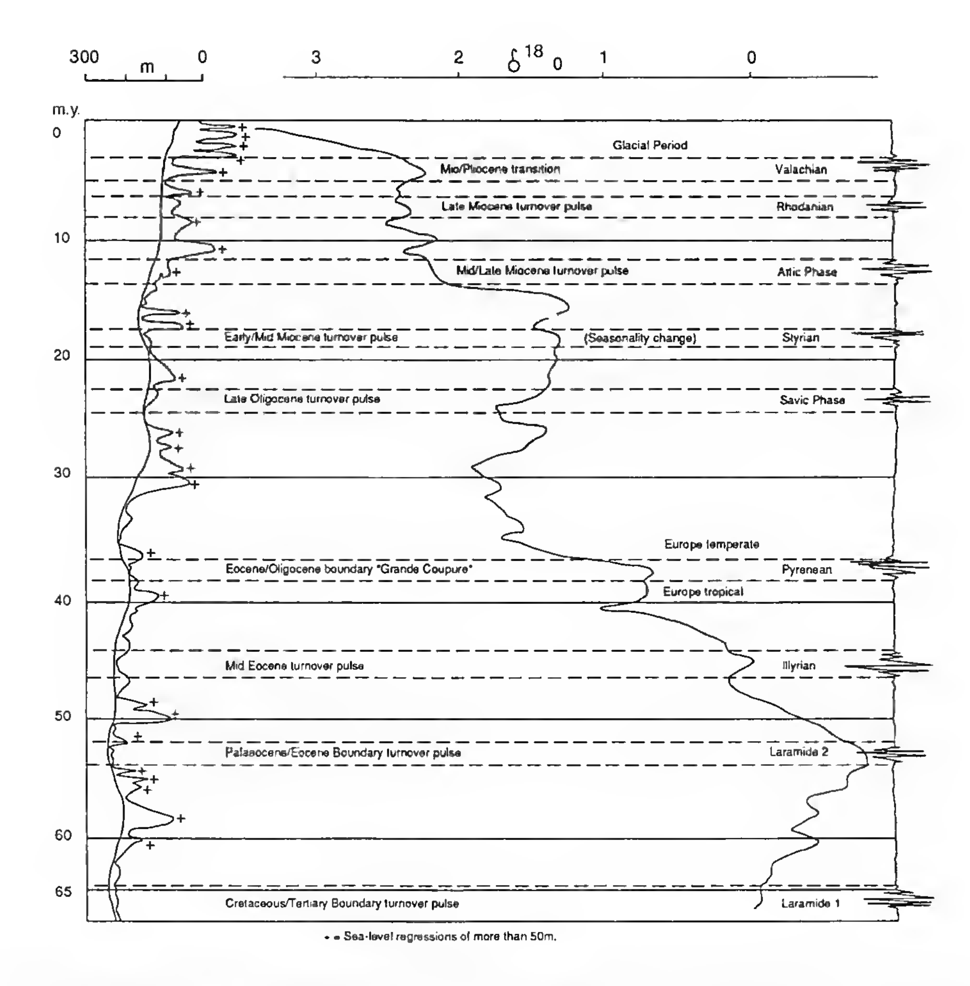


FIG. 6. — Correlation of Oxygen 18 curve (from MILLER & FAIRBANKS 1985), sea-level curve (from HAQ *et al.* 1987), tectogenic phases and faunal turnover pulses of the Tertiary and Quaternary Eras.

However, each of the 9 tectogenic phases of the Cainozoic coincides in time with high sea-levels, which are for the most part not interrupted by major regressions (more than 50 metres drop in sea-level). Out of 26 such large scale regressions which have been documented for the Cainozoic Era, only two coincide in time with a tectogenic phase as recognized in Figure 3. 24 of the 26 regressions occurred during periods of relative tectogenic quiescence. If regressions were randomly scattered through time, we would expect about 30% of them to have occurred during tectogenic phases (tectogenic activity spanned in total about 30% of Cainozoic time: 22 m.y. versus 65 m.y.) This pattern of exclusion is so strongly expressed that it seems likely that during tectogenic phases there was something that prevented or impeded great and rapid sea-level regressions, whereas during periods of tectogenic quiescence, such regressions not only became possible, but occurred relatively frequently. The post-Valachian regressions are known

to be related to the build-up and subsequent decay of polar ice caps (Quaternary Glaciations), and it has been suggested that some of the more marked regressions and transgressions during the Tertiary may also have been related to the waxing and waning of polar ice-caps. It would thus appear that the formation of polar ice-caps may have been impeded during phases of tectogenesis, and that they could only form (and then decay) during tectogenically quiet periods. However, there were probably other factors affecting sea-level, including the addition of massive volumes of neonate water to the oceans during emplacement of new lithospheric material at spreading ridges, as well as changes in rates of photo-dissociation of water molecules in the upper atmosphere, and major changes in basin shapes and depths during continental displacement activity.

The polar and equatorial radii of the Earth differ by 21,386 km (polar radius: 6357,774 km; equatorial radius: 6378.160 km). During graticule shift, changes in polar and equatorial radii of the lithosphere would lag slightly behind polar reorientation, because the lithosphere takes time to rebound isostatically (10 Ka for the rebound of Scandinavia after the waning of the last glacial cap). The radii for the hydrosphere would adjust virtually instantaneously, and the differences between the two would probably lead to short-lived (several Ka) transgressions in erstwhile polar parts of the globe and regressions in erstwhile equatorial regions, shore-line topography permitting. Transgressions and regressions would thus be taking place at the same time, albeit in different parts of the globe (WEGENER 1962). Because of this the assumption of contemporaneous same sense (either sea-level drop or sea-level increase) worldwide sea-level changes during the so-called eustatic transgressions and regressions depicted in the Vail Curve, may not be valid.

THE ATMOSPHERE

During the Cainozoic Era there were several major reorganizations of world climatic systems. During the Early (Ypresian) and Late Eocene (Priabonian), for example, Europe and North America were tropical, whereas after the Grande Coupure, which correlates in time with the Pyrenean Tectogenic Phase, they became temperate. At the end of the Lower Miocene, coincident in time with the Styrian Tectogenic Phase, worldwide seasonality increased dramatically in severity (MORALES *et al.* 1993; PICKFORD in press) and Europe became more tropical than it had been before (palm-trees grew in Poland, Germany, France and Spain; mangroves grew in France), while Central Africa became less tropical (forest in Zaire gave way to dune fields, the Namib and Sahara Deserts became humid, large rivers flowed northwards from the Sahara towards the Mediterranean, St Helena became sub-temperate, the Cape Flora occupied a much greater area than it does now) (PICKFORD 1991, 1992). At the end of the Miocene, at the time of the Rhodanian Tectogenic Phase, Europe once more became temperate and Central Africa regained its tropical character (forest returned to Zaire to grow on sand dunes over 200 metres thick, desert returned to the Sahara and Namib regions, the Cape flora was squeezed into a tiny corner of Southern Africa). At about the same time, monsoon climatic regimes were established in the Indian subcontinent (QUADE *et al.* 1989). Following the Valachian Tectogenic Phase began the Quaternary cycle of polar glaciations.

Reorganization of oceanic circulation patterns during the Cainozoic (such as occurred when the Tethys Seaway connection between the Indian and Atlantic Oceans was severed, or when

the Isthmus of Panama was closed, thereby interrupting the equatorial current that used to flow between the Pacific and the Atlantic), undoubtedly played an important role in modifying global climatic systems, but such changes would be unlikely to lead to fundamental global scale changes in degree of seasonality, because seasonality is primarily determined by the relationship of the Earth to the Sun (obliquity).

The nature of some of the global scale climatic changes that occurred during the Cainozoic, lend support to the concept that the orientation of the pole of rotation of the globe has changed, not only with respect to the globe itself (graticule shift), but also with respect to the plane of the ecliptic (obliquity shift). Two pieces of evidence lend support to this idea, and are worth repeating. The worldwide increase in seasonality that occurred at the end of the lower Miocene, at the time of the Styrian Tectogenic Phase, suggests that the relationship between the Earth and the Sun changed (its obliquity increased). At the same time, shift of the ecoclimatic belts (Europe becoming more tropical, Central Africa less tropical) indicates that the coordinate graticule shifted, so that the equator was located further north in the Old World, and further south in the New World (PICKFORD 1990b, 1991).

Earth Expansion implies an increase of the surface area over which the atmosphere is spread – present surface area of the globe is 510×10^6 km^2; Middle Miocene surface area was about 495×10^6 km^2; Oligocene surface area was about 479×10^6 km^2. The atmosphere itself probably increased in volume in phase with Earth Expansion, because of outgassing of the mantle during volcanic activity and generation of oceanic crust at spreading ridges. As the surface area of the globe increased, there would have been greater total quantities of solar energy intercepted at the Earth's surface, even if the solar flux remained constant. If solar flux remained constant at today's value of 350 watts per square metre, the total energy captured at the Earth's surface during the Early Oligocene would have been about 1.32×10^{24} joules/yr. During the Middle Miocene it would have been about 1.37×10^{24} joules/yr. Today it is about 1.4×10^{24} joules/yr. (These figures are calculated as the amount of Sun's energy impinging on a circular disc of great circle dimensions for a period of one year.) In a constant volume atmosphere, this might lead to atmospheric warming, but as far as we know, world atmospheric temperature tended to decrease during the Cainozoic. The latter, if substantiated might indicate that the volume of the atmosphere – like that of the oceans – was not constant during the Cainozoic, but further research is probably needed to settle this point.

EVIDENCE FROM THE SOLAR SYSTEM

PICKFORD (1991) recently suggested that the variety of orientations of the axes of rotation of the planets and moons in the solar system provides additional evidence in support of the idea that spin axes of heavenly bodies are not fixed, but that they change over geological time. This is not a new idea (CAREY 1988). WILLIAMS (1993) provides basic data for the solar system and discusses obliquity changes in Earth.

Uranus spins on its axis oriented at 98° to its orbital plane, and four planets, including the Earth, spin on axes which are markedly oblique to their orbital planes. In fact only two planets in the solar system (Mercury and Jupiter) rotate on axes which are nearly perpendicular to their orbital planes and spin in the same sense as the Sun. The spin axis of Venus is also perpendicular to its orbital plane, but it rotates on this axis in a retrograde sense, suggesting that it has "turned

over" since it separated from the Sun (if indeed the fission hypothesis applies to the origin of the solar system planets (MARCHAL 1968)). The satellite Triton orbits round the planet Neptune in a retrograde sense. CAREY (1988) suggests that early during its history the north rotational pole of the Earth was below the ecliptic rather than above it as it is today.

The great variety of planetary orientations and spin directions could be cited as evidence that the fission hypothesis for the origin of the solar system is incorrect. However, the fact that the orbital planes of the planets are almost parallel to one another suggests a unity of origin, probably by fission (MARCHAL 1968), in which case the varied orientations and spin directions that characterize the solar system's planets and their moons would be due to post-fission changes.

The orbital planes of the planets in the solar system are nearly parallel to one another, Pluto having the most oblique orbital plane at 17.2° from that of the Earth. If planets originally had axes of rotation perpendicular to their orbital planes, then planetary spin parameters must subsequently have changed over geologic time. Such changes would engender marked changes within the planets, including the generation of stresses and strains in the fabric of the planet, and would alter the Sun/planet relationship which would induce climatic changes on the planet (CAREY 1988; WILLIAMS 1993)

PHYSICAL BIOGEOGRAPHY

BIOPULSES

One of the more obvious kinds of biological pulsations that have occurred are "faunal turnover pulses", which are relatively brief periods during which there were widespread (intercontinental to global) changes in floras and faunas an order of magnitude greater than "normal" background evolutionary changes. First order faunal turnover pulses are known to have occurred episodically since the Vendian (Late PreCambrian), and include classic events at the PreCambrian/Cambrian boundary, at the end of the Permian and at the Lower Trias/Upper Trias boundary. More recent events such as those that occurred at the K/T boundary (Cretaceous/Tertiary Boundary) and the "Grande Coupure" (Eocene/Oligocene Boundary) are infrequent events. During the Cainozoic Era there have been fewer than a dozen which could be called major worldwide events, although there were many less important, more parochial faunal changes.

The literature contains many descriptions of these faunal turnover pulses, as well as explanations, or partial explanations of what may have caused them (VRBA 1985; ALROY 1992; MCKENNA 1985). The variety of mechanisms that have been proposed is surprisingly great, suggesting that most of them are *ad hoc* explanations. Many of them are based on events which were not global but which were too parochial in scale. For example, the Messinian event which supposedly led to the dessication of the Mediterranean at the end of the Miocene might be expected to be correlated with changes in faunas and floras in neighbouring parts of the Old World, but would it have induced changes in the New World such as was recently proposed by ALROY (1992) for the Great Plains faunas of North America? Climatic change has often been invoked to explain faunal turnover pulses, although what caused the climate to change in the first place has seldom been evinced (VRBA 1985). Changes in physical geography of the Earth

have been suggested. these changes usually being related to plate tectonic activity. Volcanism has been evoked, as have impacts of comets with the Earth and there are many other hypotheses of biological and environmental natures.

I would like to examine some of these suggestions in order to see if they can be ascribed to one or to a few basic phenomena such as tectogenic phases, eustatic history, pulsed decrease in global oceanic temperatures during the Cainozoic and others.

THE ACCORDION MODEL OF ECOCLIMATIC BELTS

Other changes which have been proposed to have occurred to latitudinal ecoclimatic belts, is that their latitudinal extent has varied over geological time, the belts becoming wider or narrower (PANTIC 1986. fig. 1). For example, for Europe to become more tropical during the Miocene period, it suffices simply to propose that the tropical belt extended to 35°-40° latitude either side of the equator. This would mean that up to 64% of the surface of the globe enjoyed a tropical climate (the area of the globe covered by the latitudinally arranged ecoclimatic belts at various times in the past can easily be calculated if their latitudinal extents are known, using the formula given in WILLIAMS (1975. 1993). The area of a low-latitude zone symmetrical about the equator is equal to the total surface of the Earth multiplied by the sine of the limiting latitude).

Changes in latitudinal width of ecoclimatic belts of the Earth could also be caused by precession and nutation of the Earth (WILLIAMS 1993) but these would be rather minor compared with changes that are reported to have occurred during the Eocene and the Miocene.

Under the accordion model of ecoclimatic belts, the present day configuration, in which the tropics cover little more than 10° of latitude either side of the equator – *i.e.* the tropics cover only 17% of the surface of the globe of which only 6% occurs on land – suggests that since the Miocene there has been a drastic reduction in the areal extent of the tropics. During the Pleistocene, with its glacial/interglacial cycles, the latitudinal widths of the ecoclimatic belts are often envisaged as having undergone several cycles of expansion and contraction, rather like the bellows of an accordion while it is being played.

At present, about 39% of solar energy reaching the atmosphere is immediately reflected back into space (CARON *et al.* 1992). If this figure were to change, then one could expect the ecoclimatic belts to become narrower or wider, as the case may be. It is doubtful, however, that widening of the tropics could be so great that Ellesmere Island at 79°N latitude would become warm-temperate or tropical without a displacement of the position of the belt, or without a change in obliquity, as has been postulated recently. It is more likely that the width of the ecoclimatic belts fluctuated by a few degrees of latitude only (PANTIC 1986), and that their position on the globe changed in phase with axial reorientation, or perhaps with *average* rotation – spin plus nutation.

The tropical belt is characterized not only by higher annual mean temperatures than temperate, boreal or polar regions, but also by a higher precipitable water content in the atmosphere (PEIXOTO & OORT 1990). In tropical zones the average precipitable water content of the atmosphere is between 45 and 50 kg m^2 yr, while near the poles values drop to as low as 2.5 kg m^2 yr. For Ellesmere Island to become tropical in terms of temperature and atmospheric water content, similar figures as occur today in the tropics would have to occur there. Under the accordion model of expanding ecoclimatic belts, huge quantities of water would have to be

transferred into the atmosphere worldwide. The volumes involved if such a model is invoked, are so great that global sea-levels would be affected. If on the other hand, one invokes a shift in the position of the ecoclimatic belt relative to the Earth's surface (*i.e.* a graticule shift), then the volumes of atmospheric water need not change very greatly in order to achieve the same result of tropicalising Ellesmere Island, as long as the graticule shift was of the appropriate direction and degree. Graticule shift would also solve the problems of "seasonality" and "polar night" that the current location of Ellesmere Island endures, which renders it unlikely that tropical conditions suitable for crocodiles and turtles could ever have been produced there without a graticule shift.

THE GRATICULE SHIFT MODEL OF ECOCLIMATIC BELTS

Repositioning of the ecoclimatic belts of the world does appear to have happened. For example, during the Eocene, Europe and North America were both endowed with tropical climates. DAWSON *et al.* (1976) report the presence of turtles, crocodiles and warm-temperate mammals in the Eocene Eureka Sound Formation at 79°N latitude. If we consider that the North American land mass has moved slightly southwards since the Eocene, consequent upon expansion of the Arctic Ocean, then at the time of sediment deposition, Ellesmere Island would have been slightly further north than it is today.

For Ellesmere Island at 80°N to be tropical or subtropical during the Eocene without axial reorientation, more than 98.4% of the Earth's surface would fall within the tropical to sub-tropical zone. Such a high figure would imply that dramatic changes occurred in the Earth/Sun energy relationship, however caused. Yet, during the same period, the distribution of oceanic organisms reveals the presence of latitudinal stratification patterns not very different from those of today's ecoclimatic belts, except that their orientation and position on the globe were different. It is thus more likely that the equatorial belt merely shifted its position on the globe so that it incorporated Ellesmere Island, without the belt itself becoming greatly widened latitudinally.

Rather abruptly – over a period of about 1 m.y. – at the Eocene/Oligocene boundary, both Europe and America became more temperate. Traditionally this change has been attributed to a narrowing of the tropical belt – the accordion model – brought about by global oceanic cooling, for which $\delta^{18}O$ data provides the most convincing support (MILLER & FAIRBANKS 1985). The accordion hypothesis would only work if the amount of solar energy being captured by the Earth varied, either because of variation in the output of energy by the Sun, or if there were changes in the retention of energy by the Earth, or if the obliquity of the Earth relative to the plane of the ecliptic changed (WILLIAMS 1993) or if there were significant precession or nutation effects.

An apparent problem is that palaeomagnetic data do not seem to indicate a major difference between the position of the poles before and after the "Grande Coupure". However, because there is today a difference of 14° between the axis of rotation and the magnetic axis, and because palaeopole positions are calculated by averaging numerous palaeomagnetic measurements – the result being assumed to coincide with the ancient rotational pole – the problem is more apparent than real. The magnetic pole could move through more than 28° of latitude relative to the rotational pole before it would show up as a measureable palaeomagnetic signature. Similarly, the rotational pole could shift through more than 28° of latitude before palaeomagnetic maps would

reveal any movement. As CAREY (1988) showed, palaeomagnetic methods are coarse tools for determining the fine points of Earth history.

Further changes in the orientation of the earth's axis of rotation during the Upper Miocene eventually led to a southwards shift of the climatic belts in the Old World towards their present day positions. Indeed, the process is still going on – in Africa the biological diversity "equator" is slightly north of the geographic equator, and is moving southwards. This is seen as a southwards "advance" of the Sahara and related belts, although this process has been greatly altered by human activity in the recent past. The present day biodiversity "equator" of South America is slightly south of the geographic equator, and is moving northwards. From this it appears that shift in the geographic position of the equator leads the shift in ecoclimatic belts. The current lag between the geographic and biodiversity equators in Africa is about 4° of latitude (about 450 km), and a similar figure characterizes South America. In South America, the geographic equator has shifted northwards since the Middle Miocene (PICKFORD 1990b). For example, Platyrrhini – the New World monkeys – used to inhabit Patagonia (55° South latitude) during the Middle Miocene, a long way south of their present day distribution limits in Argentina (35°South) (PICKFORD 1990b). During the Middle Miocene, St Helena, which is today at a latitude of 16°S and enjoys a tropical climate, was covered in plants of a subtemperate to austral kind. This suggests that St Helena lay within a subtemperate to austral ecoclimatic belt during the Miocene, and that its present day tropicality is due to a subsequent southwards shift of the tropical belt in the Old World (PICKFORD 1991). This kind of evidence appears to support the idea that both obliquity and pole position of the Earth have changed during the Tertiary Period.

OBLIQUITY AND SEASONALITY

If polar repositioning occurred, the obliquity of the Earth's axis relative to the plane of the ecliptic would change, because in rotating gyroscopes, a change in one mechanical parameter induces a change in another, causing precession, tilting, nutation and other phenomena. Seasonality is a function of the relationship between a planet and its Sun. In planets whose axes are perpendicular to the plane of the ecliptic, seasonality is minimal. In planets with low obliquity, seasonality is weakly expressed. In planets with high obliquity, seasonality is marked (TREVISAN & TONGIORGI 1987). Thus any change in obliquity of a planet will result in changes in the degree of seasonality on that planet (CAREY 1988; WILLIAMS 1993).

PICKFORD (in press), VAN DER MEULEN & DAAMS (1992) and MORALES *et al.* (1993) show that the degree of seasonality greatly increased in tropical Africa and in Spain at the end of the Lower Miocene and the beginning of the Middle Miocene. This change in seasonality was accompanied by a major latitudinal shift in African vegetation and climatic belts (PICKFORD 1992). Namibia, which today is an arid to semi-arid country, became humid during the Middle Miocene (WARD & CORBETT 1990). At the same time, Zaire, which is currently covered in tropical forest, became a dune covered desert, and Libya and Tunisia which are now arid countries, were inhabited by tropical forest plants and were traversed by Ganges-sized rivers (PICKFORD 1992). At the onset of the Middle Miocene, Europe's climate became more seasonal and more tropical. These changes in the degree of seasonality led to some dramatic, and even startling effects in the biosphere, such as the development of bony cranial appendages in numerous lineages of

herbivores and perhaps to the development of estivation behaviours among many animals, such as terrestrial gastropods (PICKFORD in press).

THE BIOSPHERE

The basis for the subdivision of geological time is biological change observed in the fossil record. While there is a relatively constant presence of background biological change in the fossil record, due mainly to autochthonous adaptive changes, there were periods in the past during which major floral and faunal changes occurred more or less at the same time in many parts of the globe and in many ecosystems, both marine and terrestrial. These are recognized as floral and faunal "turnovers" or "turnover pulses".

There are three main ways that faunas and floras respond to environmental changes. The constituent species can remain where they are and either adapt to the new conditions or go extinct, or they can shift their geographic range in order to remain within their preferred habitat type which is shifting its geographic position (PICKFORD 1990b).

In examining one of these major faunal turnovers such as the "Grande Coupure", one is not witnessing the gradual spread of species, each one of which is adapting to strange conditions in its newly colonized territory. Instead, one is in the presence of major changes in the geographic distribution of animals and plants due to major displacements of biogeographic realms. In other words, they are related to changes in the climatic and other factors responsible for maintaining the positions of biogeographic boundaries, with the result that they are displaced relative to the surface of the globe. If geography (absence of water barriers, mountain ranges) permits it, then such "pre-adapted" faunas and floras will quickly spread to the neighbouring continents or seas wherever suitable conditions exist for them. If there are none, then the species either adapt to the changed conditions or they locally go extinct.

In Figure 6, the major palaeobiological turnover pulses (most if not all of which were world-wide and which affected marine and continental faunas and floras alike) which occurred during the Cainozoic are listed, such as those that took place near the Cretaceous/Tertiary boundary, the Eocene/Oligocene boundary (the "Grande Coupure") and the Lower Miocene/Middle Miocene turnover (the great Afro-Eurasian faunal and floral interchange), among others (PICKFORD 1990b). It is evident from Figure 6 and Table 8, that each of the major faunal turnover pulses coincided in time with a tectogenic phase, which indicates that the lithosphere and the biosphere were each responding in appropriate ways to the same overall cause. It should be noted that the extinction of the dinosaurs, ammonites and belemnites at the end of the Cretaceous occurred during a tectogenic phase – the Laramide 1 Phase – and is thus not radically different in pattern or cause from other major turnover pulses such as the "Grande Coupure" (Eocene/Oligocene boundary) which occurred at the same time as the Pyrenean Tectogenic Phase. The proximal cause of the extinctions may well have been sudden change in global temperature due either to enhanced volcanism – such as the Deccan Traps which spanned the K/T faunal events – which affected the Earth's solar energy budget. The ultimate cause may be of a geotectonic nature, such as axial reorientation or tectogenesis.

During the "Grande Coupure", at least sixteen families of mammals invaded Europe, most of which probably originated in Asia (STEININGER *et al.* 1985). The invasion was part of a major

TABLE 7. — Major faunal turnover pulses of East Africa.

Period of Turnover Pulses Ma	Nature of Faunal change	Correlation to Tectogenic Phases
4 and younger	Omo mammal changes	Valachian
8 to 7	Modern lineages of African mammals replace archaic ones	Rhodanian
12 to 11	"*Hipparion*" event, Dendromurines	Attic
17 to 16	80 % change in mammal faunas	Styrian

redistribution of floras and faunas of the world. Contemporaneous effects in the seas and oceans were equally dramatic. Europe, which had been tropical during the Eocene, became temperate during the Oligocene. Thus there was an influx of proto-Palaearctic species into Europe, possibly aided by the establishment of dry land contact between Asia and Europe at about this time. At the same time, many of the mammals and reptiles adapted to tropical Europe, such as primates, crocodiles and turtles, became extinct there when its climate became temperate. These same groups continued to survive in Africa and Southern Asia which by this time were tropical in nature. Similar changes occurred in North America, which contained a rich primate fauna during the Eocene, but which had disappeared from the continent by the onset of the Oligocene.

The major changes in the distribution of land floras and faunas may have been aided by significant fluctuations in sea-level that occurred during the Pyrenean Tectogenic Phase. These sea-level changes were not caused by ice-cap formation, but may be related to transgression/regression following axial reorientation (WEGENER 1962, fig. 41) as described in detail below. It is also possible that the balance between photo-dissociation of water in the upper atmosphere and the eruption of neonate waters from the mantle into the hydrosphere was upset, a positive budget resulting in global scale transgressions, a negative budget leading to regressions.

At the end of the Lower Miocene, the great faunal interchange occurred between Africa and Eurasia, which is recognized in Europe as the base of the Middle Miocene (boundary of mammal zones MN3/MN4) (MEIN 1975). In East Africa, there was an 80% change in the mammal faunas at this time, several lineages immigrating from Europe, but many entering East Africa for the first time from other parts of the continent. This faunal turnover pulse was accompanied by floral changes (palms, mangroves and tropical hardwoods colonized Europe, while formerly forested regions of East Africa became semi-arid) which indicate that Europe became more tropical than it was during the Oligocene and Lower Miocene. In effect, large parts of Eurasia became suitable for species adapted to proto-Ethiopian biogeographic conditions (wet season/dry season cycle instead of winter/summer cycle, for example) (PICKFORD 1991, fig. 12). Interchange was probably aided by the establishment of dry land connections between Africa/Europe and Africa/Asia.

WALLACE ENVELOPES – LATITUDINAL DIVERSITY GRADIENTS

An interesting point about the mid-Miocene Afro/Eurasian vertebrate interchange is that as the diversity of some lineages of african large mammals decreased in Africa (primates and ruminants for example), (PICKFORD 1991, figs 7, 8) the same lineages tended to experience increases of diversity in Europe. In North America, large mammal faunas of the Great Plains also tended to increase in diversity from Lower Miocene to Middle Miocene times (ALROY 1992) and subsequently to decrease in Upper Miocene and Pliocene times. In the Old World, this tendency strongly suggests that the Wallace 'envelopes' which describe latitudinal taxonomic diversity gradients, shifted position, so that their peaks lay nearer Europe than they do today – currently they overlie tropical Africa near the equator. This of course implies that the position of the equator has changed (graticule change) (PICKFORD 1991, fig. 20) since the mid-Miocene.

There can be little doubt that two-way faunal interchange took place during the Middle Miocene and subsequently, but the development of dryshod access between the continental masses was not the only factor involved in the faunal interchanges. Of great importance were biological factors such as the position of zoogeographic realms relative to each other. At present, Africa and Eurasia are in dry land contact, yet almost no interchange of terrestrial forms is taking place for the simple reason that most of Africa currently lies within a different biogeographic region from Eurasia. Prevention of interchange is reinforced by the presence of the Sahara Desert and the Mediterranean Sea, but the main factor responsible for the recent lack of intermingling of and interchange between Palaearctic and Ethiopian faunas is biogeographical in origin. That the Mediterranean is not an insurpassable barrier over geologic time is shown by the fact that during the Pleistocene, each time that there was a glacial period, the Maghreb was successfully colonized by Palaearctic faunal elements including deer, wild boar and bears. Conversely, some characteristic mammals of the Ethiopian zoogeographic region such as *Hippopotamus* and *Theropithecus* (MOYA SOLA *et al.* 1989-90) crossed into Spain during interglacial periods.

For Europe to have been colonized "en masse" by proto-Ethiopian mammals the conditions in Europe would have had to have been more or less similar to those that existed in Africa. If not, only a few lineages would have made the transfer after adapting to proto-Palaearctic conditions. In fact, it is widely accepted that at the beginning of the Middle Miocene, Europe's climate became more tropical and more seasonal than it had been during the Lower Miocene period, thereby making conditions in Europe suitable for a wide variety of African mammals. Thus continental shift only partly explains the mid-Miocene Afro-Eurasian faunal interchange, and the faunal pulses that came afterwards, notably about 12 to 13 m.y. ago, 8 to 7 m.y. ago and during the Plio-Pleistocene.

In many ways, the Middle Miocene Afro/Eurasia faunal interchange resembles the Great American faunal interchange that took place during the late Cainozoic and early Quaternary (MARSHALL *et al.* 1982), which was aided by the establishment of the Isthmus of Panama between North and South America. In the case of the two Americas, however, the results of the interchange were rather one-sided, even though approximately the same number of lineages transferred in each direction. Those lineages invading North America from the south generally failed to undergo evolutionary radiations and most of them died out after a relatively short sojourn in the north. Lineages invading South America from the north, in contrast, usually experienced successful evolutionary radiations, many of which are still extant.

TABLE 8. — Summary of main tectogenic, rifting, volcanic, oceanic and faunal events of the Tertiary. Note that the absolute time scale is taken from SCHERBA (1987) which is out of date due to revision of the geological time scale. However, the changes are not incorporated into this chart, even though the author is aware of the differences, because he wishes to retain the data as close as possible to the original author's writings.

POST-VALACHIAN	Four major regressions. Cooling plunge in $\delta^{18}O$ curve.
VALACHIAN PHASE: 4+/– m.y.	Major orogenesis and olistostrome activity. Increased rifting in Western and Eastern Rifts. Uplift of Ruwenzori and associated mountains. Isthmus of Panama closed. Onset of Quaternary Glaciations after ocean warming peak.
POST-RHODANIAN/PRE-VALACHIAN	One major regression.
RHODANIAN PHASE: 4+/– m.y.	Orogenesis and olistostrome formation less than maximal but still important. Major acceleration in rifting activity in Gregory, Nyanza and Albertine Rifts. Ecoclimatic belts shift southwards in Old World, northwards in New World. Installation of "modern" mammalian lineages (including hominids) in tropical Africa. Warming peak in oceans.
POST-ATTIC/PRE-RHODANIAN	Two major regressions.
ATTIC PHASE: 12.5+/– m.y.	Major orogenesis and olistostrome activity. Plateau Phonolite eruptions. Mid-Miocene/Upper Miocene faunal changes.
POST-STYRIAN/PRE-ATTIC	Two major regressions. Warming peak in oceans followed by cooling plunge
STYRIAN PHASE: 17.5+/– m.y.	Major orogenesis and olistostrome activity. Daroca (Spain) nappe emplacement. Onset of rifting in Gregory and Nyanza Rifts. Africa "docks" to Eurasia, severing ocean circulation between Indian and Atlantic Oceans via the Mediterranean Seaway. Early Miocene/Middle Miocene faunal turnover pulse. Marked increase in seasonality worldwide. Slight ocean warming. Ecoclimatic belts shift northwards in Old World, southwards in New World. Circum-antarctic current established. Columbia River Basalts.
POST-SAVIC/PRE-STYRIAN	One major regression. Ocean temperature steady.
SAVIC PHASE: 25+/– m.y.	Widespread orogenesis and olistostrome activity. Onset of rifting in Red Sea Rift and Ethiopia. Late Oligocene faunal turnover. Warming peak in oceans.
POST-PYRENEAN/PRE-SAVIC	Five major regressions. Cooling plunge in ocean waters followed by slight cooling and warming towards end of period.
PYRENEAN PHASE: 37.5+/– m.y.	Major tectogenic activity with widespread olistostrome formation. Ural Seaway closed. Eocene/Oligocene faunal turnover pulse ("Grande Coupure"). Southwards shift of ecoclimatic belts in Europe and North America. Ocean warming peak. Eruption of Ethiopian Traps. Dog-leg in hot-spot tracks.
POST-ILLYRIAN/PRE-PYRENEAN	One major regression. Ocean cooling followed by warming at end of period.
ILLYRIAN PHASE: 47+/– m.y.	Widespread orogenesis and olistostrome activity in Alpine Fold Belt. Mid-Eocene faunal turnover pulse. Ocean warming peak.
POST-LARAMIDE 2/PRE-ILLYRIAN	Three major regressions. Ocean cooling.
LARAMIDE PHASE 2: 53+/– m.y.	Orogenesis and olistostrome activity. Palaeocene/Eocene faunal turnover pulse. Ocean warming peak.
POST LARAMIDE 1/PRE-LARAMIDE 2	Five major oceanic regressions. Warming trend in ocean waters.
LARAMIDE PHASE 1: 66.5+/– m.y.	Widespread orogenesis and olistostrome activity. Deccan Traps eruptions. South Atlantic opens. Cretaceous/Tertiary faunal turnover pulse (extinction of dinosaurs, ammonites, belemnites, rudists, etc.) Ocean warming. Dog-leg in hot-spot tracks.

The differential successes of the two American interchanging faunal groups is explained by WALLACE's Rule. In most groups of organisms on Earth, diversity is highest near the equator and is lower at higher latitudes (STEHLI 1968; PICKFORD 1991, fig. 2). North American lineages invading South America would be approaching the equator (its Early Quaternary orientation was not very far from its present position, possibly a few degrees of latitude further south than it is now), and would thus be entering the "high diversity" part of their Wallace "envelope". They would therefore have a tendency to increase in diversity (or not to decrease). In contrast, South American lineages moving northwards would be entering the low diversity parts of their Wallace "envelopes" and their diversity would naturally tend to decrease (or not to increase).

CONCLUSIONS

Several conclusions can be put forward.

1 — Of the four possible theories concerning the size of the Earth – 1) constant "r", 2) increasing "r", 3) decreasing "r" and 4) fluctuating "r" – the available evidence now favours the view that "r" has been increasing over geological time. It is less likely that "r" has remained constant, and even less likely that it has been decreasing or fluctuating.

2 — During the Cainozoic Era there have been major coincidences in the timing of world-wide changes or events in the lithosphere, biosphere, hydrosphere and atmosphere, as well as in the Earth/Sun relationships which define seasonality and the location of ecoclimatic zones on the Earth's surface. William OF OCCAM would suggest that we search for a single underlying cause, which we call Gaia's Pulse after the Greek Earth goddess.

3 — Plate Tectonics on its own in a constant dimensions globe, is unlikely to explain the pulse-like behaviour in these varied Earth Systems, nor the changes in Earth/Sun relationships. In any case, the source of power sufficient to drive the plate tectonic motors (one for each plate?) remains to be identified. geothermal energy (expressed as convection cells in the mantle which are supposed to move the crustal plates) being far to feeble to accomplish the activity observed. This suggests that Plate Tectonics on its own may well be an inappropriate mechanism to explain displacement of the continents and the origin of oceanic crust.

4 — There are two known – and possibly a third – sources of energy capable of accomplishing the work expended during continental displacement, polar repositioning, Tethyan shear and other manifestations of geotectonic activity. The two known sources are gravity and the kinetic energy of rotation of the globe. The third possible source of energy is the progressive decay of a plasma core to the atomic state which would not only lead to tremendous increase in volume (the volume of atoms is orders of magnitude greater than the volume of protons and electrons) but would also generate vast quantities of heat energy.

The pulsed nature of many of the changes indicates that kinetic energy of rotation was being tapped periodically, while gravity, the most powerful source of energy in the globe, has of course been constantly at work in maintaining the almost spherical shape of the globe against the tendency of other forces to bend it out of this shape. Volumetric increases due to decay of a plasma core to the atomic state would lead to Earth Expansion. Thus the figure of the Earth

is predominantly shaped by the interplay of at least two, and possibly three major sources of endogenetic energy and several minor ones – both endogenetic and exogenetic.

5 — There appear to have been at least five main mechanisms which have contributed to the evolution of the Earth's lithosphere during the Cainozoic:

Earth Expansion which produces an increase in the Earth's radius which leads to a net radially outward movement of the continental masses and ocean floor, causing the distance between neighbouring continents to increase. A major surface expression of this expansion is the insertion of symmetrical slices of mantle material either side of spreading axes. It also leads to the transferral of vast quantities of neonate waters from the Earth's interior to its surface, where much is subsequently lost by photo-dissociation in the upper atmosphere.

"Lead" and "Drag" effects induced in the Earth – a quasi-spherical spinning fluid mass – due to differences in radial distance of various Earth layers from the axis of rotation. One global structure possibly due to this effect is Tethyan Torsion which has produced a shear zone some 700 to 1000 km wide right round the globe in which numerous "microcontinents" have been rotated sinistrally. These include Spain and other Mediterranean microcontinents, India, Seram, New Guinea, Mesozoic Mexico, and the Greater Antilles. A second structure at right angles to the Tethyan Torsion zone is the Circum-Pacific Torsion, in which rotation of microcontinents or "terranes" has generally been dextral.

Axial reorientation which leads to pulsed changes in the lithosphere, including tectogenic activity, rifting, trap volcanism and shift of equatorial bulge, and which induces substantial changes in other Earth systems (hydrosphere, atmosphere, biosphere) and celestial parameters (graticule and obliquity changes).

Unequal disposition of spreading ridges at the Earth's surface has led to unequal expansion of the globe, producing "geotumors". The Earth's figure remains quasi-spherical despite the unequal growth, due to the action of gravity, the most powerful energy source on Earth. Due to the constraints of spherical geometry on a globe, this unequal expansion of ocean basins, especially the Pacific Ocean on the one hand and the circum-Antarctic oceans on the other soon reached the stage beyond which their Great Circle perimeters had to become smaller than Great Circles. The resulting relative compression of these Great Circle perimeters has been the formation of great circle mountain fold belts, the Cordilleran and Alpine orogenies respectively and their related thrust systems, trench systems and torsion zones. Sinistral and dextral torsion associated with these great circle compression zones may be related to the fact that the Earth's crust and mantle are not homogeneous, which would make it unlikely that compression would be perfectly vertical. A "screw" effect would thus tend to develop spontaneously, and once having developed would be maintained in the same sense during further great circle compression.

The lateral (as opposed to radial) movement of continental crust has occasionally occurred (India is the prime example, but there are many smaller terranes whose present positions are best explained by lateral movement), but on a global scale such movements of continents are less important than those due to the combination of uneven Earth Expansion and the maintainance of a quasi-spherical shape by gravity. Rotation of continental masses and smaller terranes has also occurred (Australia, Iberia, Italy, etc.) but are in total a relatively minor – even if dramatic – aspect of global geotectonics.

6 — There have been at least 9 major tectogenic phases during the Cainozoic Era, each of which lasted between 2 and 2.5 m.y. and which were separated from the others by between 4 and 11 m.y. (average 7 m.y.). Similarly episodic tectogenic activity characterized the Mesozoic Era.

7 — The extinction of dinosaurs, ammonites, belemnites and rudists at the end of the Cretaceous coincides in time with a major tectogenic phase (the Laramide 1 Phase and its associated volcanic and rifting activity). As such, the K/T faunal turnover pulse does not appear to differ radically from other major Cainozoic faunal turnover pulses that coincided with tectogenic phases, such as the "Grande Coupure" (Pyrenean Tectogenic Phase), the Lower Miocene/Middle Miocene (Styrian Tectogenic Phase) faunal turnover pulse and the End Miocene faunal turnover pulse (Rhodanian Tectogenic Phase) all of which were characterized by massive faunal turnover (up to 80% faunal change) including the extinction of numerous mammalian lineages.

8 — Several tectogenic phases coincided in time with first order fissure eruptions (Deccan Traps (65 m.y.), Ethiopian Traps (45-35 m.y.), Columbia River Basalts (16 m.y.), Plateau Phonolites (12.5 m.y.)) and with episodes of rifting activity in the African Rift System (17.5 m.y., 12.5 m.y., 7.5 m.y., 4 m.y.).

9 — Several tectogenic phases coincided in time with the abandonment of spreading ridges and the formation of new ones some distance away. The contemporaneity between tectogenesis and abandonment of spreading ridges suggests that the Earth's crust shifted with respect to the mantle, with the consequence that some of the upwelling masses at spreading ridges were shifted laterally relative to the crust, thereby forming a new spreading ridge and leaving an extinct spreading ridge off to one side.

10 — In general, periods of tectogenesis coincided with periods of high eustatic sea-levels, whereas major regressions in sea-level tended to occur during periods of prolonged tectogenic calm. During periods of polar repositioning (graticule shift) the "equatorial bulge" would change position, but because of the difference in "relax times" (adjustment to isostacy) between the lithosphere (*c.*10 Ka for Scandinavia after the waning of the last glacial cap) and the hydrosphere (0 Ka) areas near the "relaxing polar flattening" would tend to experience transgression while areas near the "relaxing equatorial bulge" would tend to experience short-lived regressions. It is noted however, that there are many causes for transgressions and regressions which operate at many scales from the very parochial (*e.g.* localized tectonic activity) to the global (*e.g.* glacial/interglacial cycles).

11 — The cooling trend that has characterized the world's oceanic waters during the past 55 m.y. is probably due to increases in the volume of the world's oceans, the "new" water having been released into the hydrosphere from the mantle at the same time as the basaltic rocks which accreted at mid-ocean ridges and elsewhere, the two being parts of the same overall process, Earth Expansion. The total amount of solar energy per square metre captured by seawaters may have remained relatively constant through geologic time, but as time passed the energy so captured was diffused through greater quantities of water ($length^2$ compared to $length^3$), hence resulting in a relatively steady cooling trend in the world's oceans throughout the Cainozoic.

12 — During the same period, pulses of energy were expended during tectogenic activity, some of which (as heat) may have contributed to ocean warming, recorded as "warming" peaks and temperature plateaux in the palaeotemperature curves of the world's oceans. Alternatively, but perhaps less likely, the Sun may have a "pulse-like" behaviour on a time scale of some 5 m.y.

13 — Major events in the biosphere and atmosphere during the Cainozoic, such as modifications in seasonality patterns, are of a type which are compatible with, if not demanding a change in the relationship between the Earth and the Sun. Three categories of global climatic change are noted:

- reorientation of ecoclimatic belts on the surface of the Earth due to graticule shift;
- seasonality changes due to obliquity shift;
- fluctuation of latitudinal width of ecoclimatic belts (see point 16 below).

14 — Major reorganizations of world ocean circulation patterns due to opening (Grahamland/Patagonia) or closing of seaways between continental masses (Asia/Europe, Africa/Eurasia, North and South America) often coincided in time with tectogenic phases, the two probably being different aspects of the same overall cause.

15 — The nature of first order faunal turnover pulses suggests that their proximate cause was large scale shift in the positions of biogeographic realms relative to the Earth's surface. Since the primary pattern of biogeographic realms is latitudinal in expression, this suggests that first order faunal turnover pulses resulted from latitudinal shifts in the boundaries between realms. This in turn indicates that polar repositioning occurred, which thereby induced graticule shift.

16 — The latitudinal extent of global ecoclimatic belts has fluctuated during the past. At times, the tropics were latitudinally wider than they are now, sometimes narrower. At times, the polar ecoclimatic belts were wider than they are now, at other times narrower. The cause of this accordion-like behaviour appears to be differential capture of solar energy at the Earth's surface (including its atmosphere), due either to fluctuations in the Sun's output of energy, or of the Earth's efficiency in capturing it, or to both. At present some 39% of the Sun's energy reaching the Earth is immediately reflected back into space. Presumably there is nothing sacrosanct about this figure, which could increase, thereby leaving the Earth with less retained solar energy, or it could decrease, in which case the Earth would retain more solar energy. These changes would probably show up as accordion-like changes in the widths of the world's ecoclimatic zones.

Acknowledgements

I am particularly anxious to thank Professor Yves COPPENS (Collège de France) for his continued help and encouragement. My sincere thanks go to Professor Philippe TAQUET (Institut de Paléontologie), Hervé LELIÈVRE, Hugh OWEN, Brigitte SENUT, Léonard GINSBURG, Christian MARCHAL and Jorge MORALES for support, discussions and encouragement. Thanks are also extended to Professor Samuel Warren CAREY (University of Hobart) and Dr Hugh OWEN (Natural History Museum, London) for solving many things about Earth History which had been troubling me, and which are now clearer in my mind, thanks to the Expanding Earth Theory. I thank Drs Miguel DOBLAS and Christian MARCHAL for reviewing the text and for making pithy and interesting comments about an earlier version of this text.

Manuscript submitted for publication on 6 January 1995; accepted on 2 October 1995.

REFERENCES

ADAMS C., GENTRY A. & WHYBROW P. 1983. — Dating the terminal Tethyan event. *Utrecht Micropaleontology Bulletin* **30**: 273-298.

ALLÈGRE C. J., SARDA P. & STAUDACHER T. 1993. — Speculations about the cosmic origin of He and Ne in the interior of the Earth. *Earth and Planetary Scientific Letter* **117**: 229-233.

ALROY J. 1992. — Conjunction among taxonomic distributions and the Miocene mammalian biochronology of the Great Plains. *Paleobiology* **18**: 326-343.

ALVAREZ W. 1990. — Geologic evidence for the plate-driving mechanism: The continental undertow hypothesis and the Australian-Antarctic discordance. *Tectonics* **9**: 1213-1233.

BARRON E. J. 1985. — Explanations of the Tertiary global cooling trend. *Palaeogeography Palaeoclimatology Palaeoecolgy* **50**: 45-61.

BARRY J., FLYNN L. & PILBEAM D. 1990. — Faunal diversity and turnover in a Miocene terrestrial sequence. *In* R. ROSS & W. ALLMON (eds). *Causes of Evolution: A Paleontological Perspective*. Chicago, Univ. Chicago Press: 381-421.

BARRY J., JOHNSON N., RAZA S. & JACOBS L. 1985. — Neogene mammalian faunal change in Southern Asia: correlations with climatic, tectonic and eustatic events. *Geology* **13**: 637-640.

BATES R. L. & JACKSON J.A. 1990. — *Glossary of Geology*, 3rd edition. Alexandria, Virginia, American Geological Institute.

BERTHELSON A. & SENGOR A. 1990. — Como se formo Europa? *In Europa Cientifica*. Barcelona, Ed. Labor, pt 3: 108-123.

BIJU-DUVAL B., DERCOURT J. & LE PICHON X. 1976. — La genèse de la Méditerranée. *La Recherche* **7**: 811-822.

CAREY S. W. 1976. — *The Expanding Earth*. Amsterdam, Elsevier: 1-488.

— 1983. — *The Expanding Earth: A Symposium*. Brunswick, Impact Printing (Vic.) Inc.

— 1988. — *Theories of the Earth and Universe*, Stanford, Stanford Univ. Press.

CARLSON R. W. 1992. — Melting of wet lithosphere. *Nature* **358**: 20-21.

CARON J. M., GAUTHIER A., SCHAAF A., ULYSSE J. & WOZNIAK J., 1992. — *Comprendre et enseigner la planète Terre*. Paris, Editions Ophrys : 1-271.

COFFIN M. F. & ELDHOLM O. 1993. — Large Igneous Provinces. *Scientific American* **269** (4): 26-33.

COLLINGBOURNE M. 1976. — Radiation and sunshine. *In* T. T. J. CHANDLER & S. GREGORY (eds). *The Climate of the British Isles*. London, Longmans **4**: 74-95.

CONDIE K. C. 1976. — *Plate Tectonics and Crustal Evolution*. New York, Pergamon: 1-288.

— 1989. — *Plate Tectonics and Crustal Evolution*, 3rd edition. Oxford, Pergamon Press.

COX, A., and HART, R. B., 1986. — *Plate Tectonics: How it works*. Boston, Blackwell: 1-392.

CREBER G. T. & CHALONER W. G. 1984. — Climatic indications from growth rings in fossil woods. *In* P. BRENCHLEY (ed.). *Fossils and Climate*. London, John Wiley and Sons: 49-74.

DAWSON M., WEST R. & WANN L. 1976. — Palaeogene terrestrial vertebrates: northernmost occurrence, Ellesmere Island, Canada. *Science* **192**: 781-782.

DEWEY J., PITMAN W., RYAN W. & BONNIN J. 1973. — Plate Tectonics and the evolution of the Alpine System. *Bulletin of the Geological Society of America* **84**: 3137-3180.

DOGLIONI C. 1993. — Geological evidence for a global tectonic polarity. *Journal of the Geological Society of London* **150**: 991-1002.

DOOLEY J. C. 1983. — A simple physical test of Earth Expansion. *In* S. W. CAREY (ed.) *The Expanding Earth: A Symposium*. Brunswick, Impact Printing (Vic.) Inc: 323-326.

DU TOIT A. L. 1937. — *Our Wandering Continents*. London, Oliver and Boyd: 1-361.

EBINGER C. J. 1989. — Tectonic development of the western branch of the East African Rift System. *Geological Society of America Bulletin* **101**: 885-903.

EGYED L. 1956. — Determination of changes in the dimensions of the Earth from paleographic data. *Nature* **178**: 534.

EYLES N. 1993. — Earth's glacial record and its tectonic setting. *Earth-Science Reviews* **35**: 1-248.

GINSBURG L. 1984. — Théories scientifiques et extinction des Dinosaures. *Comptes-Rendus de l'Académie des Sciences*, Paris, **298**: 317-320.

— 1986. — Régressions marines ou catastrophes cosmiques: Comment juger les théories sur l'extinction des Dinosaures. *Société Nationale Elf Aquitaine (Production)* **10**: 433-436.

GOLD T. 1955. — Instability of the Earth's axis of rotation. *Nature* **175**: 526-529.

GOLDREICH P. & TOOMRE A. 1969. — Some remarks on polar wandering. *Journal of Geophysical Research* **74**: 2555-2567.

HALLAM A. 1979. — Relative importance of plate movements, eustacy and climate in controlling major biogeographical changes since the Early Mesozoic. *In* G. NELSON & D. ROSEN (eds). *Vicariance Biogeography*. New York, Columbia Univ. Press: 303-330.

— 1981. — Biogeographic relations between the northern and southern continents during the Mesozoic and Cainozoic. *Aufsätze* **70**: 583-595.

HAQ B. U., HARDENBOL J. & VAIL P. R. 1987. — Chronology of fluctuating sea-levels since the Triassic. *Science* **234**: 1156-1167.

HUNT C. W., COLLINS L. G. & SKOBELIN E. A. 1992. — *Expanding Geospheres, Energy and Mass Transfers from Earth's Interior*. Calgary, Polar Publishing.

KEAREY P. & VINE F. J. 1990. — *Global Tectonics*. Oxford, Blackwell Scientific: 1-302.

KEITH M. L. 1993. — Geodynamics and mantle flow: an alternative earth model. *Earth-Science Reviews* **33**: 153-337.

LAMBECK K. 1979. — The history of the Earth's rotation. *In* M. W. MCELHINNY (ed.), *The Earth: Its Origin, Structure and Evolution*. London, Academic Press: 59-81.

LARIN V. N. 1993. — *Hydridic Earth: The New Geology of Our Primordially Hydrogen-Rich Planet*. Calgary, Polar Publishing.

LASKAR J., JOUTEL F. & ROBUTEL P. 1993. — Stabilization of the Earth's obliquity by the Moon. *Nature* **361**: 615-617.

LASKAR J. & ROBUTEL P. 1993. — The chaotic obliquity of the planets. *Nature* **361**: 608-612.

LAVALLARD J.-L. 1988. — Pourquoi la Terre tourne moins vite? *Sciences et Avenir* **494**: 34-39.

LOVELOCK J. 1990. — *The Ages of Gaia: The biography of Our Living Earth*. London, Bantam Books: 1-252.

LÜDTKE G. 1970. — The geology and structure of the area between Etjoberg and Waterberg in central South West Africa/Namibia. *Geological Survey of Namibia Open File Report*: 1-8, map.

MACDOUGALL J. D. 1988. — *Continental Flood Basalts*. Dordrecht, Kluwer Academic Publishers: 1-341.

MCKENNA M. 1985. — The great American terrestrial interchange and reorganized oceanic circulation in the latest Tertiary. *South African Journal of Science* **81**: 258.

MARCHAL C. 1968. — Figures d'équilibre séculairement stable des masses fluides hétérogènes en rotation. *Bulletin d'Astronomie* Série 3 **3**: 341-360.

— 1991. — Les causes possible de la dérive des continents. *Sciences, Publication de l'Association Française pour l'Avancement des Sciences* **91-93**: 60-72.

MARSHALL L., WEBB S., SEPKOSKI J., & RAUP D. 1982. — Mammalian evolution and the Great American Interchange. *Science* **215**: 1351-1357.

MARGULIS L. 1991. — Gaia and the colonization of Mars. *GSA today* **3** (11): 277-280 + 291.

MEIN P. 1975. — Résultats du groupe de travail des vertébrés. *Reports on R.C.M.N.S. Working Groups*, Bratislava: 79-81.

MILLER K. & FAIRBANKS R. 1985. — Cainozoic $d^{18}O$ record of climate and sea-level. *South African Journal of Science* **81**: 248-249.

MORALES J., PICKFORD M. & SORIA D. 1993. — Incremental pachyostosis in a Lower Miocene giraffid species from Spain, and its palaeobiological implications. *Geobios* **26** (2): 207-230.

MOYA SOLA S., PONS MOYA J. & KOHLER M. 1989-90. — Primates catarrinos (Mammalia) del Neogeno de la peninsula Iberica. *Paleontologia I Evolucio* **23**: 41-45.

MUTTER C. Z. & MUTTER J. C. 1993. — Variations in thickness of layer 3 dominate oceanic crustal structure. *Earth and Planet. Scientific Letter* **117**: 295-317.

NORTON I. O. 1995. — Plate motions in the North Pacific: the 43 Ma nonevent. *Tectonics* **14**: 1080-1094.

O'CONNOR J. M. & DUNCAN R. A. 1990. — Evolution of the Walvis Ridge - Rio Grande Rise Hot-Spot System: Implications for African and South American plate motions over plume. *Journal of Geophysical Research* **95**: 17,475-17,502.

O'CONNOR J. M. & LE ROEX A. P. 1992. — South Atlantic Hot-Spot-Plume systems: 1. Distribution of volcanism in time and space. *Earth and Planetary Scientific letter* **113**: 343-364.

OWEN H. G. 1976. — Continental displacement and expansion of the Earth during the Mesozoic and Cainozoic. *Philosophical Transaction of the Royal Society of London* A. **281** (1303): 223-291.

— 1981. — Constant dimensions or an expanding Earth? *In* L. R. M. COCKS (ed.). *The Evolving Earth.* London and Cambridge, Cambridge Univ. Press: 179-192.

— 1983a. — Ocean-floor spreading evidence of global expansion. *In* S. W. CAREY (ed.). *The Expanding Earth: A Symposium.* Brunswick, Impact Printing (Vic.) Inc: 31-58.

— 1983b. — *Atlas of Continental Displacement, 200 Million Years to the Present.* Cambridge, Cambridge Univ. Press: 1-159.

— 1990. — Of gaps and globes. *Journal of Biogeography* **17**: 693-695.

— 1992 — Has the Earth increased in size? *In* S. CHATTERJEE & N. HUTTON (eds). *New Concepts in Global Tectonics.* Lubbock, Texas Tech Univ. Press: 289-296.

— (in press). — *The Mesozoic to Recent Development of the Pacific Ocean: a Review of Some Ideas.*

PANTIC N. K. 1986. — Global Tertiary climatic changes, palaeophytogeography and phytostratigraphy. *Lecture Notes in Earth Sciences: Global Bio-Events.* Heidelberg, Springer-Verlag **8**: 419-427.

PATRIAT P. & ACHACHE J. 1984. — India-Eurasia collision chronology has implications for crustal shortening and driving mechanisms of plates. *Nature* **311**: 615-621.

PATTERSON C. & OWEN H. G. 1991. — Indian isolation or contact? A response to Briggs. *Systematic Zoology* **40**: 96-100.

PAVONI N. 1993. — Pattern of mantle convection and Pangaea break-up, as revealed by the evolution of the African plate. *Journal of the Geological Society of London* **150**: 953-964.

PEIXOTO J. P. & OORT A. H. 1990. — Le cycle de l'eau et du climat. *La Recherche* **221** : 570-579.

PICKFORD M. 1986a. — Première découverte d'un Hyracoïde paléogène en Eurasie. *Comptes-Rendus de l'Académie des Sciences,* Paris **303** : 1251-1254.

— 1986b. — Geochronology of the Hominoidea: a summary. *In* J. ELSE & P. LEE (eds). *Primate Evolution.* Cambridge, Cambridge Univ. Press: 123-128.

— 1987. — Révision des Suiformes (Artiodactyla: Mammalia) de Bugti (Pakistan). *Annales de Paléontologie* **73** : 289-350.

— 1988. — The age(s) of the Bugti fauna(s). *In The Palaeoenvironment of East Asia from the Mid-Tertiary.* Hong Kong, University of Hong Kong Press **2**: 937-955.

— 1990a. — Uplift of the roof of Africa and its bearing on the evolution of Mankind. *Human Evolution* **5**: 1-20.

— 1990b. — Dynamics of Old World biogeographic realms during the Neogene: implications for biostratigraphy. *European Neogene Mammal Chronology. NATO, ASI Series.* New York, Plenum: 413-442.

— 1991. — What caused the first steps towards the evolution of Walkie-Talkie primates? *Cahiers de Paléoanthropologie Editions du CNRS*: 275-293.

— 1992. — Evidence for an arid climate in western Uganda during the Middle Miocene. *Comptes-Rendus de l'Académie des Sciences* Paris **315**: 1419-1424.

— (in press). — Fossil landsnails of East Africa and their palaeoecological significance. *Cahiers de Paléontologie Editions du CNRS.* Paris.

POWELL C. McA. 1979. — A speculative tectonic history of Pakistan and surroundings: Some constraints from the Indian Ocean. *In* FARAH & DE JONG (eds). *Geodynamics of Pakistan.* Quetta, Geological Survey of Pakistan: 5-24.

QUADE J., CERLING T. & BOWMAN J. 1989. — Development of Asian monsoon revealed by marked ecological shift during the latest Miocene in northern Pakistan. *Nature* **342**: 163-166.

SAHNI A. 1984. — Cretaceous-Palaeocene terrestrial faunas of India: lack of endemism during drifting of the Indian Plate *Science* **226**: 441-443.

SCHERBA I. G. 1987. — Stages and phases of formation of Cainozoic olistostromes in the Alpine Fold Belt. *Global correlation of tectonic movements*. Chichester, John Wiley and Sons: 49-82.

SCHWANN W. 1987. — Summary of the timing of Geotectonic events during Cretaceous and Tertiary times in the Balkan Peninsula. *Global correlation of tectonic movements*. Chichester, John Wiley and Sons: 83-95.

SMITH A. G., HURLEY A. M. & BRIDEN J. C. 1981. — *Phanerozoic Paleocontinentol World Maps*. Cambridge Earth Science Series: 1-102.

STEHLI F. G. 1968. — Taxonomic diversity gradients in pole location: the recent model. *In* E.T. DRAKE (ed.). *Evolution and Environment*. New Haven and London, Yale Univ. Press: 163-219.

STEINER J. 1977. — An expanding Earth on the basis of sea-floor spreading and subduction rates. *Geology* **5**: 313-318.

STEININGER F., RABEDER G. & RÖGL F. 1985. — Land mammal distribution in the Mediterranean Neogene: a consequence of Geokinematic and climatic events. *In* D. STANLEY & F. WEZEL (eds). *Geological Evolution of the Mediterranean Basin*. New York, Springer Verlag: 559-571.

STILLE H. 1924. — *Grundfragen der vergleichenden Tektonik*. Berlin: 1-443.

TARLING D. H. & TARLING M. P. 1971. — *Continental Drift*, London, G. Bell and Sons.

TREVISAN L. & TONGIORGI E. 1987. — *Il Nostro Universo: La Terra*, Torino, Terza Edizione, UTET.

VAN COUVERING J. A. 1988. — Sea-level change, *In Encyclopedia of Human Evolution and Prehistory*. New York and London, Garland: 505-510.

VAN DER MEULEN A. & DAAMS R. 1992. — Evolution of Early-Middle Miocene rodent faunas in relation to long-term palaeoenvironmental changes. *Palaeogeography Palaeoclimatology Palaeoecology* **93**: 227-253.

VERMEERSEN L. L. A. & VLAAR N. J. 1993. — Changes in the Earth's rotation by tectonic movements. *Geophysical Research Letters* **20** (2): 81-84.

VINK G. E. 1984. — A hot spot model for Iceland and the Vöring Plateau *Journal of Geophysical Research* **89**: 9949-9959.

VRBA E. 1985. — Environment and evolution: alternative causes of the temporal distribution of evolutionary events. *South African Journol of Science* **81**: 229-236.

WARD J. & CORBETT I. 1990. — *In* M. K. SEELY (ed.). *Namib Ecology: 25 Years of Namib Research*. Transvaal Museum Monography **7**: 17-26.

WEGENER A. 1962. — *Die Entstehung der Kontinente und Ozeane*. Die Wissenschaft, Braunschweig, Friedr. Vieweg & Sohn **66**: 1-231.

WHITE R. S. 1991. — Ancient floods of fire. *Natural History* **4**: 51-60.

WILLIAMS G. E. 1975. — Late Precambrian glacial climate and the Earth's obliquity. *Geological Magazine* **112**: 441-465.

— 1993. — History of the Earth's obliquity. *Earth Sciences Reviews* **34**: 1-45.

WILSON J. T. 1965. — A new class of faults and their bearing on continental drift. *Nature* **207**: 343-347.

WILSON M. 1993. — Plate-moving mechanisms: constraints and controversies. *Journal of the Geological Society of London* **150**: 923-926.

WINDLEY B. F. 1993. — Uniformitarianism today: Plate Tectonics is the key to the past. *Journal of the Geological Society of London* **150**: 7-19.

WOODBURNE M. & SWISHER C. 1995. — Land mammal high-resolution geochronology, intercontinental overland dispersals, sea-level, climate, and vicariance. *In* Geochronology Time Scales and Global Stratigraphic Correlation. *SEPM Special Publication* **54**: 335-364.

ZIEGLER P. A. 1993. — Plate-moving mechanisms: their relative importance. *Journal of the Geological Society of London* **150**: 927-940.

Bulletin du Muséum national d'Histoire naturelle, Paris, 4ᵉ sér., **18**, 1996
Section C, nᵒˢ 2-3 : 517-554

Earth's polar displacements of large amplitude: a possible mechanism

by Christian MARCHAL

Abstract. — Earth rotation and the position of poles are essential elements of climate. For centuries the motion of the poles with respect to the Earth's surface has remained very small, but this was not necessarily the case during geological times. The orogeny of a large mountain range, such as Himalaya, modifies the Earth's moments of inertia by a few millionths and this is sufficient for a large displacement of the "stable equilibrium position" of the poles. The corresponding motion of the poles remains usually very slow, as slow as the corresponding orogeny, and the Earth's equatorial bulge doesn't forbid the transformation. This bulge is only slowly deformed until its installation in the new position of equilibrium.

Key-words. — Earth, rotation, polar motions.

Une cause probable de grands déplacements des pôles terrestres

Résumé. — La rotation de la Terre et la position des pôles sont des éléments essentiels du climat. De nos jours, les pôles terrestres se déplacent très peu par rapport à la surface du sol, mais il n'en a pas nécessairement été toujours ainsi. La surrection d'un grand massif montagneux, comme l'Himalaya, modifie de quelques millionièmes les moments d'inertie de la Terre, ce qui suffit à déplacer très largement la «position d'équilibre stable» des pôles. Bien entendu le déplacement correspondant des pôles reste généralement lent, à la mesure de la lenteur de la surrection du massif montagneux, et l'existence du renflement équatorial de la Terre n'empêche pas la transformation: ce renflement est simplement peu à peu déformé jusqu'à être installé dans la nouvelle position d'équilibre.

Mots-clés. — Terre, rotation, mouvements des pôles.

C. MARCHAL, *ONERA, F-92320 Chatillon.*

INTRODUCTION

Terra australis incognita

The idea of Earth equilibrium and of the necessity of a great southern *antarktos* goes back to the ancient Greeks and was renewed by the voyages of Colombus, Vasco da Gama, Amerigo Vespucci and Magellan. The most famous geographers of the Renaissance, Martin Waldseemüller, Gerardus Mercator, Ortelius discussed the *Terra australis incognita* and drew tentative maps. This idea remained alive for two centuries until the voyages of Cook. The *Terra australis* is a

myth but the Earth has another kind of equilibrium: its poles are, within one kilometer, at their position of stable equilibrium.

The question of the motions of the Earth axis is essential for understanding the evolution of climates and life. The long term motion of the Earth's axis with respect to the stars and to the Earth's orbital plane is now well-known, at least qualitatively (LASKAR 1993; LASKAR & ROBUTEL 1993; LASKAR *et al.* 1993). These studies show that the presence of the Moon is essential. The obliquity of planet Mars has large variations and a long-term erratic evolution while the Earth's obliquity is stabilized by the attraction of the Moon and remains in the vicinity of 23°, which is of course a decisive element for the Earth's climates. We will here specially consider the rotation of the Earth and the motions of its poles with respect to the Earth's crust.

This subject has received considerable attention for more than a century (see for instance: LOVE 1911; POINCARÉ 1952; LE MOUEL & COURTILLOT 1981; LEGROS 1987; SPADA *et al.* 1992; RICARD *et al.* 1993). Since 1900 polar motion has been very small, its amplitude is less than 15 meters, but we will see that it can sometimes have a large drift, up to 200 meters per year, when the Earth is in a state of disequilibrium. That latter velocity is much larger than the relative velocity of lithospheric plates.

The huge progress in the knowledge of Earth through geology, seismology, geophysics, plate tectonics, geodesy and space geodesy, paleogeography, analysis of polar motions, of Earth rotation, of motions of artificial satellites, etc, leads to a qualitative description of the phases of Earth disequilibrium.

There are also very large progress, in paleomagnetism (RICARD *et al.* 1993). Unfortunately the motion of the magnetic axis is poorly related to that of the geographic axis and these two axes can have a large angle (*e.g.* 60° presently for planet Uranus).

PRELIMINARY NOTICE (NUMERATION SYSTEM)

In this paper for very large and very small numbers we will use the convention of numeration by "figures and sizes":

$$\text{Mass of Earth} = M = 5.9737 \times 10^{24}\ \text{kg} = \underbrace{5.9737}_{\text{figure}}\ \underbrace{\text{p24}}_{\text{size}}\ \text{kg},$$

$$\text{Constant of NEWTON's law} = \text{CAVENDISH constant} = G = 6.6726 \times 10^{-11}\ \text{m}^3/\text{s}^2\text{kg} = \underbrace{6.6726}_{\text{figure}}\ \underbrace{\text{n11}}_{\text{size}}\ \text{m}^3/\text{s}^2\text{kg}.$$

The letter p means "positive power of ten" and the letter n means "negative power of ten", while the figure is always between one and ten (we cannot write 0.59 p25 instead of 5.9 p24). The size is thus always well defined, it is of course the most important part of very large and very small numbers, it is even sometimes the only known part.

MAIN ELEMENTS OF EARTH

We will specifically consider the following elements.

THE REFERENCE ELLIPSOID (BURSA 1992)

The international Earth reference system (I.E.R.S.) uses an oblate ellipsoid of revolution with :

(1) Earth equatorial radius R = 6 378 136 m

(2) Earth polar radius Rp = 6 356 751.3 m

(3) flattening = (R-Rp)/R = 1/298.257

MASS AND MOMENTS OF INERTIA (BURSA, 1992)

(4) Mass of Earth = M = {5.9737 p24 ± 3 p20} kg
The product of the mass M by the constant G of Newton's law is known to 9 digits:

(5) GM = Earth gravitational constant = 3.986 004 41 p14 m^3s^{-2}
The three main moments of inertia A, B, C (with A < B < C) are given by:

(6) $A/MR^2 = 0.329\,591 \pm n6$
(7) $B/MR^2 = 0.329\,599 \pm n6$ — $n6 = 10^{-6}$ (see preliminary notice)
(8) $C/MR^2 = 0.330\,678 \pm n6$

Their differences are known with much higher accuracy:

(9) $(C\text{-}A)/MR^2$ = 1.086 258 n3 ± 2n9

(10) $(C\text{-}B)/MR^2$ = 1.078 996 n3 ± 2n9

The moment C practically corresponds to the polar axis, while A corresponds to an equatorial axis with longitude 14.95° West. Hence the B axis is equatorial and has the longitude 75.05° East.

THE EARTH GRAVITATIONAL POTENTIAL

The analysis of the motions of artificial Earth satellites has led to a very accurate knowledge of the Earth's gravitational potential outside the Earth (BALMINO *et al* 1978; LERCH *et al* 1979; MARSH *et al* 1990; REIGBER *et al* 1993).

This outer potential U has several usual expressions, for instance the following one with spherical harmonics:

(11) $$U = -\frac{GM}{r}\left\{1 + \sum_{k=2}^{\infty}\sum_{n=0}^{k}\left(\frac{R}{r}\right)^k J_{kn} P_{kn}(\sin\varphi)\cos n(L - L_{kn})\right\}$$

with:

(12) GM and R given in (5) and (1)

r, φ, L are the ordinary geocentric spherical coordinates:

(13) $\begin{cases} r = \text{satellite} - \text{Earth center distance} \\ \varphi = \text{geocentric latitude (positive towards North)} \\ L = \text{geocentric longitude from Greenwich meridian (positive towards East)} \end{cases}$

$P_{kn}(\sin\varphi)$ is the Legendre polynomial or the associated function of order k, n:

(14) $$P_{kn}(\sin\varphi) = \frac{(\cos\varphi)^n}{2^k\, k\,!}\ \frac{d^{(k+n)}}{d(\sin\varphi)^{(k+n)}}\ (\sin^2\varphi - 1)^k$$

Since $-90^\circ \leq \varphi \leq +90^\circ$ we have $\cos\varphi = +\sqrt{1-\sin^2\varphi}$ and:

(15) $P_{2.0} = (3\sin^2\varphi - 1)/2$; $P_{2.1} = 3\sin\varphi\cos\varphi$; $P_{2.2} = 3\cos^2\varphi$; etc.

Finally the J_{kn} and L_{kn} are the coefficients of the Earth's potential. They are related to the distribution of masses inside the Earth.

For n = 0, with the mass dm at the point r, φ, L:

(16) $$J_{k0} = \frac{1}{MR^k}\int_M dm\, r^k\, P_{k0}(\sin\varphi)$$

and for n ≤ 1:

(17) $$\begin{cases} J_{kn}\cos nL_{kn} = \dfrac{2(k-n)\,!}{(k+n)\,!\,MR^k}\displaystyle\int_M dm\, r^k\, P_{kn}(\sin\varphi)\cos nL \\ J_{kn}\sin nL_{kn} = \dfrac{2(k-n)\,!}{(k+n)\,!\,MR^k}\displaystyle\int_M dm\, r^k\, P_{kn}(\sin\varphi)\sin nL \end{cases}$$

For the Earth, with its polar axis as the main axis of inertia, we obtain:

(18) $$\begin{cases} J_{20} = (A+B-2C)/2MR^2;\ J_{21} = 0;\ J_{22} = (B-A)/4MR^2 \\ L_{22} = -14.95^\circ = \text{longitude of the A}-\text{axis} \end{cases}$$

These expressions and accurate knowledge of the outer potential U explain why the differences (9) and (10) are known with greater accuracy than the ratios (6), (7) and (8).

The coefficients $(k-n)!/(k+n)!$ of (17) introduce artificial very small numbers that reduce the real importance of the corresponding terms.

In order to re-establish the true importance of successive terms it is customary to use the following Earth coefficients C_{kn} and S_{kn}:

(19) $$\frac{C_{kn}}{J_{kn}\cos nL_{kn}} = \frac{S_{kn}}{J_{kn}\sin nL_{kn}} = \sqrt{\frac{(k+n)\,!}{(k-n)\,!\,(2k+1)\,\nu_n}}$$

with $n = 0 \Rightarrow \nu_n = 1$

$n \geq 1 \Rightarrow \nu_n = 2$

For instance with the model Grim4 (REIGBER *et al* 1993):

$$(20)\quad \begin{cases} C_{20} = -\,4.841\,656\,236\,964\,4 \text{ n4} \\ C_{21} = S_{21} = 0 \\ C_{22} = 2.439\,315\,544 \text{ n6} \\ S_{22} = -\,1.400\,040\,70 \text{ n6}\,. \end{cases}$$

Which gives:

$$(21)\quad \begin{cases} J_{20} = C_{20}\sqrt{5} = -\,1.082\,627\,246\,95 \text{ n3} \\ J_{21} = 0 \\ J_{22} = \sqrt{5(C_{22}^2 + S_{22}^2)/12} = 1.815\,485\,964 \text{ n6} \\ L_{22} = 0.5 \text{ Arc tan } (S_{22}/C_{22}) = -\,14.926\,8^{\circ} \\ (C-A)/MR^2 = -\,J_{20} + 2J_{22} = 1.086\,258\,218\,88 \text{ n3} \\ (C-B)/MR^2 = -\,J_{20} - 2J_{22} = 1.078\,996\,275\,02 \text{ n3}\,. \end{cases}$$

These results agree with (9), (10) but their accuracy is illusory: they represent an average while the tidal variations of C_{kn} and S_{kn} correspond to the inaccuracies of (9) and (10) and are of the order of a few n9 (*i.e.* a few 10^{-9}, see preliminary notice).

These inaccuracies are well illustrated by the comparison of different models. For instance the ninth Goddard Earth Model, called GEM 9 (LERCH *et al* 1979), gives:

$$(22)\quad \begin{cases} C_{20} = -\,4.841\,655\,5 \text{ n4} \\ C_{21} = -\,2.1 \text{ n10} \\ S_{21} = -\,4.06 \text{ n9} \\ C_{22} = 2.434\,00 \text{ n6} \\ S_{22} = -\,1.397\,86 \text{ n6}\,. \end{cases}$$

The differences between the two models are indeed of the order of a few n9.

On the other hand $C_{2.1}$ and $S_{2.1}$ are not zero for the GEM 9: there is an angle of about 2.6″ between the polar axis of this model and its main axis of inertia.

These models give C_{kn} and S_{kn} for many values of k and n (for instance for all values with $n \le k \le 20$ for the GEM 9). These coefficients only have a slow decrease for large k and n and the convergence of (11) is not good: at the scale of kilometers the Earth has many irregularities. Fortunately we will not need all these coefficients.

Beyond those of (20) and (22) only two coefficients are not between + n6 and – n6:

$$(23)\quad \begin{cases} C_{31} = 2.028\,26 \text{ n6} \\ S_{33} = 1.411\,40 \text{ n6} \end{cases} \quad \text{in the GEM 9.}$$

These coefficients C_{kn} and S_{kn} allow us to draw pictures of the "geoid", as in the Figure 1.

The "geoid", very near to mean sea-level, is an equipotential surface of the difference $U - 0.5\,\omega^2 r^2 \cos^2 \varphi$, the latter term being given by the centrifugal forces with:

(24) ω = rate of rotation of Earth = 7.292 115 n5 Rd/s.

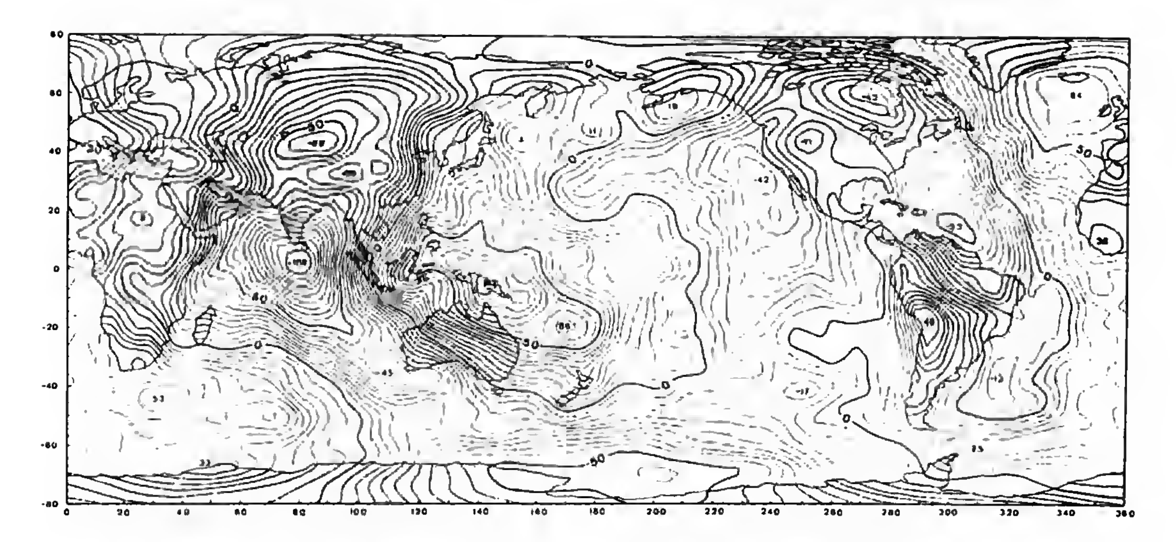


FIG. 1. — Level curves of the geoid (in meters) with respect to the following reference ellipsoid: equatorial radius = 6 378 155 m; flattening = 1/298.255 (BALMINO, REIGBER & MOYNOT 1978).

This equipotential surface can be compared to some reference ellipsoid such as (1), (2), (3) (the chosen equipotential surface is one with a volume equivalent to that of the ellipsoid). The level curves are given in meters and range from – 108 meters (near India) to + 82 meters (New Guinea).

THE POLAR MOTIONS AT THE EARTH SURFACE

The polar motions, and the corresponding variations of latitudes, have been accurately measured for a century. These motions have two main parts (Bureau des Longitudes 1984).

A short period part with two periodical components (Fig. 2)

A yearly component related to major meteorological phenomena such as the monsoon.

A component with the "Chandler period" of 435 days and corresponding to the following phenomenon. If a free body with main moments of inertia A, B, C does not exactly have pure rotation about its C-axis it will have a motion similar to the Euler-Poinsot rotation of rigid bodies. For these rigid bodies the period P of polar motion is given in terms of the period P_0 of main rotation by:

$$(25) \quad P = P_0 \sqrt{\{AB/(C-A)(C-B)\}}\ .$$

In the case of the Earth, P_0 is 23 h 56 min 4.1 s (*i.e.* one sidereal day) and (25) gives P = 303.61 days. However the Earth is not a rigid body and its properties, essentially its elasticity, enlarge the period of polar motions from P to the Chandler period of 435 days (LOVE 1911).

The second part of the motion of North Pole is a very slow drift towards Canada that remains when the short period components are removed (Fig. 3). This slow drift is certainly related to plate tectonics and to the postglacial rebound.

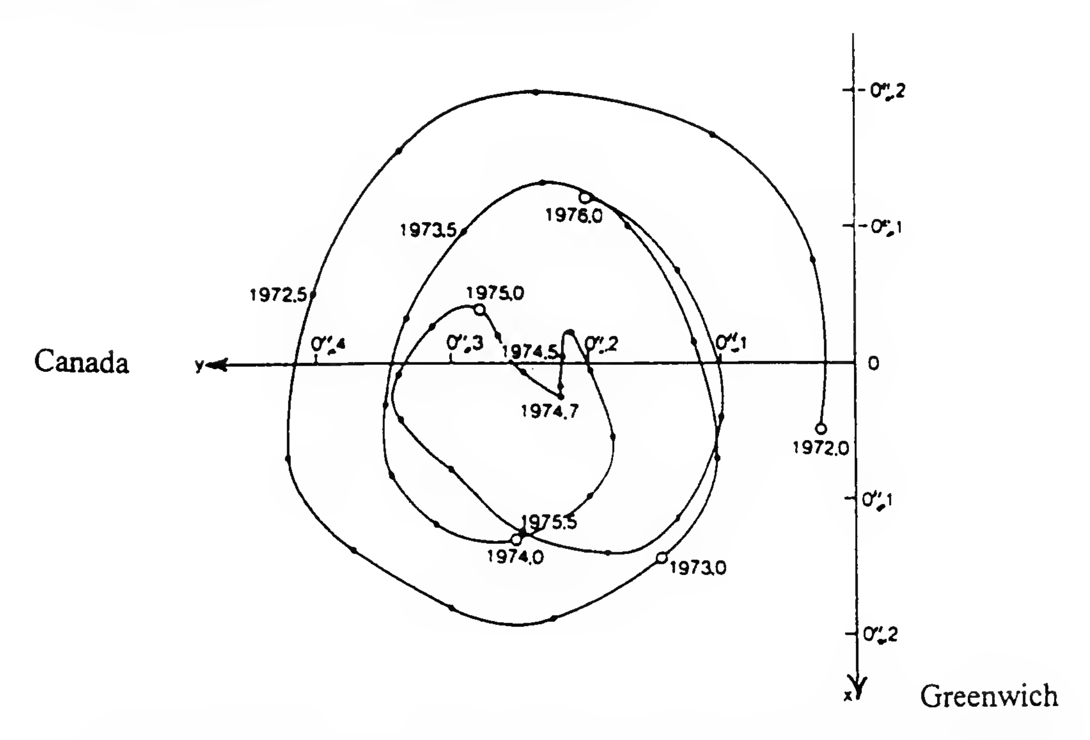


FIG. 2. — The motion of the North Pole during the four years 1972-1975. O is a conventional origin, Ox is in the direction of Greenwich and Oy in the direction of Canada. At the Earth's surface 0.1″ is only 3.1 m.

CONCERNING THE INNER STRUCTURE OF THE EARTH

The inner structure of the Earth and the distribution of its inner masses is a difficult question. A small part of our information has an astronomical and mechanical origin. The motions of the poles with respect to the stars (precession, nutation) are related to the main moments and axes of inertia, while the motions of the Moon and of the artificial satellites give us the total Earth mass and the coefficients of its outer potential. These coefficients are known functions of the inner distribution of masses (equations (16) to (19)). However they only give very partial informations, indeed an arbitrary point-mass and a spherically symmetrical distribution with the same total mass and the same center have exactly the same outer potential.

Geology and vulcanology give us much information about the Earth's crust while geodesy, and especially space geodesy, yield accurate informations about the Earth's dimensions.

Our main source of information about the interior of the Earth is seismology. The largest earthquakes give rise to powerful waves propagating in all directions up to the antipodes with

velocities depending on local conditions. The measurements of propagation durations by seismometers reveal the existence of several discontinuities at various levels within the Earth.

We are thus led to the modern Earth models such as the PREM 1s given in Table 1 (DZIEWONSKI & ANDERSON 1981). Notice that this model in terms of only one parameter, the depth, is necessarily an average approximation: the mean thickness of the lithosphere is about 217 km but it varies from a few kilometers below the oceanic ridges to about 300 km below the continents.

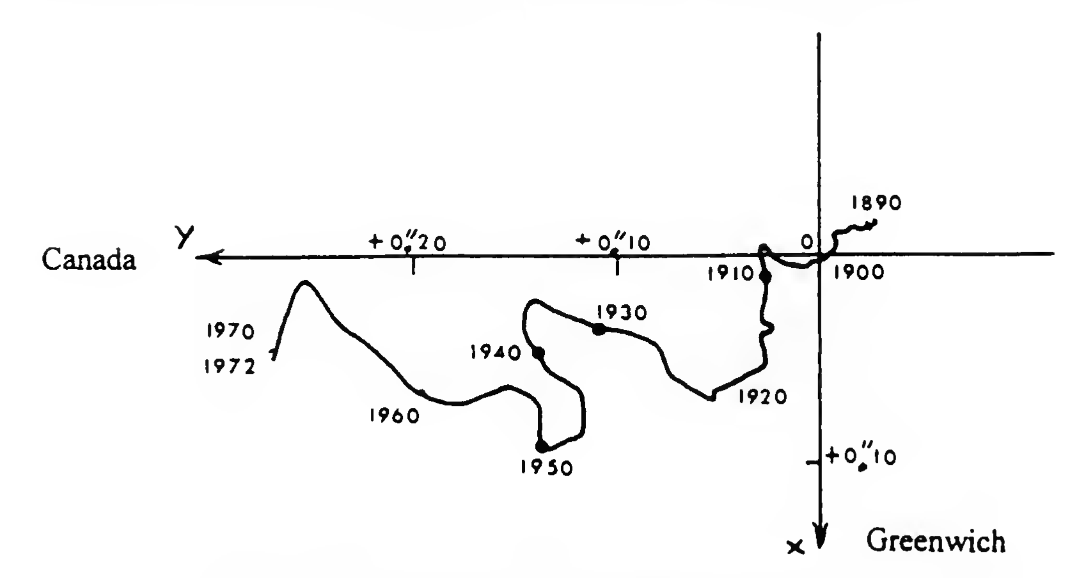


FIG. 3. — The slow drift of the North Pole towards Canada when the short period components appearing in Figure 2 are removed.

THE FOUR EARTH EQUILIBRIA

Because of the presence of outer bodies, the Sun, the Moon, etc., our planet cannot be in a state of perfect equilibrium. It permanently undergoes tides in its oceans and its crust. Furthermore its inner sources of energy draw along large masses at a very slow rate. Fortunately these phenomena remain very small, at the scale of the Earth, and we can define the four following equilibria that are more or less near to the true Earth: the hydrostatic equilibrium of a non-rotating Earth (Fig. 4A); the hydrostatic equilibrium of a rotating Earth (Fig. 4B); the isostatic equilibrium of a non-rotating Earth (Fig. 4C); the isostatic equilibrium of a rotating Earth (Fig. 4D). The last equilibrium is very near to the true Earth but notice that the first one is already good; it is the basis of the PREM 1s model of Table 1.

THE HYDROSTATIC EQUILIBRIUM OF A NON-ROTATING EARTH

This first equilibrium (Fig. 4A) is simple and well-known. It has spherical symmetry. The different layers are spherical and concentric with density increasing with depth.

THE HYDROSTATIC EQUILIBRIUM OF A ROTATING EARTH

This second equilibrium (Fig. 4B) remains simple. It has spheroidal symmetry: the axis of rotation is also an axis of symmetry of revolution; the equatorial plane (normal to the axis of rotation through the center of mass) is a plane of symmetry; on straight lines either parallel or perpendicular to the axis of rotation the density increases when we approach the center of mass. This spheroidal symmetry is very general for hydrostatic equilibria (see appendix 1).

The Earth has a rather slow rotation and its hydrostatic equilibrium has level surfaces that are concentric and coaxial oblate quasi-ellipsoids whose oblateness increases from the center to the surface. These quasi-ellipsoids are slightly depressed at mid-latitudes (the depression is only about 4.3 m at the Earth's surface at latitudes ± 45°).

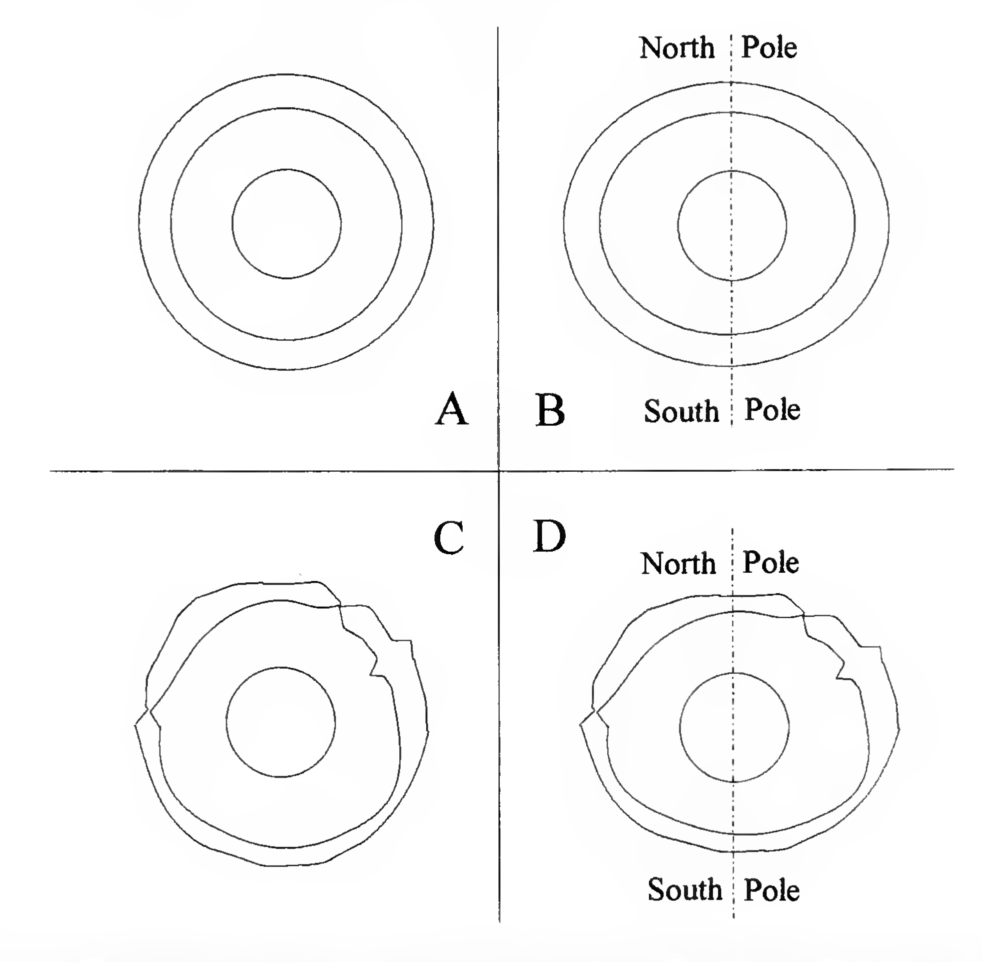


FIG. 4. — The four equilibria of Earth. A, hydrostatic equilibrium of a non-rotating Earth. The level surfaces are concentric spheres; B, hydrostatic equilibrium of a rotating Earth. The level surfaces are concentric and coaxial oblate quasi-ellipsoids (slightly depressed at mid-latitudes); C, isostatic equilibrium of a non-rotating Earth. The sea-level is almost a sphere; D, isostatic equilibrium of a rotating Earth. The sea-level is almost an oblate ellipsoid. B, D: The Earth's angular momentum H is 5.85989 p33 kg m^2/s.

TABLE 1. — The PREM 1s (Preliminary Reference Earth Model 1s). Parameters : depth z, density, seismic velocities; Vp: longitudinal waves; Vs: transversal waves; P: pressure; g: gravity; r: radius. Notice that everywhere: z + r = 6371 km = mean Earth radius. Also notice that Vs = 0 in the outer core. This layer represents 15,6% of the Earth's volume and 31% of its mass; it is considered as liquid.

	z (km)	density	Vp (km/s)	Vs (km/s)	P (kbar)	g (cm/s2)	r (km)
OCEAN							
	0	1,02	1,45	0	0	981,56	6371,0
	3	1,02	1,45	0	0,299	982,22	6368,0
LITHOSPHERE							
Upper crust	3	2,60	5,80	3,2	0,303	982,22	6368,0
	15	2,60	5,80	3,2	3,364	983,31	6356,0
Lower crust	15	2,90	6,80	3,9	3,370	983,32	6356,0
	24,4	2,90	6,80	3,9	6,040	983,94	6346,6
Upper mantle	24,4	3,38	8,11	4,49	6,043	983,94	6346,6
	40	3,37	8,11	4,48	11,239	984,37	6331,0
	60	3,37	8,08	4,47	17,891	984,93	6311,0
	80	3,37	8,07	4,46	24,539	985,53	6291,0
	80	3,37	8,07	4,46	24,546	985,53	6291,0
	115	3,37	8,05	4,45	36,183	986,64	6256,0
	150	3,36	8,03	4,44	47,824	987,83	6221,0
	185	3,36	8,01	4,43	59,466	989,11	6186,0
	220	3,35	7,98	4,41	71,108	990,48	6151,0
TRANSITION ZONE (MIDDLE MANTLE OR ASTHENOSPHERE)							
	220	3,43	8,55	4,64	71,115	990,48	6151,0
	265	3,42	8,64	4,67	86,497	992,03	6106,0
	310	3,48	8,73	4,70	102,027	993,61	6061,0
	355	3,51	8,81	4,73	117,702	995,22	6016,0
	400	3,54	8,90	4,76	133,520	996,86	5971,0
	400	3,72	9,13	4,93	133,527	996,86	5971,0
	450	3,78	9,38	5,07	152,251	997,90	5921,0
	500	3,84	9,64	5,22	171,311	998,83	5871,0
	550	3,91	9,90	5,37	190,703	999,65	5821,0
	600	3,97	10,15	5,51	210,425	1000,38	5771,0
	600	3,97	10,15	5,51	210,426	1000,38	5771,0
	635	3,98	10,21	5,54	224,364	1000,38	5736,0
	670	3,99	10,26	5,57	238,334	1001,43	5701,0
LOWER MANTLE							
	670	4,38	10,75	5,94	238,342	1001,43	5701,0
	721	4,41	10,91	6,09	260,783	1000,63	5650,0
	771	4,44	11,06	6,24	282,927	999,85	5600,0
	771	4,44	11,06	6,24	282,928	999,85	5600,0
	871	4,50	11,24	6,31	327,623	998,36	5500,0
	971	4,56	11,41	6,37	372,852	996,98	5400,0
	1071	4,62	11,57	6,44	418,606	995,73	5300,0
	1171	4,67	11,73	6,50	464,882	994,67	5200,0
	1271	4,73	11,88	6,56	511,676	993,83	5100,0
	1371	4,78	12,02	6,61	558,991	993,26	5000,0
	1471	4,84	12,16	6,67	606,830	993,01	4900,0
	1571	4,89	12,29	6,72	655,202	993,14	4800,0

1671	4,95	12,42	6,77	704,119	993,69	4700,0
1771	5,00	12,54	6,82	753,598	994,74	4600,0
1871	5,05	12,66	6,87	803,660	996,35	4500,0
1971	5,10	12,78	6,91	854,332	998,59	4400,0
2071	5,15	12,90	6,96	905,646	1001,56	4300,0
2171	5,20	13,01	7,01	957,641	1005,35	4200,0
2271	5,25	13,13	7,05	1010,363	1010,06	4100,0
2371	5,30	13,24	7,09	1063,864	1015,80	4000,0
2471	5,35	13,36	7,14	1118,207	1022,72	3900,0
2571	5,40	13,47	7,18	1173,465	1030,95	3800,0
2671	5,45	13,59	7,23	1229,719	1040,66	3700,0
2741	5,49	13,68	7,26	1229,741	1048,44	3630,0
2741	5,49	13,68	7,26	1269,742	1048,44	3630,0
2771	5,50	13,68	7,26	1287,067	1052,04	3600,0
2871	5,55	13,71	7,26	1345,619	1065,32	3500,0
2891	5,56	13,71	7,26	1357,509	1068,23	3480,0
OUTER CORE						
2891	9,90	8,06	0	1357,510	1068,23	3480,0
2971	10,02	8,19	0	1441,941	1050,65	3400,0
3071	10,18	8,36	0	1546,982	1028,04	3300,0
3171	10,32	8,51	0	1651,209	1004,04	3200,0
3271	10,46	8,65	0	1754,418	980,51	3100,0
3371	10,60	8,79	0	1856,409	955,70	3000,0
3471	10,73	8,92	0	1956,991	930,23	2900,0
3571	10,85	9,05	0	2055,978	904,14	2800,0
3671	10,97	9,16	0	2153,189	877,46	2700,0
3771	11,08	9,27	0	2248,453	850,23	2600,0
3871	11,19	9,38	0	2341,603	822,48	2500,0
3971	11,29	9,48	0	2432,484	794,25	2400,0
4071	11,39	9,57	0	2520,942	765,56	2300,0
4171	11,48	9,66	0	2606,838	736,45	2200,0
4271	11,57	9,75	0	2690,035	706,97	2100,0
4371	11,65	9,83	0	2770,407	677,15	2000,0
4471	11,73	9,91	0	2847,839	647,04	1900,0
4571	11,80	9,98	0	2922,221	616,69	1800,0
4671	11,87	10,05	0	2993,457	586,14	1700,0
4771	11,94	10,12	0	3061,461	555,48	1600,0
4871	12,00	10,18	0	3126,159	524,77	1500,0
4971	12,06	10,24	0	3187,493	494,13	1400,0
5071	12,12	10,30	0	3245,423	463,68	1300,0
5149,5	12,16	10,35	0	3288,503	440,03	1221,5
INNER CORE						
5149,5	12,76	11,02	3,50	3288,513	440,02	1221,5
5171	12,77	11,03	3,51	3300,480	432,51	1200,0
5271	12,82	11,07	3,53	3353,596	397,39	1100,0
5371	12,87	11,10	3,55	3402,383	362,03	1000,0
5471	12,91	11,13	3,57	3446,764	326,45	900,0
5571	12,94	11,16	3,59	3486,665	290,68	800,0
5671	12,98	11,18	3,61	3522,024	254,73	700,0
5771	13,01	11,20	3,62	3552,783	218,62	600,0
5871	13,03	11,22	3,64	3578,894	182,39	500,0
5971	13,05	11,23	3,65	3600,315	146,04	400,0
6071	13,06	11,24	3,65	3617,011	109,61	300,0
6171	13,07	11,25	3,66	3628,956	73,11	200,0
6271	13,08	11,26	3,66	3636,131	36,56	100,0
6371	13,08	11,26	3,66	3638,524	0	0,0

THE ISOSTATIC EQUILIBRIA

With all its mountain ranges, its continents and its oceans the Earth is of course far from hydrostatic equilibrium and a much better approximation is that of isostatic equilibrium. The idea of isostatic equilibrium comes from the large differences of viscosity and rigidity between the lithosphere and the asthenosphere. Vertical equilibrium of the lithosphere is achieved much more easily and faster than the horizontal one. The upwards motion of Scandinavia, after the recent melting of the large Quaternary glacier, is about one meter per century and corresponds to re-equilibrium on the time scale of a few millenia only.

The theory of isostatic equilibrium requires the definition of a "level of compensation", the asthenosphere, a few hundred kilometers below the surface. Above this level only vertical equilibrium is required. We thus arrive at the usual pictures with a thick lithosphere under the continents, especially the mountain ranges, and a thinner one below the oceans (Figs 4C, D). Figure 4C corresponds to the isostatic equilibrium of a non-rotating Earth. Its mean sea-level is of course almost spherical and we will see the interest of this equilibrium below. Figure 4D corresponds to the isostatic equilibrium of the Earth with its true rotation. The main feature of the surface is its oblateness (the difference between the equatorial and polar radii is 21.4 km). The mean sea-level is not exactly a "geoid" *i.e.* the equipotential surface of level zero (because of sea currents and of variations of temperature and salinity) but these two surfaces remain within meters to each other and they are close to the reference ellipsoid, as shown in Figure 1.

THE ROTATING AND NON-ROTATING SET OF AXES

For the study of the Earth's rotation and of its inner motions it is customary to use the Tisserand set of axes with origin at the center of mass and rotation such that the remaining velocities give to Earth a zero total angular momentum (LEGROS 1987).

However we are specially interested in the relative Poles-Earth crust motions and we are less interested in the oceanic currents and the motions of the Earth's mantle. Hence we will choose as Oxyz axes the reference frame ITRF (International Terrestrial Reference Frame) that is more concretely related to the crust (Fig. 5; ARIAS *et al.* 1995).

We will also use a non-rotating right tri-rectangular set of axes OXYZ (Fig. 6), with the same origin O. It is the geocentric equivalent of the reference frame ICRF (International Celestial Reference Frame; ARIAS *et al.* 1995). The relativistic corrections that are necessary between the barycentric ICRF and its geocentric version are negligible in the present study. We will define the Earth's axis and poles by the rotation vector $\vec{\omega}$ of Oxyz with respect to OXYZ. Its present module is:

(26) ω = 7.292 115 n5 Rd/s = present rate of Earth's rotation.

We will see below that the Earth's angular momentum $\vec{H}$ remains always extremely near to the direction of $\vec{\omega}$ and thus, for the study of the large polar displacements, it will be sufficient to study the evolution of $\vec{H}$.

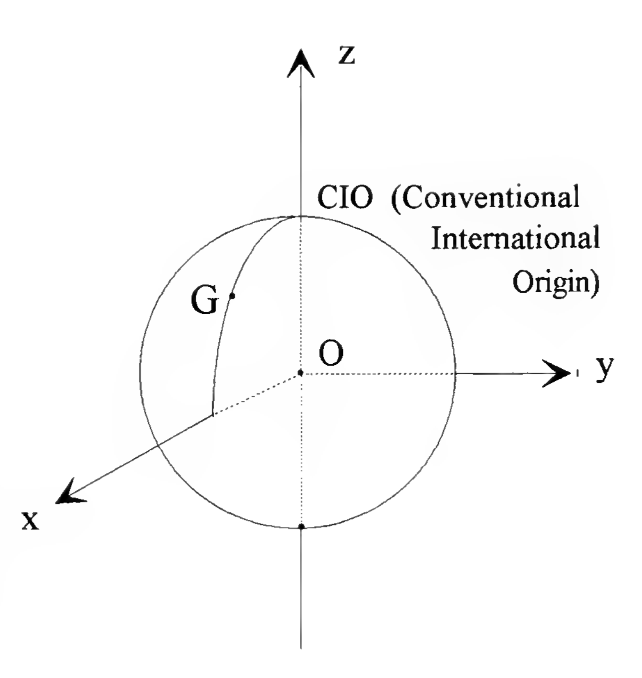


FIG. 5. — The Oxyz rotating set of axes (International Terrestrial Reference Frame). O is the Earth's center of mass. Oz passes through the Conventional International Origin (the point O of Figures 2 and 3). Oxz is along the International Reference Meridian (Greenwich). Oxyz is a right and rectangular trihedron.

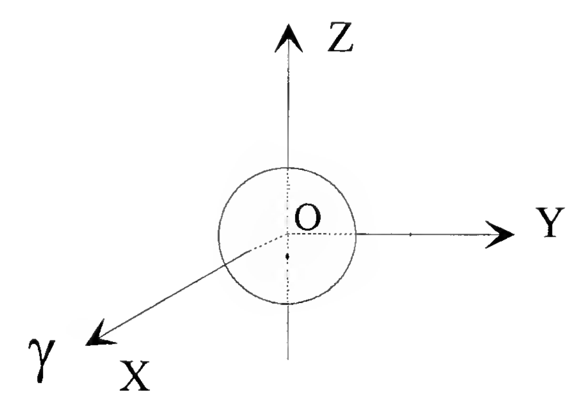


FIG. 6. — The OXYZ non-rotating set of axes. O is the Earth's center of mass. OXY is the equatorial plane of the International Celestial System. OX is the direction of the International Vernal Point.

THE EARTH'S INERTIA MATRIX M

The inertia matrix M relates the rotation vector $\vec{\omega}$ and the angular momentum $\vec{H}$ of rigid bodies rotating about their center of mass:

(27) $H = M\,\vec{\omega}$.

This relation is valid at any time and can be expressed in any set of axes, for instance Oxyz or OXYZ. The Earth is not exactly a rigid body but (27) will nevertheless be very useful (see (63)).

We will call I_{x^2}, I_{xy}, etc. the moments and products of inertia in the Oxyz axes:

$$(28)\quad I_{x^2} = \int_M x^2\,dm\,;\quad I_{xy} = \int_M xy\,dm.$$

Thus, when Oz is the main axis of largest inertia:

$$(29)\quad C = I_{x^2+y^2} = \int_M (x^2+y^2)\,dm$$

and, with (16)-(19), when Oxyz is the rotating geocentric set of axes used:

$$(30)\quad I_{xy} = MR^2 S_{2.2}\sqrt{\frac{5}{3}}\;;\; I_{xz} = MR^2 C_{2.1}\sqrt{\frac{5}{3}}\;;\; I_{yz} = MR^2 S_{2.1}\sqrt{\frac{5}{3}}\,.$$

The components of the inertia matrix M are then classically:

$$(31)\quad M = \begin{bmatrix} I_{y^2+z^2} & -I_{xy} & -I_{xz} \\ -I_{xy} & I_{x^2+z^2} & -I_{yz} \\ -I_{xz} & -I_{yx} & I_{x^2+y^2} \end{bmatrix}.$$

Hence the model Grim-4 (REIGBER *et al.* 1993) gives in its axes with (20), (21):

$$(32)\quad M = MR^2 \begin{bmatrix} U - 3.640\,248\,92\text{ n4} & 1.807\,445\text{ n6} & 0 \\ 1.807\,445\text{ n6} & U - 3.577\,266\,06\text{ n4} & 0 \\ 0 & 0 & U + 7.217\,514\,98\text{ n4} \end{bmatrix}$$

MR^2U is the average Earth moment of inertia that is less accurately known (see (6)-(8)):

$$(33)\quad MR^2U = \frac{1}{3}(A+B+C)\,;\quad U = 0.329\,956 \pm \text{n6}\,.$$

Similarly the Goddard Earth Model 9 (LERCH *et al.* 1979) gives in its own axes, with (22):

$$(34)\quad M = MR^2 \begin{bmatrix} U - 3.640\,179\,7\text{ n4} & 1.804\,63\text{ n6} & 2.7\text{ n10} \\ 1.804\,63\text{ n6} & U - 3.577\,334\,1\text{ n4} & 5.24\text{ n9} \\ 2.7\text{ n10} & 5.24\text{ n9} & U + 7.217\,513\,9\text{ n4} \end{bmatrix}$$

The differences between (32) and (34), a few n9 that is a few billionths, are essentially caused by a difference of orientation of a few seconds between the corresponding set of axes (that are both extremely near to Oxyz of Figure 5). Nevertheless there remains also an irreducible difference of a few n10, a difference related to the accuracy of present measures.

However we need not only the present expression of the matrix M but also its past and future expressions under various possible orientations of the polar axis. We will always use the Oxyz set of axes of Figure 5, that is concretely fixed to the Earth's crust; and we will consider the four equilibria of Figure 4 and the corresponding inertia matrices M_A, M_B, M_C, M_D. We are looking for M_D under various orientations of the polar axis and we know that:

M_A and M_C are, by definition, independent of the polar axis while M_B is a simple function of this axis.

The principle of small modifications allows us to write:

(35) $M_D - M_C = M_B - M_A +$ "second order".

Finally we will also need the difference $M - M_D$ that remains very small at least as long as there are no large variations of the Earth's crust; each major variation being followed by a period of reequilibrium (see below).

Notice that these variations will also modify M_C and thus our model of Earth will use:

(36) $M = M_C + (M_B - M_A) + R,$

with:

The difference $M_B - M_A$ is only a function of the direction and the modulus of the Earth's rotation vector $\vec{\omega}$.

The matrix M_C will generally have only extremely slow variations.

The remainder R will generally be very small but it will be not negligible during and just after periods of large variations of M_C, such as periods of orogeny of large mountain ranges.

THE MATRICES M_A, M_B AND $(M_B - M_A)$

The spherical symmetry of the hydrostatic and non-rotating equilibrium leads to a very simple matrix M_A:

(37) $$M_A = MR^2 \begin{bmatrix} U_A & 0 & 0 \\ 0 & U_A & 0 \\ 0 & 0 & U_A \end{bmatrix}.$$

The average moment of inertia $MR^2\, U_A$ is very near to $MR^2\, U$ of (33) and a little smaller, their relative difference is of the order of one millionth.

The spheroidal symmetry of the hydrostatic and rotating equilibrium leads to a matrix M_B that is a function of only four parameters: the smallest main moment of inertia A_B, the largest main moment of inertia C_B and the two angles giving the direction of the polar axis.

(38) $$M_B = MR^2 \begin{bmatrix} U_B & 0 & 0 \\ 0 & U_B & 0 \\ 0 & 0 & U_B \end{bmatrix} + (C_B - A_B) \begin{bmatrix} \left(\alpha^2 - \frac{1}{3}\right); & \alpha\beta\,; & \alpha\gamma \\ \alpha\beta\,; & \left(\beta^2 - \frac{1}{3}\right); & \beta\gamma \\ \alpha\gamma\,; & \beta\gamma\,; & \left(\gamma^2 - \frac{1}{3}\right) \end{bmatrix}$$

with:

(39) $$\begin{cases} MR^2U_B = \text{average moment of inertia} = (2A_B + C_B)/3 \\ U_A < U_B < U : \text{these three numbers are almost equal} \end{cases}$$

and:

$$(40)\quad \begin{cases} (\alpha,\ \beta,\ \gamma) = \text{components of the unit vector of polar axis in the rotating Oxyz set of axes} \\ (\alpha,\ \beta,\ \gamma) = \dfrac{\vec{\omega}}{\omega}\ ;\ \alpha^2+\beta^2+\gamma^2=1\ ;\ \text{with } \vec{\omega} = \text{rotation vector of Oxyz with respect OXYZ.} \end{cases}$$

We can verify that in the present state:

$$(41)\quad M_B = \begin{bmatrix} A_B & 0 & 0 \\ 0 & A_B & 0 \\ 0 & 0 & C_B \end{bmatrix}.$$

The values of A_B and C_B depend upon the Earth model considered, such as the PREM 1s model of Table 1.

The depth of inner discontinuities are accurately known but the knowledge of inner densities remains weak. Fortunately the influence of this ignorance remains small in our problem. Let us assume for instance that we only know the following.

(42)
- The total Earth mass $M = 5.9737$ p24 kg.
- The equatorial radius $R = 6\,378\,136$ m and the mean radius $R_M = 6\,371\,200$ m (including the volume of continents).
- The average moment of inertia: $(2A_B + C_B)/3 = MR^2U_B \approx MR^2U = 0.329\,956\,MR^2$.
- The present Earth angular momentum $H_p = 5.859\,89$ p33 kg m^2/s
- $H_p = C\omega$; with $C = 0.330\,678\,MR^2$, $\omega = 7.292\,115$ n5 Rd/s.
- The first layer (the water, essentially the oceans): density 1.02 g/cm^3 ; global mean depth 2750 m.
- The following limits on inner densities: 2.6 g/cm^3 $\leq$ density $\leq$ 15 g/cm^3.

The limits on $(C_B - A_B)$ are then given by the two extreme cases with only three homogenous layers the outer one being the ocean.

Maximum of $C_B - A_B$:

(43)

radius (km)	density (g/cm^3)
6371.2	
	1.02
6368.45	
	4.266 843
3112.732	
	15
0	

$C_B - A_B = 1.077\,408$ n3 MR^2

Minimum of $C_B - A_B$:

$$(44)\quad \left\{\begin{array}{ll} \text{radius (km)} & \text{density (g/cm}^3\text{)} \\ 6371.2 & \\ & 1.02 \\ 6368.45 & \\ & 2.6 \\ 5225.794 & \\ & 7.885\,025 \\ 0 & \end{array}\right\} C_B - A_B = 1.070\,805\ \text{n3}\ MR^2 .$$

In these conditions the realistic model with ten homogeneous layers presented in appendix 2 gives an accurate result, very near to the minimum (44):

$$(45)\quad C_B - A_B = 1.070\,978\ \text{n3}\ MR^2.$$

These results (43)–(45) correspond to the present value H_P of the Earth's angular momentum H. They would be practically proportional to H^2 for neighbouring values of H.

We are thus led to the following expression of $M_B - M_A$:

$$(46)\quad M_B - M_A = MR^2 \left\{ (U_B - U_A) \begin{bmatrix} 1 & 0 & 0 \\ 0 & 1 & 0 \\ 0 & 0 & 1 \end{bmatrix} + 1.070\,978\ \text{n3}\ \frac{H^2}{H_P^2} \begin{bmatrix} \left(\alpha^2 - \frac{1}{3}\right); & \alpha\beta\,; & \alpha\gamma \\ \alpha\beta\,; & \left(\beta^2 - \frac{1}{3}\right); & \beta\gamma \\ \alpha\gamma & \beta\gamma & \left(\gamma^2 - \frac{1}{3}\right) \end{bmatrix} \right\}$$

$U_B - U_A$ is of the order of n6 and we will see in the next two sections that this difference is useless while the accuracy of (45) and (46) is superabundant.

The remaining matrix R

The "remaining matrix R" of (36) is composed of two terms: the second order terms of (35) and the difference $M - M_D$.

The second order terms are of the order of $(M_B - M_A)(M_D - M_B)/MR^2$ that is about n8 MR^2, *i.e.* less than $M - M_D$. The difference $M - M_D$ is given by the discrepancies between the true Earth and its isostatic equilibrium.

The discrepancy corresponding to the CHANDLER effect (see above with (25)) is very small, a few n10 MR^2, but it will become of the order of the above terms for large disequilibria. The discrepancy corresponding to re-equilibrium motions such as the recent upward motion of Scandinavia are of the order of a few n8 MR^2, and their time scale is only a few millenia. The global discrepancies can be larger but their time scale is only about one century (these discrepancies have a time scale proportional to the inverse of their width).

Hence we can model the remaining matrix R as follows. During the periods of tectonic quiescence on Earth the matrix M_C is quasi-constant and R is at most of the order of n7 MR^2. If the Earth and the matrix M_C undergo large variations (*i.e.* variations larger than n7 MR^2 per millenium) the remaining matrix R can be larger than n7 MR^2 and can remain above this level for a few centuries after the period of large variations.

THE MATRIX M_C

The matrix M_C is quasi-constant during the periods of tectonic quiescence on Earth and, with (32), (36), (41), (46) we can obtain its present value corresponding to $\alpha = \beta = 0$; $\gamma = 1$:

(47) $M_C = M - (M_B - M_A) - R; \qquad R = O\,(\text{n7 } MR^2).$

Hence:

$$(48)\quad M_C = MR^2 \begin{bmatrix} U_C - 7.032\,\text{n6} & 1.807\,\text{n6} & 0 \\ 1.807\,\text{n6} & U_C - 7.34\,\text{n7} & 0 \\ 0 & 0 & U_C + 7.766\,\text{n6} \end{bmatrix} + O\,(\text{n7}.MR^2)$$

with:

(49) $U_C = U - U_B + U_A = 0.329\ 956 \pm \text{n6}.$

The corresponding main moments of inertia are then:

$$(50)\quad \begin{cases} A_C = (U_C - 7.514\,\text{n6} \pm \text{n7})\,MR^2 \\ B_C = (U_C - 2.52\,\text{n7} \pm \text{n7})\,MR^2 \\ C_C = (U_C + 7.766\,\text{n6} \pm \text{n7})\,MR^2\,. \end{cases}$$

Thus C_C is the largest main moment of inertia and its axis is along the present Earth's axis of rotation. This classical situation of stability will be shown essential for the present stability of the Earth's rotation.

THE EARTH INERTIA MATRIX M

Let us recall that M is given by (36) that is by:

(51) $M = M_C + (M_B - M_A) + R,$

with $(M_B - M_A)$ given in (46) where (α, β, γ) is the unit vector of the Earth's axis of rotation.

During the periods of tectonic quiet on Earth the matrix M_C is almost constant while R remains smaller than n7 MR^2. But R can be larger when M_C has variations faster than n7 MR^2 per millenium.

The mean values U, U_A, U_B, U_C are all within $0.329956 \pm$ n6. They are thus less accurately known but this will have no effect.

The present value of M is given in (32) with an accuracy of a few n10 MR^2 except for U. This allows us to obtain, with (46), the matrix M with almost the same accuracy for directions (α, β, γ) different from (0, 0, 1):

$$(52)\quad M = MR^2 \left\{ \begin{bmatrix} U - 3.640249\text{n}4 & 1.8074\text{n}6 & 0 \\ 1.8074\text{n}6 & U - 3.577266\text{n}4 & 0 \\ 0 & 0 & U + 7.217515\text{n}4 \end{bmatrix} + 1.070978\text{n}3 \begin{bmatrix} \alpha^2 & \alpha\beta & \alpha\gamma \\ \alpha\beta & \beta^2 & \beta\gamma \\ \alpha\gamma & \beta\gamma & \gamma^2 - 1 \end{bmatrix} \right\}$$

with U = 0.329 956 ± n6.

THE ANGLE BETWEEN THE ROTATION VECTOR $\vec{\omega}$ AND THE EARTH'S ANGULAR MOMENTUM $\vec{H}$

The vector $\vec{\omega}$ is the rotation vector of the rotating set of axes Oxyz of Figure 5 with respect to the non-rotating set of axes OXYZ of Figure 6.

We will call ω_1, ω_2, ω_3 the components of $\vec{\omega}$ in Oxyz; hence from (40):

$$(53)\quad \vec{\omega} = (\omega_1, \omega_2, \omega_3) = (\omega\alpha, \omega\beta, \omega\gamma).$$

Let us consider an element dm of the Earth's mass with a radius vector $\vec{r}(t)$ in the Oxyz rotating set of axes. This mass dm will have a relative velocity $\vec{v}$ with respect to Oxyz and an absolute velocity $\vec{V}$ with respect to OXYZ.

$$(54)\quad \begin{cases} \vec{v} = \dfrac{d\vec{r}}{dt} \\ \vec{V} = \vec{\omega} \times \vec{r} + \vec{v}. \end{cases}$$

In the analysis of $\vec{v}$ we find:

The motions related to plate tectonics (velocity: a few centimeters per year);

The general motion of Earth mantel (velocity: a few meters per year);

The quasi-periodic motions related to the tides of the crust (amplitude up to one meter; periods from a few hours to a few years);

The motions of the oceans and the atmosphere: quasi-periodic tidal motions, permanent currents and winds, seasonal currents and winds, meteorology.

Let us call $\vec{H}$ the angular momentum of Earth.

$$(55)\quad \vec{H} = \int_M dm\, \vec{r} \times \vec{V}; \qquad M = \text{mass of Earth}.$$

Since $\vec{V} = \vec{\omega} \times \vec{r} + \vec{v}$ we can write:

$$(56)\quad \vec{H} = \vec{H}_\omega + \vec{H}_v$$

with, M being the Earth's inertia matrix:

(57) $\vec{H}_\omega = \int_M dm\, \vec{r} \times (\vec{\omega} \times \vec{r}) = M\vec{\omega}$

and:

(58) $\vec{H}_v = \int_M dm\, \vec{r} \times \vec{v}$.

The z-component of $\vec{H}_\omega$ is about 5.859 89 p33 kg m^2 s^{-1} and we can decompose $\vec{H}_v$ into a main quasi-periodic part $\vec{H}_{qp}$ given by the tides and a remaining erratic part $\vec{H}_{er}$ given mostly by the oceanic currents. For instance the famous "Pacific Equatorial Under-Current" gives a component of about 1.5 p24 kg m^2 s^{-1} that is more than the combined effects of plate tectonics and motions in the Earth's mantle. The Gulf Stream and the Kuro Shivo give, in other directions, components of the same order of magnitude. The general tidal motions give a much larger component, up to p27 kg m^2 s^{-1}, and we can thus model $\vec{H}_v$ by the following:

(59) $\vec{H}_v = \vec{H}_{qp} + \vec{H}_{er}$,

$\vec{H}_{qp}$: quasi-periodic component, periods from a few hours to a few years, modulus < p27 kg m^2 s^{-1},

$\vec{H}_{er}$: erratic and long period component, modulus < 5 p24 kg m^2 s^{-1}.

For the angle $(\vec{H}, \vec{\omega})$ we find:

The angle $(\vec{H}, \vec{H}_\omega)$ remains smaller than or equal to $|\vec{H}_v|/|\vec{H}_\omega|$ that is less than 2 n7 radian.

The angle $(\vec{H}_\omega, \vec{\omega})$ given by:

(60) $\begin{cases} \vec{H}_\omega = M\vec{\omega} \\ M = M_C + (M_B - M_A) + R . \end{cases}$

The main part of M is, by far, M_C, while $(M_B - M_A)\,\vec{\omega}$ is parallel to $\vec{\omega}$.

The component $R\vec{\omega}$ introduces a new angle less than 3 n7 radian and the typical example (48) giving the present M_C shows that the angle $(M_C\,\vec{\omega}, \vec{\omega})$ remains small, less than a few n5 radian, *i.e.* a few seconds of arc.

Hence, at least during the periods of tectonic quiet on Earth, the angle $(\vec{H}, \vec{\omega})$ remains extremely small, smaller than 5″ or 10″. This limit is of course larger when the Earth's crust and the matrix M_C have fast variations but 1′ or 2′ seems a good upper limit for all cases.

Thus, in order to know the motions of the poles with respect to the Earth's crust with an accuracy of 1′ or 2′, it is sufficient to look for the evolution of the Earth angular momentum $\vec{H}$ with respect to the set of axes Oxyz rotating with Earth.

EVOLUTION OF THE EARTH'S ANGULAR MOMENTUM $\vec{H}$ WITH RESPECT TO THE ROTATING SET OF AXES OXYZ

Case of an isolated Earth

If the Earth were isolated its angular momentum $\vec{H}$ would be constant in the non-rotating axes OXYZ and its evolution with respect to the axes Oxyz rotating with Earth would be simple.

(61) $$0=\left(\frac{d\vec{H}}{dt}\right)_{OXYZ}=\left(\frac{d\vec{H}}{dt}\right)_{Oxyz}+\vec{\omega}\times\vec{H}$$

that is:

(62) $$\left(\frac{d\vec{H}}{dt}\right)_{Oxyz}=-\vec{\omega}\times\vec{H}=\vec{H}\times\vec{\omega}.$$

However, with (56), (57) (59):

(63) $$\begin{cases}\vec{H}=\vec{H}_{\omega}+\vec{H}_{qp}+\vec{H}_{er}\\ \vec{H}_{er}:\ \text{erratic component smaller than } 5\,\text{p}24\ \text{kg m}^2\,\text{s}^{-1}\\ \vec{H}_{qp}:\ \text{quasi-periodic component smaller than p}27\ \ \text{kg m}^2\,\text{s}^{-1}\\ \vec{H}_{\omega}=M\vec{\omega}:\ \text{modulus about } 5.86\,\text{p}33\ \text{kg m}^2\,\text{s}^{-1}\end{cases}$$

and thus:

(64) $$\left(\frac{d\vec{H}}{dt}\right)_{Oxyz}=(M\vec{\omega}+\vec{H}_{qp}+\vec{H}_{er})\times\vec{\omega}.$$

The term $\vec{H}_{er}\times\vec{\omega}$ is very small (an erratic polar displacement of less than 13 m per year).

The term $\vec{H}_{qp}\times\vec{\omega}$ is larger but quasi-periodic with an average equal to zero. Its average effect in one month is already very small and its average effect in a few years is negligible.

The remaining term $(M\vec{\omega})\times\vec{\omega}$ can be considered accurately with the present expression of M given in (52).

This expression gives a negligible polar displacement for the present polar position, but it also gives a polar displacement of almost 340 km per year for poles at the worst position (This large velocity is of course theoretical, see for instance the analysis presented with Figure 10.)

This result emphasizes the importance of the notion of "stable equilibrium position" of the poles.

Let us neglect the $\vec{H}_{qp}$ and $\vec{H}_{er}$ terms and let us use the decomposition (51):

(65) $M = M_C + (M_B - M_A) + R.$

The product $[(M_B - M_A)\,\vec{\omega}]\times\vec{\omega}$ is always zero and thus the main term of $\frac{d\vec{H}}{dt}$ in Oxyz is:

(66) $$\left(\frac{d\vec{H}}{dt}\right)_{Oxyz}=\{M_C\vec{\omega}+R\vec{\omega}+\vec{H}_{qp}+\vec{H}_{er}\}\times\vec{\omega}\approx\{M_C\vec{\omega}\}\times\vec{\omega}.$$

This equation, with constant M_C, also appears in the classic Euler-Poinsot theory of the rotation of a free and invariable solid (with inertia matrix M_C) about its center of mass. Hence the stable equilibrium positions of the poles are on the main axis of largest inertia of M_C and this is precisely the situation of Earth as shown by (48)–(50). The consideration of outer torques in the next section will not modify this result.

INFLUENCE OF OUTER TORQUES

The Earth is not isolated, it undergoes many torques.

The main torques are given by the attraction of outer bodies, especially the Sun and the Moon. The other torques, such as the electromagnetic torque due to the solar electromagnetic field, are much smaller (at most a few billionths of the main torques) and we will neglect them.

Let us first consider the solar gravitational torque $\vec{T}_S$.

S is the Earth-Sun distance and $\vec{S}$ the Earth-Sun vector (Fig. 7).

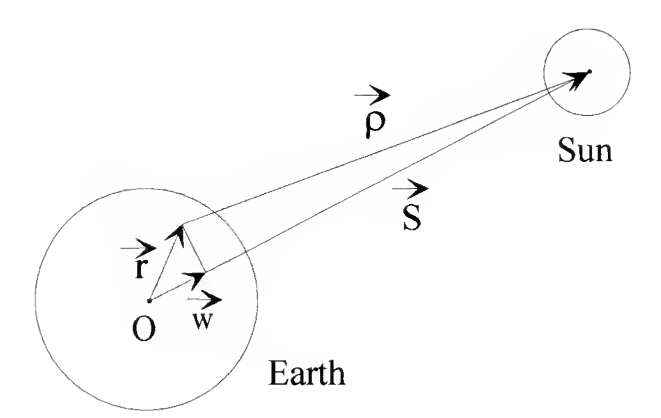


FIG. 7. — Study of the solar gravitational torque $\vec{T}_S$.

The elementary mass dm is at the radius vector $\vec{r}$ and the classical expression of the solar tidal force $\vec{F}_S$ dm is:

(67) $$\vec{F}_S\,dm = \mu_S\,dm\left(\frac{\vec{\rho}}{\rho^3} - \frac{\vec{S}}{S^3}\right)$$

with:

(68) $$\begin{cases} \mu_S = 1.327\,124\,38\text{ p}20\text{ m}^3\,\text{s}^{-2} = \text{solar gravitational constant} \\ \vec{\rho} = \vec{S} - \vec{r} = \text{vector from the mass dm to the Sun} \\ \rho = |\vec{\rho}| \end{cases}$$

Let us put:

(69) $$\vec{w} = \left(\frac{\vec{r}\vec{S}}{S}\right).\frac{\vec{S}}{S} = \text{projection of } \vec{r} \text{ on } \vec{S}.$$

Then:

(70) $$\vec{F}_S\,dm = \frac{\mu_S}{S^3}\,dm\left[3\,\vec{w} - \vec{r} + O\left(\frac{r^2}{S}\right)\right]$$

and the solar gravitational torque $\vec{T}_S$ is:

$$(71)\quad \vec{T}_S = \int_{\text{Earth mass}} \vec{r} \times \vec{F}_S \, dm \approx \frac{3\mu_S}{S^3} \int_M \vec{r} \times \vec{w} \, dm.$$

Let us call $\vec{u} = (u_1, u_2, u_3)$ the unit vector of the direction of the Sun in the Oxyz set of axes.

$$(72)\quad \vec{u} = \frac{\vec{S}}{S}; \quad \vec{w} = \vec{u}(\vec{r} \cdot \vec{u}); \quad u_1^2 + u_2^2 + u_3^2 = 1.$$

Hence, with the approximation of (71):

$$(73)\quad \vec{T}_S = \frac{3\mu_S}{S^3} \int_M dm \begin{pmatrix} x \\ y \\ z \end{pmatrix} \times \begin{pmatrix} u_1 \\ u_2 \\ u_3 \end{pmatrix} \cdot (xu_1 + yu_2 + zu_3),$$

that is:

$$(74)\quad \vec{T}_S = \frac{3\mu_S}{S^3} \begin{cases} (u_1u_3I_{xy} - u_1u_2I_{xz} + u_2u_3I_{y^2-z^2} + (u_3^2 - u_2^2)\, I_{yz}) \\ (u_1u_2I_{yz} - u_2u_3I_{xy} + u_1u_3I_{z^2-x^2} + (u_1^2 - u_3^2)\, I_{xz}) \\ (u_2u_3I_{xz} - u_1u_3I_{yz} + u_1u_2I_{x^2-y^2} + (u_2^2 - u_1^2)\, I_{xy})\,. \end{cases}$$

In the set of axes Oxyz used the components u_1, u_2, u_3 and the torque $\vec{T}_S$ have very fast daily variation. However, if we only consider the outer torque $\vec{T}_S$, the equations (61), (62) become:

$$(75)\quad \vec{T}_S = \left(\frac{d\vec{H}}{dt}\right)_{OXYZ} = \left(\frac{d\vec{H}}{dt}\right)_{Oxyz} + \vec{\omega} \times \vec{H},$$

$$(76)\quad \left(\frac{d\vec{H}}{dt}\right)_{Oxyz} = \vec{H} \times \vec{\omega} + \vec{T}_S.$$

The term $\vec{H} \times \vec{\omega}$ has already been analysed in the previous section. Its main part is $(M_C\,\vec{\omega}) \times \vec{\omega}$ equivalent to $(M_C\,\vec{\omega}) \times \vec{\omega}$.

The daily variations of $\vec{T}_S$ have little importance of course, and we essentially need the daily averaged value of $\vec{T}_S$.

We will assume that the Oxyz rotation vector $\vec{\omega}$, that is also practically the Earth's rotation vector, is in the direction of Oz or in its immediate vicinity. Since the orientation of Oxyz is arbitrary this condition can always be satisfied after, if necessary, a suitable modification of the Oz direction.

The component u_3 is then fixed, or very slowly variable, while u_1 and u_2 essentially have a daily sinusoidal evolution.

The daily averaged values of u_1u_2, u_1u_3 and u_2u_3 are almost zero while these of u_1^2 and u_2^2 are $(1 - u_3^2)/2$.

Hence, with these Oxyz axes:

$$(77) \quad \vec{T}_{S,\,\text{daily averaged}} \approx \frac{3\mu_S}{S^3}\,\frac{1-3u_3^2}{2}\begin{pmatrix} -I_{yz} \\ I_{xz} \\ 0 \end{pmatrix}.$$

Notice that with the same Oxyz axes:

$$(78) \quad \vec{H} \times \vec{\omega} \approx (M\vec{\omega}) \times \vec{\omega} = \omega^2 \begin{pmatrix} -I_{yz} \\ I_{xz} \\ 0 \end{pmatrix}.$$

These two vectors appearing in (76) have the same direction but the second is much larger: at least 40 000 times larger. The effect of the solar gravitational torque $\vec{T}_S$ is negligible and this conclusion remains true even if we take into account the final term that was neglected in (70).

The same analysis can be done, with a similar conclusion, for the lunar gravitational torque and for all outer torques undergone by Earth.

Notice that this conclusion would not be true for an analysis of the evolution of the angular momentum $\vec{H}$ with respect to the non-rotating set of axes OXYZ. In this set of axes the components of the unit vector $\vec{u}$, equal to $\frac{\vec{S}}{S}$, would not have a fast daily variation and we would thus reach the motions of the poles with respect to the stars: nutation and precession.

MODIFICATIONS OF THE EARTH'S INERTIA MATRIX BY THE OROGENY OF A LARGE MOUNTAIN RANGE

It is essential to take the isostatic equilibrium into account in the analysis of the variations of the Earth's inertia matrix. This equilibrium reduces very much the possible variations that nevertheless are not at all negligible.

Let us consider the orogeny of the Himalaya range. That range is classically considered as the result of the collision between the plates of Asia and India (Fig. 8).

Between the two plates the northward motion of India pushes the Earth's crust partly upwards and partly downwards (because of the isostatic compensation); while behind India we have the opposite transformation: a thin oceanic crust takes the place of a thick continental crust. These two opposite evolutions combined with the isotatic equilibrium reduce to almost nothing (about a billionth) the variations of the average Earth's moment of inertia that is (A + B + C)/3. However this is not true for each moment of inertia and also for the products of inertia.

Let us for instance consider the product of inertia I_{yz}.

Let us call v the local volumic mass, g the local intensity of gravity and h the local altitude.

If D is the depth of the compensation level, the isostatic equilibrium can be written along any vertical:

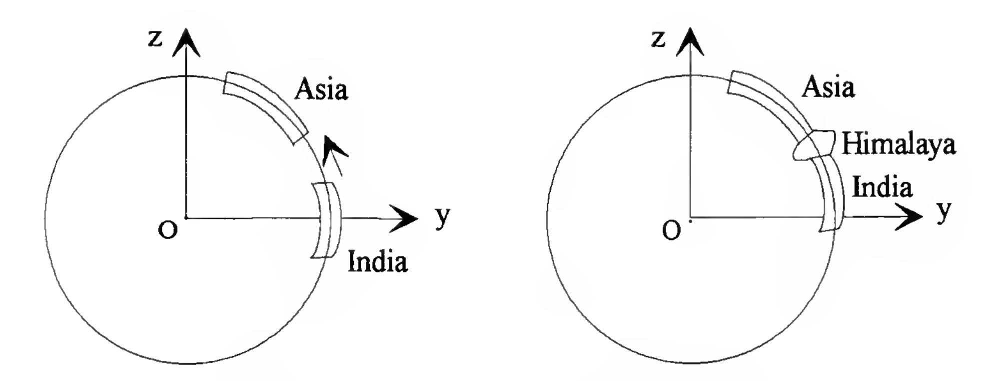


FIG. 8. — The Asia-India collision and the orogeny of Himalaya.

(79) $\int_{-D}^{+50\,km} v\, g\, dh = P_c$ = pressure at the compensation level

(above 50 km, in the stratosphere, the volumic mass v is negligible).

Hence along any vertical the passage from the volumic mass $v_1(h)$ to the volumic mass v_2 (h) must satisfy the following isostatic condition:

(80) $\int_{-D}^{+50\,km} (v_2 - v_1)\, g\, dh = 0.$

The product of inertia I_{yz} is defined by:

(81) $I_{yz} = \int_{Earth's\,volume} v\, y\, z\, dx\, dy\, dz.$

That is, with the ordinary geocentric spherical coordinates r, φ, L defined in (13):

(82) $$\begin{cases} y = r \cos \varphi \sin L\,; \quad z = r \sin \varphi \\ dx\ dy\ dz = r^2 \cos \varphi\, dr\, d\varphi\, dL \\ I_{yz} = \int_{Earth's\ volume} v\, r^4 \cos^2 \varphi \sin \varphi \sin L\, dr\, d\varphi\, dL \end{cases}$$

and the variation of the product of inertia I_{yz} is then:

(83) $\Delta I_{yz} = (I_{yz})_2 - (I_{yz})_1 = \int_{Earth's\ volume} (v_2 - v_1)\, r^4 \cos^2 \varphi \sin \varphi \sin L\, dr\, d\varphi\, dL.$

We must of course take the isostatic condition (80) into account along any vertical.
This condition gives along any radial direction:

(84) $\int_{R_{p-D}}^{R+50\,km} (v_2 - v_1)\, g \cos \varepsilon\, dr = 0$

with:

(85) $\begin{cases} R = \text{equatorial radius} = 6\,378\,136 \text{ m} \\ R_p = \text{polar radius} = 6\,356\,751.3 \text{ m} \\ \varepsilon = \text{angle between the vertical and the radial directions.} \end{cases}$

The angle ε remains everywhere smaller than 13′ and its cosine remains between 1 and 0.999992.

With $v_2 - v_1 = 0$ when $r < R_P - D$ and with the definition of triple integrals this equation (84) leads to:

(86) $\int_{\text{Earth's volume}} (v_2 - v_1)\ g \cos\varepsilon\ dr.\ \cos^2\varphi \sin\varphi \sin L\ d\varphi\ dL = 0.$

In a small dφdL pyramid starting from the center of mass the coefficient of $(v_2 - v_1)$ $\cos^2\varphi \sin\varphi \sin L\ dr d\varphi dL$ is r^4 in (83) and $g \cos\varepsilon$ in (86).

These two coefficients vary in opposite directions when r varies in the range

$$R_P - D < r < R + 50 \text{ km}$$

(even if $g \cos\varepsilon$ is there almost constant as shown in Table 1).

It is this variation of the ratio $r^4/g \cos\varepsilon$ in terms of r that is the source of the variations of the Earth's moments and products of inertia. Without it the Earth's inertia matrix would be constant for all states of isostatic equilibrium and, since there exist isostatic equilibria with a symmetry of revolution about the polar axis, all isostatic equilibria would then have equal equatorial main moments of inertia instead of the present difference $B - A = 7.26$ n6 MR^2 (with M = mass of the Earth).

Which value can we give to the difference $(v_2 - v_1)$?

In the orogeny of the Himalaya range and its vicinity the seabed (average depth 3.8 km) has been pushed up over a large region.

That region – Himalaya range, Tibet plateau, Hindu-Kush, Karakoram, Pamir, Kunlun, Chamdo, Quinghai, etc. – has an area of about 10 millions of square kilometers and an average altitude of 2800 m (The average altitude of all Asia is 1000 m while that of Europe is only 300 m).

Thus over that region that we will call "H" we can estimate ΔI_{yz} with:

(87) $\begin{cases} v_2 - v_1 = 2600 \text{ kg/m}^3 \text{ between the altitudes 0 and 2800 m} \\ v_2 - v_1 = 1600 \text{ kg/m}^3 \text{ between the altitudes } -3800 \text{ m and 0.} \end{cases}$

Of course, because of (84) that is of the isostatic equilibrium, the difference $(v_2 - v_1)$ must be negative somewhere below, around the bottom of average continental plates at depths of about 300 km.

Hence for the Himalaya region and its surroundings, the region "H", we can write with (83), (86) and with an arbitrary constant K:

(88) $\Delta I_{yz} = \int_H (v_2 - v_1)\ dr\ d\varphi\ dL \cos^2\varphi \sin\varphi \sin L\ [r^4 - K\ g \cos\varepsilon].$

We will choose K such that the factor ($r^4 - K\ g \cos \varepsilon$) is zero in the middle of the depths where ($v_2 - v_1$) is negative. Hence for these depths the integral ΔI_{yz} will be negligible.

We can also neglect the small variations of g cos ε and since these variations are in the opposite direction of the variations of r^4 our computation will give a lower bound of ΔI_{yz}.

Hence, with $K\ g \cos \varepsilon = r_0^4$:

$$(89) \quad \Delta I_{yz} \approx \int_{R_M-3800\ m}^{R_M+2800\ m} (v_2 - v_1)\, dr\, (r^4 - r_0^4) \int_H \cos^2 \varphi \sin \varphi \sin L\, d\varphi dL$$

with:

$$(90) \quad \begin{cases} R_M = \text{mean Earth radius} = 6371\ \text{km} \\ r_0 = R_M - 300\,\text{km} \\ \begin{cases} (v_2 - v_1) = 2600\text{kg/m}^3 & \text{for} \quad R_M < r < R_M + 2800\,\text{m} \\ \qquad\qquad = 1600\,\text{kg/m}^3 & \text{for} \quad R_M - 3800\,\text{m} < r < R_M \end{cases} \\ \int_H \cos \varphi\, d\varphi\, dL = (\text{area of H})/R_M^2 = \text{p7 km}^2/[6371\ \text{km}]^2 \\ \cos \varphi \sin \varphi \sin L = yz/r^2 : \text{ with an average value of } 0.45 \text{ in H}. \end{cases}$$

We thus obtain finally for the H region:

$$(91) \quad \Delta I_{yz} = 4.28\ \text{p32 kg.m}^2 = 1.76\ \text{n6 MR}^2.$$

To this variation of the product of inertia I_{yz} in the region H we must add the variation obtained behind the Indian plate where a thin oceanic plate takes the place of a thick continental plate.

The signs of ($v_2 - v_1$) are there opposite but so are the signs of the factor cosφ sinφ sinL with a negative sin φ. Hence the two variations ΔI_{yz} have the same sign and their sum is about 3 n6 MR^2, which is of course a rough estimation. (Notice the essential role of the factor cos φ sin φ sin L that is yz/r^2. Without that factor the computation would give the variation of the average moment of inertia (A + B + C)/3 and we have seen that this variation is negligible; its two components, before and behind the Indian plate, are almost opposite.)

The Earth's crust can easily bear such a dissymmetry, even under the condition of isostatic equilibrium; today it bears the larger difference B – A = 7.26 n6 MR^2 between its two equatorial main moments of inertia. But the Earth's rotation reacts rapidly to this non-zero product of inertia I_{yz} as we will see in the next section.

Variations of the Earth's moments of inertia of the same order of magnitude, or even a little larger, are obtained in the outstanding study of RICARD *et al.* (1993). However these authors consider that the main source of these variations is the motion of downgoing slabs during subductions.

Whatever the source of these variations they imply large polar displacements.

REACTION OF THE EARTH'S ROTATION TO A DISSYMMETRY OF THE EARTH'S INERTIA MATRIX

The Earth's reaction to a dissymmetry of its inertia matrix is of course a very complex phenomenon. We have already considered that reaction and we can at least notice the following points.

The equations (61)-(66) and (75)-(78) are obtained by the application of the general theorems of Mechanics. They are rigorous and can be applied to any type of body: rigid, elastic, plastic, viscous, fluid, mixed, etc. These equations are in agreement with the Euler linearized equations, and this was of course a necessary condition, but they are valid even for a viscous Earth and for a large drift of the poles. They are of course the only equations that can be written for a viscous Earth without a detailed rheology study. The main discussion is that of the relative importance of the four terms of (66) that is:

$$(92) \quad \left(\frac{d\vec{H}}{dt}\right)_{Oxyz} = \{M_C\vec{\omega} + R\vec{\omega} + \vec{H}_{qp} + \vec{H}_{er}\} \times \vec{\omega} \approx \{M_C\vec{\omega}\} \times \vec{\omega}\,.$$

For a long-term uniform rotation about a fixed Earth's axis the main term of (92) is, by far, the term $M_C\vec{\omega}$ and this shows that the stable Earth's rotation is about the main axis of largest inertia of matrix M_C. Notice that this rotation corresponds also, very naturally, to the minimum of mechanical energy for a given angular momentum.

This rotation is precisely that given by the Earth's model Grim4 (REIGBER *et al.* 1993) with its coefficients given in (20). It is also extremely near to the rotation given by the GODDARD Earth's model 9 (LERCH *et al.* 1979) with its coefficients given in (22): there is then less than 100 m between the poles and their positions of stable equilibrium. This present Earth's situation is obviously a very strong indication.

The existence of a large equatorial bulge of course opposes a strong resistance to the motion of the poles towards a new position of stable equilibrium after the orogeny of a large mountain range; and it is precisely because the Earth is viscous (on the long term) that its poles can move towards the new position of stable equilibrium with successive isostatic deformations of the equatorial bulge.

In the discussion of the motion given by (92) the three small terms can become more important when the rotation is not a pure rotation about a fixed Earth's axis, especially the $R\vec{\omega}$ term that is related to the successive deformations of the equatorial bulge. However these three small terms correspond to losses of energy and these losses are large for non-stable rotations. The march towards stability is then unavoidable even if the path followed by the poles depend very much on the Earth's properties (Fig. 9).

Let us look more carefully at the influence of the equatorial bulge. Let us assume for instance that at some initial time t_0 the Earth has a stable rotation about the axis leading from the city of Madrid to its antipode in the North island of New Zealand, and let us assume that suitable orogenies give to its crust a new shape corresponding to the present matrix M_C of the "non-rotating Earth in isostatic equilibrium" (Fig. 4C). Hence the theoretical stable rotation becomes about the present North Pole-South Pole axis. This is of course a very artificial assumption but it will allow to give a better idea of the reaction of the Earth's rotation.

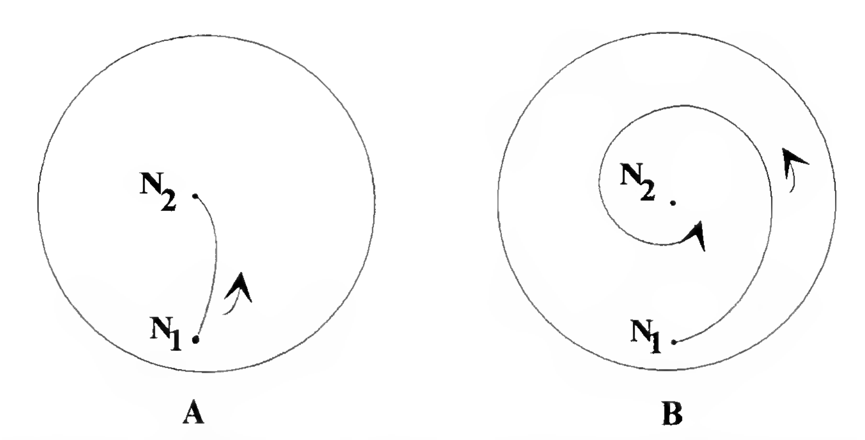


FIG. 9. — March of the North pole towards a new position N_2 of stable equilibrium after a variation of the Earth's crust. A, march for a very viscous Earth. B, march for a very fluid Earth. In the absence of a detailed rheology study it is impossible to guess the path that will be followed, however the large losses of energy corresponding to non-pure stable rotations will lead more or less rapidly to the vicinity of the stable equilibrium.

At the initial time t_0 the Earth has a large equatorial bulge corresponding to the Madrid-New Zealand axis and very similar to the present equatorial bulge. This bulge stabilizes the Earth's rotation very much and, since it is about 300 times larger than the considered Earth's modifications, the variations of the Earth's rotation are initially weak. Under the condition of isostatic equilibrium the initial Earth's inertia matrix M is given in (52) with the direction cosines α, β, γ corresponding to the geocentric direction of Madrid ($\alpha_M = 0.76189$; $\beta_M = -0.04949$; $\gamma_M = 0.64581$).

If the Earth were rigid after t_0 its rotation would be an Euler-Poinsot motion corresponding to the inertia matrix M: the North pole would remain in the vicinity of Madrid and starting from Madrid it would describe a small "polhode" that is then almost a circle with center near the small city of Torrelaguna at the point T (Fig. 10). That point T corresponds to the main axis of smallest inertia, it is only 44.0 km north of Madrid and 6.3 km east of Madrid. The motion of the North pole would be counter-clockwise along the polhode with a period given by (25) that is about 300 days.

If the Earth were perfectly elastic the motion would be similar but with a longer period (CHANDLER effect), a period of 400 or 450 days.

However the Earth is neither rigid nor perfectly elastic and we can expect the two following effects.

Notice that between a pole at M (Madrid) and at the opposite point N (Fig. 10) the equilibrium sea-level has variations reaching almost 300 meters. The Earth's elasticity reduces these variations to about 200 meters, but nevertheless they are sufficiently large to give a great complexity to the Earth's rotation and the corresponding large losses of energy lead to a North Pole at a medium position in the vicinity of T.

Meanwhile the condition of isostatic equilibrium slightly modifies the equatorial bulge. The local isostatic re-equilibria, as the present upward motion of Scandinavia, have a rather short relaxation time (a few millenia for Scandinavia) and the global isostatic re-equilibria, as the modification of the equatorial bulge, have a shorter relaxation time of one or two centuries only (because this relaxation time is roughly proportional to the width of the affected zone).

Hence after one or two centuries the equatorial bulge corresponds to a North Pole in the vicinity of T, instead of M (Fig. 10) and the Earth's inertia matrix M given in (52) must now use the direction cosines α_T, β_T, γ_T instead of α_M, β_M, γ_M. This matrix M gives a main axis of largest inertia corresponding to a point in the vicinity of N, instead of T, and thus another move of the pole towards north must be expected in the next centuries for exactly the same reasons.

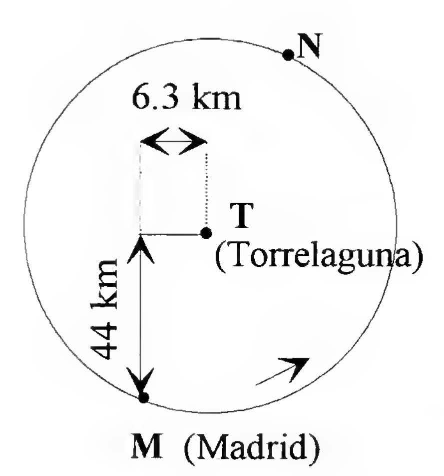


FIG. 10. — Hypothesis of a rigid Earth; an example of polhode (curve described by the North Pole). The period of this motion is about 300 days.

This evolution is repeated again and again as long as the axis of the equatorial bulge differs from the main axis of largest inertia, that is until the arrival of the poles at their position of stable equilibrium and there is no such position before the present position poles.

Thus, in spite of the existence of a large equatorial bulge, the viscosity of the Earth and its tendency to the isostatic equilibrium allow a more or less fast move of the two poles towards their positions of stable equilibrium, positions that correspond to the main axis of largest inertia of the "non-rotating Earth in isostatic equilibrium" (Fig. 4C).

Of course the complexity of the Earth's inner motions, with its elasticity, its plasticity and its viscosity, as well as the large transgressions and regressions of sea-level that must be expected during the phases of variable rotation and of isostatic re-equilibria forbid to obtain a simple description of the evolution.

Our only solid elements are the general theorems of Mechanics, explicited in (61)-(66) and (75)-(78), and the tendency towards the state of minimum energy (for the given value of the Earth's angular momentum) because of the large losses of energy associated to non-pure rotations.

This section allows us to give an approximate value of the relaxation time of the march of the pole towards its position of stable equilibrium. If B_C and C_C are the two largest main moments of inertia of the "non-rotating Earth in isostatic equilibrium" the relaxation time is roughly proportional to $[C_C - B_C]^{-1}$ and it is about 100000 years when the difference $C_C - B_C$ is a few n6 MR^2.

A variation of moments and products of inertia of the order of n6 MR^2 (that is a millionth of the product MR^2) requires a very powerful orogeny, as shown in the previous section. Such

an orogeny will usually take millions of years and then the poles will follow very nearly and very slowly their position of stable equilibrium.

Notice that the drift of the poles can be large, for instance the orogeny of the Himalaya range (analysed above, Fig. 8) has modified A_C, B_C, C_C, M_C by about 3 n6 MR^2, even if we only consider isostatic situations. This must be compared to the present $C_C - A_C$ (*i.e.* 1.53 n5 MR^2) and $C_C - B_C$ (8.02 n6 MR^2). A modification of about 20° in the position of the North Pole (from Siberia to the present position) was likely if it was not offset by other orogenies. (The present matrix M_C is given in (48) and its $(-I_{yz})$ components are zero. The main effect of the Himalaya orogeny is an increase of the product of inertia I_{yz} of about 3 n6 MR^2 and hence the $(-I_{yz})$ components were about 3 n6 MR^2 before the orogeny. The corresponding matrix M_C had a main axis of largest inertia (eigenvector of the largest eigenvalue) oriented toward the point 72° North and 83° East near the present mouth of the Yenisei river.)

Also notice that, with the difference $C_C - B_C$ having the large value 8.02 n6 MR^2, the Earth presently has a rather good stability without immediate threat of large disequilibrium. However with a much smaller difference $C_C - B_C$ (and the hydrostatic equilibrium gives $A_C = B_C = C_C$) the position of the poles would be very unstable. This was perhaps the case at some past periods.

CONCLUSION

The study of the Earth's rotation and of the displacement of its poles over geological time is a complex but also very beautiful undertaking implying many domains of science from astronomy, mechanics and space dynamics to geology, geophysics, rheology and seismology. The positions of poles at the Earth's surface are usually very near to their positions of stable equilibrium which are given by the main axis of largest inertia of the "non-rotating Earth in isostatic equilibrium". The corresponding relaxation time is usually about 100 000 years.

The stable equilibrium positions depend very much on the variations of the Earth's crust and the poles have certainly moved much more than the different lithospheric plates. Large orogenies and/or large subductions can move the poles by tenths of degrees within a few million years. We can hope that plate tectonics and paleogeography will be able to yield an accurate description of the successive polar shifts.

Acknowledgements – Remerciements

Je suis heureux de pouvoir remercier ici Messieurs Hervé LELIÈVRE et Martin PICKFORD du Laboratoire de Paléontologie du Muséum national d'Histoire naturelle qui m'ont donné l'idée de ce travail et la possibilité de le publier. Je tiens aussi beaucoup à exprimer ma gratitude à mes collaborateurs de l'Office National d'Etudes et de Recherches Aérospatiales, M. Nguyen VAN-NHÂN et Bruno CHRISTOPHE dont l'aide m'a été très précieuse. Je remercie enfin vivement M. Jean-Louis LE MOUEL, Jean-Paul POIRIER et J. CALMUSCKI de l'Institut de Physique du Globe de Paris, M. Hilaire LEGROS de l'Institut de Physique du Globe de Strasbourg, M. François BARLIER de l'Observatoire de la Côte d'Azur et MM. Bruno MORANDO, Jacques LASKAR, Olivier NÉRON DE SURGY et Pierre BRETAGNON du Bureau des Longitudes qui m'ont transmis un très grand nombre de renseignements indispensables.

Manuscript submitted for publication on 19 September 1995; accepted on 31 January 1996.

REFERENCES

ARIAS E. F., CHARLOT P., FEISSEL M. & LESTRADE J.-F. 1995. — The extragalactic reference system of the International Earth Rotation Service, I.C.R.S. *Astronomy and Astrophysics* **303**: 604.

BALMINO G., REIGBER Ch. & MOYNOT B. 1978. — Le modèle de potentiel gravitationnel terrestre GRIM2. *Annales de Géophysique* **34** (2): 55-78.

BUREAU DES LONGITUDES 1984. — *Encyclopédie scientifique de l'Univers. La Terre, les eaux, l'atmosphère.* GAUTHIER VILLARS (eds).

BURSA M. 1992. — Parameters of common relevance of Astronomy, Geodesy and Geodynamics. *In* C. C. TSCHERNING (ed.). *Geodetic Bulletin, The Geodesist's Handbook.* **66** (2).

CAREY S. W. 1958. — The tectonic approach to continental drift: *Symposium on Continental Drift*. Hobart: 177-355.

— 1976. — *The Expanding Earth. Developments in Geotectonics* 10. Elsevier Scientific Publishing Company. Amsterdam, Oxford, New York, 488 p.

DZIEWONSKI A. M. & ANDERSON D. L. 1981. — Preliminary reference Earth model. *Physics of the Earth and Planetary Interiors* **25**: 297-356.

HILGENBERG O. 1933. — *Vom Wachsenden Erdball*. Berlin, 50 p.

JEANS J. H. 1917. — *Memoirs of the Royal Astronomical Society* **62**.

LASKAR J. 1993. — La Lune et l'origine de l'homme. *Pour la science*, hors série, août: 14-21.

LASKAR J. & ROBUTEL P. 1993. — The chaotic Obliquity of the Planets. *Nature* **361**: 608-612.

LASKAR J., JOUTEL F. & ROBUTEL P. 1993. — Stabilization of Earth's Obliquity by the Moon. *Nature* **361**: 615-617.

LEGROS H. 1987. — *Sur quelques problèmes de dynamique planétaire*. Thèse de doctorat. Université Louis Pasteur de Strasbourg, Institut de Physique du Globe, Laboratoire de Géodynamique, 16 septembre.

LE MOUEL J.-L. & COURTILLOT V. 1981. — Core motions, electromagnetic core mantle and variations in the Earth's rotation: new constraints. *Physics of the Earth and Planetary Interiors* **24**: 236-241.

LERCH F. J., KLOSKO S. M., LAUBSCHER R. E. & WAGNER C. A. 1979. — Gravity model improvement using GEOS-3 (GEM-9 and 10). *Journal of Geophysical Resarch* **84**: 3897-3915.

LICHTENSTEIN L. 1933. — *Gleichgewichtsfiguren rotierender Flussigkeiten*. Leipzig.

LOVE A. E. H. 1911. — *Some Problems of Geodynamics*. Cambridge University Press.

MARCHAL C. 1968. — Figures d'équilibre séculairement stables des masses fluides hétérogènes en rotation. *Bulletin astronomique*, série 3, 3 (3): 341-360.

MARSH J. G., LERCH F. J., PUTNEY B. H., FELSENTREGER T. L., SANCHEZ B. V., KLOSKO S. M., PATEL G. B., ROBBINS J. W., WILLIAMSON R. G., ENGELIS T. L., EDDY W. F., CHANDLER N. L., CHINN D. S., KAPOOR S., RACHLIN K. E., BRAATZ L. E. & PAVLIS E. C. 1990. — The GEM-T2 Gravitational Model. *Journal of Geophysical Research*, December 10, 95 (B13): 22043-22071.

OWEN H. G. 1981. — Ocean floor spreading evidence of Global Expansion. *In* S. W. CAREY (ed.). *The Expanding Earth. A Symposium at University of Sydney*, February 10-14, University of Tasmania.

— 1984. — The Earth is expanding and we don't know why. *New Scientist* November 22.

— 1989. — La Terre en expansion. *107e Congrès de l'Association Française pour l'Avancement des Sciences*, Orléans 23-25 novembre.

POINCARÉ H. 1952. — Formes d'équilibre d'une masse fluide en rotation. *In* GAUTHIER VILLARS (ed.). *Œuvres de H. POINCARÉ*. Paris 7:14-219.

REIGBER C., SCHWINTZER P., BARTH W., MASSMANN F. H., RAIMONDO J. C., BODE A., LI H., BALMINO G., BIANCALE R., MOYNOT B., LEMOINE J. M., MARTY J. C., BARLIER F. & BOUDON Y. 1993. — Grim4-C1-C2p: Combination solutions of the global Earth gravity field. *Surveys in Geophysics* **14**: 381-393.

RICARD Y., SPADA G. & SABADINI R. 1993. — Polar wandering of a dynamic Earth. *International Geophysical Journal* **113**: 284-298.

SPADA G., RICARD Y. & SABADINI R. 1992. — Excitation of true polar wander by subduction. Letter to Nature. *Nature* **360**: 452-454.

APPENDIX 1

STABLE HYDROSTATIC EQUILIBRIUM OF A ROTATING PLANET AND SPHEROIDAL SYMMETRY

Stable hydrostatic equilibria

A rotating planet has a negative gravitational energy (it requires energy to disperse all its parts) and a positive kinetic energy of rotation. The sum of these two energies is the (negative) mechanical energy while the stable hydrostatic equilibria correspond to the local minima of that mechanical energy under the following conditions.

The planet is isolated, very far from other celestial bodies.

The total angular momentum $\vec{H}$ of the planet is given and cannot be modified.

The planet is composed of undilatable and incompressible fluids. Notice that this third condition is not restrictive since for ordinary fluid planets, composed of dilatable and compressible fluids, any stable hydrostatic equilibrium corresponds also to a particular stable hydrostatic equilibrium in the above meaning.

The general properties of stable hydrostatic equilibria are as follows:

The planet has no inner motion, it rotates uniformly as an invariable solid about its main axis of largest inertia that we will call Oz, with O being the center of mass. Oz is of course in the direction of the angular momentum $\vec{H}$ and we will use an ordinary rotating set of axes with Ox along the main axis of smallest inertia and Oy along the main axis of mean inertia.

The equatorial plane Oxy is a plane of symmetry (LICHTENSTEIN symmetry, LICHTENSTEIN 1933) and on straight lines parallel to Oz the density increases, or is at least is non-decreasing, when $|z|$ decreases.

It seems that all stable hydrostatic equilibria have a second plane of symmetry: the meridian plane Oxz (with the corresponding density property). However, this property has only been partially demonstrated (see for instance condition (A5) below).

The spheroidal symmetry

A planet with spheroidal symmetry not only has the above LICHTENSTEIN symmetry about the equatorial plane but also has a symmetry of revolution about the polar axis Oz. Furthermore on z = constant planes the density is non-decreasing when we approach Oz.

Domain of spheroidal symmetry

For centuries, until the JACOBI counter-example given below, it was believed that all stable hydrostatic equilibria must have spheroidal symmetry. Nevertheless the domain of this symmetry remains large.

Let us call:

(A1)
$$\begin{cases} G \text{ the constant of Newton's law} \\ M \text{ the total mass of the planet} \\ \rho \text{ its mean density } (\rho = M/\text{volume}) \\ \omega \text{ its rate of rotation} \\ D \text{ its "diameter" (largest distance between two points)} \\ R \text{ its "radius" (largest distance between the center of mass O and the surface), hence} \\ R < D \leq 2R \\ A, B, C \text{ the main moments of inertia, with } A \leq B \leq C \\ \Delta = \sqrt[3]{(GM/\omega^2} = \text{average distance of "planetostationary" and "planetosynchronous" satellites.} \end{cases}$$

The angular momentum H is equal to $C\omega$ and it is easy to verify that:

$2C \leq A + B + C \leq 2MR^2$.

For an homogeneous planet the figures with stable hydrostatic equilibrium are either oblate MacLaurin ellipsoids or three axis Jacobi ellipsoids. All Poincaré figures are unstable (Jeans 1917).

The stable oblate MacLaurin ellipsoids have spheroidal symmetry, a ratio major axis/minor axis in the range 1 to 1.71608 and a slow rotation: they exist only if

$$H \leq 0.23924\ G^{\frac{1}{2}} M^{\frac{5}{3}} \rho^{-\frac{1}{6}}$$

(see the next appendix). The one-parameter family of stable three-axis Jacobi ellipsoids follows that of MacLaurin ellipsoids without discontinuity. These Jacobi ellipsoids have a ratio major axis / minor axis in the range 1.71608; 2.8983. (The ratio r_2 = (mean axis/minor axis) is almost exactly given in terms of the ratio r_1 = (major axis/minor axis) by the relation $(r_1 - \alpha)(r_2 - \alpha) = 0.581415$; with $\alpha = 0.953572$.) They exists only when the number without dimension $H\,G^{-\frac{1}{2}} M^{-\frac{5}{3}} \rho^{\frac{1}{6}}$ is in the range 0.23924; 0.30684. Beyond the upper limit an homogeneous planet has too fast a rotation and generally undergoes fission into two very unequal parts (Marchal 1968).

These results can be extended to heterogeneous planets and the following partial but already very general results can be demonstrated.

All stable hydrostatic equilibria verifying:

(A2) $D \leq \Delta$

have spheroidal symmetry (Marchal 1968).

All stable hydrostatic equilibria verifying:

(A3) $2MR^2 + A + B + 5C \leq 2M\Delta^2$

also have spheroidal symmetry (which implies of course $A = B$).

All stable hydrostatic equilibria verifying:

(A4) $2MR^2 - A + 3B + 3C \leq 2M\Delta^2$

have at least the "tri-symmetry" already encountered for three-axis JACOBI ellipsoids. The three main planes Oxy, Oxz and Oyz are planes of symmetry and the density is non-decreasing when one moves towards these planes on a straight line parallel to one of the three axes.

Finally if:

(A5) $2MR^2 + 3A - B + 3C \leq 2M\Delta^2$

it is easy to demonstrate the "bi-symmetry" that was conjectured above for all stable hydrostatic equilibria.

All known stahle hydrostatic equilibria with only bi-symmetry are very far from spheroidal symmetry. They always verify $4A \leq B$.

For the Earth: $D = 2R$ and $\Delta = 6.61\,R$ (= distance of geostationary satellites). The inequality (A2) is widely satisfied.

This condition $D \leq \Delta$ is satisfied by all planets but Saturn (for which $D = 1.07\,\Delta$). Fortunately Saturn, and all other planets, verify (A3) and thus all planets of the solar system have an hydrostatic equilibrium with spheroidal symmetry.

APPENDIX 2

STUDY OF THE STABLE HYDROSTATIC EQUILIBRIUM OF AN EARTH MODEL

We have seen above that with only the information (42) we can already obtain very narrow limits (43), (44) on the difference $(C_B - A_B)$. A better Earth model than the limiting cases used in (43), (44) will then give $(C_B - A_B)$ with excellent accuracy.

Let us consider for instance the following ten homogeneous layer Earth model (Table 2) that is a simplification of the model presented in BUREAU DES LONGITUDES 1984. Notice that the third and fourth layers are given with extremely accurate densities: these two layers correspond to the largest Earth zone, the lower mantle (55% of the volume, 49% of the mass); and the two densities are chosen in order to keep the following accurately known elements of Earth: the total mass and the average moment of inertia. These accurate densities are not at all an indication of the degree of our knowledge of Earth, they are there only to give us a better value of the difference $(C_B - A_B)$ that we are looking for.

We can then research the stable hydrostatic equilibrium of this model of Earth. A first approximation is to consider that all level surfaces are oblate ellipsoids. We will then need the gravitational potential of an homogeneous oblate ellipsoid, that is of a MACLAURIN ellipsoid already considered in appendix 1. Let us call a the semi-major axis of this oblate ellipsoid (equatorial radius), c its semi-minor axis (polar radius), R its average radius (with $R^3 = a^2 c$), e the eccentricity of its meridians (with $c = a\sqrt{(1 - e^2)}$ and ρ its density. With Oz in the polar direction we obtain the following classical expression of the inner gravitational potential U:

$$\text{(A6)}\quad U = GM\left[-\frac{3}{2ae}\,\text{Arcsin}\ e + \frac{x^2 + y^2 + z^2}{2R^3} + \frac{2z^2 - x^2 - y^2}{4R^3}\,F(e)\right]$$

with:

$$\text{(A7)}\begin{cases} G = \text{constant of NEWTON's law} \\ M = \text{mass of the ellipsoid} = 4\pi R^3\rho/3 = 4\pi a^2 c\rho/3 \\ a = R(1-e^2)^{-\frac{1}{6}}\ ;\ c = R(1-e^2)^{\frac{1}{3}} \\ F(e) = \dfrac{3}{e^2} - 1 - \dfrac{3}{e^3}\sqrt{(1-e^2)}\cdot \text{Arcsin } e = \dfrac{2}{5}e^2 + \dfrac{2\times 4}{5\times 7}e^4 + \dfrac{2\times 4\times 6}{5\times 7\times 9}e^6 + \ldots \end{cases}$$

(For an isolated MACLAURIN ellipsoid the rate of rotation ω is given by the uniformity of the total potential $U - 0.5\ \omega^2(x^2 + y^2)$ along the surface. This leads to:
$\omega^2 = 2\pi G\rho\ [2e^2 + (2e^2 - 3)\ F(e)] / 3$.

This oblate MACLAURIN ellipsoid is stable if and only if:

$(3e + 10e^3)\sqrt{(1-e^2)} \geq (3 + 8e^2 - 8e^4)$. Arcsin e; that is $e \leq e_f = 0.812\,670\,01\ldots$

The last stable MACLAURIN ellipsoid, obtained for $e = e_f$, is also the first JACOBI ellipsoid.)

It is then easy to obtain the total gravitational energy E_G of the system of the ten ellipsoidal layers. Notice first that we can consider this system as a system of ten homogeneous concentric ellipsoids (with a spatial superposition of these ellipsoids); the k[th] ellipsoid having the density $\delta_k = \rho_k - \rho_{k+1}$ and the mass $M_k = \dfrac{4\pi}{3} R_k^3\,\delta_k$.

Then, with the function F(e) of (A7):

$$\text{(A8)}\begin{cases} E_G = \dfrac{G}{10}\displaystyle\sum_{1\leq j<k\leq 10} M_j M_k \left[\dfrac{R_j^2}{R_k^3}\,\dfrac{3 - e_j^2\,(1 + F(e_k))}{(1-e_j^2)^{\frac{1}{3}}} - \dfrac{15}{R_k}\,\dfrac{(1-e_k^2)^{\frac{1}{6}}}{e_k}\ \text{Arcsin } e_k\right] - \\ -\dfrac{3G}{5}\displaystyle\sum_{k=1}^{10}\dfrac{M_k^2}{R_k}\,\dfrac{(1-e_k^2)^{\frac{1}{6}}}{e_k}\ \text{Arcsin } e_k \end{cases}$$

We also need the kinetic energy of rotation E_C:

$$\text{(A9)}\quad E_C = \frac{H^2}{2C_B} = \frac{5H^2}{4\displaystyle\sum_{k=1}^{10} M_k R_k^2\,(1-e_k^2)^{-\frac{1}{3}}}$$

with:

$$\text{(A10)}\begin{cases} H = \text{Earth's angular momentum} = 5.859\,893\,762\text{p}33\ \text{kg m}^2\,\text{s}^{-1} \\ C_B = \text{polar moment of inertia of the system of the ten homogeneous ellipsoids} \\ \quad = \dfrac{2}{5}\displaystyle\sum_{k=1}^{10} M_k R_k^2\,(1-e_k^2)^{-\frac{1}{3}} \end{cases}$$

The mechanical energy $E = E_G + E_C$ is then a function of 22 known quantities (G, H, the ten M_k, the ten R_k) and ten unknown quantities (the eccentricities e_k). The minimisation of the mechanical energy E with respect to the ten eccentricities gives the stable hydrostatic equilibrium. These minimising eccentricities are given in the fourth column of Table 2; they increase from e_1 to e_{10} and correspond to the oblateness: $\left(1 - \sqrt{1 - e_{10}^2}\right) = 1/299.8115$.

The corresponding difference $(C_B - A_B)$ between the main moments of inertia is the following (as already presented in (45)).

$$\text{(A11)} \begin{cases} C_B - A_B = \frac{1}{5} \sum_{k=1}^{10} M_k R_k^2 \left[(1 - e_k^2)^{-\frac{1}{3}} - (1 - e_k^2)^{\frac{2}{3}} \right] = \frac{1}{5} \sum_{k=1}^{10} M_k R_k^2 \, e_k^2 \, (1 - e_k^2)^{-\frac{1}{3}} \\ \quad = 2.602\,623 \text{ p35 kg m}^2 = 1.070\,978 \text{ n3 } MR^2 . \end{cases}$$

The true stable hydrostatic equilibrium has level surfaces that are only quasi-ellipsoids. These quasi-ellipsoids are slightly depressed at mid-latitudes but the depressions are extremely small. The largest one, at the Earth's surface, reaches the proportion 6.7 n7 only of the corresponding radius, that is only 4.3 meters. The corresponding modification of the difference $C_B - A_B$ is negligible, it doesn't modify the digits given in (A11).

Table 2. Study of an Earth model with ten homogeneous layers.
Notice 1: the radius R_{10} takes the volumes of continents into account.
Notice 2: the accuracy of ρ_3 and ρ_4 is artificial and doesn't reflect our uncertain knowledge of Earth. These densities of the two main layers (corresponding to the lower mantle) allows us to keep the two essential parameters: the total mass $M = \sum M_k = 5.973\ 698\ 985$ p24 kg and the average moment of inertia $= \frac{2}{5} \sum M_k R_k^2 = 8.018\ 385\ 949$ p37 kg m² (these two parameters themselves have a superabundant accuracy which allows at least a direct comparison with the extreme cases presented in (43) and (44) and which leads to the best possible value of the difference $(C_B - A_B)$ we were looking for).

average radius (in km)	density of the layer (in g/cm3)	mass M_k (in 10^{24} kg) $M_k = \frac{4}{3} \pi R_k^3 (\rho_k - \rho_{k+1})$	eccentricity of the meridian ellipses (after minimisation of the mechanical energy)
R_0 = 0			
R_1 = 1221.5	ρ_1 = 12.90	M_1 = 0.015 192 250	e_1 = 0.069 801 515 54
R_2 = 3480	ρ_2 = 10.91	M_2 = 0.974 226 590	e_2 = 0,072 035 569 37
R_3 = 4845	ρ_3 = 5.391 340 009	M_3 = 0.461 997 078	e_3 = 0.075 994 548 44
R_4 = 5701	ρ_4 = 4.421 568 826	M_4 = 0.435 357 701	e_4 = 0.079 157 866 65
R_5 = 5971	ρ_5 = 3.86	M_5 = 0.338 854 626	e_5 = 0,080 133 114 66
R_6 = 6151	ρ_6 = 3.48	M_6 = 0.107 230 536	e_6 = 0.080 790 375 46
R_7 = 6346.6	ρ_7 = 3.37	M_7 = 0.503 280 205	e_7 = 0.081 515 276 99
R_8 = 6356	ρ_8 = 2.9	M_8 = 0.322 672 185	e_8 = 0.081 550 310 60
R_9 = 6368.45	ρ_9 = 2.6	M_9 = 1.709 412 701	e_9 = 0.081 596 868 85
R_{10} = 6371.2	ρ_{10} = 1.02	M_{10} = 1.104 975 112	e_{10} = 0.081 607 191 58

APPENDIX 3

ABOUT THE HYPOTHESIS OF EARTH EXPANSION

In 1912, A. WEGENER presented his Theory of Continental Drift now subsumed by the Theory of Plate Tectonics. But this theory was so new and so audacious that it was discarded by most scientists until the end of the sixties and the discovery of a possible motor: the motions of convection in the Earth's mantle. These motions are envisaged as being produced by the heat supplied essentially by the Earth's natural radioactivity.

Similarly, after the pioneering works of O. HILGENBERG (1933), A. DUTOIT, S. W. CAREY (1958, 1976), the theory of Earth Expansion has been promoted by H. G. OWEN (1981, 1984, 1989). This theory helps to explain a wide variety of geological features; however, in the absence of a plausible explanation, it remains discarded by most scientists.

Nevertheless, let us consider Table 1 of inner Earth, and let us examine the two main layers, *i.e.* the lower mantle (55% of Earth's volume and 49% of Earth's mass) and the outer core (16% of Earth's volume and 31% of Earth's mass).

The boundary between these two layers is particularly abrupt and well-defined, its position is well-known and it separates two media with very different densities and very different seismic velocities. Notice that the velocity V_S of transversal waves is 7 km/s in the lower mantle and 0 in the outer core as if the lower mantle were solid and the outer core liquid.

In these conditions it is reasonable to envisage that the lower mantle and the outer core are composed of the same material under two different phases, the solid phase (lower mantle) floating above the liquid phase (outer core) exactly as in the polar oceans in which the ice-cap is floating on water.

If this is true, in a slowly cooling Earth, the outer core can progressively transform into lower mantle and the volume of Earth will expand slowly and continuously. The average density of the outer core is 10.9 and that of the lower mantle is 4.9. If we keep these same average densities during the transformation, the volume of Earth can expand from 70% of its present value (when all the lower mantle was liquid) to 119% of its present value (when all the outer core will be solid). The corresponding radii are 0.89 R and 1.06 R which seems in good agreement with OWEN's theory of Earth Expansion. If that slow transformation can be extended to the transition zone (middle mantle), the initial volume of the Earth could have been as low as 58% of its present value.



Date de distribution le 30 juillet 1996

Le fascicule n° 1 1996 a été distribué le 29 février 1996.

LOUIS-JEAN
avenue d'Embrun, 05003 GAP cedex
Tél. : 92.53.17.00
Dépôt légal : 547 — Juillet 1996
Imprimé en France

Mémoires du Muséum national d'Histoire naturelle
Série C - Sciences de la Terre

À partir de 1993, les *Mémoires du Muséum national d'Histoire naturelle* ne paraissent plus en quatre séries séparées (A, B, C, D), mais en une seule série. Le nom de la revue devient *Mémoires du Muséum national d'Histoire naturelle* (ISSN 1243-4442). La numérotation commence au tome 155.

164 **Broutin, J.** *et al.* 1995. La Flore fossile du bassin houiller de Saint-Étienne.

165 **Marshall, L. G., Muizon Ch. de & Sigogneau-Russell D.,** 1995. *Pucadelphys andinus* (Marsupialia, Mammalia) from the Early Paleocene of the Santa Lucia Formation, Bolivia.

Bulletin du Muséum national d'Histoire naturelle

Les gisements de mammifères du Miocène supérieur de Kemiklitepe, Turquie. 4e série, **16**, 1994, section C, n° 1, 240 p.

VIIe Symposium International, Parc de Miguasha, Québec, Études sur les Vertébrés inférieurs. *Coordonné par Marius Arsenault, Hervé Lelièvre et Philippe Janvier*, 4e série, **17** (1-4), 1995, section C, 530 p., ca. 200 figures.

Vente en France

MUSÉUM NATIONAL D'HISTOIRE NATURELLE

Éditions Scientifiques du Muséum, Paris
Diffusion Delphine Henry
57, rue Cuvier, 75005 Paris, France
Tél.: [33] (1) 40.79.37.00
Fax : [33] (1) 40.79.38.40
Internet http://www.mnhn.fr

Sales Office (France excluded)

UNIVERSAL BOOK SERVICES

Dr W. Backhuys
P.O. Box 321 2300 AH Leiden
The Netherlands
Tel.: [31] (71) 5 17 02 08
Fax : [31] (71) 5 17 18 56
Internet backhuys @ euronet.nl


MUSEUM
NATIONAL
D'HIST. NAT.